

# Chapter 4

## Taxonomy of soil ciliates (Ciliophora) from Australia and some other parts of the world<sup>1</sup>

Wilhelm Foissner

University of Salzburg, Hellbrunnerstrasse 34, 5020 Salzburg, Austria

<http://www.foissner.at>

<https://orcid.org/0000-0003-4528-0176>

ZooBank registration of present chapter: [urn:lsid:zoobank.org:pub:3D9A9E74-4463-458F-9292-BB78E435A32A](https://zoobank.org/pub:3D9A9E74-4463-458F-9292-BB78E435A32A)

### 4.1 Summary of taxa described in this work and of nomenclatural acts<sup>2</sup>

Within each category (e.g., genus) the taxa are arranged alphabetically. All taxa are ciliates, unless otherwise indicated.

#### 4.1.1 New subspecies

*Circinella filiformis australiensis* nov. sspec. (p. 209); *Enchelys polynucleata hollandica* nov. sspec. (p. 65); *Mixophrya pantanalensis australiensis* nov. sspec. (p. 256); *Mixophrya pantanalensis pantanalensis* nov. sspec. (p. 253); *Oxytricha africana australiensis* nov. sspec. (p. 290); *Rimaleptus similis australiensis* nov. sspec. (p. 129).

#### 4.1.2 New species

*Afrogonostomum alveum* nov. spec. (p. 205); *Apobryophyllum pinetum* nov. spec. (p. 116); *Apooxytricha bromelicola* nov. spec. (p. 276); *Bophrya costata* nov. spec. (p. 135); *Bothrix africana* nov. spec. (p. 234); *Bryophyllum australiense* nov. spec. (p. 125); *Bursaria africana* nov. spec. (p. 157); *Bursaria americana* nov. spec. (p. 163); *Bursaria fluviatilis* nov. spec. (p. 185); *Bursaria salisburgensis* nov. spec. (p. 179); *Bursaria uluruensis* nov. spec. (p. 181); *Conothrix australiensis* nov. spec. (p. 267); *Crassienchelys oriclavata* nov. spec. (p. 92); *Enchelariophrya jamaicensis* nov. spec. (p. 58); *Enchelys australiensis* nov. spec. (p. 73); *Enchelys bivacuolata* nov. spec. (p. 79); *Enchelys polyvacuolata* nov. spec. (p. 84); *Gastronauta insula* nov. spec. (p. 194); *Levispatha australiensis* nov. spec. (p. 100); *Microsporidium protocyclidicola* nov. spec. (Microsporida; p. 201); *Mixophrya pantanalensis* nov. spec. (p. 248); *Monomicrocaryon australiense* nov. spec. (p. 283); *Protocyclidium bimacronucleatum*

<sup>1</sup> This chapter should be referenced as follows: Foissner W. (2021): Taxonomy of soil ciliates (Ciliophora) from Australia and some other parts of the world. – In: Foissner W. & Berger H. (Eds): Terrestrial ciliates (Protista, Ciliophora) from Australia and some other parts of the world. — Series Monographiae Ciliophorae, Number 5: 55–345.

<sup>2</sup> Note by H. Berger: I have written this part of this chapter.

© Verlag Helmut Berger 2021

W. Foissner & H. Berger (Eds), *Terrestrial ciliates (Protista, Ciliophora) from Australia and some other parts of the world*, Series Monographiae Ciliophorae, Number 5

nov. spec. (p. 199); *Protocyclidium namibiense* nov. spec. (p. 198); *Pseudofuscheria magna* nov. spec. (p. 111); *Tachysoma setifera* nov. spec. (p. 293); *Urosoma australiensis* nov. spec. (p. 212); *Urosoma pelobia* nov. spec. (p. 217); *Urosomoida bromelicola* nov. spec. (p. 229); *Urosomoida uluruensis* nov. spec. (p. 225); *Wolfkosia acuta* nov. spec. (p. 141); *Wolfkosia pantanalensis* nov. spec. (p. 147).

#### 4.1.3 New genera

*Afrogonostomum* nov. gen. (p. 203); *Apooxytricha* nov. gen. (p. 276); *Bophrya* nov. gen. (p. 133); *Bothrix* nov. gen. (p. 232); *Conothrix* nov. gen. (p. 261); *Crassienchelys* nov. gen. (p. 89); *Levispatha* nov. gen. (p. 99); *Mixophrya* nov. gen. (p. 245); *Protospatha* nov. gen. (p. 100); *Pseudofuscheria* nov. gen. (p. 109); *Spinispatha* nov. gen. (p. 100).

#### 4.1.4 New combination

*Enchelariophrya micrographica* (Foissner, 2010) nov. comb. (p. 57); *Mixophrya gigantea* (Horváth, 1933) nov. comb. (p. 246).

#### 4.1.5 New status

*Enchelys polynucleata polynucleata* (Foissner, 1984) Foissner, Agatha & Berger, 2002 nov. stat. (p. 63); *Rimaleptus similis similis* (Foissner, 1995) Vďačný & Foissner, 2012 nov. stat. (p. 129).

#### 4.1.6 New subfamily

Territrichinae nov. subfam. (p. 275).

#### 4.1.7 New families

Bophryidae nov. fam. (p. 133); Bothrigidae nov. fam. (p. 232); Conotrichidae nov. fam. (p. 261).

#### 4.1.8 Redescriptions, emendations, remarks

*Arcuospathidium* Foissner, 1984 (p. 99); *Bursaria* Müller, 1773 (p. 149); *Bursaria caudata* Dragesco, 1972 (p. 176); *Bursaria ovata* Beers, 1952 (p. 173); *Bursaria truncatella* Müller, 1773 (p. 155); *Enchelariophrya* Foissner, 2016 (p. 57); *Enchelys megaspinata* Jang, Vďačný, Shazib & Shin, 2017 (p. 73); *Enchelys polynucleata* (Foissner, 1984) Foissner, Agatha & Berger, 2002 (p. 63); *Exocolpoda augustini* (Foissner, 1987a) Foissner, Agatha & Berger, 2002 (p. 193); *Gonostomum affine* (Stein, 1859) Sterki, 1878 (p. 203); *Hemiurosoma similis* (Foissner, 1982) Foissner, Agatha & Berger, 2002 (p. 221); *Monomicrocaryon opisthomuscorum* (Foissner, Blatterer, Berger & Kohmann, 1991) Foissner, 2016 (p. 290); *Oxytricha lithofer* Foissner, 2016 (p. 292); *Pattersoniella* Foissner, 1987a (p. 298); *Pattersoniella* (*Pattersoniella*) Foissner, 1987a (p. 298); *Pattersoniella* (*Pattersoniellides*) Kumar & Foissner, 2016 (p. 298); *Pattersoniella* (*Pattersoniellides*) *australiensis* Kumar & Foissner, 2016 (p. 297); *Wolfkosia* Foissner, Agatha & Berger, 2002 (p. 141).

#### 4.1.9 Type slides and accession numbers

The slides of the species described in the present chapter are shown in Chapter 5. The type slides are deposited in the Upper Austrian Museum in Linz (LI); for accession numbers see Table 1 in Chapter 5.

## 4.2 Description of taxa<sup>1</sup>

### 4.2.1 Gymnostomatea

For some recent comments on this taxon by W. Foissner, see Foissner (2016, p. 49).

#### *Enchelariophrya* Foissner, 2016

**Remarks:** The new species discovered, *Enchelariophrya jamaicensis*, stimulated me to re-investigate the materials from *Enchelys micrographica* Foissner, 2010, especially the oral structures which are very difficult to recognize due to the narrow setting between oral bulge and body proper (Fig. 1a–c, 2a–c, e, 3a, d, e, j, k, m, q, r). However, with some effort, I could produce very detailed photographs, showing a single dikinetid, which produces an oral basket rod at anterior end of each ciliary row and close to the first kinetid of the ciliary rows (Fig. 1d, 3e, f, j, k, m, n, q, r). Thus, oralized somatic kinetids, as suggested by Foissner (2010, Fig. 12), are absent.

A very similar pattern occurs in the genus *Semispathidium* Foissner, Agatha & Berger, 2002. However, *Semispathidium* species still have a minute gap between the somatic kineties and the circumoral kinety (Foissner et al. 2002, 2010; Vd'ačný & Foissner 2013; Vd'ačný et al. 2014a) and have much more circumoral dikinetids than somatic kineties. Further, all described *Enchelariophrya* species have a pyriform body shape and an acentric oral opening while *Semispathidium* species are rod-shaped and have a central oral opening. Thus, it is unlikely that *Enchelariophrya* is a junior synonym of *Semispathidium*.

#### *Enchelariophrya micrographica* (Foissner, 2010) nov. comb.

(Fig. 1a, f, 2g, j, 3j–r, 9g–k; Table 1 on p. 308)

2010 *Enchelys micrographica* nov. spec. — Foissner, MittBl. Mikroskop. Ges. Wien, Festschrift, November 2010: 72 (original description).

**Remarks:** The discovery of  $\rightarrow$  *Enchelariophrya jamaicensis* stimulated me to re-investigate the live micrographs of the extrusomes (Fig. 2j) and the protargol preparations of *Enchelariophrya micrographica*. As concerns the extrusomes, they are thicker in *E. micrographica* than in *E. jamaicensis* (in vivo  $3.0\text{--}4.0 \times 0.5\text{--}0.8 \mu\text{m}$  vs. about  $3.0 \times 0.4 \mu\text{m}$ ; cp. Fig. 1f, 2j with Fig. 1e, 2h). The second problem, viz., the structure of the oral ciliature, could be solved by stacked micrographs of *E. micrographica* and *E. jamaicensis* (see above and Fig. 1d, 2e, f, j, k, m, q, r).

---

<sup>1</sup> Note by H. Berger: The arrangement (classification) of the taxa within this work was not yet fixed by W. Foissner. Thus, I arranged them basically as in Foissner et al. (2002) and Foissner (2016). In addition, W. Foissner did not yet write comments to the higher taxa as he did it in Foissner (2016). I added some brief hints (see, for example, chapter 4.2.1 above). An arrow ahead of a certain taxon means that it is described in the present work. The “Type locality” and “Occurrence and ecology” sections sometimes contain sample numbers (e.g., “Australian site (30)”). Foissner did not yet compile a table/list with a detailed description of these samples as he did it in his other monographs (e.g., Foissner 2016). I did not delete them, although they have no meaning in the present work. Perhaps I can provide such a list in a later work. The present chapter also contains the description of a new *Microsporidium* species, which follows immediately the host species, a new *Protocyclidium* species.

The work contains 204 plates, but relatively little text. Therefore I have added the tables with the morphometric characterisations (Tables 1–37) at the end of the chapter (p. 307–345).

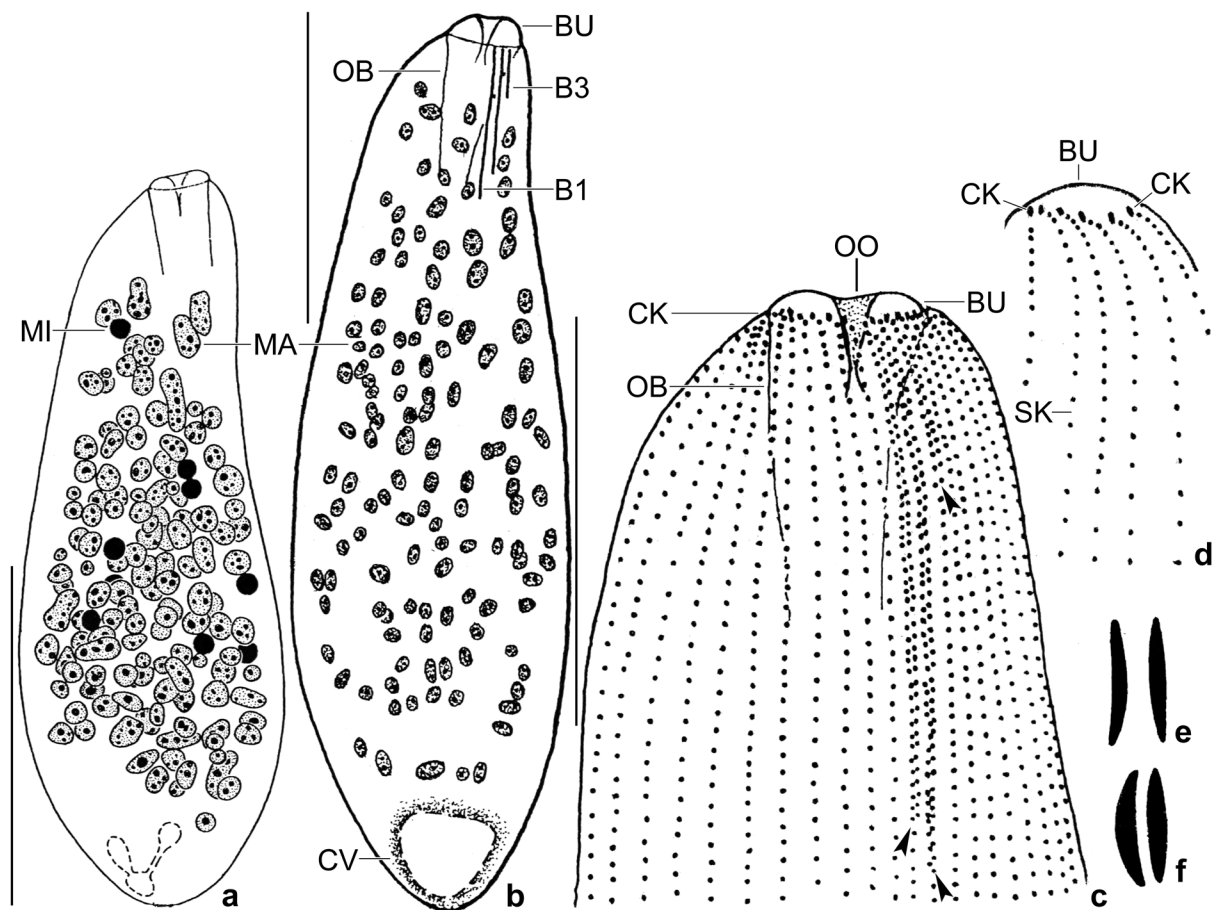


**Fig. 1a–f.** *Enchelariophrya jamaicensis* (b–e) and *Enchelariophrya micrographica* (a, f, from Foissner 2010). **a, b:** *Enchelariophrya micrographica* has only half of the macronuclear nodules of *E. jamaicensis* (only half of the nodules is shown!) but the nodules are twice as large as in *E. jamaicensis*. **c:** Dorsal view of anterior body portion of holotype specimen, showing the posterior end of the dorsal brush rows (arrowheads) and the narrow spacing of the brush dikinetids. **d:** Structure of circumoral kinety in *Enchelariophrya*. **e, f:** The extrusomes of *E. jamaicensis* (e) are thinner than those of *E. micrographica* (f), i.e., about  $3.0 \times 0.4 \mu\text{m}$  vs.  $3.0\text{--}4.0 \times 0.5\text{--}0.8 \mu\text{m}$ . B1, 3 – dorsal brush rows, BU – oral bulge, CK – circumoral ciliature, CV – contractile vacuole, MA – macronuclear nodules, MI – micronucleus, OB – oral basket, OO – oral opening, SK – somatic kinety. Scale bars  $50 \mu\text{m}$  (a, b) and  $20 \mu\text{m}$  (c).

***Enchelariophrya jamaicensis* nov. spec.**

(Fig. 1b, c, e, 2a–i, 3a–i; Table 1 on p. 308)

**Diagnosis:** Size in vivo about  $135 \times 45 \mu\text{m}$ . Usually pyriform with oral opening distinctly out of pole centre. On average about 260 macronuclear nodules  $3.8 \times 3.2 \mu\text{m}$  in size. Extrusomes bluntly fusiform and slightly curved, about  $3.0 \times 0.4 \mu\text{m}$  in size. Cortical granulation very dense, plate-like. On average 41 ciliary rows; middle row of dorsal brush extends about 32% of body length. Spines of resting cyst about  $13 \mu\text{m}$  long.

**Type locality:** Humous surface soil (0–5 cm) around an *Aechmea paniculigera* (Bromeliaceae) in the outskirts of the village of Quick Step in Cockpit Country, Jamaica,  $18^{\circ}17'N$ ,  $77^{\circ}41'W$ .

**Type material:** The slide containing the holotype (Fig. 1c, 3d) and three paratype slides with protargol-impregnated specimens have been deposited in the Biology Centre of the Upper Austrian Museum in Linz (LI). The holotype and all paratype specimens have been marked with black ink circles on the coverslip. For slides, see Fig. 1a–e in Chapter 5.

**Etymology:** Named after the country discovered, i.e., Jamaica.

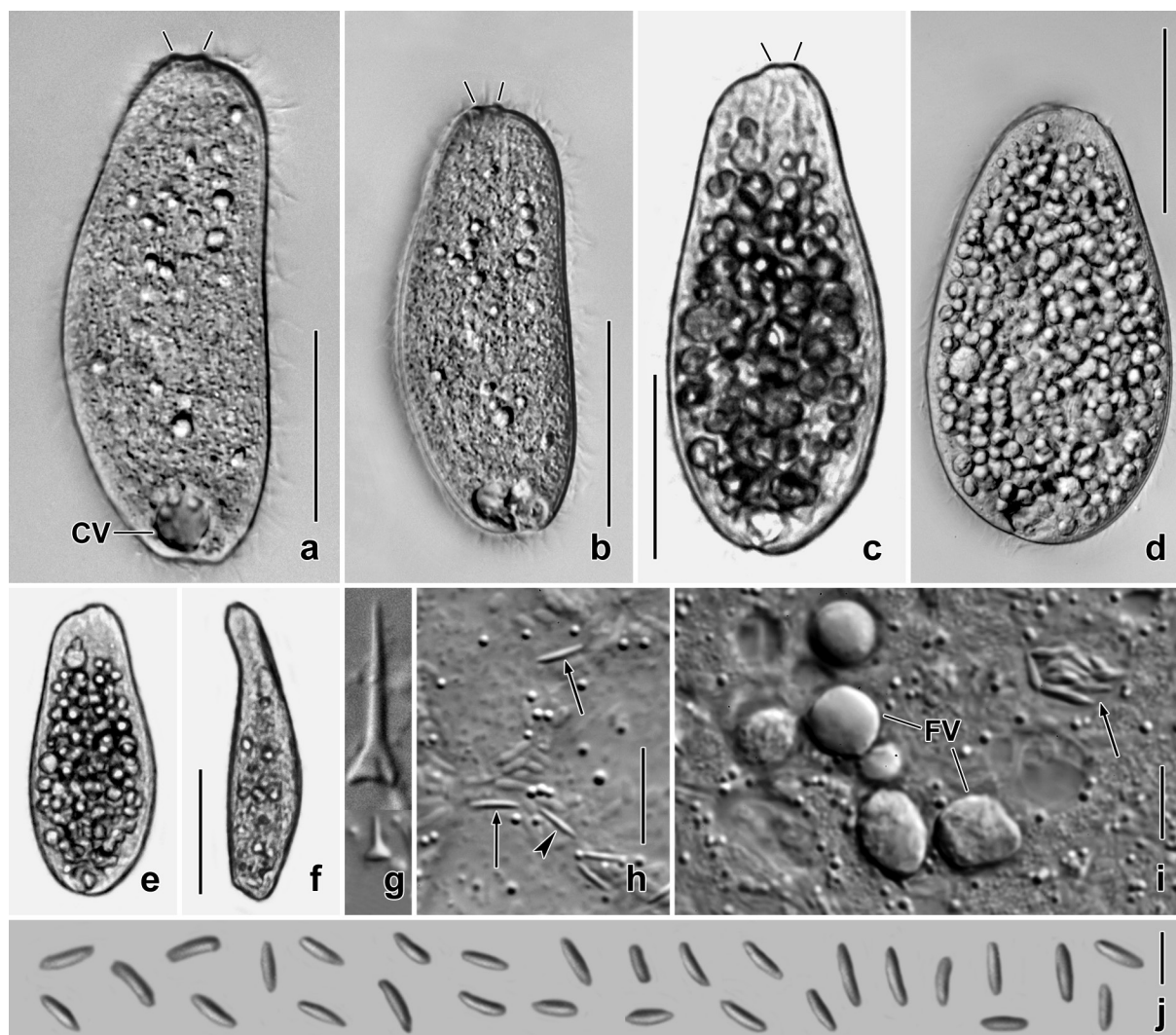


**Fig. 2a–j.** *Enchelariophrya jamaicensis* (a–f; g, upper spine; h, i) and *E. micrographica* (g, lower spine; j) from life. **a–c, e, f:** Freely motile specimens, showing the acentric location of the minute oral apparatus (oblique lines) and the pyriform body shape (b, c, e). The cells are flattened about 2:1, even when they have many food vacuoles (e, f). **d:** A slightly pressed specimen, showing many bright globules, very likely food vacuoles in advanced digestion. **g:** Comparison of cyst spines of *E. jamaicensis* (upper spine) and *E. micrographica* (lower spine), made to scale. **h:** Extrusomes of *E. jamaicensis*, narrow (arrowhead) and broad side (arrows) views, size about  $3.0 \times 0.4 \mu\text{m}$ . **i:** Part of cytoplasm, showing compact food vacuoles and a vacuole (arrow) with prey (*Frontonia depressa*) trichocysts, suggesting organelle sorting. **j:** Extrusomes of *E. micrographica*, size  $3.0\text{--}4.0 \times 0.5\text{--}0.8 \mu\text{m}$ ; magnified with the computer. CV – contractile vacuole, FV – food vacuoles. Scale bars  $50 \mu\text{m}$  (a–f),  $13 \mu\text{m}$  (h),  $10 \mu\text{m}$  (i), and  $5 \mu\text{m}$  (j).

**Description and comparison with *Enchelariophrya micrographica*:** Unfortunately, *Enchelariophrya jamaicensis* was very rare and the protargol preparations were mediocre. Thus, the morphometry is incomplete (Table 1).

As concerns the general morphology and the *in vivo* aspect, I refer the reader to Figures 1 and 4 of *E. micrographica* in Foissner (2010). Details of *E. jamaicensis* and a comparison with *E. micrographica* are shown by micrographs, the figure explanations, and the morphometric table. Generally, the morphology of *E. jamaicensis* is highly similar to that of *E. micrographica*, both *in vivo* and in protargol preparations. For feeding of *E. micrographica*, see → *Enchelys australiensis* (Fig. 8g–k). Here, I mention only those features that help to separate *E. jamaicensis* from *E. micrographica* (lined up according to importance; averages are given, see Table 1; *E. jamaicensis* ahead): resting cyst spines (*in vivo*  $13 \mu\text{m}$  vs.  $3 \mu\text{m}$ ; seen within cytoplasm and in a single mature

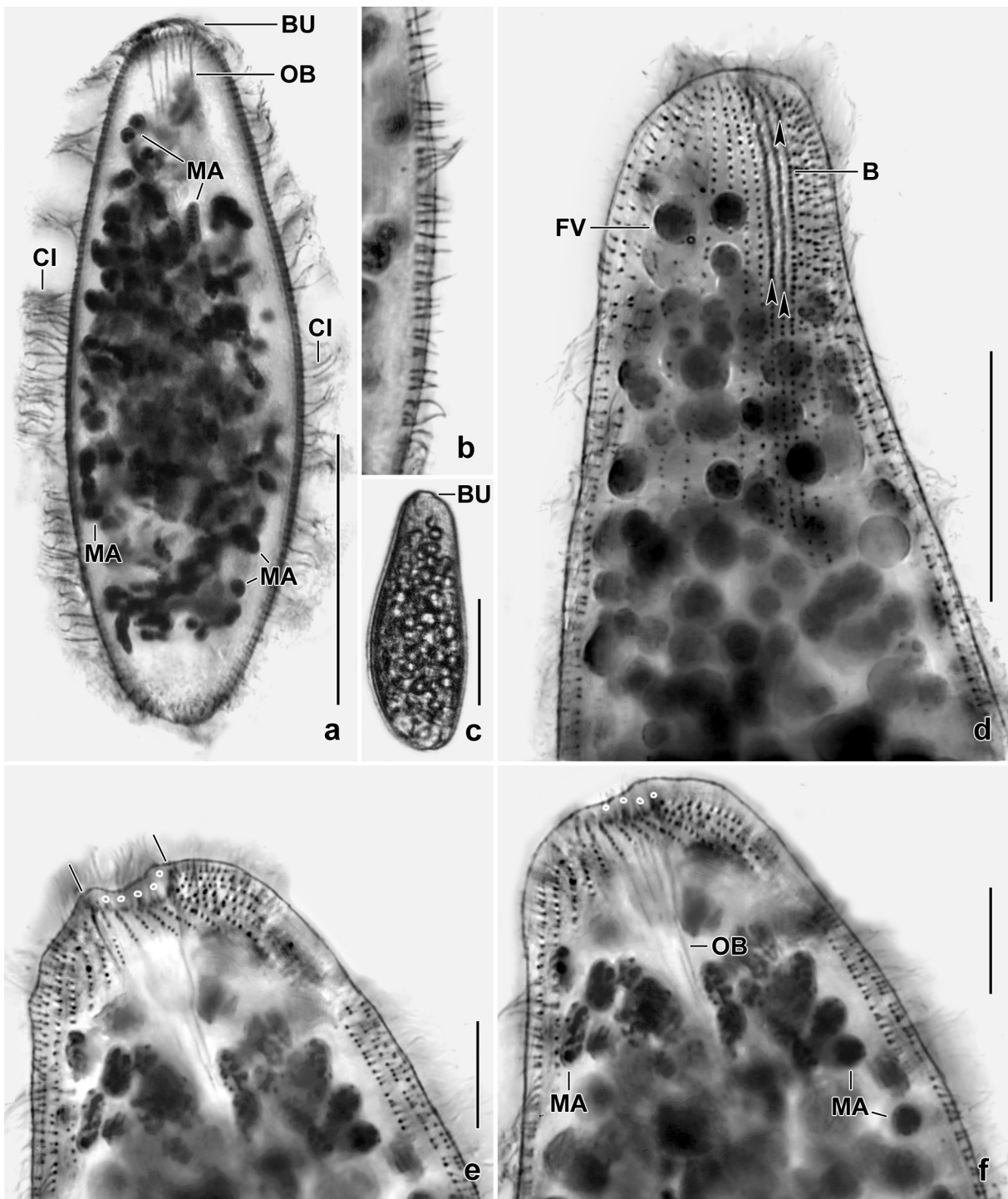


**Fig. 3a–f.** *Enchelariophrya jamaicensis* from life (c) and after protargol impregnation (a, b, d–f). **a:** Overview, showing the dense ciliature and many macronuclear nodules. **b:** A somatic kinety. The cilia are narrowly and irregularly arranged mainly in anterior half of body (see also Fig. 3e, f). **c:** A typical, freely motile specimen showing the minute oral bulge. **d:** Dorsal view of anterior third of holotype specimen, showing the three dorsal brush rows (posterior ends marked by arrowheads) with very narrowly spaced dikinetids (cp. Fig. 1c). **e, f:** Lateral view at two focal planes, showing the oral bulge (margin marked by lines) and a dikinetid each in between two ciliary rows (dots). B – dorsal brush, BU – oral bulge, CI – cilia, FV – food vacuoles, MA – macronuclear nodules, OB – oral basket. Scale bars 50  $\mu\text{m}$  (a, c), 30  $\mu\text{m}$  (d), and 10  $\mu\text{m}$  (e, f).

cyst; Fig. 2g); number of macronuclear nodules in protargol preparations (260.0 vs. 116.7; Fig. 1a, b, 3a, e–i; Table 1); number of dikinetids in dorsal brush rows 1–3 (very narrowly spaced; 42.0 vs.

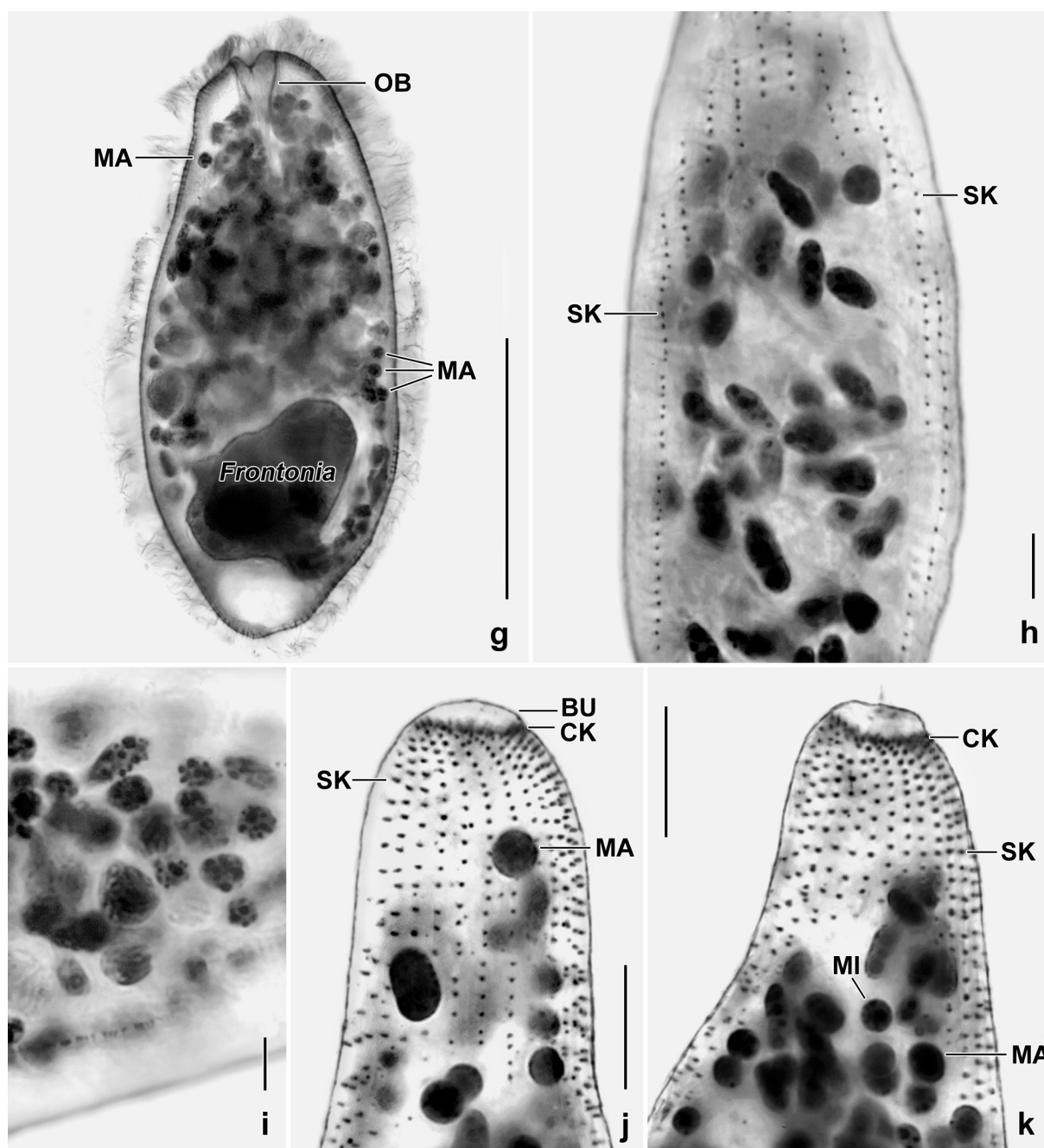


**Fig. 3g–k.** *Enchelariophrya jamaicensis* (g–i) and *E. micrographica* (j, k) after protargol impregnation. **g:** Overview, showing a large food vacuole containing a decaying *Frontonia depressa*. This is remarkable, showing that the minute oral bulge (Fig. 2a–c, e) can open widely. Note the globular to broadly ellipsoid macronuclear nodules. **h, i:** A specimen with mainly elongate ellipsoid macronuclear nodules (h,  $6.4 \times 2.8 \mu\text{m}$ ,  $n = 9$ ; in two out of five cells) and another with globular to broadly ellipsoid nodules (i,  $3.8 \times 3.2 \mu\text{m}$ ; Table X; in three out of five cells). **j, k:** Lateral views of anterior body portion of *E. micrographica*, showing the oral and circumoral ciliature, i.e., the circumoral kinety (for details, see next plate) and the anteriorly curved somatic kineties, a spathidid character. Compared to *E. jamaicensis* (g–i), the macronuclear nodules are larger and rarer. BU – oral bulge, CK – circumoral kinety, MA – macronuclear nodules, OB – oral basket, SK – somatic kineties. Scale bars  $50 \mu\text{m}$  (g),  $10 \mu\text{m}$  (j, k),  $7 \mu\text{m}$  (h), and  $5 \mu\text{m}$  (i).

23.7, 40.0 vs. 28.9, 16.0 vs. 11.4; Fig. 3d, n; Table 1); number of ciliary rows (41.4 vs. 34.9; Table 1); size of macronuclear nodules in protargol preparations ( $3.8 \times 3.2$  vs.  $6.5 \times 4.1$ ; Table 1); and body length in protargol preparations ( $118.8 \mu\text{m}$  vs.  $107.2 \mu\text{m}$ ; Table 1). Basically, these differences suggest subspecies rank but the considerable difference in the length of the cyst spines as well as in the number and size of macronuclear nodules suggest species rank.

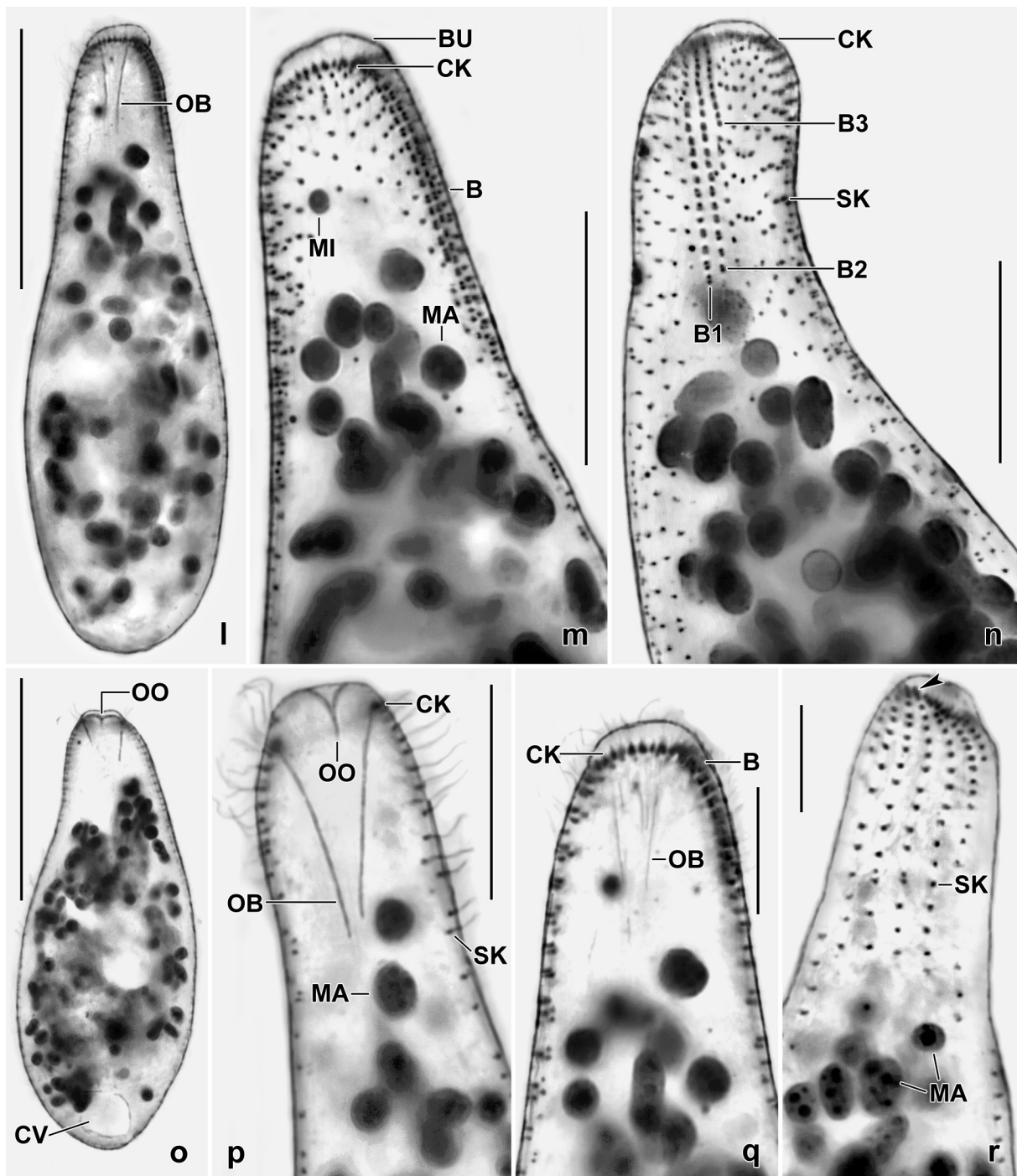


**Fig. 31–r.** *Enchelariophrya micrographica* after protargol impregnation. **l, o:** Overviews, showing the pyriform body shape. **m, q, r:** Lateral views of anterior body portion (m and q from same specimen at two focal planes). The circumoral dikinetids are comparatively large because of the adjacent anteriormost ordinary monokinetid of the ciliary rows. When seen obliquely and due to the rather distinctly curved anterior region of the ciliary rows, the circumoral dikinetids appear as minute rods between the beginning of the ciliary rows (Fig. 3e, f, Fig. 3r, arrowhead). **n:** Dorsal view, showing the dorsal brush where the dikinetids are much wider spaced than in *E. jamaicensis* (Fig. 3d). **p:** Oral apparatus. B – dorsal brush, BU – oral bulge, B1,2,3 – dorsal brush rows, CK – circumoral kinety, CV – contractile vacuole, MA – macronuclear nodules, MI – micronuclei, OB – oral basket, OO – oral opening, SK – somatic kineties. Scale bars 50  $\mu\text{m}$  (l, o) and 20  $\mu\text{m}$  (m, n, p–r).

**Ecology and distribution:** As yet found only at type locality. Was not present in the bromeliad tank water investigated three times during a period of three weeks.

**Remarks:** The third species, *Enchelariophrya wolffi* Foissner, 2016, is type of the genus and occurs at the same locality as *E. jamaicensis*. This species is much smaller than *E. micrographica* and *E. jamaicensis* ( $64.3 \times 14.2 \mu\text{m}$  vs.  $118.8 \times 40.4 \mu\text{m}$  in protargol preparations), has only 23.0 vs. 41.4 ciliary rows, and 45 vs. 260 macronuclear nodules and occurs not only in Jamaica but also in the Morrocoy National Park in Venezuela (Foissner 2016).

***Enchelys polynucleata* (Foissner, 1984) Foissner, Agatha & Berger, 2002**

(Table 2 on p. 309)

**Improved diagnosis** (averages are provided): Size in vivo about  $130 \times 65 \mu\text{m}$ ; bursiform. More than 100 macronuclear nodules. Oral bulge extrusomes rod-shaped, indistinctly curved,  $10 \mu\text{m}$  long. On average 35 ciliary rows, three anteriorly differentiated to a dorsal brush. Oral bulge about  $30 \mu\text{m}$  long in vivo, ordinary or formed like a propeller blade; temporary cytostome near centre of oral bulge or neighboured dorsal margin. Resting cyst globular and with distinct spines  $5\text{--}15 \mu\text{m}$  long.

**Remarks:** Over the years, I studied five *Enchelys polynucleata*-like populations. Originally, I classified most as *E. polynucleata*, including two new Australian species, viz.,  $\rightarrow$  *Enchelys australiensis* and  $\rightarrow$  *Crassienchelys oriclavata*. Jang et al. (2017) discovered a further species, viz.,  $\rightarrow$  *Enchelys megaspinata*, briefly described below. Very likely, all belong to the *E. polynucleata*-complex, possibly except of *Crassienchelys*, which is thus not contained in the diagnosis of the complex.

***Enchelys polynucleata polynucleata* (Foissner, 1984) Foissner, Agatha & Berger, 2002 nov. stat.**

(Fig. 4a–e, 5a–d; Table 2 on p. 309)

- 1984 *Enchelydium polynucleatum* nov. spec. — Foissner, Stapfia, 12: 37 (supplemented with micrographs, Fig. 4a–e).  
1985 *Enchelydium polynucleatum* Foissner, 1984 — Foissner W. & Foissner I., J. Protozool., 32: 712 (transmission electron microscopy).  
1996 *Enchelydium polynucleatum* Foissner, 1984 — Foissner, Biol. Fertil. Soils, 23: 284 (Gough Island in the Southern Atlantic Ocean; here supplemented with micrographs, Fig. 5a–d).  
2002 *Enchelys polynucleata* Foissner (1984) nov. comb. — Foissner, Agatha & Berger, Denisia, 5: 121, 127 (record from Namibia).  
2006 *Enchelys polynucleata* (Foissner, 1984) Foissner, Agatha & Berger 2002 — Strüder-Kypke, Wright, Foissner, Chatzinotas & Lynn, Protist, 157: 271 (molecular taxonomy).  
2008 *Enchelydium polynucleatum* Foissner, 1984 and *Enchelys polynucleata* (Foissner, 1984) Foissner, Agatha & Berger, 2002 — Berger & Al-Rasheid, Denisia, 23: 77, 91 (Festschrift).  
2016 *Enchelys polynucleata* (Foissner, 1984) Foissner, Agatha & Berger, 2002 — Foissner, Denisia, 35: 28 (record from Venezuela).

**Diagnosis** (includes the population from Gough Island): Size in protargol preparations  $96\text{--}140 \times 38\text{--}77 \mu\text{m}$ , on average  $120 \times 55 \mu\text{m}$ . Oral bulge ordinary, temporary cytostome in or near centre of oral bulge ( $0\text{--}7 \mu\text{m}$ , average  $1\text{--}3 \mu\text{m}$  out of bulge centre). Spines of resting cyst  $<10 \mu\text{m}$  long; cyst wall colourless.

**Type locality:** Soil of an intensely farmed field in Lower Austria, Tullnerfeld, near the village of Bierbaum,  $48^{\circ}23'N$ ,  $15^{\circ}56'E$ .

**Type material:** The holotype slide (1984/22; see Aescht 2008, p. 174) with protargol-impregnated specimens has been deposited in the Biology Centre of the Upper Austrian Museum in Linz (LI). Here, I add three paratype slides from the type population. Further, I add three voucher slides with protargol-impregnated specimens from Gough Island. Important specimens have been marked by black ink circles on the coverslip. For slides, see Fig. 2a–f in Chapter 5.

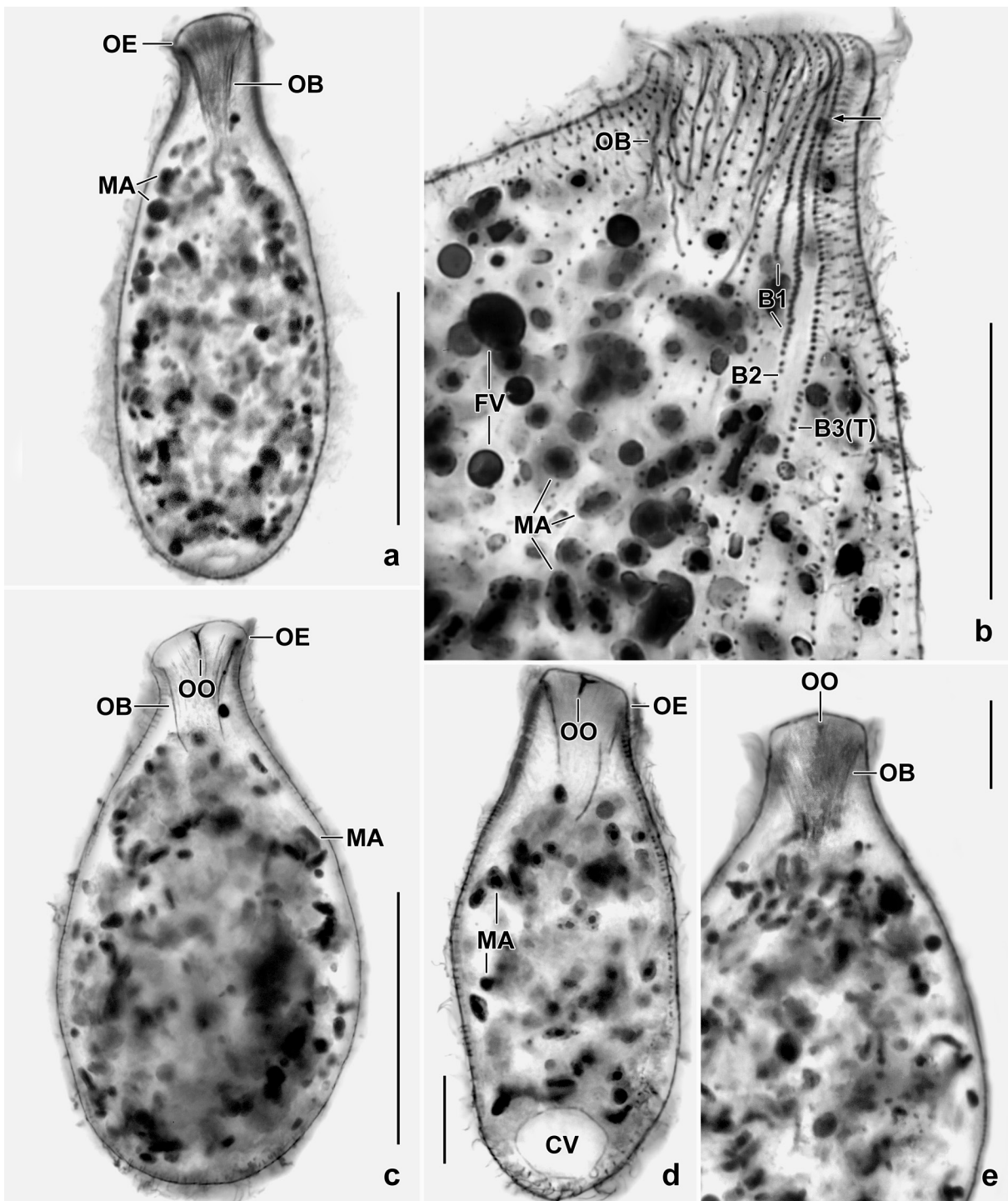


**Fig. 4a–e.** *Enchelys polynucleata polynucleata*, Austrian type population after protargol impregnation. **a, c:** Left and right side view of a moderately and of an overfed specimen becoming broadly bottle-shaped. **b:** Dorsolateral view, showing the dorsal brush; row 3 has a long, monokinetal bristle tail, B3(T). The arrow in (b) marks the transition zone of dikinetids and monokinetids. **d, e:** Focused on temporary cytostome in centre of oral bulge. B1–3 – dorsal brush rows, B3(T) – bristle tail of brush row 3, CV – contractile vacuole, FV – food vacuoles, MA – macronuclear nodules, OB – oral basket, OE – oral bulge, OO – temporary cytostome. Scale bars 50 µm (a, c), 30 µm (b), and 20 µm (d, e).

**Remarks:** The records from Namibia and Venezuela remain uncertain because the location of the temporary cytostome was not investigated and protargol preparations were not available. Possibly, the population from Gough Island is also a distinct subspecies; however, the extremes overlap suggesting conspecificity with *Enchelys polynucleata polynucleata*.

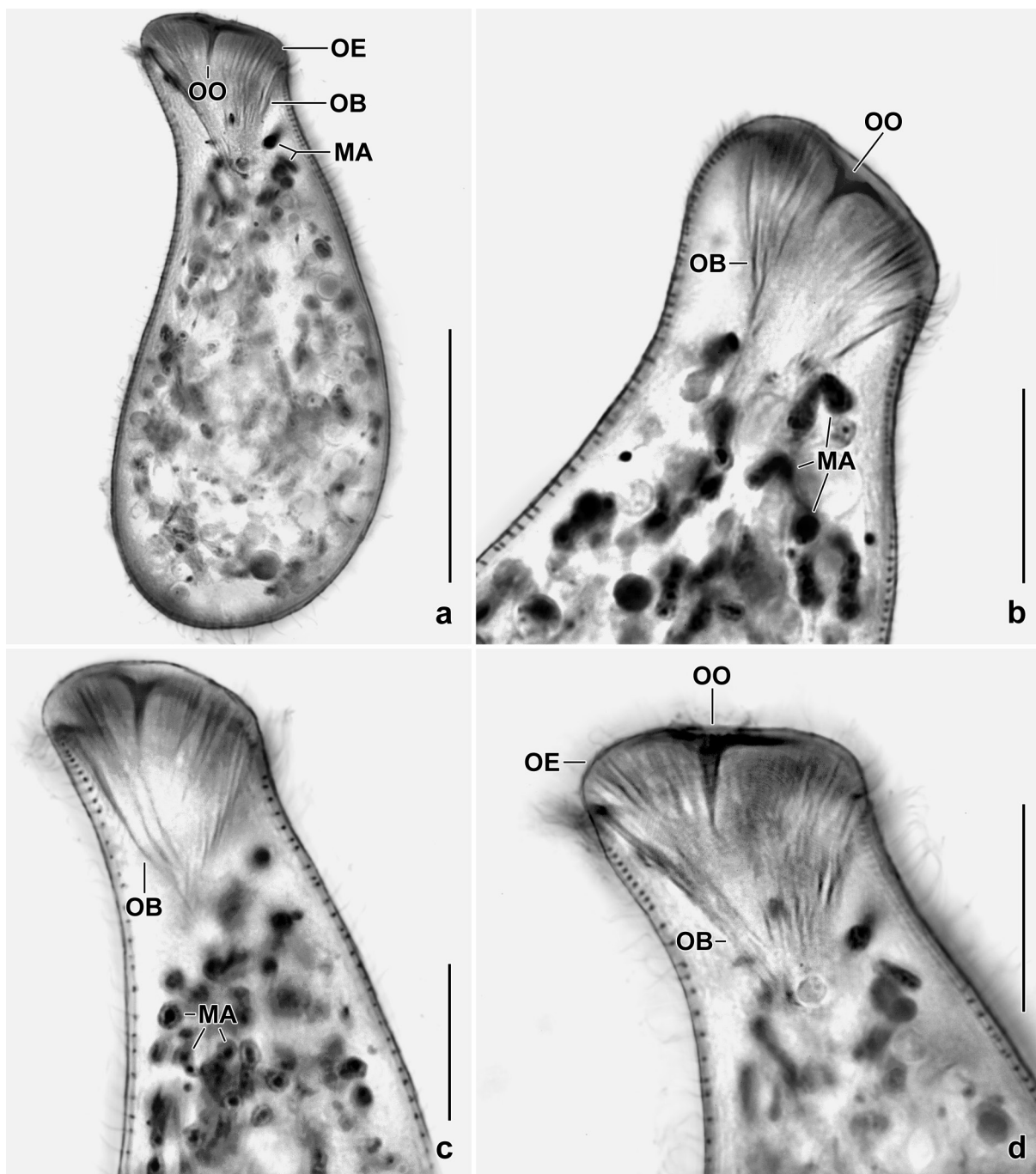


**Fig. 5a–d.** *Enchelys polynucleata polynucleata*, protargol-impregnated specimens from Gough Island in the sub-Antarctic region. **a:** A typical, bursiform specimen, showing the distinct oral basket and the temporary cytostome. **b–d:** This subspecies has the temporary cytostome in the centre of the oral bulge (b) or slightly neighbored the dorsal side (a, c, d), an important character. MA – macronuclear nodules, OB – oral basket, OE – oral bulge, OO – temporary cytostome. Scale bars 50  $\mu\text{m}$  (a) and 20  $\mu\text{m}$  (b–d).

***Enchelys polynucleata hollandica* nov. subsp.**

(Fig. 6a–h, 7a–u; Table 2 on p. 309)

2007 *Enchelys polynucleata* (Foissner 1984) Foissner et al. 2002 — Foissner & Al-Rasheid, Acta Protozool., 46: 209 (description of population from The Netherlands).

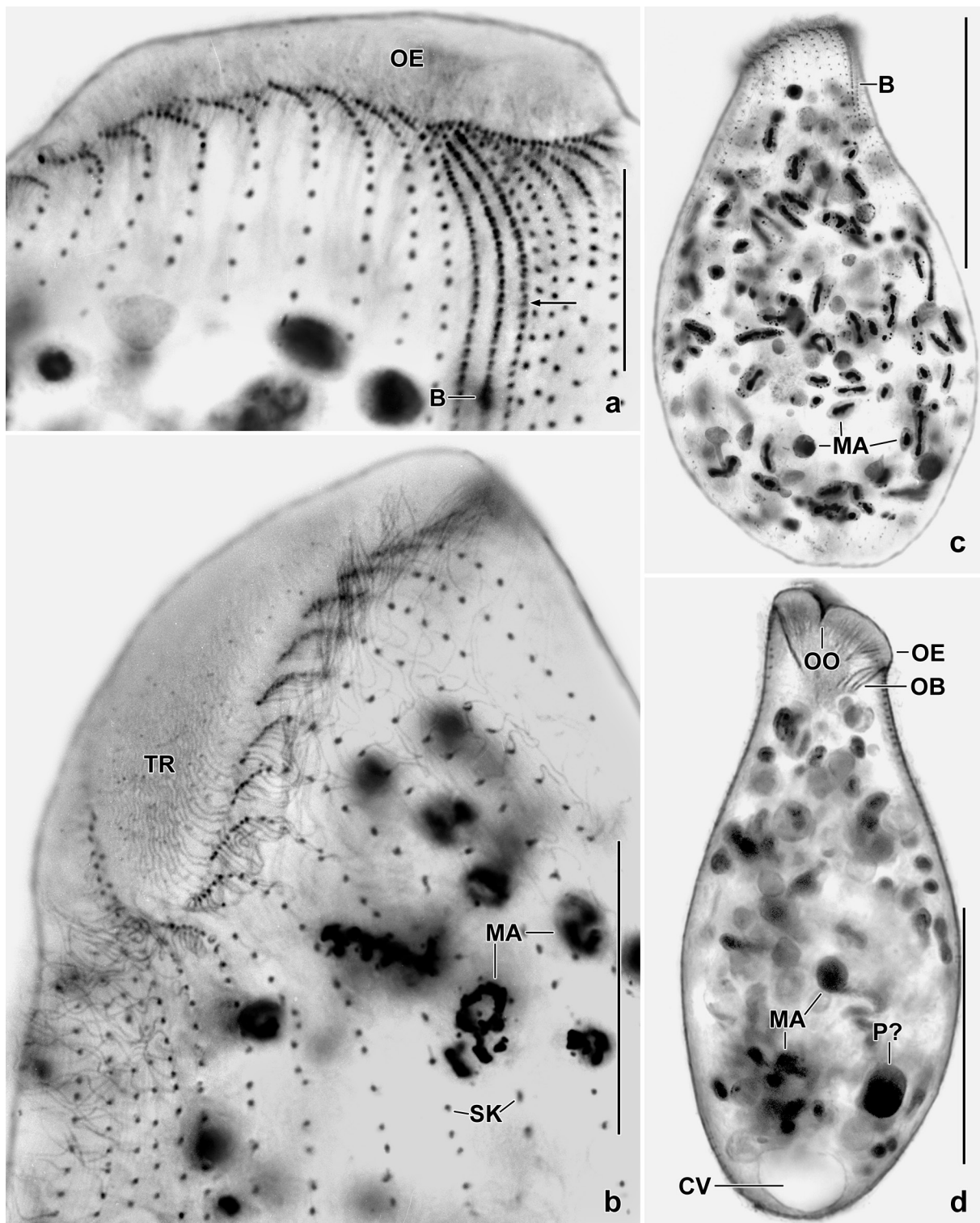


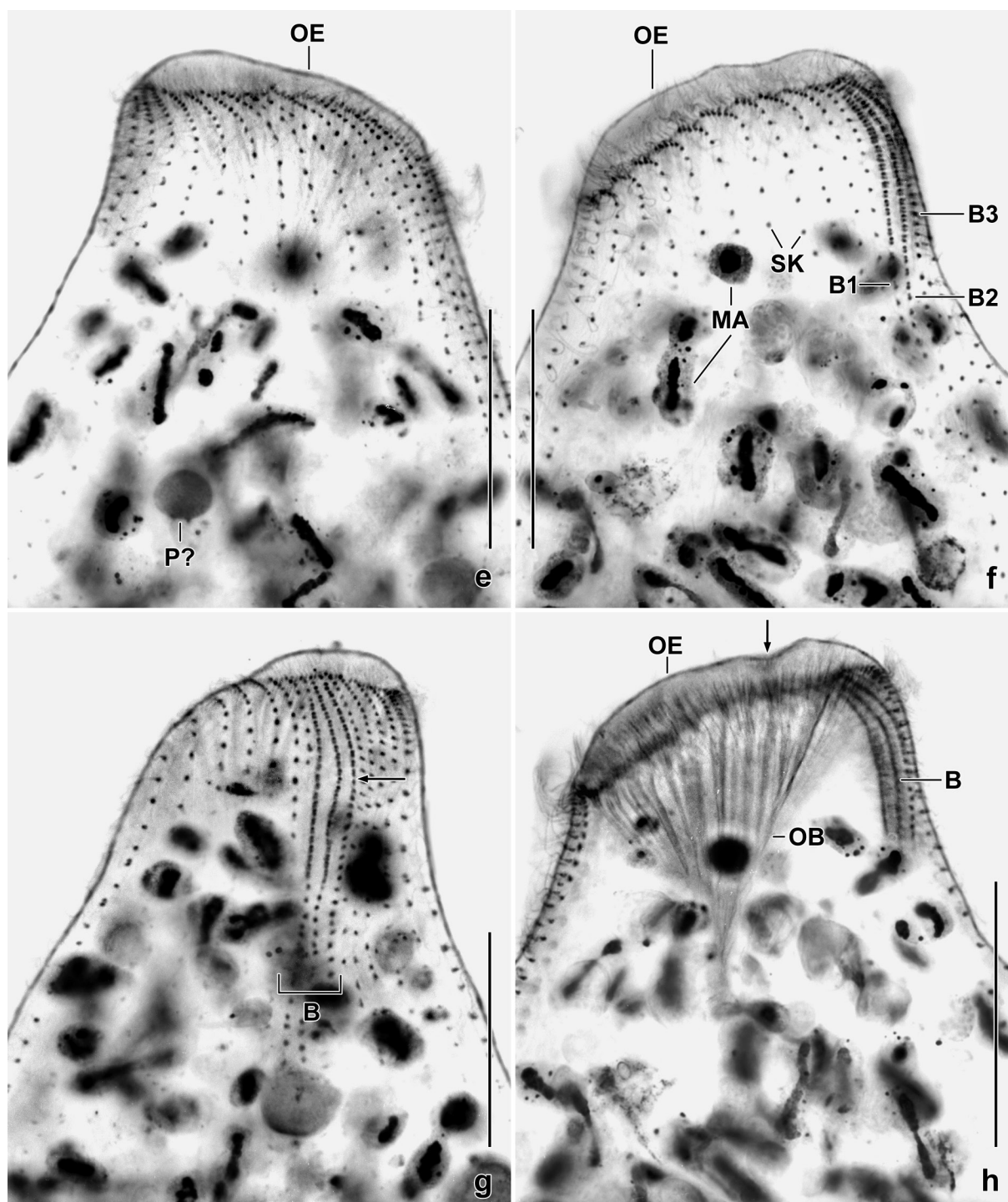
**Fig. 6a–d.** *Enchelys polynucleata hollandica* after protargol impregnation. Specimens in (a–c) pressed to show details. **a:** Dorsal view showing anterior region of dorsal brush. The arrow marks the transition of dikinetids to a monokinetal bristle tail. **b:** Ventrolateral view, showing the densely ciliated curved anterior portion of the ciliary rows. **c, d:** Overviews. The temporary cytostome is distinctly out of bulge centre (d). B – dorsal brush, CV – contractile vacuole, MA – macronuclear nodules, OB – oral basket, OE – oral bulge, OO – temporary cytostome, P – parasite, SK – somatic kineties, TR – transverse microtubule ribbons in oral bulge. Scale bars 50  $\mu\text{m}$  (c, d), 20  $\mu\text{m}$  (b), and 10  $\mu\text{m}$  (a).

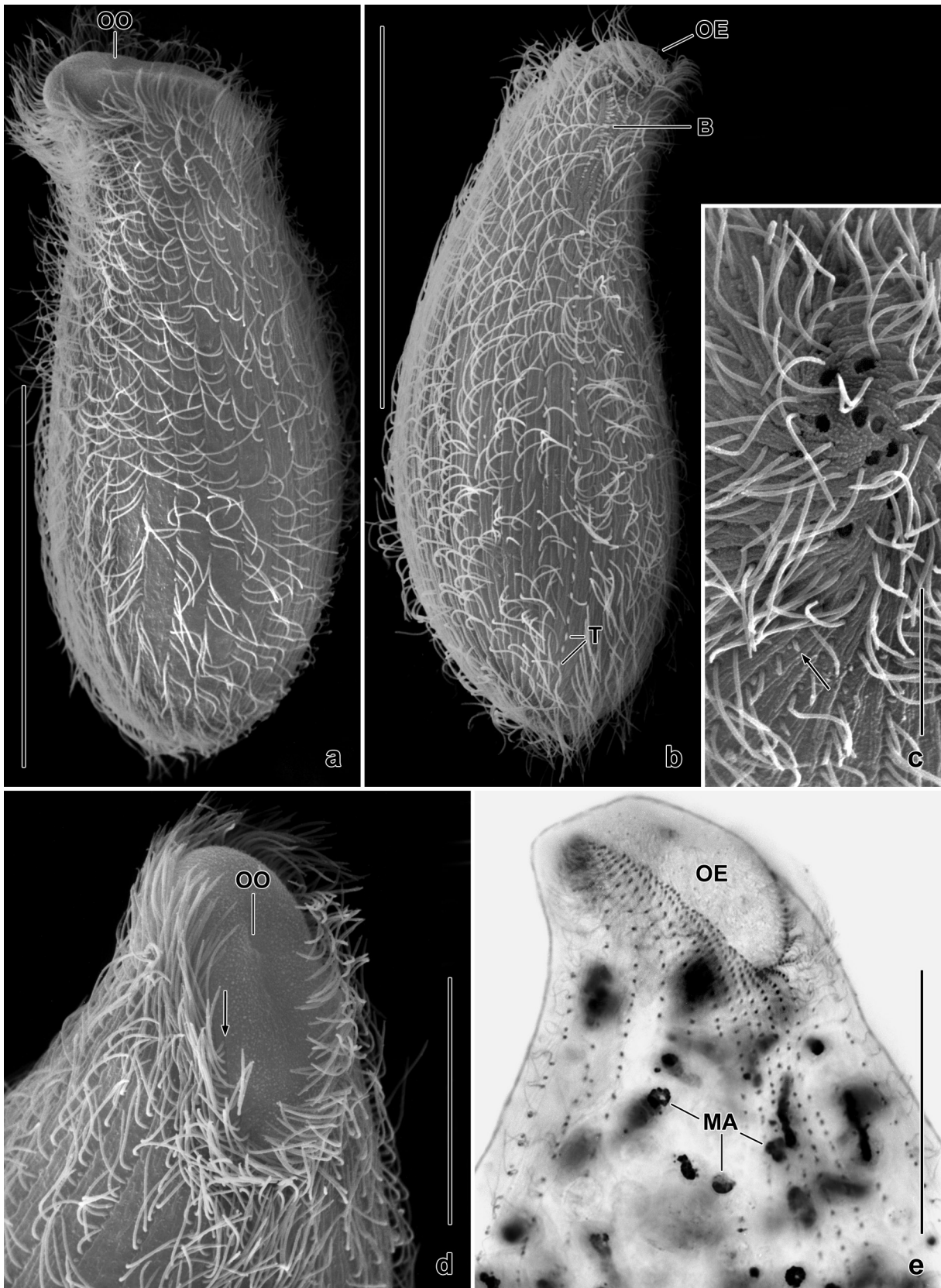
**Fig. 6e–h.** *Enchelys polynucleata hollandica* after protargol impregnation. **e, f, h:** Right and left side focused on cell surface (e, f) and on oral basket (h). The ciliary rows are distinctly curved and the basal bodies are condensed in the anterior region. The arrow in (h) marks the temporary cytostome. **g:** Dorsal view, showing the three-rowed dorsal brush and the transition of dikinetids into a monokinetal tail in brush row 3 (arrow). B – dorsal brush, B<sub>1,2,3</sub> – dorsal brush rows, OB – oral basket, OE – oral bulge, P – parasite, SK – somatic kineties. Scale bars 25  $\mu\text{m}$  (g) and 20  $\mu\text{m}$  (e, f, h).

**Diagnosis:** Size in protargol preparations  $96\text{--}131 \times 38\text{--}66 \mu\text{m}$ , on average about  $115 \times 53 \mu\text{m}$ . Oral bulge ordinary, temporary cytostome out of bulge centre by  $4\text{--}8 \mu\text{m}$ , on average by  $5.5 \mu\text{m}$  (22%) in protargol preparations. Wall of resting cyst yellow, with short ( $1\text{--}4 \mu\text{m}$ ) and long ( $4\text{--}7 \mu\text{m}$ ) spines.

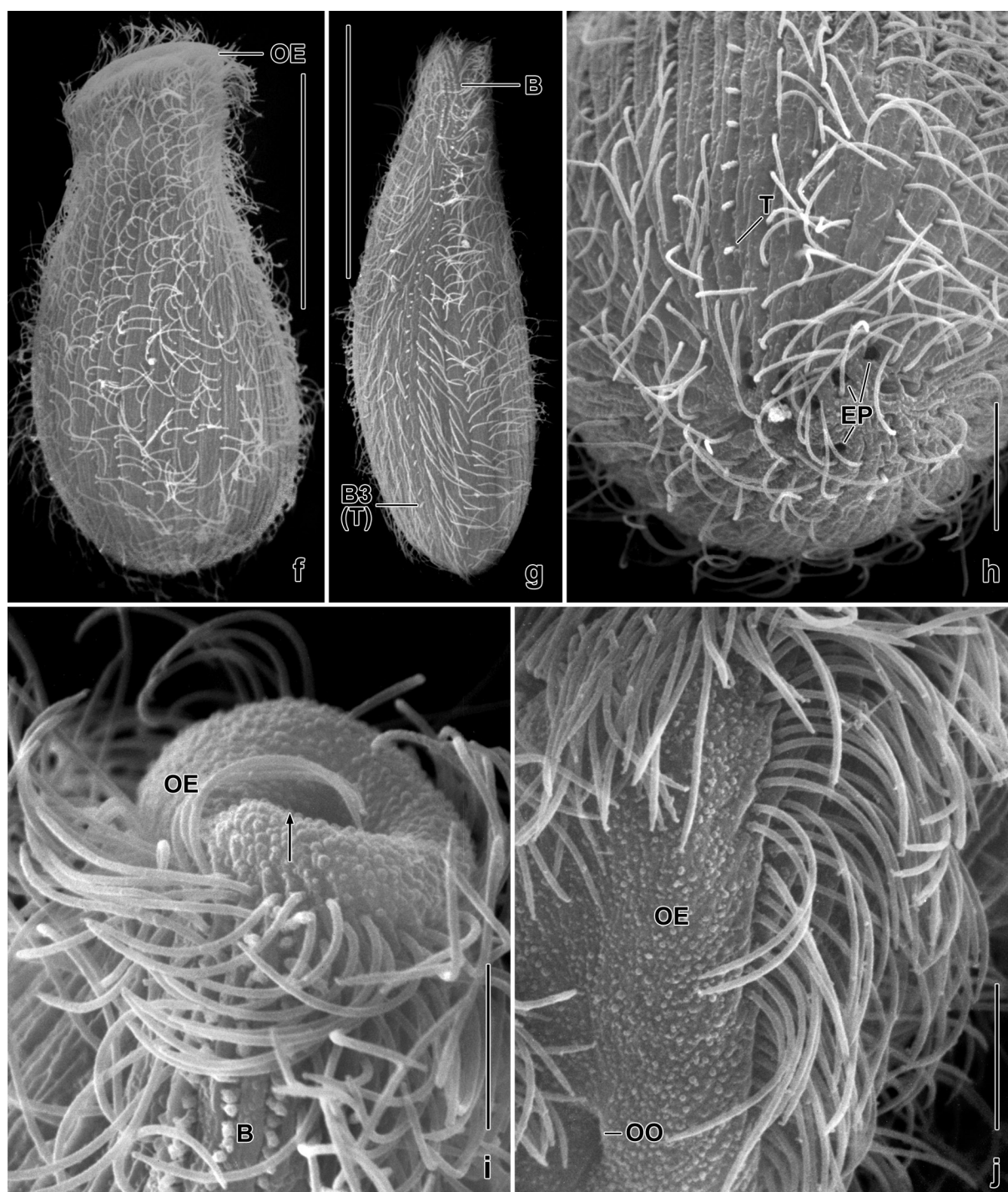
**Type locality:** Soil and leaf litter from an inland sand dune in the Hoge Veluwe National Park, The Netherlands (Hollandia),  $52^{\circ}04'N$ ,  $05^{\circ}43'E$ , i.e., between the villages of Ede and Otterloo, about 50 m aside the road to the Kröller-Müller Museum.

**Type material:** The holotype slide and two paratype slides with protargol-impregnated specimens have been deposited in the Biology Centre of the Upper Austrian Museum in Linz (LI). Important specimens have been marked by black ink circles on the coverslip. For slides, see Fig. 3a–d in Chapter 5.





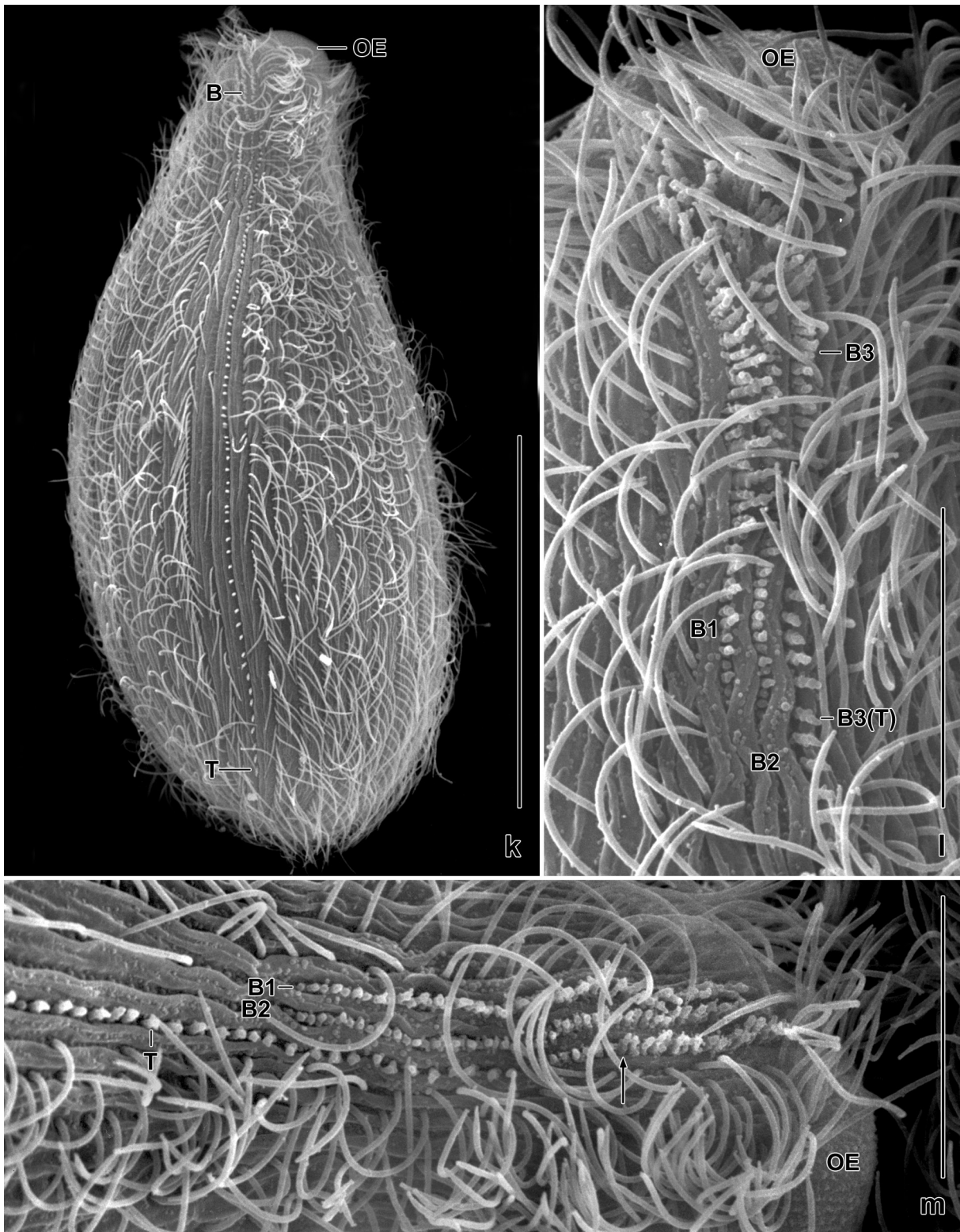
**Fig. 7a–e.** *Enchelys polynucleata hollandica* in the scanning electron microscope (a–d) and after protargol impregnation (e). **a, b:** Right side and dorsal view, showing body shape (a) and monokinetal bristle tail of dorsal brush row 3 (b). **c:** Posterior polar view, showing 10 pores of the contractile vacuole and the end of the monokinetal bristle tail of brush row 3 (arrow). **d, e:** Ventrolateral views, showing the curved, condensed ciliature around the oral bulge. The arrow in (d) marks the anterior end of a ciliary row. B – dorsal brush, MA – macronuclear nodules, OE – oral bulge, OO – temporary cytostome. Scale bars 50  $\mu\text{m}$  (a, b), 20  $\mu\text{m}$  (d, e), and 10  $\mu\text{m}$  (c).



**Fig. 7f–j.** *Enchelys polynucleata hollandica* in the scanning electron microscope. **f, g:** Left side and dorsal overview, showing the bursiform body shape (f), the lateral flattening (g), and the tail of dorsal brush row 3 (g). **h:** Oblique polar view, showing pores of contractile vacuole and posterior end of bristle tail of dorsal brush row 3. **i:** Dorsal view of oral bulge, showing the temporary cytostome (arrow). **j:** The ciliary rows extend onto the margin of the oral bulge. B – dorsal brush, B3(T) – tail of dorsal brush row 3, EP – pores of contractile vacuole, OE – oral bulge, OO – temporary cytostome, T – posterior end of tail of dorsal brush row 3. Scale bars 50  $\mu\text{m}$  (f, g), 10  $\mu\text{m}$  (h), and 5  $\mu\text{m}$  (i, j).

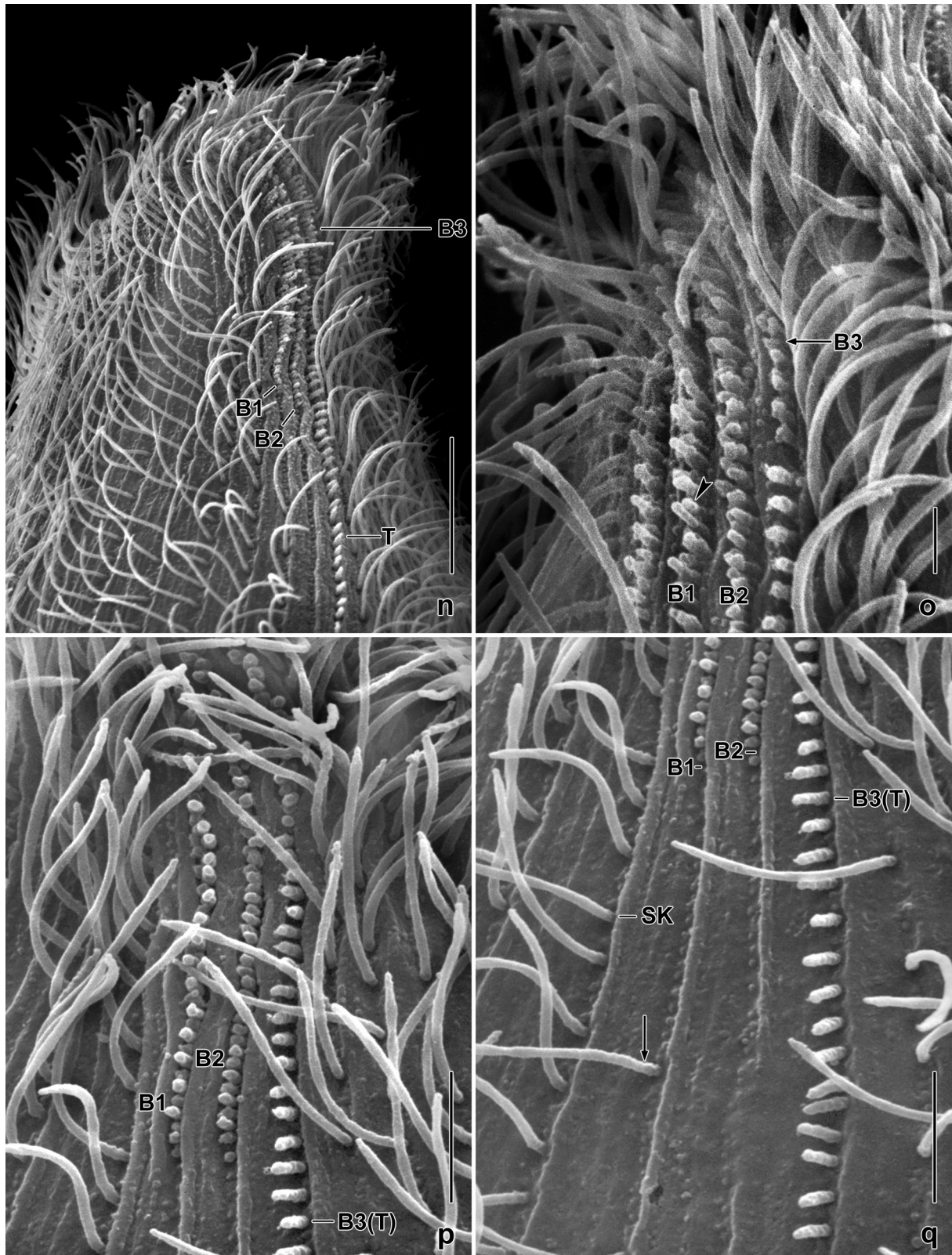
**Etymology:** *Hollandica* is the adjective of Hollandia and refers to the country the species was discovered.

**Description:** This has been provided by Foissner & Al-Rasheid (2007, p. 209). Here, I add some micrographs from protargol impregnated specimens and many SEM micrographs. Further, a morphometric analysis is provided (Table 2).



**Fig. 7k–q.** *Enchelys polynucleata hollandica*, dorsal brush in the scanning electron microscope, showing the following details: the three brush rows are narrower spaced than ordinary lateral kineties (l, n); the rows extend in shallow furrows flattening posteriorly (k–q); the brush ridges undulate in the dikinetal portion (l, m, n, p); of 10 specimens investigated, all have few to many, frequently loosely spaced ordinary monokinetal cilia posterior of brush rows 1 and 2 (k, m, n, q, arrow); brush row 3 has slightly elongated bristles posterior the level of rows 1 and 2 (n, q); the anterior bristle of the dikinetids is slightly shorter than the posterior (l, o, arrowhead, q); bristle length decreases from anterior to posterior in rows 1 and 2 (l–o); anterior of the brush rows are some monokinetal, ordinary cilia (Fig. 3a, g). B – dorsal brush, B1,2,3 – dorsal brush rows, B3(T) – tail of brush row 3, SK – ordinary ciliary rows, T – tail of brush row 3. Scale bars in (k–m): 50 µm (k) and 10 µm (l, m); in (n–g): 10 µm (n), 5 µm (p, q), and 2 µm (o).

**Remarks:** Foissner & Al-Rasheid (2007, p. 211) already suggested that this population could be a distinct subspecies of *Enchelys polynucleata* because the temporary cytostome is rather near to the dorsal end of the oral bulge (see diagnosis above). All other morphostatic features match *E. polynucleata polynucleata*.



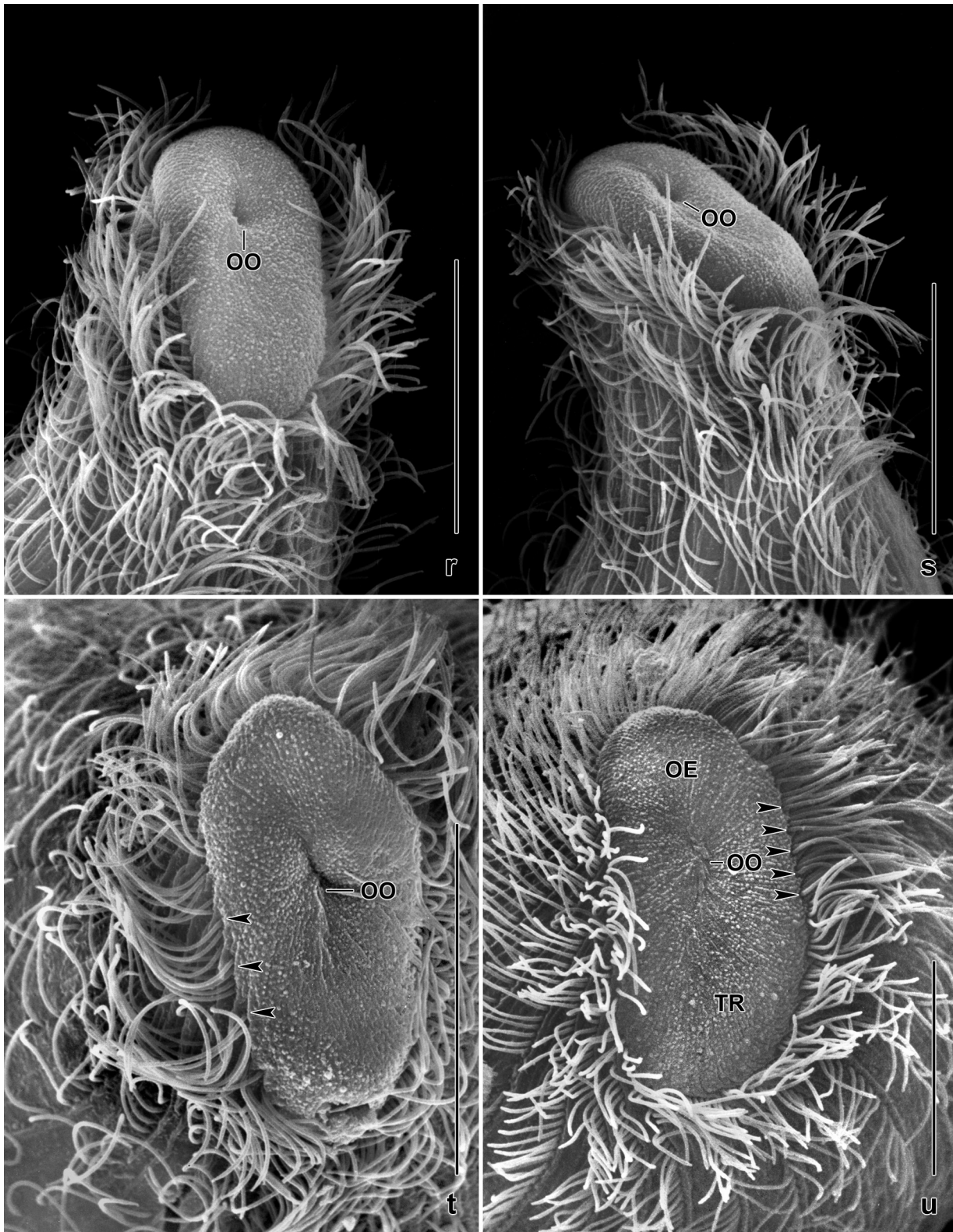


**Fig. 7r–u.** *Enchelys polynucleata hollandica* in the scanning electron microscope. The cilia are very narrowly spaced in the anterior region of the rows, producing a dense ciliature around the oral bulge. **r, s:** Ventrolateral views, showing the temporary cytostome shifted to the dorsal end of the oral bulge. **t, u:** Frontal views, showing almost closed temporary cytostomes out of the centre of the oral bulge. The striation of the bulge is caused by the transverse microtubule ribbons originating from the anterior end of the ciliary rows (cp. Fig. 3b). The arrowheads mark the anterior end of some ciliary rows on the margin of the oral bulge. OE – oral bulge, OO – temporary cytostome, TR – transverse microtubule ribbons. Scale bars 20  $\mu\text{m}$ .

***Enchelys megaspinata* Jang, Vd'áčný, Shazib & Shin, 2017**

**Diagnosis** (adapted to this review): Size in protargol preparations 90–150 × 31–74 µm, on average 130 × 47 µm; body slenderly bursiform. 85–148 macronuclear nodules. On average 30 ciliary rows. Oral bulge ordinary, 23 µm long on average; temporary cytostome in or near bulge centre. Resting cyst wall with 8–13 µm long spines.

**Type locality:** Leaf litter and soil from the surroundings of the Junggol reservoir, Mugeo-dong, Namgu, Ulsan, Korea, 35°32'35"N, 129°15'04"E.

**Type material:** The holotype slide (NIBRPR0000107176) and one paratype slide (NIBRPR0000107176) with protargol-impregnated specimens have been deposited in the Natural Institute of Biological Resources, Incheon, South Korea. One additional paratype slide has been deposited in the Laboratory of Biodiversity, Department of Biological Science, College of Natural Sciences, University of Ulsan, South Korea. Relevant specimens have been marked by black ink circles on the coverslip (Jang et al. 2017, p. 942).

**Description and remarks:** *Enchelys megaspinata* has been well described and documented by Jang et al. (2017). Thus, I refer the reader to their paper for details.

*Enchelys megaspinata* clearly belongs to the *Enchelys polynucleata*-complex and is morphologically most near to → *E. polynucleata polynucleata* because the temporary cytostome is in or near the centre of the oral bulge (Fig. 1f–h, 2b, g in Jang et al. 2017). Some other features of *E. megaspinata* are slightly different from those of *E. polynucleata*: body length:width ratio 2.9:1 vs. 1.9:1, thus slenderly bursiform vs. bursiform; number of macronuclear nodules (85–148, on average 108 vs. >200); number of ciliary rows (24–33, on average 29.7 vs. 30–45, on average 35), and length of cyst spines (8–13 µm vs. 5–9 µm).

***Enchelys australiensis* nov. spec.**

(Fig. 8a–l, 9a–s; Tables 2, 3 on p. 309, 310)

**Diagnosis:** Size in vivo about 150 × 40 µm; bursiform and 2:1 flattened. About 150–300 ellipsoid to elongate-ellipsoid macronuclear nodules. Extrusomes rod-shaped and slightly curved, 10 µm long. Ciliary pattern as typical for genus, on average 42 ciliary rows, three modified anteriorly to a dorsal brush, middle row about 32 µm long, row 3 distinctly shortened. Oral bulge width about 35 µm, in frontal view curved like a propeller blade; temporary cytostome about 9 µm out of bulge centre, i.e., neighboured dorsal side.

**Type locality:** Upper soil layer (0–5 cm) of a small swamp near the village of Eubenangee, south of the town of Cairns, Australia, 17°05'S, 145°00'E.

**Type material:** The slide containing the holotype and three paratype slides with protargol-impregnated specimens have been deposited in the Biology Centre of the Upper Austrian Museum in Linz (LI). Relevant specimens have been marked by black ink circles on the coverslip. For slides, see Fig. 4a–f in Chapter 5.

**Etymology:** *australiensis* refers to the continent the species was discovered.

**Description:** Only 13 specimens were found in eight protargol slides; fortunately, most specimens were excellently impregnated; however, most cells appear inflated (CV of body width 37.6%). Thus, the morphometry is incomplete.

Body length in vivo 120–190 µm, on average about 150 × 40 µm, as calculated from some in vivo measurements and the morphometric data (Table 2) adding 15% preparation shrinkage. Body shape basically bursiform but rather variable, i.e., ordinarily to broadly bursiform, more or less curved and flattened laterally, neck indistinct, anterior quarter hyaline, further on studded with food vacuoles

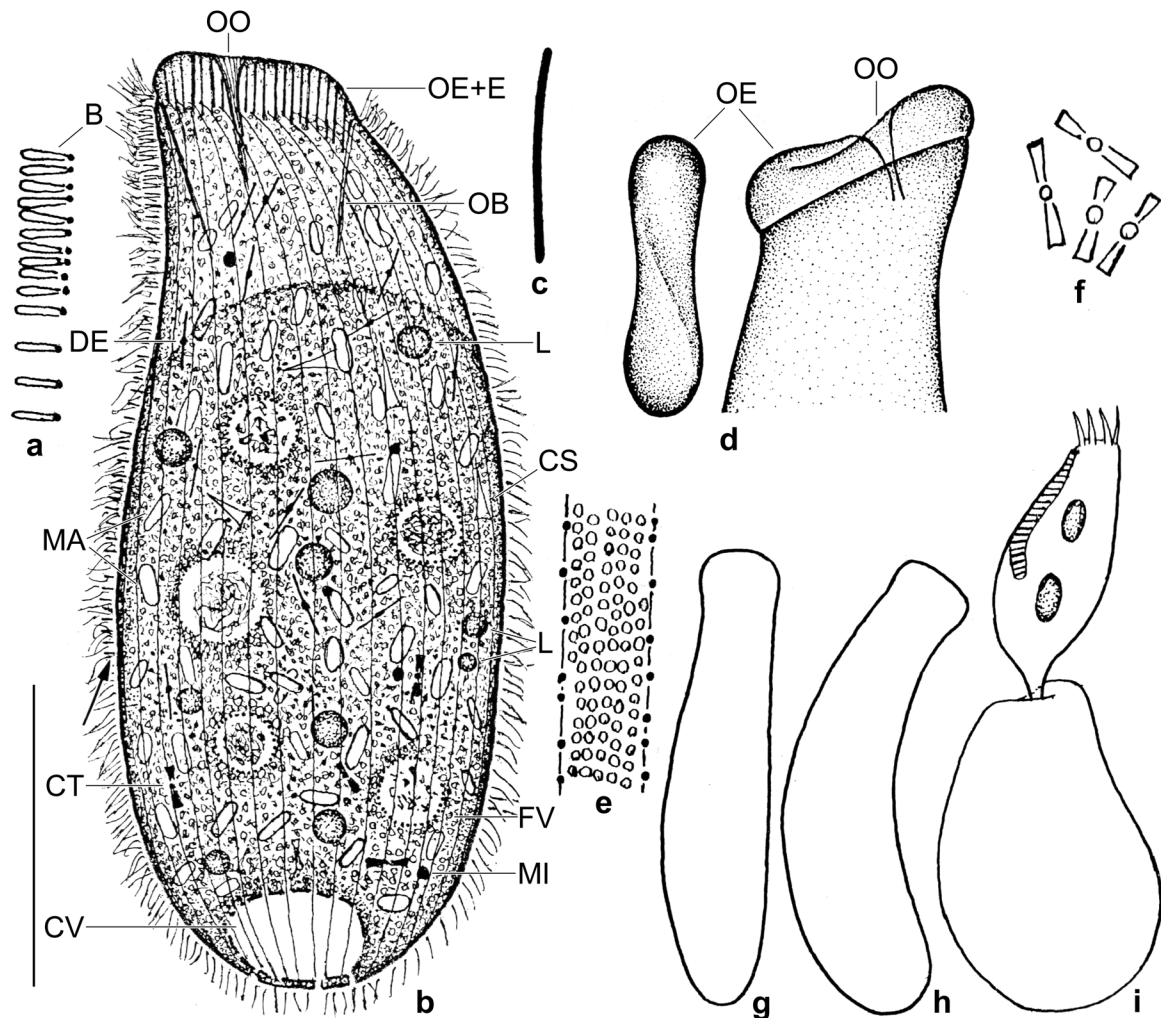


**Fig. 8a-i.** *Enchelys australiensis* from life. **a:** Anterior portion of dorsal brush row 3, which changes from dikinetids to a monokinetal bristle tail (posterior end marked by arrow). **b:** Right side view of a representative specimen, length 155  $\mu\text{m}$ . The location of the oral opening is distinctly decentral. Only part of the macronuclear nodules is shown in outline view. Shape of oral bulge simplified (cp. Fig. 8d). **c:** Oral bulge extrusomes are slightly curved, about 10  $\mu\text{m}$  long rods. **d:** Frontal and lateral view of oral bulge (from Foissner & Xu 2007). Note decentral oral opening. **e:** Cortical granulation. **f:** Cytoplasmic crystals. **g, h:** Dorsal views showing lateral flattening and, occasionally, a flat right side. **i:** A specimen just catching a *Gonostomum affine* (cp. Fig. 9d). The predator's body is distinctly contracted. B – dorsal brush, CS – cyst spine, CT – cytoplasmic crystal (cp. Fig. 8f), CV – contractile vacuole, DE – developing extrusome, E – extrusomes, FV – food vacuole, L – lipid droplet, MA – macronuclear nodules, MI – micronucleus, OB – oral basket, OE – oral bulge, OO – oral opening. Scale bar 50  $\mu\text{m}$ .

(Fig. 8b, g, h, j, 9a–f, n, p; Table 2). Macronuclear nodules scattered, in some specimens ellipsoid to broadly ellipsoid, in others ellipsoid to elongate ellipsoid or with some long strands; nucleoli of ordinary size and number (Fig. 8b, k, 9a–c, l, o, p–s; Table 2). A single contractile vacuole in rear body end. Oral bulge extrusomes (toxicysts) rod-shaped, slightly curved, 10.0–11.0  $\times$  0.5  $\mu\text{m}$  in size; developing extrusomes as usual, viz., scattered in cytoplasm and with a deeply impregnating granule in mid of length (Fig. 8b–d, k, 9a–c, p, r). Cytoplasm turbid due to countless granules about 0.5  $\mu\text{m}$  in size, contains some crystals 3–5  $\mu\text{m}$  in size, resting cyst spines 7–9  $\mu\text{m}$  long, some lipid droplets 3–10  $\mu\text{m}$  across, and food vacuoles 10–20  $\mu\text{m}$  in size (Fig. 8b, e, f, 9a–f). Feeds on cysts of flagellates and on moderately-sized ciliates, such as *Frontonia depressa*, *Gonostomum affine*, and *Colpoda lucida* (Fig. 8i, 9d–k). Glides slowly on microscope slides and between soil particles.

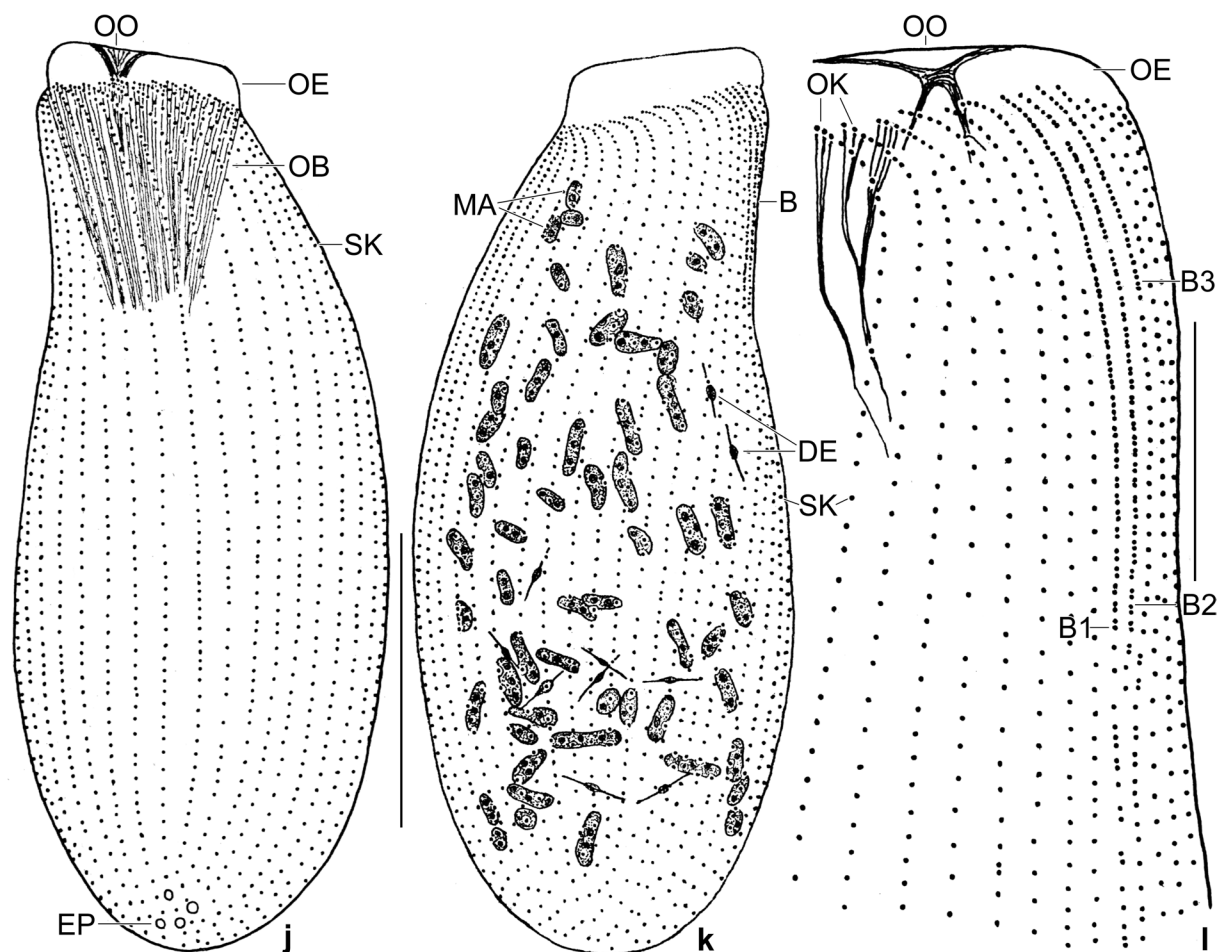


**Fig. 8j-l.** *Enchelys australiensis* after protargol impregnation. **j, k:** Right and left side view of holotype specimen, length 155  $\mu\text{m}$ . The oral opening is distinctly decentral, i.e. neighboured the dorsal side, an important feature of this species. Only few of the many macronuclear nodules are shown (cp. Table 2). **l:** Dorsolateral view, showing the three-rowed dorsal brush, the decentral oral opening, and the oralized somatic monokinetids at begin of the ciliary rows. B – dorsal brush, B1–3 – dorsal brush rows, DE – developing extrusomes, EP – excretory pore of contractile vacuole, MA – part of macronuclear nodules, OB – oral basket, OE – oral bulge, OK – oralized somatic monokinetids producing the oral basket, OO – oral opening, SK – somatic kineties. Scale bars 50  $\mu\text{m}$  (j, k) and 20  $\mu\text{m}$  (l).

Ciliature as typical for genus, i.e., circumoral kinety absent, oral basket rods thus made by two to seven oralized somatic monokinetids at beginning of ciliary rows anteriorly curved dorsally on right side while ventrally on left side (Fig. 8b, j–l, 9o, q–s). Anteriorly, the rows commence unequally due to the special shape of the oral bulge (see next paragraph). Cilia in vivo 10  $\mu\text{m}$  long, arranged in an average of 42 ordinarily spaced rows with ordinarily spaced cilia (basal bodies), except in anterior portion where they are very narrowly spaced. Three dorsal ciliary rows anteriorly modified to a dikinetid brush with 3  $\mu\text{m}$  long slightly inflated bristles, each row commences with some monokinetids; brush isomorphic and distinctly heterostichad, kinetids narrowly spaced; rows 1 and 2 about 32  $\mu\text{m}$  long, row 3 distinctly shortened but with a monokinetid bristle tail extending to near rear body end (Fig. 8a, b, k, l, 9q–s; Table 2).

Oral bulge conspicuous because 6–9  $\mu\text{m}$  high in vivo; screwed like a propeller blade in frontal view while like a recumbent number 8 in lateral view (Fig. 8d); and the distinct, funnel-shaped, decentral temporary cytostome neighbouring dorsal side and widely open when feeding on ciliate prey (Fig. 8b, d, j–k, 9a, f–j, l–o; Table 3); shape of oral bulge mainly in vivo and, less distinctly, in protargol preparations recognizable (Fig. 8d, j, k; overlap (j, k) to recognize the shape of the

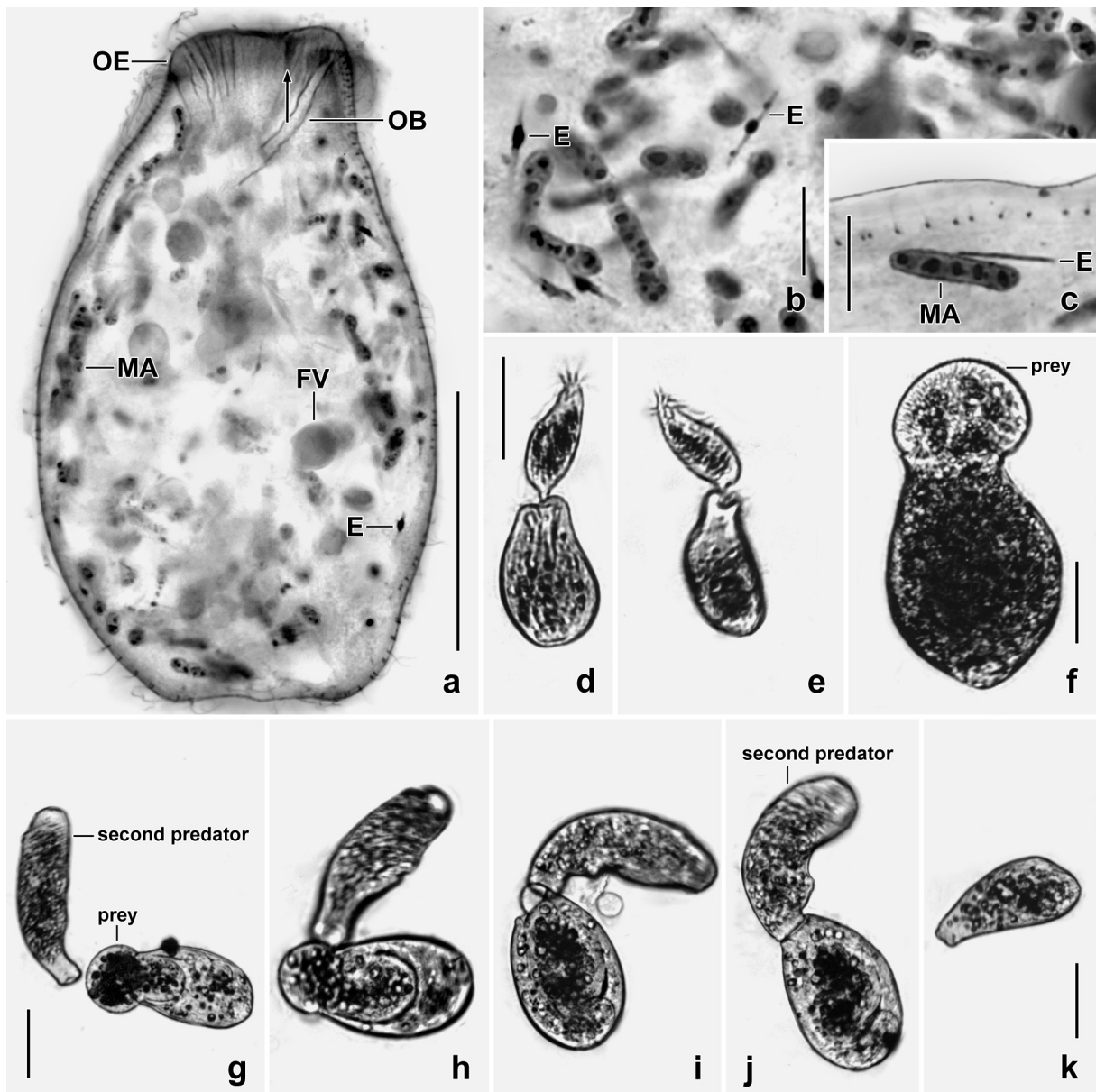


**Fig. 9a-k.** *Enchelys australiensis* (a–f) and  $\rightarrow$  *Enchelariophrya micrographica* (previously *Enchelys micrographica*) (g–k) from life (d–k) and after protargol impregnation (a–c). **a:** An inflated specimen, showing the general organization and temporary cytostome (arrow). **b, c:** The macronuclear nodules are ellipsoid to elongate ellipsoid (c). Mature extrusomes are about 10  $\mu\text{m}$  long (c), developing extrusomes have a central widening (b). **d–f:** *Enchelys australiensis* is a violent predator feeding on other ciliates, such as *Gonostomum affine* (d, e) and *Frontonia depressa* (f). **g–k:** Venezuelan specimens of *Enchelariophrya micrographica* feeding on *Colpoda* sp., whereby the oral bulge opens widely, just as in *E. australiensis* (f). In this case, two *Enchelys* fight for a single prey specimen. Finally, the first predator takes the prey in dissolved condition (j, k). E – developing and mature extrusomes, FV – food vacuole, MA – macronuclear nodules, OB – oral basket, OE – oral bulge. Scale bars 100  $\mu\text{m}$  (d, e), 50  $\mu\text{m}$  (a, f, k), and 10  $\mu\text{m}$  (b, c, g–j).

bulge). Oral basket rods comparatively short, viz., 30–60  $\mu\text{m}$ , originate from 2–7 oralized somatic monokinetids (Fig. 8j, l, 9o–s).

**Occurrence and ecology:** I found *Enchelys australiensis* in Australian samples (107, swamp soil) and (169, bark from trees in the botanical garden in the town of Sydney). These are very different habitats, indicating a broad niche.

**Remarks:** *Enchelys australiensis* is highly similar to several middle and large-sized spathidiids mainly due to the specific oral bulge so far known only from a few spathidiids (for reviews, see

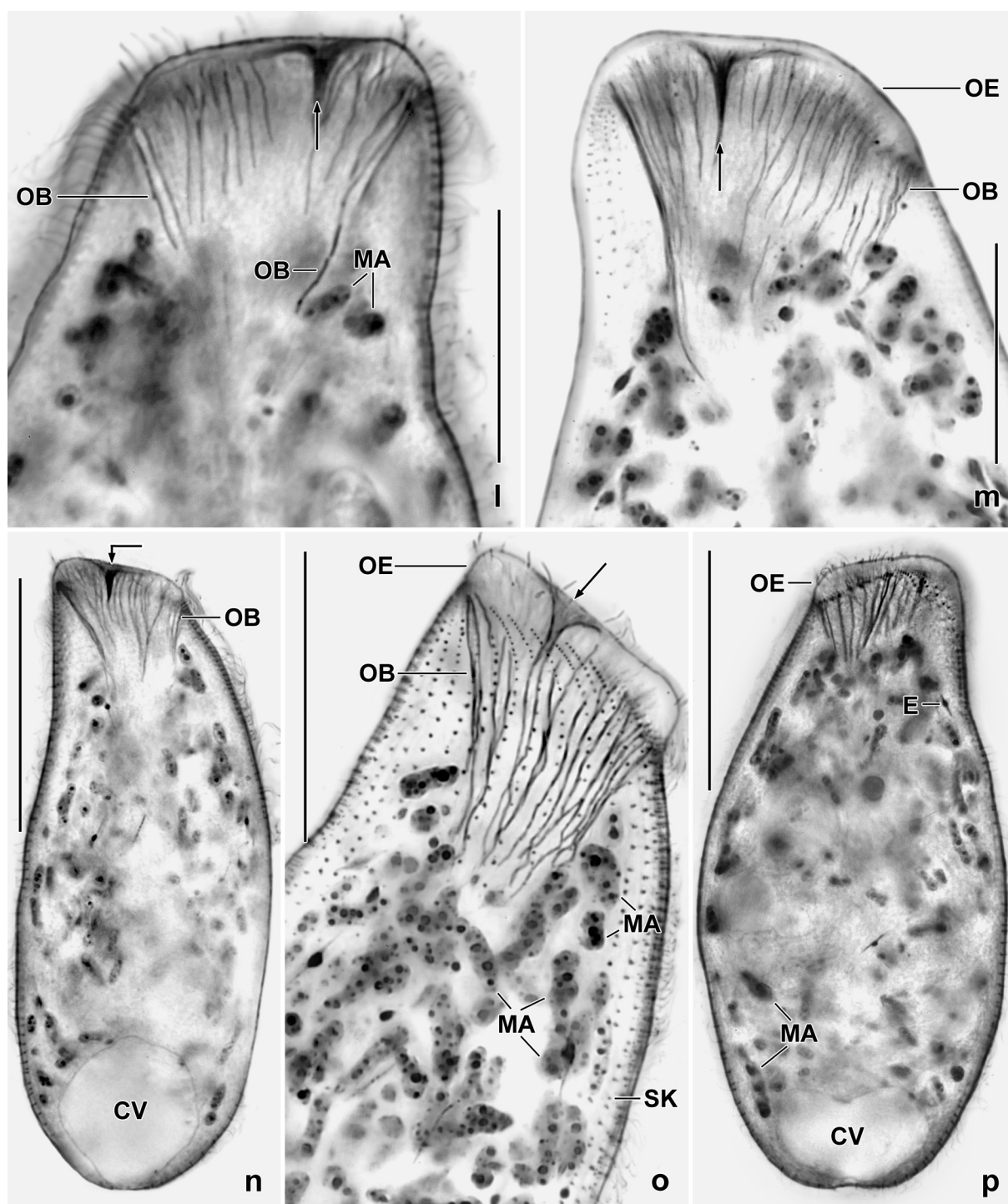


**Fig. 9l–p.** *Enchelys australiensis* after protargol impregnation. **l, m, o:** Anterior body regions, showing the temporary cytostome (arrows) that is not in the centre of the oral bulge but is neighbouring the dorsal side. The location of the temporary cytostome is an important species character. Note the distinct oral rods producing the oral basket (for details, see next plate). **n, p:** Overviews, showing the bursiform body, the temporary cytostome (n, arrow) and the oral basket rods (for details, see next plate). CV – contractile vacuole, E – developing extrusome, MA – macronuclear nodules, OB – oral basket, OE – oral bulge, SK – somatic kineties. Scale bars 50  $\mu\text{m}$  (l, m, n, p) and 40  $\mu\text{m}$  (o).

Foissner & Xu 2007 and Kahl 1927, 1943). Actually, *E. australiensis* is the sole described *Enchelys* with such an oral bulge. Recognizing the absence of a circumoral kinety needs protargol preparation.

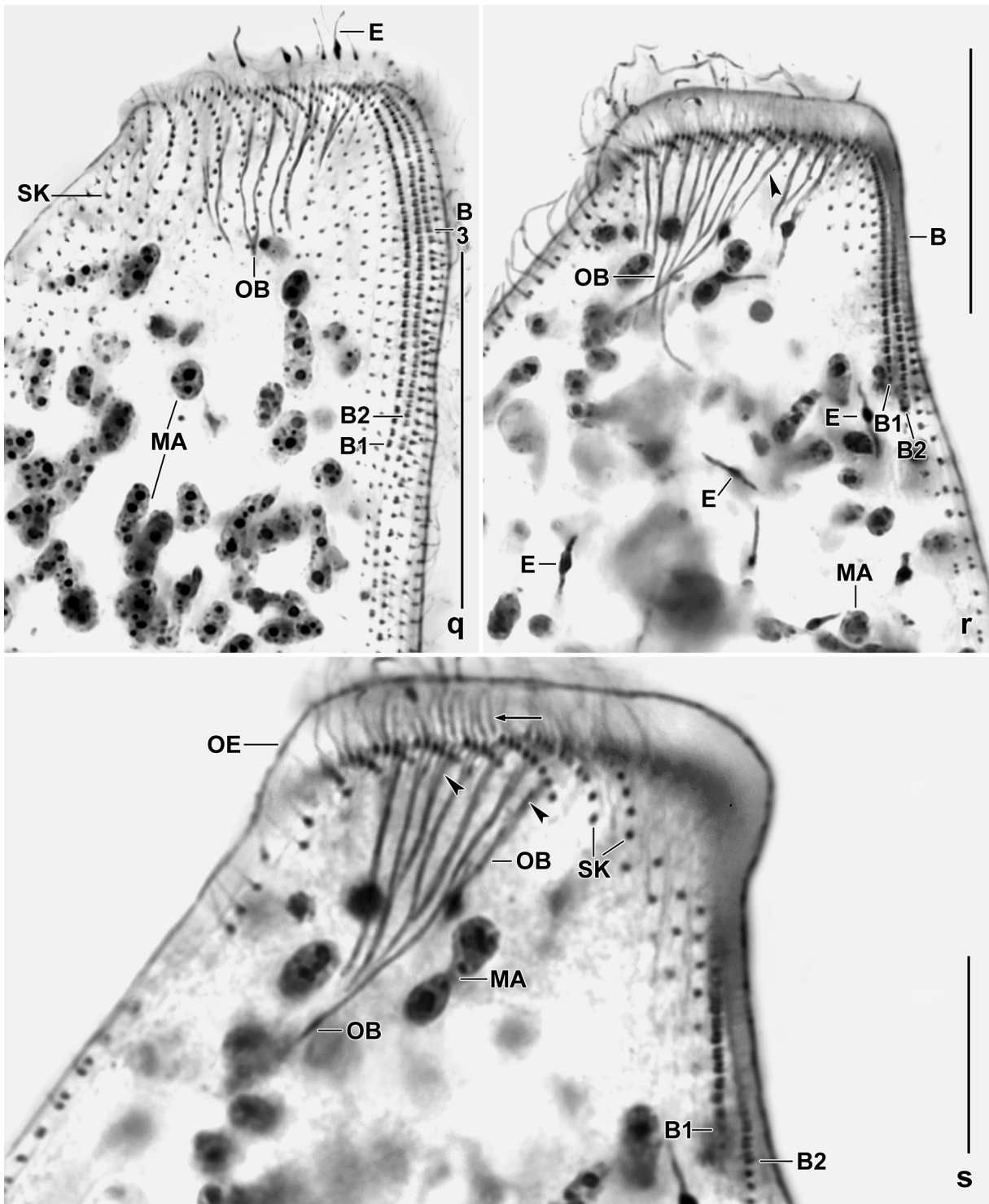


**Fig. 9q–s.** *Enchelys australiensis*, anterior body region after protargol impregnation. These figures show the three-rowed dorsal brush (q, r), the origin of the oral basket rods from very narrowly spaced, oralized somatic monokinetids in the anterior, curved region of all ciliary rows (r, s, arrowheads; same specimen at low and high magnification), and the transverse microtubule ribbons in the oral bulge (s, arrow). B – dorsal brush, B1–3 – dorsal brush rows, E – developing and extruded toxicysts, MA – macronuclear nodules, OB – oral basket, OE – oral bulge, SK – somatic kineties. Scale bars 30  $\mu\text{m}$  (q, r) and 15  $\mu\text{m}$  (s).

**Fig. 10a–d.** *Enchelys bivacuolata* (Australian site 111) from life (a, b) and after protargol impregnation (c, d). **a:** Right side view of a representative specimen, showing the main character, viz., the two contractile vacuoles, length 215  $\mu\text{m}$ . **b:** Oral bulge extrusome, 10  $\mu\text{m}$ . **c, d:** Right side views of holotype specimen, showing shortened ciliary rows (arrowheads) and the nuclear apparatus. B – dorsal brush, CV – contractile vacuoles, FV – food vacuole, L – lipid droplet, MA – macronuclear nodules, MI – micronuclei, OE + E – oral bulge and extrusomes. Scale bars 100  $\mu\text{m}$ .

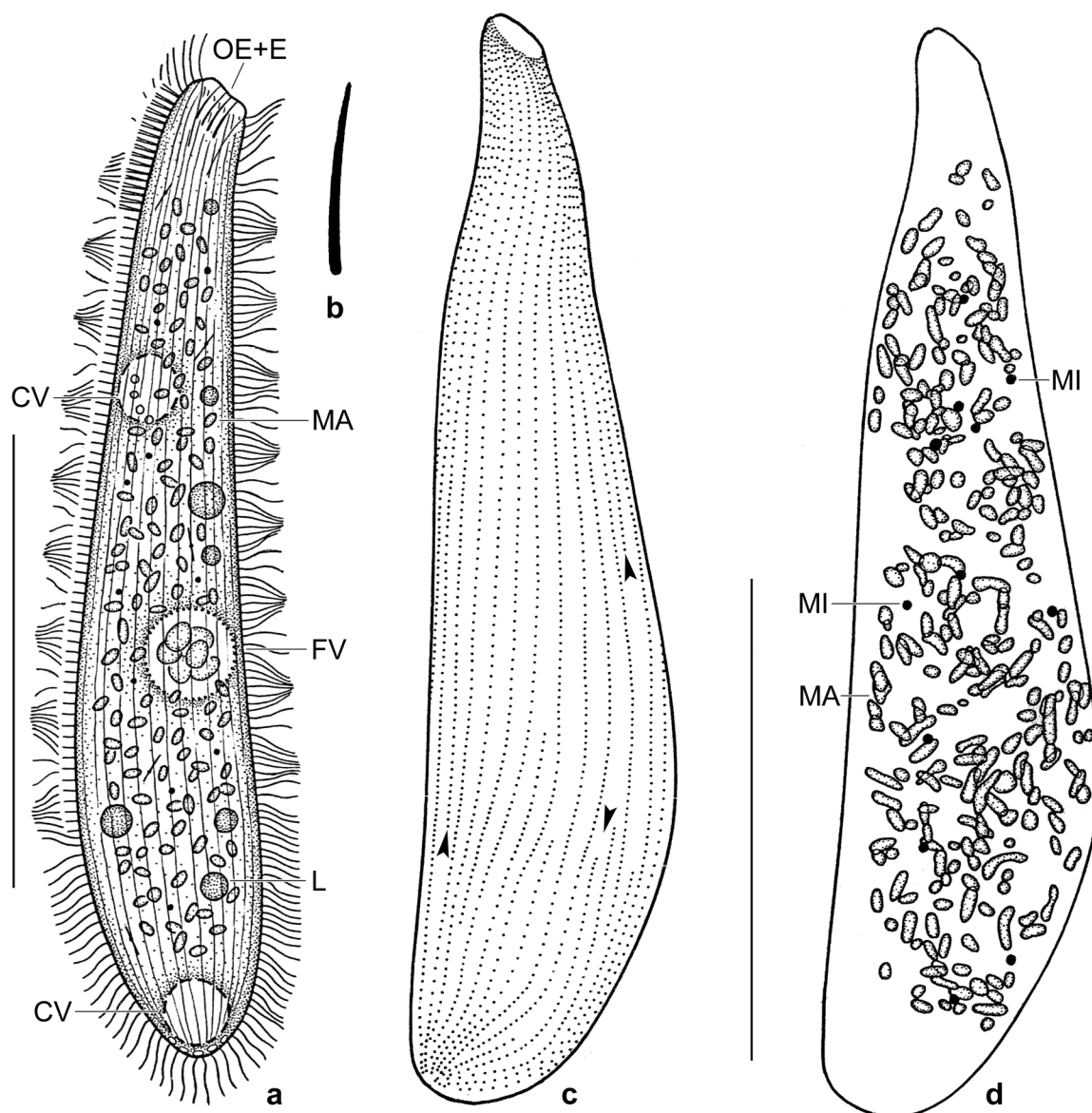
*Enchelys bivacuolata* nov. spec.

(Fig. 10a–v, 11a–s; Table 4 on p. 310)

**Diagnosis:** Size in vivo about  $220 \times 40 \mu\text{m}$ ; body very elongate ovate or elongate bursiform with oblique anterior end occupied by oral bulge. About 260 scattered, ellipsoid macronuclear nodules and about 11 globular micronuclei. Two contractile vacuoles, one at begin of second third of cell, another in posterior body end. Extrusomes form a bundle in centre of oral bulge, thorn-shaped and slightly curved, about  $9 \mu\text{m}$  long in vivo. On average 26 longitudinal ciliary rows, three anteriorly modified to a monomorphic dorsal brush with up to  $5 \mu\text{m}$  long, slightly inflated bristles. Oral bulge broadly ellipsoid, indistinct because only  $1.5\text{--}3.0 \mu\text{m}$  high.

**Type locality:** Australian site 111, i.e., soil from woodland in the surroundings of the town of Alice Springs,  $24^{\circ}\text{S}$ ,  $134^{\circ}\text{E}$ .

**Type material:** The slide containing the holotype and five paratype slides with protargol-impregnated specimens have been deposited in the Biology Centre of the Upper Austrian Museum in Linz (LI). The holotype and paratype specimens have been marked by black ink circles on the coverslip. For slides, see Fig. 5a–i in Chapter 5.



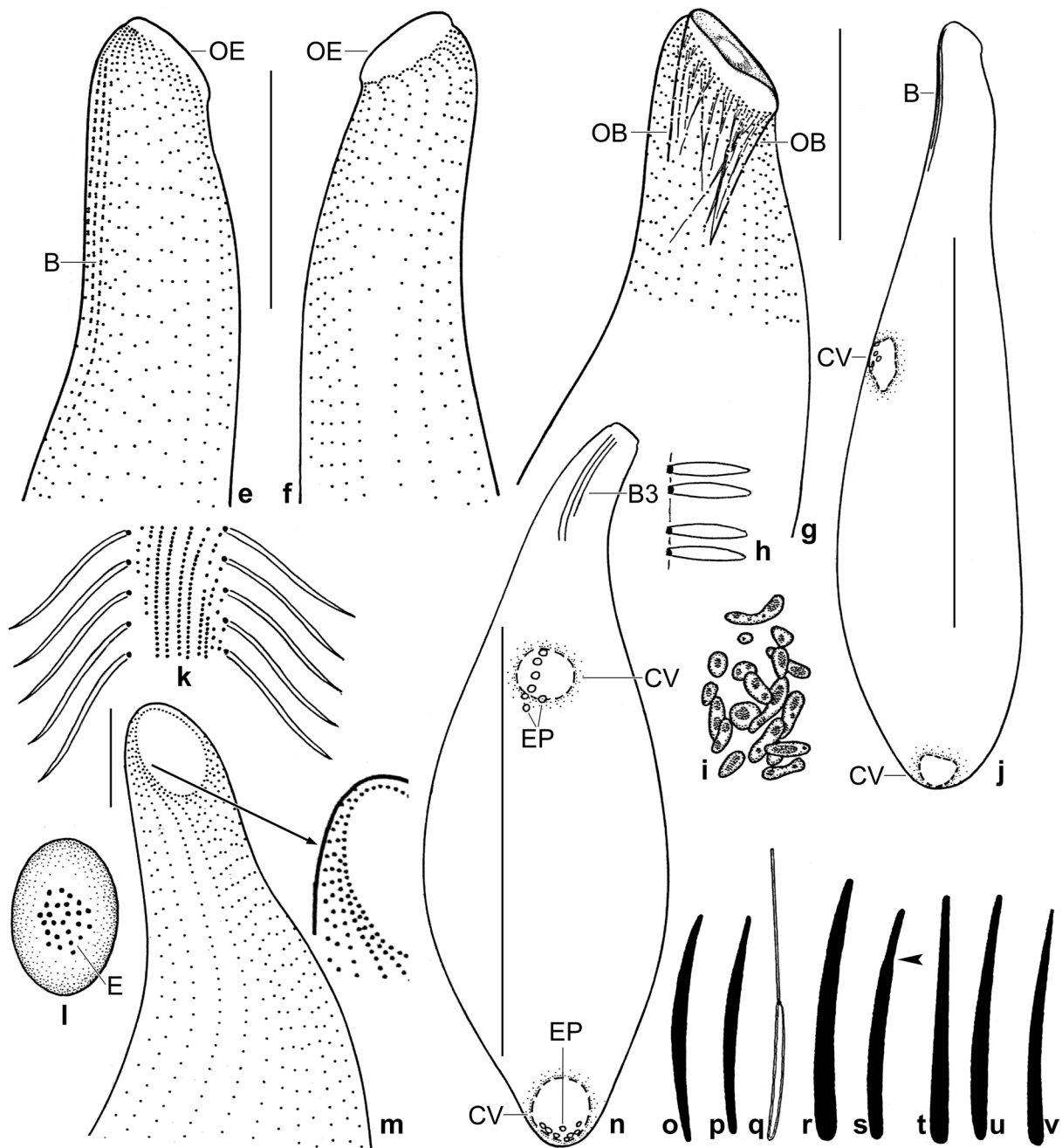


**Fig. 10e–v.** *Enchehlys bivacuolata* from life (h, k, l, o–v) and after protargol impregnation (e–g, i, j, m, n). **e, f:** Dorsolateral and ventrolateral view of anterior body portion, showing the absence of a circumoral kinety. **g:** Right side view, showing the oral basket made of oralized somatic monokinetids at the anterior end of each ciliary row. **h:** Dorsal brush bristles, 5  $\mu\text{m}$ . **i:** Macronuclear nodules. **j, n:** Lateral and dorsal view, showing two contractile vacuoles and their pores in each specimen. **k:** Surface view, showing cortical granulation. **l:** Frontal view of the broadly ellipsoid oral bulge, showing the central extrusome bundle. **m:** Ventral view, showing the broadly ellipsoid oral bulge and the absence of a circumoral kinety. **o–v:** Variability of extrusome shape in specimens from Australian sites (o–s: 152, 155, 160, 149) and t: 159, u, v: 111, length 7–12  $\mu\text{m}$ . The arrowhead marks a sudden narrowing of extrusomes from site (149). B – dorsal brush, CV – contractile vacuole, E – extrusomes, EP – pores of contractile vacuoles, OB – oral basket, OE – oral bulge. Scale bars 100  $\mu\text{m}$  (j, n), 20  $\mu\text{m}$  (e, f, g), and 10  $\mu\text{m}$  (m).

**Etymology:** *bivacuolata* refers to the two contractile vacuoles, a distinct feature not known from any congener.

**Description:** The species was rare at all sites. Thus, the morphometry is slightly incomplete. Most characteristics are highly variable (CV>15%), very likely due to fixation problems because

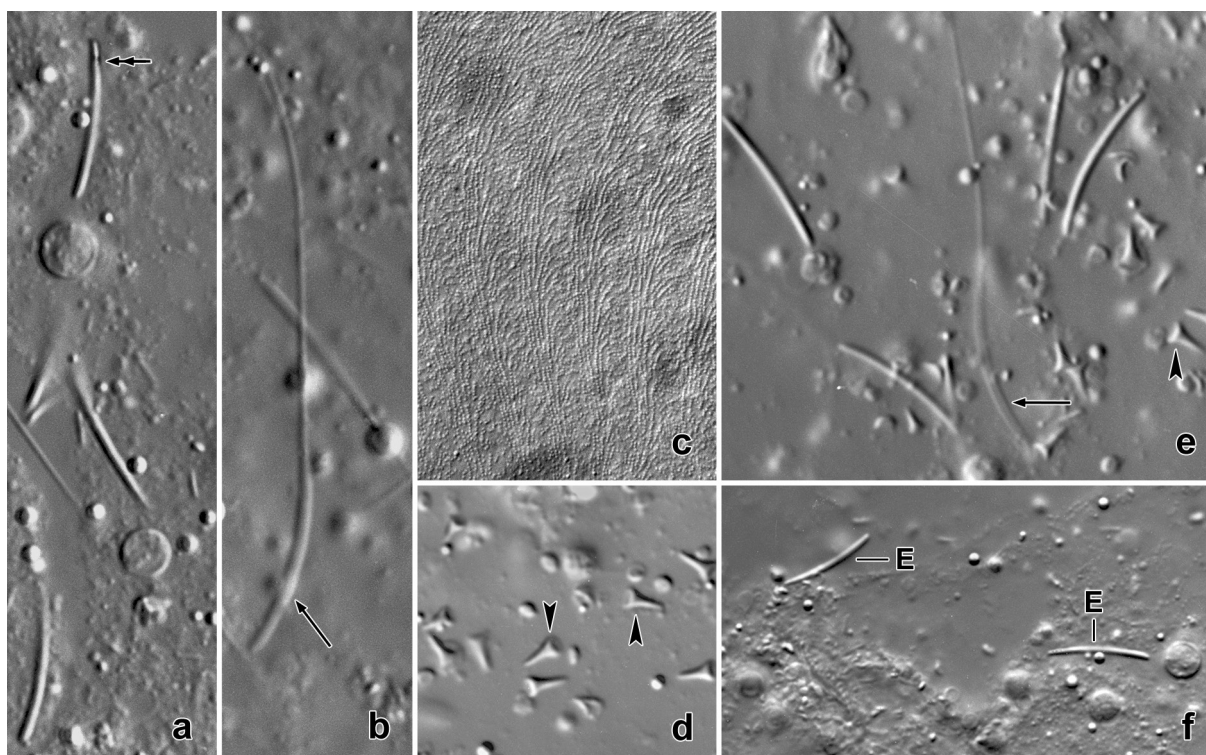


**Fig. 11a–f.** *Enchelys bivacuolata* from life. **a, b, e, f:** Extrusomes (toxicysts) of specimens from sites 149 (a), 111 (f), and 155 (e), length 8–12  $\mu\text{m}$ . The arrows in (b, e) mark exploded toxicysts. **c:** Surface view, showing cortical granulation. **d, e:** Cyst spines in the cytoplasm (arrowheads).

one of the most important features, the number of ciliary rows, has an ordinary variability (CV = 6.3%, Table 4).

Size in vivo 160–275  $\times$  30–50  $\mu\text{m}$ , on average 220  $\times$  40  $\mu\text{m}$ , as calculated from some live measurements and protargol-impregnated cells adding 15% preparation shrinkage (Table 4). Body very elongate ovate or elongate bursiform, rarely cylindroid (length: width ratio 5.5:1), usually slightly curved, anterior end obliquely truncate (Fig. 10a, c–e, j, n, 11g, h, k–m; Table 4). Nuclear apparatus scattered throughout cell, composed of an average of 250 macronuclear nodules 4–7  $\times$  2–3  $\mu\text{m}$  in size, studded with minute and moderately-sized nucleoli; shape and size highly variable. About 10 globular micronuclei difficult to separate from cytoplasmic inclusions (Fig. 10a, d, i, 11g, h, j–r; Table 4). Two contractile vacuoles, each with several pores; anterior vacuole posterior to dorsal brush between first and second third of cell to near mid-body; second vacuole invariably in posterior end of cell (Fig. 10a, j, n, 11h, i, l, m). Extrusomes restricted to centre of oral bulge, forming a rather conspicuous bundle, in some specimens faintly impregnated in posterior third; in type population thorn-shaped, slightly curved, and about 9  $\mu\text{m}$  long (Fig. 10a, b, 11f); in other populations 8–10  $\times$  0.5–1  $\mu\text{m}$  in size (Fig. 10o–v, 11a, e, f). When exploded with typical toxicyst structure (Fig. 10q, 11b, e); developing toxicysts common in cytoplasm, fusiform (Fig. 11o, p, r). Cortex very flexible and rather fragile, most cells thus more or less inflated in protargol preparations. About 10 rows of colourless cortical granules between two ciliary rows, 0.7–1.0  $\mu\text{m}$  in size, do not impregnate with the protargol method used (Fig. 10k, 11c). Cytoplasm usually studded with lipid droplets 3–8  $\mu\text{m}$  across, some 20  $\mu\text{m}$ -sized food vacuoles, macronuclear nodules and developing toxicysts (Fig. 10a, d, 11g, k, m–o); some cells with spiny resting cyst precursors 5–8  $\mu\text{m}$  long (Fig. 11e, d, j). Creeps and swims rather slowly changing body shape from cylindroid to distinctly curved.

Cilia about 10  $\mu\text{m}$  long in vivo, narrowly to ordinarily spaced, form 23–28, on average 25.5 longitudinal, narrowly spaced rows anteriorly curved dorsally on right side while ventrally on left,

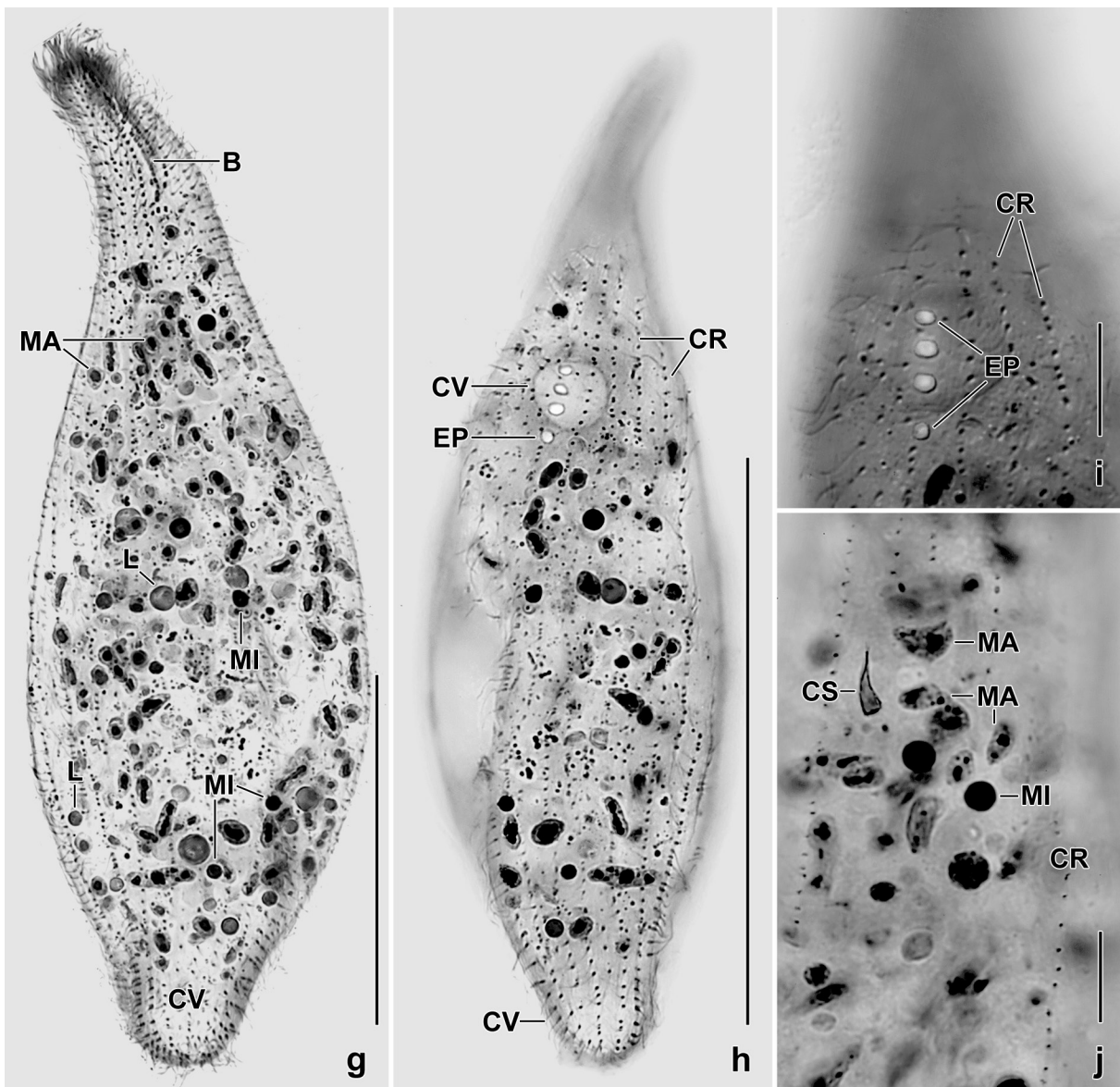


**Fig. 11g–j.** *Enchelys bivacuolata* after protargol impregnation. **g, h:** Dorsal view of inflated specimens, showing the dorsal brush (g) and the two contractile vacuoles (h). **i:** Detail from (h), showing the excretory pores of the anterior contractile vacuole. **j:** Cytoplasmic inclusions. Note a developing spine for the resting cyst. B – dorsal brush, CR – ordinary somatic ciliary rows, CS – cyst spine, CV – contractile vacuoles, EP – pores of anterior contractile vacuole, L – lipid droplets, MA – macronuclear nodules, MI – micronuclei. Scale bars 100  $\mu\text{m}$  (h), 50  $\mu\text{m}$  (g), 20  $\mu\text{m}$  (i), and 10  $\mu\text{m}$  (j).

some shortened or broken (Fig. 10a, c, e–g, 11m, n, r; Table 4); produce a “false” circumoral kinety due to the very narrowly spaced cilia at begin of rows (Fig. 10m, 11q, r). Three rows anteriorly modified to a monomorphic, heterostichad, dikinetid dorsal brush, each row commences with 1–3 monokinetids; row 1 longest, i.e., 38  $\mu\text{m}$  on average, row 2 slightly shorter than row 1, row 3 shortened posteriorly by about 30% but extending to near posterior body end with 3  $\mu\text{m}$  long, monokinetid bristles; dikinetids ordinarily spaced, have about 3  $\mu\text{m}$  long, slightly inflated bristles, not studied in detail (Fig. 10a, e, j, n, 11g, m, n; Table 4).

Oral bulge indistinctly separate from body proper, broadly ellipsoid, centre brownish and occupied by a bundle of toxicysts described above. Oral basket made by 1–5 oralized somatic kinetids at anterior end of ciliary rows, basket rods 10–30  $\mu\text{m}$  long; circumoral kinety absent (Fig. 10a, c, e–g, m, 11m, n, q, r; Table 4).

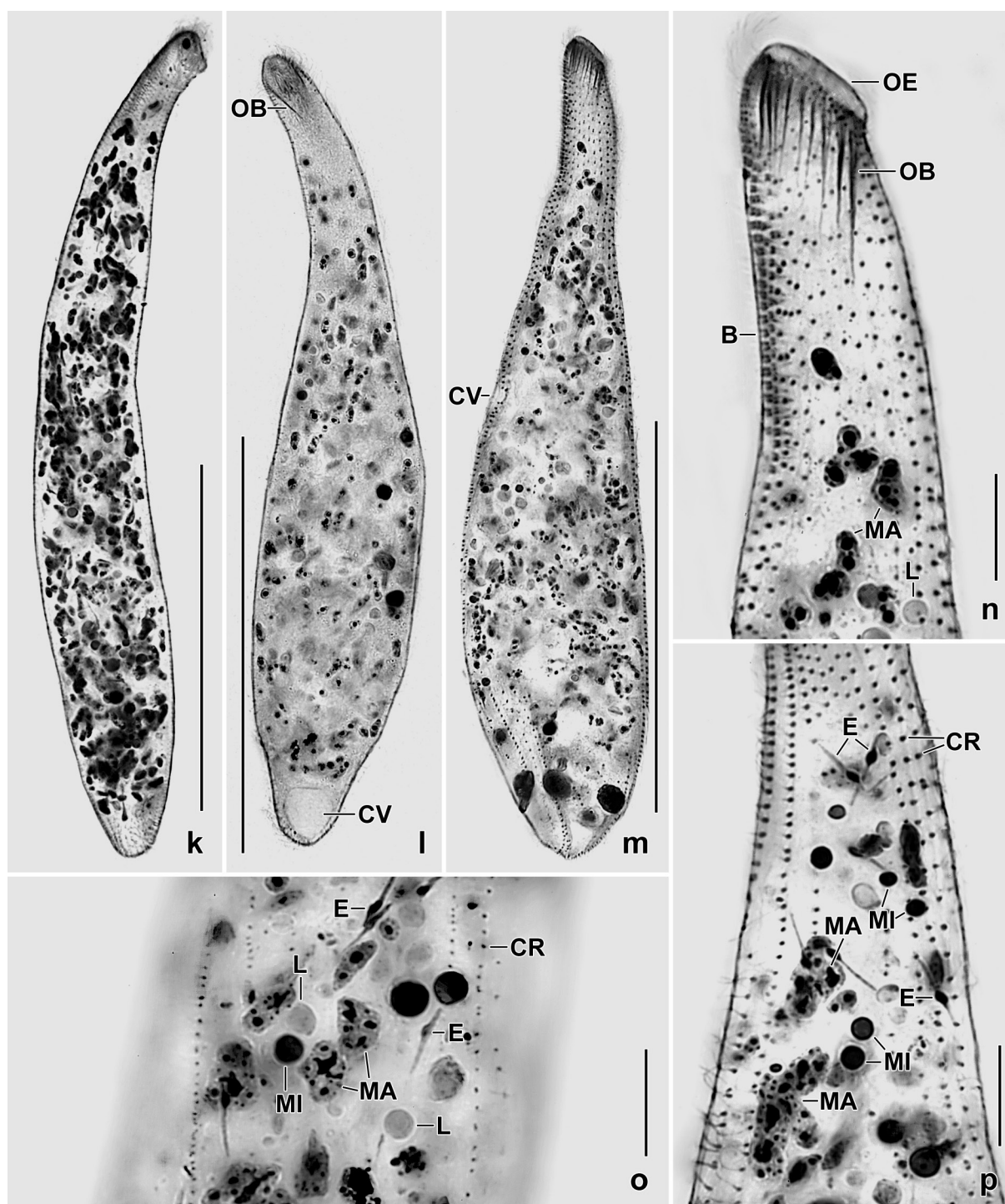


**Fig. 11k–p.** *Enchelys bivacuolata* after protargol impregnation. **k–n:** Well preserved specimens, showing body shape, nuclear apparatus, dorsal brush, the low oral bulge, and the oral basket (m, n) made of nematodesmata originating from oralized somatic monokinetids at the anterior end of the somatic kineties. Fig. (m, n) are from holotype. **o, p:** Cytoplasmic inclusions. B – dorsal brush, CR – ordinary ciliary rows, CV – anterior (m) and posterior (l) contractile vacuole, E – developing extrusomes with a central thickening, L – lipid droplets, MA – macronuclear nodules, MI – micronuclei, OB – oral basket, OE – oral bulge. Scale bars 100  $\mu\text{m}$  (k–m) and 10  $\mu\text{m}$  (n–p).

**Occurrence and ecology:** Common in soil from woodlands and savannas in the surroundings of the towns of Alice Springs and Eralunda (sites 111, 149, 155) but also in the floodplain of the Murray River (sites 159, 160). Possibly, also in the Pantanal of Brazil (but cells  $\sim 370 \mu\text{m}$  long) and in surface soil of a deciduous forest in Slovakia, i.e. a quite similar species with two contractile

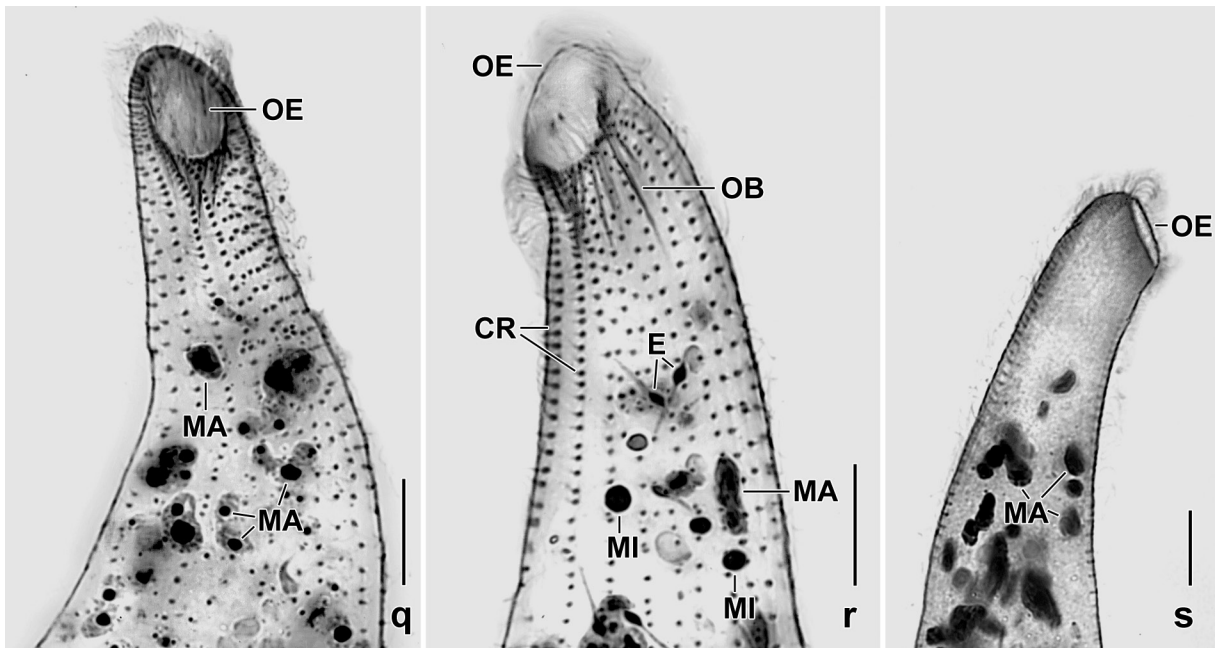


**Fig. 11q–s.** *Enchelys bivacuolata* after protargol impregnation. Several views of anterior body region, showing the broadly ellipsoid oral bulge (q, r) and its tiny height (s). CR – somatic ciliary rows, E – developing extrusomes, MA – macronuclear nodules, MI – micronuclei, OB – oral basket, OE – oral bulge. Scale bars 10  $\mu\text{m}$ .

vacuoles. This indicates an insular distribution because it was absent in over 1000 samples studied by me. Never abundant in the non-flooded Petri dish cultures; pure cultures failed. Food not identifiable in the vacuoles of impregnated specimens. Very likely, *Enchelys bivacuolata* lives in the litter layer, as indicated by the long and slender body.

**Remarks:** *Enchelys bivacuolata* is easily identified because all described congeners have only one contractile vacuole in posterior body end, except of the polyvacuolate  $\rightarrow$  *E. polyvacuolata* (Berger et al. 1984; Dragesco & Dragesco-Kernéis 1979; Foissner 1984, 2010; Foissner & Al-Rasheid 2007; Foissner et al. 2002; Jang et al. 2017; Kahl 1930; Mermod 1914; Vuxanovici 1963). The genus *Enchelys* is very distinct because it lacks a circumoral kinety. However, this must be verified by silver impregnation. The extrusome shape is highly variable (Fig. 10o–v) possibly indicating subspecies rank or a high natural variability. The same has been described in *Pseudoholophrya terricola* (Foissner et al. 2002).

***Enchelys polyvacuolata* nov. spec.**

(Fig. 12a–f, h, j, k, 13a–m; Table 4 on p. 310)

**Diagnosis:** Size in vivo about  $270 \times 40 \mu\text{m}$ ; body slender to vermiform, with oblique anterior end occupied by oral bulge. About 500 ellipsoid macronuclear nodules. At least five contractile vacuoles posterior to dorsal brush. Extrusomes form a bundle in centre of oral bulge, very elongate fusiform, slightly curved and  $8\text{--}10 \mu\text{m}$  long. On average 21 ciliary rows extending longitudinally, three anteriorly modified to a monomorphic, heterostichad, dikinetid dorsal brush. Oral bulge broadly ellipsoid, moderately distinct.

**Type locality:** Rare in grassland soil from the Garajan Cape of the Island of Madeira in the Atlantic Ocean,  $32^{\circ}\text{N}$ ,  $17^{\circ}\text{W}$ .

**Type material:** The slide containing the holotype and three paratype slides with protargol-impregnated specimens have been deposited in the Biology Centre of the Upper Austrian Museum

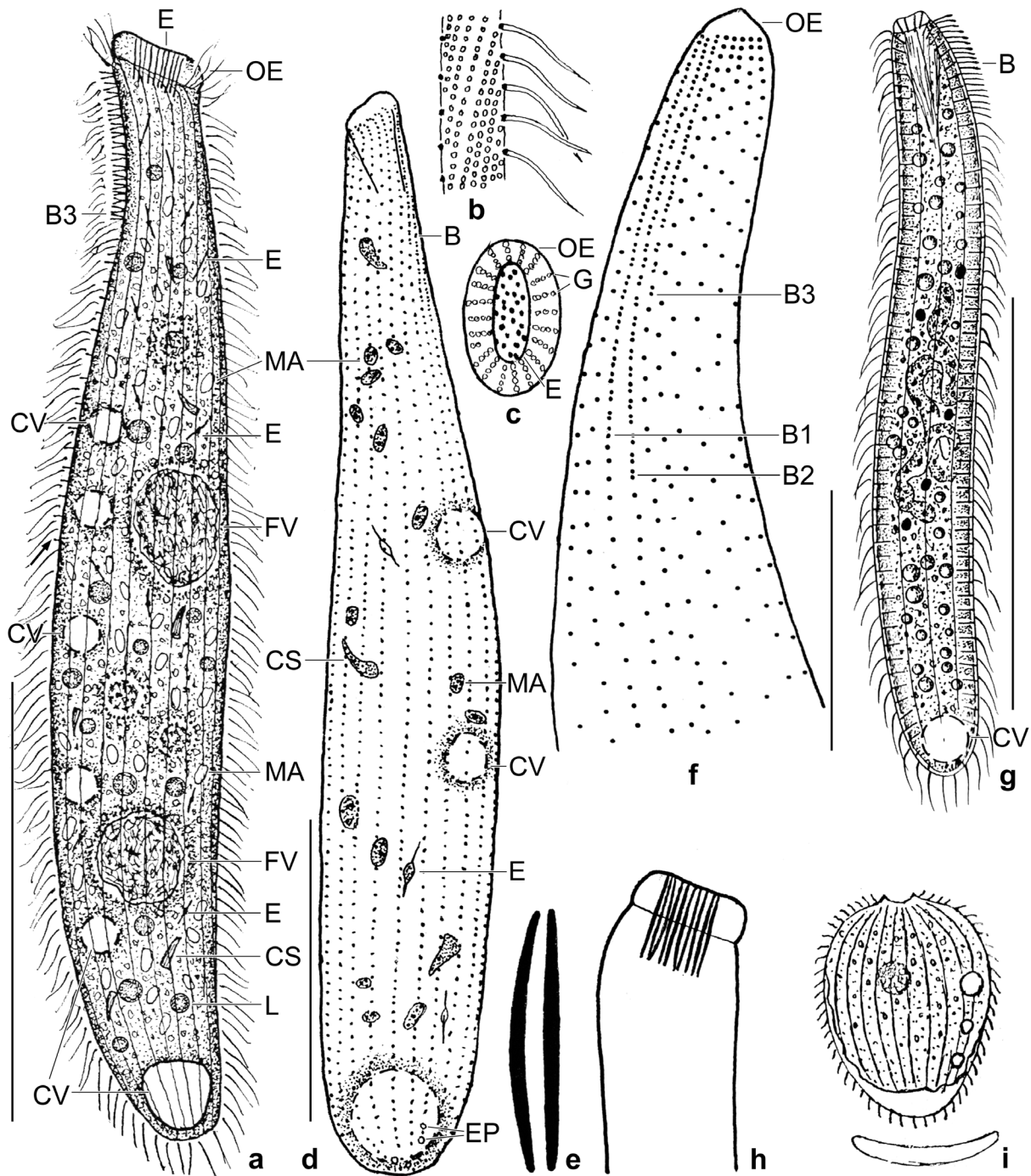


**Fig. 12a-i.** *Enchelys polyvacuolata* (a-f, h), *E. vermiformis* (g, from Foissner 1987c) and *E. multivacuolata* (i, from Vuxanovici 1963) from life (a-c, e, g-i) and after protargol impregnation (d, f). **a, d, f:** Right side (a, length 280  $\mu\text{m}$ ), left side (d, 200  $\mu\text{m}$ ) and dorsal view (f), showing the infraciliature, the nuclear apparatus, the end of the monokinetal bristle tail of brush row 3 (a, arrow), and the dorsal row of contractile vacuoles, the main species character. Only few of many macronuclear nodules are shown in (a, d; cp. Fig. 2a-d). **b:** Surface view showing cortical granulation. **c:** Frontal view of anterior body end, showing the granulated oral bulge and the central extrusome bundle. **e:** Oral bulge extrusomes are slightly curved in lateral view and are 8-10  $\mu\text{m}$  long. **g:** *Enchelys vermiformis* resembles *E. polynucleata* but has only a posterior contractile vacuole, somatic extrusomes, and a moniliform macronucleus, length 180  $\mu\text{m}$ . **h:** Anterior region, showing the oblique oral bulge and the oral extrusome bundle in centre of oral bulge. **i:** Lateral and transverse view of *E. multivacuolata*, length 70  $\mu\text{m}$ . B - dorsal brush, B1-3 - dorsal brush rows, CS - cyst spines, CV - contractile vacuoles, E - extrusomes, EP - pores of posterior contractile vacuole, FV - food vacuoles, G - cortical granules, L - lipid droplets, MA - macronuclear nodules, OE - oral bulge. Scale bars 110  $\mu\text{m}$  (a), 100  $\mu\text{m}$  (g), 55  $\mu\text{m}$  (d), 25  $\mu\text{m}$  (f).

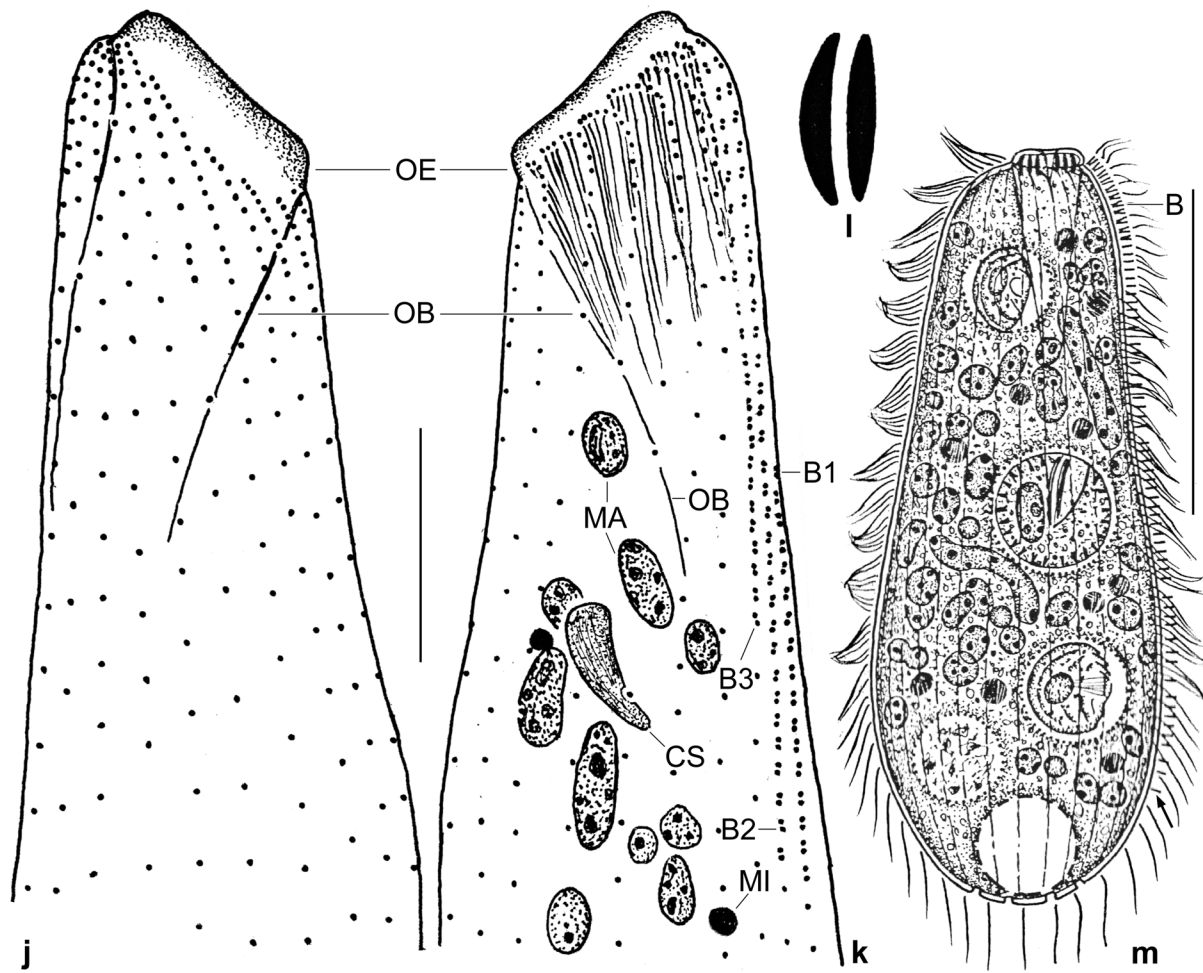


**Fig. 12j–m.** *Enchelys polyvacuolata* (j, k) and  $\rightarrow$  *Enchelariophrya micrographica* (l, m, from Foissner 2010) from life (l, m) and after protargol impregnation (j, k). **j, k:** Right and left side view of anterior body region, showing the oral bulge and the oralized somatic monokinetids that produce the oral basket rods. Through an optical effect, dorsal brush row 3 is not right but left of rows 1 and 2. **l:** The oral bulge extrusomes of  $\rightarrow$  *Enchelariophrya micrographica* are thick, slightly curved, and only 3–4  $\mu\text{m}$  long (vs. thin and about 10  $\mu\text{m}$  long in *Enchelys polyvacuolata*). **m:**  $\rightarrow$  *Enchelariophrya micrographica* resembles *Enchelys polyvacuolata* but has only a posterior contractile vacuole (vs. several along dorsal side), a bursiform body (vs. elongate bursiform or vermiform), and the oral opening is decentral (vs. central). The arrow marks the posterior end of the monokinetal bristle tail of brush row 3. B – dorsal brush, B1–3 – dorsal brush rows, CS – cyst spine, MA – macronuclear nodules, MI – micronucleus, OB – oral basket, OE – oral bulge. Scale bars 50  $\mu\text{m}$  (m) and 10  $\mu\text{m}$  (j, k).

in Linz (LI). The holotype and some paratype specimens have been marked by black ink circles on the coverslip. For slides, see Fig. 6a–f in Chapter 5.

**Etymology:** *polyvacuolata* (with more than two contractile vacuoles) refers to the increased number of contractile vacuoles.

**Description:** The species was rare. Thus, the morphometry is slightly incomplete. Most features are highly variable ( $\text{CV} > 15\%$ ), very likely due to fixation problems because one of the most important features, the number of ciliary rows, has an ordinary variability ( $\text{CV} = 7.1\%$ ).

Size in vivo 225–320  $\times$  30–60  $\mu\text{m}$ , on average 270  $\times$  40  $\mu\text{m}$ , as calculated from some live measurements and protargol-impregnated cells adding 15% preparation shrinkage (Table 4); one specimen 430  $\times$  30  $\mu\text{m}$  in vivo, a well-fed specimen ellipsoid and 200  $\times$  85  $\mu\text{m}$  in size (Fig. 13d). Body slender to vermiform, length:width ratio 6.3:1 on average, both ends narrowed, anterior end slightly inflated and obliquely truncate, with rather distinct, moderately flattened neck (Fig. 12a,

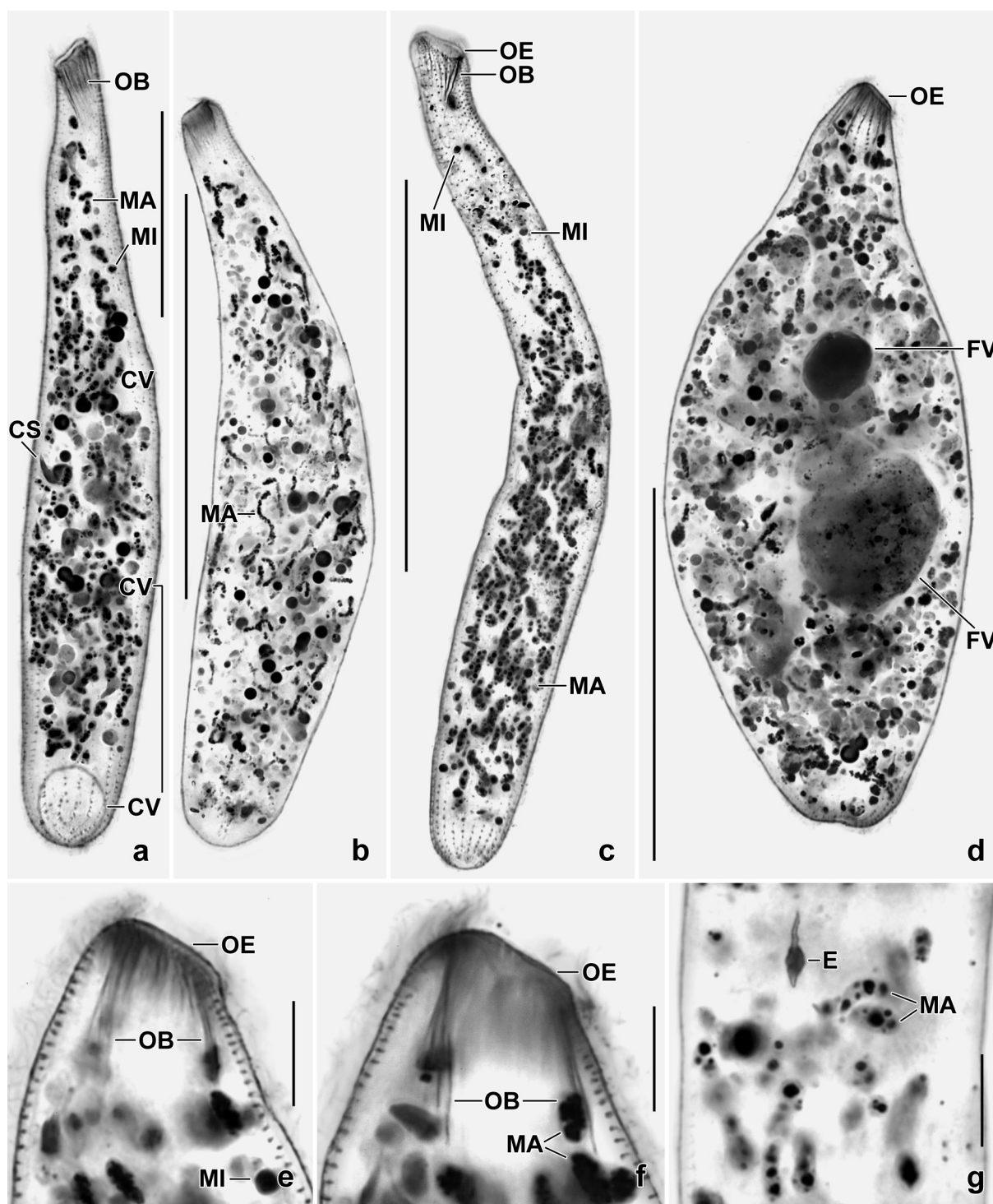


**Fig. 13a–g.** *Enchelys polyvacuolata* after protargol impregnation. **a–d:** Overviews showing variability of body shape and three contractile vacuoles (a), size 190–220 μm. **e, f:** Anterior region, showing the low oral bulge. **g:** Cytoplasmic inclusions. CS – cyst spine, CV – contractile vacuoles, E – developing extrusome, FV – food vacuoles, MA – macronuclear nodules, MI – micronuclei, OB – oral basket, OE – oral bulge. Scale bars 100 μm (b–d), 50 μm (a), 10 μm (e–g).

d, f, h, j, k, 13a–c, h, i; Table 4). About 500 globular to elongate ellipsoid macronuclear nodules  $4.0\text{--}8.0 \times 1.5\text{--}3.0 \mu\text{m}$  in protargol preparations, scattered throughout cell, studded with minute nucleoli; two specimens with ordinary and much longer nodules (Fig. 12a, d, k, 13a–j, l; Table 4). Very likely many micronuclei difficult to separate from lipid droplets in protargol preparations (Fig. 13a, c, j, l). At least five contractile vacuoles posterior to dorsal brush; pores unfortunately not recognizable because cells impregnated too faintly. However, pores were recognizable in vivo

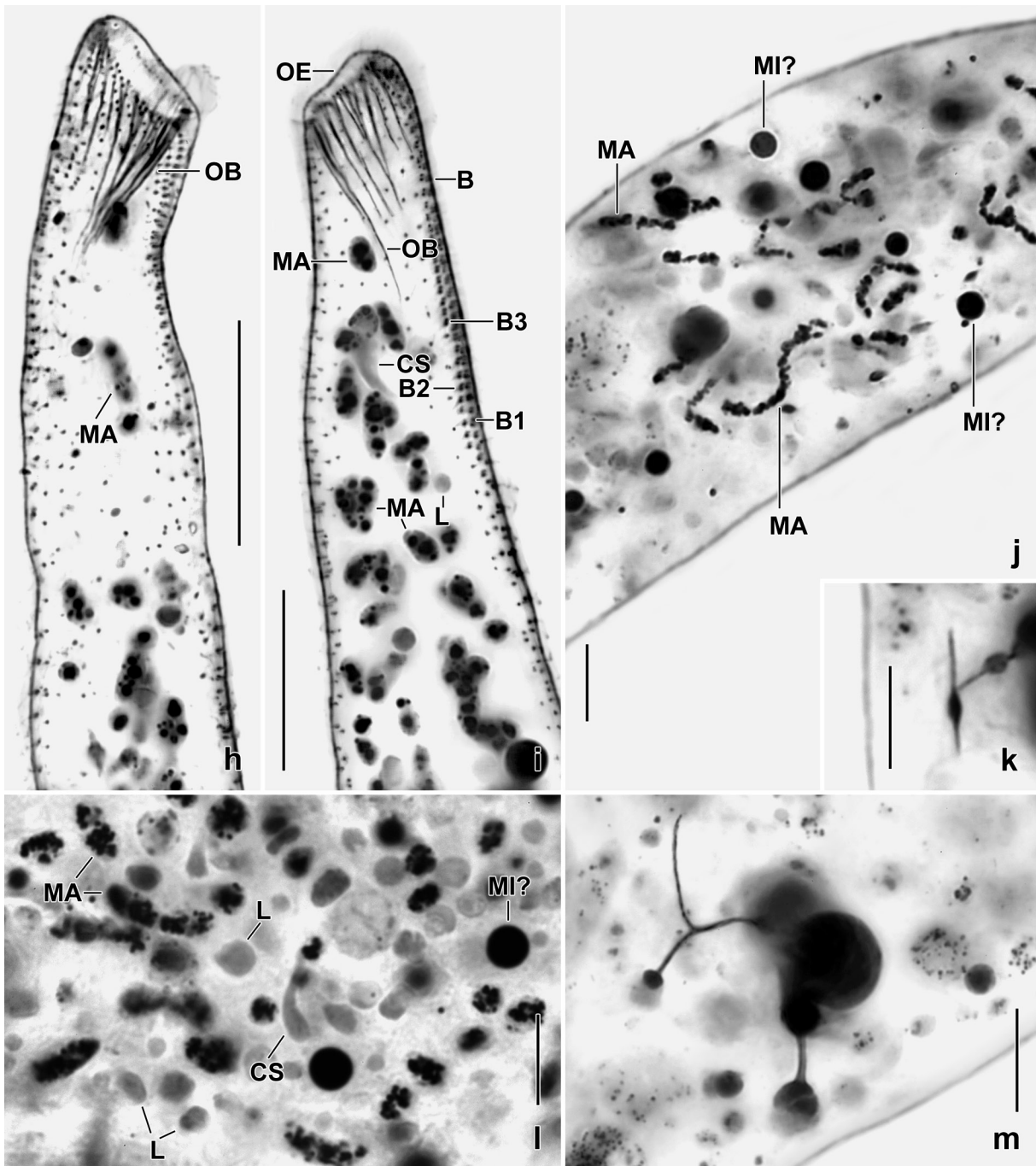


**Fig. 13h–m.** *Enchelys polyvacuolata* after protargol impregnation. **h, i:** Right and left side view of anterior body portion, showing the oral and somatic infraciliature and some of many macronuclear nodules. The dorsal brush (B1–3) is, through an optical effect, partially on the left body side causing that row 3 is not right but left of rows 1 and 2. **j:** Nuclear apparatus. Whether or not the globular, deeply impregnated structures are micronuclei or lipid droplets needs further investigation. **k:** Developing toxicysts have a thickened mid. **l:** Cytoplasmic inclusions. **m:** A curious structure, possibly a fungal parasite. B – dorsal brush, B1–3 – dorsal brush rows, CS – cyst spines, L – lipid droplets, MA – macronuclear nodules, MI? – supposed micronuclei, OB – oral basket, OE – oral bulge. Scale bars 20  $\mu\text{m}$  (h, i), 10  $\mu\text{m}$  (j, l, m), 5  $\mu\text{m}$  (k).

in specimens from Australian site (111). Extrusomes (toxicysts) restricted to centre of oral bulge, forming a rather conspicuous bundle; very elongate fusiform and slightly curved, 4–7  $\mu\text{m}$  long in protargol preparations (Fig. 12a, c, h); developing toxicysts scattered throughout cytoplasm, with a fusiform widening in or posterior of centre (Fig. 13g, k). Cortex very flexible and rather fragile, most prepared cells appear slightly inflated; studded with colourless granule rows (Fig. 12b, c), do

not impregnate with the protargol method used. Cytoplasm colourless, usually studded with lipid droplets up to 5  $\mu\text{m}$  across and 10  $\mu\text{m}$ -sized food vacuoles containing only a single type of prey organelles, e.g., trichocysts of *Frontonia* (Fig. 12a, 13a, i, l). Some cells contain horn-shaped resting cyst precursors 8–12  $\mu\text{m}$  long (Fig. 12a, d, k, 13a, i, l), and one specimen has a ramified inclusion, possibly a parasitic fungus (Fig. 13m). Feeds mainly on middle-sized ciliates, such as *Frontonia depressa* and *Colpoda lucida* (Fig. 12a, 13d). Glides and swims rather slowly.

19–23, on average 21 ordinarily spaced ciliary rows with cilia densely spaced in oral region; anteriorly curved dorsally on right side while ventrally on left; some shortened or broken (Fig. 12a, d, j, k, 13c, h, i; Table 4). Three rows anteriorly modified to a monomorphic, heterostichad, dikinetid dorsal brush each commencing with some monokinetids (Fig. 12a, f, k, 13i; Table 4): row 1 slightly shorter than row 2, row 3 shortened posteriorly by about 42% but extending beyond mid-body with 3  $\mu\text{m}$  long monokinetid bristles; dikinetids ordinarily spaced, have 2–3  $\mu\text{m}$  long bristles, not studied in detail.

Oral bulge rather distinctly separate from body proper because slightly wider than neck and up to 4  $\mu\text{m}$  high, elliptic in frontal view, centre occupied by a bundle of toxicysts described above. Oral basket made by some oralized somatic kinetids at anterior end of ciliary rows, basket rods up to 40  $\mu\text{m}$  long; circumoral kinety absent (Fig. 12a, c, d, h, j, k, 13a, c, e, f, h, i; Table 4).

**Occurrence and ecology:** The type locality is covered with grass and *Opuntia*. The soil is slightly red brown and has pH 4.8 in water. The sample was collected on 21.7.1985 by Dr. Wolfgang Petz (Salzburg, Austria). The same or a rather similar species occurs at Australian sites 111 (soil from woodland in the surroundings of the town of Alice Springs) and 159 (soil from floodplain of the Murray River; about 300  $\mu\text{m}$  in vivo, extrusomes thorn-shaped) as well as in the Pantanal (Brazil). Thus, *Enchelys polyvacuolata* or a very similar species has a wide ecological range and cosmopolitan distribution.

**Remarks:** *Enchelys polyvacuolata* is a conspicuous species with several contractile vacuoles while all described congeners have only one or two (Berger et al. 1984; Dragesco & Dragesco-Kernéis 1979; Foissner 1984, 1987c, 2010; Foissner et al. 2002; Kahl 1930;  $\rightarrow$  *E. bivacuolata*) except of *E. multivacuolata* Vuxanovici, 1963 which, however, is only 70  $\mu\text{m}$  long and broadly elliptic (Fig. 12i). Another species, *E. vermiformis* Foissner, 1987c has a similar size and shape as *E. polyvacuolata* but has rows of somatic extrusomes and a moniliform macronucleus (Fig. 12g).

### ***Crassienchelys* nov. gen.**

**Diagnosis:** Medium-sized Enchelyidae Ehrenberg, 1838 with cuneate oral bulge and a comparatively large temporary cytostome near dorsal margin of oral bulge. Left side ciliary rows distinctly curved and condensed anteriorly while moderately curved and condensed on right side. Dorsal brush three- or four-rowed, i.e., composed of one or two short rows and two long rows. Resting cyst wall spinous.

**Type species:**  $\rightarrow$  *Crassienchelys oriclavata* nov. spec.

**Etymology:** Composite of the Latin adjective *crassus* (thick), the thematic vowel *-i-*, and the genus-group name *Enchelys* (eel), meaning a “thick *Enchelys*”. Feminine gender.

**Species assignable:**  $\rightarrow$  *Crassienchelys oriclavata* nov. spec.

**Remarks:** At first glance, *Crassienchelys* looks like *Cranotheridium* Schewiakoff, 1892, a rather superficially described genus from Australia (Schewiakoff 1892, 1893, 1896). It has a single main characteristic, viz., a specific structure in anterior dorsal margin of cell and resembling the basket found in nassulids (Fig. 14a). However, Kahl (1930) interpreted the “basket” as a bundle of trichocysts. I agree.

In 1984, Wirnsberger, Foissner & Adam used protargol for redescribing *Pseudoprorodon foliosus* Foissner, 1983a and suggested a spathidid relationship because it has a circumoral kinety and a

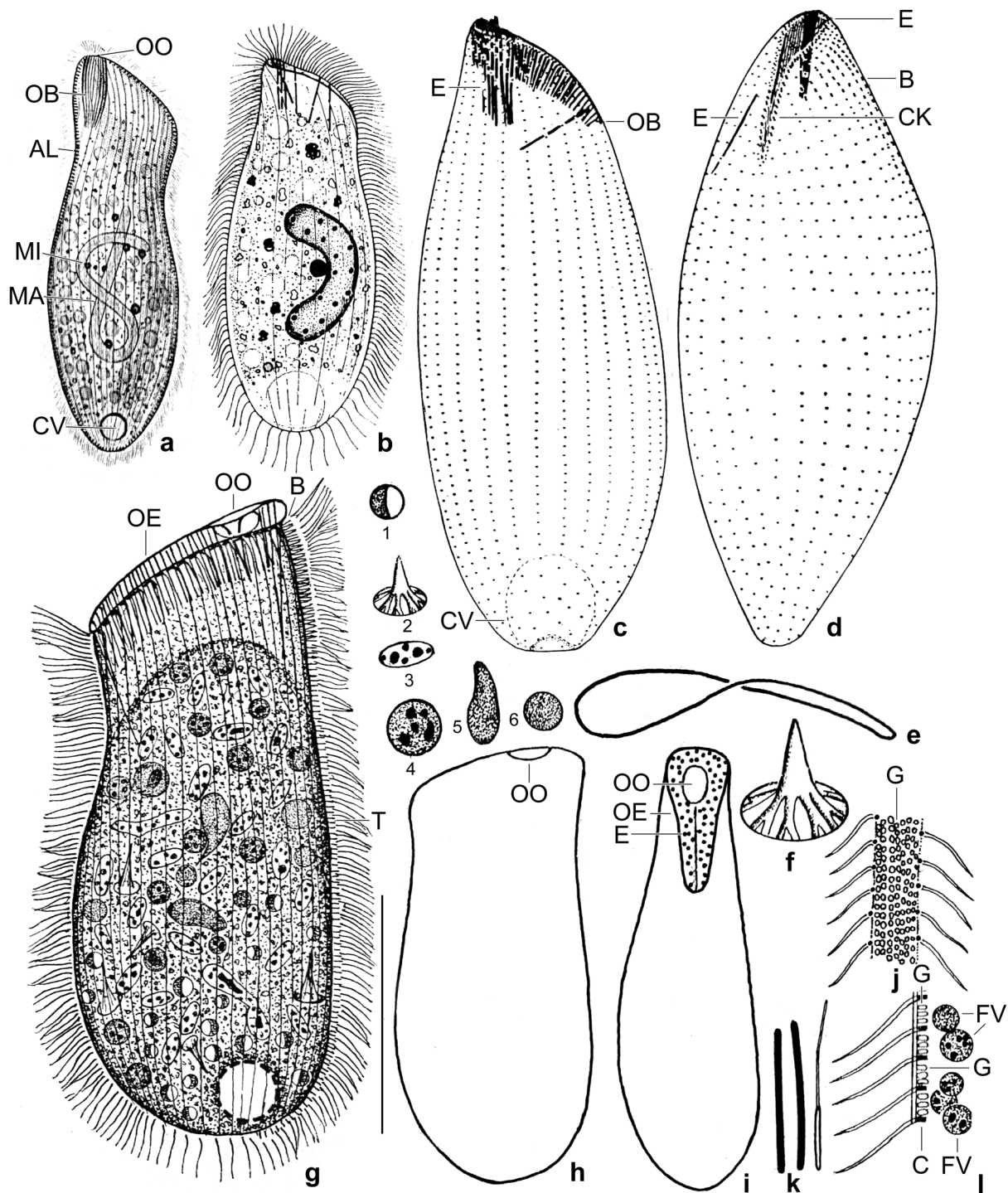


**Fig. 14a-l.** *Cranotheridium* (a) and *Cranotheridium*-like (b-l) haptorids. **a:** *Cranotheridium taeniatum*, right side view, length 170  $\mu\text{m}$  (from Schewiakoff 1896). Note the nassulid oral basket which is very likely an extrusome bundle. **b-d:** *Cranotheridium foliosum* in vivo (b, right side view, length about 100  $\mu\text{m}$ ) and after protargol impregnation (c, d, right side view and ventrolateral view, length about 80  $\mu\text{m}$ ; from Wirnsberger et al. 1984). Note the circumoral kinety (d). **e-l:** *Crassienchebys oriclavata* in vivo (g-k) and after protargol impregnation (originals; e, l; numerals 1-6). **e:** Lateral view, showing the propeller-shaped circumoral kinety. **f:** Mature cyst scale (lepidosome), height 10  $\mu\text{m}$ . **g and numerals 1-6:** Left side overview (g), scale bar 50  $\mu\text{m}$ , and cytoplasmic inclusion – developing (1) and mature (2) lepidosomes; 3 – macronuclear nodule; 4-6 – food vacuoles with selected prey pieces. **h, i:** Left side and ventral overview of same specimen, length 120  $\mu\text{m}$ . **j, l:** Cortical granulation, surface view and optical section. **k:** Mature extrusome seen from two sides (13  $\mu\text{m}$ ) and an exploded toxicyst (length 30  $\mu\text{m}$ ). AL – alveolar layer, b – dorsal brush, C – cortex, CK – circumoral kinety, CV – contractile vacuole, E – extrusomes, FV – food vacuoles, G – cortical granules, MA – macronucleus (macronuclear nodules), MI – micronucleus, OP – oral basket, OE – oral bulge, OO – oral opening (temporary cytostome), T – tail of dorsal brush row 3.

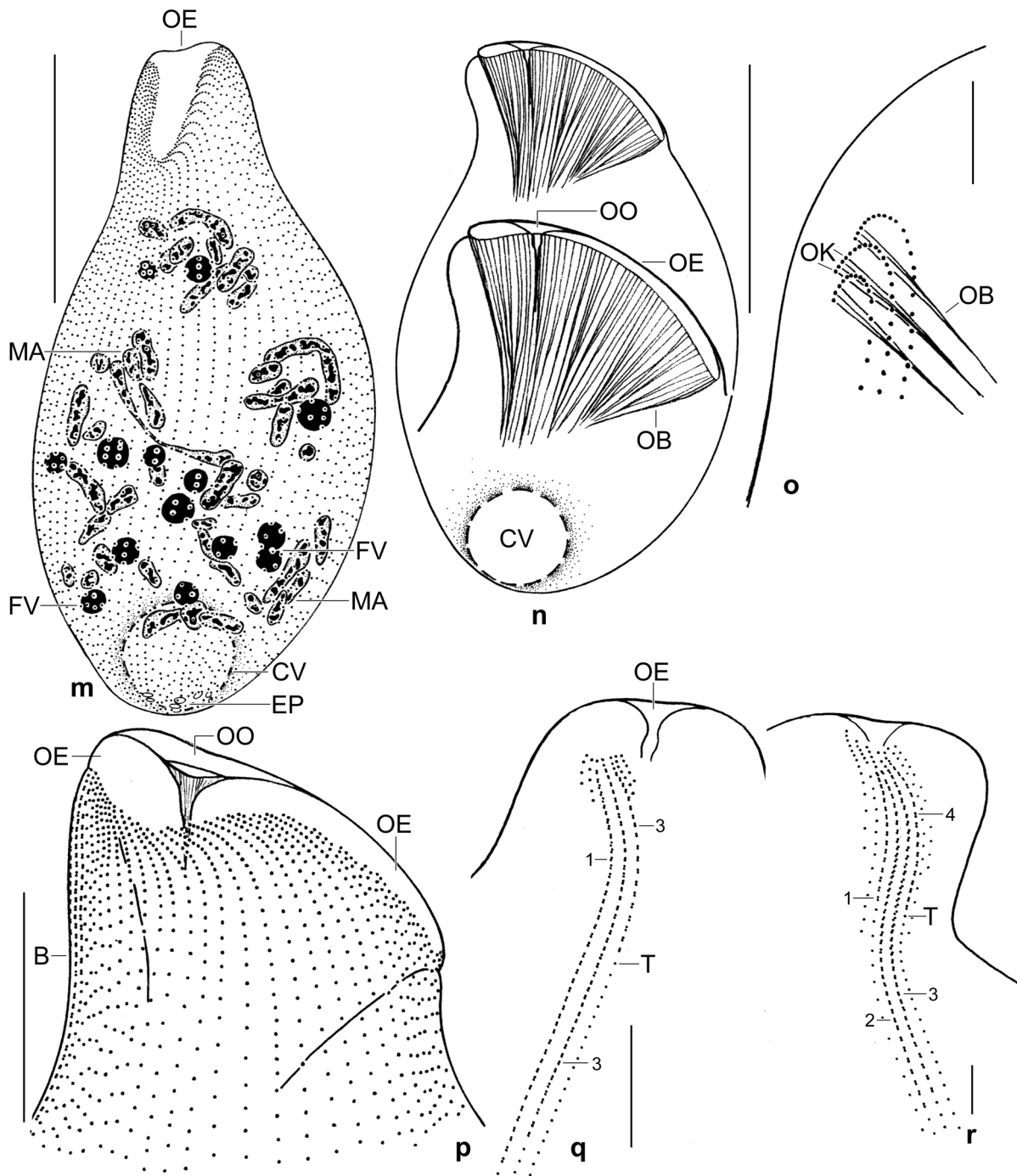


**Fig. 14m-r.** *Crassienchelys oriclavata*, ciliary and nuclear pattern after protargol impregnation. **m:** Ventral view of a representative specimen, showing the cuneate oral bulge and the anteriorly strongly curved left side ciliary rows. Only a minor portion of macronuclear nodules and food vacuoles are shown. **n:** Right side view of a thick specimen, showing the oral structures. **o:** The oral basket rods are produced by a few oralized somatic monokinetids at anterior end of the ciliary rows. **p:** Right side view of oral portion, showing the conspicuous oral opening (temporary cytostome). **q, r:** Most specimens have a four-rowed dorsal brush (r), in a few cells it is three-rowed. B – dorsal brush, CV – contractile vacuole, EP – pores of contractile vacuole, FV – food vacuoles, MA – macronuclear nodules, OB – oral basket, OE – oral bulge, OK – oralized somatic monokinetids, OO – oral opening (temporary cytostome), 1–4 – dorsal brush rows. Scale bars 50  $\mu\text{m}$  (m, n), 20  $\mu\text{m}$  (p), and 10  $\mu\text{m}$  (o, q, r).

dorsal brush while the dorsal bundle of trichocysts indicated an affinity to *Cranotheridium* (Fig. 14b–d). *Crassienchelys* differs from the *Cranotheridium* of Wirnsberger et al. (1984) by the absence of a circumoral kinety and the strongly curved and condensed anterior region of the left side ciliary

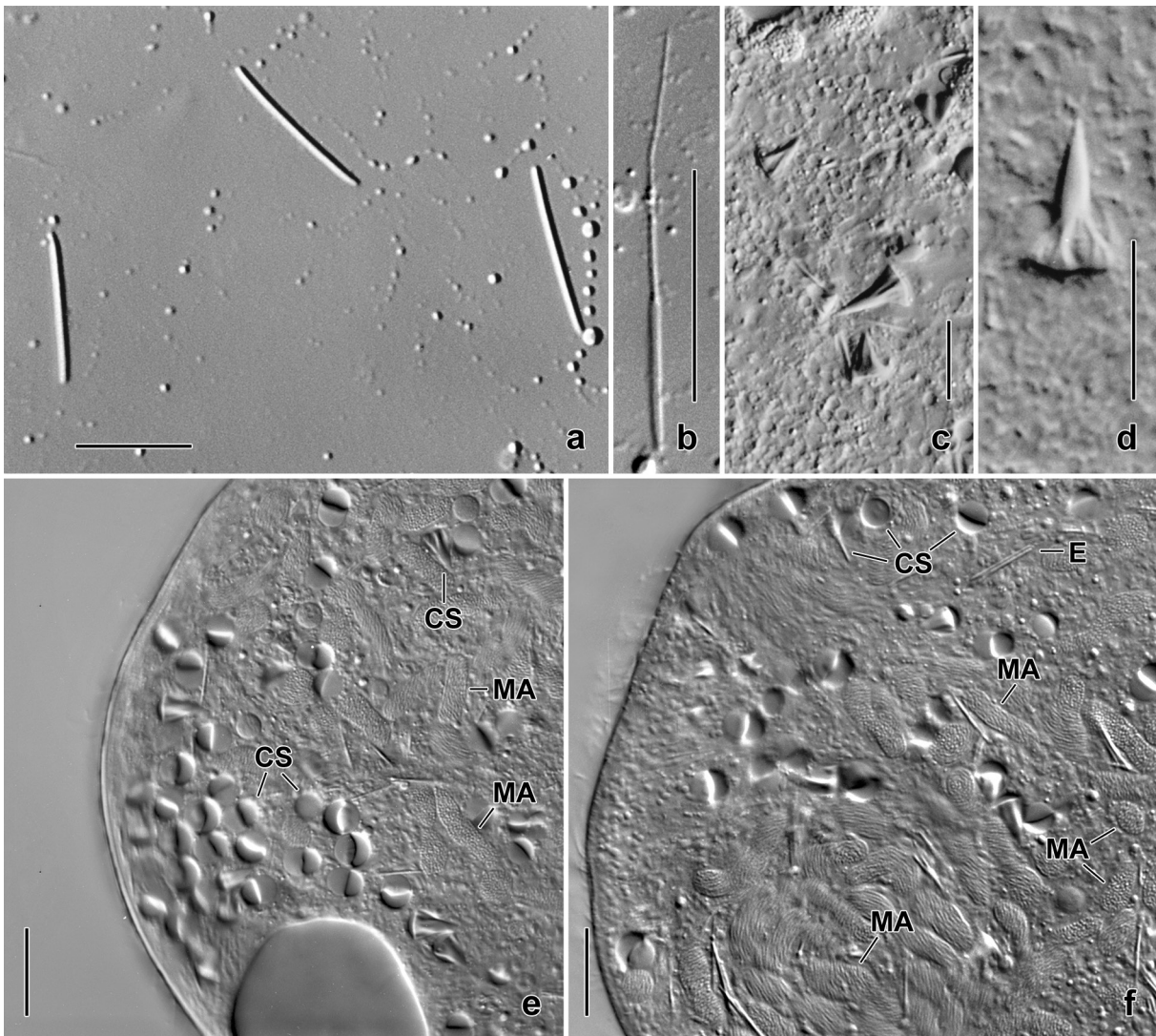


**Fig. 15a–f.** *Crassienchelys oriclavata* from life. **a:** Extrusomes (toxicysts), length 13–15  $\mu\text{m}$ . **b:** Exploded toxicyst, 30–50  $\mu\text{m}$ . **c, d:** Mature cyst scales in the cytoplasm. **e, f:** Macronuclear nodules and developing cyst scales in the cytoplasm. The scales develop in vacuoles partially filled with highly refractive, smooth material; the spine develops later. CS – developing and mature cyst scales, E – extrusome (toxicyst), MA – macronuclear nodules. Scale bars 20  $\mu\text{m}$  (b), 12  $\mu\text{m}$  (d), and 10  $\mu\text{m}$  (a, c, e, f).

rows (Fig. 14b–d). The classification into *Cranotheridium* of the ciliate studied by Wirnsberger et al. (1984) can be accepted when the basket of the ciliate studied by Schewiakoff (1892) is interpreted as a bundle of extrusomes.

Another similar ciliate is *Prorodon deflandrei* discovered by Dragesco (1960) in the fine coastal sands of Lake Geneva. It matches *Crassienchelys* roughly by body shape and the clavate oral bulge while the ciliary rows are not curved anteriorly; in addition, it possesses symbiotic green algae (zoochlorelles). Further investigations on the shape of the ciliary rows are required.

***Crassienchelys oriclavata* nov. spec.**

(Fig. 14e–r, 15a–x; Table 5 on p. 311)

**Diagnosis:** Size in vivo about 140  $\times$  60  $\mu\text{m}$ , bursiform and slightly flattened. Around 100 ellipsoid macronuclear nodules. Extrusomes rod-shaped and slightly curved, 13.0–15.0  $\times$  0.7–0.9  $\mu\text{m}$  in size.

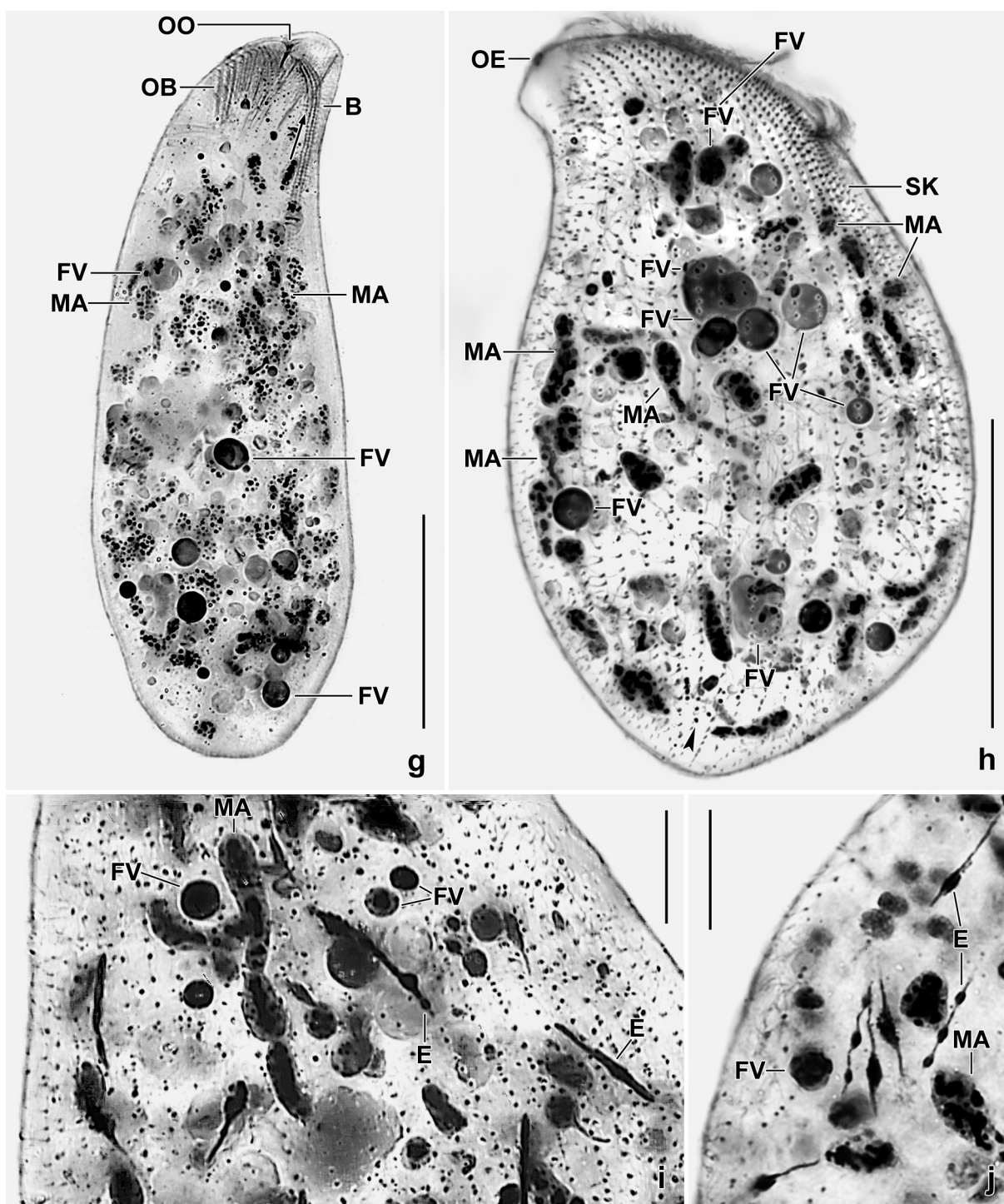


**Fig. 15g–j.** *Crassienchelys oriclavata* after protargol impregnation. **g:** Dorsolateral view of a specimen with four brush kineties; arrow marks the strongly shortened row 1. The specimen appears slender when compared with (h) because it is flattened laterally. **h:** Right side view, showing that the shape of the ciliary rows follows the shape of the oral bulge. The arrowhead marks a slightly shortened ciliary row. **i, j:** Cytoplasmic inclusions: long and short macronuclear nodules, food vacuoles, and extrusomes with 1–3 spindle-shaped widenings. B – dorsal brush, E – extrusomes, FV – food vacuoles with selected prey components, MA – macronuclear nodules, OE – oral bulge, OO – oral opening (temporary cytostome), SK – ordinary somatic ciliary rows. Scale bars 50  $\mu\text{m}$  (g, h), 15  $\mu\text{m}$  (j), and 10  $\mu\text{m}$  (i).

On average 61 ciliary rows, four, rarely three anteriorly modified to a dorsal brush with 3  $\mu\text{m}$  long bristles. Oral bulge slightly propeller-shaped, more or less oblique and moderately convex producing an about 45  $\mu\text{m}$  long cord; temporary cytostome conspicuous because distinctly concave and about

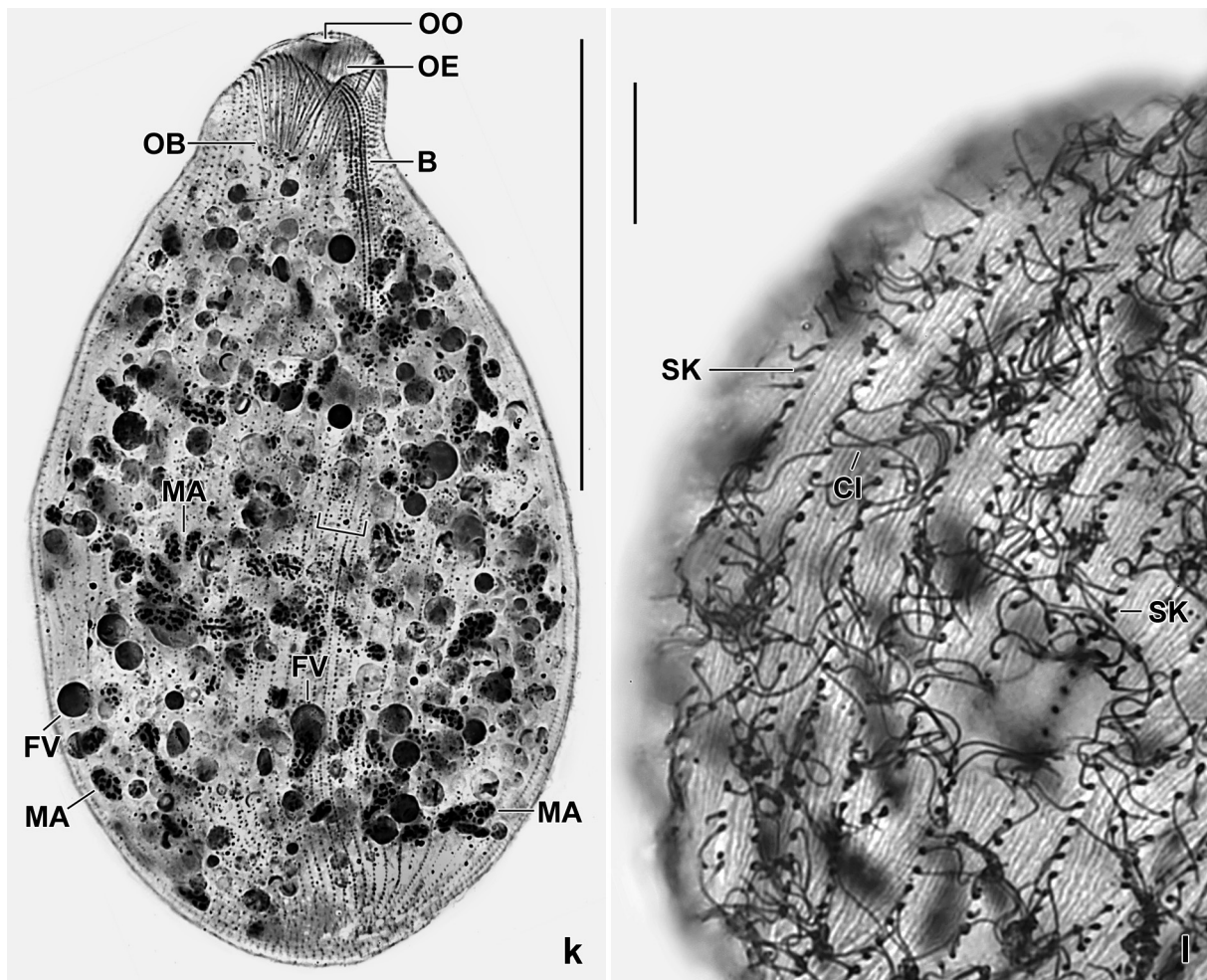


**Fig. 15k, l.** *Crassienchelys oriclavata* after protargol impregnation. **k:** A large specimen with many macronuclear nodules, four dorsal brush rows, and many small food vacuoles with selected prey components. The bracket in mid-body shows the narrow spacing of the ciliary rows posterior of the dorsal brush. **l:** Part of cortex, showing the comparatively thick postciliary microtubular ribbons originating from the basal bodies of the cilia and extending between the ciliary rows. B – dorsal brush, CI – somatic cilia, FV – food vacuoles, MA – macronuclear nodules, OB – oral basket, OE – bulge, OO – oral opening (temporary cytostome), SK – ordinary somatic kineties. Scale bars 90  $\mu\text{m}$  (k) and 10  $\mu\text{m}$  (l).

10  $\mu\text{m}$  in size, on average 12  $\mu\text{m}$  distant from dorsal bulge margin. Cyst scales conical.

**Type locality:** Australian site (96), i.e., near to the town of Darwin, entrance to the Foog Dam (12°33'29"S, 131°17'50"E); litter and soil from a young *Eucalyptus* forest.

**Type material:** The slide containing the holotype and six paratype slides with protargol-impregnated specimens have been deposited in the Biology Centre of the Upper Austrian Museum in Linz (LI). The holotype and paratype specimens have been marked by black ink circles on the coverslip. For slides, see Fig. 7a–m in Chapter 5.

**Etymology:** *oriclavata* is a composite in genitive case of *os* – *oris* (mouth) and the participial adjective *clavatus* -a -um, meaning a ciliate with clavate mouth.

**Description:** Few specimens were present, when I cleared the non-flooded Petri dish culture most cells had produced cyst scales; re-watering did not revive the population. The high coefficients of variability (most >15%) suggest that *Crassienchelys oriclavata* is rather variable (Table 5), very likely also due to insufficient fixation. Thus, measurements must be interpreted with care (Table 5).

Size in vivo 100–190  $\times$  55–110  $\mu\text{m}$ , on average about 140  $\times$  60  $\mu\text{m}$ , as calculated from some live measurements and protargol-impregnated cells adding 15% preparation shrinkage (Table 5). Body

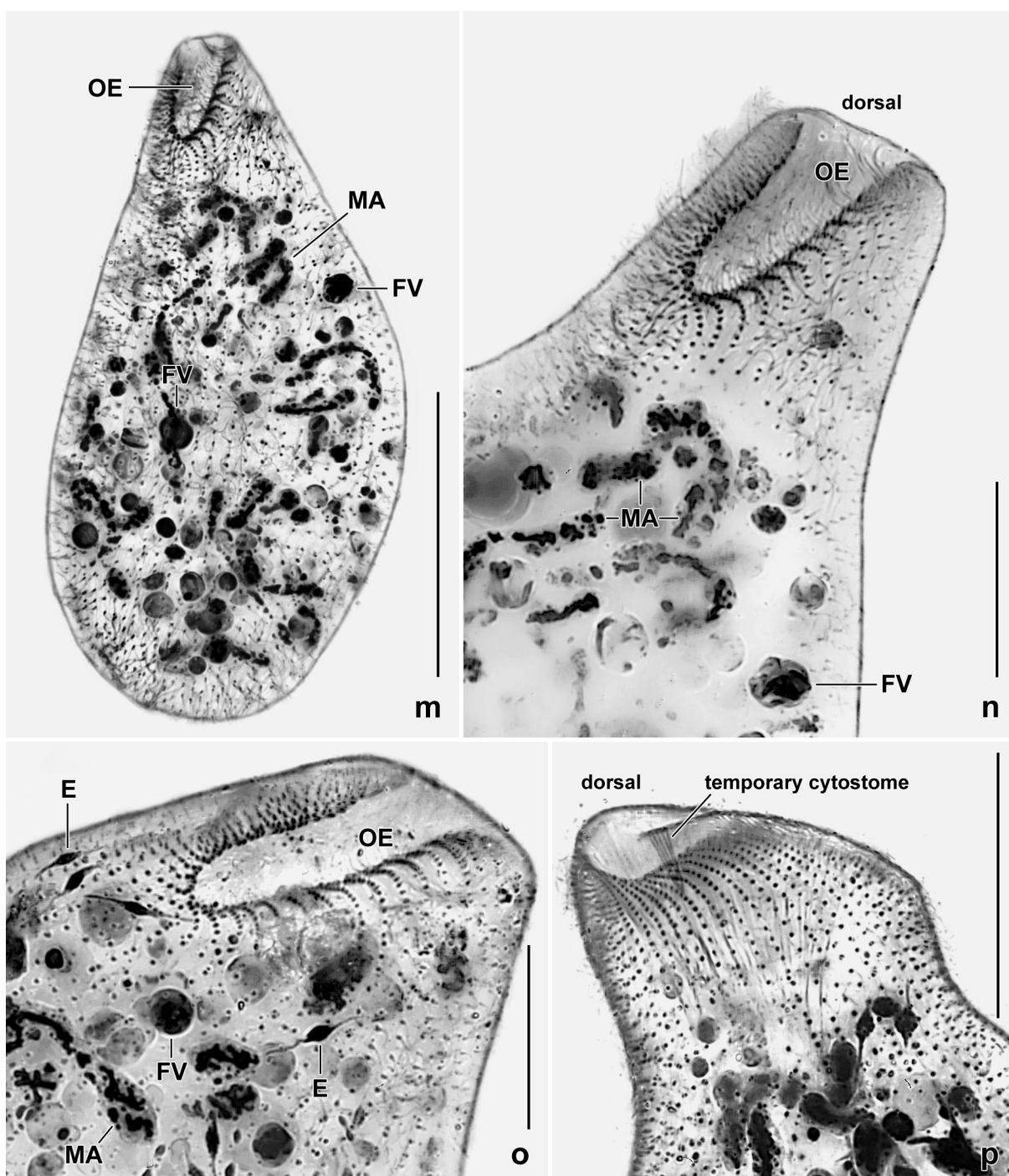


**Fig. 15m–p.** *Crassienchelys oriclavata* after protargol impregnation. **m:** Ventral view of holotype specimen, length 130  $\mu\text{m}$ . **n–p:** Anterior body region, showing the clavate oral bulge and the strongly curved and condensed ciliary rows along the left side of the oral bulge (n, o) while those of the right side are moderately curved but condensed for a longer distance (p). E – developing extrusomes, FV – food vacuoles, MA macronuclear nodules, OE – oral bulge. Scale bars 50  $\mu\text{m}$  (m), 40  $\mu\text{m}$  (p), and 20  $\mu\text{m}$  (n, o).

bursiform, usually dark due to masses of inclusions except in narrowed, transparent anterior quarter; left side distinctly flattened, right moderately to strongly convex, depending on food inclusions; anterior end slightly to distinctly oblique, posterior broadly rounded (Fig. 14g–i, m, n, p, 15g, h, k, m, n, r, t, w). About 100 macronuclear pieces scattered throughout body; nodules ellipsoid to elongate ellipsoid, on average  $9 \times 4 \mu\text{m}$  in protargol preparations; usually also some up to 30  $\mu\text{m}$  long macronuclear strands; size and number of nucleoli ordinary (Fig. 14g, m, 15e–k, m–o, q–t, x;

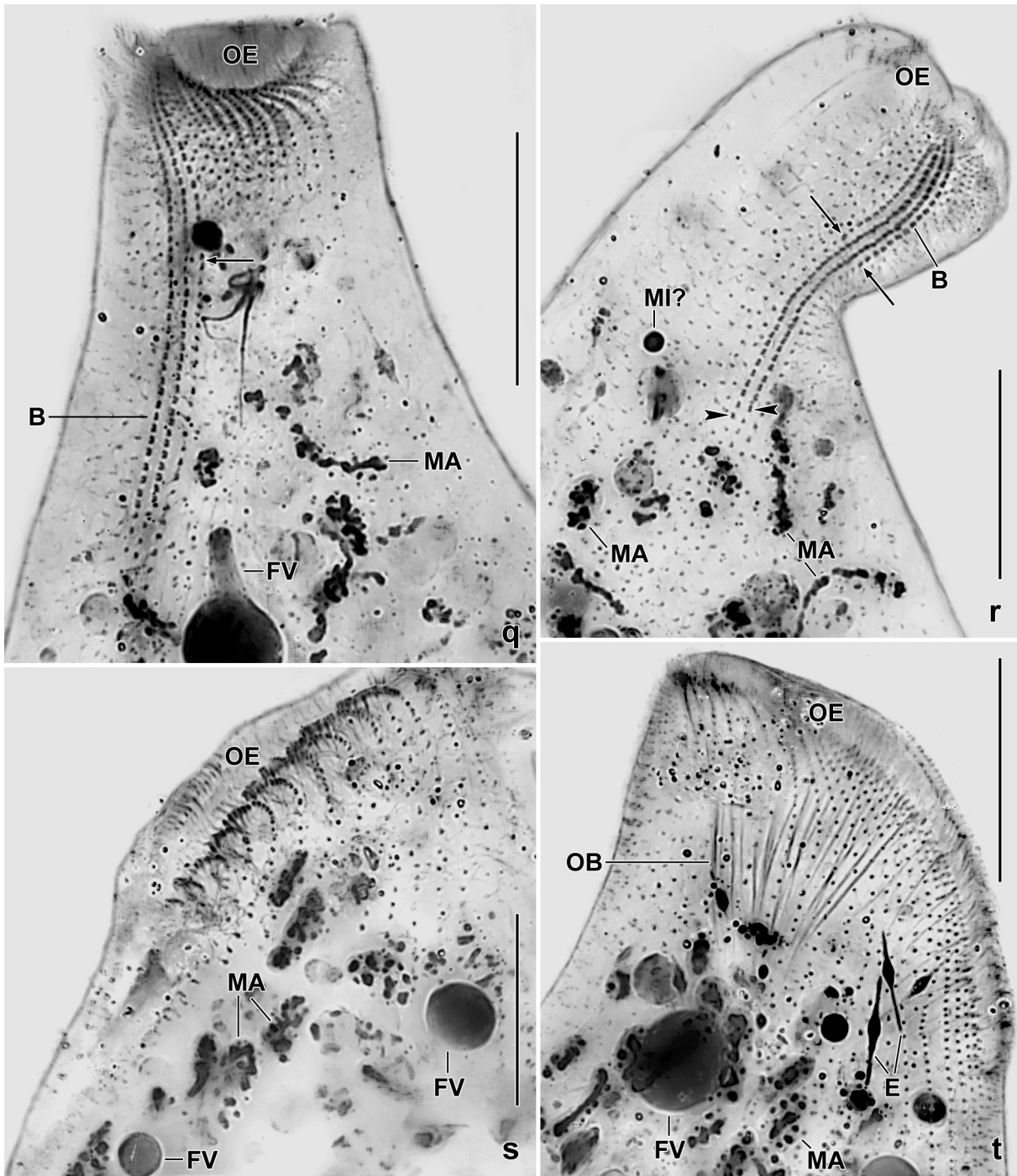


**Fig. 15q–t.** *Crassienchelys oriclavata*, oral ciliature and dorsal brush after protargol impregnation. **q:** A specimen with a three-rowed dorsal brush; rows 1 and 2 have a similar length while row 3 (arrow) is distinctly shortened. Note the conspicuous, pumpkin-shaped food vacuole. **r:** Most specimens have a four-rowed dorsal brush; rows 1 and 4 (arrows at end of dikinetal portion) are distinctly shortened, rows 2 and 3 (arrowheads) are much longer and end at same level. **s, t:** Left and right side view of oral region. On the left side, the ciliary rows are markedly curved and condensed anteriorly (s), on the right the ciliary rows are moderately curved and condensed (t). B – dorsal brush, E – developing extrusomes, FV – food vacuoles, MA – macronuclear nodules, MI? – supposed micronucleus, OB – oral basket, OE – oral bulge, OK – oralized somatic kinetids. Scale bars 50  $\mu\text{m}$  (q, r), 35  $\mu\text{m}$  (t), and 20  $\mu\text{m}$  (s).

Table 5). Very likely several micronuclei not clearly separable from other cytoplasmic inclusions. Contractile vacuole in posterior body end slightly left of midline (Fig. 14g, m, n). Mature extrusomes studded in oral bulge, much longer than bulge height, rod-shaped and slightly curved,  $13.0\text{--}15.0 \times 0.7\text{--}0.9 \mu\text{m}$  in size, when extruded with typical toxicyst structure and up to 50  $\mu\text{m}$  long in vivo (Fig.

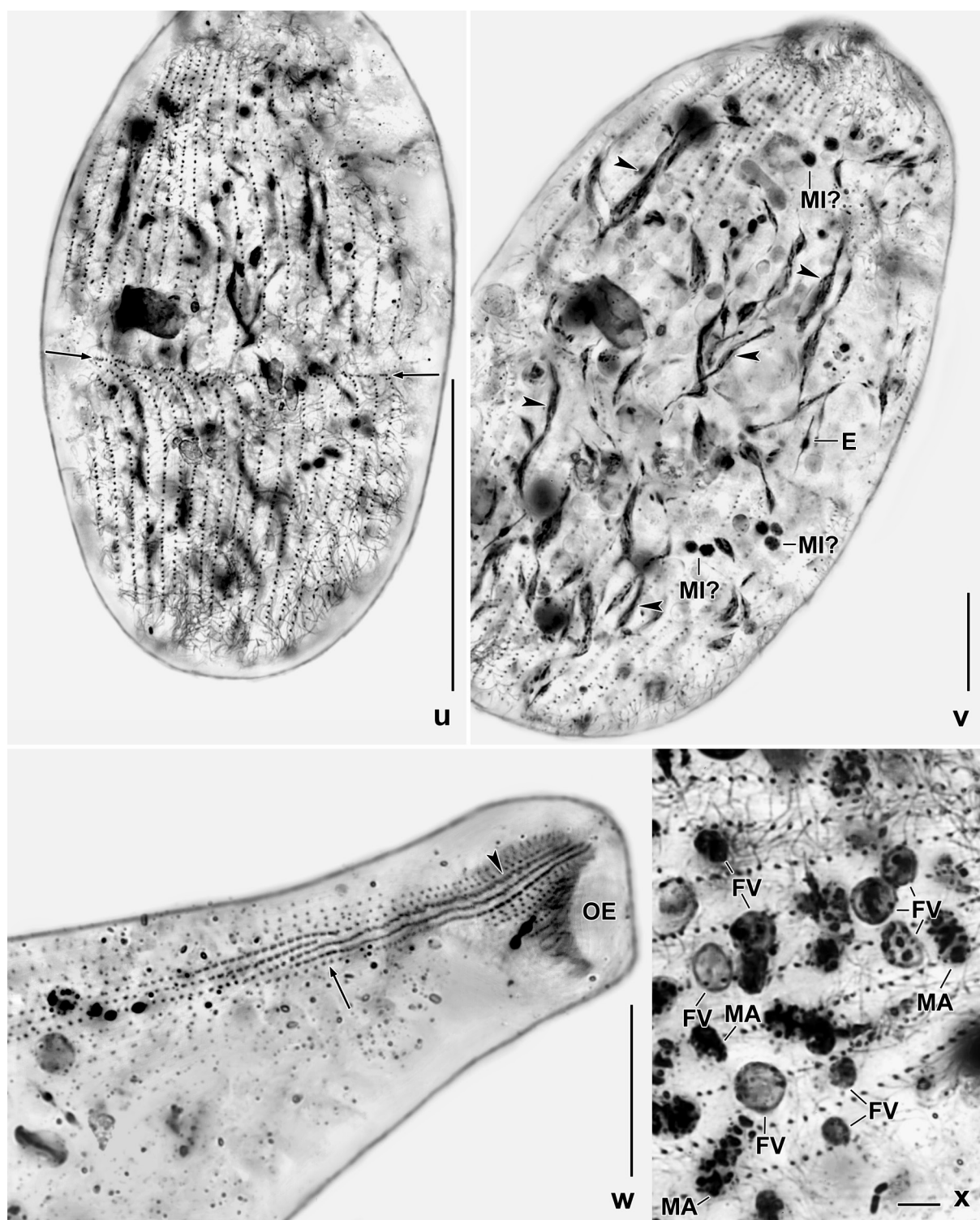


**Fig. 15u–x.** *Crassienchelys oriclavata* after protargol impregnation. **u, v:** An early mid-divider (**u**, divided ciliary rows marked by arrows), showing curious spindle-shaped macronuclear nodules some marked by arrowheads in (**v**). **w:** Dorsal view of a specimen with damaged(?) dorsal brush forming three rows in anterior half (arrowhead) while four rows in last third (arrow). **x:** Food vacuoles with selected prey components. **E** – developing extrusome, **MA** – macronuclear nodules, **MI?** – supposed micronuclei, **OE** – oral bulge. Scale bars 70  $\mu\text{m}$  (**u**), 20  $\mu\text{m}$  (**v, w**), and 5  $\mu\text{m}$  (**x**).

14g, k, 15a, f). Developing extrusomes scattered throughout cell, with 1–3 fusiform extensions in central quarters, 12–14  $\mu\text{m}$  long (Fig. 14k, 15i, j, o, t, v). Cortex 1.0–1.5  $\mu\text{m}$  thick, contains about eight rows of granules 0.8  $\times$  0.5  $\mu\text{m}$  in size and massive postciliary microtubule ribbons between two ciliary rows each (Fig. 14j, l, 15l). Cytoplasm colourless, postorally studded with three kinds

of inclusions: (i) many macronuclear nodules as described above; (ii) many developing and some mature cyst scales (lepidosomes), developing scales 3–5  $\mu\text{m}$  across, one half filled with smooth, refractive material, the other half hyaline looking empty (Fig. 14e–g); mature scales about 10  $\mu\text{m}$  high, conical with circular base plate, both showing minute ridges bifurcated distally (Fig. 14f, 15c–e); such scales have been observed mainly in haptorids and enchelydids (see this monograph and Foissner 2016); (iii) many globular and some tear-shaped structures 3–10  $\mu\text{m}$ , respectively up to 20  $\mu\text{m}$  in size; impregnate faintly to deeply, many contain deeply impregnated granules and granular accumulations resembling nuclear material, and a few look like dividers producing dumb-bell-shaped figures (Fig. 14g, l, 15a–k, m–o, q, s, t, x).

Originally, I classified these granular globules as coccidian parasites; however, now I interpret them as minute food vacuoles containing selected prey. This is supported by the absence of classical food vacuoles larger than 20  $\mu\text{m}$ , indicating that prey is lysed outside and then ingested and sorted according to materials, such as extrusomes, lipid droplets, and nuclear pieces. Swims and creeps rather fast.

Only one early mid-divider is contained and marked in the protargol slides. While the ciliary pattern seems to divide ordinarily (Fig. 15u), the ellipsoid macronuclear nodules become long and fusiform (Fig. 15v), as in some dileptids (for a review, see Vd'ačný & Foissner 2012).

Ciliary pattern epispathidid but without circumoral kinety, left side ciliary rows anteriorly distinctly curved and condensed, right side rows only condensed anteriorly and gradually abutting on oral bulge (Fig. 14g, m, p, 15h, k, m–p, s, t). Cilia of oral area about 14  $\mu\text{m}$  long, decrease to 11  $\mu\text{m}$  near posterior end of cell, all ciliary and dorsal brush rows begin with 3–6 very narrowly spaced oralized somatic monokinetids, producing the oral basket rods (Fig. 14g, o, 15s). On average 62 narrowly to very narrowly spaced, densely ciliated rows abutting on oral bulge, four, rarely only three rows anteriorly modified to an isomorphic, distinctly heterostichad dorsal brush composed of ordinarily to narrowly spaced dikinetids having about 3  $\mu\text{m}$  long bristles in vivo, monokinetal tail of leftmost row with fusiform bristles gradually shortened to 2  $\mu\text{m}$  in posterior third (Fig. 14g, p–r, 15g, k, q, r, w; Table 5).

Oral bulge moderately convex, cord of curve about 45  $\mu\text{m}$  long in protargol preparations, slightly to distinctly oblique, clavate and about 13  $\mu\text{m}$  wide near dorsal end, about 2  $\mu\text{m}$  high at ventral end while about 6  $\mu\text{m}$  at dorsal end, slightly screwed like a propeller blade in frontal view while like a recumbent number 8 in lateral view (Fig. 14g, e, h, 15m, n, p–t; Table 5; cp.  $\rightarrow$  *Enchelys australiensis*). Temporary cytostome on average 14  $\mu\text{m}$  distant from dorsal margin of oral bulge, obconical with wide end on surface of bulge, about 10  $\times$  8  $\mu\text{m}$  in size and more conspicuous in vivo than in protargol preparations (Fig. 14g, h, n, p–r, 15g, h, k, p; Table 5).

**Occurrence and ecology:** As yet found only at type locality and very likely also in the Brazilian Pantanal where very few specimens occurred; the only difference in life observation was the length of the extrusomes (11  $\mu\text{m}$  vs. 13–15  $\mu\text{m}$ ). *Crassienchelys oriclavata* is a massive, conspicuous species possibly endemic to Gondwana.

**Remarks:** *Crassienchelys oriclavata* is easily recognized by the comparably large temporary cytostome, the many macronuclear nodules, and the moderate body length (~100–150  $\mu\text{m}$ ). There is no other haptorid with such a combination of features. See also “Remarks” to genus.

## Nomenclatural corrections and new spathidid genera

Foissner (2016) created the spathidid genus *Facetospatha* (species with arcuospathidid ciliary pattern and faceted cyst wall) with *Arcuospathidium cultriforme* (Penard, 1922) Foissner, 1984 as type species. However, Helmut Berger (Salzburg) recognized that I used *Spathidium cultriforme* Penard,

1922 previously as type species for the genus *Arcuospathidium* Foissner, 1984. Thus, *Facetopatha* Foissner, 2016 has to be suppressed and the character “faceted cyst wall” added to the diagnosis of *Arcuospathidium*. A new genus is required for arcuospathidids that have another cyst wall (see below).

As yet, the resting cyst of most spathidid genera and species is not known because it never has been used as a generic character though it is of paramount significance for dispersal and survival (Foissner 2011). Based on this knowledge, I created three spathidid genera in 2016: *Mamillospatha*, *Columnnospatha* and *Facetopatha* (Foissner 2016). Here, I add three new genera diagnosed below and provide an improved diagnosis for *Arcuospathidium*.

### ***Levispatha* nov. gen.**

**Diagnosis:** Spathidiidae Kahl in Doflein & Reichenow, 1929 with arcuospathidid ciliary pattern and smooth cyst wall.

**Type species:** *Levispatha tristicha* (Foissner et al., 2002) nov. stat., nov. comb. (original combination: *Arcuospathidium namibiense tristicha* Foissner, Agatha & Berger, 2002).

**Species assignable:** *Levispatha tristicha* (type species); *Levispatha muscorum* (Dragesco & Dragesco-Kernéis, 1979) nov. comb. (original combination: *Spathidium muscorum* Dragesco & Dragesco-Kernéis, 1979); → *Levispatha australiensis* nov. sp.

**Etymology:** *Levispatha* is a composite of the Latin adjective *levis* (smooth) and the Latinized Greek noun *spatha* (spathula; Hentschel & Wagner 1996), referring to the smooth cyst wall. Feminine gender.

**Remarks:** There are now three arcuospathidid genera: *Arcuospathidium* (with faceted cyst wall; junior objective synonym *Facetopatha* Foissner, 2016); *Columnnospatha* (cyst wall with pillar-shaped lepidosomes), and *Levispatha* (cyst wall smooth).

### ***Arcuospathidium* Foissner, 1984**

1984 *Arcuospathidium* nov. gen. — Foissner, Stapfia, 12: 74. Type species (by original designation): *Spathidium cultriforme* Penard, 1922.

2007 *Arcuospathidium* Foissner, 1984 — Foissner & Xu, Monogr. Biol., 81: 156 (detailed revision).

2007 *Arcuospathidium* Foissner, 1984 — Jankowski, Phylum Ciliophora, p. 565 (generic revision).

2016 *Facetopatha* nov. gen. — Foissner, Denisia, 35: 187. Type species (by original designation): *Spathidium cultriforme* Penard, 1922 (junior objective synonym, that is, illegitimate because based on same type species as *Arcuospathidium*).

**Improved diagnosis:** Spathidiidae Kahl in Doflein & Reichenow, 1929 with arcuospathidid ciliary pattern and thick, faceted cyst wall.

**Type species:** *Arcuospathidium cultriforme* (Penard, 1922) Foissner, 1984 (original combination: *Spathidium cultriforme* Penard, 1922).

**Species assignable:** So far only the type species.

**Etymology:** The name is a composite of the Latin noun *arcus* (arc, curve) and the genus-group name *Spathidium*, referring to the often long and curved oral bulge and the similarity to the genus *Spathidium*. Neuter gender (from Foissner & Xu 2007).

**Remarks:** Foissner & Xu (2007) recognized three subspecies in *A. cultriforme* but the cyst structure is known only from *Arcuospathidium cultriforme cultriforme*.

***Protospatha* nov. gen.**

**Diagnosis:** Spathidiidae Kahl in Doflein & Reichenow, 1929 with protospathidid ciliary pattern and smooth cyst wall.

**Type species:** *Protospatha terricola* (Foissner, 1998) nov. comb. (original combination: *Protospathidium terricola* Foissner, 1998).

**Species assignable:** *Protospatha terricola* (Foissner, 1998) nov. comb.

**Etymology:** *Protospatha* is a composite of the Latin comparative *proto* (the first) and the Latinized Greek noun *spatha* (*spathula*; Hentschel & Wagner 1996), referring to the supposed plesiomorphic genus *Protospathidium*. Feminine gender.

**Remarks:** The type species of *Protospathidium* Dragesco & Dragesco-Kernéis, 1979 is *P. muscicola* Dragesco & Dragesco-Kernéis, 1979, which has nipple-shaped cyst scales matching the protospathidid genus *Mamillospatha* Foissner, 2016.

***Spinispatha* nov. gen.**

**Diagnosis:** Spathidiidae Kahl in Doflein & Reichenow, 1929 with protospathidid ciliary pattern and a spiny cyst wall.

**Type species:** *Spinispatha serpens* (Kahl, 1930) nov. comb. (original combination: *Spathidium serpens* Kahl, 1930).

**Species assignable:** *Spinispatha serpens* (Kahl, 1930) nov. comb.

**Etymology:** *Spinispatha* is a composite of the Latin adjective *spinus* (thorny, spiny) and the Latinized Greek noun *spatha* (*spathula*; Hentschel & Wagner 1996), referring to the spiny cyst wall. Feminine gender.

**Remarks:** The Antarctic *Protospathidium serpens* (Kahl, 1930) Foissner, 1981 has a different cyst and is thus very likely another species, viz., *P. fraterculus* Xu & Foissner, 2005 (for details, see Foissner & Xu 2007, p. 130).

***Levispatha australiensis* nov. spec.**

(Fig. 16a–l, 17a–x, 18a–k, 19; Table 6 on p. 312)

**Diagnosis:** Size in vivo about  $100 \times 20 \mu\text{m}$ . Narrowly spatulate with oblique to strongly oblique, very narrowly cuneate oral bulge about  $2 \mu\text{m}$  wide and high and 1.2 times longer than widest trunk region. Macronucleus usually oblong; single micronucleus. Extrusomes slightly curved rods with a size of about  $8.0 \times 0.3 \mu\text{m}$ , attached only to right half of oral bulge and absent from dorsal bulge region. On average 13 ciliary rows, three anteriorly differentiated to a heterostichad dorsal brush occupying 15% of body length. Brush bristles up to  $3 \mu\text{m}$  long; rows 1 and 2 each composed of an average of 12 dikinetids, row 3 of seven followed by a monokinetid bristle tail extending to second quarter of cell.

**Type locality:** Soil from floodplain of the Murray River near to the town of Albury (Australia), waterside of Ryans Road.<sup>1</sup>

**Type material:** The slide containing the holotype and three paratype slides with protargol-impregnated specimens have been deposited in the Biology Centre of the Upper Austrian Museum

<sup>1</sup> Note by H. Berger: Foissner did not provide geographic co-ordinates. According to Google Maps, the sample site must be at or near the following point:  $36^{\circ}06'49.342''\text{S}$ ,  $146^{\circ}58'13.966''\text{E}$ . This is very likely also the type locality of  $\rightarrow$  *Bursaria fluviatilis* and  $\rightarrow$  *Pseudofuscheria magna*.

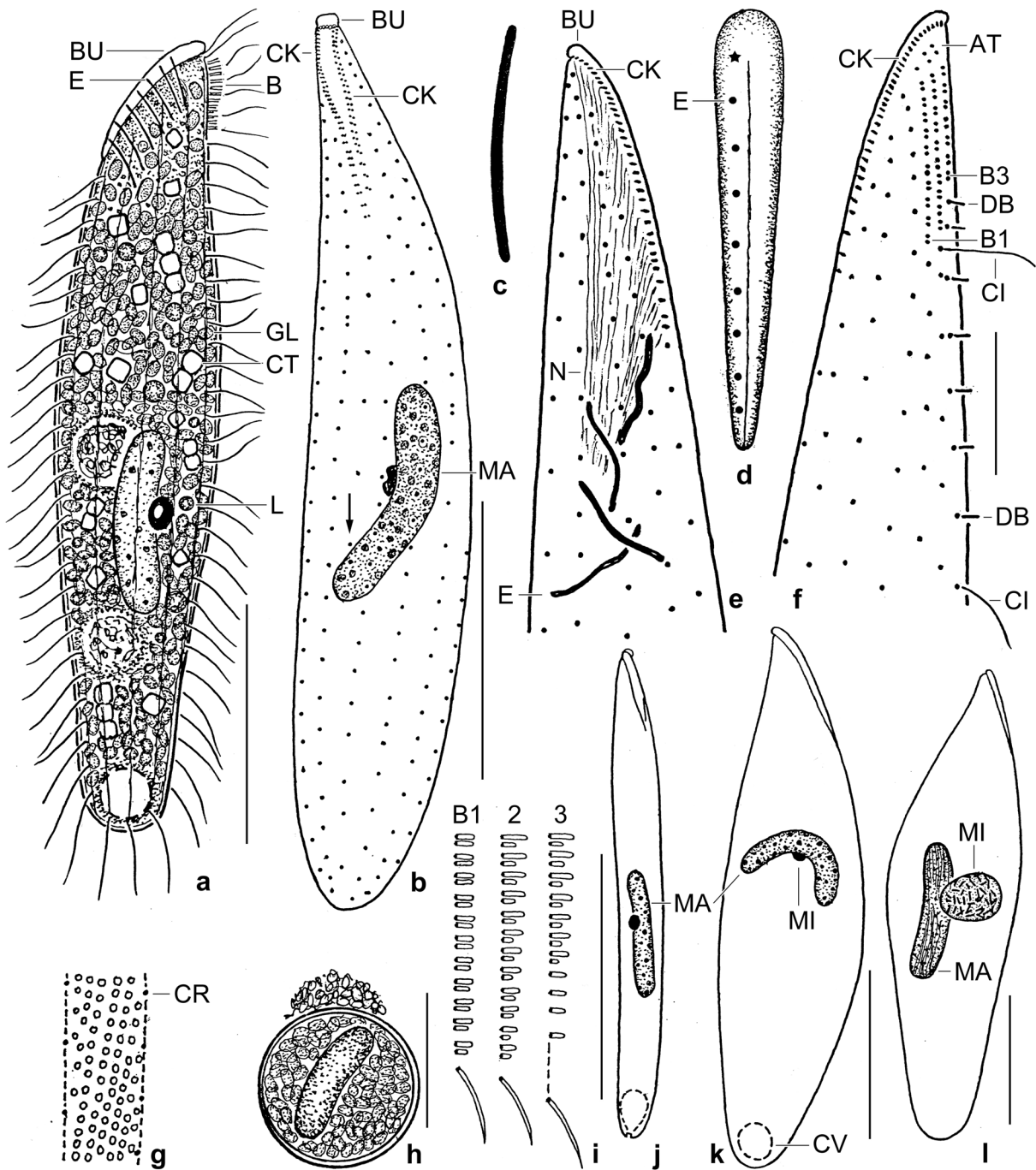


**Fig. 16a–l.** *Levispatha australiensis* from life (a, c, d, g–i) and after protargol impregnation (b, e, f, j–l). **a:** Left side view of a representative specimen, length 100  $\mu\text{m}$ . The cell is studded with granules, crystals, and lipid droplets. **b:** Ventral view, showing the basal body (ciliary) and nuclear pattern. **c:** Extrusome,  $8.0 \times 0.3 \mu\text{m}$ . **d:** Frontal view of oral bulge, showing absence of extrusomes in dorsal region (asterisk) and in left half of bulge. **e, f:** Right and left side view of infraciliature in anterior body region. **g:** Cortical granulation. **h:** Resting cyst. **i:** Dorsal brush. **j, k:** The most slender specimen and the largest cell found. **l:** A very early divider with strongly inflated micronucleus. AT – anterior tail of dorsal brush rows, B – dorsal brush, B1–3 – dorsal brush rows, BU – oral bulge, CI – ordinary somatic cilia, CK – circumoral kinety, CR – ciliary row, CT – crystals, CV – contractile vacuole, DB – bristles of dorsal brush row 3, E – extrusomes, GL – granular inclusions, L – lipid droplet, MA – macronucleus, MI – micronucleus, N – nematodesmata. Scale bars 10  $\mu\text{m}$  (e, f), 25  $\mu\text{m}$  (l), 30  $\mu\text{m}$  (a, b, h), and 50  $\mu\text{m}$  (j, k).

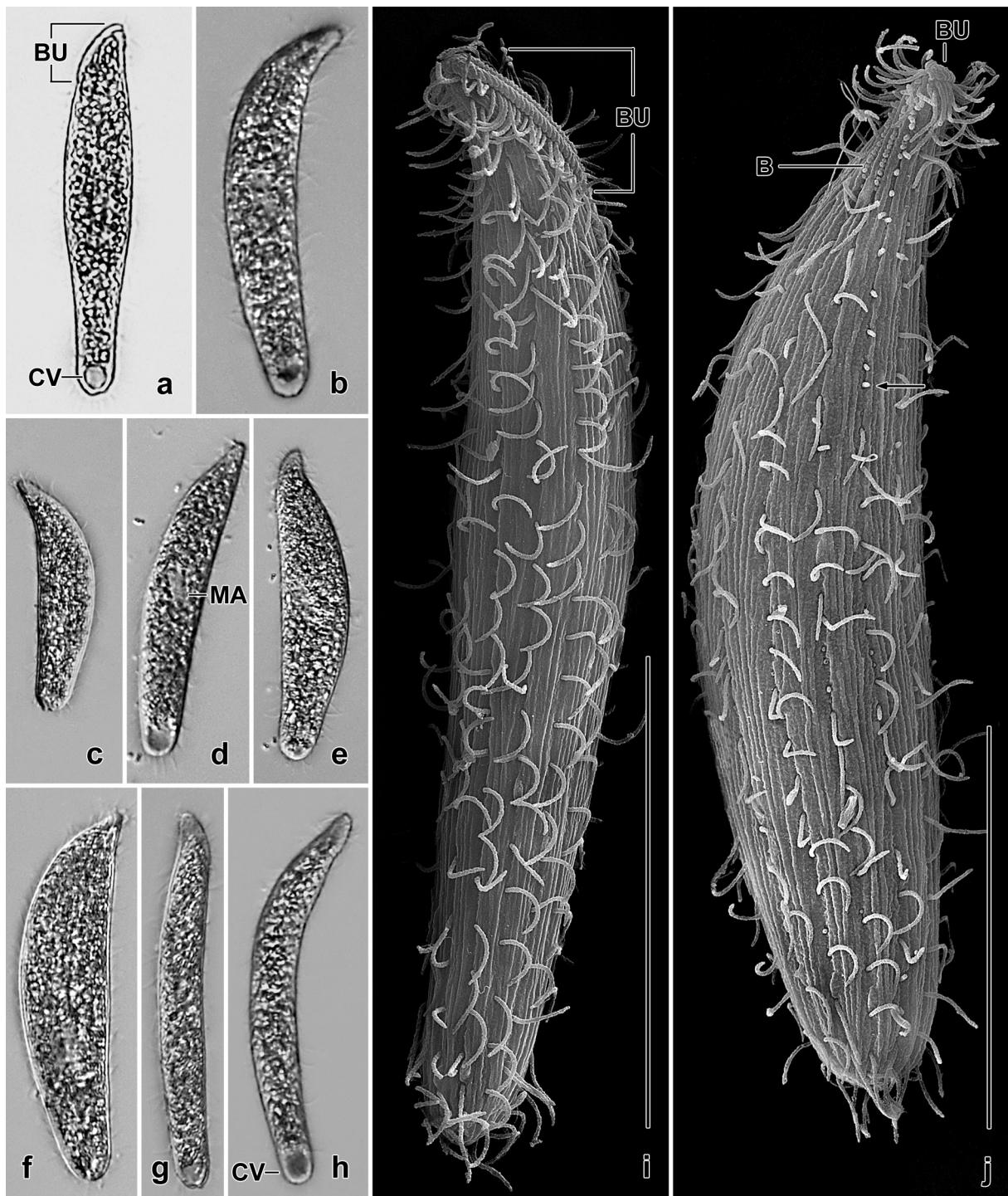


**Fig. 17a–j.** *Levispatha australiensis* from life (a–h) and in the SEM (i, j). **a–h:** Overviews, length 70–120  $\mu\text{m}$ . The cells are flattened in the oral area (b, c, d, g) and rather dark because they are studded with inclusions (see next plate). The length:width ratio is highly variable, depending on the amount of food ingested. **i, j:** Right side and dorsal overview, showing the very short oral bulge and dorsal brush. The arrow marks the posterior end of the bristle tail of brush row 3. The longitudinal striation is caused by the postciliary microtubule bundles. B – dorsal brush, BU – oral bulge, CV – contractile vacuole, MA – macronucleus. Scale bars 40  $\mu\text{m}$  (i, j).

in Linz (LI).<sup>1</sup> The holotype and relevant paratype specimens have been marked with black ink circles on the coverslip. For slides, see Fig. 8a–g in Chapter 5.

<sup>1</sup> Note by H. Berger: The slide is labelled with *Arcuospathidium australiense* (see Fig. 8a–g in Chapter 5). This name is disclaimed for nomenclatural purposes (ICZN 1999, Article 8.3).

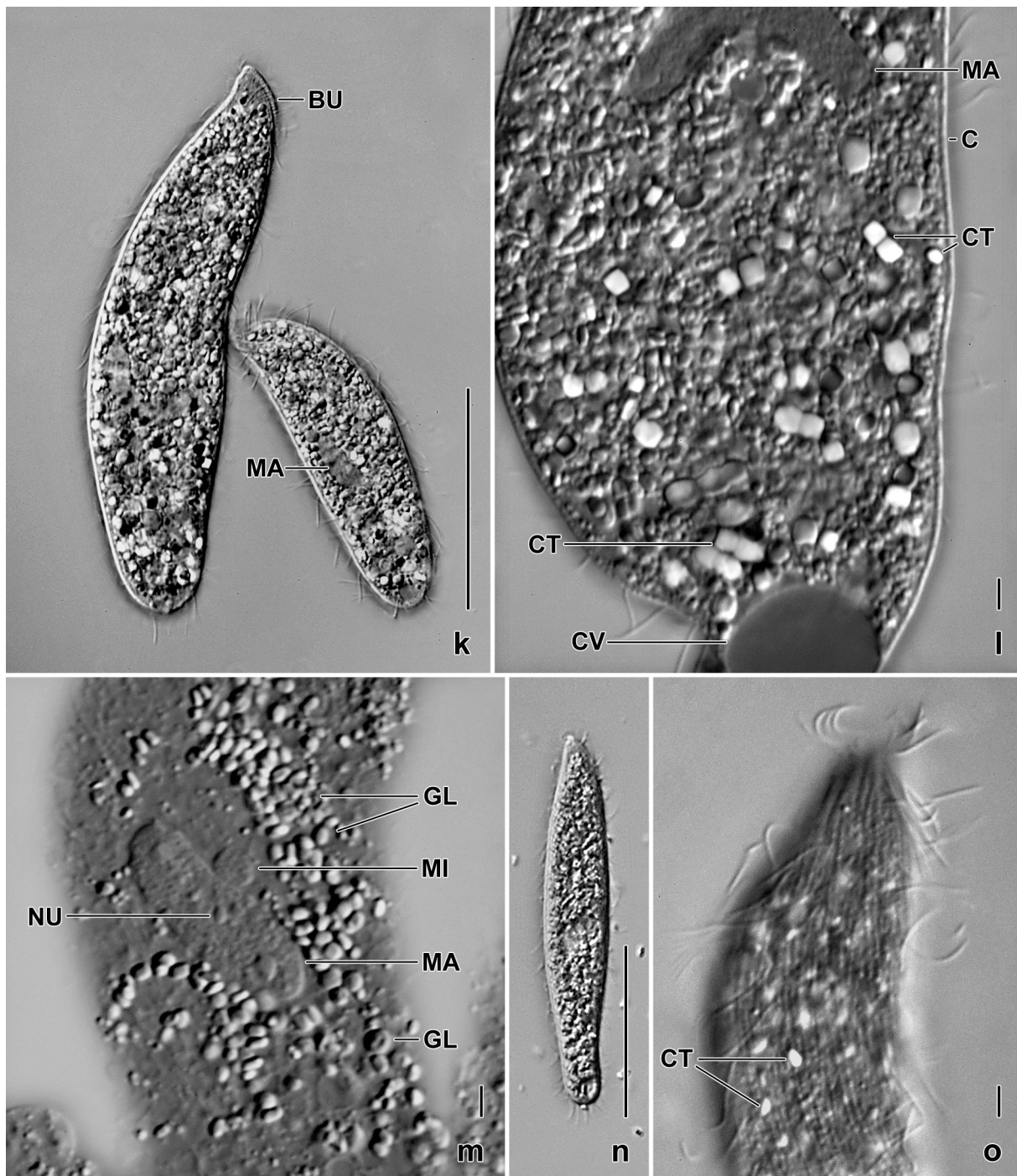


**Fig. 17k–o.** *Levispatha australiensis* from life (interference contrast). **k, n:** Right side overviews, showing the cells studded with various inclusions. Note the length difference in (k). **l:** Posterior region of a pressed specimen, showing many cubic crystalline inclusions sparkling under interference contrast. Note the reniform macronucleus. **m:** Mid-body of a strongly pressed specimen, showing innumerable refractive granules and the nuclear apparatus. **o:** Surface view of dorsal anterior body region, showing rows of cortical granules and some bright crystals as described above. BU – oral bulge, C – cortex, CT – crystals, CV – contractile vacuole, GL – granular inclusions, MA – macronucleus, MI – micronucleus, NU – nucleolus. Scale bars 5  $\mu\text{m}$  (l, m, o) and 40  $\mu\text{m}$  (k, n).

**Etymology:** Named after the continent discovered.

**Description:** Size in vivo 60–150  $\times$  10–40  $\mu\text{m}$ , usually about 100  $\times$  20  $\mu\text{m}$ , as calculated from live measurements and two different preparations adding 15% for shrinkage, altogether 53 individuals; values agree well for the different methods (Table 6). Forms theronts and trophonts

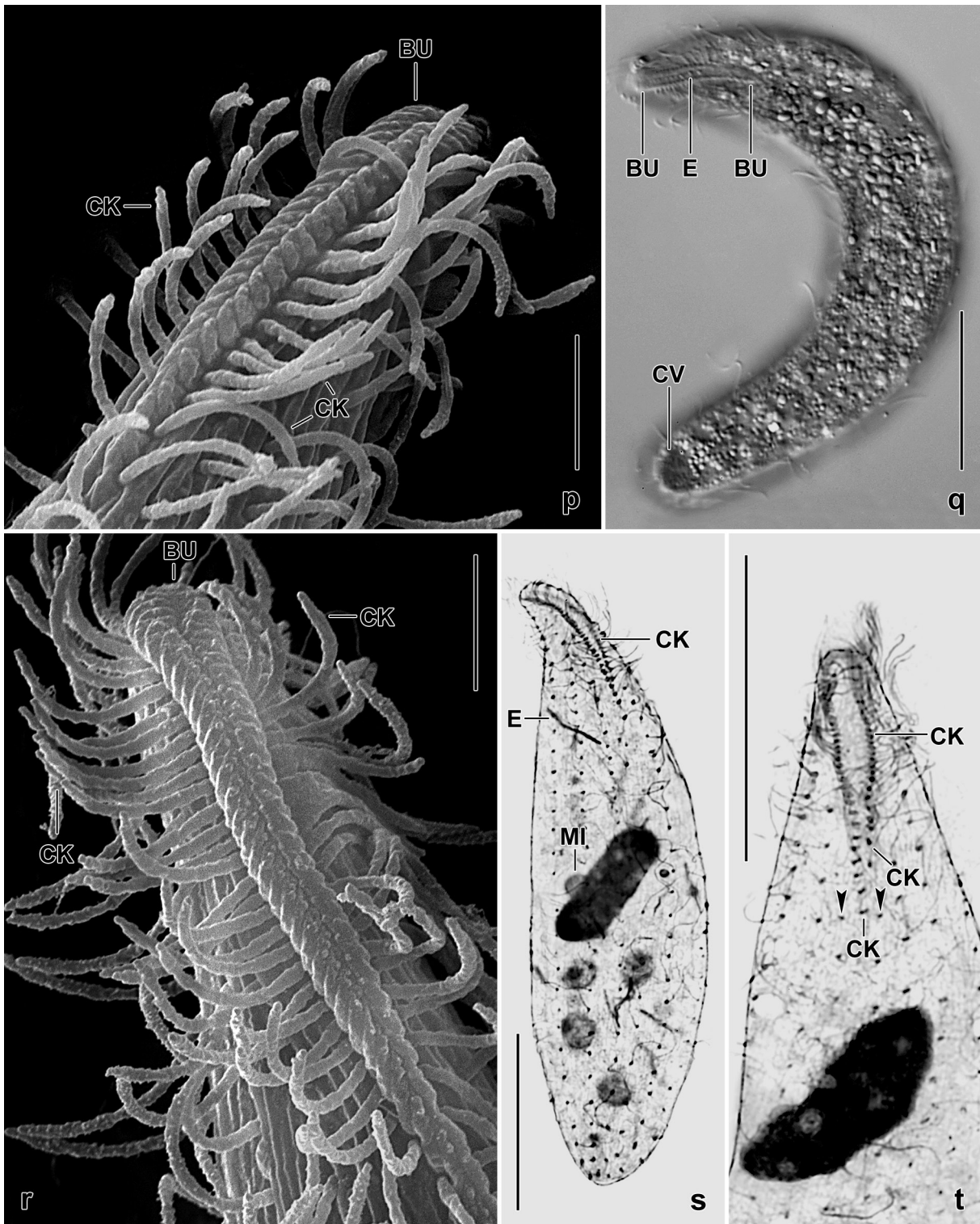


**Fig. 17p–t.** *Levispatha australiensis* in vivo (q), after protargol impregnation (s, t; pressed), and in the SEM (p, r). These figures show the oral bulge. Arrowheads (t) mark the beginning of the first ciliary row right and left of the circumoral kinety. BU – oral bulge, CK – circumoral kinety, CV – contractile vacuole, E – developing extrusome, MI – micronucleus. Scale bars 4  $\mu\text{m}$  (p, r), 20  $\mu\text{m}$  (q), and 30  $\mu\text{m}$  (s, t).

differing markedly in shape and length:width ratio; basically narrowly spatulate to cylindrical, ends slightly narrowed, flattened only in oral region; variability coefficients ordinary for body length (CV  $\sim$ 15%) while high (CV  $\sim$ 25–30%) for body width (Fig. 16a, b, j, k, 17a–j, n, u; Table 6). Theronts very slender with a length:width ratio up to 12:1; trophonts with more or less convex ventral and

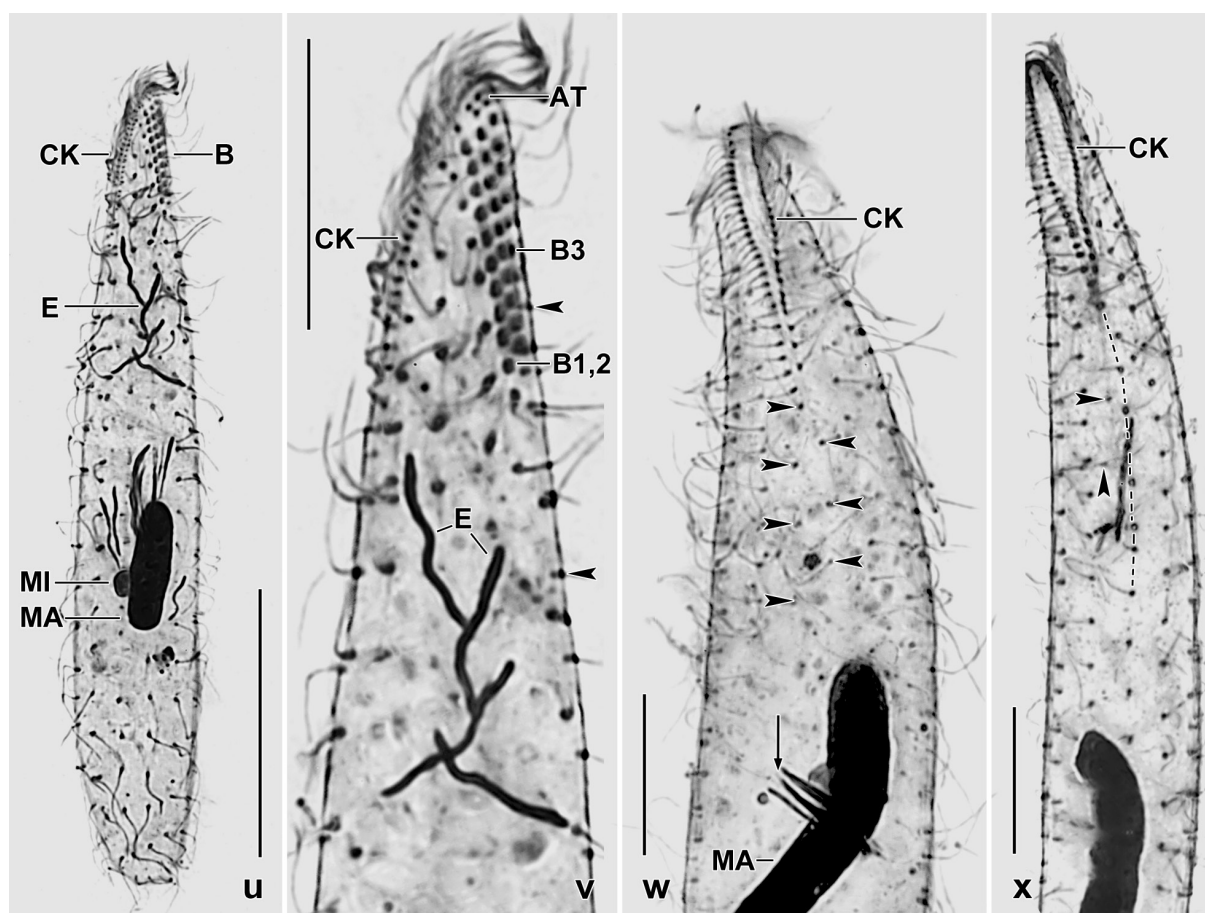


**Fig. 17u–x.** *Levispatha australiensis*, infraciliature after protargol impregnation. **u, v:** Overview and detail of dorsal brush, showing body shape, nuclear apparatus, developing extrusomes, and the anterior tail of the dorsal brush rows. The arrowheads mark some of the monokinetidal bristles of the posterior tail of brush row 3. **w, x:** Ventral views of anterior body half. The circumoral kinety is more or less clavate in the protargol preparations. However, this is very likely an artifact because it is very elongate cuneate in the scanning electron microscope (Fig. 17p, r). The arrow in (w) marks a small extrusome bundle; the arrowheads denote kineties posterior of the circumoral kinety. The dashed line in (x) shows a kinety associated with the right branch of the circumoral kinety. AT – anterior tail of dorsal brush rows, B – dorsal brush, B1–3 – dorsal brush rows, CK – circumoral kinety, E – developing extrusomes, MA – macronucleus, MI – micronucleus. Scale bars 10  $\mu\text{m}$  (v–x) and 25  $\mu\text{m}$  (u).

straight to slightly convex dorsal side, length:width ratio up to 3:1 (Fig. 16a, j, k, 17a–j, k, n, q, u; Table 6). Nuclear apparatus posterior of mid-body on average, composed of a single macronucleus and micronucleus (Fig. 16a, b, j, k, 17d, k–m, s–w, 18a; Table 6). Macronucleus in most specimens oblong or slightly reniform, rarely horseshoe-shaped; nucleoli numerous and minute, i. e., up to 2  $\mu\text{m}$  across. Micronucleus attached to mid of macronucleus, globular to broadly ellipsoidal. Contractile vacuole in posterior end of body, two excretory pores seen in one specimen (Fig. 16a, j, k, 17a, h, l, q). Extrusomes, very likely toxicysts, in curious pattern seen in three specimens: attached to right half of oral bulge but absent from dorsal bulge region (Fig. 16a–d, 17q). Mature extrusomes in vivo slightly curved rods with rounded ends, about  $8.0 \times 0.3 \mu\text{m}$  in size (Fig. 16c); do not impregnate with the method used; various deeply impregnated developmental stages scattered through cytoplasm, some in small bundles, about  $8 \times 1 \mu\text{m}$  in size (Fig. 16e, 17s, v, w, 18a, c). Cortex very flexible, distinct, about eight rows of granules between two ciliary rows each; individual granules about 0.3  $\mu\text{m}$  across, rather pale and thus inconspicuous (Fig. 16g, 17l, o). Cytoplasm colourless, with three prominent inclusions (Fig. 16a, 17k–m, q): (i) many cube-shaped crystals, some forming short arrays, scattered through body and highly refractive under interference contrast, 3–4  $\mu\text{m}$  in

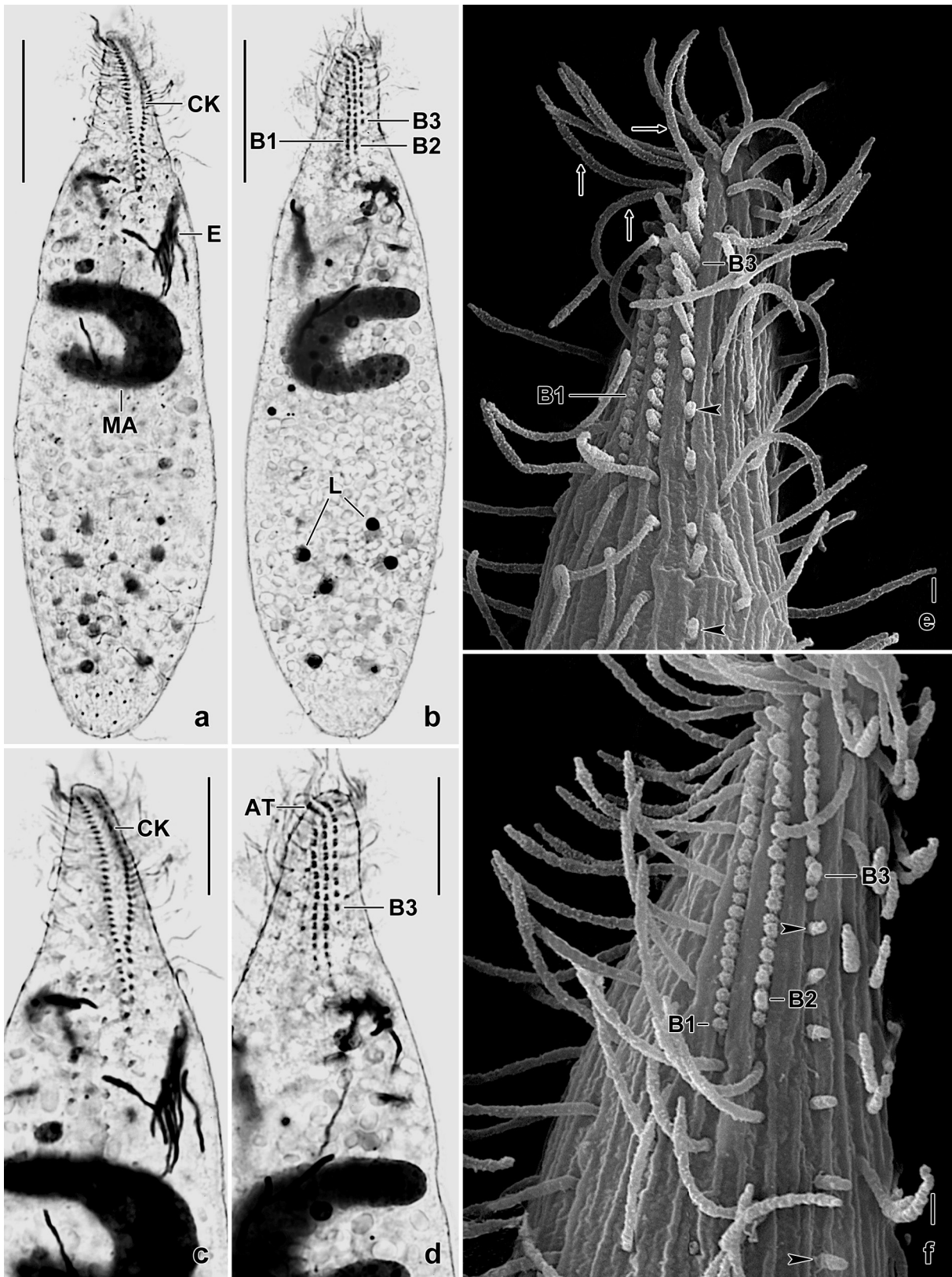


**Fig. 18a–f.** *Levispatha australiensis* after protargol impregnation (a–d) and in the scanning electron microscope (e, f). a–d: Ventral and dorsal overview and details in anterior body region of a single specimen. The circumoral kinety is slightly inflated and the short dorsal brush consists of three rows: row 1 and 2 have the same length, row 3 is shortened by about 40%. Note the horseshoe-shaped macronucleus. e, f: Compared to body length, the dorsal brush and its bristles are very short. The arrowheads mark the monokinetidal bristle tail of brush row 3. The arrows denote cilia of the anterior tail of the dorsal brush rows. AT – anterior tail of dorsal brush rows, B1–3 – dorsal brush rows, CK – circumoral kinety, E – developing extrusomes, L – lipid droplets, MA – macronucleus. Scale bars 1  $\mu\text{m}$  (e, f), 10  $\mu\text{m}$  (c, d), and 20  $\mu\text{m}$  (a, b).

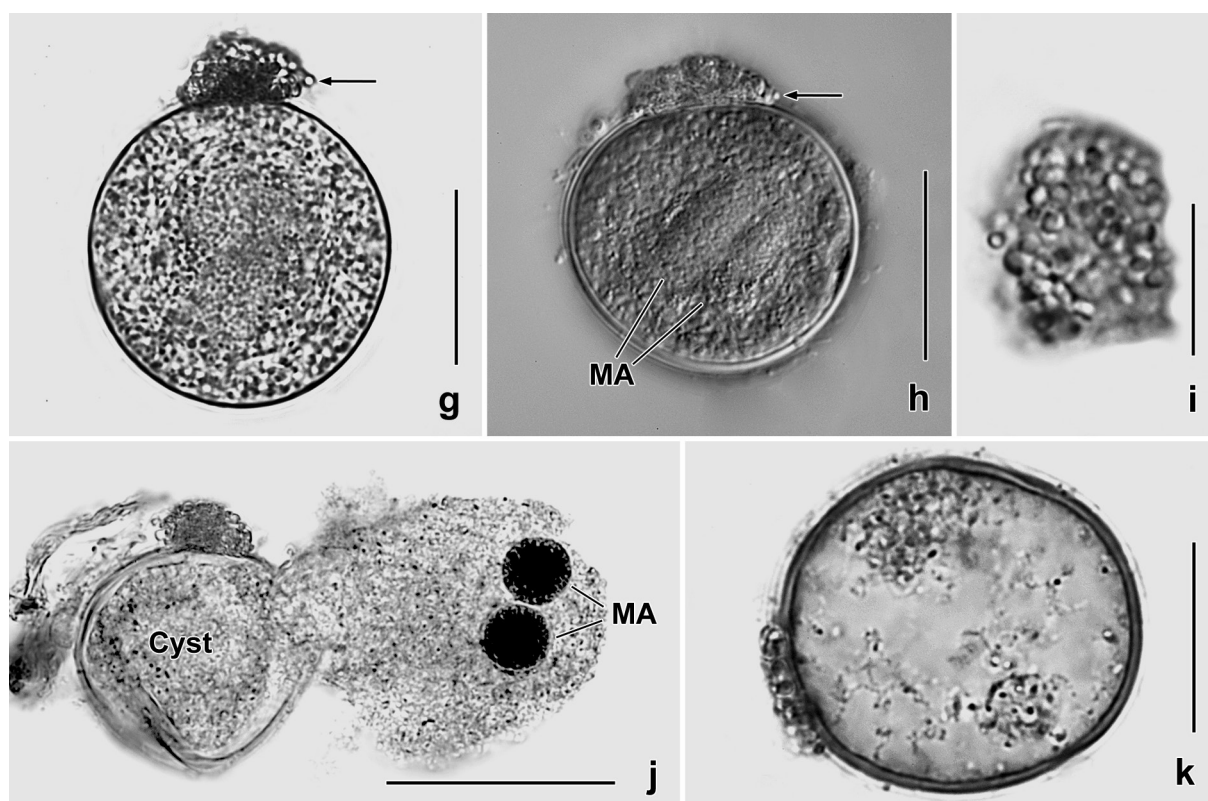


**Fig. 18g–k.** *Levispatha australiensis*, resting cysts from life (g–i) and after methyl green-pyronin staining (j, k). **g–i:** The cyst, which has an average diameter of 35  $\mu\text{m}$  has a thin, smooth wall. Usually, there is a heap of slime and granules (i), which highly resemble those in the cytoplasm, attached to the wall (arrows). **j:** Many of the cysts are from post-conjugants because they have two globular macronuclear nodules. **k:** The cyst wall is about 1  $\mu\text{m}$  thick and consists of two deeply staining, membranous layers. MA – macronuclear nodules. Scale bars 10  $\mu\text{m}$  (i), 20  $\mu\text{m}$  (g, h, k), and 30  $\mu\text{m}$  (j).

size; (ii) innumerable moderately refractive granules 2.0–3.0  $\times$  1.0–1.5  $\mu\text{m}$  in size making cells dark at low magnification; (iii) in trophonts many lipid droplets some impregnating with protargol (Fig. 18b). Feeds on heterotrophic euglenids, viz., *Peranema* sp. and *Cyclidiopsis* sp. Movement without peculiarities.

Cilia about 8  $\mu\text{m}$  long in vivo and in protargol preparations, on average 31 cilia in a lateral row; arranged in an average of 13 equidistantly and ordinarily spaced rows in typical *Arcuospathidium* pattern, i. e., do not touch the circumoral kinety and their length increases gradually from ventral to dorsal end of oral bulge (Fig. 16a, b, e, f, 17i, s, u, v, 18c; Table 6). Dorsal brush three-rowed, occupies only 15% of body length, heterostichad because row 3 shorter than rows 1 and 2 by an average of 32%, isomorphic, dikinetids ordinarily spaced (1.1–1.3  $\mu\text{m}$ ); rows 1 and 2 of same length each composed of an average of 12 dikinetids, row 3 composed of about seven dikinetids, continues to second quarter of body with an average of eight monokinetidal bristles (Fig. 16a, f, 17j, u, v, 18b, d–f; Table 6). Brush bristles oblong, distal end knob-like inflated when disturbed. Anterior bristles of row 1 dikinetids about 2  $\mu\text{m}$  long, posterior bristles of same length as anterior bristles in upper half of row gradually decreasing to about 1  $\mu\text{m}$  in posterior half. Bristles of rows 2 and 3 very similar, i. e., anterior bristles of dikinetids 2.5–3.0  $\mu\text{m}$  long in upper half of rows gradually decreasing to about 1  $\mu\text{m}$  in posterior half; posterior bristles of dikinetids about 1  $\mu\text{m}$  long in anterior half of rows gradually decreasing to about 0.5  $\mu\text{m}$  in posterior half (Fig. 16a, f, i, 17j, 18e, f). Anterior tail of brush row 1 composed of one or two ordinary cilia; tail of row 2 composed of an average of two cilia; tail of row 3 composed of 1–3 cilia (Fig. 16a, f, 17u, v, 18d, e; Table 6).



a usual basket rarely impregnating with protargol. Rarely, specimens with two mouths, one after the other, the anterior more or less disturbed.

**Resting cyst:** *Levispatha australiensis* makes type III cysts (Foissner & Xu 2007), usually with a heap of extruded slime and bright cytoplasmic granules 0.5–2.0 µm across; rarely, the granules are distributed around the cyst (Fig. 16h, 18g–k). Mature cysts spherical, on average 35 µm across, colourless; wall about 1 µm thick and composed of two membranous layers staining red with methylgreen-pyronin; without slime cover. Macronucleus oblong or, in encysted postconjugants, in two globular nodules (Fig. 16h, 18g–k; Table 6).

**Division:** The protargol slides contain several dividers. Here, only a very early stage with greatly inflated micronucleus is shown (Fig. 16l), just as described in *Cultellothrix coemeterii* (Kahl, 1943) (for revision, see Foissner & Xu 2007, p. 275).

**Conjugation:** The protargol slides contain some conjugating specimens and many post-dividers with two globular macronuclear nodules. All were excluded from the morphometric analysis. The cells unite with the oral bulge in the ventral-to-dorsal mode (Foissner & Xu 2007).

**Phylogeny:** The small subunit rDNA gene shows that *Arcuospathidium* is polyphyletic, appearing in several clades of the haptorian phylogenetic tree (Vďačný et al. 2014; Fig. 19). *Levispatha australiensis* forms a distinct clade and is sister to a rather large clade containing *Arcuospathidium cultriforme* and *A. namibiense* Foissner et al., 2002. However, this may change because the statistical support is low.

**Occurrence and ecology:** As yet found only at type locality, i. e., in a non-flooded Petri dish culture with litter and soil from the floodplain of the Murray River. Thus, *Levispatha australiensis* might be a limnetic species. It grew well for two months so that it could be studied in detail.

**Remarks:** There are several spathidids which resemble *Levispatha australiensis* but none has the same combination of characters (for a review, see Foissner & Xu 2007). For instance, *Arcuospathidium cooperi* Foissner, 1996b, which has a similar shape, size, and cytoplasmic inclusions lacks extrusomes (for a review, see Foissner & Xu 2007, p. 157). *Armatospathula periarmata* Foissner & Xu, 2007 has a similar size and shape but has somatic extrusomes (Foissner & Xu 2007, p. 308). *Edaphospathula gracilis* Foissner & Xu, 2007 is also slender but possesses lenticular extrusomes and a different circumoral ciliary pattern (Foissner & Xu 2007, p. 88).

*Levispatha australiensis* resembles *Cultellothrix coemeterii* in that the micronucleus becomes enormously inflated during early division (Fig. 16l). Indeed, *C. coemeterii* is sister to *L. australiensis* in the phylogenetic tree (Fig. 19). A further peculiarity is the ornamentation of the oral bulge. Usually, this is an arrowhead-like pattern with thin arms (Foissner & Xu 2007) while *L. australiensis* and *Arcuospathidium cooperi* have thick arms.

### ***Pseudofuscheria* nov. gen.**

**Diagnosis:** Fuscheriidae Foissner, Agatha & Berger, 2002 with oral nematodesmal bundles originating from circumoral dikinetids and oralized somatic monokinetids. Extrusomes nail-shaped. Polymerizations in right side kineties present (vs. absent in *Fuscheria* Foissner, 1983a).

**Type species:** *Pseudofuscheria magna* nov. spec.

**Etymology:** Composite of the Greek comparative *pseudo* (resembling but not equalling) and the genus-group name *Fuscheria*, indicating a similarity to this genus. Feminine gender.

**Species assignable** (Table 7): *Pseudofuscheria magna* nov. spec.; *Pseudofuscheria terricola* (Berger, Foissner & Adam, 1983) nov. comb. (original combination: *Fuscheria terricola* Berger, Foissner & Adam, 1983).

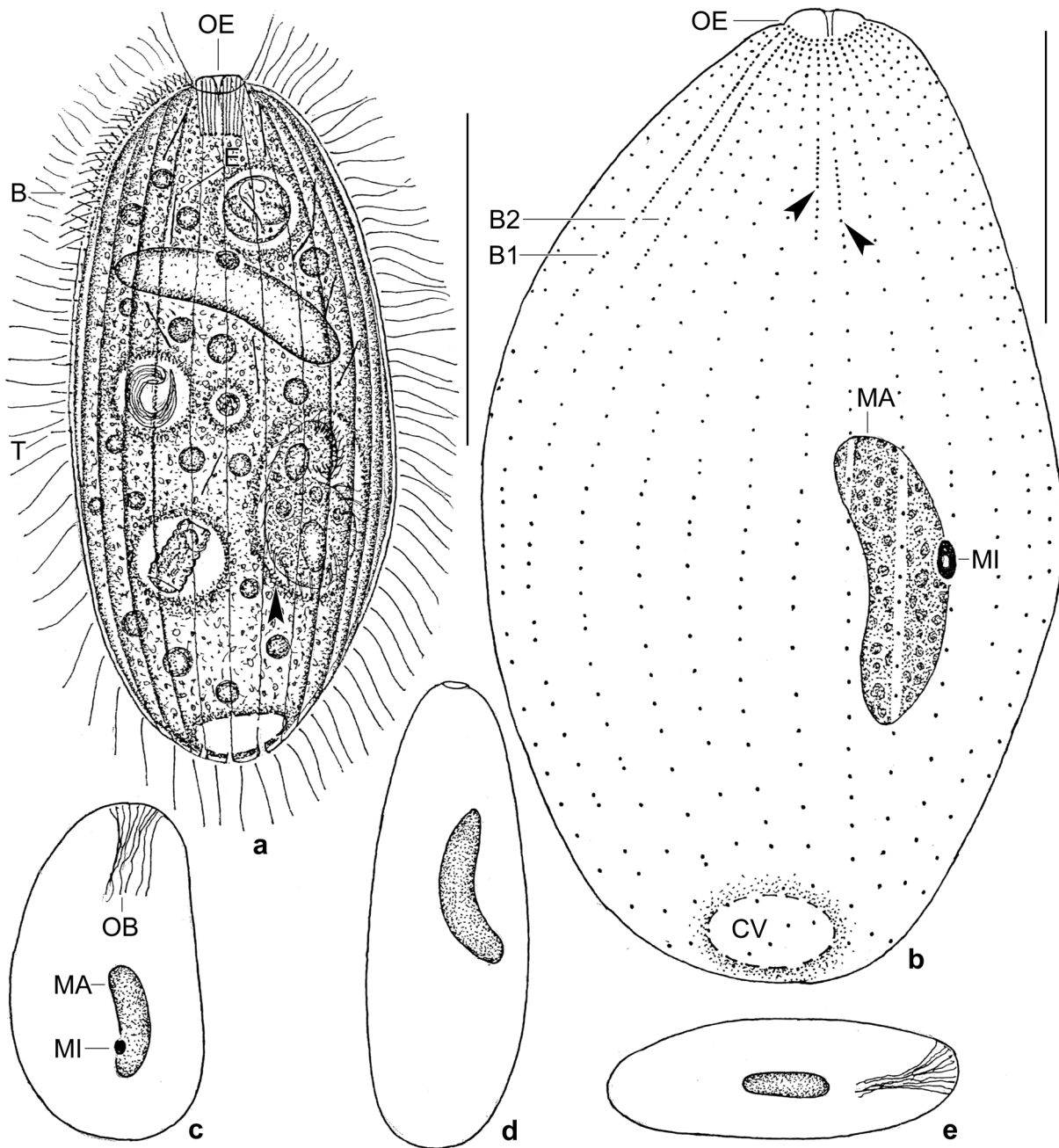


**Fig. 20a–e.** *Pseudofuscheria magna* from life (a) and after protargol impregnation (b–e). **a:** Right lateral view of a representative specimen, length 140 µm. Note the nail-shaped extrusomes (main character of genus) in the oral basket; the dorsal brush; the comparatively short, oblong macronucleus; many lipid droplets and some small food vacuoles; some large food vacuoles containing a hypotrich ciliate (*Gonostomum* sp.); a zooid and a swarmer of *Vorticella* sp.; and a euglenid (*Peranema* sp.). **b:** Right lateral view of holotype specimen (length 100 µm), showing the short, oblong macronucleus and the infraciliature including the widely spaced ciliary rows two of which have a polymerized spot of monokinetids (arrowheads). **c–e:** Variability of body and macronucleus shape. B1, 2 – dorsal brush rows, CV – contractile vacuole, E – extrusomes, MA – macronucleus, MI – micronucleus, OB – oral basket, OE – oral bulge, T – monokinetal tail of dorsal brush row 2. Scale bars 30 µm (b) and 50 µm (a).

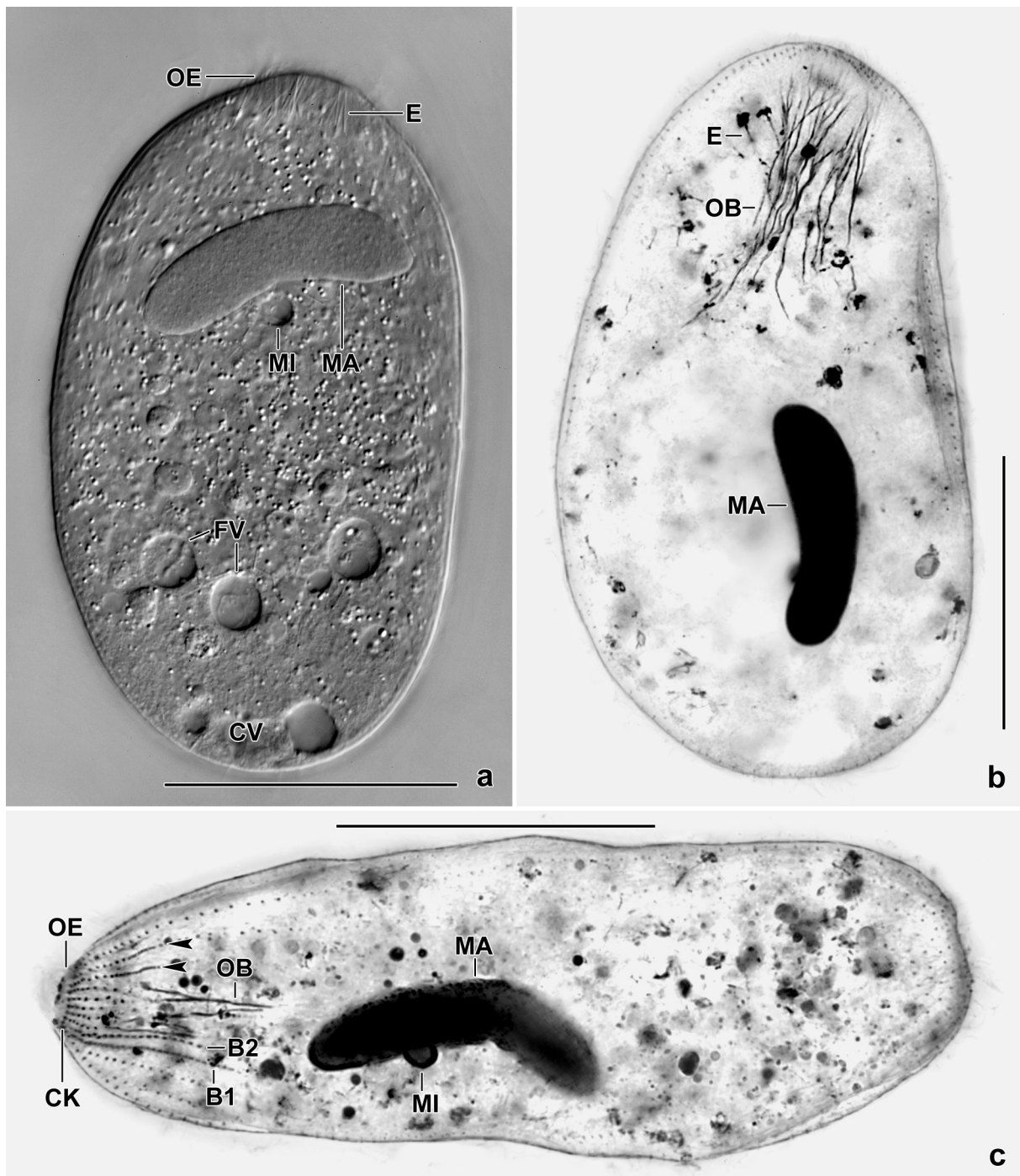
**Fig. 21a–c.** *Pseudofuscheria magna* from life (a) and after protargol impregnation (b, c). **a:** A specimen slightly flattened → by the coverslip to show details, such as the nuclear apparatus; the very low oral bulge; the basket extrusomes, and small food vacuoles containing heterotrophic flagellates. **b, c:** One of the fattest and most slender specimens contained in eight protargol slides, showing the great variability in body shape. The arrowheads in (c) mark two lateral ciliary rows with a spot of polymerized monokinetids; there are five ordinary ciliary rows between the dorsal brush and the polymerization. The oblong, slightly curved macronucleus is comparatively short. B1,2 – dorsal brush rows, CK – circumoral kinety, CV – contractile vacuole, E – mature and developing extrusomes, FV – food vacuoles, MA – macronucleus, MI – micronucleus, OB – oral basket, OE – oral bulge. Scale bars 50 µm.

**Remarks:** Possibly, this is a weak genus, differing from *Fuscheria* by the presence of polymerizations in some right lateral ciliary rows (Fig. 20b, 21c, s). The polymerizations are ciliated but their genesis and function is not known. However, there is some relation to the lifestyle: *Fuscheria* species prefer limnetic habitats while *Pseudofuscheria* species prefer terrestrial habitats.

*Pseudofuscheria magna* nov. spec.

(Fig. 20a–e, 21a–s; Tables 7, 8 on p. 313, 314)

**Diagnosis:** Size in vivo about  $140 \times 60 \mu\text{m}$ ; broadly to slenderly ellipsoid. Macronucleus short compared to cell size, i.e., about  $45 \mu\text{m}$  in vivo, usually slightly curved. On average 28 ordinarily to



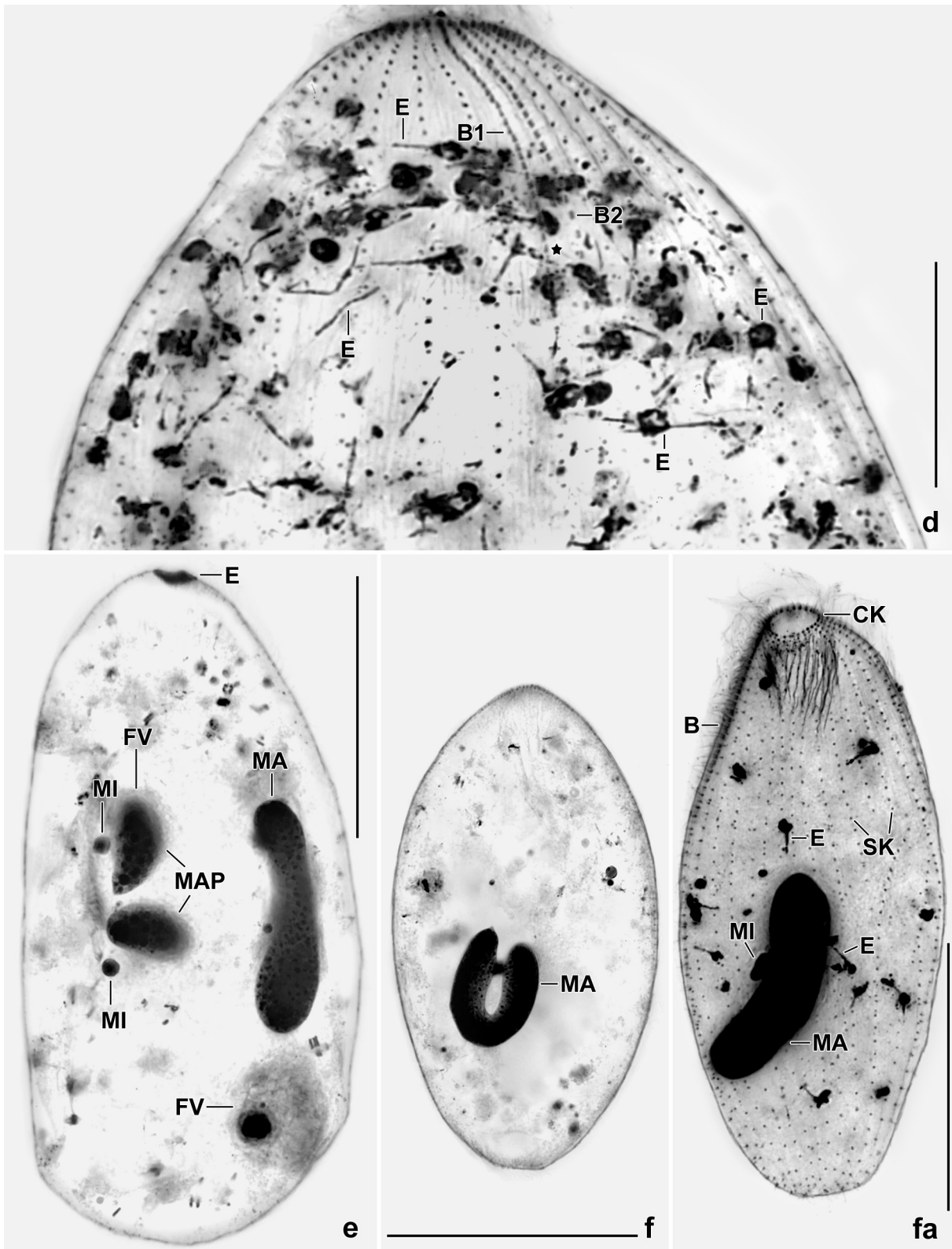


**Fig. 21d–fa.** *Pseudofuscheria magna* after protargol impregnation. **d:** Dorsal view, showing the two-rowed dorsal brush (for details, see Fig. 21p–s) and many developing extrusomes with the posterior end showing a roughly globular, fluffy structure 2–4  $\mu\text{m}$  in size, very likely the developing head; other extrusomes are up to 10  $\mu\text{m}$  long rods without inflated end. The asterisk marks the proximal end of brush row 1. **e:** A specimen with two food vacuoles of which one is large and contains *Gonostomum* sp., whose nuclear apparatus is still recognizable. **f:** A specimen with horseshoe-shaped macronucleus. **fa:** Right side overview of a specimen without polymerizations in the ciliary rows. Note the flattened micronucleus. B1, 2 – dorsal brush rows, CK – circumoral kinety, E – mature and developing extrusomes, FV – food vacuoles, MA – macronucleus, MAP – macronuclear nodules of prey, MI – micronucleus, OB – oral basket, SK – somatic kineties. Scale bars 25  $\mu\text{m}$  (d) and 50  $\mu\text{m}$  (e, f, fa).

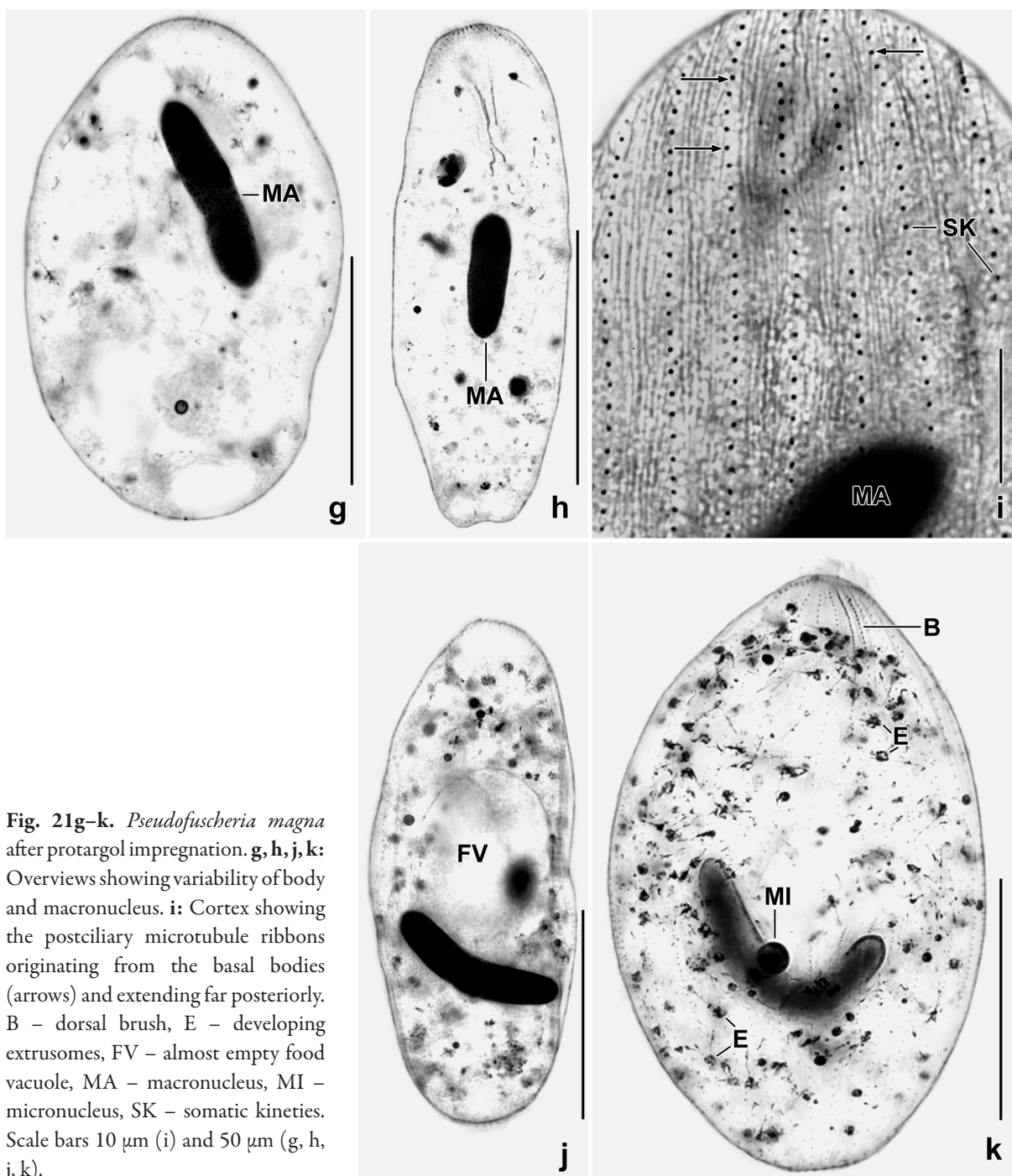


**Fig. 21g–k.** *Pseudofuscheria magna* after protargol impregnation. **g, h, j, k:** Overviews showing variability of body and macronucleus. **i:** Cortex showing the postciliary microtubule ribbons originating from the basal bodies (arrows) and extending far posteriorly. B – dorsal brush, E – developing extrusomes, FV – almost empty food vacuole, MA – macronucleus, MI – micronucleus, SK – somatic kineties. Scale bars 10  $\mu\text{m}$  (i) and 50  $\mu\text{m}$  (g, h, j, k).

widely spaced ciliary rows; dorsal brush isostichad, row 1 with an average of 28 dikinetids, row 2 with 23 dikinetids; five kineties between brush row 2 and first polymerized spot of monokinetids on right side. Oral bulge diameter about 10  $\mu\text{m}$ , height about 2  $\mu\text{m}$ .

**Type locality:** Soil and litter from floodplain of the Murray River near to the town of Albury, waterside of Ryans road, 37°S, 147°E.<sup>1</sup>

**Type material:** The slide containing the holotype (Fig. 20b) and three paratype slides with protargol-impregnated specimens have been deposited in the Biology Centre of the Upper Austrian Museum in Linz (LI). The holotype and other relevant specimens have been marked by black ink circles on the coverslip.<sup>2</sup> For slides, see Fig. 9a–g in Chapter 5.

<sup>1</sup> Note by H. Berger: See footnote at  $\rightarrow$  *Levispatha australiensis*.

<sup>2</sup> Note by H. Berger: These slides also contain specimens of the hypotrich  $\rightarrow$  *Conothrix australiensis*.

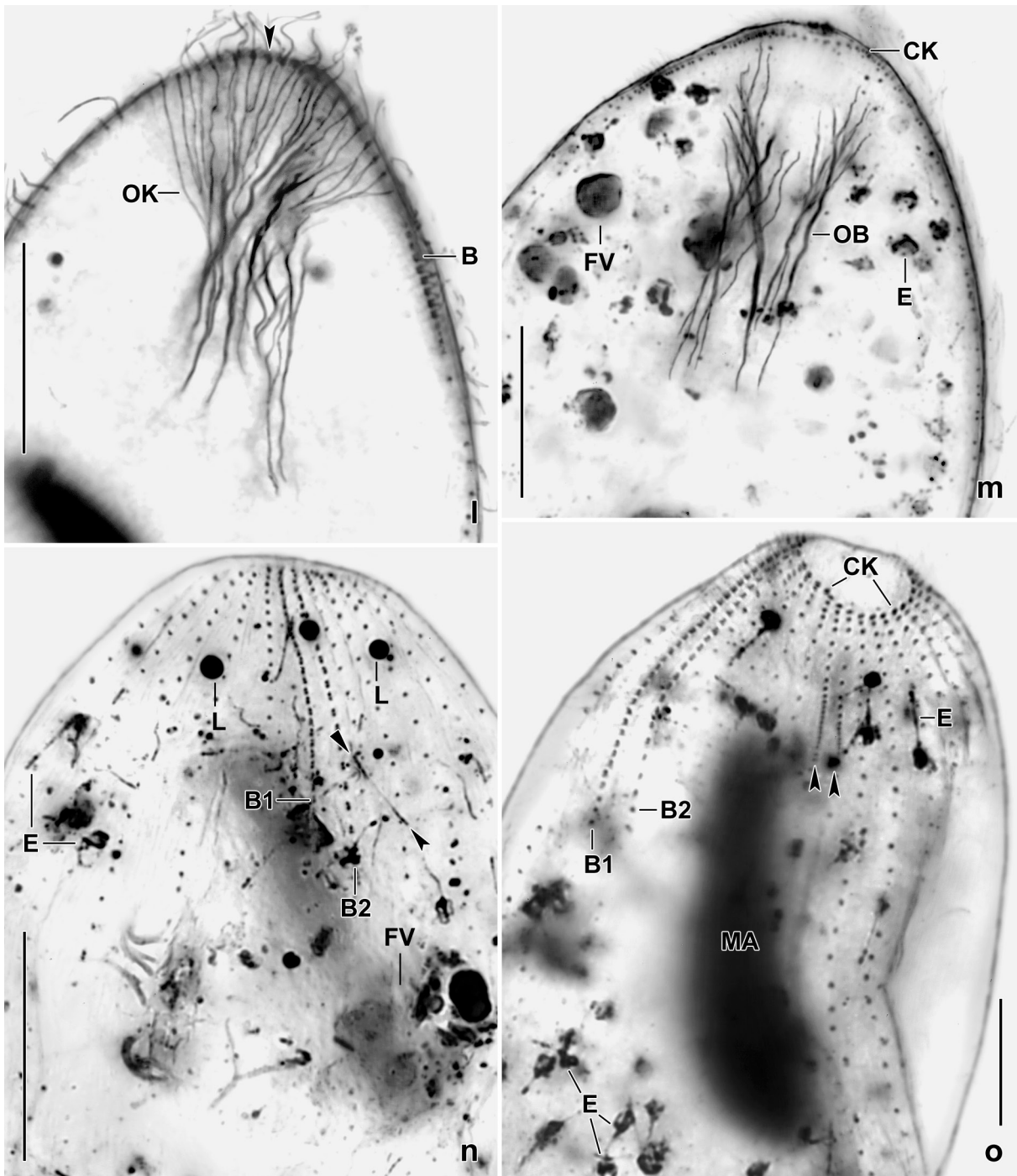


**Fig. 211–o.** *Pseudofuscheria magna* after protargol impregnation. **l, m:** At the anterior body end, the oral basket has a diameter of about 40  $\mu\text{m}$  because not only the circumoral dikinetids (arrowhead) produce basket rods but also the monokinetids in the anterior region of the ciliary rows (oralized somatic monokinetids). **n:** Dorsal view of anterior body region, showing the isostichad dorsal brush and developing extrusomes some of which are deeply impregnated at both ends (arrowhead). **o:** Dorsolateral view, showing the dorsal brush and two kineties with a spot of very narrowly spaced monokinetids (arrowheads). B1, 2 – dorsal brush rows, CK – circumoral kinety, E – developing extrusomes, FV – food vacuoles, L – lipid droplet, MA – macronucleus, OB – oral basket, OK – oral basket rods from oralized somatic monokinetids. Scale bars 10  $\mu\text{m}$  (o) and 20  $\mu\text{m}$  (l–n).

**Etymology:** The species-group name *magna* (Latin adjective) refers to the comparatively large body size.

**Description:** This species is highly variable because most features investigated have a CV > 15% (Table 8). This is common in haptorids because many features are influenced by the nutrition state:

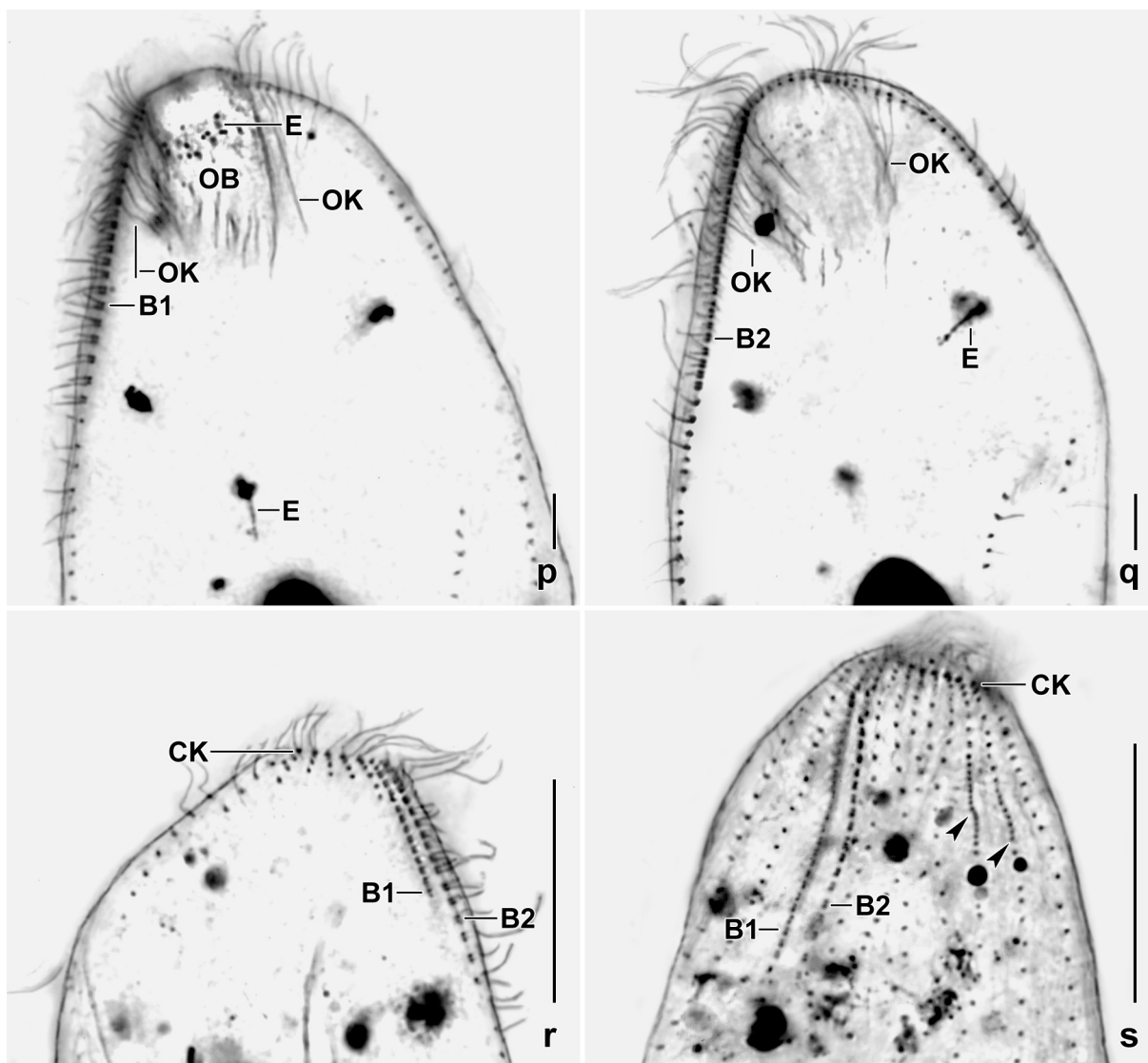


**Fig. 21p–s.** *Pseudofuscheria magna* after protargol impregnation. **p, q:** Same specimen at two focal planes to show details of the two dorsal brush rows. The posterior bristles of the dikinetids of row 1 are 4–6  $\mu\text{m}$  long, the anterior bristles are 3–4  $\mu\text{m}$ . Long postciliary microtubular ribbons originate from the anterior kinetids of the dorsal brush and the anterior monokinetids of the somatic kineties and contribute to the oral basket. **r, s:** Dorsal brush. The space between the dikinetids is larger in the posterior than the anterior half of the rows. The dikinetids of the circumoral kinety are deeper impregnated and slightly larger than the monokinetids of the ciliary rows. The arrowheads mark polymerizations in two right side kineties. B1, 2 – dorsal brush rows 1 and 2, CK – circumoral kinety, E – oral bulge and developing extrusomes. The mature extrusomes are nail-shaped, the nailhead is recognizable (p), OB – oral basket, OK – oralized somatic monokinetids. Scale bars 10  $\mu\text{m}$  (p, q), 20  $\mu\text{m}$  (s) and 30  $\mu\text{m}$  (r).

the more food ingested the higher the variability. Fortunately, three important characteristics have – beside the generic features – a CV < 15%, viz., body length (12.7%), shape and size of macronucleus (small compared to body size and congeners), and the number of ciliary rows (6.8%).

Size in protargol preparations on average 118  $\times$  58  $\mu\text{m}$  (length:width ratio 2.1:1, Table 8) and 136  $\times$  67  $\mu\text{m}$  when 15% preparation shrinkage is added. Body shape slenderly to broadly ellipsoid (Fig. 20a, b, d, e, 21a, c, f, fa, g, h) or indistinctly ovate (Fig. 20c, 21b, e); unflattened. Macronucleus usually in anterior body half, rarely in mid-body or in posterior body half, on average 42  $\times$  10  $\mu\text{m}$  in size (Table 8), i.e., short compared to cell size and similar species from other genera; shape rather stable, usually oblong and slightly curved (71% out of 38 specimens, Fig. 20a–d, 21a–c, e, fa, j, k), rarely cylindroid (18.4%, Fig. 20e, 21g, h), horseshoe-shaped or semi-circular (10.5%,

Fig. 21f). Micronucleus attached to curved centre of macronucleus, rarely to convex side; discoid, i.e., about 5.0  $\mu\text{m}$  across and 2.5  $\mu\text{m}$  thick (Fig. 20a–c, 21a, c, fa, k; Table 8). Two micronuclei in two out of 38 specimens. Contractile vacuole in posterior body end, several excretory pores (Fig. 20a, b, 21a). Cortex very flexible, about 1.5  $\mu\text{m}$  thick, contains countless ellipsoid granules and a conspicuous fibre system produced by the postciliary microtubule ribbons (Fig. 21i). Extrusomes nail-shaped, about 7  $\mu\text{m}$  long, concentrated in oral basket, anterior and posterior end slightly to deeply impregnated with protargol (Fig. 20a, 21a, e, p). Developing extrusomes about 7  $\mu\text{m}$  long in protargol preparations, one end with a 2–3  $\mu\text{m}$ -sized, fluffy, drumstick-shaped structure, very likely the developing nail head of the mature organelle (Fig. 20a, 21b, d, k, m, o–q; Table 8); rarely, an earlier(?) stage is recognizable, viz., about 9  $\mu\text{m}$  long rods with both ends deeper impregnated than the middle third (Fig. 21n). Cytoplasm colourless, usually studded with developing extrusomes and small to large food vacuoles when sufficient prey is available; when hungry studded with refractive granules 1–3  $\mu\text{m}$  across (Fig. 20a, 21a, e). Swims slowly, showing pronounced flexibility when moving in organic masses.

Somatic and oral infraciliature as typical for genus and haptorids in general (Vďačný & Foissner 2012). Cilia about 9  $\mu\text{m}$  long in protargol preparations, arranged in an average of 28 ordinarily to widely ( $\sim 5 \mu\text{m}$ ) spaced rows beginning with a circumoral dikinetid and 10–15 oralized somatic monokinetids having about 40  $\mu\text{m}$  long rods contributing to the oral basket; more densely spaced in perioral area (Fig. 20a, b, 21o, s; Table 8). Dorsal brush isostichad, composed of two short rows of dikinetids continuing as ordinary ciliary rows to posterior end of cell. Row 1 composed of an average of 28 dikinetids with anterior bristle approximately 2.8  $\mu\text{m}$  long and posterior about 2.4  $\mu\text{m}$ . Row 2 composed of an average of 23 dikinetids with anterior bristle about 1.8  $\mu\text{m}$  long and posterior approximately 3.6  $\mu\text{m}$ ; has a monokinetal tail extending to about mid-body with circa 3  $\mu\text{m}$  long bristles. On average five ciliary rows between dorsal brush row 2 and polymerization 1 comprising about 13 narrowly spaced monokinetids while polymerization 2 consists of only nine monokinetids (Fig. 20a, b, 21c, o, s; Table 8); polymerization absent in two out of 38 specimens investigated (Fig. 21fa).

Oral bulge very inconspicuous because only about 10  $\mu\text{m}$  across and 2  $\mu\text{m}$  high but can open widely because large prey, e.g., the hypotrich *Gonostomum* sp., is ingested alive (Fig. 20a, b, d, 21a, e, o, p; Table 8). Circumoral kinety composed of distinct dikinetids from anterior end of each ciliary row, their number thus equalizing ciliary rows; each dikinetid produces an about 40  $\mu\text{m}$  long rod contributing to oral basket (Fig. 20c, d, 21c, l, m, p, q; Table 8).

**Occurrence and ecology:** As yet found only at type locality, i.e., soil and litter from a floodplain in Australia. Shape and size indicate that it is a limnetic litter species (Foissner 1987b).

**Remarks:** *Pseudofuscheria magna* differs from *P. terricola* by the large body size, the shape of the macronucleus, and the much higher number of brush dikinetids and ciliary rows (Table 7).

Among *Fuscheria*, which has also nail-shaped extrusomes, only *Fuscheria nodosa salisburgensis* Foissner & Gabilondo in Gabilondo & Foissner, 2009 has as similar body size and number of ciliary rows while the number of brush dikinetids and the shape of the macronucleus are distinctly different (Table 7). The family Pleuroplitidae should be mentioned because *Pleuroplitoides smithi* Foissner, 1996a has a great overall similarity to *Pseudofuscheria magna*, differing in the location of the extrusomes, i.e., apical in the oral basket (fuscheriids) vs. far subapical between two ciliary rows (pleuroplitids).

#### *Apobryophyllum pinetum* nov. spec.

(Fig. 22a–p, 23a–u, 24a–f; Tables 9, 10 on p. 315)

**Diagnosis:** Size in vivo about 135  $\times$  45  $\mu\text{m}$ . Elongate lanceolate with an average length:width ratio of 3:1. Macronucleus moniliform with about 19 ellipsoid nodules often forming a globular cluster

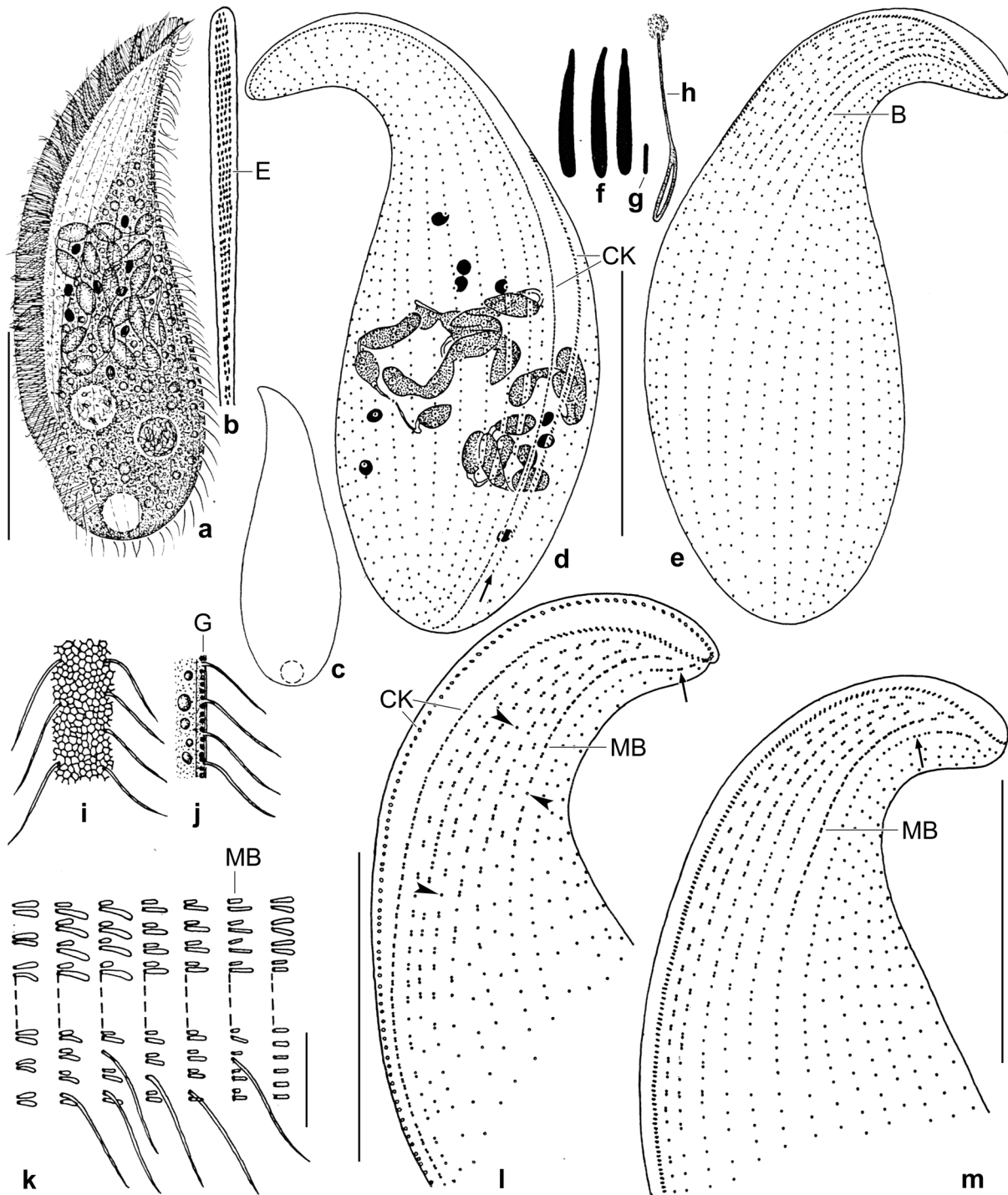


**Fig. 22a-m.** *Apobryophyllum pinetum* from life (a-c, f-k) and after protargol impregnation (d, e, l, m). **a:** Left side view of a representative specimen, length 140  $\mu\text{m}$ . Note the moniliform macronucleus and the compact micronuclei. **b:** Oral bulge with extrusome rows. **c:** Shape variant. **d, e:** Right and left side view of holotype specimen. Arrow marks posterior end of left branch of circumoral kinety. **f, h:** Resting (8  $\mu\text{m}$ ) and exploded ( $\sim 30 \mu\text{m}$ ) type I extrusomes. **g:** A type II extrusome, length 2  $\mu\text{m}$ . **i, j:** Surface view and optical section of cortex. **k:** Scheme of dorsal brush. **l, m:** Left side view, showing dorsal brush. The arrows mark the very short last row of dikinetids; the arrowheads denote monokinetids with ordinary cilia in between dikinetids with 1-3  $\mu\text{m}$  long bristles. B - dorsal brush, CK - circumoral kinety, E - type I extrusomes, G - cortical granules, MB - main brush row. Scale bars 50  $\mu\text{m}$  (a, d, e), 40  $\mu\text{m}$  (l, m), and 5  $\mu\text{m}$  (k).

in mid-body; on average nine ellipsoid micronuclei. Type I extrusomes asymmetrical, that is, slightly curved rods with conical anterior region, in vivo 7-10  $\mu\text{m}$  long; type II rod-shaped, fine, about 2  $\mu\text{m}$  long. On average 28 somatic ciliary rows, eight anteriorly modified to a heteromorphic, complex

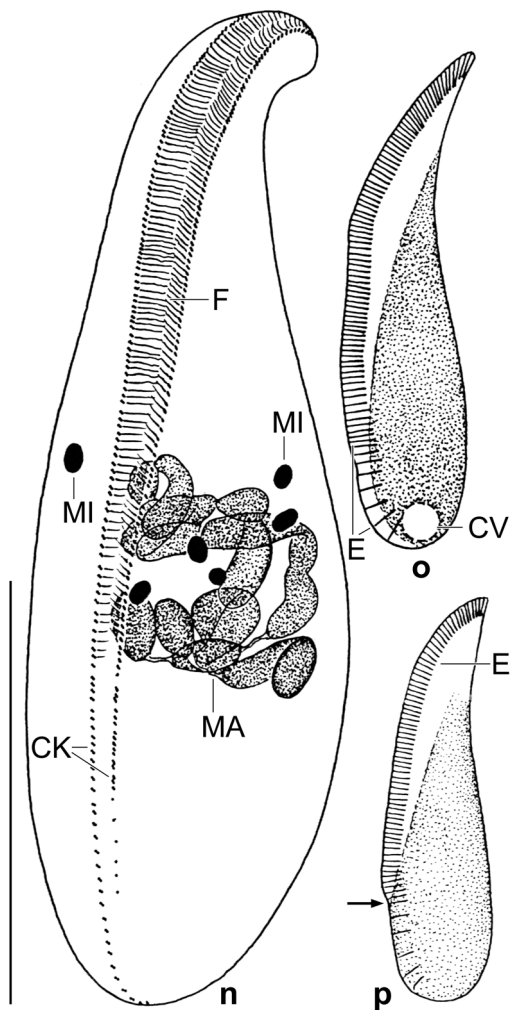


**Fig. 22n–p.** *Apobryophyllum pinetum* from life (o, p) and after protargol impregnation (n). **n:** Ventral view, showing the moniliform macronucleus and the gradually narrowing oral bulge and circumoral kinety the left branch of which ends subterminally. **o, p:** Left side views, showing body shape, the convex portion of the surface, and the end of the oral bulge where the outline has a minute break (arrow) and the extrusomes are very sparse. CK – circumoral kinety, CV – contractile vacuole, E – extrusomes, F – fibres originating from circumoral dikinetids, MA – macronucleus, MI – micronuclei. Scale bar 50  $\mu\text{m}$ .

dorsal brush. Oral bulge ends subterminally.

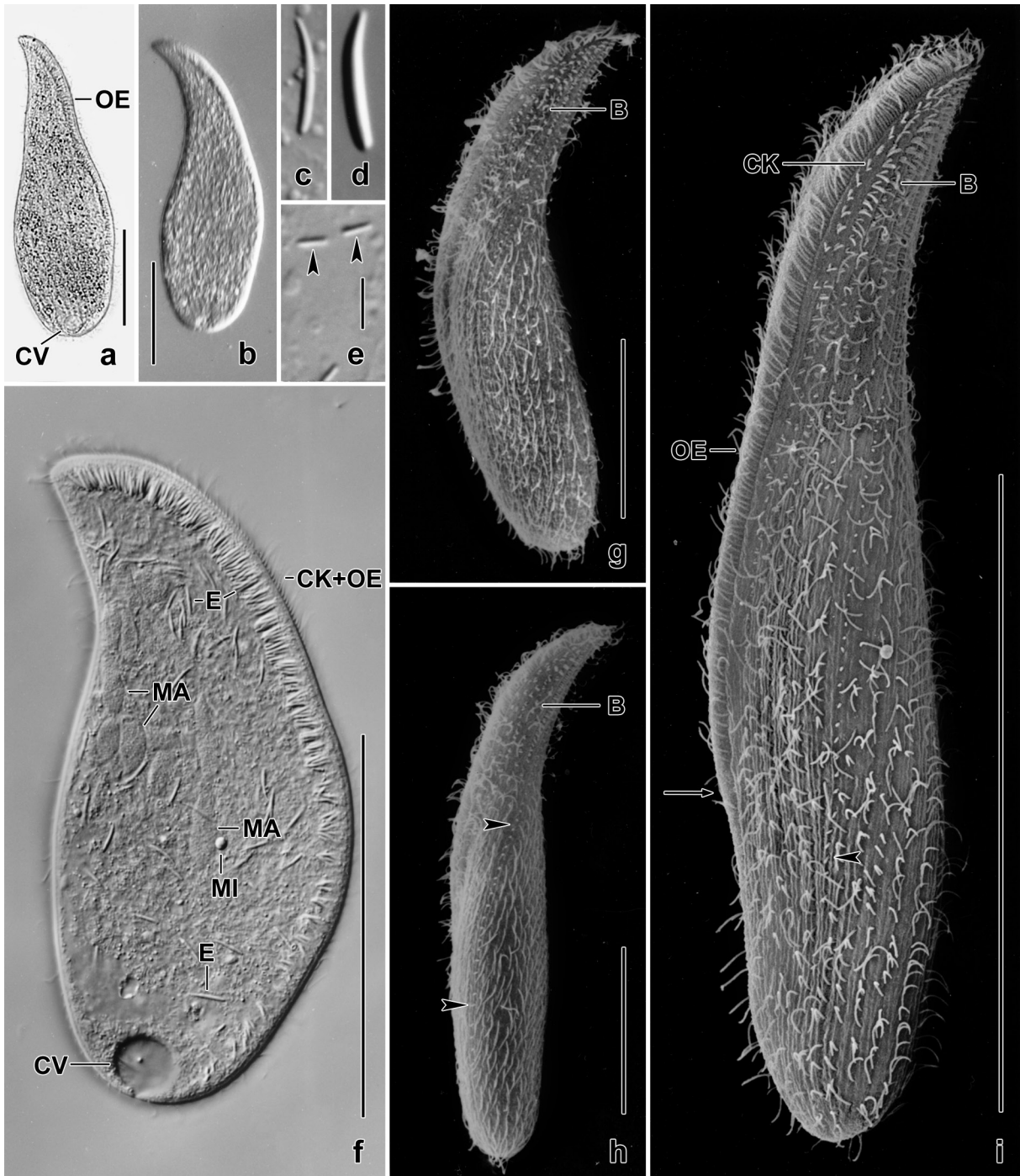
**Type locality:** Leaf litter, surface soil (0–10 cm), and some moss from a primeval (undisturbed for at least 100 years) spruce-fir-beech forest in Styria, Austria, 47°46'N, 15°07'E.

**Type material:** Unfortunately, I lost the slide with the holotype specimen (Fig. 22d, e); possibly, I put it in the wrong box.<sup>1</sup> Thus, I deposited three slides with protargol-impregnated specimens from the type series in the Biology Centre of the Upper Austrian Museum in Linz (LI). Some well-impregnated specimens have been marked by black ink circles on the coverslip. For slides, see Fig. 10a–c in Chapter 5.

**Etymology:** *Pinetum* is the Latin noun for a spruce forest where the species was discovered.

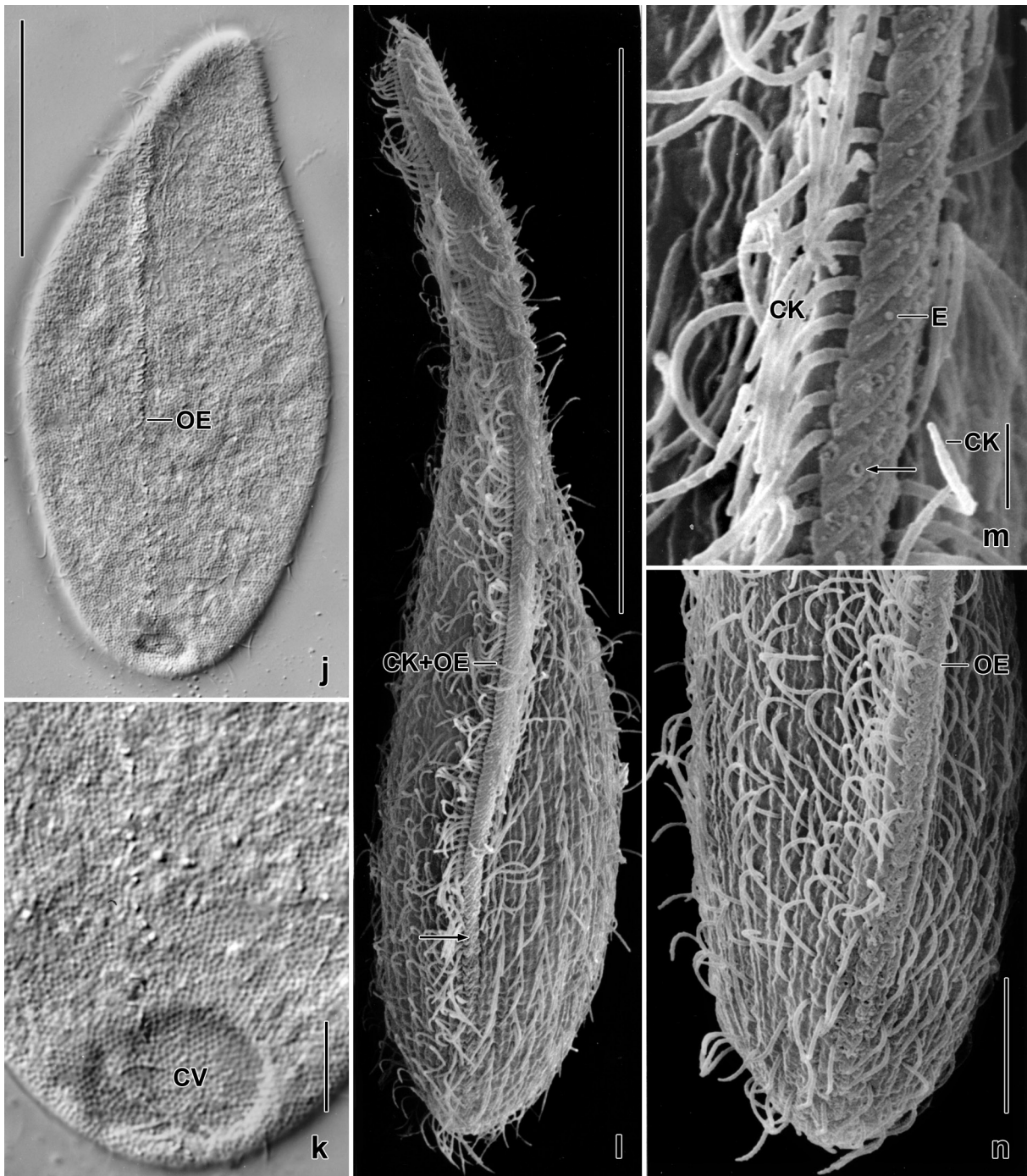
**Description:** Most features investigated have a coefficient of variation >15%, suggesting high variability of the species. Size in vivo 144 × 50  $\mu\text{m}$  (n = 5) on average; in protargol preparations 116.9 × 39.5  $\mu\text{m}$  (n = 19); when 15% preparation shrinkage is added, in vivo values are obtained matching well those provided above: 101–196 × 35–61  $\mu\text{m}$ , on average 134 × 45  $\mu\text{m}$  (Table 9). Body shape rather variable, basically slenderly to broadly lanceolate with length:width ratios of 2.3–4.5:1, on average 3.1:1 (Fig. 22a, c, d, o, p, 23a, b, g–i; Table 9). Ventral margin moderately to distinctly convex, dorsal margin sigmoid due to a slight to distinct concavity between first and second third of body. Both sides moderately convex (Fig. 23l, 24a); anterior third and ventral margin leaf-like flattened and thus hyaline; posterior body region frequently slightly narrowed due to the thinning oral bulge (Fig. 22a, o, p, 23i, l). Nuclear apparatus in middle third of body (Fig. 22a, d, n, 23f, 24c–f; Table 9). Macronucleus moniliform with an average of 19 nodules producing a discoid or globular irregular cluster; nodules 11 × 5  $\mu\text{m}$  on average; in some cells composed of pieces with 2–4 nodules. Nine broadly ellipsoid micronuclei on average, scattered in and around macronuclear cluster. Contractile vacuole in midline of posterior body end (Fig. 22a, o, 23a, f, j, k).

<sup>1</sup> Note by H. Berger: For nominal species-group taxa established after 1999, name-bearing types must be fixed originally (ICZN 1999, article 72.3). According to article 73.1.4, the designation of an illustration of a single specimen as a holotype is to be treated as designation of the specimen illustrated; the fact that the specimen no longer exists or cannot be traced does not of itself invalidate the designation. This indicates that the new species is valid, although the slide containing the holotype specimen was “lost” (see above). The name on the three slides (which are obviously paratype slides) from the type series is “*Bryophyllum pinetum*” (this name is disclaimed for nomenclatural purposes; ICZN 1999, article 8.3).



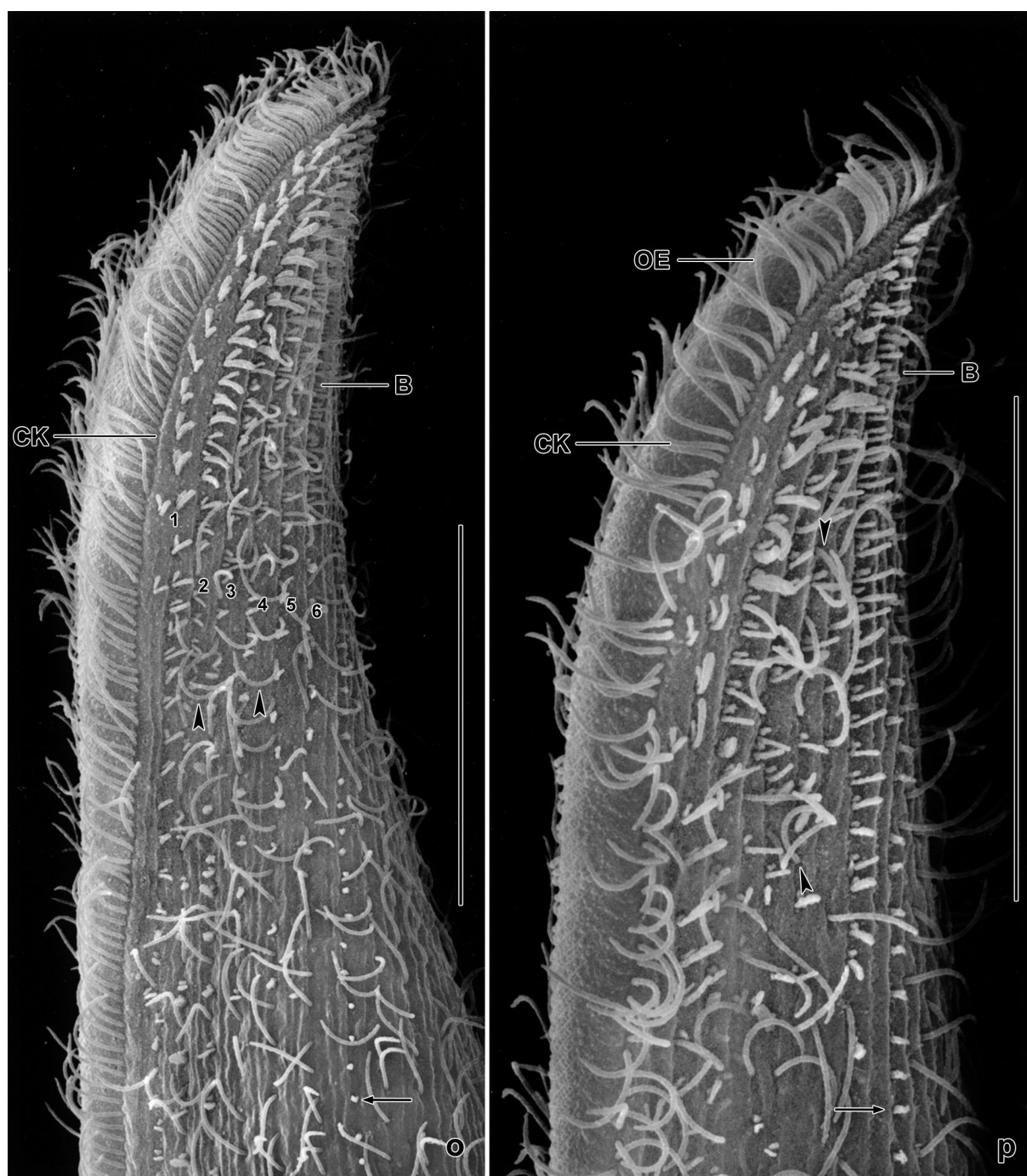
**Fig. 23a–i.** *Apobryophyllum pinetum* from life (a–f) and in the SEM (g–i). **a, b:** Shape of freely motile specimens. **c, d:** Type I extrusomes, 7–10  $\mu\text{m}$  long. **e:** Type II extrusomes, about 2  $\mu\text{m}$  long (arrowheads). **f:** Right side view of a slightly pressed specimen, showing the conspicuous extrusome fringe in the oral bulge and the nuclear apparatus. **g, h:** Shape variants. The arrowheads in (h) mark the monokinetal bristle tail of the last row of the dorsal brush. **i:** Left side view, showing the thinning oral bulge (arrow), the dorsal brush (B), and the end of the monokinetal bristle tail of the last brush row (arrowhead). B – dorsal brush, CK – circumoral kinety, CK + OE – circumoral kinety and oral bulge, CV – contractile vacuole, E – extrusomes, MA – macronucleus, MI – one of several micronuclei, OE – oral bulge. Scale bars 100  $\mu\text{m}$  (f, i), 50  $\mu\text{m}$  (a, b, g, h), and 4  $\mu\text{m}$  (e).

Two types of extrusomes in oral bulge and cytoplasm, do not impregnate with the protargol method used (Fig. 22a, b, f–h, o, p, 23c–f, m, q, s, 24a): type I conspicuous because 7–10  $\times$  1  $\mu\text{m}$  in size, compact and thus highly refractive, studded in anterior thirds of oral bulge, forming oblique rows each consisting of 4–7 extrusomes, loosely scattered in posterior third where the bulge is thinning



**Fig. 23j–n.** *Apobryophyllum pinetum* from life (j, k) and in the scanning electron microscope (l–n). **j, k:** Ventral surface views, showing the plate-like cortical granulation and the posteriorly thinning oral bulge. **l, n:** Ventral overview and detail, showing the leaf-like flattened anterior body half and the disappearing oral bulge (arrow) which does not surround the posterior body end. **m:** High magnification of the oral bulge, showing oblique ridges between short extrusome rows (cp. Fig. 1b); the arrow marks the hole remaining from a just released extrusome. CK – circumoral kinety, CK + OE – circumoral kinety and oral bulge, CV – contractile vacuole, E – type I extrusome, OE – oral bulge. Scale bars 50  $\mu\text{m}$  (j, l), 10  $\mu\text{m}$  (n), 5  $\mu\text{m}$  (k), and 2  $\mu\text{m}$  (m).

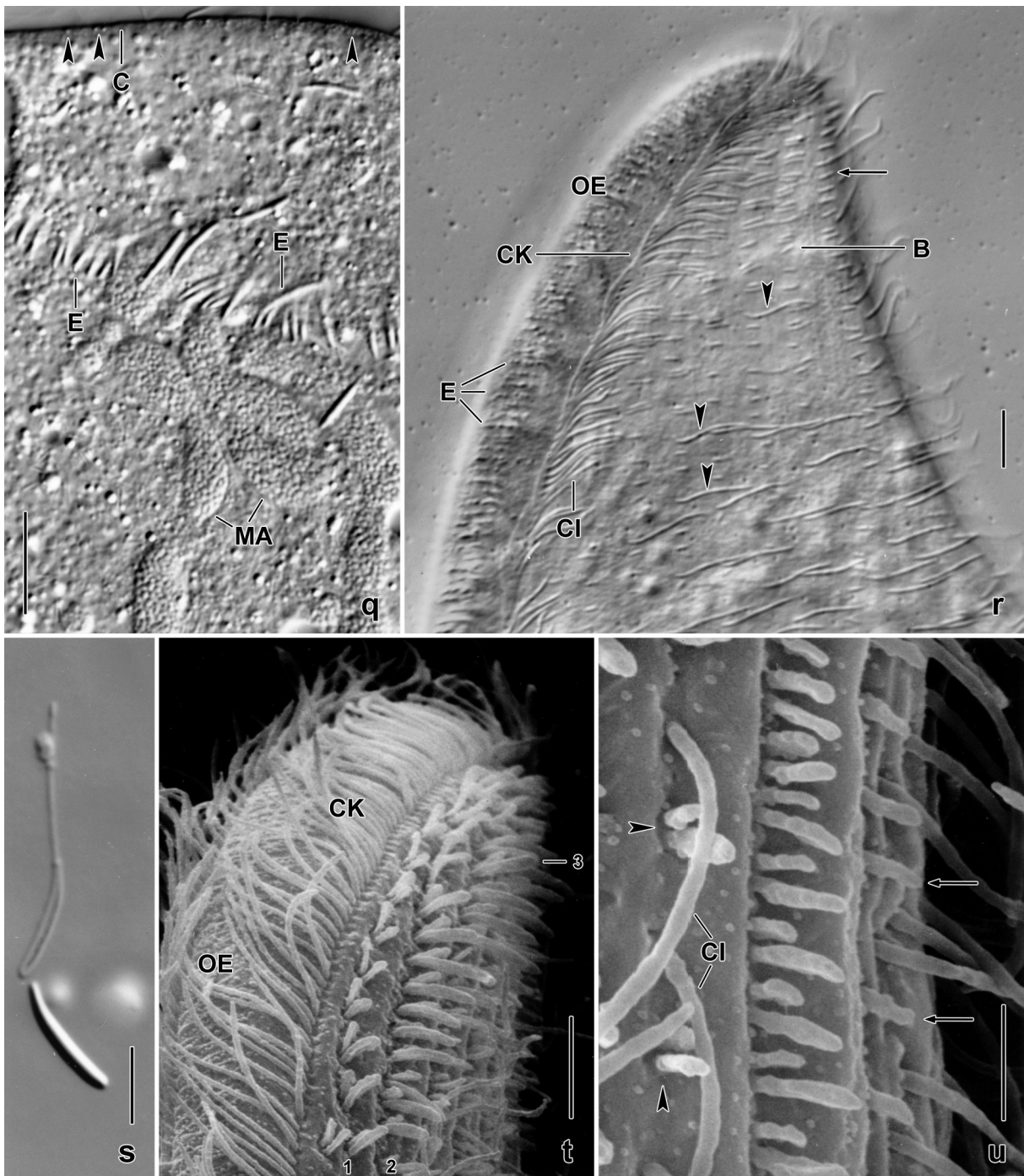
(Fig. 22a, f, o, p, 23f, j, l–n, 24a); individual type I extrusomes asymmetric, i.e., slightly curved rods with conical tip and rounded posterior end (Fig. 22f, 23c, d, f). Type II extrusomes also rod-shaped, but only  $2.0 \times < 0.3 \mu\text{m}$  in size and thus difficult to recognize (Fig. 22g, 23e). Cortex very flexible but not contractile, studded with minute ( $\sim 1 \mu\text{m}$ ) alveoli containing so closely spaced granules that



**Fig. 23o, p.** *Apobryophyllum pinetum*, dorsal brush in the scanning electron microscope; compare with scheme Fig. 22k. The heteromorphic brush is the genus character (cp. with → *Bryophyllum australiense*) and is very complex because monokinetal, ordinary cilia (arrowheads) are mixed with dikinetal, minute bristles which are slightly to greatly different in the individual brush rows and in anterior and posterior region of the brush; posterior of the brush, the rows continue as ordinary somatic kineties except of the last row which has a monokinetal bristle tail extending to near posterior end of cell (arrows). B – dorsal brush, CK – circumoral kinety, OE– oral bulge, 1–6 – brush rows. Scale bars 30  $\mu$ m.

a plate-like structure is produced (Fig. 22i, j, 23j, k). Cytoplasm colourless, posterior left quadrant of cell usually packed with globular and irregular fat droplets up to 10  $\mu$ m in size (Fig. 24b). Feeds very likely on ciliates lysed outside the cell because no prey could be detected inside the cells. Glides slowly and elegantly on microscope slides and soil particles, showing great flexibility but no undulating ventral margin; when swimming, rotates around main body axis.

Cilia 8–10  $\mu\text{m}$  long in vivo, arranged in an average of 28 longitudinal rows rather evenly spaced, those of right side abutting to anterior third of circumoral kinety while extending to posterior end of cell (Fig. 22d, e, 23i). Anterior third of 6–10, on average eight left lateral ciliary rows modified to a heterostichid dorsal brush, i.e., with ordinary, monokinetal cilia between dikinetal bristles. Anterior quarter of brush rows usually composed of only dikinetids. Bristle structure rather different in the individual rows: bristles of row 1 of same length ( $\sim 3 \mu\text{m}$ ), of rows 2 and 3 of different length (anterior much shorter than inflated posterior up to  $5 \mu\text{m}$  long), of rows 4–7 similar to rows 2 and 3 but posterior bristles not inflated and shorter ( $\sim 3 \mu\text{m}$ ), dikinetids more narrowly spaced in second or third row (“main brush row”) left of last row similar to first row but composed of only few dikinetids anteriorly and followed by a monokinetal bristle tail extending to near posterior body



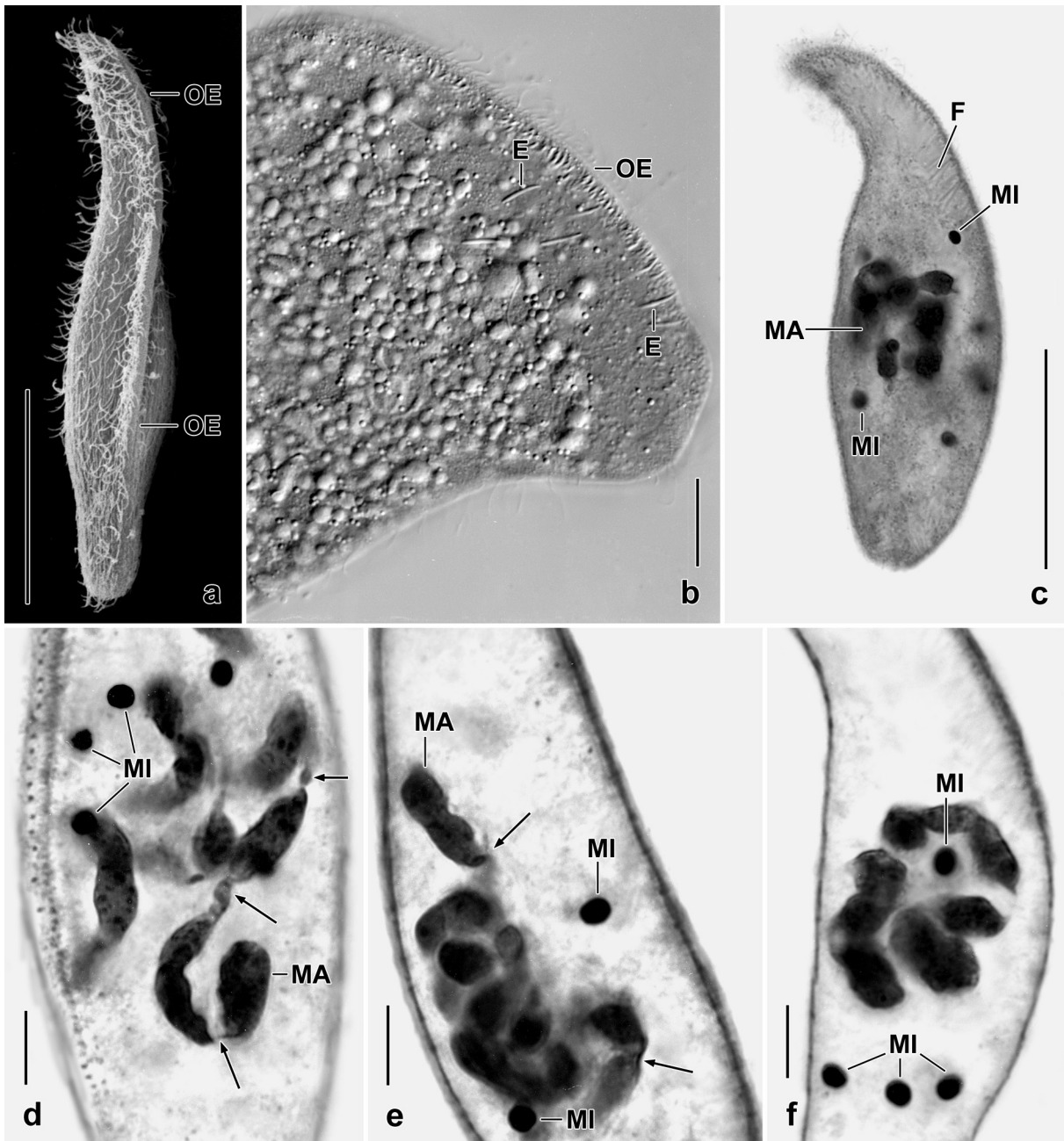


**Fig. 24a-f.** *Apobryophyllum pinetum* in the scanning electron microscope (a), from life (b), and after protargol impregnation (c-f). **a:** Ventral view of a specimen with flattened posterior region (cp. Fig. 21!). **b:** Anterior region of a specimen studded with globular and irregular inclusions, likely from a just ingested ciliate. **c, f:** *Apobryophyllum pinetum* is the sole member of the family that has a globular moniliform macronuclear mass comparable with *Stentor polymorphus* (Foissner et al. 1992). The micronuclei are inside and outside of the globe. **d, e:** As Fig. 3c, f, but macronuclear mass ellipsoid. Arrows denote fine bridges between the macronuclear nodules. E – type I extrusomes, F – pharyngeal fibres, MA – macronucleus, MI – micronuclei, OE – oral bulge. Scale bars 50  $\mu\text{m}$  (a, c), 15  $\mu\text{m}$  (b), and 10  $\mu\text{m}$  (d-f).

- ← **Fig. 23q-u.** *Apobryophyllum pinetum* from life (q-s) and in the SEM (t, u). **q:** Ventral view, showing cortical granulation (arrowheads) and part of the moniliform macronucleus. **r:** Anterior left side, showing part of the dorsal brush. The arrowheads mark ordinary, monokinetal cilia in between dikinetal, minute brush bristles. The arrow marks the last brush row, which consists almost entirely of monokinetal bristles (cp. Fig. 1k-m). **s:** A resting and an exploded type I extrusome with toxicyst structure. **t:** Anterior region of left side, showing that bristles of brush row (1) are shorter than those of rows (2) and (3). **u:** Mid of dorsal brush, showing ordinary cilia (CI) between dikinetal brush bristles (arrowheads); the penultimate brush row is composed of dikinetal bristles of which the anterior is shorter than the posterior. The last row consists mainly of monokinetal bristles (arrows). B – dorsal brush, CK – circumoral kinety, CI – ordinary cilia, E – extrusomes (q) and minute rows of type I extrusomes (r), MA – macronucleus, OE – oral bulge, 1, 2, 3 – dorsal brush rows. Scale bars 10  $\mu\text{m}$  (q, s), 5  $\mu\text{m}$  (r), and 2  $\mu\text{m}$  (t, u).

end. Bristles gradually decrease in length from anterior to posterior by about 50% (Fig. 22e, k–m, 23h, i, o, p, r, t, u; Table 9).

Oral apparatus as in congeners, e.g., *Apobryophyllum schmidingeri* Foissner & Al-Rasheid, 2007. Thus, I refer to the figures in *A. pinetum* (Fig. 22a, b, d, l, m–p, 23a, b, f, i, j, l–r, t, 24a, b; Tables 9, 10).

**Occurrence and ecology:** See Tables 1 and 4 in Foissner et al. (2005) for detailed site data (pH, organic C, etc.). Some kilometres distant occurs *A. schmidingeri* Foissner & Al-Rasheid, 2007 in a commercial spruce forest. Further, I found *A. pinetum* in forest soil from the surroundings of the town of Uema, Sweden.

**Remarks:** *Apobryophyllum pinetum* can be probably confused with *A. schmidingeri* and *Bryophyllum lingua multistriatum*; see Table 10 for separation. The best character is the moniliform, globular macronuclear mass (Fig. 22a, d, n, 23f, q, 24c–f). I introduced the term “main brush row” because the last three brush kineties of *Apobryophyllum* match the three-rowed dorsal brush of many other haptorids, especially in the order Spathidiida (for a review, see Foissner & Xu 2007). Accordingly, the complex brush pattern of *Apobryophyllum* is very likely derived.

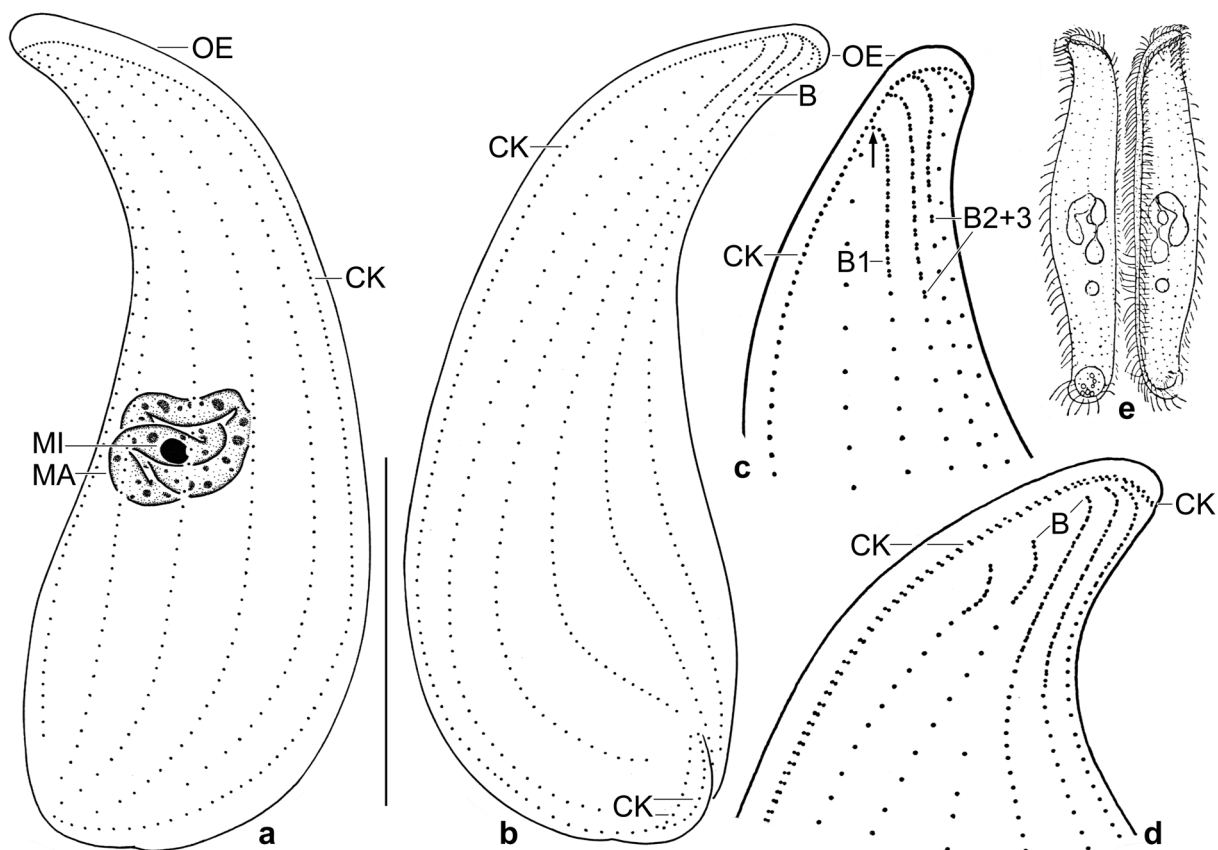


**Fig. 25a–e.** *Bryophyllum australiense* (a–c), *Neobryophyllum paucistriatum* (d, from Foissner et al. 2002), and *Bryophyllum hyalinum* (e, from Gelei 1936) after protargol impregnation (d) and Gentiana violet staining (e). **a–c:** Right and left side view of a representative specimen, showing body shape, ciliary pattern, and nuclear apparatus, length 100  $\mu\text{m}$ ; (c) is a magnification from (b), showing details of the dorsal brush such as some ciliated monokinetics at the beginning of the dikinetal dorsal brush rows (arrow). **d:** *Neobryophyllum* has four or five dorsal brush rows while *Bryophyllum* has three (c). The circumoral kinety consists of dikinetids in both genera. **e:** *Bryophyllum hyalinum* is much more slender than *B. australiense* (5.8:1 vs. 3.5:1). B – dorsal brush (rows), CK – circumoral kinety, MA – macronucleus, MI – micronucleus, OE – oral bulge. Scale bar 40  $\mu\text{m}$ .

***Bryophyllum australiense* nov. spec.**

(Fig. 25a–c, 26a–j; Table 11 on p. 316)

**Diagnosis:** Size in vivo about  $115 \times 35 \mu\text{m}$ , elongate lanceolate ( $\sim 3.5:1$ ). Macronuclear strand highly tortuous, composed of about five indistinct nodules. Main oral bulge extrusomes rod-shaped  $5\text{--}6 \mu\text{m}$  long. 9–11, on average 10 ciliary rows, three anteriorly modified to an isomorphic dorsal brush with  $2\text{--}3 \mu\text{m}$  long bristles. Oral apparatus as typical for genus.

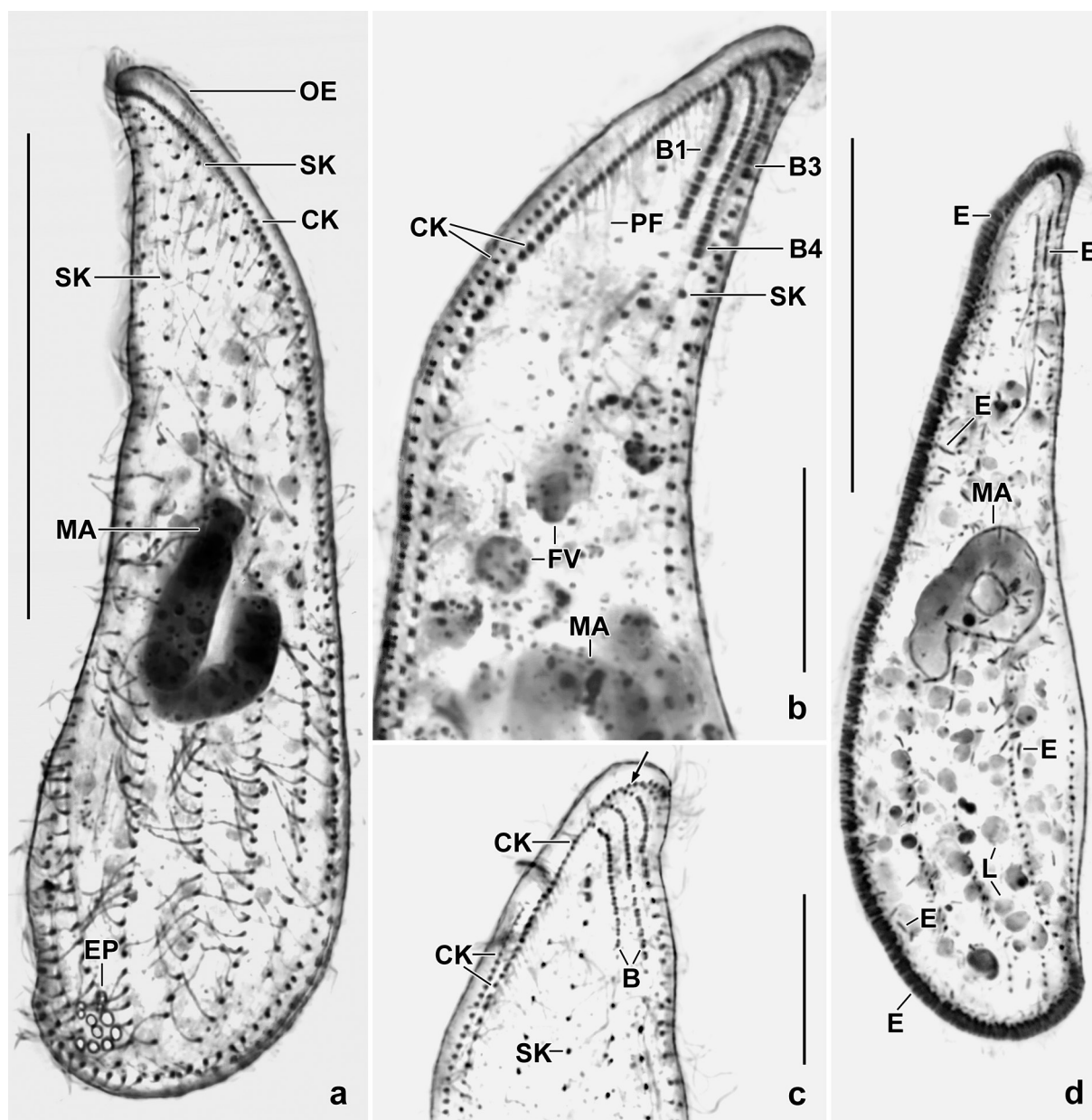


**Fig. 26a–d.** *Bryophyllum australiense* after protargol impregnation. **a, b, d:** Right and left side view, showing body shape, ciliary pattern, and macronucleus. Only type II extrusomes, which are in the oral bulge and the cytoplasm, occasionally impregnate deeply (d). **c:** Left side view of anterior body region, showing the dikinetal dorsal brush rows which begin with some ciliated monokinetids (arrow). B – dorsal brush (rows), CK – circumoral kinety, E – type II extrusomes in oral bulge and, less abundant, in the cytoplasm, EP – excretory pores of the contractile vacuole, FV – food vacuoles, L – lipid droplets, MA – macronucleus, OE – oral bulge, PF – pharyngeal fibres, SK – somatic ciliary rows. Scale bars  $40 \mu\text{m}$  (a, d) and  $15 \mu\text{m}$  (b, c).

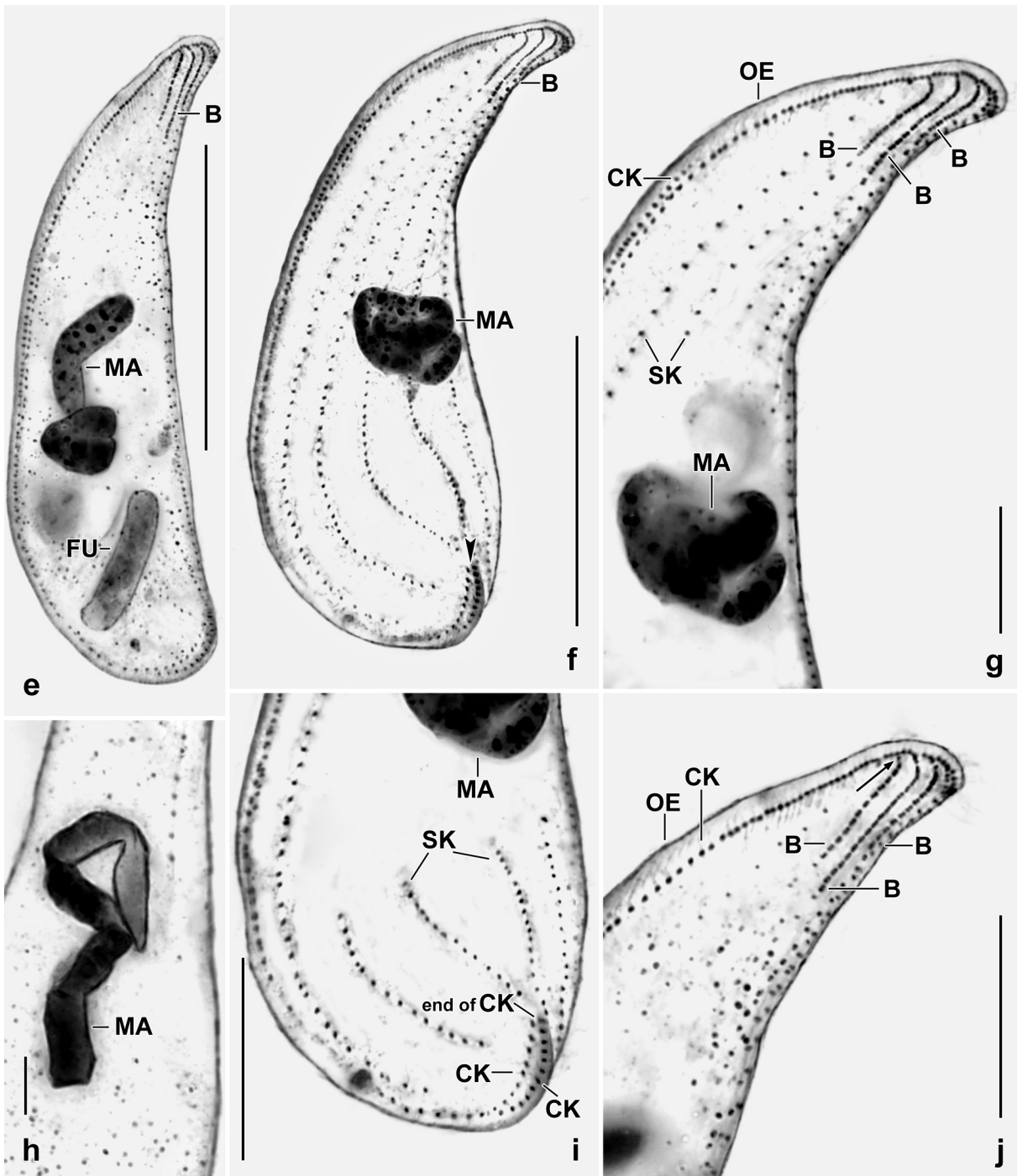


**Fig. 26e–j.** *Bryophyllum australiense* after protargol impregnation. **e–g, i:** Left side views, showing variability of body shape, ciliary pattern, and the highly tortuous macronucleus having four indentations, i.e., five nodules; (**g**) is a higher magnification of (**f**) where the arrowhead marks the posterior end of the oral bulge and the circumoral kinety. **h:** The macronucleus shows five nodules produced by four indentations. **j:** Left side view of anterior body region, showing some ciliated monokinetids between circumoral kinety and dikinetal brush rows (arrow). B – dorsal brush (rows), CK – circumoral kinety, FU – a piece of a fungus(?), MA – macronucleus, OE – oral bulge, SK – somatic ciliary rows. Scale bars 40  $\mu\text{m}$  (**e, f**), 20  $\mu\text{m}$  (**i, j**), and 5  $\mu\text{m}$  (**h**).

**Type locality:** Litter and upper soil layer (0–5 cm) of a *Eucalyptus* forest about 10 m distant from the seacoast in the surroundings of the town of Eubenangee south of the town of Cairns, Australia, 17°S, 145°E.

**Type material:** The slide containing the holotype and one paratype slide with protargol-impregnated specimens have been deposited in the Biology Centre of the Upper Austrian Museum in Linz (LI). Relevant specimens have been marked by black ink circles on the coverslip. For slides, see Fig. 11a–e in Chapter 5.

**Etymology:** *australiense* refers to the continent the species was discovered.

**Description:** In vivo, I misidentified this species as *Neobryophyllum paucistriatum* (Foissner et al., 2002) Foissner & Lei, 2004 when I made the species list in 1985 because both have a great overall similarity. Thus, detailed live observations were not performed. However, *Bryophyllum australiense* is a typical member of the genus and thus it is reasonable to describe the species despite the lack of detailed live observations.

Except of body length and number of ciliary rows, all features investigated are highly variable, i.e., have coefficients of variation >15% (Table 11).

Size in protargol preparations 67–122 × 23–44 µm, on average 98 × 29 µm (Table 11). When 15% preparation shrinkage is added, in vivo values are obtained: 77–140 × 23–44 µm, on average about 115 × 35 µm. Body shape as typical for genus, i.e., slenderly to very slenderly lanceolate (2.4–5:1), usually 3.5:1, i.e., slenderly lanceolate; anterior end bluntly acute and more or less curved dorsally, posterior end broadly rounded with a small dorsal indentation where the oral bulge ends; ventral margin slightly to distinctly convex, dorsal margin straight to slightly convex or concave; laterally distinctly flattened (Fig. 25a–c, 26a–g, i, j; Table 11). Nuclear apparatus in middle third of body (Fig. 25a, 26a, d–f; Table 11). Macronucleus about 60 µm long, usually highly tortuous having about five, usually indistinct nodules; nucleoli numerous and small. Micronucleus often within tortuous macronuclear strand and thus difficult to recognize, globular to broadly ellipsoid, on average 3.6 × 2.4 µm in protargol preparations. Contractile vacuole near posterior dorsal margin of cell, about 8–12 excretory pores on right side of body, i.e. left of rear end of oral bulge (Fig. 26a). Two types of oral bulge and cytoplasmic extrusomes: main type I rod-shaped to indistinctly fusiform, 5–6 µm long, does not impregnate with the protargol method used but recognizable in most protargol-impregnated specimens with interference contrast; type II fine, about 2 µm long rods occasionally deeply impregnating with the protargol method used (Fig. 26d). Cortex very flexible and colourless.

Cilia about 8 µm long in protargol preparations, arranged in five left side and five right side rows in typical *Bryophyllum* pattern (Foissner et al. 2002; Foissner & Lei 2004), intrakinetid distances about twice as large in anterior than posterior thirds of cell; three dorsal rows anteriorly modified to a dorsal brush with 2–3 µm long bristles, middle row, on average, slightly longer than right and left row, each row commences with 1–6 monokinetids; two or three right side rows slightly shortened due to the pores of the contractile vacuole (Fig. 25a–c, 26a–g, j; Table 1).

Oral apparatus as described by Foissner et al. (2002) for *Bryophyllum paucistriatum* (now *Neobryophyllum paucistriatum*) (Fig. 25a–c, 26a–g; Table 11).

**Occurrence and ecology:** This was a species-rich sample (for details, see type locality.<sup>1</sup> *Bryophyllum australiense* appeared 4 d after rewetting the sample and developed moderate abundances the following three weeks.

**Remarks:** None of the bryophyllids listed in the study of Foissner & Lei (2004) is identical with *Bryophyllum australiense*. However, at first glance the Australian species highly resembles *B. paucistriatum* Foissner et al., 2002, which has been transferred to *Neobryophyllum* by Foissner & Lei (2004) because it has four or five (vs. usually three) isomorphic brush rows (cp. Fig. 25c with

---

<sup>1</sup> Note by H. Berger: The original (incomplete) sentence by W. Foissner reads as follows: “This was a rich sample (for details, see type locality) with XX species of which XX were undescribed.” (XX = number of species not yet mentioned in the manuscript). I could not locate the numbers in reasonable time, thus, I shortened the sentence.

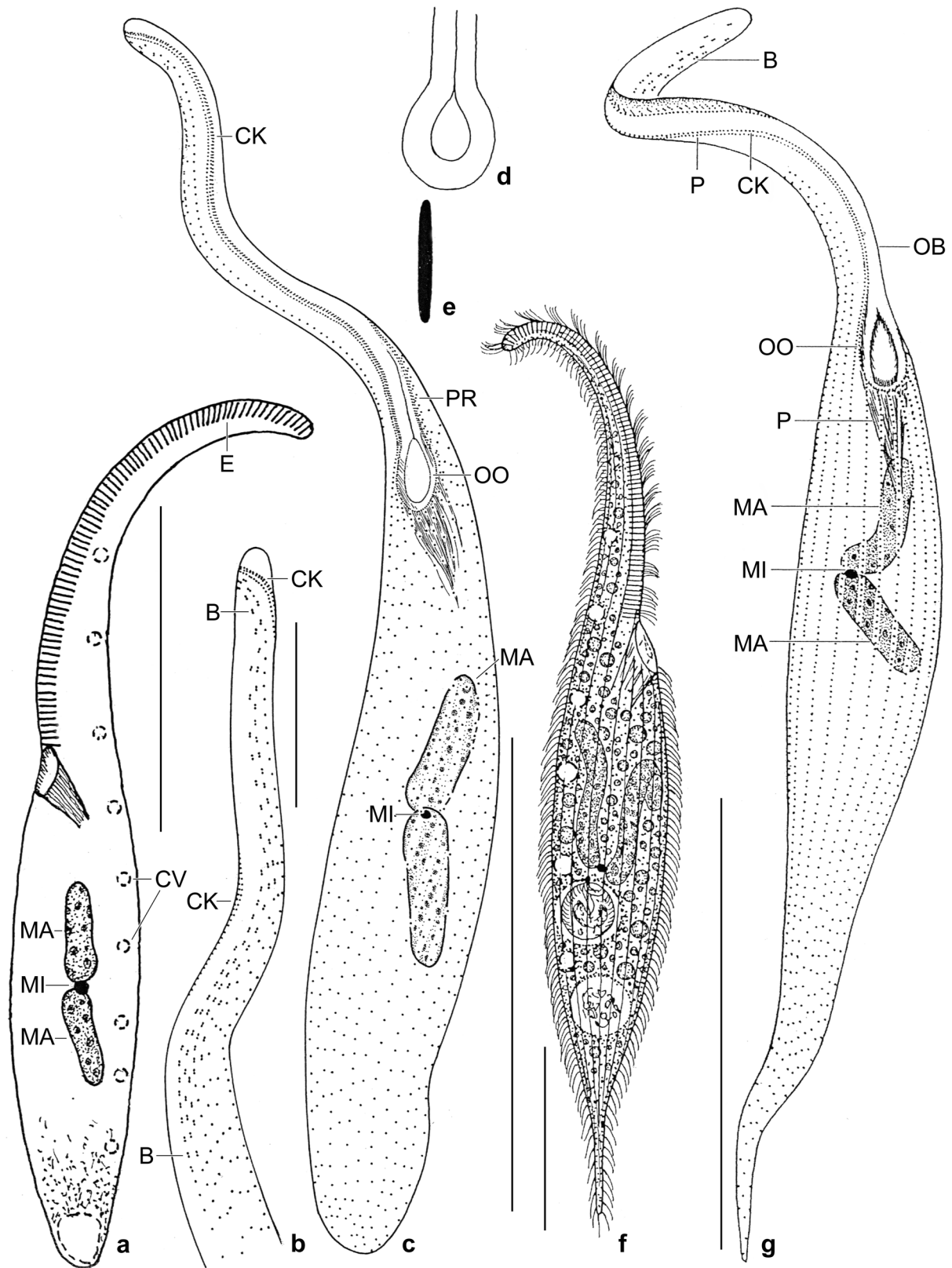


**Fig. 27a–g.** *Rimaleptus similis australiensis* (a–e) and *R. mucronatus* (f, g; from Vd'ačný & Foissner 2012) from life (a, d–f) and after protargol impregnation (b, c, g). **a:** Left side view of a representative specimen, size and shape according to the morphometric data, length 300  $\mu\text{m}$ . **b:** Dorsal brush in anterior half of proboscis. **c:** Ventral view of infraciliature, length 277  $\mu\text{m}$ . **d, e:** Oral opening and oral bulge extrusome, 6  $\mu\text{m}$ . **f, g:** *Rimaleptus mucronatus* differs from *R. similis australiensis* mainly by the tailed body (g, 330  $\mu\text{m}$ ). B – dorsal brush, CK – circumoral kinety, CV – contractile vacuoles, E – extrusomes, MA – macronuclear nodules, MI – micronucleus, OB – oral bulge, OO – oral opening, PB – pharyngeal basket, PE – perioral kinety, PR – preoral kineties. Scale bars 25  $\mu\text{m}$  (b) and 100  $\mu\text{m}$  (a, c, f, g).

Fig. 25d). Another species, not yet investigated with modern methods, is *Bryophyllum hyalinum* Gelei, 1936 (Fig. 25e). It is a *Sphagnum* species much more slender than *B. australiense* (average length:width ratio 5.8:1 vs. 3.5:1). All other characteristics are highly similar though slight differences occur in the number of macronuclear nodules (four vs. five) and ciliary rows (12 vs. 10). Unfortunately, Gelei (1936) did not report on the extrusomes.

***Rimaleptus similis similis* (Foissner, 1995) Vďačný & Foissner, 2012 nov. stat.**

1995 *Dileptus similis* nov. sp. — Foissner, Arch. Protistenk., 145: 43 (type population from Costa Rica).

1999 *Dileptus similis* Foissner, 1995 — Foissner, Biodivers. Conserv. 8: 334 (description of population from Kenya).

**Diagnosis:** See diagnosis of *Rimaleptus similis australiensis* nov. ssp. for differences.

**Remarks:** The Australian subspecies (see below) is clearly different from the Costa Rican and the Kenyan populations representing the nominotypical subspecies of *Rimaleptus similis* (Foissner, 1995) Vďačný & Foissner, 2012. However, there is only one “strong” character, viz., the number of somatic ciliary rows, suggesting subspecies classification (Table 12 on p. 317).

***Rimaleptus similis australiensis* nov. ssp.**

(Fig. 27a–e, 28a–r; Table 12 on p. 317)

**Diagnosis:** As nominal subspecies but with a body size of  $255 \times 35 \mu\text{m}$  (vs. about  $219 \times 57 \mu\text{m}$  in Costa Rican population and  $245 \times 43 \mu\text{m}$  in Kenyan population) in protargol preparations, a length:width ratio of 7.3:1 (vs. 4.0:1 and 5.7:1), and with an average of 19 (vs. 29 and 31) somatic ciliary rows.

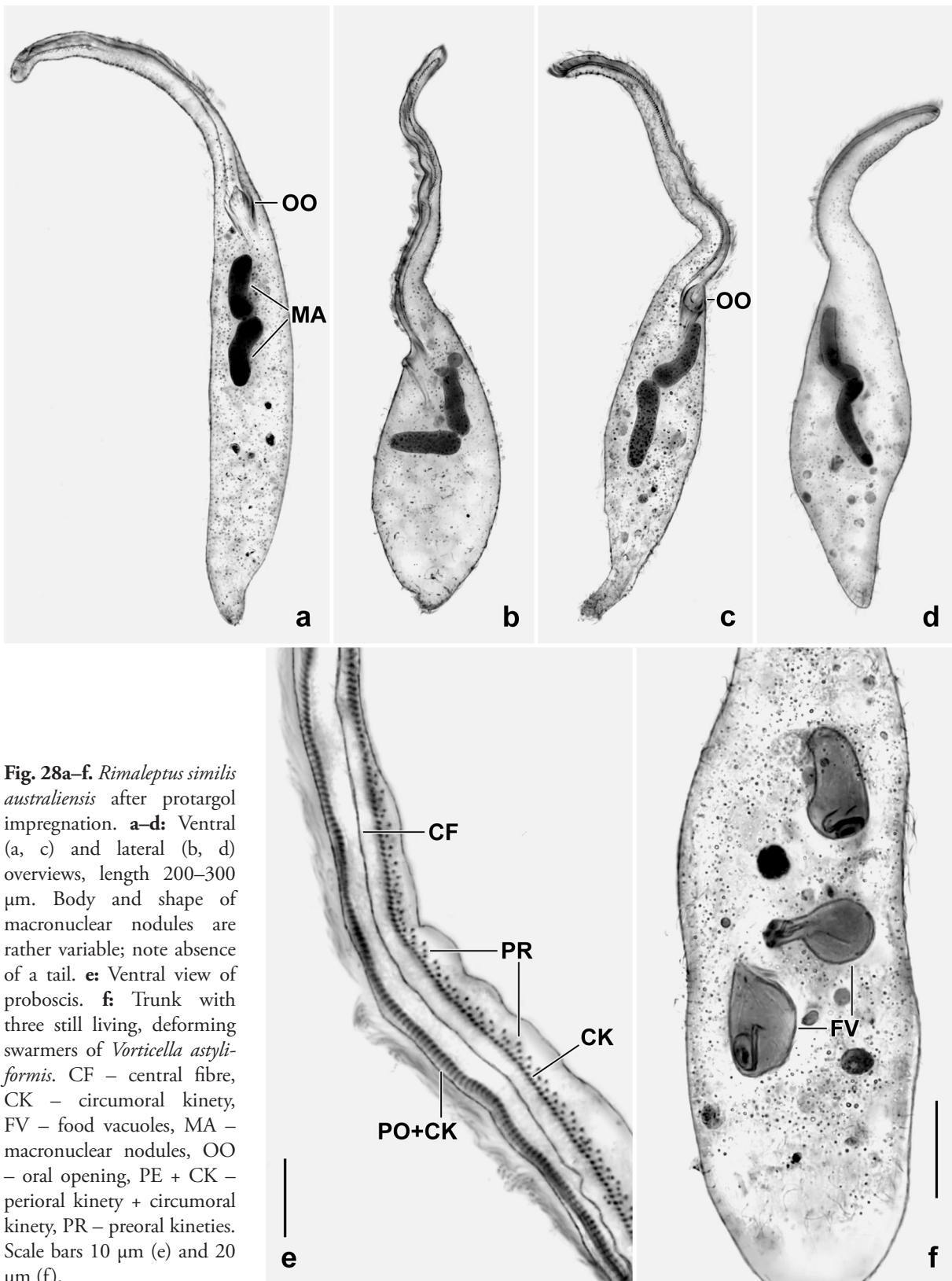
**Type locality:** Australian site (27), i.e., litter and surface soil from Green Island east of the town of Cairns,  $17^{\circ}02'07''\text{S}$ ,  $145^{\circ}05'09''\text{E}$ .

**Type material:** The slide containing the holotype and two paratype slides with protargol-impregnated specimens have been deposited in the Biology Centre of the Upper Austrian Museum in Linz (LI). Relevant specimens have been marked by black ink circles on the coverslip. For slides, see Fig. 12a–f in Chapter 5.

**Etymology:** *australiensis* refers to the continent the species was discovered.

**Description:** Of 12 features investigated, five have a coefficient of variation >15%, indicating a rather distinct variability. As *Rimaleptus similis australiensis* is rather similar to the nominal subspecies, I provide only a schematic in vivo illustration and a brief description. Identification needs protargol impregnation and morphometry. For terminology, see Vďačný & Foissner (2012).

Size in protargol preparations  $197\text{--}322 \times 25\text{--}53 \mu\text{m}$ , on average  $256 \times 36 \mu\text{m}$  (Table 12). When 15% preparation shrinkage is added, in vivo values are obtained:  $225\text{--}370 \times 29\text{--}60 \mu\text{m}$ , on average  $300 \times 35 \mu\text{m}$ . Body shape rather variable, i.e., very narrowly dileptid with a length:width ratio of about 7.3:1. Proboscis of ordinary length, i.e., 43% of body length on average (Fig. 27a; Table 12). Posterior body end rounded, never tailed (Fig. 27a, c, 28a–d, g, j–o; Table 12). Two slightly drumstick-shaped macronuclear nodules slightly anterior of mid-trunk. Micronucleus in between macronuclear nodules, globular (Fig. 27a, c, 28a–d, g–o; Table 12). About eight contractile vacuoles in proximal portion of proboscis and dorsal side of trunk; pores usually single in proboscis, two or three pores in trunk (Fig. 27a, 28p). Oral bulge extrusomes very narrowly ellipsoid, about  $6 \mu\text{m}$  long in vivo (Fig. 27a, e). I did not look for the minute, fine extrusomes present in two populations of the nominal subspecies (Vďačný & Foissner 2012). Cortex very flexible, ordinarily granulated, i.e.,



about five granule rows between two ciliary rows. Cytoplasm with countless granules 1–2  $\mu\text{m}$  in size, concentrated in posterior region of trunk; rather many lipid droplets 2–6  $\mu\text{m}$  in size; numerous vacuoles with fluffy contents; occasionally one or several food vacuoles with swarms of *Vorticella astyliiformis* (Fig. 28f, k).

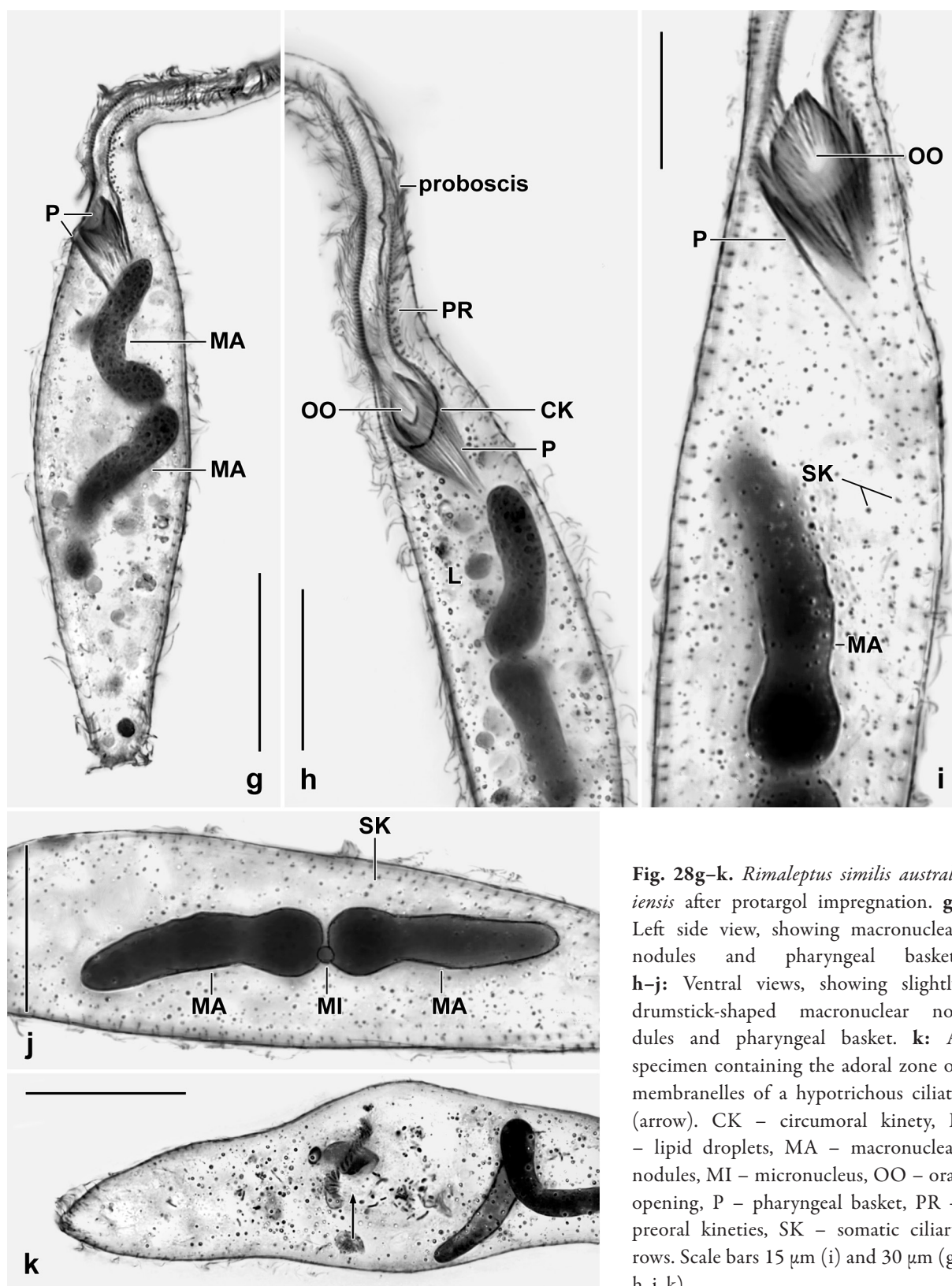


**Fig. 28g–k.** *Rimaleptus similis australiensis* after protargol impregnation. **g:** Left side view, showing macronuclear nodules and pharyngeal basket. **h–j:** Ventral views, showing slightly drumstick-shaped macronuclear nodules and pharyngeal basket. **k:** A specimen containing the adoral zone of membranelles of a hypotrichous ciliate (arrow). CK – circumoral kinety, L – lipid droplets, MA – macronuclear nodules, MI – micronucleus, OO – oral opening, P – pharyngeal basket, PR – preoral kineties, SK – somatic ciliary rows. Scale bars 15  $\mu\text{m}$  (i) and 30  $\mu\text{m}$  (g, h, j, k).

Somatic and oral infraciliature as typical for genus (Vďačný & Foissner 2012). On average 19 ciliary rows on trunk, 3–6 modified to a heterostichad, multi-rowed and staggered dorsal brush anteriorly. Right and left of circumoral kinety a rather narrow, blank stripe. Preoral kineties each composed of three cilia. Oral opening circular to narrowly ovate (Fig. 27a, c, d, 28c, e, g–i, p, q, r; Table 12).

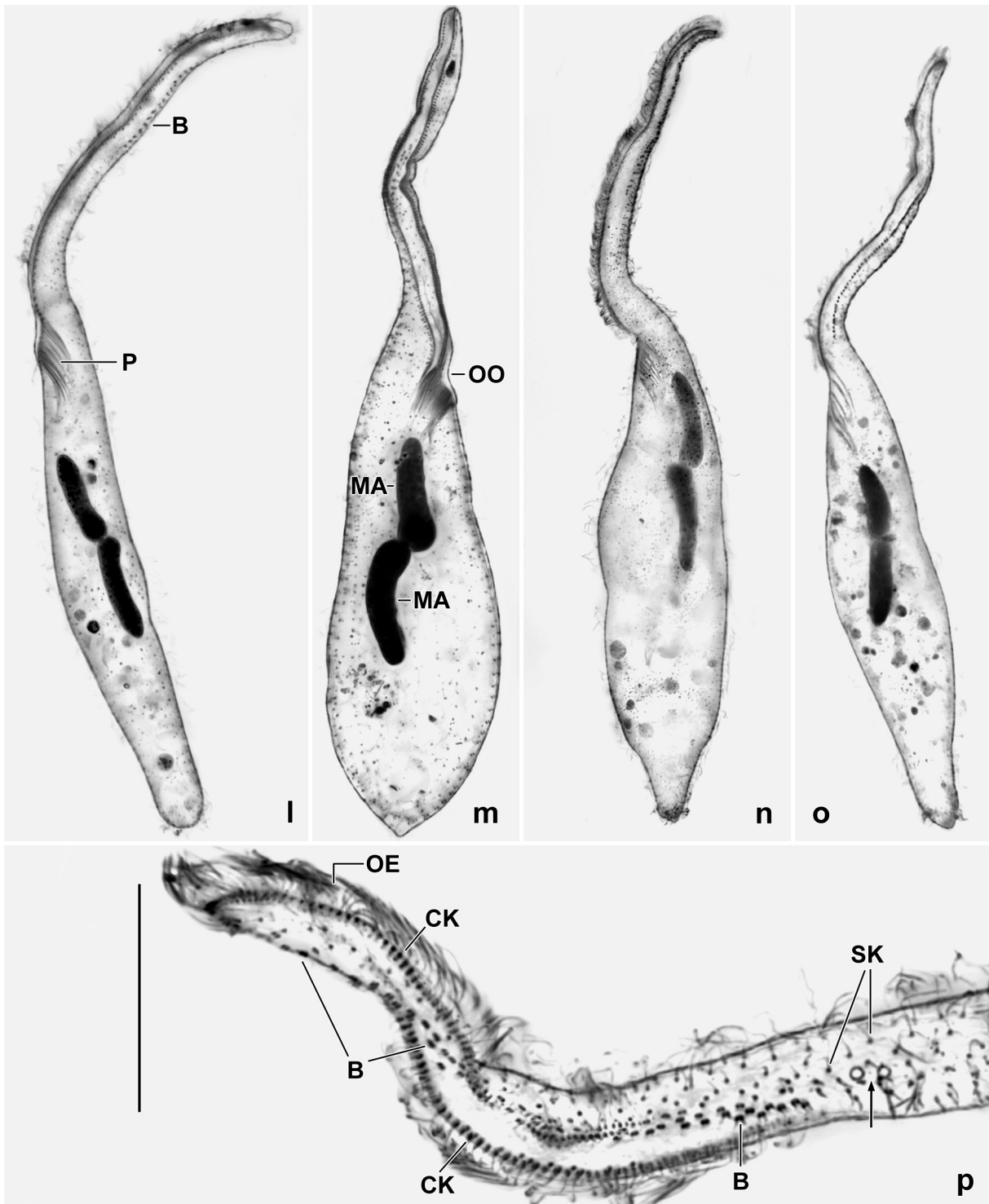


**Fig. 281–p.** *Rimaleptus similis australiensis* after protargol impregnation. **I–o:** Variability of body shape and nuclear apparatus, length 200–300  $\mu\text{m}$ . Note lack of a tail. **p:** Spiralized anterior half of proboscis, showing dorsal brush made of dikinetids and two excretory pores of a contractile vacuole (arrow). B – dorsal brush, CK – circumoral kinety, MA – macronuclear nodules, OE – oral bulge, OO – oral opening, P – pharyngeal basket, SK – ordinary somatic kineties. Scale bar 20  $\mu\text{m}$  (p).

**Occurrence and ecology:** As yet found only at the slightly saline type locality. Grew well in the non-flooded Petri dish culture where it appeared 3 d after rewetting the sample. Laurasian records of *R. similis* not known, suggesting restricted Gondwanan distribution.

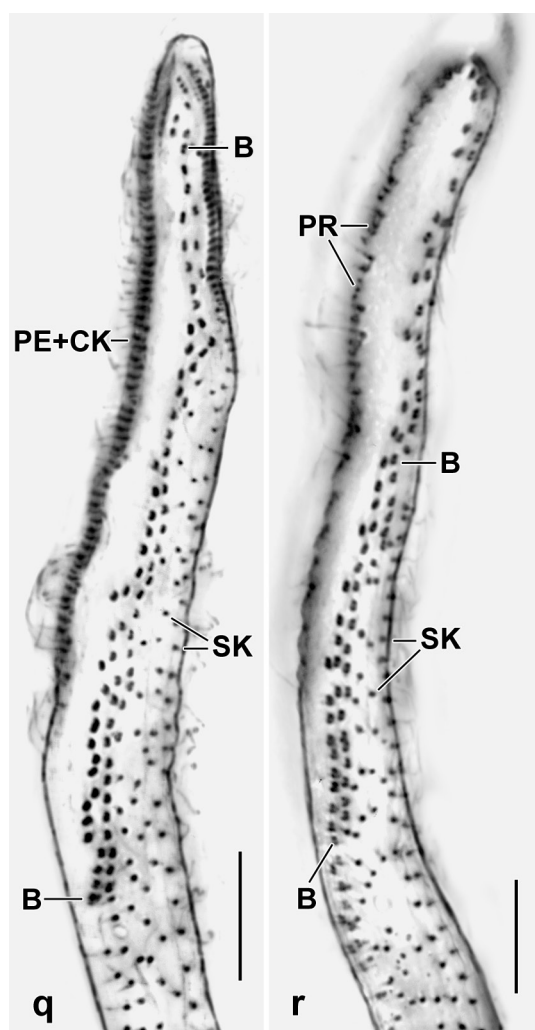


**Fig. 28q, r.** *Rimaleptus similis australiensis*, dorsal brush after protargol impregnation. The brush is composed of 3–6 staggering dikinetid rows extending almost total length of proboscis. B – dorsal brush, PE + CK – perioral kinety + circumoral kinety, PR – preoral kineties, SK – ordinary somatic kineties. Scale bars 10  $\mu$ m.

**Remarks:** There is only one species that could be confused with *Rimaleptus similis australiensis*, viz., *R. mucronatus* (Fig. 27f, g). They differ by the absence vs. presence of a tail. See Vd'ačný & Foissner (2012) for a revision of the dileptids.

#### 4.2.2 Nassulia

For some comments on this taxon by W. Foissner, see Foissner et al. (2002, p. 409).

#### **Bophryidae nov. fam.**

**Diagnosis:** Colpodidiida with a single, complete adoral organelle 3; horizontally oriented paroral membrane; and a contractile vacuole close posterior to oral apparatus. Usually with conspicuous, trichocyst-like extrusomes and a fine-meshed silverline pattern. Buccal cavity absent.

**Type genus:** *Bophrya* nov. gen.

**Genera assignable:**  $\rightarrow$  *Bophrya* nov. gen.;  $\rightarrow$  *Wolfkoscia* Foissner et al., 2002; *Parafurgasonia* Foissner & Adam, 1981.

**Remarks:** There is no doubt that the genera mentioned above belong to the class Nassophorea Small & Lynn, 1981 and that their closest relatives are members of the order Colpodidiida Foissner et al., 2002. The Bophryidae differ from the Colpodidiidae by the absence vs. presence of a buccal cavity and the horizontally vs. laterally located paroral membrane.

The “single, complete adoral organelle 3” is a very specific feature of the genera mentioned above. Traditionally, the “complete” organelle is termed “nassulid organelle 3” because organelles 1 and 2 are highly reduced or even absent (Foissner et al. 2002).

#### ***Bophrya* nov. gen.**

**Diagnosis:** Moderately-sized, ellipsoid and laterally flattened, holotrichously ciliated Nassophorea with broad cortical stripes containing globular anterior end (“head”) of cortical mitochondria each associated with a membranous, minute cone causing a serrate cell outline. Oral apparatus with a unique, convex shield (scutum) extending over adoral organelles and entrance to oral basket lengthening horizontally to dorsal side where it curves posteriorly.

**Type species:** *Bophrya costata* nov. spec.

**Etymology:** *Bophrya* is a composite of *Bo* (Botswana, the country where the type species was discovered), and the Greek noun *phrya* (eyebrow ~cilia ~ciliate), meaning a ciliate from Botswana. Feminine gender.

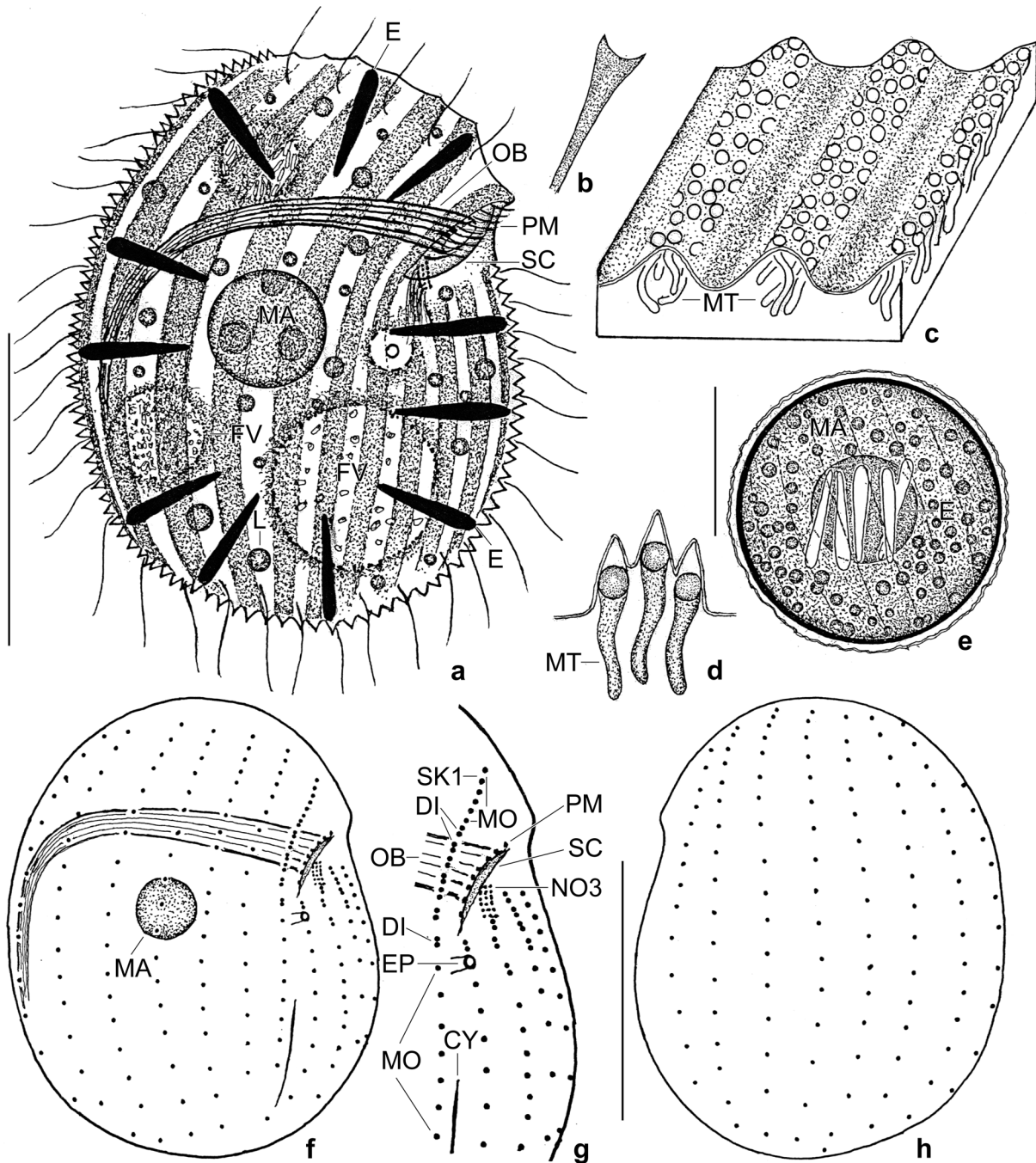


**Fig. 29a–h.** *Bophrya costata* from life (a–e) and after Chatton-Lwoff silver nitrate and silver carbonate (oral structures, partially) impregnation (f–h). **a:** Semischematic right side view of a representative specimen, length 50  $\mu\text{m}$ . **b:** Distal end of a basket rod. **c, d:** Surface and transverse view of cortex, showing location (c) and shape (d) of the headed mitochondria. **e:** Resting cyst. **f–h:** Somatic and oral ciliary pattern of right and left side of holotype. CY – cytophyge, DI – dikinetids, E – extrusomes, EP – pore of contractile vacuole, FV – food vacuoles, L – lipid droplet, MA – macronucleus, MO – monokinetids, MT – mitochondria, NO3 – nassulid adoral organelle 3, OB – oral basket, PM – paroral membrane, SC – scutum, SK1 – somatic kinety 1. Scale bars 15  $\mu\text{m}$  (e) and 25  $\mu\text{m}$  (a, f, h).

**Species assignable:**  $\rightarrow$  *Bophrya costata* nov. spec. (type species).

**Remarks:** *Bophrya* appears as a curious “composite” of several nassophorid genera: body flattened as in the Microthoracida (Foissner 1985); ciliature holotrichous as common in the Nassulida (Foissner et al. 2002); broad cortical stripes, a rare feature found only in two other genera, viz., *Pseudomicrothorax* (Foissner et al. 1994) and *Lopezoterenia* Foissner, 1997c; large, trichocyst-like extrusomes as, e.g., in

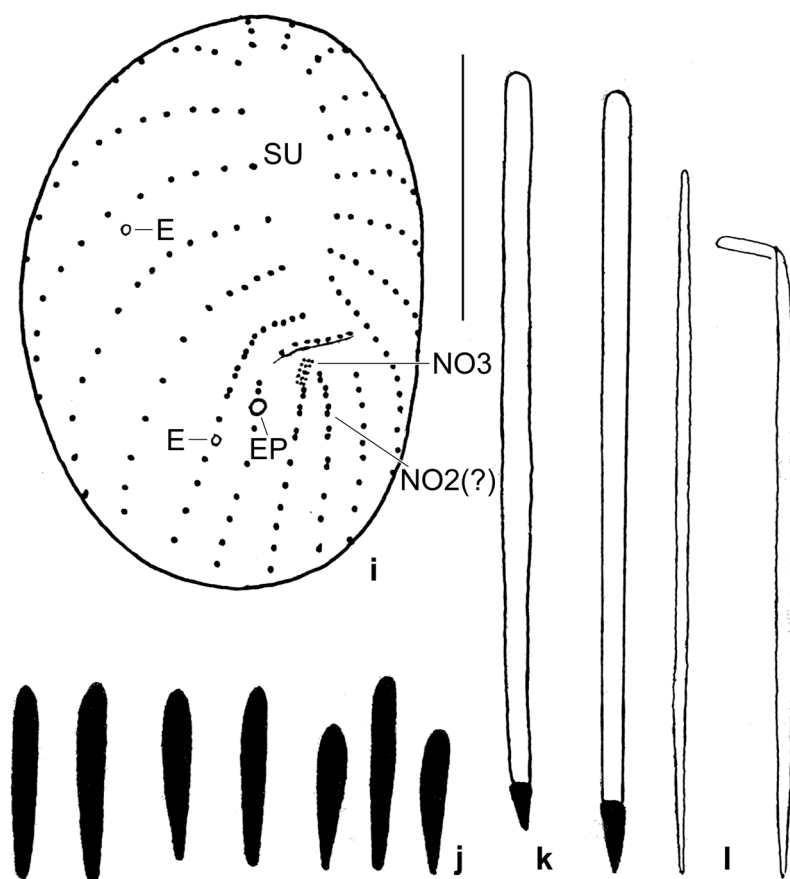


**Fig. 29i-l.** *Bophrya costata* from life (j-l) and after Chatton-Lwoff silver nitrate impregnation (i). **i:** Oblique ventral view, showing the clavate preoral suture and the ciliary pattern. **j:** Variability of resting extrusomes, copied from micrographs, size  $\sim 7-10 \times 1-2 \mu\text{m}$ . **k:** Released extrusomes with posterior end not spread, thus looking like exploded extrusomes from hymenostome ciliates, e.g., *Paramecium*, size  $\sim 40 \times 2-4 \mu\text{m}$ . **l:** Fully exploded extrusomes, length up to  $80 \mu\text{m}$ . E – extrusome holes, EP – pore of contractile vacuole, NO2, 3 – nassulid adoral organelles, SU – preoral suture. Scale bar  $20 \mu\text{m}$ .

→ *Wolkosia* and *Apocolpodidium* (*Phagoon*) *macrostoma* Foissner et al., 2002; contractile vacuole close posterior to oral apparatus, as in → *Wolkosia* and the Colpodidiidae; a horizontally oriented paroral membrane as

in → *Wolkosia* and *Parafurgasonia* Foissner & Adam, 1981; only a single, complete adoral organelle, as in → *Wolkosia* and *Colpodidium*. Unique features are the oral shield and the vermiform mitochondria with a globular anterior end (Fig. 29c, d, 31a, b, d, h).

***Bophrya costata* nov. spec.**

(Fig. 29a-l, 30a-t, 31a-h; Table 13 on p. 318)

**Diagnosis:** Size in vivo about  $50 \times 40 \mu\text{m}$ . Broadly ellipsoid with an inconspicuous concavity in oral area far subapically. Nuclear apparatus in mid-body. Extrusomes very narrowly cuneate, conspicuous because about  $10.0 \times 1.5 \mu\text{m}$  in size. Cortex, somatic and oral infraciliature, and location of contractile vacuole as diagnosed for family and genus. 18 slightly convex ciliary rows: seven each on right and left side, four postoral; somatic ciliary row 1 with ciliated dikinetids at level of oral apparatus; preoral suture clavate. Nassulid organelle 3 minute, composed of six vertical ciliary rows. Paroral membrane oblique, composed of about 18 dikinetids each having ciliated only one basal body. Oral basket in vivo about  $5 \mu\text{m}$  wide distally, composed of about 12 rods. Resting cyst about  $30 \mu\text{m}$  across; wall  $1.5-2.0 \mu\text{m}$  thick, composed of two distinct layers.

**Type locality:** Soil from floodplain of the Chobe River, Kabolebole Peninsula, Botswana,  $25^{\circ}\text{S}$ ,  $17^{\circ}50'\text{E}$ .

**Type material:** The slide containing the holotype (Fig. 29f-h) and two paratype slides with silver nitrate impregnated specimens (Chatton-Lwoff method) and one slide with protargol-impregnated cells have been deposited in the Biology Centre of the Upper Austrian Museum in Linz (LI). Relevant specimens have been marked by black ink circles on the coverslip. For slides, see Fig. 13a-f in Chapter 5.

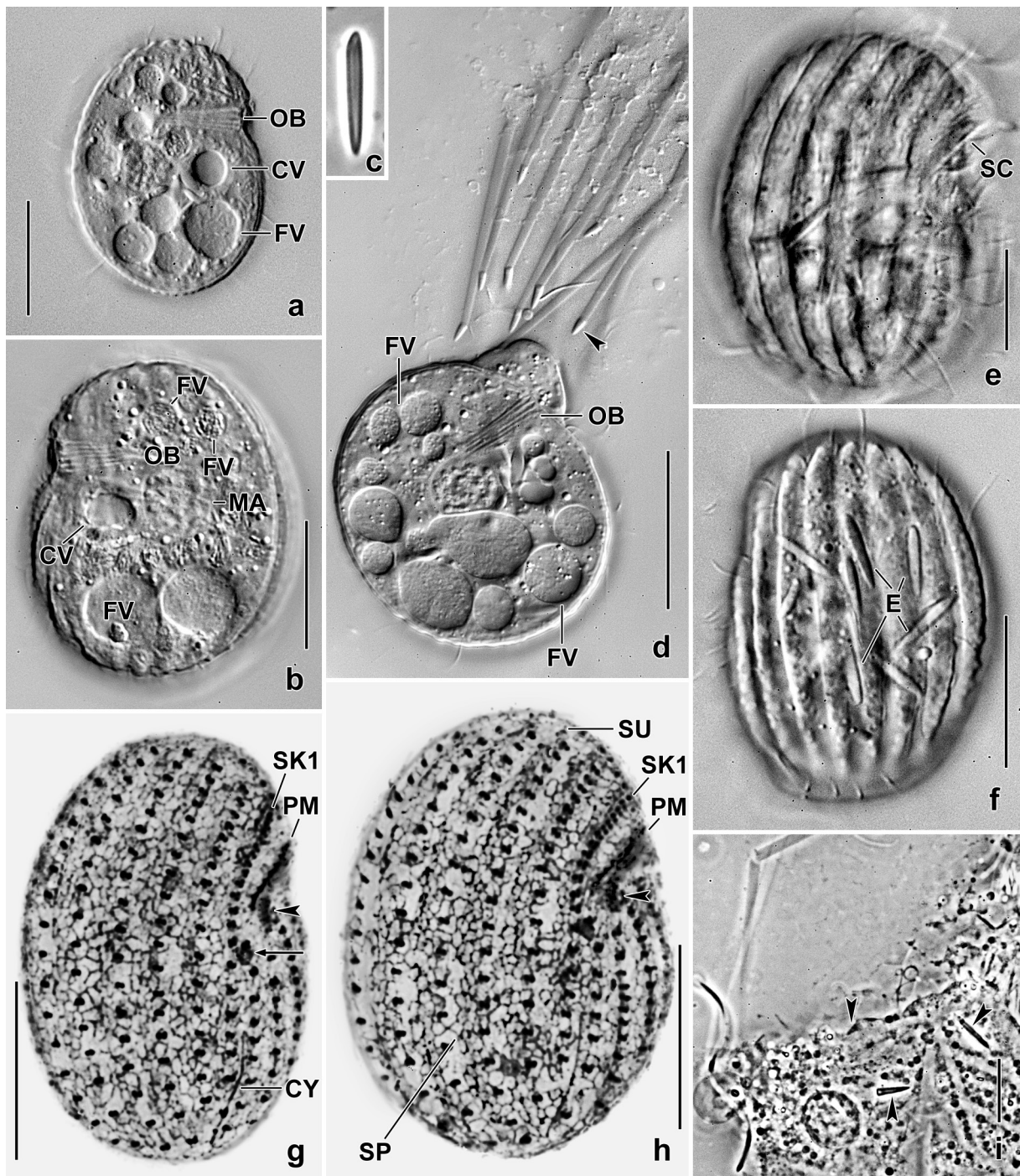


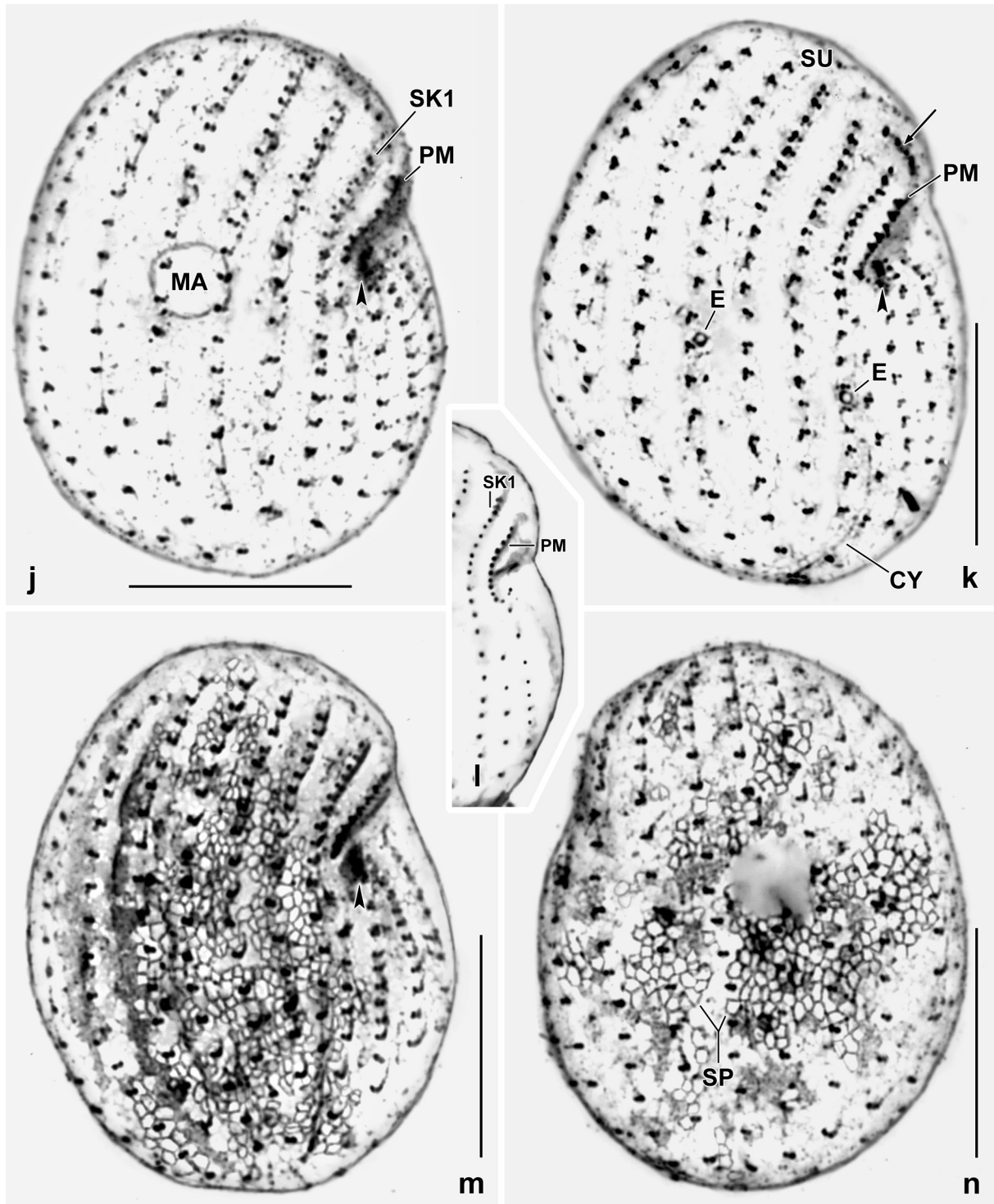
**Fig. 30a–i.** *Bophrya costata* from life (a–f, i) and after Chatton-Lwoff silver nitrate impregnation (g, h). **a, e:** Right side views. Note the distinct ridges (e) and the broadly ellipsoid body shape (a). **b, f:** Left side views, showing the conspicuous extrusomes (f) and food vacuoles (b) with granular contents, i.e., minute bacteria. **c:** Resting extrusomes. **d, i:** A squashed specimen with extrusomes having a strongly refractive posterior end (arrowheads), i.e., a non-exploded portion. **g, h:** Right side views, showing the fine-meshed silverline pattern, the pore of the contractile vacuole (g, arrow), and nassulid adoral organelle 3 (arrowheads). CV – contractile vacuole, CY – cytophyge, E – extrusomes, FV – food vacuoles, MA – macronucleus, OB – oral basket, PM – paroral membrane, SC – scutum, SP – silverline pattern, SK1 – somatic kinety 1, SU – preoral suture. Scale bars 5  $\mu\text{m}$  (i) and 20  $\mu\text{m}$  (a, b, d–h).

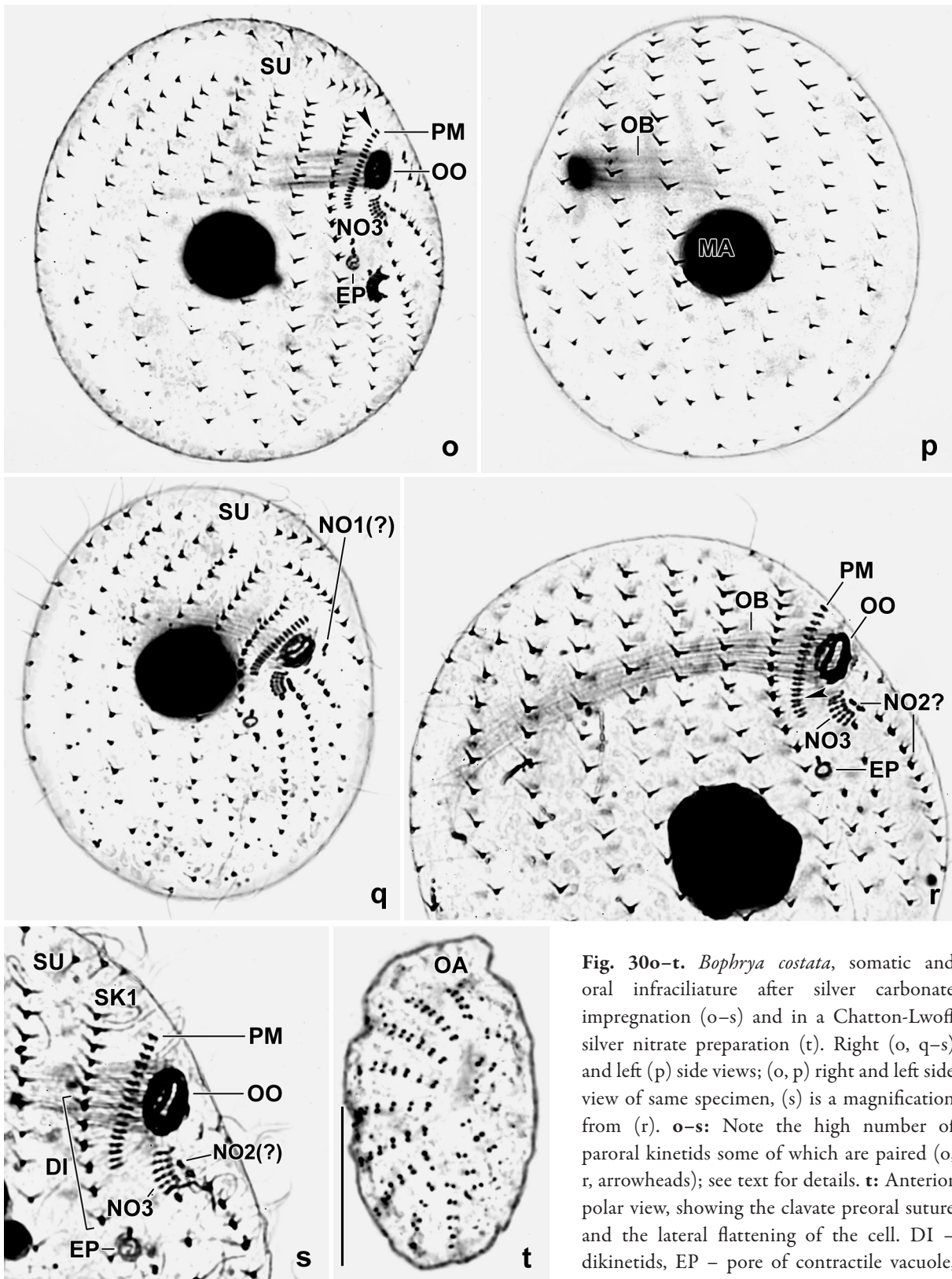
**Fig. 30j–n.** *Bophrya costata* after Chatton-Lwoff silver nitrate impregnation (j, k, m, n) and in a protargol preparation (l). One of the two granules composing the “dikinets” in silver nitrate preparations is very likely a parasomal sac or an alveolar cyst. **j, k, m:** Right side views, showing the somatic and oral infraciliature. Arrowheads mark nassulid organelle 3; the arrow in (k) denotes the anterior portion of a left side kinety. **l:** Protargol preparations show more paroral kinetids than silver nitrate preparations. **n:** Left side view. CY – cytophyge, E – extrusome hole, MA – macronucleus, PM – paroral membrane, SK1 – somatic kinety 1, SP – silverline pattern, SU – preoral suture. Scale bars 20  $\mu\text{m}$ .

**Etymology:** *Costata* is a Latin adjective referring to the cortical ridges.

**Description:** *Bophrya costata* is a conspicuous species due to the broad cortical stripes and the nearly discoid body shape. It has a low variability: of 24 features investigated, only two (number of monokinetids in somatic kinety 3, mesh size of silverline pattern) have a coefficient of variation higher than 15% (Table 13).

Size in vivo about  $50 \times 40 \mu\text{m}$  and  $47.3 \times 36.7 \mu\text{m}$  on average in Chatton-Lwoff silver nitrate preparations; adding 5% preparation shrinkage (Foissner 2014) results in  $49.7 \times 38.5 \mu\text{m}$  matching well the in vivo measurements (Table 13). Body broadly ellipsoid or almost discoid because flattened laterally about 2:1, or broadly ovate because moderately narrowed preorally. Dorsal side more convex





than ventral in about half of specimens. On ventral side a slight concavity marking oral area, anterior margin of concavity bordered by a slightly projecting cortical stripe (Fig. 29a, f, 30a, b, f-h, j-n, 31a, b, g; Table 13). Nuclear apparatus in or near body centre. Macronucleus in vivo

**Fig. 30o-t.** *Bophrya costata*, somatic and oral infraciliature after silver carbonate impregnation (o-s) and in a Chatton-Lwoff silver nitrate preparation (t). Right (o, q-s) and left (p) side views; (o, p) right and left side view of same specimen, (s) is a magnification from (r). o-s: Note the high number of paroral kinetids some of which are paired (o, r, arrowheads); see text for details. t: Anterior polar view, showing the clavate preoral suture and the lateral flattening of the cell. DI - dikinetids, EP - pore of contractile vacuole, MA - macronucleus, NO1, 2(?) - nassulid adoral organelles 1 and 2, NO3 - nassulid adoral organelle 3, OA - ventral side with oral apparatus, OB - oral basket, OO - oral opening, PM - paroral membrane, SK1 - somatic kinety 1, SU - preoral suture. Scale bar 15  $\mu$ m for (t), others without bar because heavily pressed with coverslip.

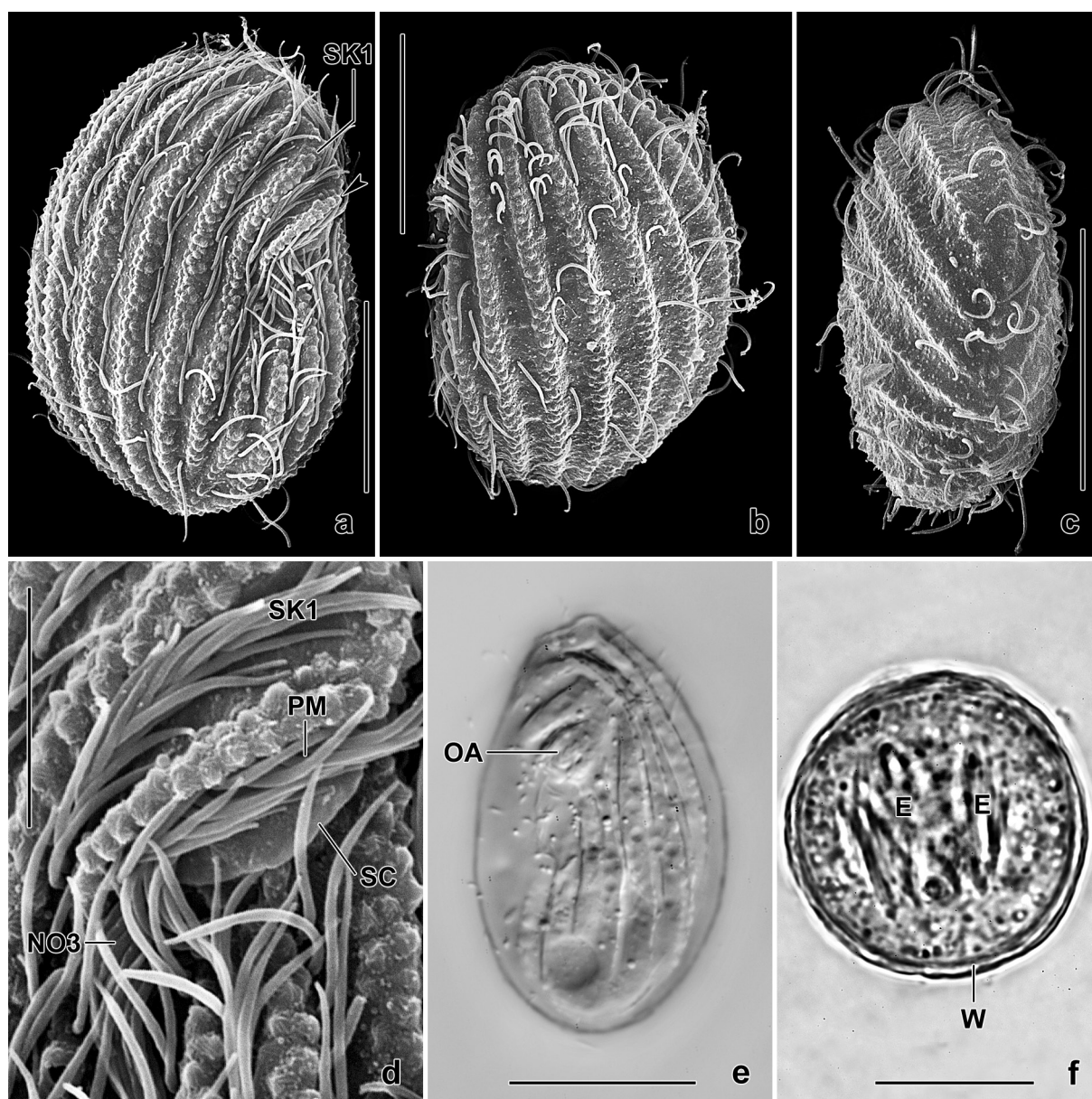


**Fig. 31a–f.** *Bophrya costata* from life (e, f) and in the scanning electron microscope (a–d). **a, b:** Right and left side view, showing the distinct cortical furrows and ridges containing the mitochondrial heads on which the cortex makes minute cones producing the serrate outline of the cell. The ciliature is sparse on the left side. The arrowhead in (a) marks the ridge covering the base of the paroral membrane. **c:** Oblique posterior polar view, showing the lateral flattening of the cell. **d:** Circumoral details. The most curious structure is the convex oral shield extending over the opening of the oral basket and the bases of the adoral organelles. The base of the paroral membrane is covered by a ridge. Somatic kinety 1 has ciliated dikinetids right of the oral area. **e:** Ventral view of a slightly pressed specimen. **f:** Resting cyst, diameter about 30  $\mu\text{m}$ . The large extrusomes arrange around the macronucleus in the centre of the cyst. E – extrusomes, NO3 – nassulid adoral organelle 3, OA – oral apparatus, PM – paroral membrane, SC – scutum, SK1 – somatic kinety 1, W – cyst wall. Scale bars 5  $\mu\text{m}$  (d), 15  $\mu\text{m}$  (a, b, f), and 20  $\mu\text{m}$  (c, e).

about 12  $\mu\text{m}$  across, in silver nitrate preparations only 7–8  $\mu\text{m}$  indicating considerable preparation shrinkage. Micronucleus not recognizable, neither in vivo nor in silver preparations (Fig. 29a, f, 30b, j, o; Table 13). Pore of contractile vacuole close posterior of right end of paroral membrane, i.e., slightly anterior of mid-body within or left of first postoral kinety (Fig. 29a, f, g, i, 30a, b, g, o, q–s; Table 13). Only 15–25 very narrowly cuneate extrusomes, conspicuous because about 10  $\mu\text{m}$  long (Fig. 29a, j, 30c, f; Table 13); split into sharp-edged pieces when pressed with coverslip. When

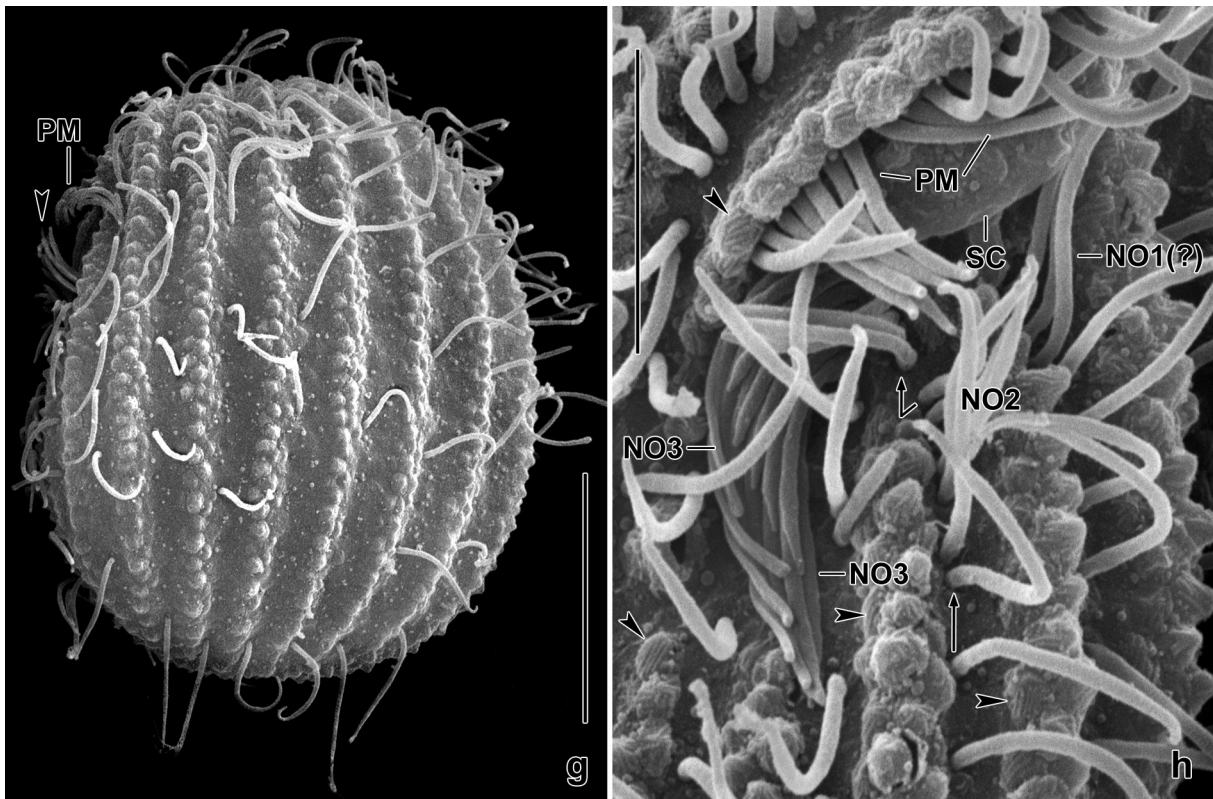


**Fig. 31g, h.** *Bophrya costata* in the scanning electron microscope. **g:** Left side view, showing the pronounced cortical furrows and ridges which contain the mitochondrial heads. The arrowhead marks cilia of nassulid adoral organelle 3. **h** (cp. Fig. 3d): Oral area, showing the nassulid adoral organelles 1, 2 (uncertain), and 3, the convex oral scutum covering the entrance to the oral basket, and supporting the paroral membrane the base of which is covered by a cortical ridge. The arrows mark dikinetids probably belonging to nassulid adoral organelle 2. The arrowheads denote a fine, longitudinal striation of the cortical cones on the mitochondrial heads. The cones produce the serrate outline of the cell (g). NO1–3 – nassulid adoral organelles, PM – paroral membrane, SC – scutum. Scale bars 5  $\mu\text{m}$  (h) and 20  $\mu\text{m}$  (g).

exploded, extrusome holes occasionally recognizable within and left of somatic kineties (Fig. 29i, 30k). Posterior end sometimes not unfolded and thus looking like tip of hymenostome trichocysts, e.g., from *Paramecium* (Fig. 29k, 30d, i). Fully exploded extrusomes acicular and up to 80  $\mu\text{m}$  long (Fig. 29l). Cortex colourless, strongly furrowed by broad pustulate stripes/ribs due to mitochondrial “heads” associated with minute cones hardly recognizable in vivo where cell margin appears studded with small convexities produced by mitochondrial heads. Cones generated by cortex, 0.5–1.5  $\mu\text{m}$  high, longitudinally striated. Mitochondria vermiform, up to 8  $\mu\text{m}$  long, with a conspicuous “head” 1.0–1.5  $\mu\text{m}$  across (Fig. 29a, c, d, 30a, b, e, f, 31a–d, g, h). Cytoplasm colourless, contains many lipid droplets 1–3  $\mu\text{m}$  across and some food vacuoles 3–10  $\mu\text{m}$  in diameter and filled with minute bacteria providing contents with a granular appearance (Fig. 29a, 30a, b, d). Silverline pattern narrowly meshed, individual meshes 0.5–2.0  $\mu\text{m}$  in size (Fig. 30g, h, m, n; Table 13). Movement inconspicuous, i.e., creeps and swims moderately rapid rotating about longitudinal axis.

Cilia about 8  $\mu\text{m}$  long in vivo and in SEM micrographs, arranged in 18 longitudinal, slightly curved rows: seven each on right and left side, four postoral; commence slightly subapical producing cuneate preoral suture. Ciliature rather sparse, many left side kinetids not ciliated; monokinetal except of some ciliated dikinetids in kinety 1 right of oral apparatus; intrakinetidal space increasing from anterior to posterior (Fig. 29a, f–i, 30e–h, j–t, 31a–e; Table 13).

Oral apparatus inconspicuous but rather complex, in shallow concavity far subapical (Fig. 29a, f, g, i, 30a, b, e, g, h, j–m, o–s, 31a, d, e, h; Table 13). Very likely three adoral organelles but only

organelle 3, near right end of paroral membrane, complete and thus distinct, composed of three rows of basal bodies each having six cilia up to 8  $\mu\text{m}$  long in vivo (Fig. 29a, 31d, h). Organelles 1 and 2 appear as dikinetids at anterior end of postoral kineties 4 and 3; organelle 1 (Fig. 30q) usually absent. Paroral membrane in vivo and in silver nitrate preparations about 10  $\mu\text{m}$  long, obliquely arranged and composed of about nine rather thick granules each with a 4  $\mu\text{m}$  long cilium; in silver carbonate and protargol preparations about 18 dikinetids arranged in indistinct pairs (Fig. 30j–o, q–s; Table 13); details should be clarified by TEM investigations. Oral field with a convex shield (scutum) extending over bases of adoral organelles and opening of oral basket in vivo about 6  $\mu\text{m}$  wide at distal end, extends to dorsal side where it curves to near posterior body end becoming gradually very narrow ( $\sim 1 \mu\text{m}$ ); composed of about 12 rods with concave distal end (Fig. 29b); basket opening deeply impregnating with silver carbonate possibly due to a ring of basal bodies (Fig. 30o, s).

**Resting cyst:** Inconspicuous because in vivo only 30  $\mu\text{m}$  across and a 1.5–2.0  $\mu\text{m}$  thick, externally slightly wrinkled wall (Fig. 29e, 31f). Studded with 0.5–2.0  $\mu\text{m}$ -sized lipid droplets and 15–25 extrusomes most around macronucleus. Cell or wall with very fine longitudinal lines, very likely caused by somatic kineties; rarely recognizable.

**Occurrence and ecology:** As yet found only at type locality. *Bophrya costata* appeared 5 d after rewetting the sample and reached moderate abundance in the non-flooded Petri dish culture after 10 d.

**Remarks:** This ciliate is easily identified because it has several uncommon features: a discoid body shape, large extrusomes, and broad cortical stripes. Such stripes occur only in two other nassophoreans, viz., *Pseudomicrothorax* (for a review, see Foissner et al. 1994), which has three complete nassulid adoral organelles left of the oral basket entrance (vs. one close posterior to right end of paroral membrane) and in *Lopezoterenia* Foissner, 1997. Further, *Pseudomicrothorax* has a smooth cortex while that of *Bophrya* is pustulate due to the headed mitochondria, a unique feature not known from any other ciliate. The same applies to the oral shield unique in nassophoreans.

### ***Wolfkoscia* Foissner, Agatha & Berger, 2002**

Although I did not (yet?) find *Wolfkoscia* in Australia, I describe a new species each from Botswana and the Brazilian Pantanal. The type species, *W. loeffleri*, was discovered in Costa Rica and occurs also in two African sites, viz., in Saudi Arabia and Namibia (Foissner et al. 2002). These data suggest a Gondwanan distribution of the genus because I did not find it in hundreds of Laurasian samples.

#### ***Wolfkoscia acuta* nov. spec.**

(Fig. 32a–f, 33a–n; Table 14 on p. 319)

**Diagnosis** (averages are provided): Size in vivo 70  $\times$  25  $\mu\text{m}$ ; oblongate with posterior end bluntly acute. Macronucleus usually in posterior half of cell. Extrusomes normally cuneate, 9  $\mu\text{m}$  long. 18 somatic ciliary rows and 10 vertical ciliary rows in nassulid organelle 3. Paroral membrane dome-shaped, composed of 13 dikinetids.

**Type locality:** Soil from the floodplain of the Chobe River, Kaborobole Peninsula, Botswana, 25°S, 17°50'E.

**Type material:** The slide containing the holotype (Fig. 32b, d, e) and four paratype slides with Chatton-Lwoff silver nitrate-impregnated specimens have been deposited in the Biology Centre of

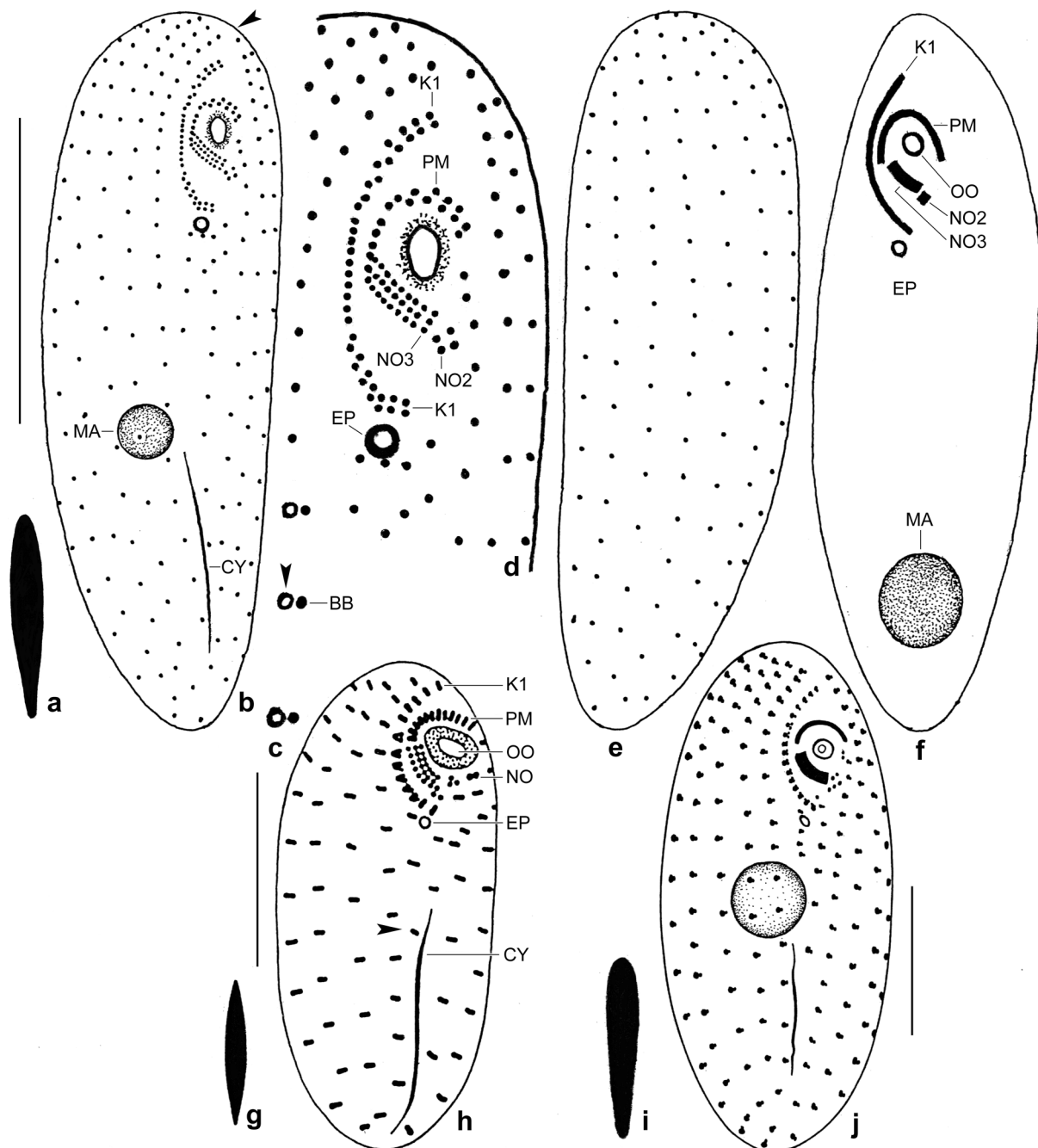


**Fig. 32a–j.** Comparison of *Wolfkosia acuta* (a–f), *W. loeffleri* (g, h), and *W. pantanalensis* (i, j) after Chatton-Lwoff silver nitrate impregnation. **a:** Extrusome, length 8  $\mu\text{m}$ . **b, d, e:** Ventral and dorsal views of holotype specimen, length 70  $\mu\text{m}$ . The arrowhead in (b) marks the preoral suture. Note the acute posterior end. **c:** Kinetid structure, showing parasomal sac (arrowhead) and basal body. **f:** Ventral view of a paratype specimen, showing the dome-shaped paroral membrane and nassolid organelle 2 which consists of four basal bodies (d). Note the subterminal location of the macronucleus. **g, h:** Extrusome, length 4  $\mu\text{m}$ , and ventrolateral view of infraciliature. **i, j:** Extrusome, length 9  $\mu\text{m}$ , and ventral view of infraciliature. BB – basal body, CY – cytophyge, EP – excretory pore of contractile vacuole, K1 – kinety 1, MA – macronucleus, NO2, 3 – nassolid organelles, OO – oral opening, PM – paroral membrane. Scale bars 30  $\mu\text{m}$  (b, e, f) and 15  $\mu\text{m}$  (h, j).

the Upper Austrian Museum in Linz (LI). Relevant specimens have been marked by black ink circles on the coverslip. For slides, see Fig. 14a–h in Chapter 5.

**Etymology:** Named after the acute posterior body end.

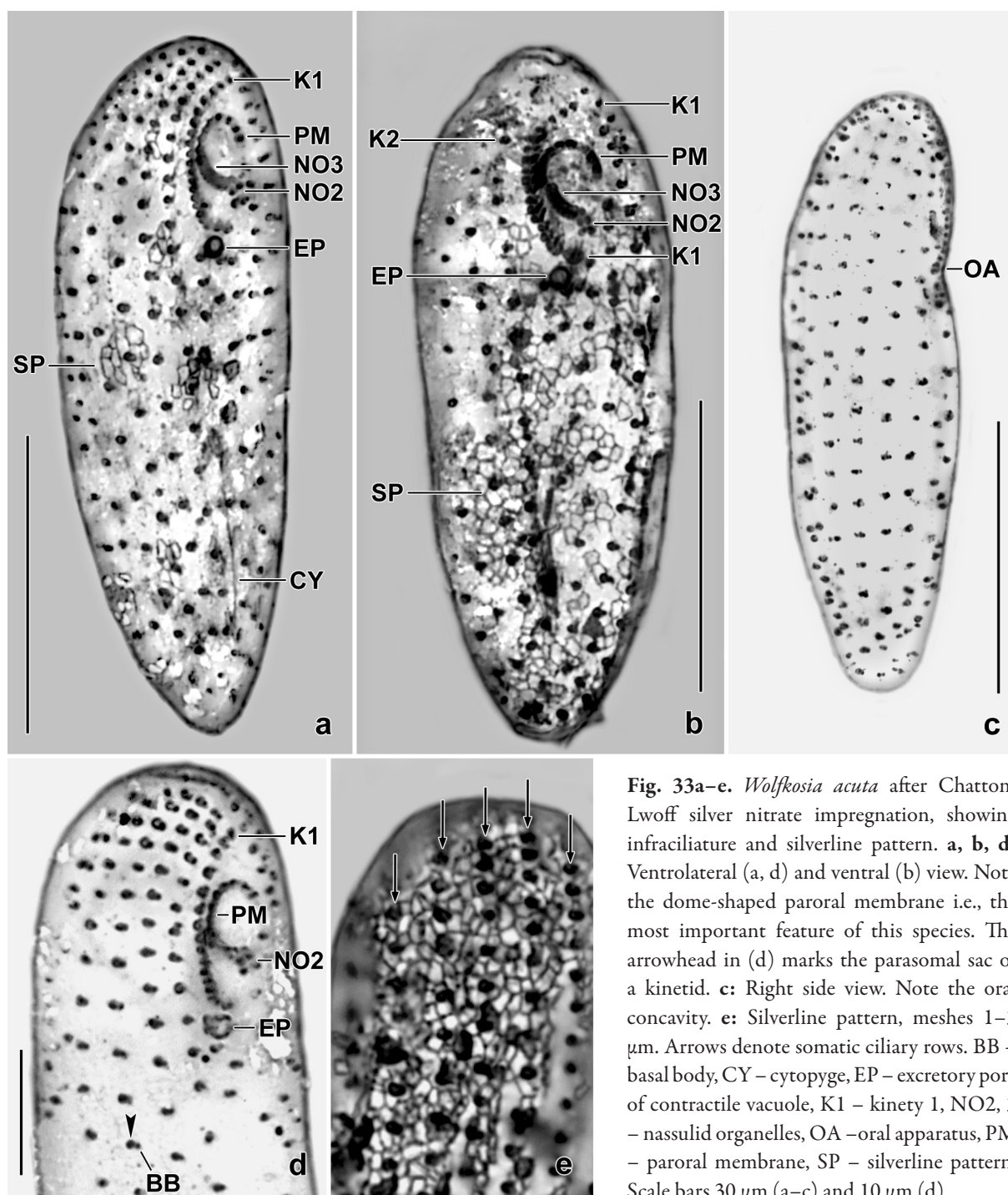


**Fig. 33a-e.** *Wolfkoscia acuta* after Chatton-Lwoff silver nitrate impregnation, showing infraciliature and silverline pattern. **a, b, d:** Ventrolateral (a, d) and ventral (b) view. Note the dome-shaped paroral membrane i.e., the most important feature of this species. The arrowhead in (d) marks the parasomal sac of a kinetid. **c:** Right side view. Note the oral concavity. **e:** Silverline pattern, meshes 1–3  $\mu\text{m}$ . Arrows denote somatic ciliary rows. BB – basal body, CY – cytophyge, EP – excretory pore of contractile vacuole, K1 – kinety 1, NO2, 3 – nassulid organelles, OA – oral apparatus, PM – paroral membrane, SP – silverline pattern. Scale bars 30  $\mu\text{m}$  (a–c) and 10  $\mu\text{m}$  (d).

**Description:** This species was very rare in the non-flooded Petri dish culture, i.e., I found only a single specimen and thus live observation is incomplete. Fortunately, I found nearly 20 specimens in the silver nitrate preparations; together, the observations provide a solid description.

Of 18 features measured, six have a coefficient of variation >15%, suggesting moderate variability (Table 14).

Size in vivo 60–75  $\times$  15–30  $\mu\text{m}$ , on average about 70  $\times$  25  $\mu\text{m}$  when 5% preparation shrinkage have been added. Body usually oblongate, rarely elongate ellipsoid or ellipsoid; posterior end usually bluntly acute, rarely narrowly rounded (Fig. 32b, f, 33a–c, f, k, l; Table 14). Nuclear apparatus in rear body half, in some specimens even subterminal (Fig. 32b, f, 33f, l; Table 14); macronucleus globular, about 9  $\mu\text{m}$  across; single micronucleus in small concavity of macronucleus. Excretory

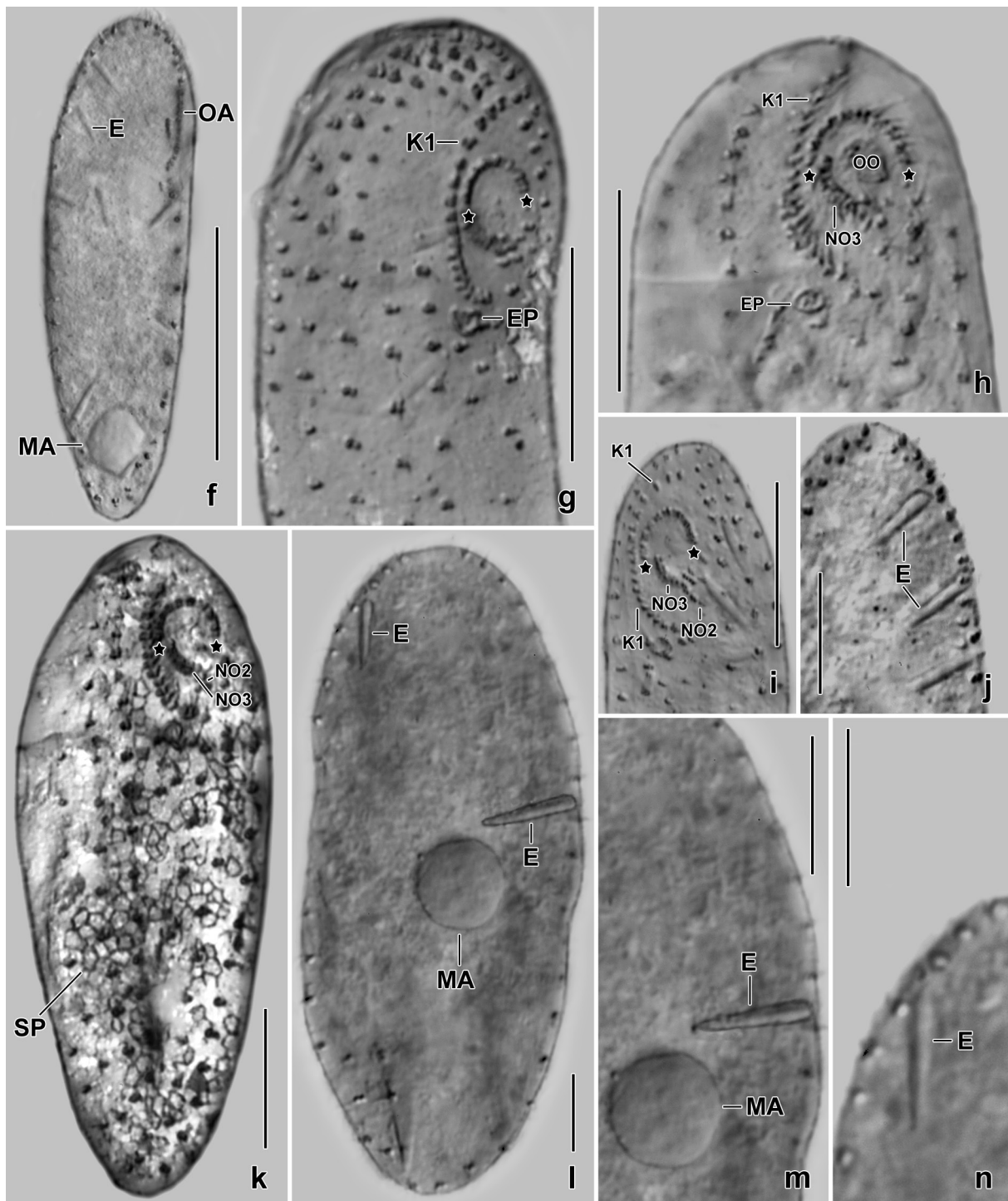


**Fig. 33f–n.** *Wolkosia acuta* after Chatton-Lwoff silver nitrate impregnation; contrast enhanced in under-impregnated specimens and extrusomes by interference contrast microscopy (f–j, l–n). **f:** A specimen with subterminally located macronucleus. **g, h, i, k:** Oral apparatus showing, inter alia, a main character of *W. acuta*, viz., the dome-shaped paroral membrane (ends marked by asterisks). **j, l–n:** Extrusomes 7–9  $\mu\text{m}$  long, (m) and (n) from (l). E – extrusomes, EP – excretory pore of contractile vacuole, K1 – kinety 1, MA – macronucleus, NO2, 3 – nassulid organelles, OA – oral apparatus, OO – oral opening, SP – silverline pattern. Scale bars 30  $\mu\text{m}$  (f), 15  $\mu\text{m}$  (g, h, i, k), and 10  $\mu\text{m}$  (j, l–n).

pore of contractile vacuole at end of dikinetal part of somatic kinety 1 (Fig. 32b, d, f, 33a, b, d, g, h; Table 14). Extrusomes of trichocyst type, narrowly cuneate, 6–9  $\mu\text{m}$  long (Fig. 32a, 33j, l–n).

Somatic and oral infraciliature and silverline pattern as in congeners (Foissner et al. 2002), except of some morphometrics and the dome-shaped paroral membrane (Fig. 32b–f, 33a–d, g–i, k;

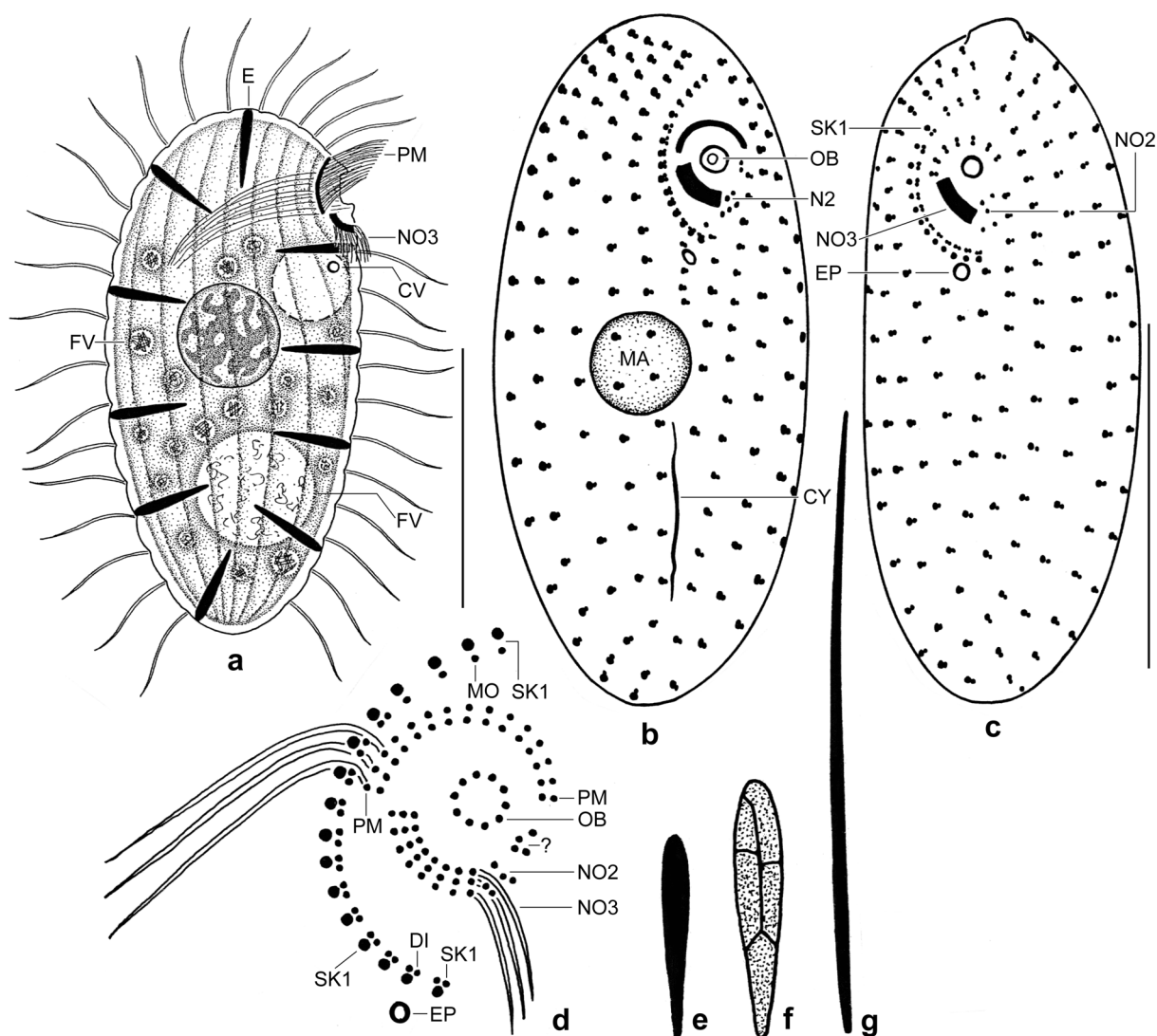


**Fig. 34a–g.** *Wolfkosia pantanalensis* from life (a, d [pro parte, e–g]) and after silver nitrate impregnation (Chatton-Lwoff method). **a:** Right side view of a representative specimen, length 60  $\mu\text{m}$ . **b, c:** Ventral view of the holotype and a paratype specimen, showing the somatic and oral infraciliature. **e, f:** Resting (10  $\mu\text{m}$ ) and squashed resting extrusome (cp. Fig. 35f), showing sharp-edged fragmentation. **g:** Exploded extrusome (up to 80  $\mu\text{m}$  long). CV – contractile vacuole and its excretory pore, CY – cytopyge silver line, DI – dikinetid, E – extrusome, EP – excretory pore of contractile vacuole, FV – food vacuoles, MA – macronucleus, MO – monokinetid, NO – nassulid organelles 2 and 3, OB – oral basket, PC – parasomal sac, PM – paroral membrane, SK1 – somatic kinety 1, ? – nassulid organelle 1. Scale bars 30  $\mu\text{m}$  (a) and 25  $\mu\text{m}$  (b, c).

Table 14). Oral area slightly concave (Fig. 33c); very fine nematodesmata forming an inconspicuous basket.

**Occurrence and ecology:** As yet found only at type locality. In the non-flooded Petri dish, it appeared 24 h after rewetting the sample, indicating a r-selected way of life. The abundance was very low and the species did not re-appear after looting the culture for preparations.

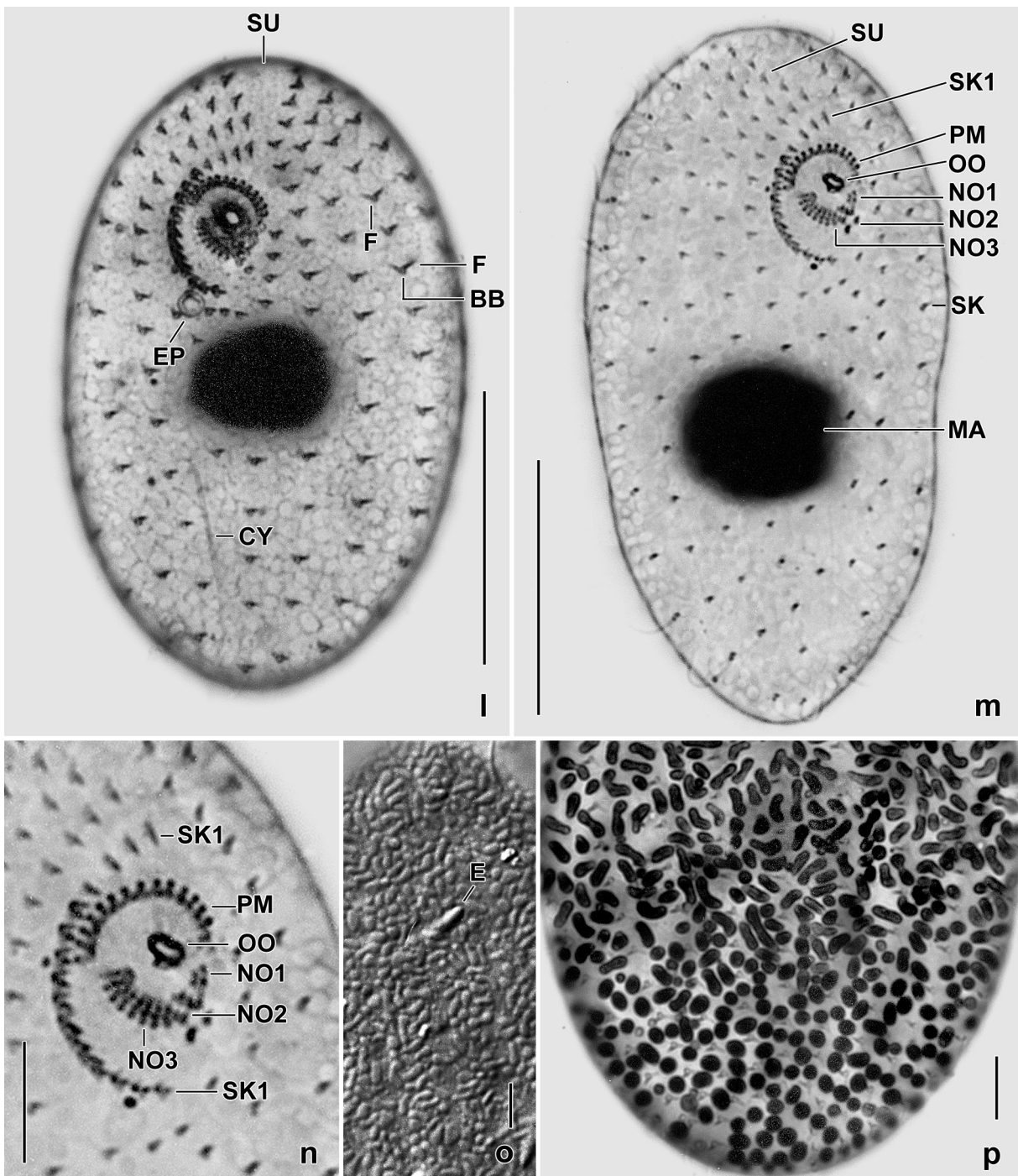
**Remarks:** *Wolfkosia acuta* is possibly most closely related to  $\rightarrow$  *W. pantanalensis* (Fig. 32b, j, 33a–c, f–h, k; Table 14). Morphologically, these species differ by body shape (with acute vs. broadly rounded posterior region; Fig. 32b, j) and the paroral membrane which is inverted U-shaped vs. moderately convex (Fig. 32f, j). Morphometrically, they differ by body length (67  $\mu\text{m}$  vs. 53  $\mu\text{m}$ ), by the ratio body length:width (2.9:1 vs. 2.4:1) and by the distance between anterior body end and macronucleus (38  $\mu\text{m}$  vs. 23  $\mu\text{m}$ ). The most conspicuous differences are the acute (vs. ellipsoid) body shape and the inverted U-shaped (vs. moderately convex) paroral membrane.



*Wolfkoscia pantanalensis* nov. spec.  
(Fig. 34a–g, 35a–v; Table 14 on p. 319)

**Diagnosis:** Size in vivo about  $55 \times 25 \mu\text{m}$ . Ellipsoid with posterior third usually slightly narrowed. Nuclear apparatus in mid-body. Pore of contractile vacuole close underneath posterior region of somatic kinty 1. Extrusomes narrowly obovate or cuneate, about  $10 \mu\text{m}$  long in vivo. 18 somatic ciliary rows and eight vertical ciliary rows in nassulid organelle 3. Paroral membrane distinctly convex, composed of about eight dikinetids.

**Type locality:** Floodplain soil from the Paraná River at Porto Rico Island, Paraná state, Pantanal of Brazil,  $23^{\circ}17'20''\text{S}$ ,  $53^{\circ}27'16''\text{W}$ . Sample kindly provided by Dr. Machado Velho.



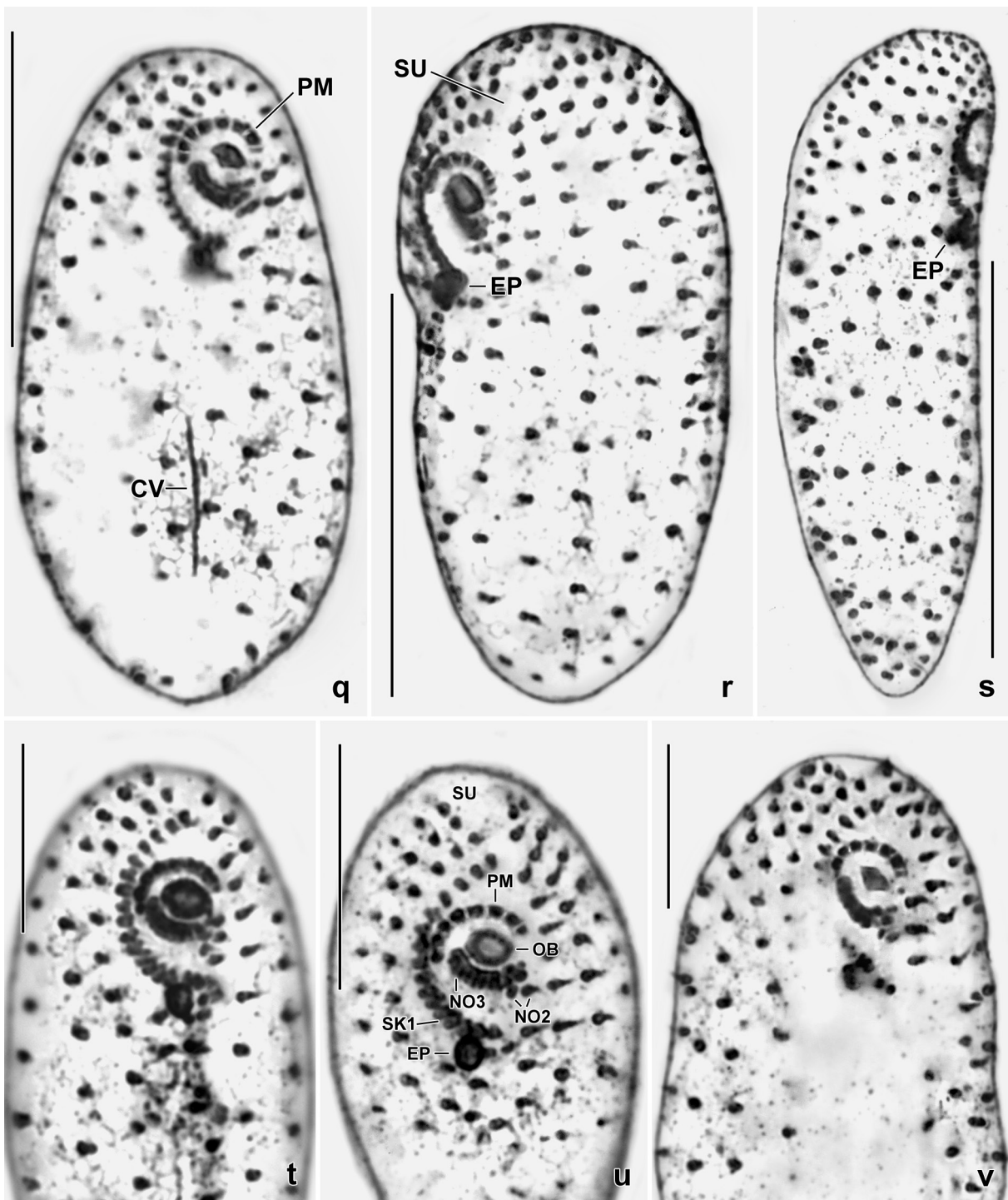


**Fig. 35q–v.** *Wolfkoscia pantanalensis* after Chatton-Lwoff silver nitrate impregnation. In this preparation (cp. Fig. 351–p) details of the oral apparatus are well recognizable, for instance, the paroral membrane which consists of seven or eight dikinetids forming minute squares (q, u, v). Nassulid organelle 3 is composed of eight kineties with three basal bodies each (u) while organelle 2 consists of five scattered granules (q, t–v). The posterior half of somatic kinety 1 consists of zigzagging dikinetids (t, u). The pore of the contractile vacuole is close to the posterior end of somatic kinety 1 (r–u). Body shape is ovate in ventral view (q) while obovate in left side view (r). The shape of the specimen in (s) highly resembles → *Wolfkoscia acuta*. CY – cytophyge, EP – excretory pore of contractile vacuole, NO2,3 – nassulid organelles, OB – oral basket, PM – paroral membrane, SK1 – somatic kinety 1, SU – preoral suture. Scale bars 30  $\mu\text{m}$  (q–s) and 15  $\mu\text{m}$  (t–v).

**Type material:** The slide containing the holotype (Fig. 34b, c) and four paratype slides with silver nitrate-impregnated specimens have been deposited in the Biology Centre of the Upper Austrian

Museum in Linz (LI). Relevant specimens have been marked by black ink circles on the coverslip. For slides, see Fig. 15a–g in Chapter 5.

**Etymology:** Named after the region discovered, i.e., the famous Pantanal wetland in Brazil.

**Description:** This species was rare in the non-flooded Petri dish culture. Of 20 features measured, only the location of the macronucleus and the number of paroral dikinetids have a coefficient of variation >15%, indicating low variability.

Size in vivo  $45\text{--}65 \times 20\text{--}30 \mu\text{m}$ , as calculated from some in vivo measurements and the morphometric data in Table 14. In lateral view ellipsoid or slightly obovate; slightly flattened, ventral view thus ellipsoid or slightly elongate ellipsoid (Fig. 34a–c, 35e, g; Table 14). Nuclear apparatus in mid-body, in vivo about  $15 \mu\text{m}$  across while only  $8 \mu\text{m}$  in silver nitrate preparations very likely due to strong shrinkage, as in congeners; nucleolus reticulate (Fig. 34a, b, 35b, k; Table 14); a minute micronucleus in small concavity of macronucleus. Contractile vacuole posterior of oral apparatus, excretory pore underneath posterior region of somatic kintety 1 (Fig. 34a–c, 35a, b, l; Table 14). Cytopyge in line with excretory pore, extends in posterior half of cell (Fig. 34b, 35l). Resting extrusomes attached almost perpendicularly to cortex, narrowly obovate or cuneate, conspicuous because about  $10.0 \times 1.5\text{--}2.0 \mu\text{m}$  in vivo and in silver nitrate preparations, comparatively rare and thus not forming a fringe; breaks into sharp-edged pieces when strongly pressed with coverslip; when expelled, cell performs a jerky movement and the extrusome elongates to an about  $80 \mu\text{m}$  long rod with acute ends (Fig. 34a, e–g, 35a, d, h–j; Table 14). Cortex bright and about  $1 \mu\text{m}$  thick, with distinct ciliary pits providing outline with many minute convexities (Fig. 34a, 35d, g). Most mitochondria underneath cortex, conspicuous because numerous and  $4\text{--}6 \mu\text{m}$  long, many serpentine (Fig. 35a, o, p). Cytoplasm colourless, usually studded with food vacuoles only  $2\text{--}3 \mu\text{m}$  across and containing  $2\text{--}6$  minute, ellipsoid bacteria; usually some larger vacuoles about  $15 \mu\text{m}$  across and with loose contents (Fig. 34a, 35a–c). Moves rapidly appearing like a swimming ellipsoid.

Somatic and oral ciliature as well as silverline pattern as in type species (Foissner et al. 2002), except of some morphometrics (Fig. 34b–d, 35l–n, q–v; Table 14). Some additional data (Fig. 34a–d, 35l, m): distal end of oral basket hardly projecting and cornered, composed of  $10\text{--}12$  rods extending to dorsal side and forming an indistinct basket; paroral cilia about  $7 \mu\text{m}$  long, only one basal body of dikinetids ciliated; cilia of nassulid organelle 3 about  $4 \mu\text{m}$  long in vivo.

**Occurrence and ecology:** As yet found only at type locality. Recognized 7 d after rewetting the dry sample, indicating a k-selected lifestyle. The abundance was low and the species did not recover after looting the culture for preparations. More detailed site and sample data, see Foissner (2003).

**Remarks:** At first glance, *W. pantanalensis* highly resembles *W. loeffleri*, type species of the genus discovered in Costa Rica, Central America (Foissner et al. 2002). However, there is at least one distinct difference validated by a reinvestigation of the type species *W. loeffleri*, viz., the shape and size of the extrusomes (narrowly cuneate or obovate and  $10 \mu\text{m}$  long vs. fusiform and  $4\text{--}5 \mu\text{m}$  long (compare Fig. 106f in Foissner et al. 2002 and Fig. 34g, 35h; Table 14). Three morphometric differences support this decision (Table 14): body length  $55 \mu\text{m}$  vs.  $45 \mu\text{m}$ ; anterior body end to nassulid organelle 3 ( $12 \mu\text{m}$  vs.  $8 \mu\text{m}$ ); number of somatic ciliary rows ( $18$  vs.  $14$ ).

### 4.2.3 Colpodea

For some recent comments on this taxon by W. Foissner, see Foissner (2016, p. 264).

#### *Bursaria* Müller, 1773

**Diagnosis:** Moderately large to very large, bursiform Bursariidae (Colpodea) with keyhole-shaped oral aperture extending from anterior body end to mid-body or to near posterior end. Paroral

formation (right oral polykinetid) on edge and inner side of dorsal and right wall of buccal cavity, consists of many rather regularly spaced kineties forming a curved ribbon (septum). Adoral zone very large, composed of many equidistantly spaced polykineties forming a sigmoid, proximally slightly to strongly recurved ribbon.

**Type species:** *Bursaria truncatella* Müller, 1773 (by subsequent designation by Apstein 1915, p. 122; see Aescht 2001, p. 35).

**Remarks:** The present investigations confirm the characterization by Foissner (1993), who distinguished two species, viz., *B. truncatella* and *B. ovata* Beers, 1952, the second redescribed by Foissner (2016). Here, five further species are described from Africa, Austria, the USA, and Australia, based on morphologic and morphometric differences summarized in Fig. 36a–h, 37a, Table 15, and the identification key (see below).

**Discussion of main features:** *Bursaria* species are rather difficult to investigate due to their large size. A combination of live observation and various silver techniques is indispensable. The basic morphology, as described by Foissner (1993), is very similar in the seven species distinguished while pronounced morphometric differences are frequent (Table 15). For instance, the large *B. ovata* has the smallest adoral polykineties.

Each species is characterized morphometrically and shown by a multitude of figures. Based on these data, the valuable features shown in Table 15 were selected.

**Body size:** The smallest species are → *B. africana* (~305 µm) and *B. truncatella* (376 µm; Table 15), the largest are → *B. fluviatilis* (681 µm) and → *B. americana* (~500 µm). Although body size depends on various environmental conditions, the considerable distance (400 µm) between the smallest and the largest species suggests body size as a valuable feature for some species (Fig. 37a).

**Anterior body end to posterior end of oral (ventral) cleft in percent of body length:** Surprisingly, this feature is very variable and rather similar in all species, suggesting it as a minor character for species identification. The smallest value is 48% in *B. fluviatilis*, the largest value is 64% in *B. ovata*.

**Posterior body end to deepest point of left oral polykinetid in percent of body length:** The lowest values belong to → *B. americana* (10%) and → *B. truncatella* (17%) while the highest values occur in the Australian species → *B. fluviatilis* (31%) and → *B. uluruensis* (29%). The considerable differences between the lowest and highest value suggests this as a valuable species character.

**Number of ciliary rows:** Although the ciliary rows are difficult to count, they are a valuable feature: the lowest value (215 rows in the Austrian *B. truncatella*) is much smaller than the highest (581 rows) in → *B. americana*.

**Number of polykineties in left oral polykinetid:** This is a very valuable character because it separates → *B. fluviatilis* (72) clearly from, e.g. → *B. ovata* (148), → *B. uluruensis* (103), and → *B. salisburgensis* (101).

**Maximum width of adoral polykineties:** This is also a valuable character because it separates → *B. fluviatilis* (63 µm), → *B. uluruensis* (62 µm), and → *B. americana* (64) from → *B. ovata* (33 µm), → *B. truncatella* (50 µm), and → *B. salisburgensis* (51). Briefly, the width of the largest polykineties is >60 µm in the first group while about ≤50 µm in the second group.

**Shape of the left oral polykinetid:** It is distinctly recurved in → *B. ovata* (Fig. 36f; Foissner 2016), → *B. uluruensis* (Fig. 36d), → *B. americana* (Fig. 36g, h), and → *B. salisburgensis* (Fig. 36e) while not or indistinctly recurved in → *B. fluviatilis* (Fig. 36c), → *B. africana* (Fig. 36b), and *B. truncatella* (Fig. 36a). This is an important feature because it separates, e.g., *B. truncatella* from *B. salisburgensis*.

**Extrusome shape and height of cortical extrusome fringe:** There are three types of extrusomes (rod-like, globular, unstructured) which distinguish several species very clearly (Fig. 27b) but the investigation is difficult in the rod-shaped type.

**Barren stripe along right oral polykinetid:** Possibly, this is an important feature because the stripe is absent in two of the four populations investigated in the scanning electron microscope (Table 15). Unfortunately, data are lacking for the other species.

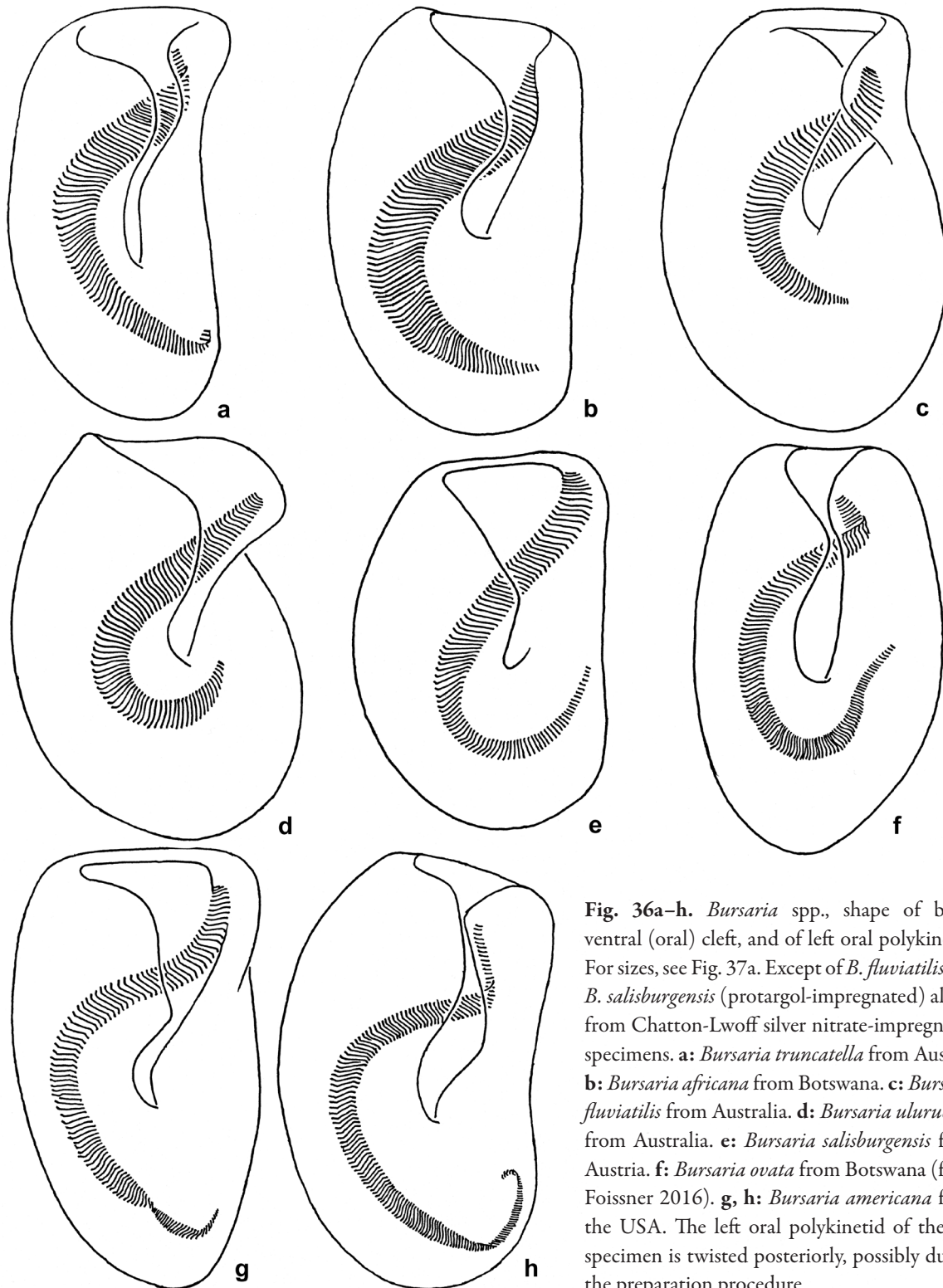


**Fig. 36a–h.** *Bursaria* spp., shape of body, ventral (oral) cleft, and of left oral polykinetid. For sizes, see Fig. 37a. Except of *B. fluviatilis* and *B. salisburgensis* (protargol-impregnated) all are from Chatton-Lwoff silver nitrate-impregnated specimens. **a:** *Bursaria truncatella* from Austria. **b:** *Bursaria africana* from Botswana. **c:** *Bursaria fluviatilis* from Australia. **d:** *Bursaria uluruensis* from Australia. **e:** *Bursaria salisburgensis* from Austria. **f:** *Bursaria ovata* from Botswana (from Foissner 2016). **g, h:** *Bursaria americana* from the USA. The left oral polykinetid of the left specimen is twisted posteriorly, possibly due to the preparation procedure.

*Granular cortex vacuoles* (Fig. 46p, q): This organelle, first described by Foissner (2016), has been observed in → *B. salisburgensis*, → *B. uluruensis*, and → *B. ovata* (Foissner 2016) when cells were fixed in Stieve’s fluid. In → *B. americana* fixed with this fluid, granular vacuoles were absent, indicating that these vacuoles could be a valuable species feature.

*Shape and size of resting cyst:* Distinct morphological differences are absent while the size, e.g., is conspicuously smaller in → *B. africana* (153 μm) than in the other species (190–328 μm).

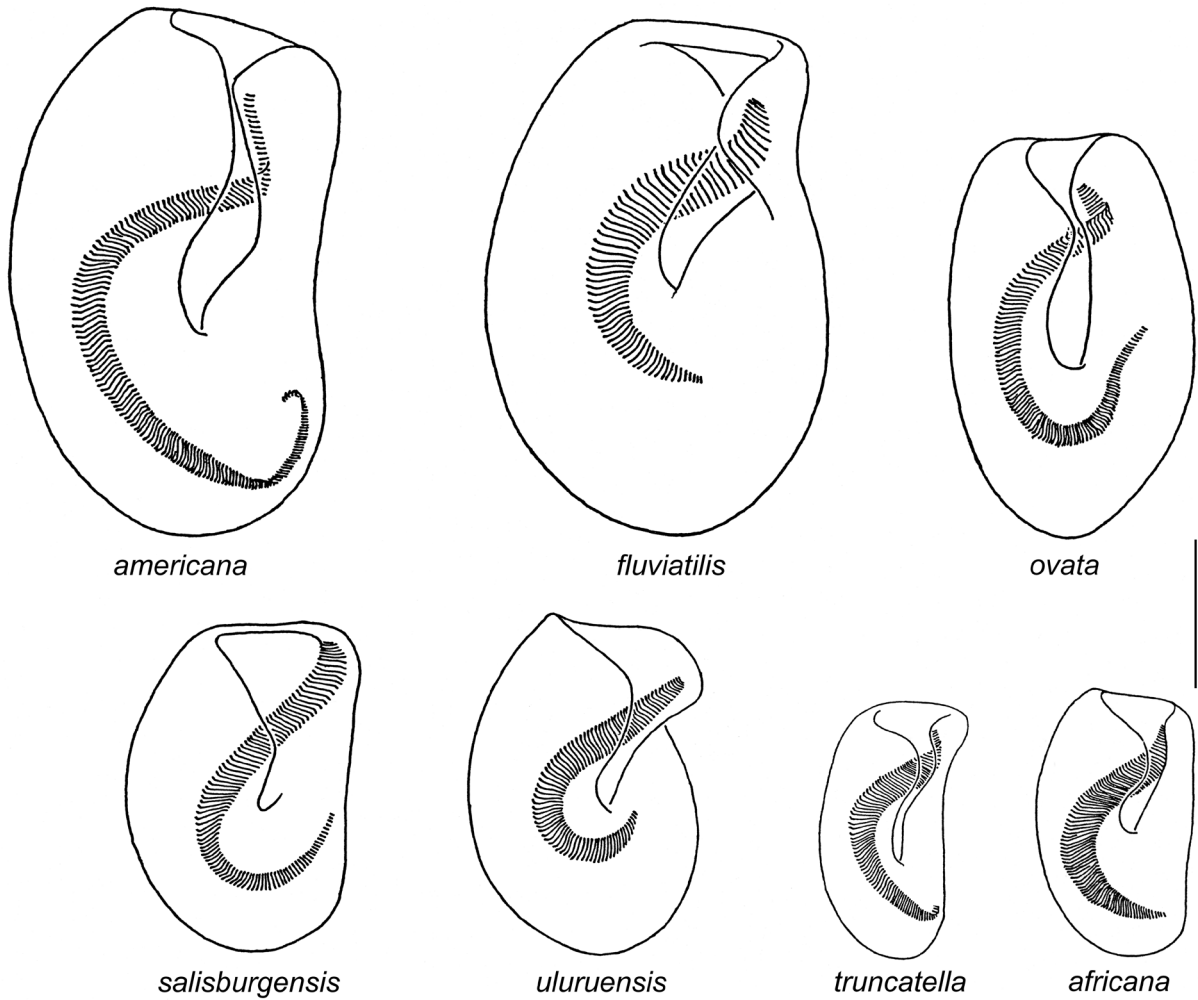


Fig. 37a. Average size comparison of the seven *Bursaria* species recognized. Drawn to scale, bar 200  $\mu\text{m}$ .

**Molecular phylogeny** (Fig. 38): The five species investigated differ only slightly in the nuclear SSU-DNA. Two clades can be recognized: one contains the species with rod-shaped extrusomes, viz.,  $\rightarrow$  *B. ovata* and  $\rightarrow$  *B. americana* while the other clade contains the species with globular or unstructured ( $\rightarrow$  *B. salisburgensis*) extrusomes, viz.,  $\rightarrow$  *B. truncatella*,  $\rightarrow$  *B. fluviatilis*, and  $\rightarrow$  *B. uluruensis*. The two last mentioned species as well as  $\rightarrow$  *B. truncatella* have very similar nuclear sequences although they are distinct morphospecies.

### Key to *Bursaria* species

The key uses only three features shown in Fig. 37a, b: the shape of the left polykinetid, the distance from posterior body end to the deepest point of the left oral polykinetid (% of body length), and the shape of the extrusomes (careful live observation indispensable, left row in Fig. 37b drawn to scale, 20  $\mu\text{m}$ ). For details, see description of individual species and Tables 15–18.

- 1 Left oral polykinetid recurved, i.e.,  $\pm$  U-shaped because posterior region recurved to or near to mid-body ..... 2
- Left oral polykinetid indistinctly recurved ..... 5
- 2 Extrusomes cylindroid or globular ..... 3
- Extrusomes form a structureless, 3–4  $\mu\text{m}$  thick plate ..... *B. salisburgensis*

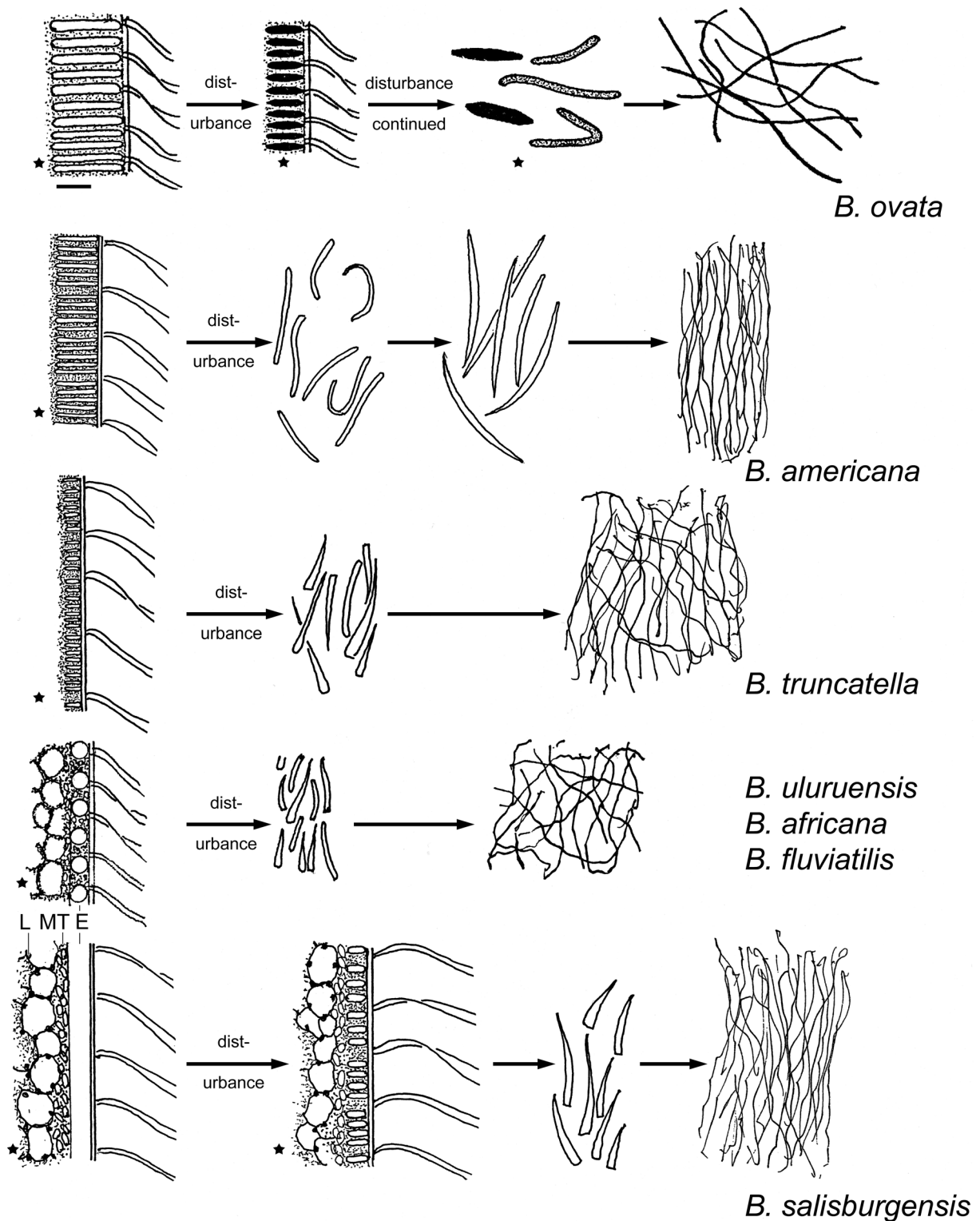
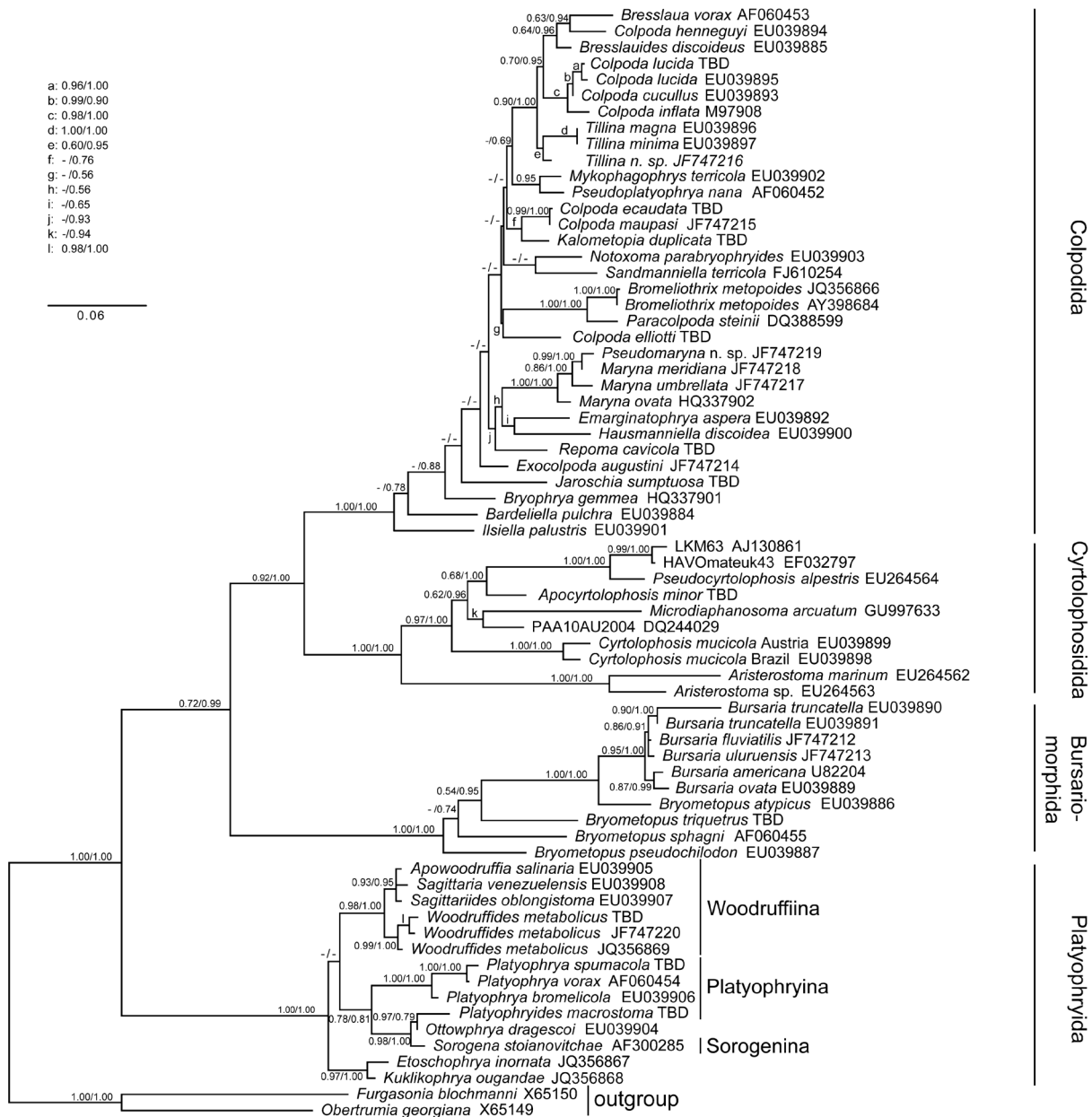


Fig. 37b. Extrusomes in the seven *Bursaria* species recognized. Drawn to scale, bar 20 µm. Asterisks: from in vivo observation, the other after methyl green-pyronin staining.

- |   |  |                      |
|---|--|----------------------|
| 3 | Extrusomes cylindroid, about 10 µm or 3–5 µm long .....  | 4                    |
| – | Extrusomes ~20 µm long, vacuole-like, become about 10 µm long, refractive rods in early explosion stages, body size 521 × 323 µm ..... | <i>B. ovata</i>      |
| 4 | Extrusomes about 10 µm long, body size 692 × 427 µm .....  | <i>B. americana</i>  |
| – | Extrusomes globular, 3–5 µm across; deepest point of left oral polykinetid at 29% of body length; body size 442 × 256 µm .....         | <i>B. uluruensis</i> |



**Fig. 38.** Molecular phylogeny of *Bursaria* species, based on Foissner et al. (2011). EU039890 and EU039891: *Bursaria truncatella* from Etosha Pan, Namibia. JF747212: *Bursaria fluviatilis* from Darling River in Australia. JF747213: *Bursaria uluruensis* from Uluru (Ayers Rock) in Australia. U82204: *Bursaria americana* from the USA, Carolina population. EU 039889: *Bursaria ovata* from Niger River, West Africa.

- 5 (1) Extrusomes globular, about 3  $\mu\text{m}$  across; deepest point of left oral polykinetid at 31% of body length ..... *B. fluviatilis*
- Extrusomes cylindroid, 3–5  $\mu\text{m}$  long or globular and 3–4  $\mu\text{m}$  across ..... 6
- 6 Extrusomes cylindroid, 3–5  $\mu\text{m}$  long ..... *B. truncatella*
- Extrusomes globular, 3–4  $\mu\text{m}$  across ..... *B. africana*

**Geographic distribution:** Over the years, I found many *Bursaria* populations but only some I investigated in detail. This showed at least seven species one of which,  $\rightarrow$  *B. ovata*, has been redescribed by Foissner (2016). I discovered also a new cortical organelle, viz., granular (“curious”) vacuoles in most species (Fig. 46p, q). These vacuoles become recognizable only after

Stieve fixation; they are about  $20 \times 15 \mu\text{m}$  in size and are distinctly granulated by argyrophilic material (Foissner 2016).

*Bursaria* species have resting cysts with a thick wall that has an escape opening (Fig. 42a, b, f–i, 44n, q, 48s, t, v, Table 15). In spite of this, only  $\rightarrow B. truncatella$  and  $\rightarrow B. ovata$  have a wide distribution. The former has been reported from Central Europe (this paper), Namibia (Foissner et al. 2002), the Neotropis (Foissner 2016), and very likely from Antarctica (for a review, see Foissner 1993). The latter has been reported from Europe and Russia, the USA, Botswana (Africa), and the Neotropis (for reviews, see Foissner 1993, 2016, Foissner et al. 2002). The unique Australian species ( $\rightarrow B. fluviatilis$  and  $\rightarrow B. uluruensis$ ) suggest a restricted distribution of at least some species.

There are many reports on  $\rightarrow B. truncatella$  (for a review, see Foissner 1993). Very likely, most are misidentifications, e.g., the New Zealand population studied by Bary (1950), which is very likely  $\rightarrow B. fluviatilis$  or  $\rightarrow B. uluruensis$  as indicated by the short left oral polykinetid. However, usually it is impossible to re-identify the old descriptions mainly because the extrusomes have been not or insufficiently described.

### Description of *Bursaria* species

#### *Bursaria truncatella* Müller, 1773

(Fig. 36a, 37a, b, 38, 39a–g; Tables 15, 16 on p. 321, 322)

**Material:** The population described was found in a temporary, eutrophic (by excrements of grazing cows) pond in the Austrian Central Alps ( $47^{\circ}\text{N}$ ,  $12^{\circ}47'\text{E}$ ) about 2000 m above sea level (detailed description, see Foissner 1980, Weidetümpel 1).

**Improved diagnosis** (excludes all literature data; measurements are from silver nitrate-impregnated specimens, add 5% preparation shrinkage to obtain in vivo values; averages are given, see Table 16 for extremes): Bursiform with left side flat or slightly concave, right side more or less convex; body size  $376 \times 190 \mu\text{m}$ ; ventral cleft extends 54% of body length. Left oral polykinetid not recurved, consists of 83 polykineties with a maximum width of  $50 \mu\text{m}$ , deepest point at 17% of body length. About 215 ciliary rows. Extrusomes slenderly ellipsoid, 3–4  $\mu\text{m}$  long. Resting cyst about 140  $\mu\text{m}$  in vivo.

**Type locality:** Surroundings of the town of Copenhagen ( $55^{\circ}41'\text{N}$ ,  $12^{\circ}35'\text{E}$ ), Denmark, where Müller (1786) discovered rich populations in ditches and shady swamps containing decaying beech leaves.

Possibly, the species should be neotypified but this should await further investigations of populations from Central Europe or, ideally, from the type area. The Austrian population described here is possibly a mountain variety, as mentioned below.

**Voucher material:** Six slides of the Austrian population with silver nitrate-impregnated specimens (Chatton-Lwoff method) have been deposited in the Biology Centre of the Upper Austrian Museum in Linz (LI). Relevant specimens have been marked by black ink circles on the coverslip. For slides, see Fig. 16a–g in Chapter 5.

**Etymology:** Not given in original description; *truncatella* is a Latin diminutive meaning “a minute trunk with blunt anterior end”.

**Remarks:** The Austrian population of *B. truncatella* is rather similar to the Botswanan  $\rightarrow B. africana$  but differs significantly in the shape of the extrusomes: 3–4  $\mu\text{m}$  long rods vs. 3–4  $\mu\text{m}$ -sized globules (Fig. 37b, c, 39l, 40p–v, 41a–d, f). Of the other characteristics compiled in Table 15, the following might be of value although they overlap more or less distinctly: length:width ratio 2.0:1 vs. 1.6:1 (Fig. 36a, b, 37a, 39a, b, d, 40a–k, 41e, i, j, Table 15); deepest point of left polykinetid 17%

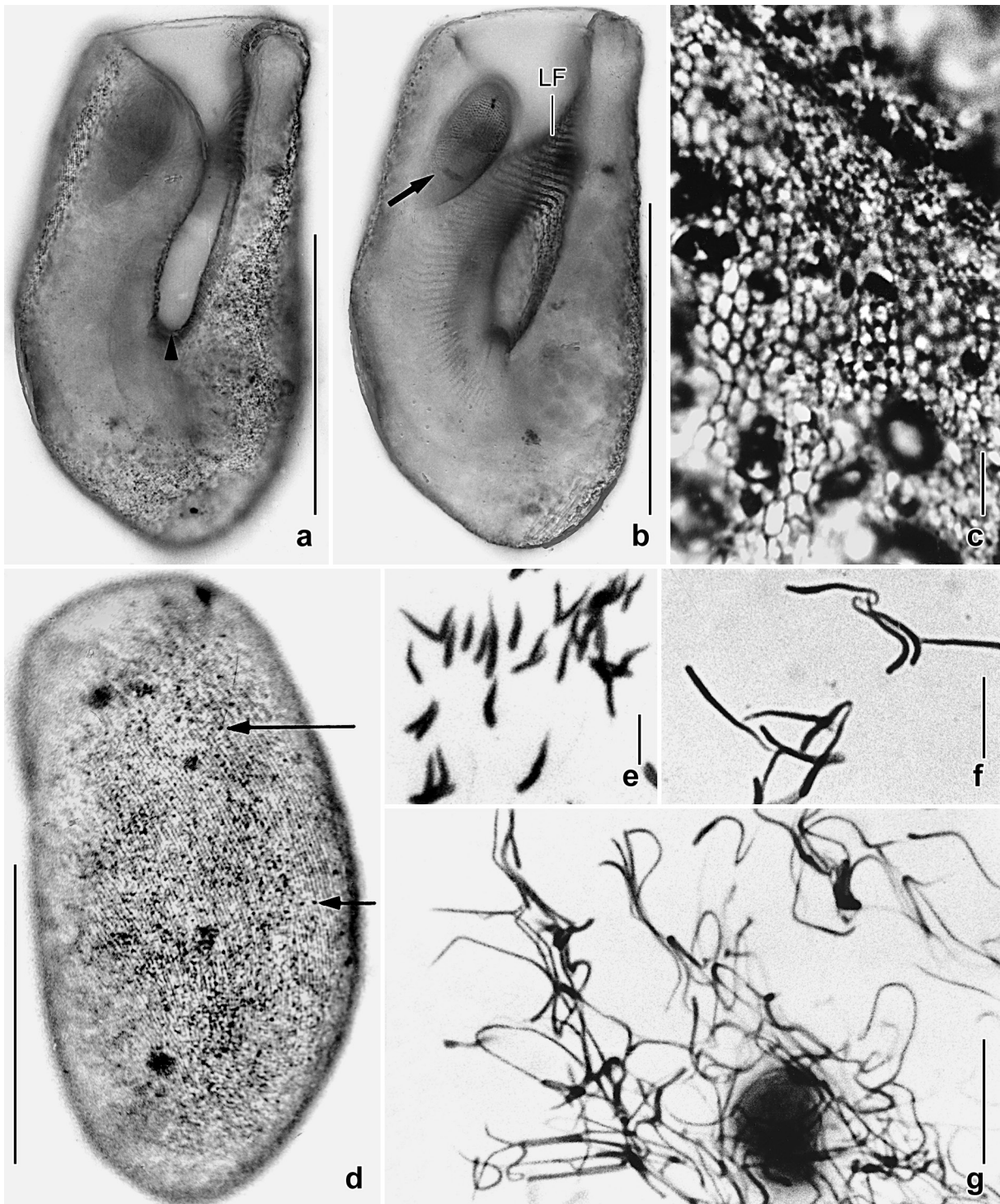


**Fig. 39a–g.** *Bursaria truncatella* from an astatic pool in the Austrian Central Alps (Foissner 1980, 1980a) after silver nitrate impregnation (a–d) and methyl green-pyronin staining (e–g). **a, b:** Ventral surface view and optical section of same specimen. Arrowhead marks posterior end of ventral cleft while the arrow denotes a just engulfed ciliate. **c:** Silverline pattern in dorsal wall of buccal cavity. **d:** Dorsal surface view, showing the very narrowly spaced ciliary rows and some (arrows) of many excretory pores of the contractile vacuoles. **e–g:** When the dye is added, the extrusomes are released (e) and elongate (f) to a dense reticulum (g). LF – left oral polykinetid. Scale bars 5  $\mu\text{m}$  (e), 10  $\mu\text{m}$  (c, f), 20  $\mu\text{m}$  (g), and 200  $\mu\text{m}$  (a, b, d).

vs. 11% of body length (Fig. 36a, b, 39h, 40b, c, g, 41e; Tables 15, 16); and number of somatic ciliary rows, i.e., 215 vs. 282 (Fig. 39d, 40f, 41g; Tables 15, 16).

*Bursaria truncatella* and  $\rightarrow$  *B. africana* are distinctly smaller than the other species (Fig. 37a; Table 16). Possibly, the Austrian population of *B. truncatella* is a mountain variety. In the literature,

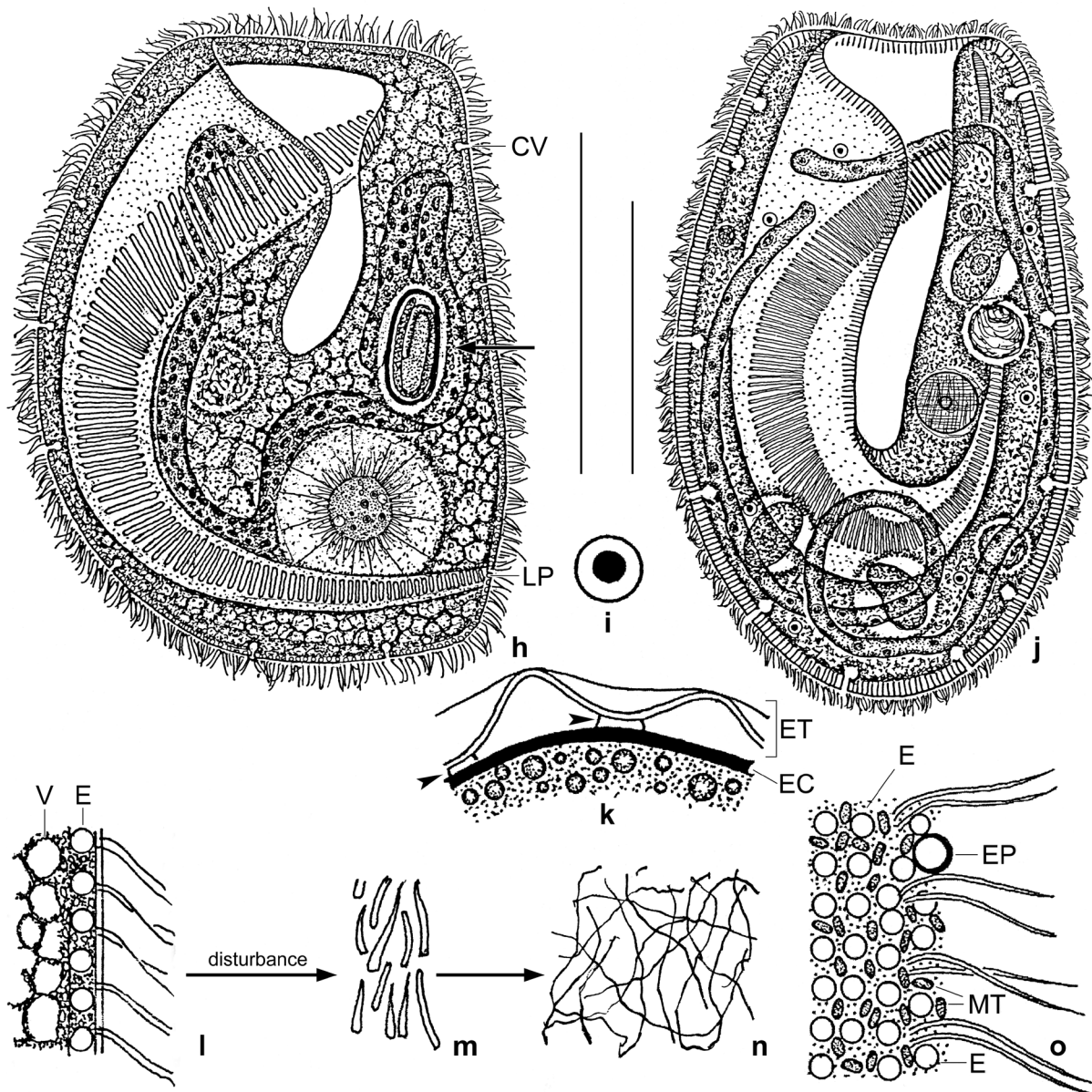


**Fig. 39h–o.** *Bursaria africana* (h, l–n) and *B. ovata* (i–k, o; from Foissner 2016) from Botswana in vivo (h–l, o) and after methyl green-pyronin staining (m, n). **h:** Ventral view of a representative specimen, length 360  $\mu\text{m}$ . The arrow marks an egg of a nematode. **i:** Micronucleus, diameter 7  $\mu\text{m}$ . **j:** Ventral view of a representative specimen, length 500  $\mu\text{m}$ . **k:** Part of resting cyst with bridges (arrowheads) connecting ecto- and endocyst. **l–n:** *Bursaria africana* has globular, 3–4  $\mu\text{m}$ -sized extrusomes which form a dense reticulum of long threads when fully exploded (cp. Fig. 40r). **o:** Surface view of cortex. CV – contractile vacuole, E – extrusomes, EC – endocyst, EP – excretory pore of a contractile vacuole, ET – ectocyst, LP – left oral polykinetid, MT – mitochondria, V – cytoplasmic vacuoles. Scale bars 200  $\mu\text{m}$ .

usually higher values have been reported, e.g., 500–1000  $\mu\text{m}$  by Kahl (1932). On the other hand, several authors mentioned small (fit to my data) and large (up to 1700  $\mu\text{m}$ ) varieties (for a review, see Foissner 1993), indicating that the population from the Austrian Alps is not an exception.

***Bursaria africana* nov. spec.**

(Fig. 36b, 37a, b, 39h, l–n, 40a–v, 41a–w, 42a–k; Tables 15, 16 on p. 321, 322)

**Material:** Floodplain soil in the surrounding of the Kwai River Lodge, Botswana (19°05'S, 23°45'E). The soil, which was very fine and almost black, is covered with *Sphaeranthus incisus* and a dry,

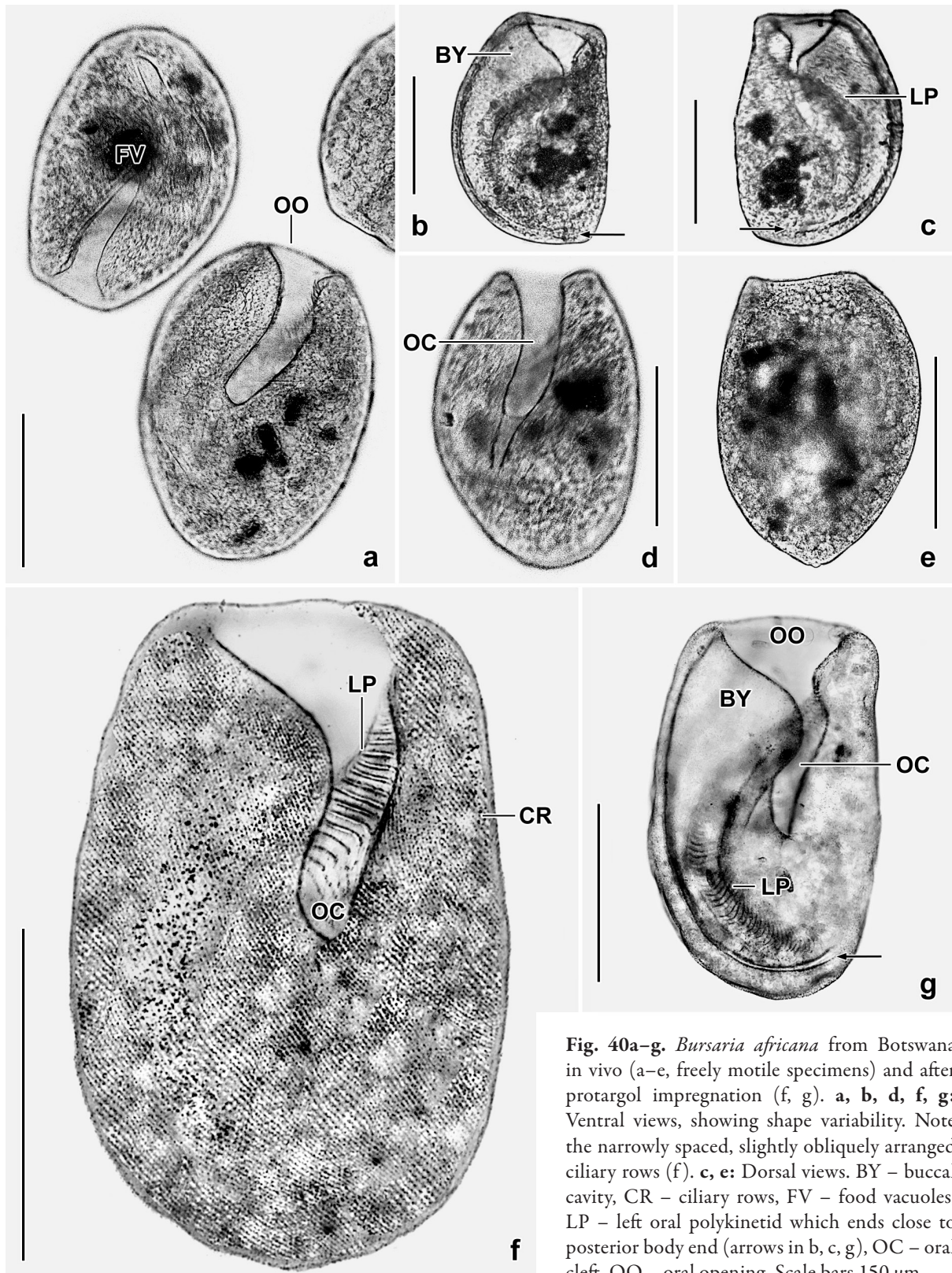


**Fig. 40a-g.** *Bursaria africana* from Botswana in vivo (a-e, freely motile specimens) and after protargol impregnation (f, g). **a, b, d, f, g:** Ventral views, showing shape variability. Note the narrowly spaced, slightly obliquely arranged ciliary rows (f). **c, e:** Dorsal views. BY – buccal cavity, CR – ciliary rows, FV – food vacuoles, LP – left oral polykinetid which ends close to posterior body end (arrows in b, c, g), OC – oral cleft, OO – oral opening. Scale bars 150  $\mu\text{m}$ .

paper-thick algal layer; pH 5.3 in water. *Bursaria africana* occurred together with  $\rightarrow$  *B. ovata* and was cultivated in tap water enriched with some milliliters eluate from the non-flooded Petri dish culture and some squashed wheat grains to stimulate bacterial production and growth of indigenous protists and of *Colpidium colpoda* which was added as food.

**Diagnosis** (most measurements are from silver nitrate-impregnated specimens; add 5% preparation shrinkage to obtain in vivo values; averages are given, see Tables 15, 16 for extremes):

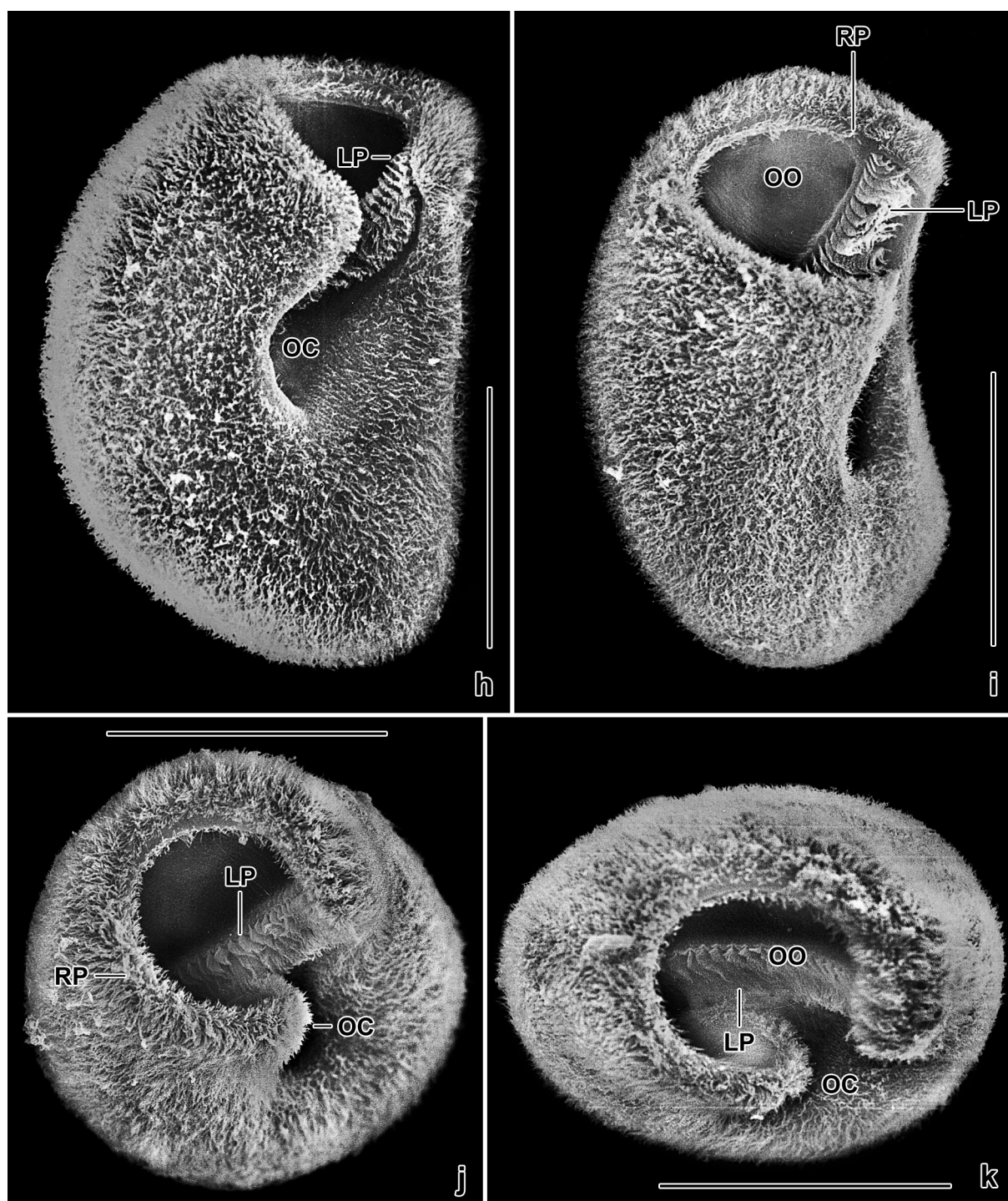


**Fig. 40h–k.** *Bursaria africana* from Botswana in the scanning electron microscope. **h:** Ventrolateral view, showing the oral cleft which merges into the left oral polykinetid. **i:** Right lateral view, showing the left oral polykinetid commencing near anterior body end and close to the right oral polykinetid. **j, k:** Frontal views, showing the circular or broadly ellipsoid oral opening and the traversing left oral polykinetid. KP – left oral polykinetid, LP – left oral polykinetid, OC – oral cleft, OO – oral opening, RP – right oral polykinetid. Scale bars 150  $\mu\text{m}$ .

Bursiform, frequently slightly curved dorsoventrally; body size  $305 \times 190 \mu\text{m}$ ; ventral cleft extends 57% of body length. Left oral polykinetid not recurved, consists of 91 polykineties with a maximum width of  $49 \mu\text{m}$ , deepest point at 11% of body length. About 282 ciliary rows. Extrusomes globular, 3–4  $\mu\text{m}$  across. Diameter of resting cyst  $153 \mu\text{m}$  in vivo.

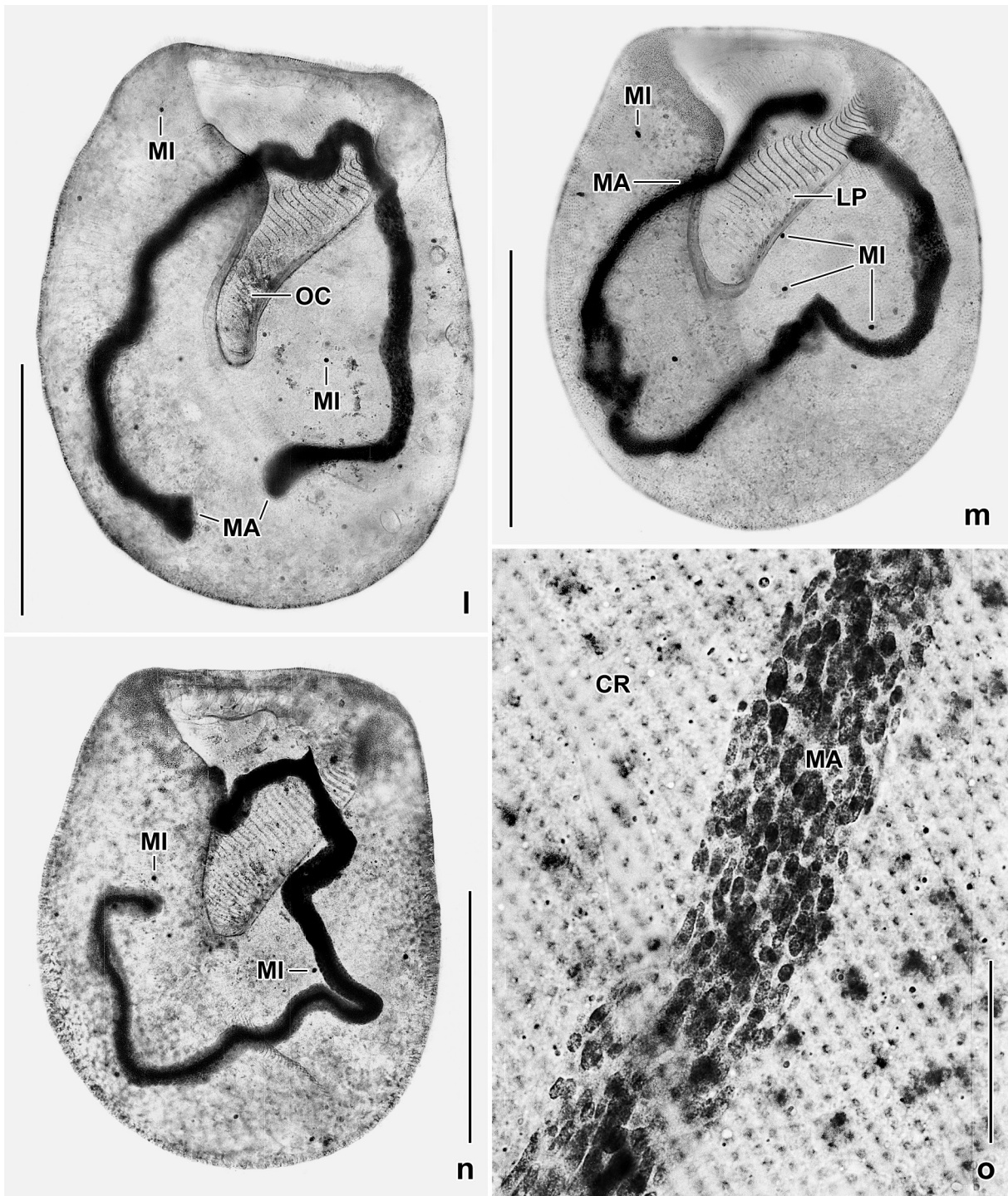


**Fig. 401–o.** *Bursaria africana*, flattened specimens (by coverslip) from Botswana after protargol impregnation. **i–n:** Overviews showing variability of macronucleus and micronuclei. **o:** The macronucleus consists of ellipsoid structures. CR – basal bodies of ciliary rows, LP – left oral polykinetid, MA – macronucleus, MI – micronuclei, OC – oral cleft. Scale bars 20 µm (o) and 200 µm (i–n).

**Type locality:** Floodplain soil from the surroundings of the Kwai River Lodge, Botswana, 19°05'S, 23°45'E.

**Type material:** The Chatton-Lwoff slide containing the holotype and 11 paratype slides (three Chatton-Lwoff; five protargol; three silver carbonate) have been deposited in the Biology Centre of the Upper Austrian Museum in Linz (LI). The holotype and other relevant specimens have been marked by black ink circles on the coverslip. For slides, see Fig. 17a–m in Chapter 5.

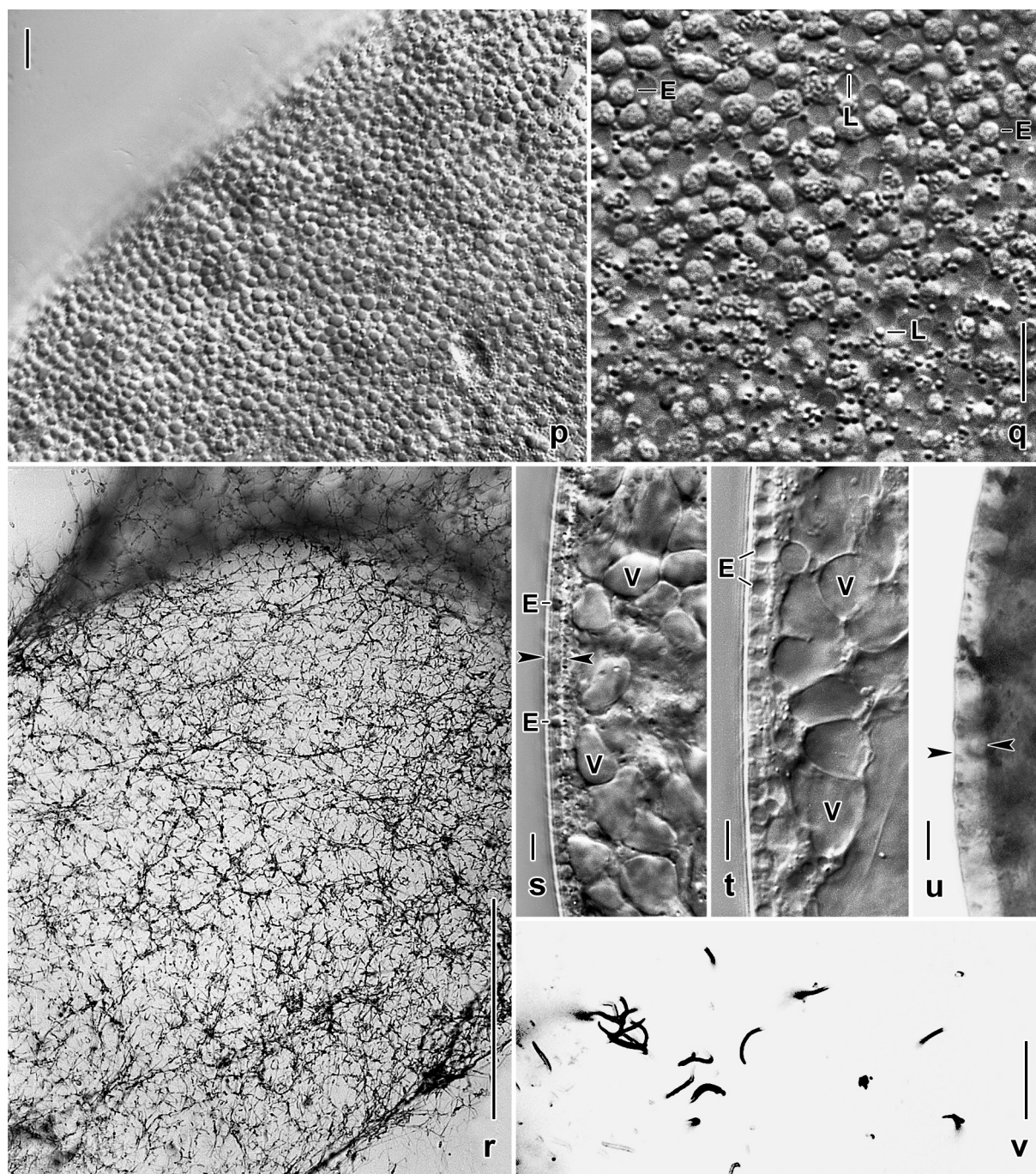


**Fig. 40p–v.** *Bursaria africana*, Botswanan specimens from life (p, q, s, t), after protargol impregnation (u), and methyl green-pyronin staining (r, v). **p–v:** Surface views (p, q) and optical sections (s–u), showing the 3–4  $\mu\text{m}$  thick alveolar layer (opposed arrowheads in s, u). The alveoli (p, s, t) contain globular mucocysts (q, s, t) which are extruded when methyl green-pyronin is applied (v), and then they elongate, forming a three-dimensional reticulum (r). E – extrusomes (mucocysts), L – lipid droplets, V – cytoplasmic vacuoles. Scale bars 5  $\mu\text{m}$  (s–u), 10  $\mu\text{m}$  (p, q, v), and 100  $\mu\text{m}$  (r).

**Etymology:** The Latin adjective *africana* means “belonging to or from Africa”.

**Remarks:** In vivo body size about 320–400  $\times$  220–300  $\mu\text{m}$  (n = 5), which matches the size in preparations (Tables 15, 16). Specimens from the non-flooded Petri dish culture contained food vacuoles with the testate amoeba *Arcella* sp., the ciliate *Urosoma* sp., heliozoans, and eggs of nematodes (Fig. 39h).

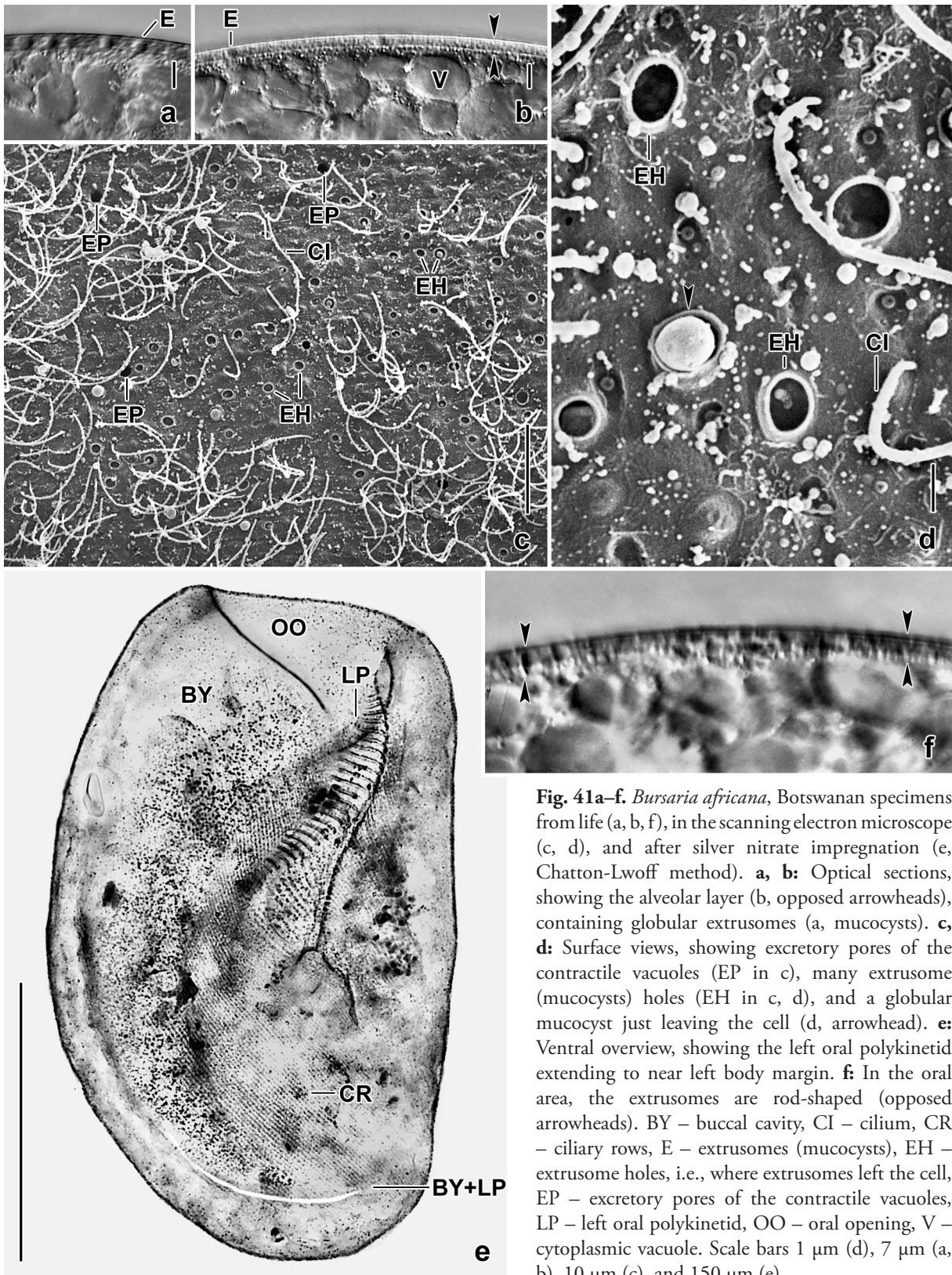


**Fig. 41a–f.** *Bursaria africana*, Botswanan specimens from life (a, b, f), in the scanning electron microscope (c, d), and after silver nitrate impregnation (e, Chatton-Lwoff method). **a, b:** Optical sections, showing the alveolar layer (b, opposed arrowheads), containing globular extrusomes (a, mucocysts). **c, d:** Surface views, showing excretory pores of the contractile vacuoles (EP in c), many extrusome (mucocysts) holes (EH in c, d), and a globular mucocyst just leaving the cell (d, arrowhead). **e:** Ventral overview, showing the left oral polykinetid extending to near left body margin. **f:** In the oral area, the extrusomes are rod-shaped (opposed arrowheads). BY – buccal cavity, CI – cilium, CR – ciliary rows, E – extrusomes (mucocysts), EH – extrusome holes, i.e., where extrusomes left the cell, EP – excretory pores of the contractile vacuoles, LP – left oral polykinetid, OO – oral opening, V – cytoplasmic vacuole. Scale bars 1  $\mu\text{m}$  (d), 7  $\mu\text{m}$  (a, b), 10  $\mu\text{m}$  (c), and 150  $\mu\text{m}$  (e).

*Bursaria africana* is morphologically most closely related to  $\rightarrow$  *B. truncatella*, e.g., in body size, in the number of somatic ciliary rows, the shape of the adoral polykinetid, and the number and size of the adoral polykineties (Tables 15, 16). Main differences are the extrusome shape (globular vs. rod-like) and the small (11% vs. 17% of body length) distance between posterior body end and the deepest point of the adoral polykinetid (Fig. 36b, 37b, 39h, 40b, c, g, 41e; Tables 15, 16).

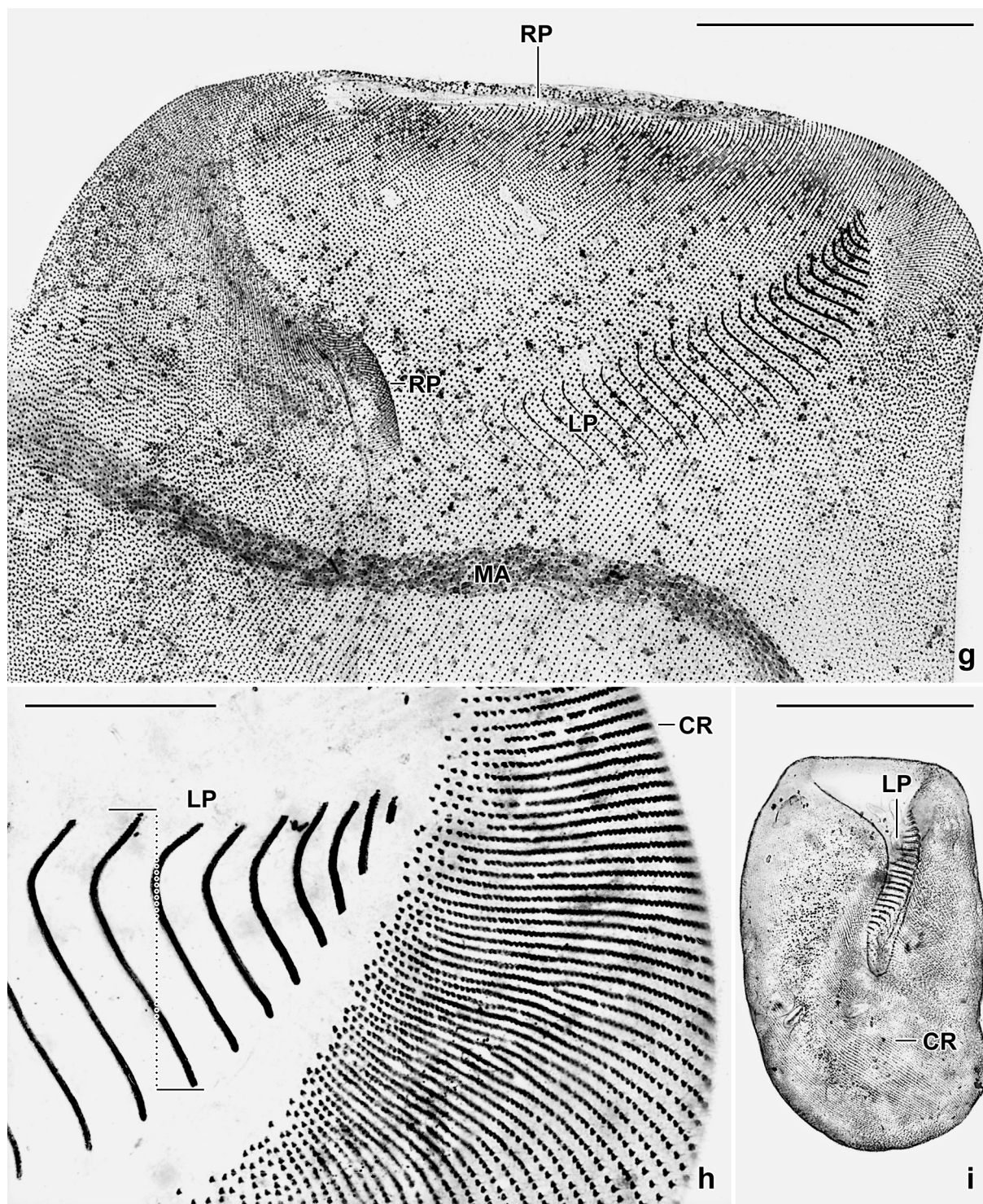


**Fig. 41g-i.** *Bursaria africana*, Botswanan specimens after silver carbonate (f, g) and silver nitrate (h) impregnation. **g:** Dorsal anterior body region, showing the enormous number of ciliary rows. **h:** Anterior region of left oral polykinetid; dotted line shows measurement of length of polykineties. **i:** Ventral overview. CR – ciliary rows, LP – left oral polykinetid, MA – macronucleus, RP – right oral polykinetid. Scale bars 30  $\mu\text{m}$  (h), 80  $\mu\text{m}$  (g), and 150  $\mu\text{m}$  (i).

***Bursaria americana* nov. spec.**

(Fig. 36g, h, 37a, b, 38, 43a–z, 44a–r; Tables 15, 17 on p. 321, 323)

**Material:** This species (“Carolina population” in Foissner 1993) was obtained from the Carolina Biological Supply Company, Burlington, North Carolina 27215, USA. The provider and Foissner

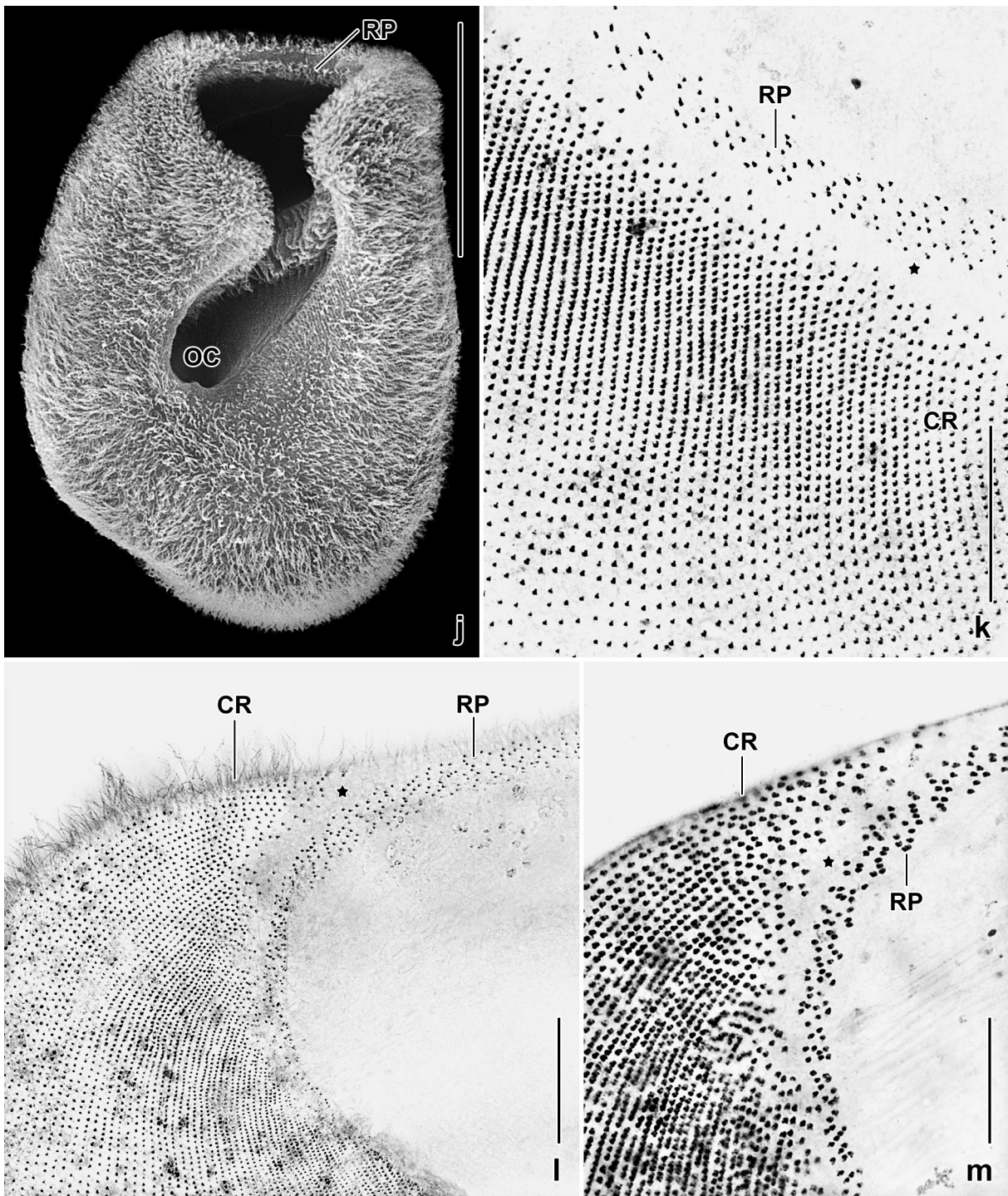


**Fig. 41j–m.** *Bursaria africana*, Botswanan specimens in the scanning electron microscope (j) and after silver carbonate impregnation (k–m). **j:** Ventral overview, showing the conspicuous oral cleft. **k–m:** Anteriorly, the right oral polykinetid extends to the left margin of the oral opening (j) and is separated from the ordinary somatic ciliary rows by a narrow, naked stripe (asterisks). CR – somatic ciliary rows, OC – oral cleft, PR – right oral polykinetid. Scale bars 25  $\mu\text{m}$  (k–m) and 150  $\mu\text{m}$  (j).

(1993, p. 426) misidentified it as *Bursaria truncatella*. Lynn (1980) and Stechmann et al. (1998) studied the fine structure and the genomic sequence.

**Diagnosis** (most measurements are from silver nitrate-impregnated specimens; add 5% preparation shrinkage to obtain in vivo values; averages are given, see Table 17 for extremes): Bursiform or cylindroid; left margin frequently concave, right more or less convex; dorsal side

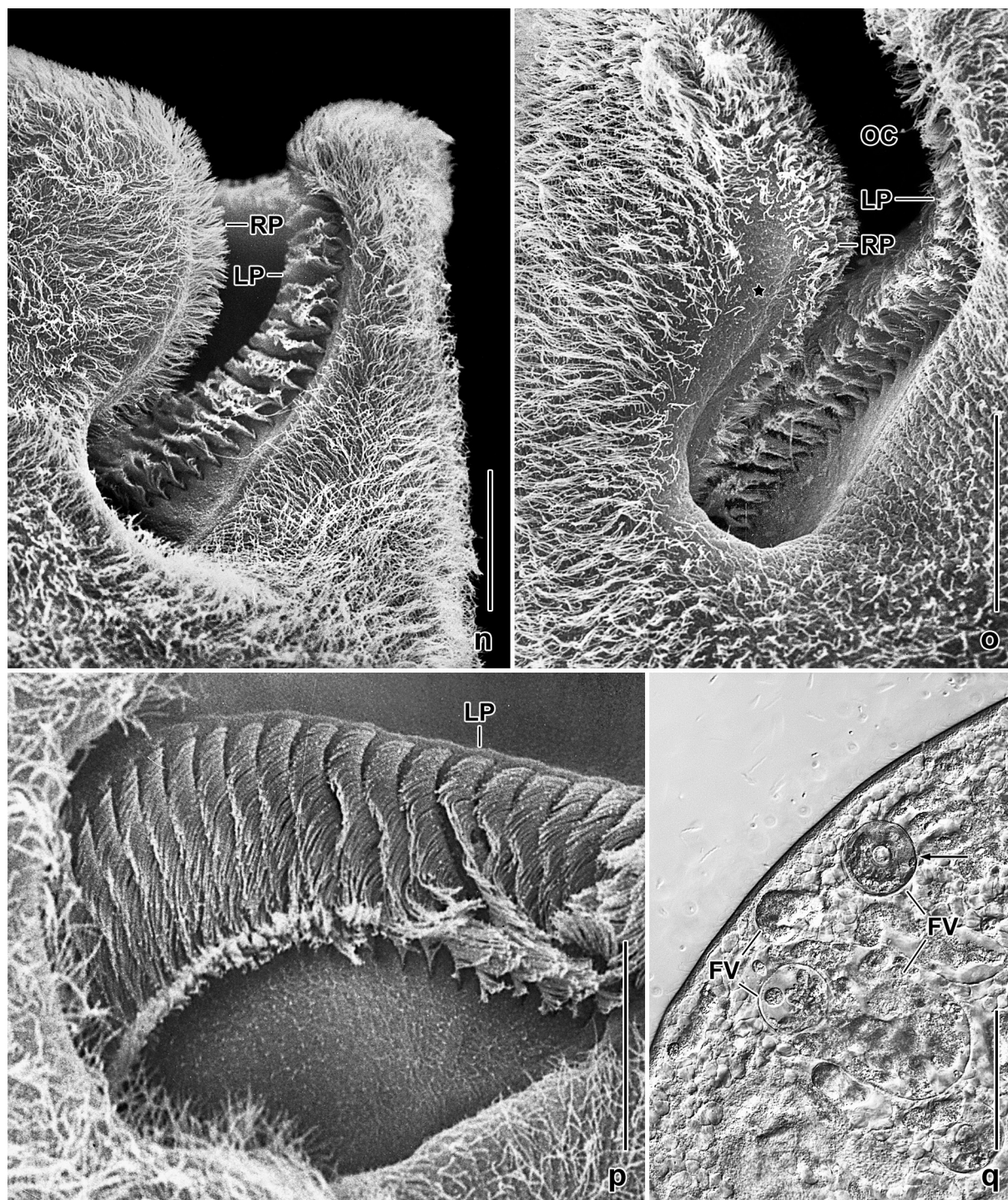


**Fig. 41n–q.** *Bursaria africana*, Botswanan specimens in the scanning electron microscope (n–p) and from life (q). **n–p:** Ventral views, showing the anterior region of the left oral polykinetid. Both polykineties are densely ciliated and extend to near posterior end (for details, see next plates). The asterisk in (o) marks the naked stripe between somatic ciliary rows and the right oral polykinetid (cp. previous plate). **q:** The cytoplasm is studded with food vacuoles one containing a testate amoeba (arrow, *Arcella* sp.). FV – food vacuoles, LP – left oral polykinetid, OC – oral cleft, RP – right oral polykinetid. Scale bars 40  $\mu\text{m}$  (o), 50  $\mu\text{m}$  (n, p), and 100  $\mu\text{m}$  (q).

flat, ventral convex; body size 692  $\times$  427  $\mu\text{m}$ ; ventral cleft extends 62% of body length. Left oral polykinetid recurved, consists of 132 polykineties with a maximum width of 64  $\mu\text{m}$ , deepest point at 10% of body length. About 581 ciliary rows. Extrusomes cylindroid, about 10  $\mu\text{m}$  long. Resting cyst 328  $\mu\text{m}$  across in vivo.

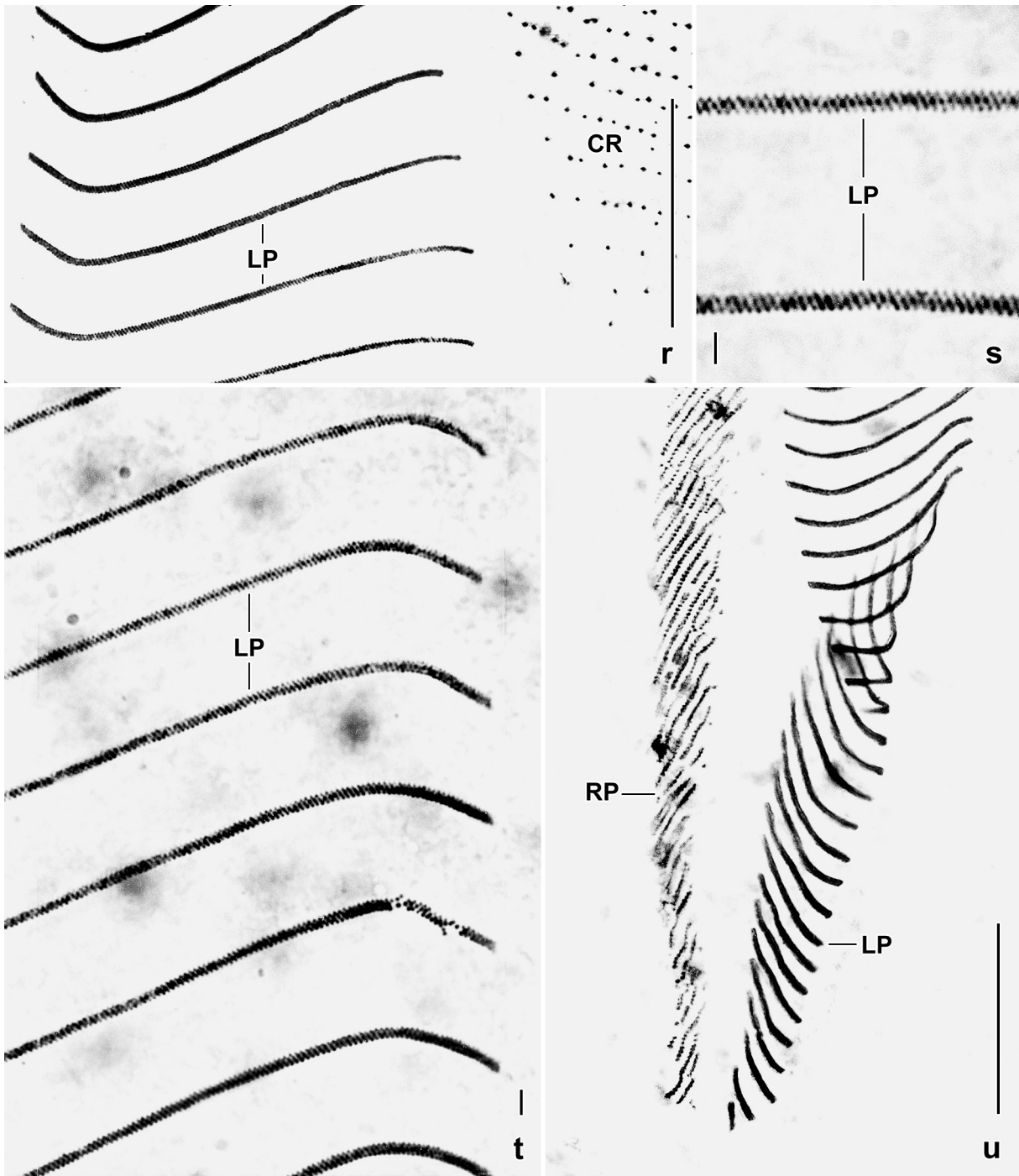


**Fig. 41r-u.** *Bursaria africana*, details of oral structures from Botswanan specimens after silver carbonate impregnation. **r-t:** Left oral polykinetid at low (r), moderate (t), and high (s) magnification. The individual polykinetids consist of narrowly spaced oblique, minute kineties. **u:** Proximal end of the left and right oral polykinetid. The kineties of the right polykinetid are slightly disordered. CR – ordinary somatic ciliary rows, LP – left oral polykinetid, RP – right oral polykinetid. Scale bars 3  $\mu\text{m}$  (r), 5  $\mu\text{m}$  (s, t), and 25  $\mu\text{m}$  (u).

**Type locality:** Not given by the provider (see Material above). Likely, North Carolina, USA.

**Type material:** The protargol slide containing the holotype and seven paratype slides (three protargol; four Chatton-Lwoff) have been deposited in the Biology Centre of the Upper Austrian Museum in Linz (LI). The holotype and other relevant specimens have been marked by black ink circles on the coverslip. For slides, see Fig. 18a–i in Chapter 5.

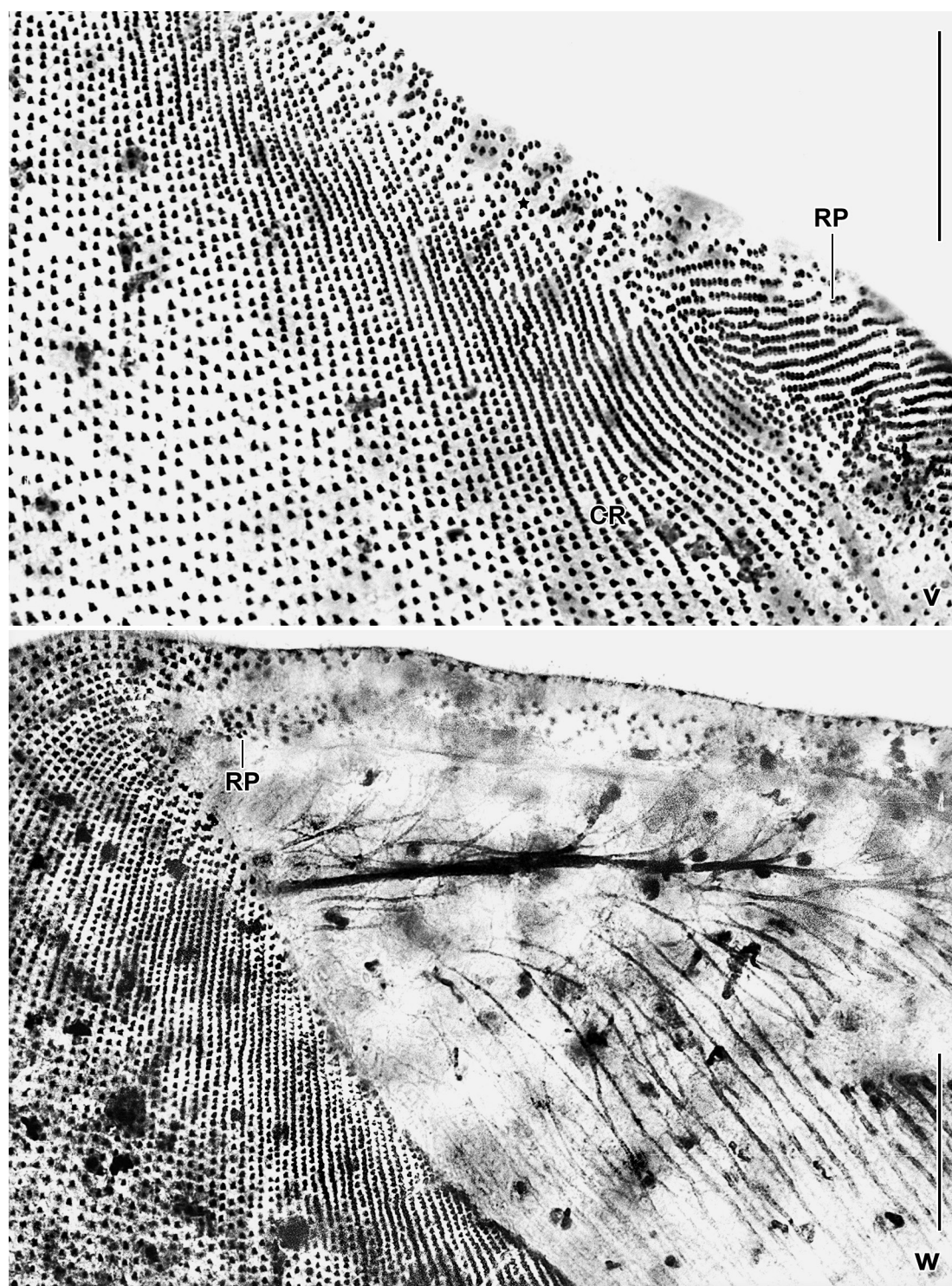


**Fig. 41v, w.** *Bursaria africana*, Botswanan specimens after silver carbonate impregnation. **v:** frontal view of ciliary pattern in dorsal anterior region. The kineties of the right oral polykinetid are fragmented and rather disordered. **w:** Ventral view, showing the conspicuous fibre bundle in anterior dorsal wall of buccal cavity. CR – ordinary somatic kineties of ventral side, RP – right oral polykinetid. Scale bars 25  $\mu$ m.

**Etymology:** The Latin adjective *americana* means “belonging to America”.

**Remarks:** *Bursaria americana* is the largest species in the genus. It is rather similar to  $\rightarrow$  *B. ovata*, as redescribed by Foissner (2016), with which it forms a molecular clade (Fig. 3). Main differences (Table 15) are body length (692  $\mu$ m vs. 521  $\mu$ m), deepest point of left oral polykinetid (10% vs. 19% of body length), the number of somatic ciliary rows (581 vs. 417), the width of the adoral

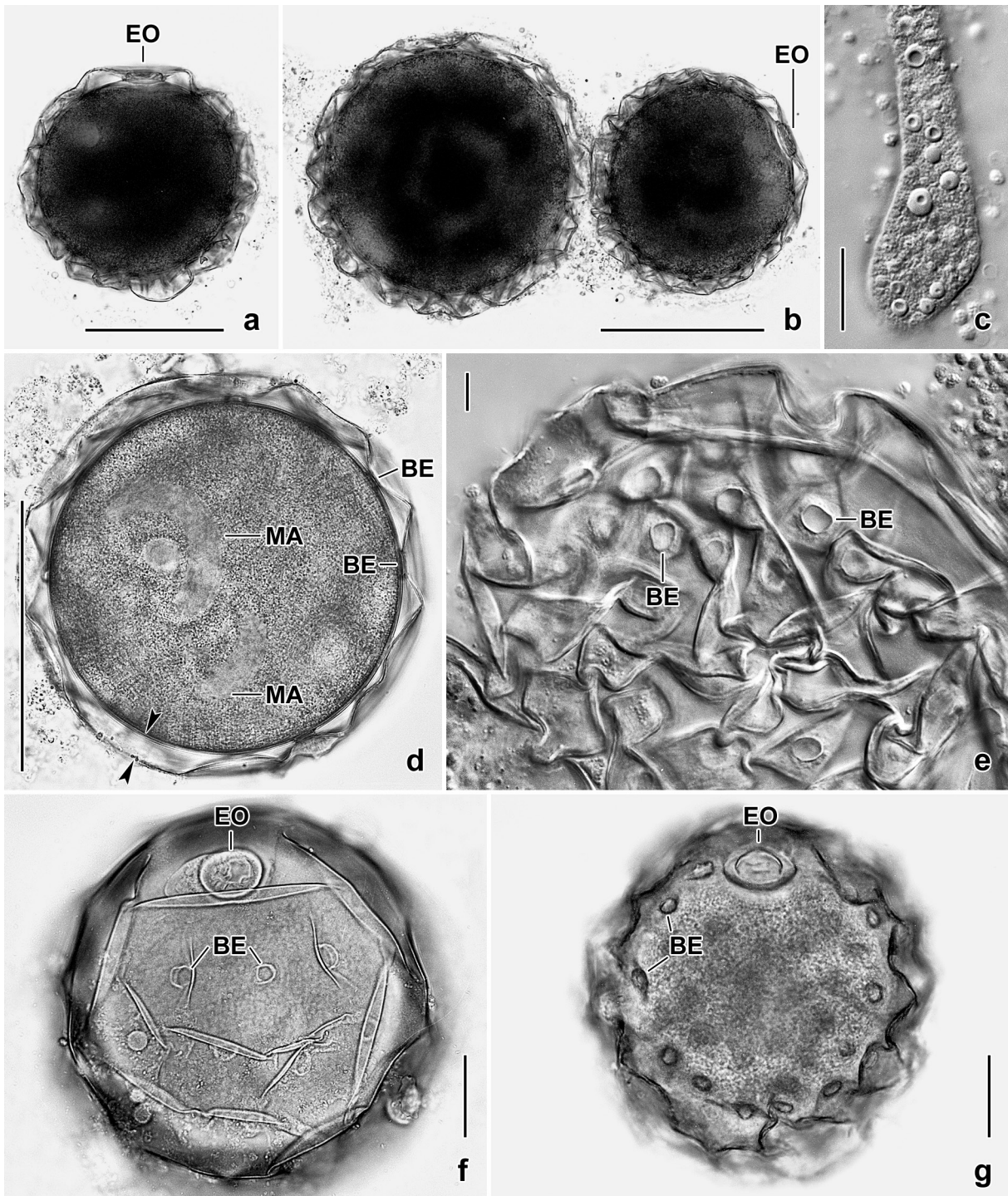


**Fig. 42a–g.** *Bursaria africana*, resting cyst of Botswanan specimens from life (see also next plate). **a, b:** At low magnification, the cysts appear dark because they are large ( $\sim 150\ \mu\text{m}$ ) and have a condensed cytoplasm. **c:** Part of the macronucleus which has ring-shaped nucleoli. **d–g:** The cyst wall consists of two distinct layers. The thick, faceted external layer (d, opposed arrowheads) is connected to the internal layer by ring-shaped, 2–3  $\mu\text{m}$  high bridges. The escape apparatus has about 25  $\mu\text{m}$  in diameter (Table 1). The cytoplasm consists of lipid droplets 1–5  $\mu\text{m}$  in size (d, g). BE – bridges connecting external and internal cyst wall, EO – escape apparatus, MA – macronucleus. Scale bars 10  $\mu\text{m}$  (e), 20  $\mu\text{m}$  (c), 30  $\mu\text{m}$  (f, g), and 100  $\mu\text{m}$  (a, b, d).

polykineties (64  $\mu\text{m}$  vs. 33  $\mu\text{m}$ ), and the height of the extrusome fringe (10  $\mu\text{m}$  vs. 20  $\mu\text{m}$ ). The most important difference is the width of the adoral polykineties which are remarkably narrow in  $\rightarrow B. ovata$  (64 vs. 33  $\mu\text{m}$ ).

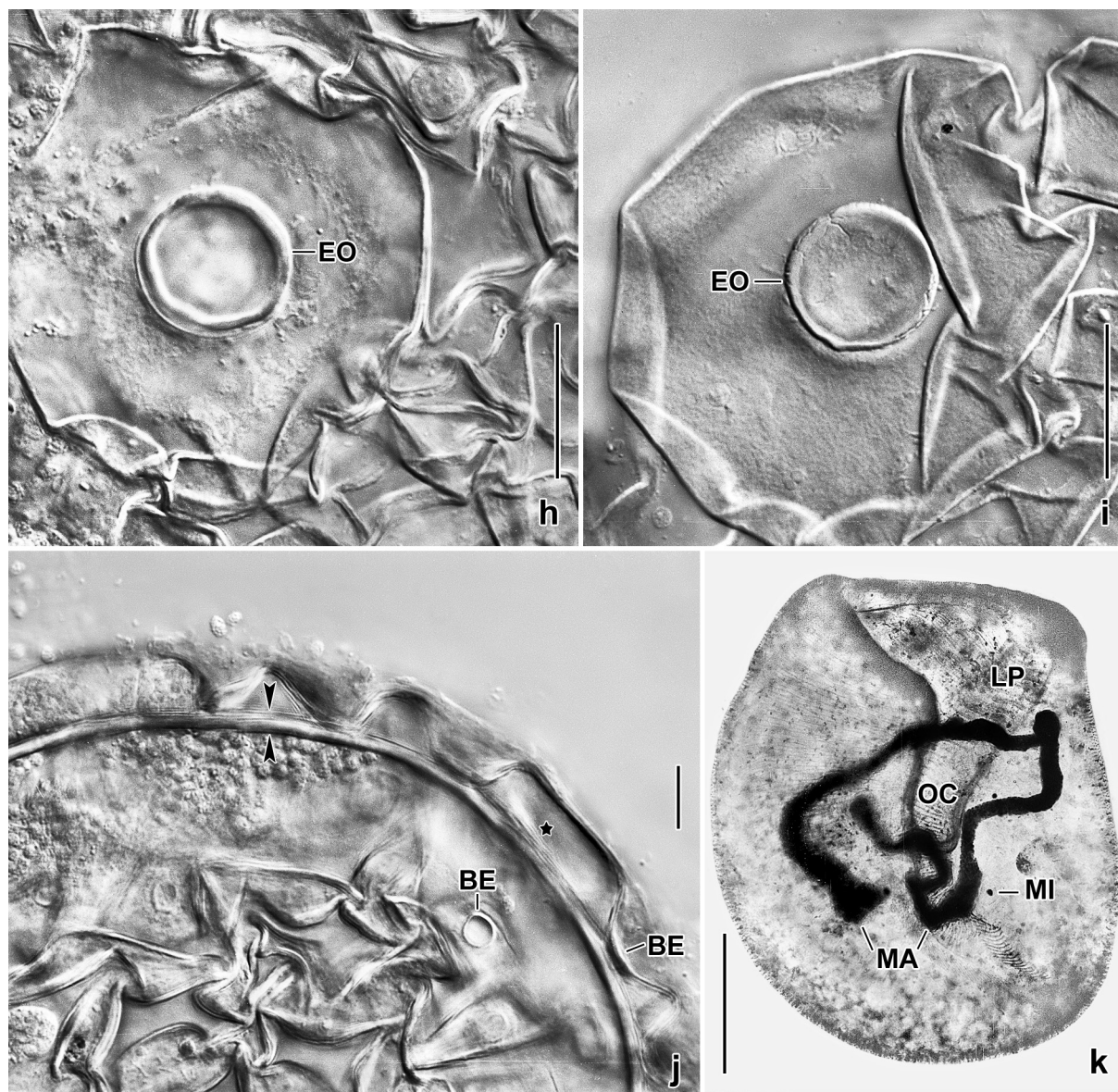


**Fig. 42h–k.** *Bursaria africana* from life (h–j) and after protargol impregnation (k). **h, i:** Escape apparatus of resting cysts which consists of a thick, ring-shaped structure closed by a concave (h) or flat (i) membrane. The apparatus is surrounded by a large facet. **j:** Part of a resting cyst at high magnification, showing the faceted external wall which is connected to the smooth and thin internal wall (opposed arrowheads) by 2–3  $\mu\text{m}$  high cylindric bridges. The asterisk marks a large facet surrounding the escape apparatus. **k:** Ventral view, showing the tortuous macronucleus. BE – bridges, EO – escape apparatus, LP – left oral polykinetid, MA – macronucleus, MI – micronucleus, OC – oral cleft. Scale bars 15  $\mu\text{m}$  (j), 30  $\mu\text{m}$  (h, i), and 100  $\mu\text{m}$  (k).

The morphology of *B. americana* is quite similar to that of the congeners and documented by a multitude of Figures (Fig. 43a–z, 44a–r). The preparations are very clear and thus one can see the cortical fibre system (Fig. 43d, 44b, c, i) and the reticular silverline pattern in the cortex of the buccal cavity (Fig. 43p, 44k–m); it extends also between the adoral polykineties (Fig. 44k). The huge buccal cavity is very distinct (Fig. 43a, b) while the adoral polykinetid is not as distinctly recurved as in  $\rightarrow$  *B. ovata* (Fig. 43v, w, 44a). Very likely, *B. americana* lacks granular vacuoles. Description of resting cyst, see Foissner (1993).

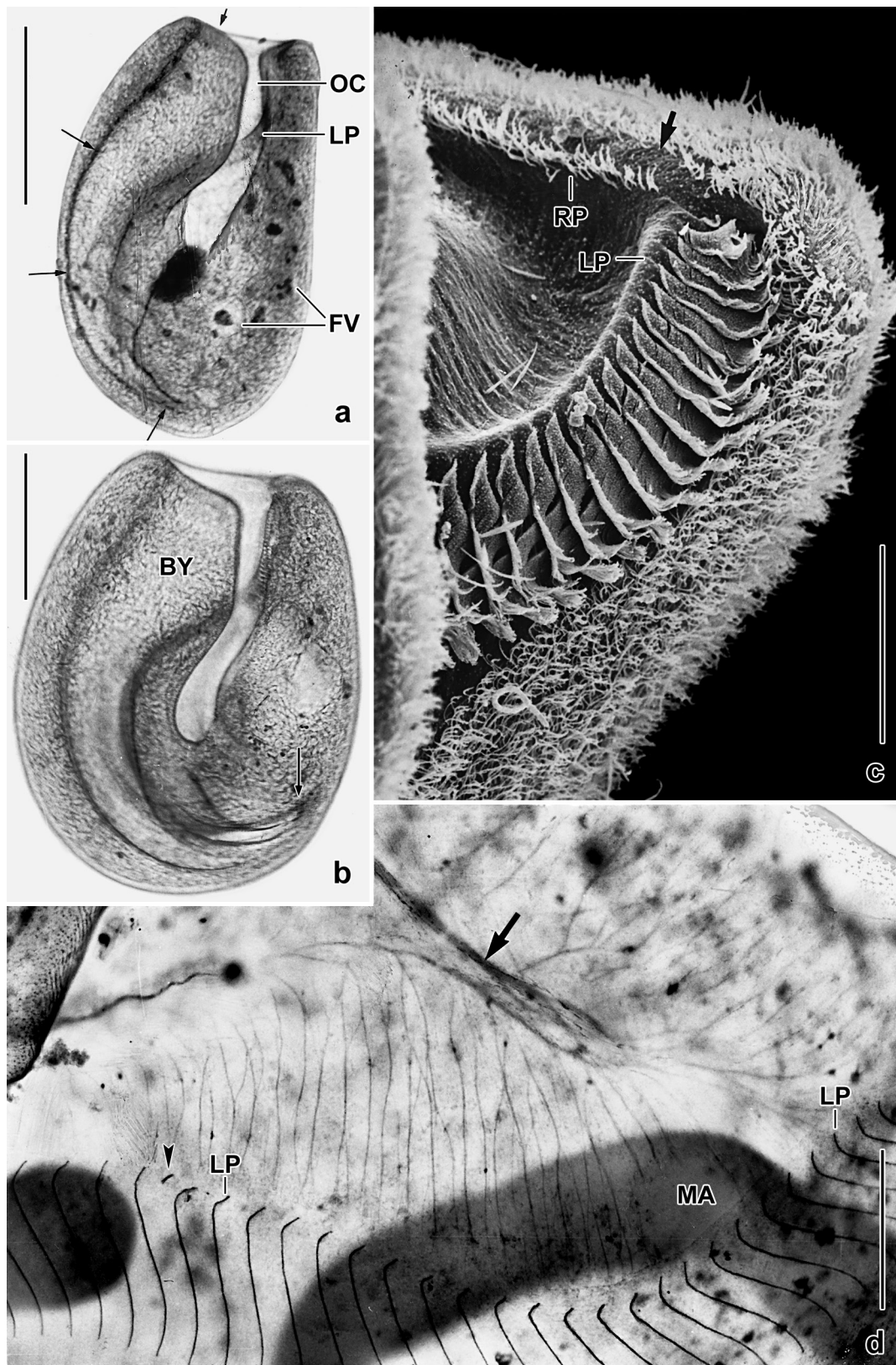


**Fig. 43a–d.** *Bursaria americana* from life (a, b), in the scanning electron microscope (c), and after protargol impregnation (d). **a, b:** Ventral view of a typical and of a broad specimen, both showing the large, horn-shaped buccal cavity (margins and proximal end marked by arrows). **c:** Left anterior portion, showing the distal end of the oral polykinetids. The right polykinetid is separated from the somatic ciliature by a narrow, unciliated stripe (arrow). **d:** Anterior end of dorsal buccal wall. The arrow marks a thick fibre formed by thin fibres originating from the oral polykineties. The arrowhead denotes a minute polykinetid. BY – buccal cavity, FV – food vacuoles, LP – left oral polykinetid, MA – macronucleus, OC – oral cleft, RP – right oral polykinetid. Scale bars 50  $\mu\text{m}$  (c, d) and 300  $\mu\text{m}$  (a, b).

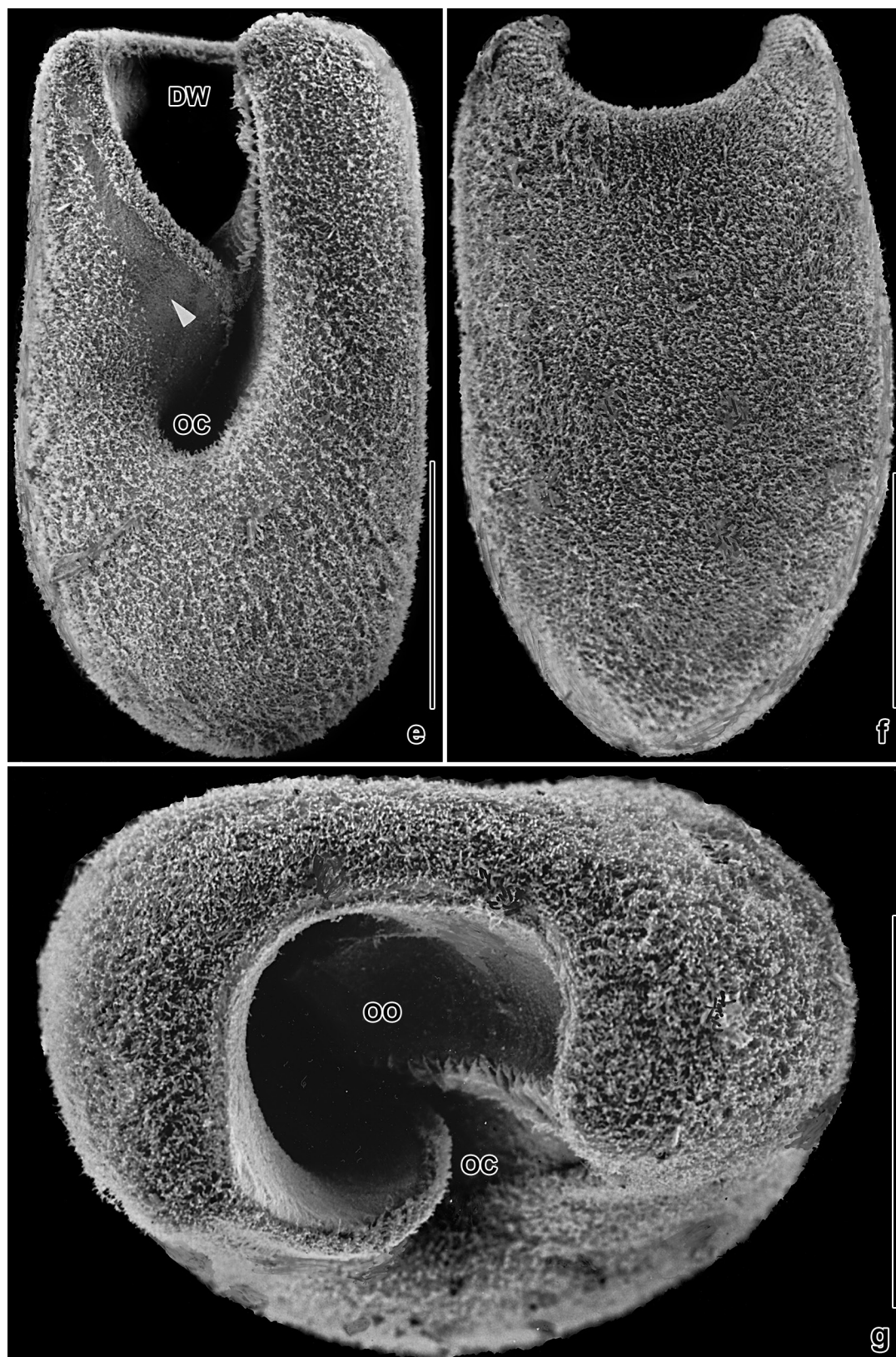


**Fig. 43e-g.** *Bursaria americana* in the scanning electron microscope. Ventral (e), dorsal (f), and frontal (g) overview. Triangle in Fig. 43e marks the barren stripe. DW – dorsal wall, OC – coral cleft, OO – oral opening. Scale bars 200  $\mu$ m.

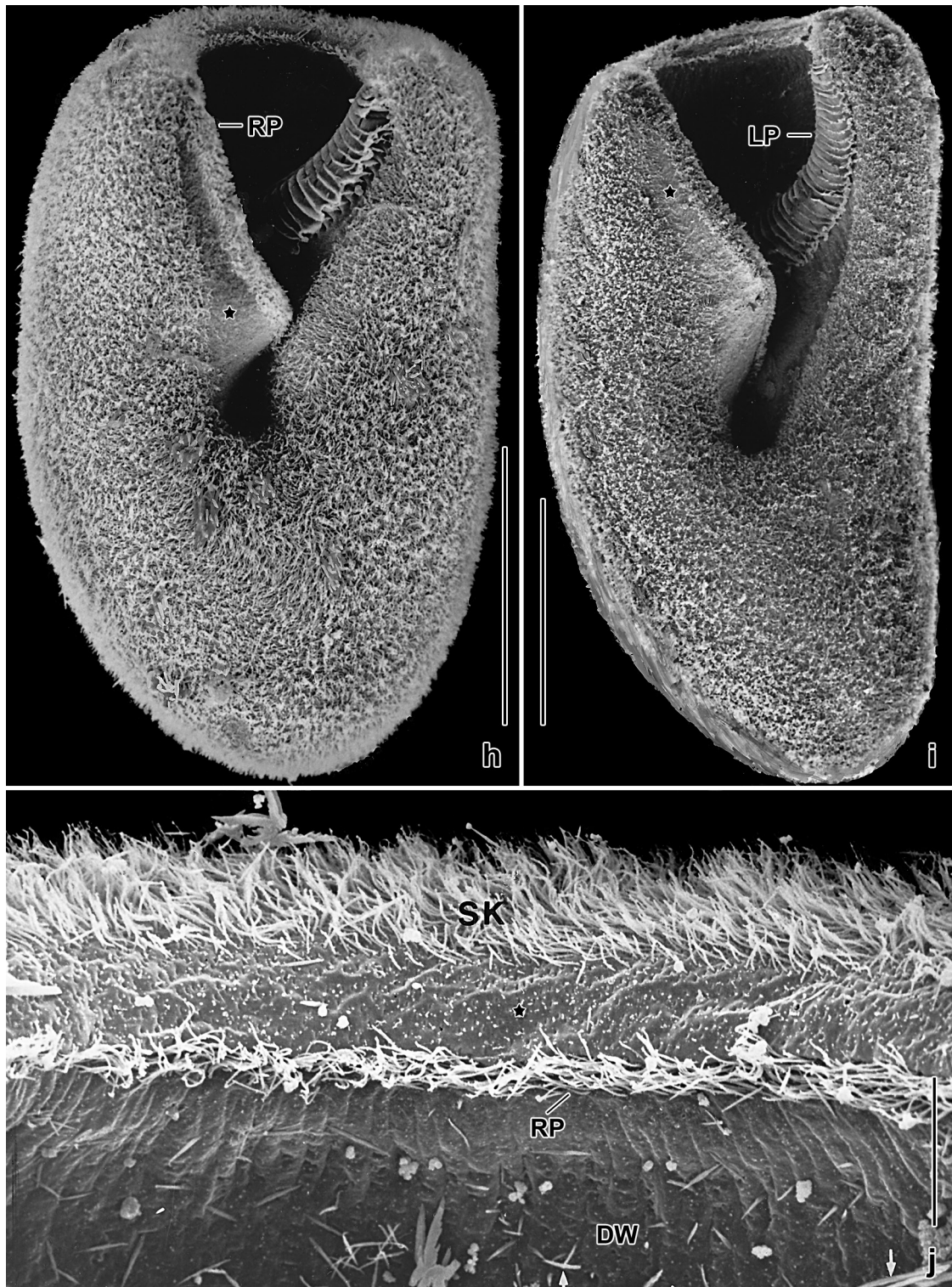


**Fig. 43h–j.** *Bursaria americana* in the scanning electron microscope. The asterisks mark the unciliated stripe between the somatic ciliature and the right oral polykinetid. **h, i:** An ordinary and a slender specimen. **j:** Anterior dorsal wall of buccal cavity. The somatic kineties and the right oral polykinetid are separated by a barren stripe. DW – dorsal wall of buccal cavity, LP, RP – left and right oral polykinetid, SK – somatic kineties. Scale bars 20  $\mu\text{m}$  (j) and 200  $\mu\text{m}$  (h, i).

**Fig. 43k–m.** *Bursaria americana* in the SEM (k, m) and after protargol impregnation (l). **k, m:** The somatic ciliature and the right oral polykinetid are separated by a narrow, unciliated stripe. The thick arrows denote excretory pores of the contractile vacuoles while the thin arrows mark holes remaining from just extruded mucocysts. **l:** Trikinetids (arrows) occur between the ordinary dikinetids. LP, RP – left and right oral polykinetid, SK – somatic kineties. Scale bars 10  $\mu\text{m}$  (l), 30  $\mu\text{m}$  (m), and 50  $\mu\text{m}$  (k).

***Bursaria ovata* Beers, 1952**

(Fig. 36f, 37a, b, 38; Table 15 on p. 321)

**Remarks:** This species has been carefully redescribed by Foissner (2016), based on a population from Botswana (site description, see → *B. africana*). Thus, I provide only a diagnosis as used for the other species.

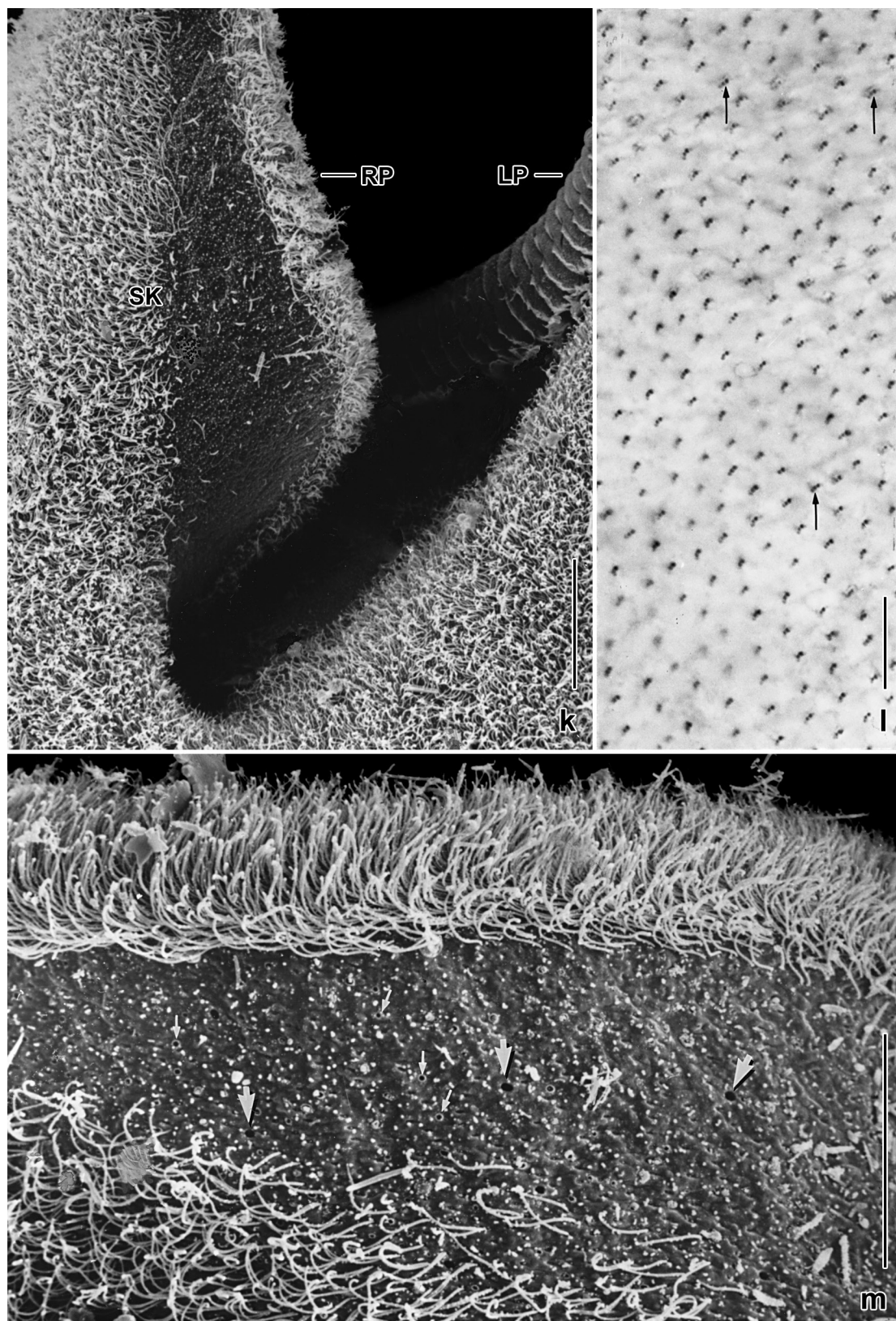




**Fig. 43n–p.** *Bursaria americana*, cortex after silver nitrate impregnation (Chatton-Lwoff method). **n, o:** The cortex is studded with narrowly spaced ciliary rows and holes (arrows) left by just extruded mucocysts. **p:** The unciliated dorsal wall of the buccal cavity contains a fine net of silverlines. BB – basal bodies (somatic dikinetids). Scale bars 10  $\mu\text{m}$  (n, o) and 20  $\mu\text{m}$  (p).

**Improved diagnosis** (most measurements are from silver nitrate-impregnated specimens; add 5% preparation shrinkage to obtain in vivo values; averages are given, see Table 15 for extremes): Body bursiform with anterior end transversely truncate and posterior bluntly pointed; precystic specimens distinctly narrowed posteriorly; left body margin usually less convex than right, laterally flattened up to 2:1. Ventral cleft extends 64% of body length. Left oral polykinetid recurved, consists

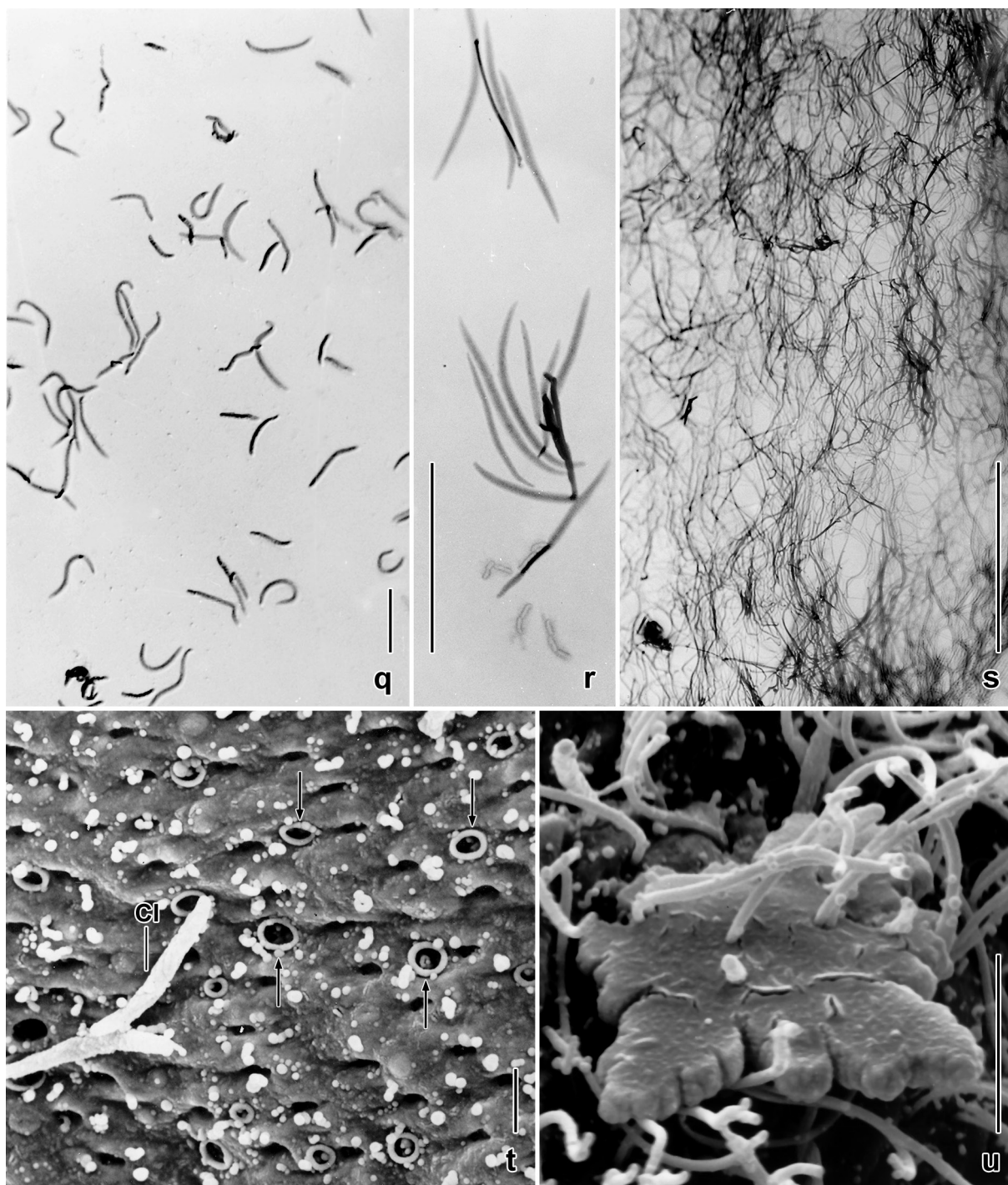


**Fig. 43q–u.** *Bursaria americana* after methyl green-pyronin staining (q–s) and in the SEM (t, u). **q–s, u:** When the dye is added, the mucocysts are extrude (q) and elongate (r) to a dense, three-dimensional network (s) which develops to a plate-like structure (u). **t:** Emerging and just extruded mucocysts produce distinct holes (arrows). CI – cilium. Scale bars 5  $\mu\text{m}$  (u), 10  $\mu\text{m}$  (q, t), 30  $\mu\text{m}$  (r), and 50  $\mu\text{m}$  (s).

of 148 polykinetids with a maximum width of only 33  $\mu\text{m}$ , deepest point at 19% of body length. About 417 ciliary rows. Extrusomes rod-shaped, about  $20 \times 2 \mu\text{m}$  in size, produce a distinct cortical fringe, shorten to about 10  $\mu\text{m}$  when disturbed; with “granular vacuoles”. Resting cyst 193  $\mu\text{m}$  across in vivo.

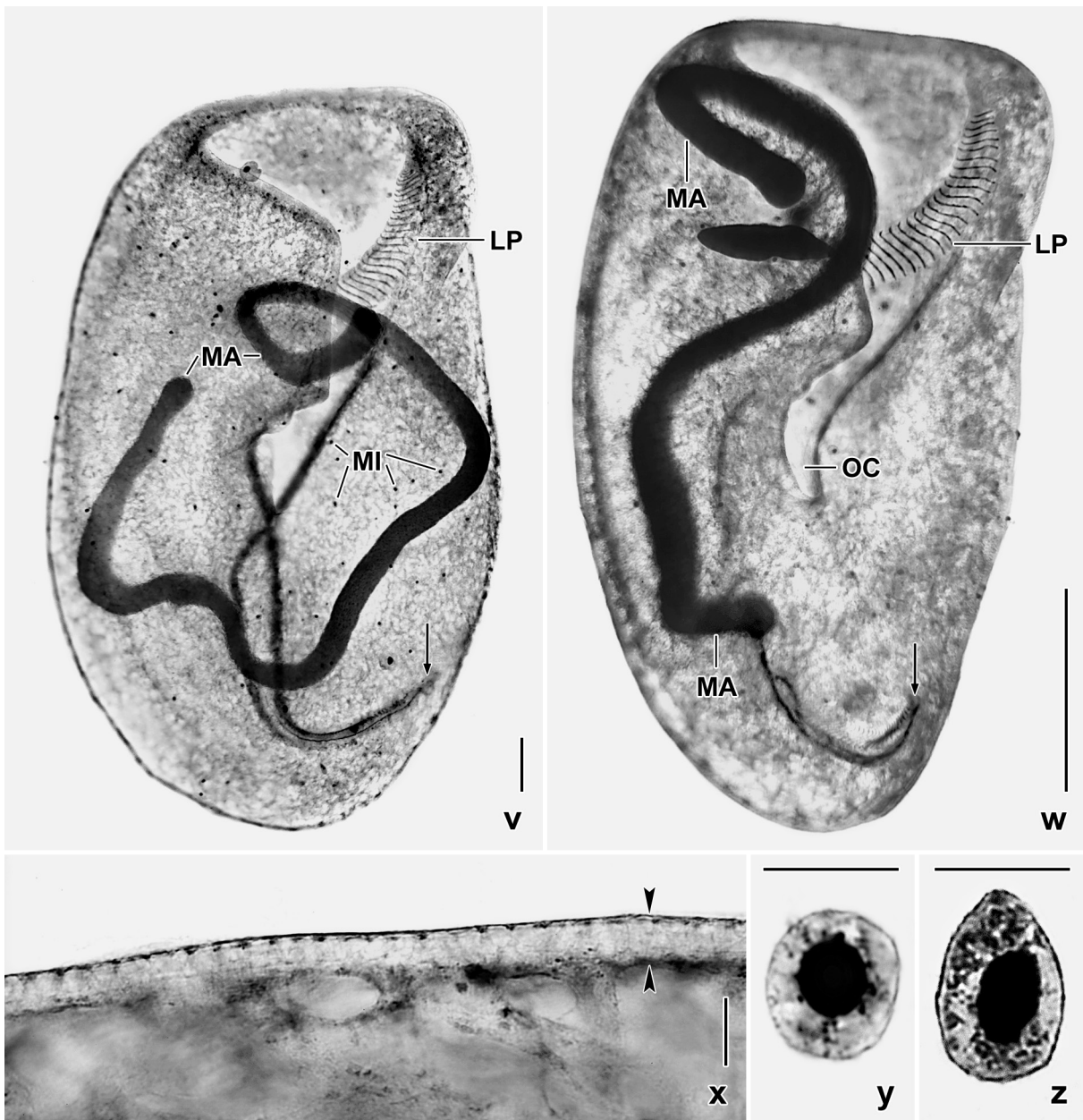


**Fig. 43v-z.** *Bursaria americana* after protargol impregnation. **v, w:** Ventral views, showing the nuclear apparatus (**v**) and the left oral polykinetid which extends to the left body margin where it recures anteriorly (arrows). **x:** The in vivo 10  $\mu\text{m}$  long mucocysts produce a distinct cortical fringe (opposed arrowheads). **y, z:** The large micronuclei contain a deeply impregnated, globular structure connected with the micronuclear membrane by a granular reticulum. LP – left oral polykinetid, MA – macronucleus, MI – micronuclei, OC – oral clef. Scale bars 10  $\mu\text{m}$  (**x-z**), 50  $\mu\text{m}$  (**v**), and 200  $\mu\text{m}$  (**w**).

### *Bursaria caudata* Dragesco, 1972

**Remarks:** For a review, see Foissner (1993). This poorly described African species differs from the other species by a tail-like or acute posterior end. I have observed similar shapes in the big species under strong starvation. The size in vivo is 1000–1500  $\mu\text{m}$ , matching the  $\rightarrow$  *B. ovata* of Beers (1952) and suggesting synonymy with that species.

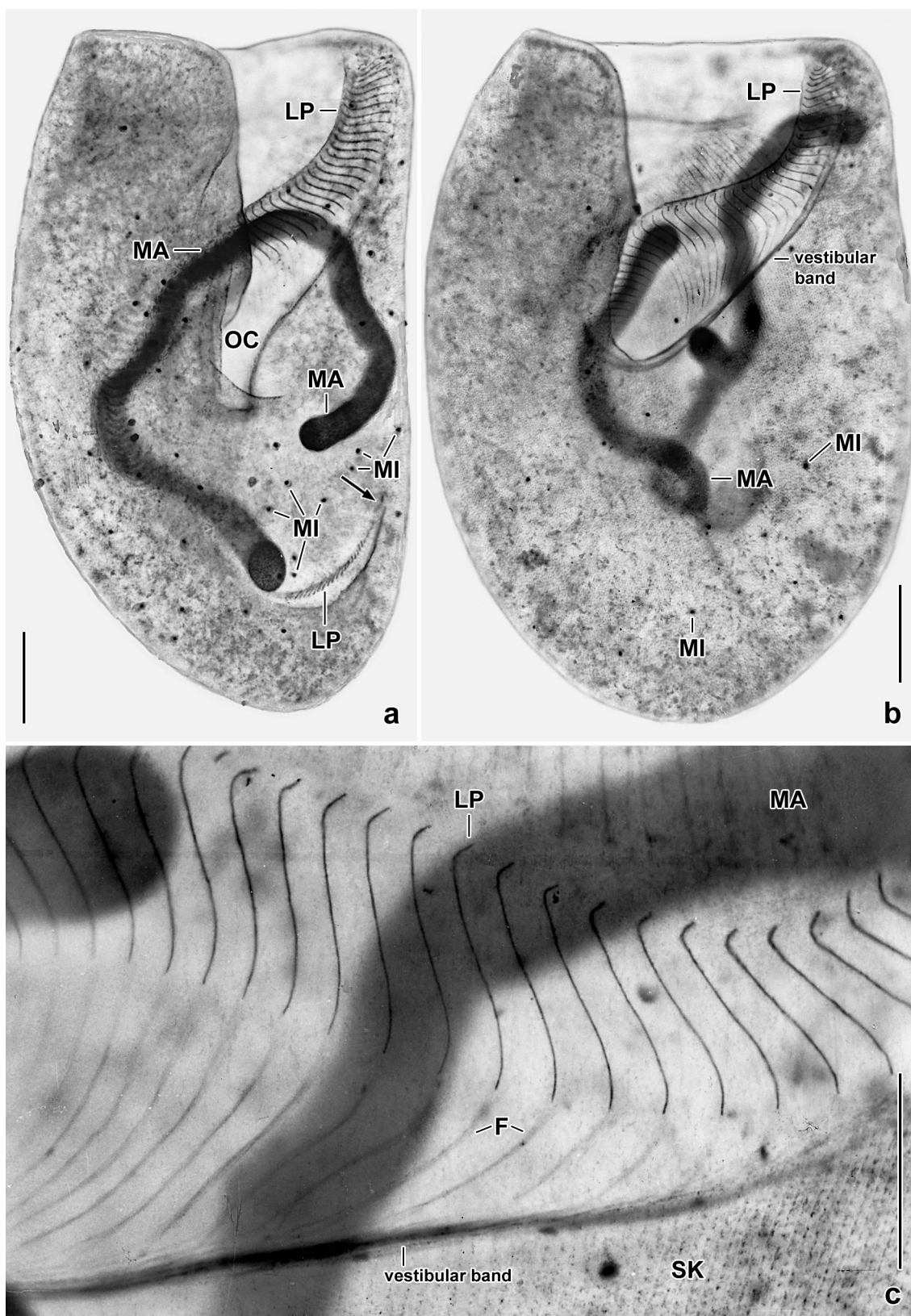


**Fig. 44a–c.** *Bursaria americana* after protargol impregnation. **a, b:** Ventral views, showing the nuclear apparatus, the oral cleft, and the left oral polykinetid that extends to near body end where it recurves to mid-body (**a**, arrow). **c:** Distal portion of left oral polykinetid. Fibres originate from the left end of the individual polykineties and extend to the left margin of the oral cleft where they unite to form a compound structure, the “vestibular band”. F – fibres, LP – left oral polykinetid, MA – macronucleus, MI – micronuclei, OC – oral cleft, SK – ordinary somatic kineties. Scale bars 50  $\mu\text{m}$  (**c**) and 100  $\mu\text{m}$  (**a, b**).

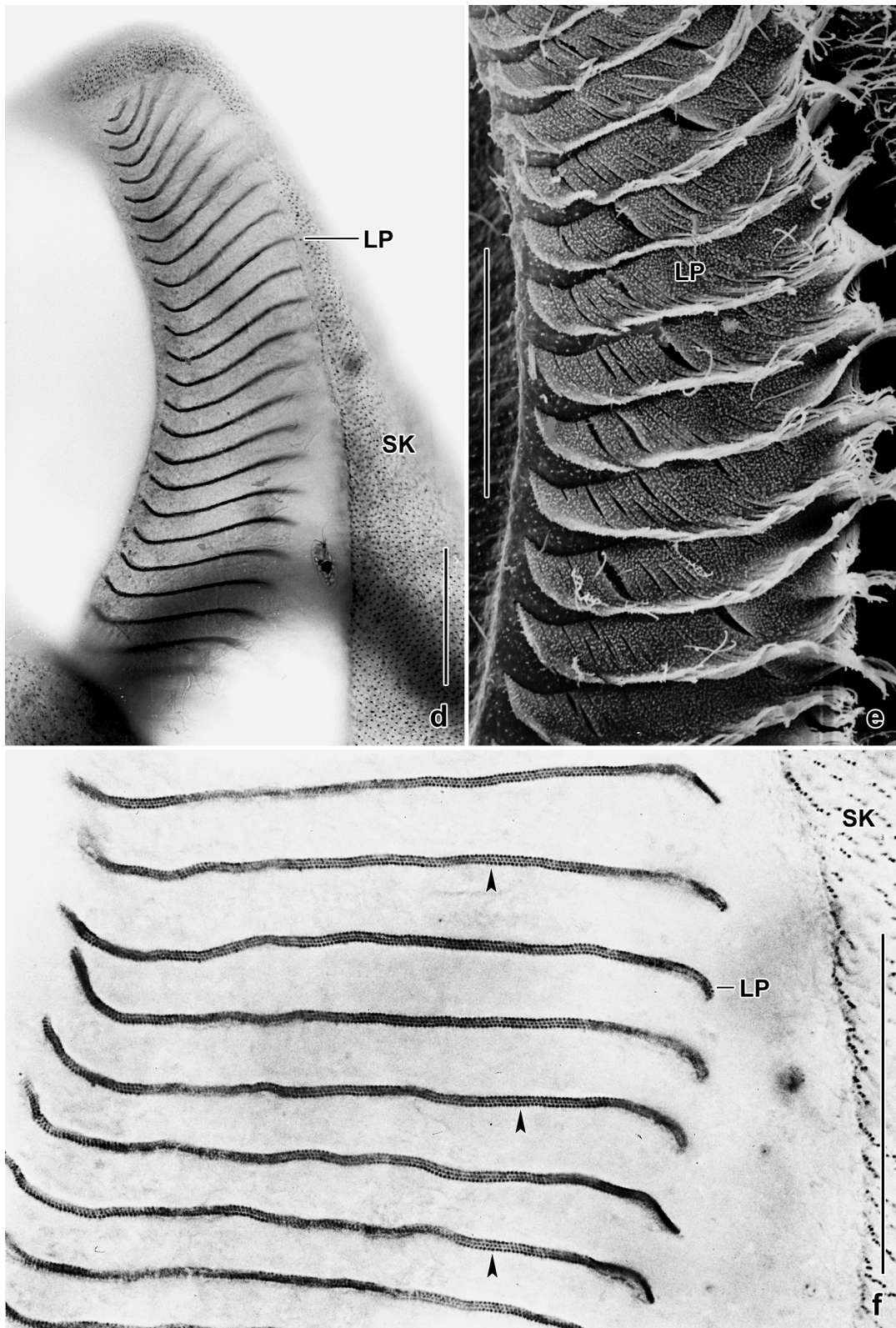


**Fig. 44d-f.** *Bursaria americana*, oral structures after protargol impregnation (d, f) and in the scanning electron microscope (e). **d-f:** Overview of distal portion (d) and details of left oral polykinetid (e, f). The individual polykineties consist of three rows of basal bodies, forming minute, oblique kineties (f, arrowheads) with about 10  $\mu\text{m}$  long cilia (e). LP – left oral polykinetid, SK – somatic kineties. Scale bars 30  $\mu\text{m}$  (d) and 40  $\mu\text{m}$  (e, f).

**Fig. 44g, h.** *Bursaria americana*, oral structures after protargol impregnation. **g, h:** Right and left oral polykinetid in anterior half of cell. The right polykinetid consists of fragmented rows of dikinetids (see also Fig. 44j) while the left polykinetid has a unique structure (see Fig. 44d-f). LP – left oral polykinetid, MA – macronucleus, RP – right oral polykinetid, SK – somatic kineties. Scale bars 40  $\mu\text{m}$ .

***Bursaria salisburgensis* nov. spec.**

(Fig. 36e, 37a, b, 45a–e; Tables 15, 17 on p. 321, 323)

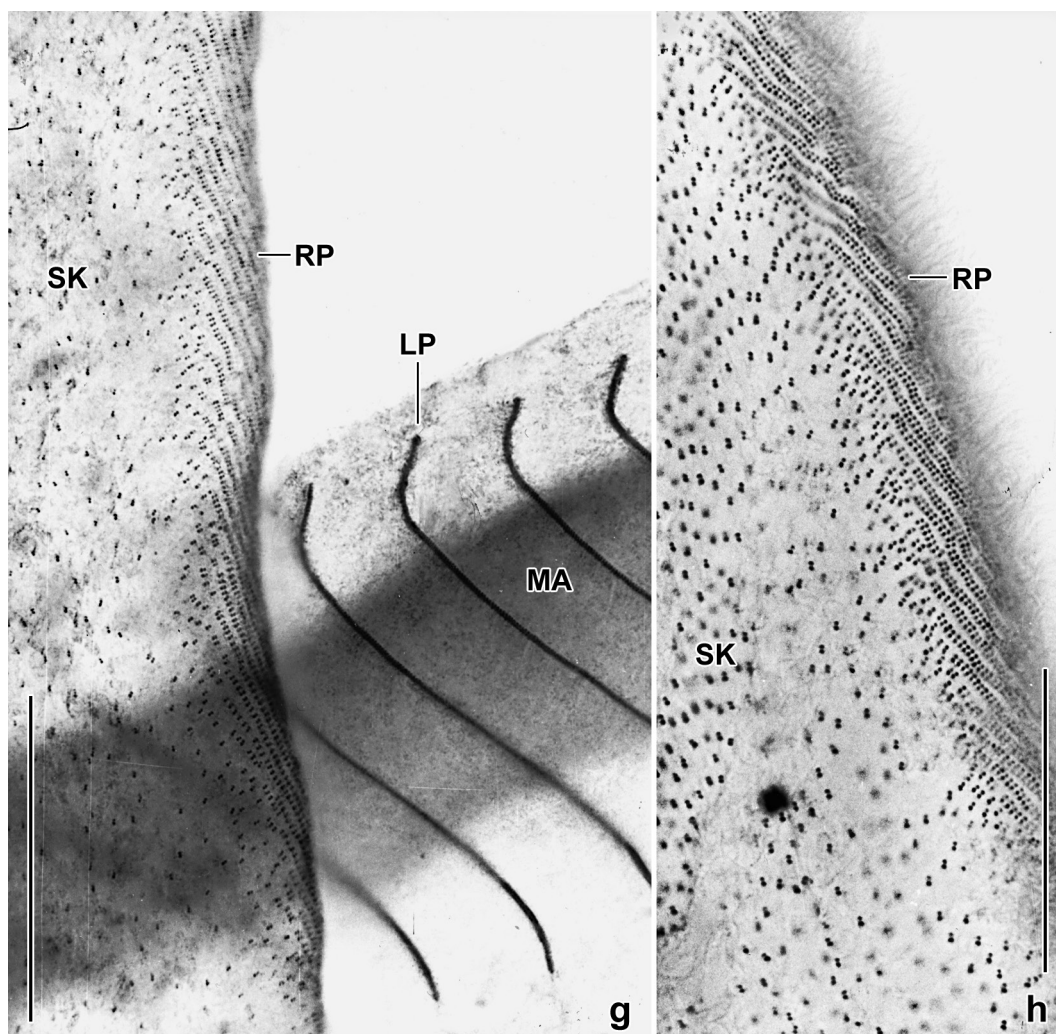
**Material:** This species was discovered in the surrounding of the town of Salzburg, Austria, i.e., in a small, permanent forest pond on the hill to the Neuhaus castle. Environmental specimens were used for most investigations.

**Diagnosis** (most measurements are from protargol-impregnated specimens; add 20% preparation shrinkage to obtain in vivo values; averages are given, see Tables 15, 17 for extremes): Broadly lenticular or ellipsoid, ventrally flattened, dorsally convex; body size  $444 \times 289 \mu\text{m}$ ; ventral cleft extends 53% of body length. Left oral polykinetid recurved, consists of 101 polykineties with a maximum width of  $51 \mu\text{m}$ , deepest point at 20% of body length. 455 ciliary rows. Extrusomes form a  $3\text{--}4 \mu\text{m}$ , structureless plate; when disturbed  $5 \mu\text{m}$  long rods become recognizable. With “granular vacuoles”.

**Type locality:** Permanent forest pond in the surrounding of the town of Salzburg, Austria,  $47^{\circ}47'\text{N}$ ,  $13^{\circ}02'\text{E}$ .

**Type material:** The protargol slide containing the holotype and six paratype slides with protargol-impregnated specimens have been deposited in the Biology Centre of the Upper Austrian Museum in Linz (LI). The holotype and other relevant specimens have been marked by black ink circles on the coverslip. For slides, see Fig. 19a–h in Chapter 5.

**Etymology:** The Latin adjective *salisburgensis* means “belonging to or from the Salzburg region”.



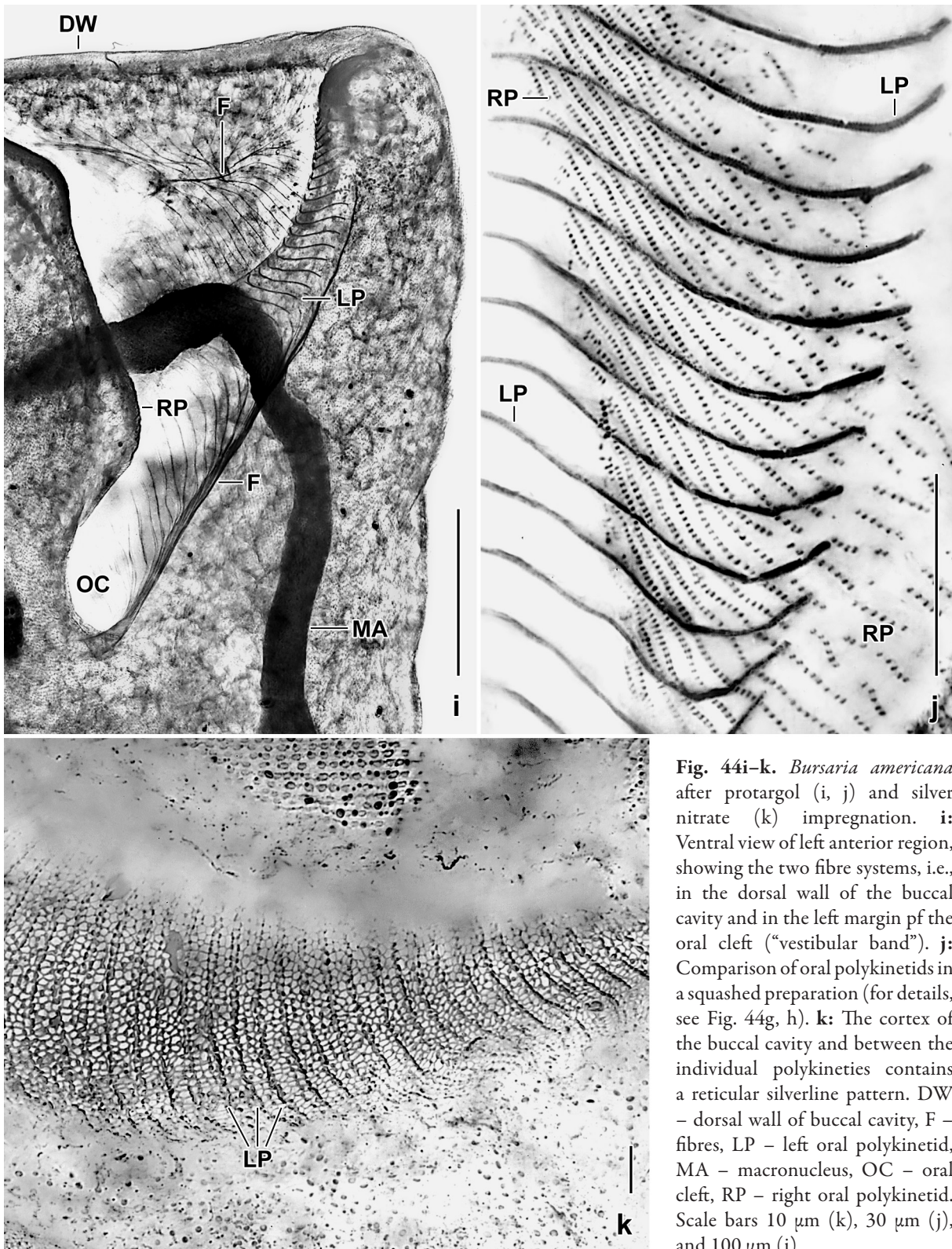


**Fig. 44i-k.** *Bursaria americana* after protargol (i, j) and silver nitrate (k) impregnation. **i:** Ventral view of left anterior region, showing the two fibre systems, i.e., in the dorsal wall of the buccal cavity and in the left margin of the oral cleft (“vestibular band”). **j:** Comparison of oral polykinetids in a squashed preparation (for details, see Fig. 44g, h). **k:** The cortex of the buccal cavity and between the individual polykineties contains a reticular silverline pattern. DW – dorsal wall of buccal cavity, F – fibres, LP – left oral polykinetid, MA – macronucleus, OC – oral cleft, RP – right oral polykinetid. Scale bars 10  $\mu\text{m}$  (k), 30  $\mu\text{m}$  (j), and 100  $\mu\text{m}$  (i).

**Remarks:** *Bursaria salisburgensis* differs from all congeners by the extrusomes which form a 3–4  $\mu\text{m}$  thick, structureless plate in the cortex. Only when disturbed 4–5  $\times$  2  $\mu\text{m}$ -sized rods become recognizable (Fig. 37b). I checked this carefully in three specimens, and the observations were confirmed in protargol-impregnated specimens, showing a structureless, not impregnated, 3–8  $\mu\text{m}$  thick zone in the periphery of the cortex (Fig. 45e). In most other characteristics, *B. salisburgensis* resembles  $\rightarrow$  *B. uluruensis*, except of the much longer left oral polykinetid (Fig. 37b; Table 15). *Bursaria salisburgensis* has “granular (curious) vacuoles” very similar to those of  $\rightarrow$  *B. uluruensis*.

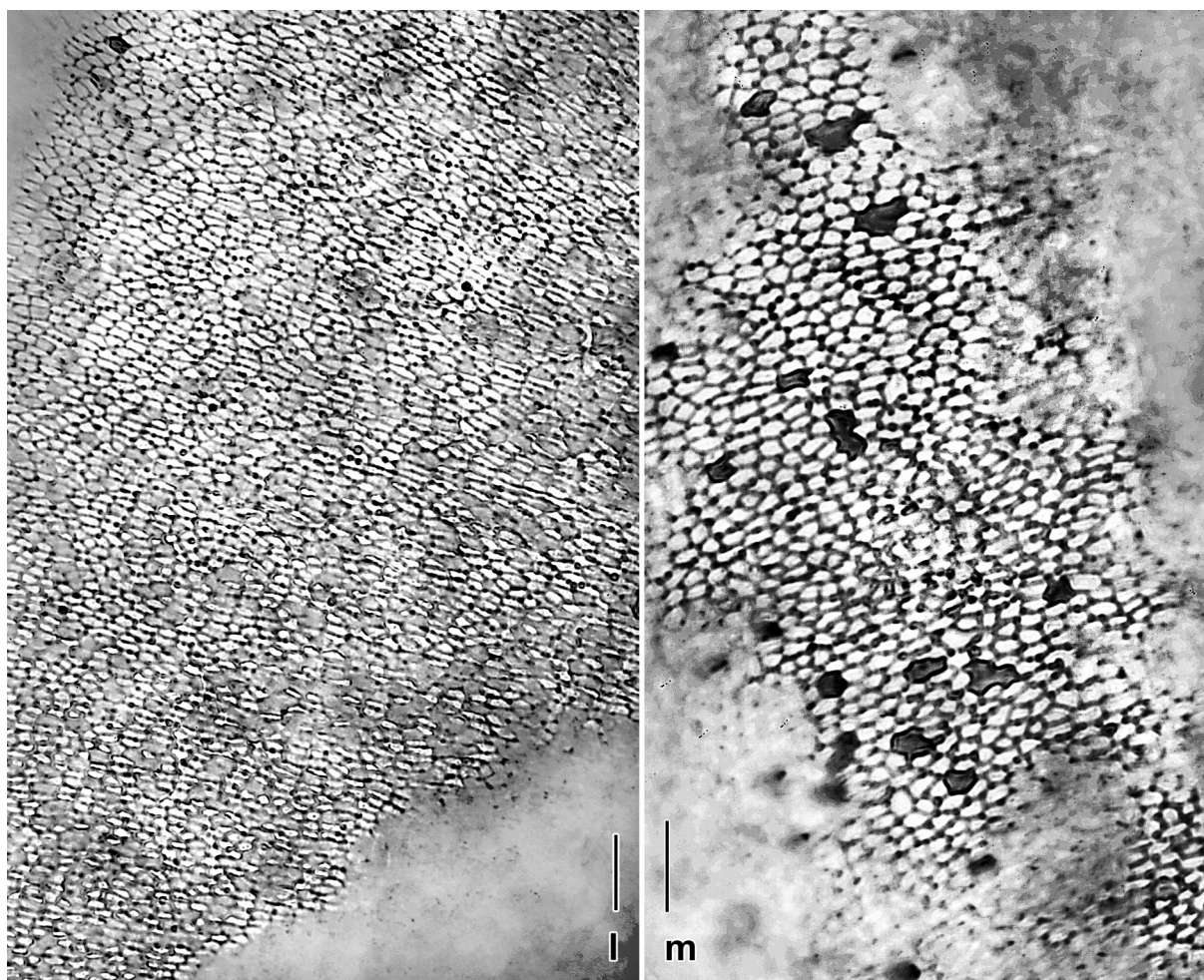


Fig. 441, m. *Bursaria americana*, variability of silverline pattern in buccal wall. Scale bars 10  $\mu\text{m}$  (l) and 12  $\mu\text{m}$  (m).

The cytoplasm is strongly vacuolated and contains food vacuoles with anaerobic ciliates, e.g., *Caenomorpha* sp. When feed with *Colpidium colpoda*, up to 100  $\mu\text{m}$ -sized food vacuoles are formed, each containing about 10 colpidia. Found in the anoxic mud and in the plankton.

***Bursaria uluruensis* nov. spec.**

(Fig. 36d, 37a, b, 46a–q, 47g–k; Tables 15, 18 on p. 321, 324)

**Material:** Australian site (170), i.e., ephemeral puddles on top of Ayers Rock 863 m above sea-level, Tjuta National Park, Australia. Cultivated with *Paramecium aurelia* as food.

**Diagnosis** (most measurements are from silver nitrate-impregnated specimens; add 5% preparation shrinkage to obtain in vivo values; averages are given, see Table 18 for extremes): Bursiform with left margin more or less concave and right convex, dorsoventrally flattened up to 2:1 and slightly twisted; body size 442  $\times$  256  $\mu\text{m}$ ; oral cleft extends 57% of body length. Left polykinetid recurved, consists of 103 polykineties with a maximum width of 62  $\mu\text{m}$ , deepest point at 30% of body length. About 328 ciliary rows. Extrusomes globular, 3–5  $\mu\text{m}$  in size. Resting cyst 223  $\mu\text{m}$  across in vivo.

**Type locality:** Ephemeral ponds on top of Ayers Rock, Australia, 25°20'42"S, 131°02'10"E.

**Type material:** Seven and four slides with protargol- and silver nitrate-impregnated specimens, respectively, have been deposited in the Biology Centre of the Upper Austrian Museum in Linz

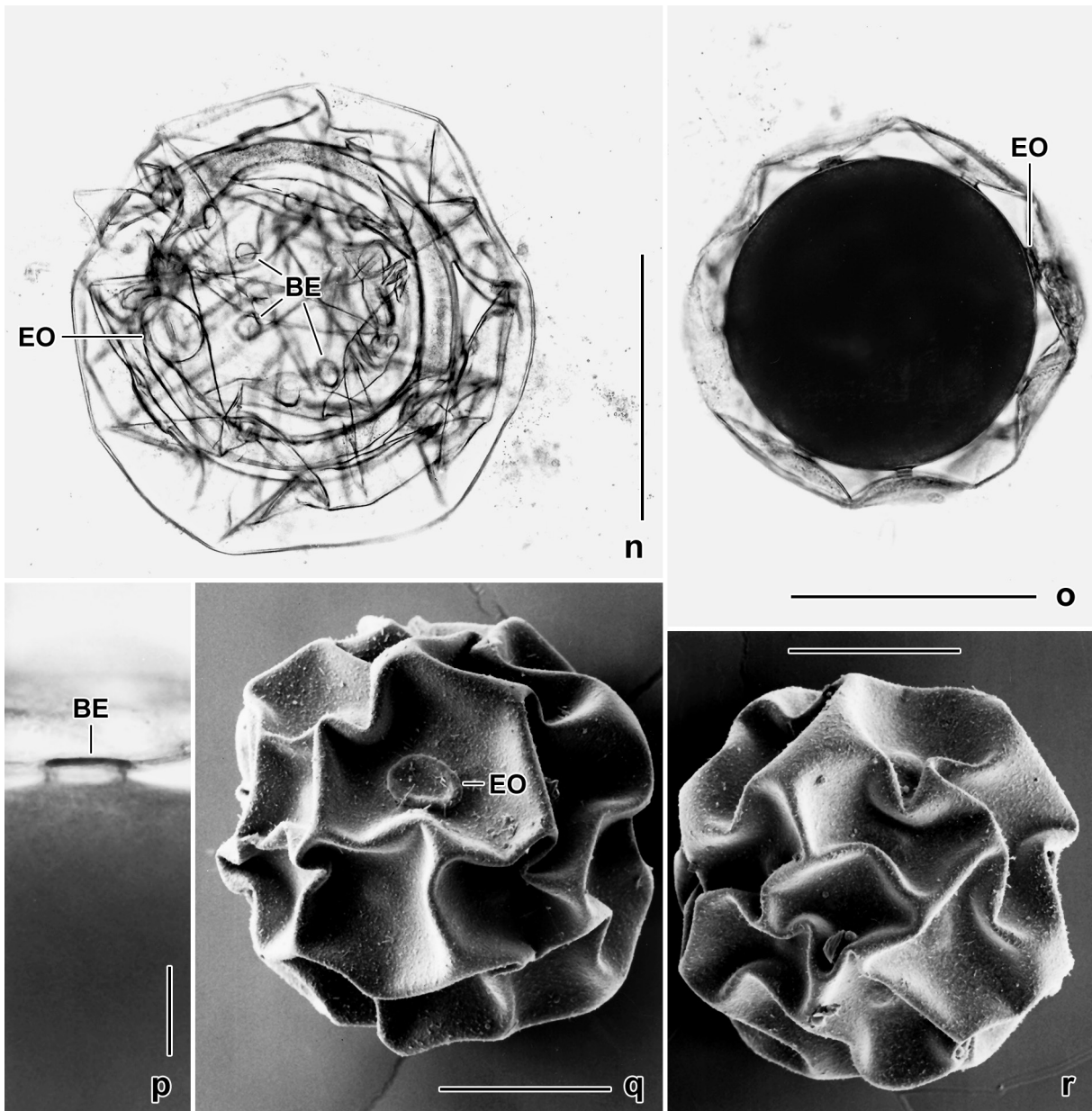


**Fig. 44n-r.** *Bursaria americana*, resting cysts in the light- and scanning electron microscope. **n:** A squashed cyst, showing the escape opening and the bridges connecting ectocyst and endocyst. **o, p:** Under transmitted light, the resting cyst appears dark due to the dense contents. The cyst wall contains an escape opening and low bridges (4–13 µm) that connect ectocyst and endocyst. **q, r:** The cyst surface is faceted and shows the escape opening. See Foissner (1993, p. 451) for a detailed description of the resting cyst of *B. americana*. BE – bridges connecting ectocyst and endocyst, EO – escape opening. Scale bars 20 µm (p), 100 µm (q, r), and 200 µm (n, o).

(LI). The holotype (protargol) and other relevant specimens have been marked by black ink circles on the coverslip. For slides, see Fig. 20a–l in Chapter 5.

**Etymology:** Named after the site discovered, i.e., the aboriginal noun *Uluru* (Ayers Rock) which is the type locality.

**Remarks:** *Bursaria uluruensis* is a “typical” congener (see diagnosis) and could be cultivated with *Paramecium aurelia* as food. Like some congeners, it has granular vacuoles in the cortex (Fig. 46p, q). The extrusomes belong to the globular type and are 3–5 µm across (Fig. 37b, 46c, 47g). When disturbed, the globules become 3–4 µm long rods (Fig. 27b, 46d–f, 47h–j) highly similar to those in undisturbed → *B. truncatella*. When the rods are extruded, they become slenderly conical (Fig.

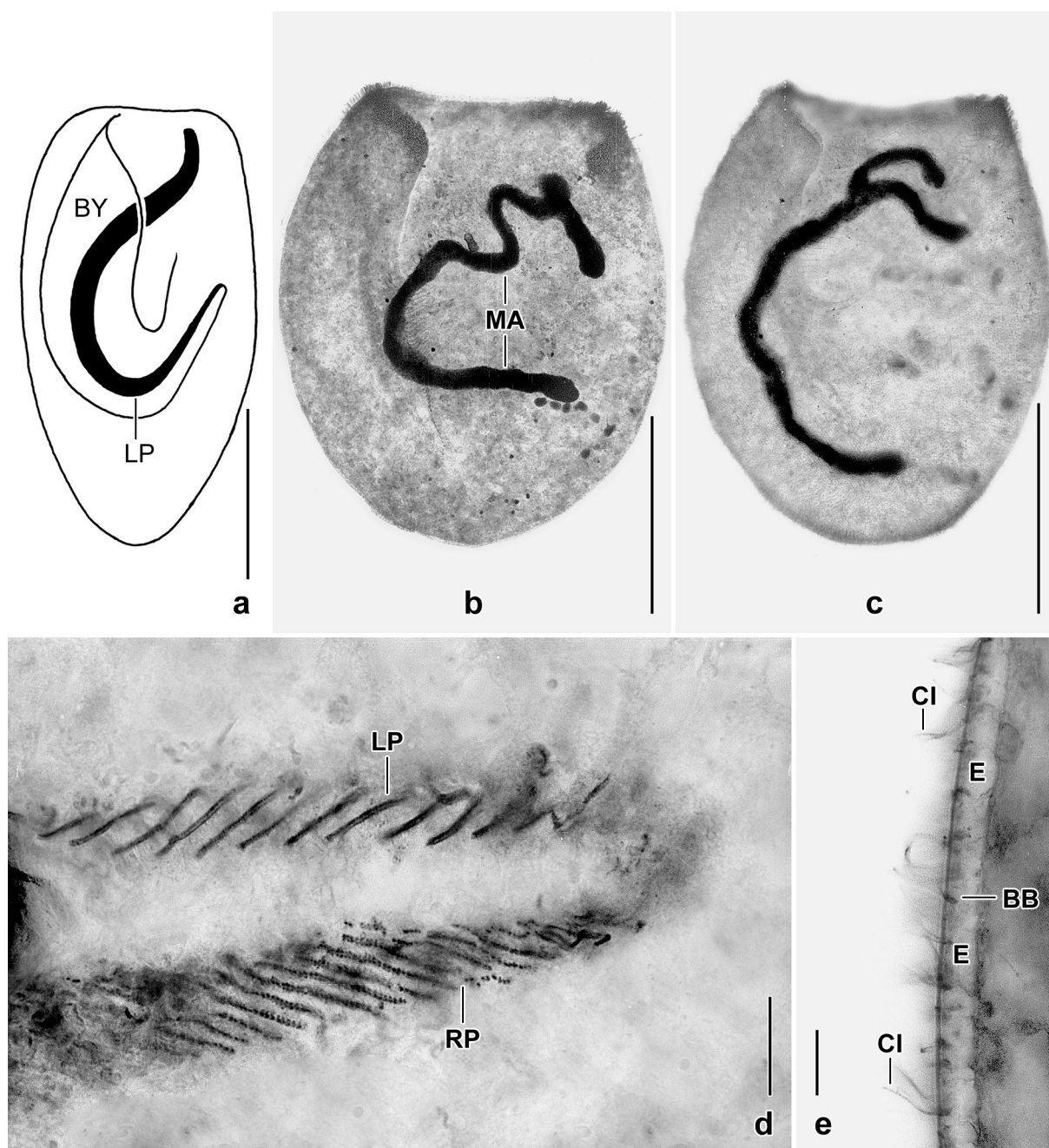


**Fig. 45a–e.** *Bursaria salisburgensis* from Austria in a Stieve-fixed preparation (a) and after protargol impregnation (a–e). **a:** A well-preserved, lenticular or ellipsoid specimen with recurved left oral polykinetid, length 510  $\mu\text{m}$ . **b, c:** Ethanol-fixed, slightly squashed specimens to show the macronucleus which is bifurcated in the right cell. **d:** Proximal region of a squashed specimen to show the oral polykinetids which are very similar in all species investigated except of the shape (recurved or not recurved). **e:** The cortex has a 3–8  $\mu\text{m}$  wide, bright, structureless zone, i.e., plate-like arranged mucocysts, a main diagnostic feature. BB – basal bodies, BY – buccal cavity, CI – cilia, E – extrusome zone, LP – left oral polykinetid, MA – macronucleus, RP – right oral polykinetid. Scale bars 10  $\mu\text{m}$  (d, e) and 200  $\mu\text{m}$  (a–c).

46k, 47j). Next, the cones develop to about 50  $\mu\text{m}$  long threads forming a dense envelope around the cell (Fig. 46l, m, 47k).

*Bursaria uluruensis* is rather similar to the second Australian species,  $\rightarrow$  *B. fluviatilis*: both have a short oral polykinetid (Table 15) which, however, is recurved only in *B. uluruensis*; furthermore, they have a different number of oral polykineties (103 vs. 72) and ciliary rows (328 vs. 455).

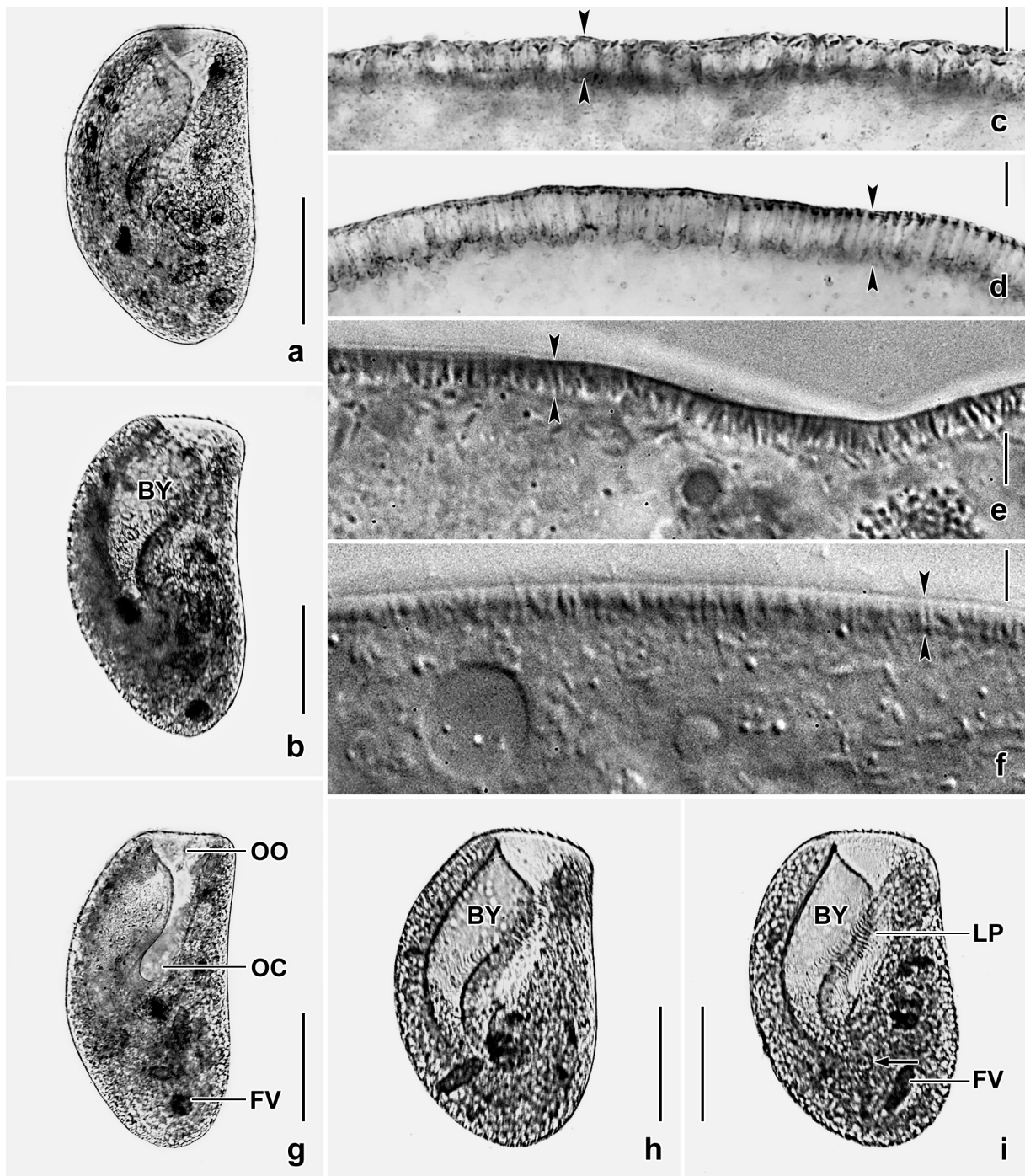


**Fig. 46a–i.** *Bursaria uluruensis* from life (a–c, e–i) and after protargol impregnation (d). **a, b, g–i:** Ventral views of freely motile specimens, showing variability of body shape and the huge buccal cavity (b, h, i). The arrow in (i) marks the deepest point of the left oral polykinetid, i.e., the site where it commences recurving; compared to most congeners, this is far away from the posterior body end and thus an important feature of this species. **c–f:** *Bursaria uluruensis* has a 3–4  $\mu\text{m}$  thick extrusome fringe marked by opposed arrowheads. When resting, the extrusomes are globular and about 3  $\mu\text{m}$  across (c). When the cell is slightly disturbed, the extrusomes explode becoming 3–5  $\mu\text{m}$  long rods (d–f). See Fig. 37b and 46k–m for further information. BY – buccal cavity, FV – food vacuoles, LP – left oral polykinetid, OC – oral cleft, OO – oral opening. Scale bars 5  $\mu\text{m}$  (c–f) and 200  $\mu\text{m}$  (a, b, g–i).

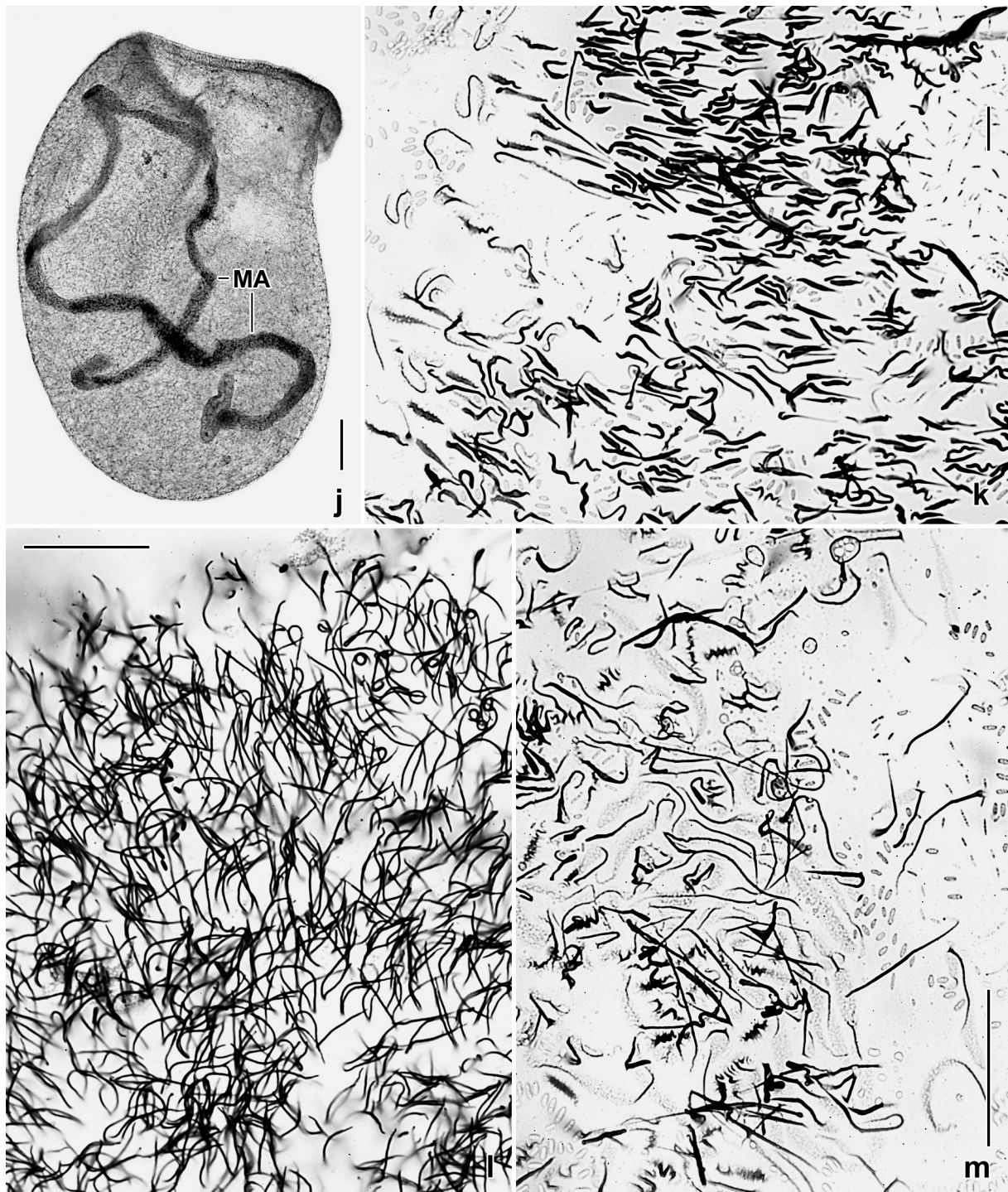
**Fig. 46j–m.** *Bursaria uluruensis* in a silver carbonate impregnation (j) and in methyl green-pyronin stains (k–m). **j:** → Ventral view showing the long macronucleus. **k:** *Bursaria uluruensis* has thousands of extrusomes (mucocysts) in the cortex. When just extruded, the extrusomes are narrowly conical. **l, m:** Fully exploded extrusomes become up to 50  $\mu\text{m}$  long, flexible filaments which swell to a thick, slimy envelope. The minute, faintly impregnated structures in the background are bacteria. MA – macronucleus. Scale bars 10  $\mu\text{m}$  (k) and 50  $\mu\text{m}$  (j, l, m).

*Bursaria fluviatilis* nov. spec.

(Fig. 36c, 37a, 47a–f, 48a–x; Tables 15, 18 on p. 321, 324)

**Material:** *Bursaria fluviatilis* was discovered in soil from the floodplain of the Murray River near to the town of Albury, southern Australia. It was also observed in the plankton of this river. The species was cultivated in dirty cultures set up with a few milliliters from the non-flooded Petri dish culture and feed with some squashed wheat grains.

**Diagnosis** (measurements are from protargol-impregnated specimens; add 15% preparation shrinkage to obtain in vivo values; averages are given, see Tables 15 and 18 for extremes): Bursiform, left margin frequently concave, right more or less convex; body size  $681 \times 442 \mu\text{m}$ ; oral cleft extends



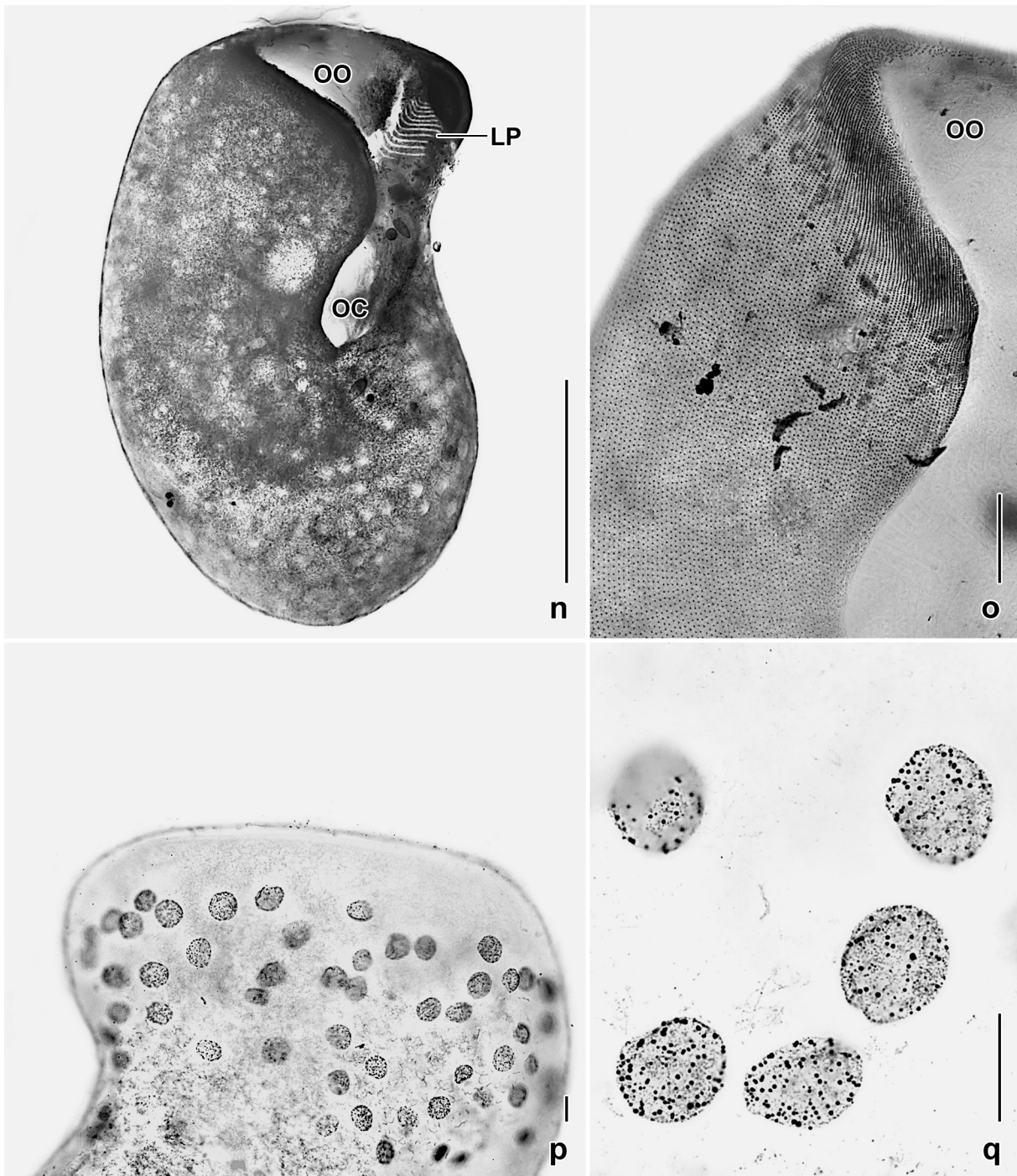


**Fig. 46n–q.** *Bursaria uluruensis* after protargol (n, p, q) and silver carbonate (o) impregnation. **n:** Ventrolateral view of a specimen with strongly concave ventral side. Live shape, see Fig. 46a, b, g–i. **o:** Ventral view of the right anterior quadrant of a cell, showing the narrowly spaced ciliary rows with cilia very narrowly spaced around the oral opening. **p, q:** Dorsal view of anterior body region, showing the granular (“curious” in Foissner 2016) vacuoles, a new organelle with unknown function. These vacuoles, which have a size of about 15  $\mu\text{m}$  (Table 18), contain minute, strongly protargol-affine granules (q). LP – left oral polykinetid, OC – oral cleft, OO – oral opening. Scale bars 15  $\mu\text{m}$  (p, q), 50  $\mu\text{m}$  (o), and 200  $\mu\text{m}$  (n).

48% of body length. Left oral polykinetid not recurved, short, i.e., deepest point 31% away from posterior body end, consists of 72 polykineties with a maximum width of 63  $\mu\text{m}$ . About 403 ciliary rows. Extrusomes globular, about 3  $\mu\text{m}$  across. Resting cyst 232  $\mu\text{m}$  in diameter in vivo.

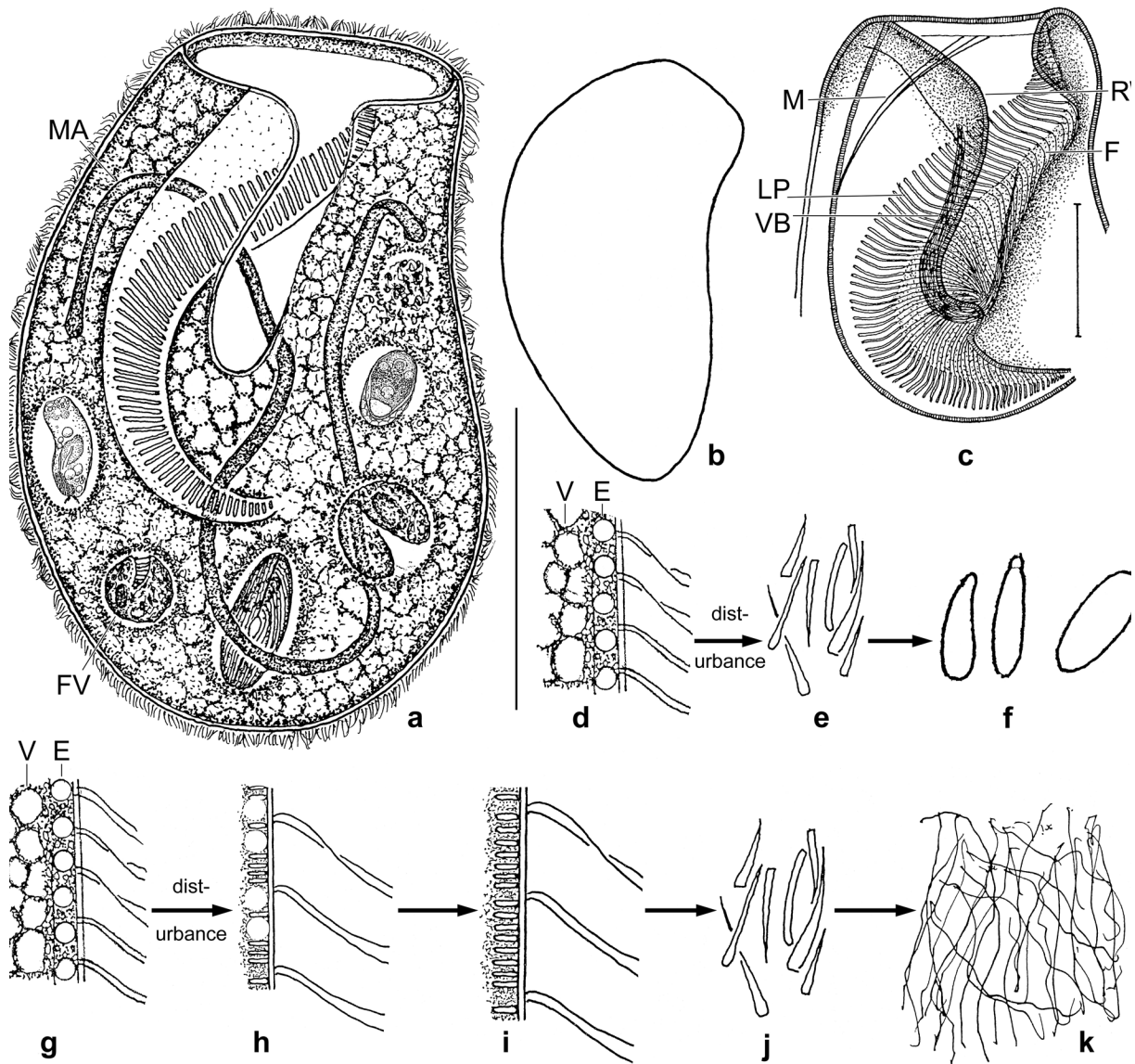


**Fig. 47a–k.** *Bursaria fluviatilis* (a–f) and *B. uluruensis* (g–k) from life (a, b, d, g–i), after hematoxylin staining (c, from Bary 1950), and in methyl green-pyronin stains (e, f, j, k). **a:** Ventral view of a representative specimen with several food vacuoles containing ciliates, testate amoebae, and rotifers; length 700  $\mu\text{m}$ . Note the short left oral polykinetid and the strongly vacuolated cytoplasm. **b:** Shape variant. **c:** The short left oral polykinetid of the New Zealand *B. truncatella* suggests that it is *B. fluviatilis* or *B. uluruensis*. **d–f:** *Bursaria fluviatilis* has globular extrusomes (d), which become slenderly conical (e) and inflated (f) when the dye is added. **g–k:** *Bursaria uluruensis* has also globular extrusomes (g) which transform to 3–4  $\mu\text{m}$  long rods (h, i) when the cell is disturbed by slight coverslip pressure. When the dye is added, the extrusomes are extruded and become slenderly conical (j) and, finally, long threads (k). E – extrusomes, F – fibres, FV – food vacuoles, LP – left oral polykinetid, M – “Mundspalte”, MA – macronucleus, RW – right wall of buccal cavity, V – cytoplasmic vacuole, VB – “vestibular” band. Scale bars 105  $\mu\text{m}$  (c) and 300  $\mu\text{m}$  (a).

**Type locality:** Floodplain soil from the Murray River near to the town of Albury, waterside of Ryans road, Australia, 37°S, 147°E. See also footnote at  $\rightarrow$  *Levispatha australiensis* nov. spec.

**Type material:** Six slides with protargol-impregnated specimens have been deposited in the Biology Centre of the Upper Austrian Museum in Linz (LI). The holotype and other relevant specimens have been marked by black ink circles on the coverslip. For slides, see Fig. 21a–g in Chapter 5.

**Etymology:** The Latin adjective *fluviatilis* (pertaining to rivers) refers to the habitat the species was discovered.

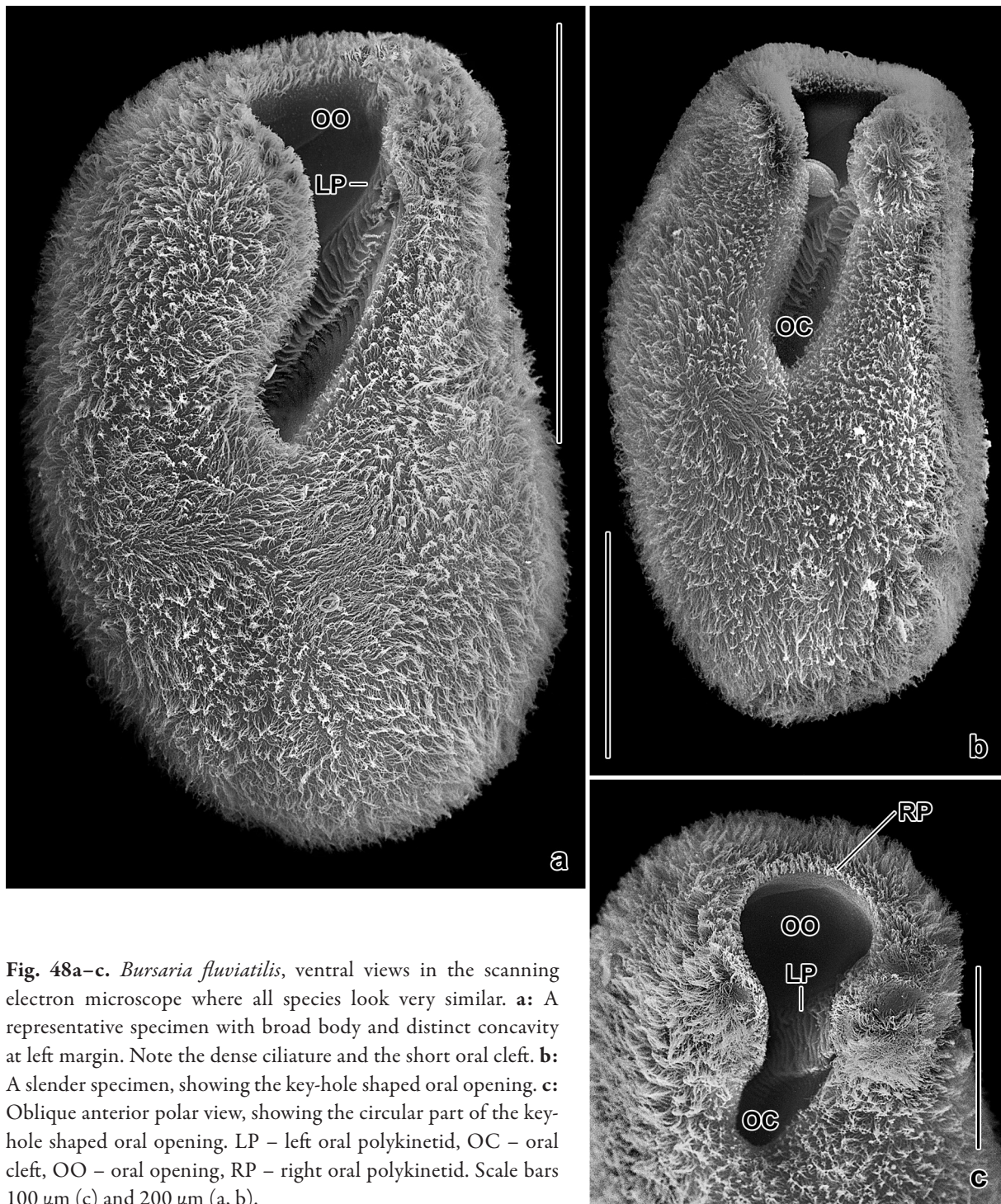


**Fig. 48a–c.** *Bursaria fluviatilis*, ventral views in the scanning electron microscope where all species look very similar. **a:** A representative specimen with broad body and distinct concavity at left margin. Note the dense ciliature and the short oral cleft. **b:** A slender specimen, showing the key-hole shaped oral opening. **c:** Oblique anterior polar view, showing the circular part of the key-hole shaped oral opening. LP – left oral polykinetid, OC – oral cleft, OO – oral opening, RP – right oral polykinetid. Scale bars 100  $\mu\text{m}$  (c) and 200  $\mu\text{m}$  (a, b).

**Remarks:** The body is flattened ventrally and has a more or less distinct subapical concavity along the left body margin (Fig. 47a, b, 48a, b, j, l). The macronucleus (Fig. 47a, 48f, n, o) as well as the somatic and oral infraciliature are as in congeners (Fig. 48a, b, i, j, l, m, p–r). The cytoplasm is distinctly vacuolated and studded with minute lipid droplets between the vacuoles. Feeds on the hypotrich ciliate  $\rightarrow$  *Urosoma australiensis*, testate amoebae, and rotifers; in cultures it takes *Paramecium* (Fig. 47a). The extrusomes are globular and 3–4  $\mu\text{m}$  across (Fig. 47d, 48e–g); when disturbed, extruded and developing to up to 15  $\mu\text{m}$  long, slender cones (Fig. 37b, 47e, 48h–k). Then, cones become inflated (Fig. 47f) and possibly develop to long threads; a rod-shaped stage, as in  $\rightarrow$  *B. uluruensis*, was not observed. Granular cortex vacuoles possibly absent.

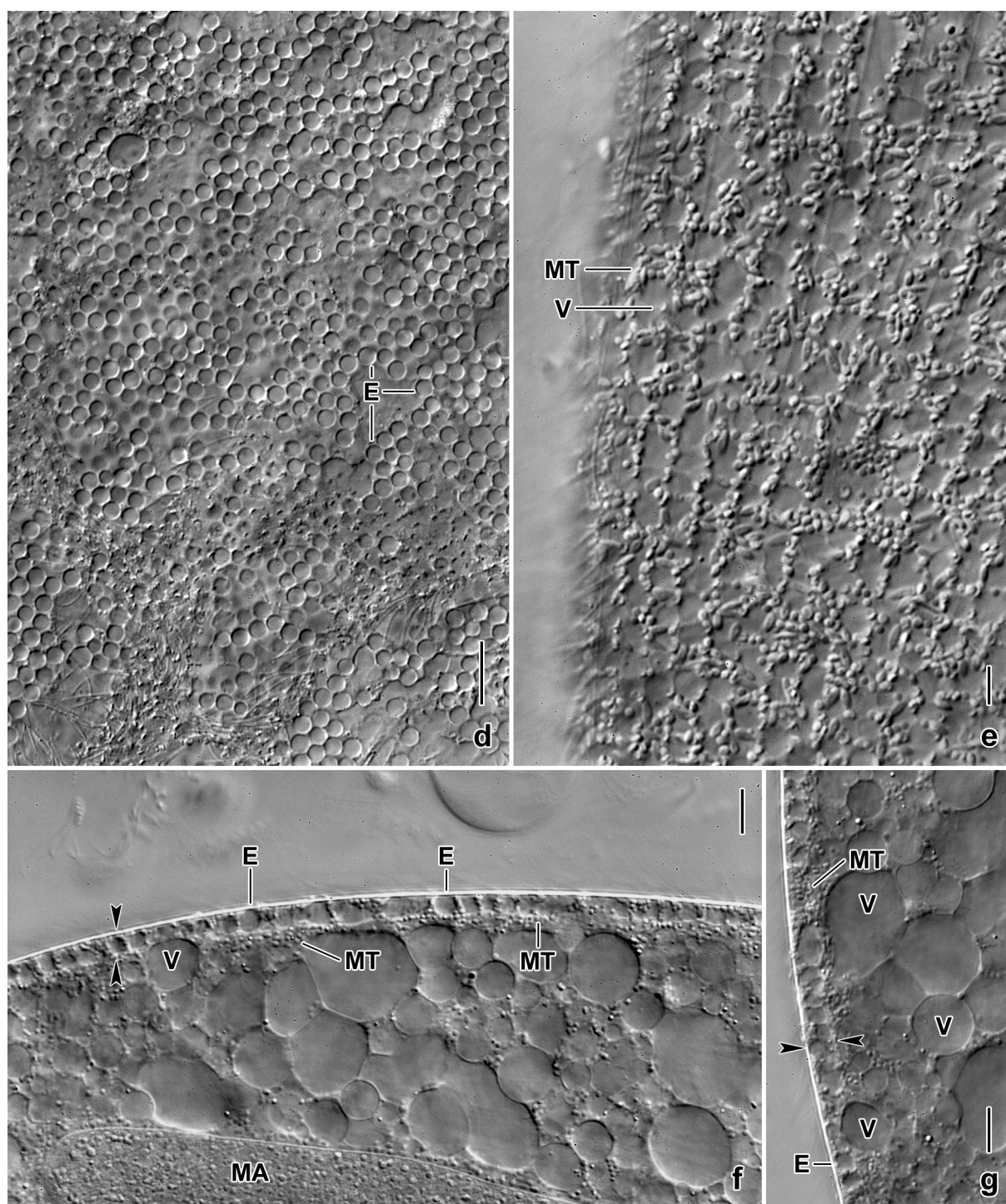


**Fig. 48d–g.** *Bursaria fluviatilis*, showing extrusomes from life. All *Bursaria* species have extrusomes of the mucocyst type. Three subtypes can be distinguished: globular, rod-shaped, and plate-like. *Bursaria fluviatilis* belongs to the globular subtype seen at two focal planes in (d, e) where they appear as small, round vacuoles (d) proximally surrounded by countless mitochondria (e). **f, g:** Optical section of cell periphery, showing the cortex (opposed arrowheads) containing countless globular mucocysts. The cytoplasm is strongly vacuolated. E – extrusomes, MA – macronucleus, MT – mitochondria, V – cytoplasmic vacuoles. Scale bars 3  $\mu\text{m}$  (e), 5  $\mu\text{m}$  (f, g), and 10  $\mu\text{m}$  (d).

The resting cyst is globular, rarely slightly elliptic (Fig. 48s–u). The bridges between ectocyst and endocyst have a diameter of about 10  $\mu\text{m}$ . The endocyst is inconspicuous because only 2–3  $\mu\text{m}$  thick (Fig. 48u). The cytoplasm appears homogenous because studded with 2–4  $\mu\text{m}$ -sized granule aggregates composed of minute granules 1–2  $\mu\text{m}$  across (Fig. 48x). The macronucleus is irregularly

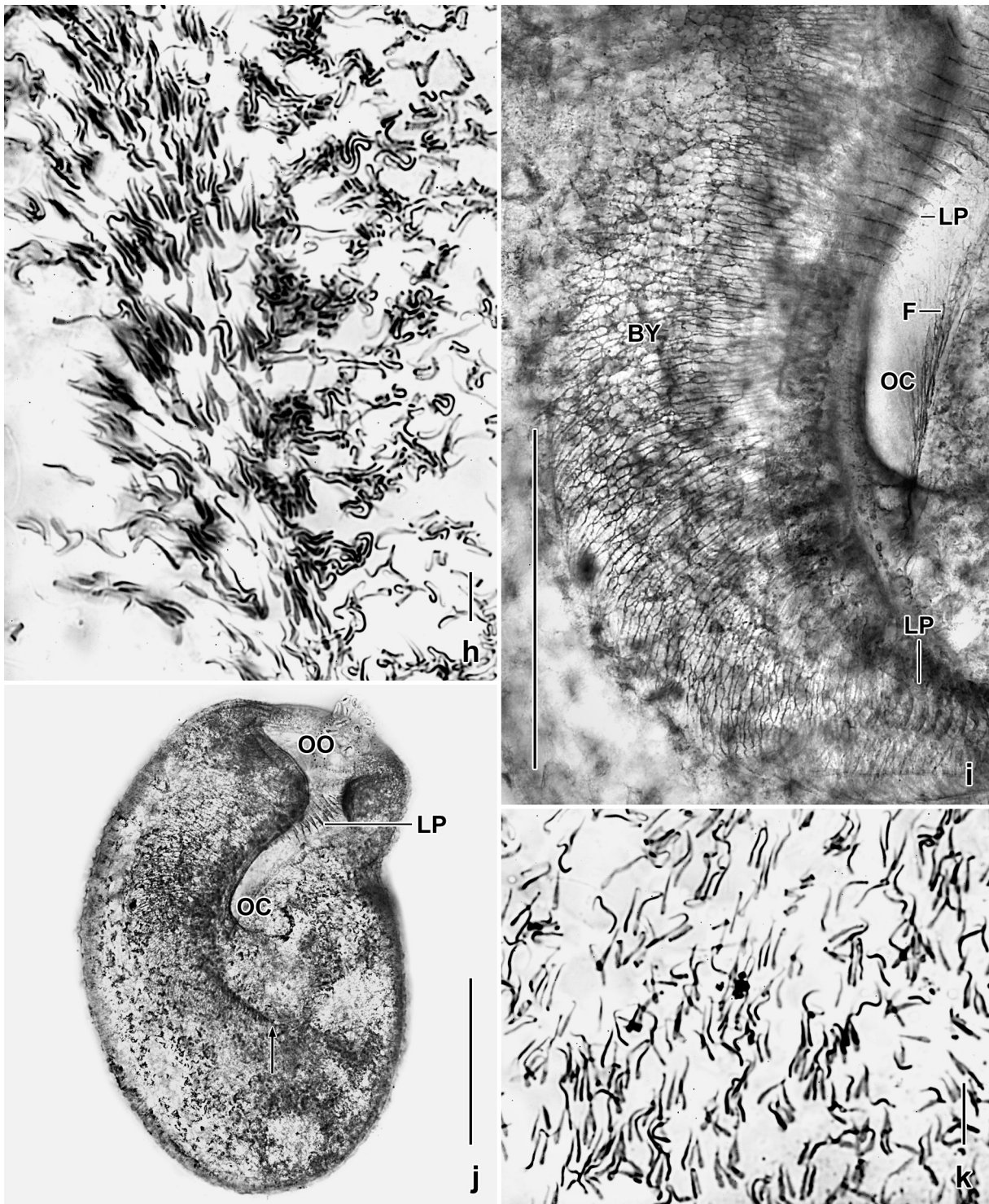


**Fig. 48h-k.** *Bursaria fluviatilis* in methyl green-pyronin (h, k) and protargol (i, j) preparations. **h, k:** When just extruded, the mucocysts are narrowly conical. **i:** Fibre system in right buccal wall and right of the left oral polykinetid. **j:** Ventral view, showing the proximal end (arrow) of the left oral polykinetid far away from the posterior end of the cell; this is a main diagnostic feature. BY – buccal cavity, F– fibres, LP – left oral polykinetid, OC – oral cleft, OO – oral opening. Scale bars 10 µm (h, k) and 200 µm (i, j).

curved. The emergence pore is 30–40 µm in size, circular to elliptic, and its surface is wrinkled or has some minute holes (Fig. 48s, t, v, w).

Of the species investigated, *B. fluviatilis* has the shortest oral cleft (48% of body length) and adoral polykinetid (Fig. 37a, 48j, l, q; Table 15). Thus, it is rather easily identified. The most similar

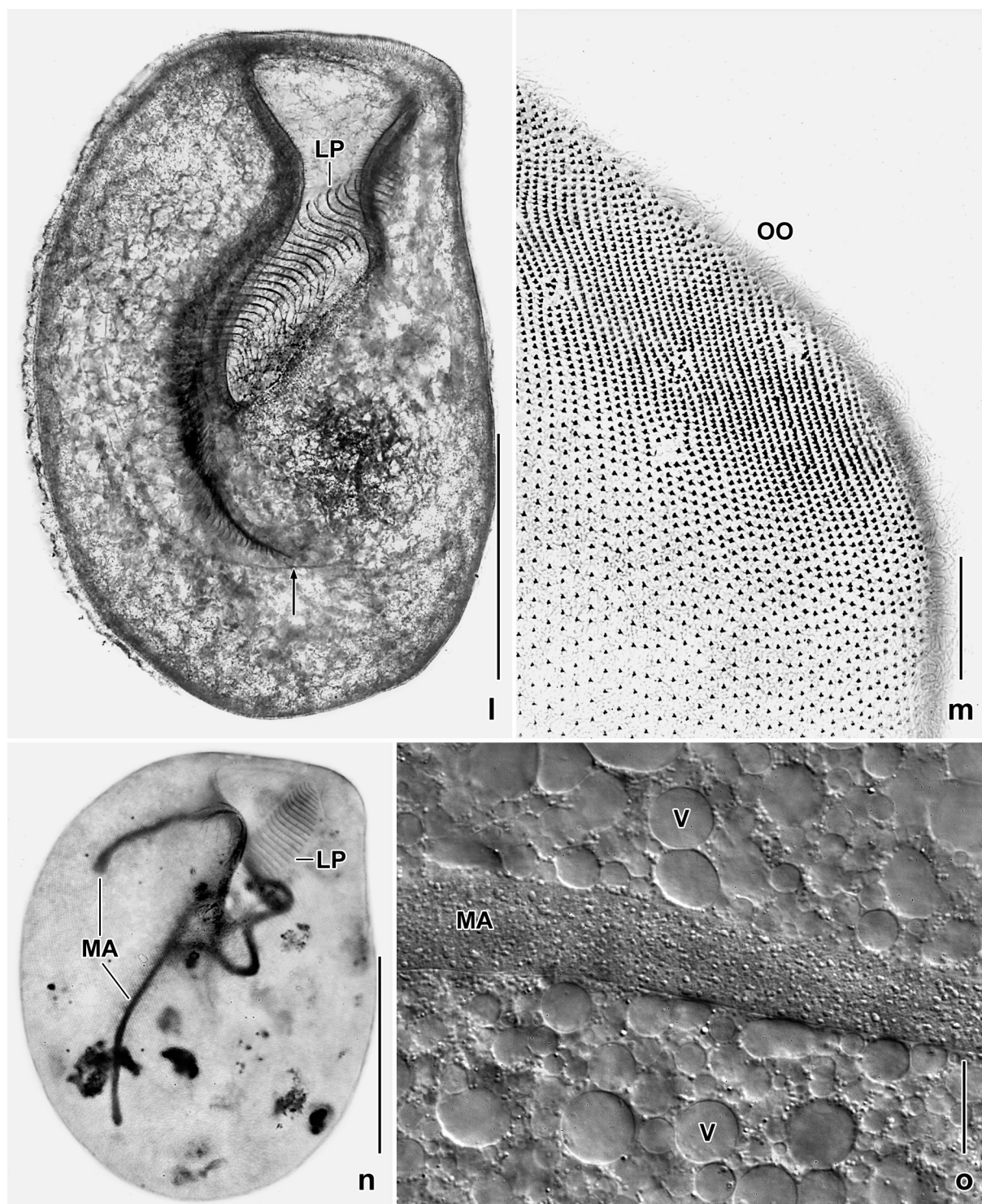


**Fig. 481-o.** *Bursaria fluviatilis* after protargol (l) and silver carbonate (m, n) impregnation and from life (o). **l:** Ventral view showing the proximal end of the left oral polykinetid (arrow) far away from rear end of body, a main diagnostic feature. **m:** A piece of the anterior kinety pattern. **n:** Overview showing the macronucleus. **o:** Macronucleus and the strongly vacuolated cytoplasm. LP – left oral polykinetid, MA – macronucleus, OO – oral opening, V – cytoplasmic vacuoles. Scale bars 20  $\mu\text{m}$  (o), 25  $\mu\text{m}$  (m), and 200  $\mu\text{m}$  (l, n).

species is  $\rightarrow$  *B. uluruensis* which differs by the recurved adoral polykinetid (vs. not recurved; Fig. 1c, d), the number of polykineties comprising the polykinetid (103 vs. 72; Table 15), and the number of ciliary rows (328 vs. 403; Table 15). The extrusomes are also slightly different (Fig. 47d–f vs. 47g–k).

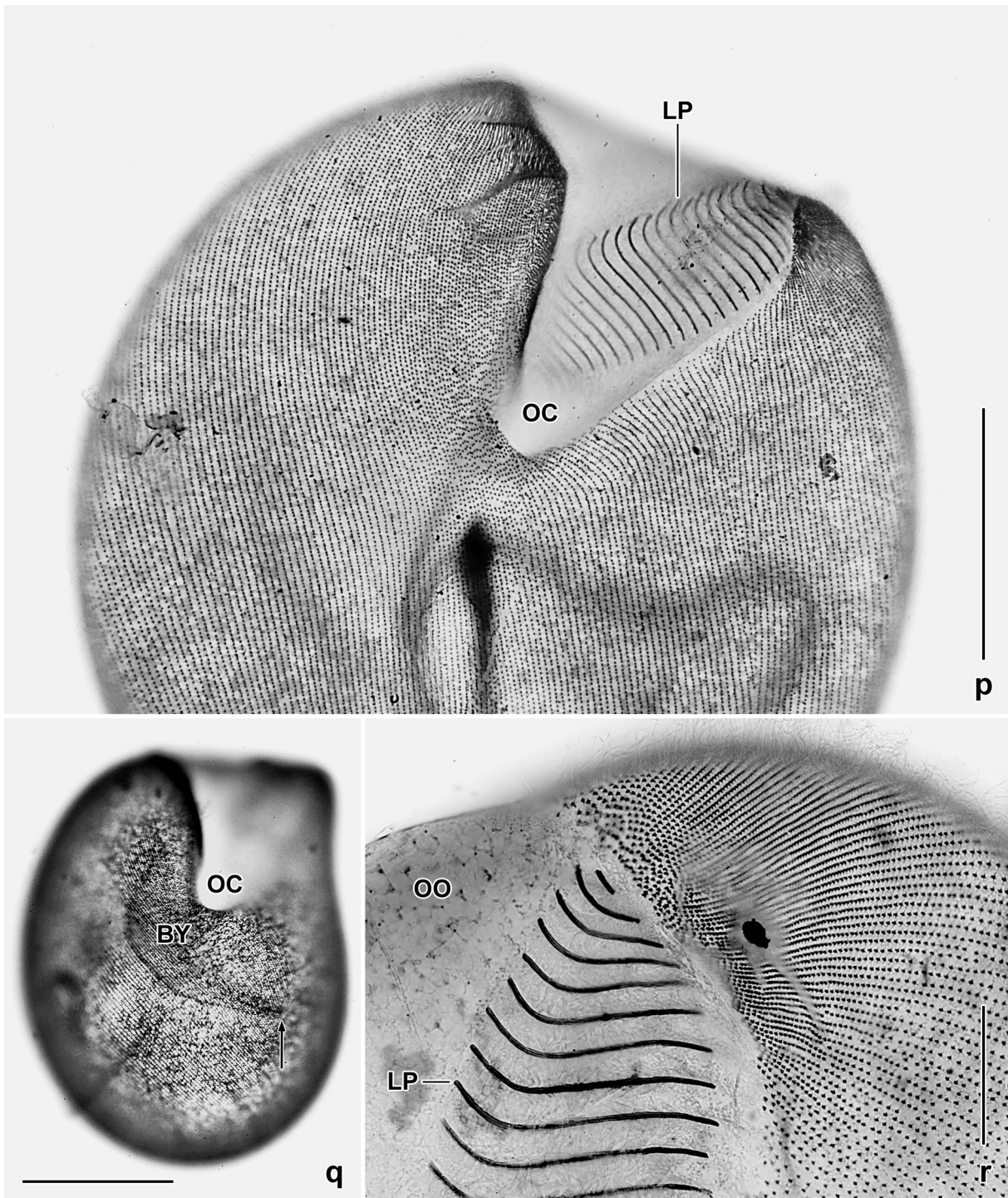


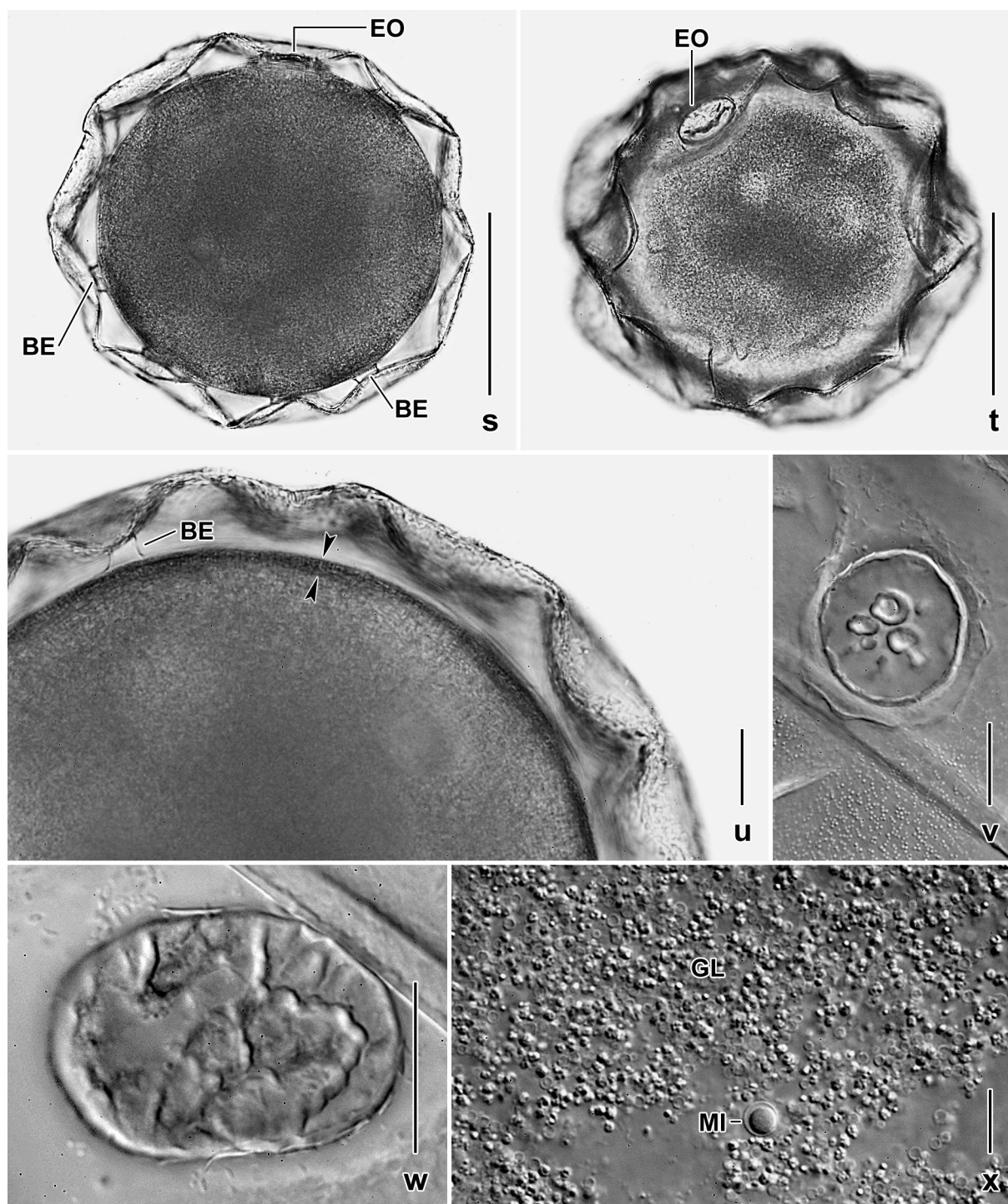
**Fig. 48p-r.** *Bursaria fluviatilis*, ventral views after silver carbonate impregnation. **p:** Anterior body half, showing about 130 kineties. Note the narrowly spaced kinetids within the ciliary rows. **q:** Overview showing the ciliary rows and the proximal end of the left oral polykinetid (arrow) which is far away from the posterior end of the cell. This is an important character of this species. **r:** Begin of the left oral polykinetid. The full width of the oral polykineties is obtained posterior of the first third of the polykinetid. BY – buccal cavity, LP – left oral polykinetid, OC – oral cleft, OO – oral opening. Scale bars 20  $\mu\text{m}$  (r), 100  $\mu\text{m}$  (p), and 200  $\mu\text{m}$  (q).

**Fig. 48s-x.** *Bursaria fluviatilis*, resting cysts from life. The cysts are globular and colourless but the contents appears dark because it is thick and refractive. **s, t:** Optical sections, showing the thick, faceted cyst wall, bridges connecting ectocyst and endocyst, and the emergence pore. **u:** High magnification of cyst wall, showing a bridge and the endocyst (opposed arrowhead). **v, w:** The emergence pore is circular (v) or elliptic (w) and its surface has minute holes (v) or is strongly wrinkled (w). **x:** Granular cyst contents and micronucleus with distinct membrane. BE – bridges, EO – emergence pore, GL – granules, MI – micronucleus. Scale bars 10  $\mu\text{m}$  (x), 20  $\mu\text{m}$  (u-w), and 100  $\mu\text{m}$  (s, t).

*Exocolpoda augustini* (Foissner, 1987) Foissner, Agatha & Berger, 2002

(Fig. 49a–d)

- 1987 *Colpoda augustini* nov. spec. — Foissner, Zool. Beitr., 31: 249 (original description).  
1993 *Colpoda augustini* Foissner, 1987 — Foissner, Protozoenfauna Vol. 4/1: 135 (review and first SEM micrographs).  
2002 *Exocolpoda augustini* (Foissner, 1987) nov. comb. — Foissner, Agatha & Berger, Denisia 5: 921 (review and transfer to *Exocolpoda*; redescription from a Namibian population; ontogenesis using silver nitrate impregnation and SEM; morphometry).  
2011 *Exocolpoda augustini* — Foissner, Dispersal of protists: the role of cysts and human introductions. — In: Fontaneto D. (ed.): Biogeography of microscopic organisms. Is everything small everywhere? — Cambridge Univ. Press, Cambridge, UK, p. 67 (resting cyst).



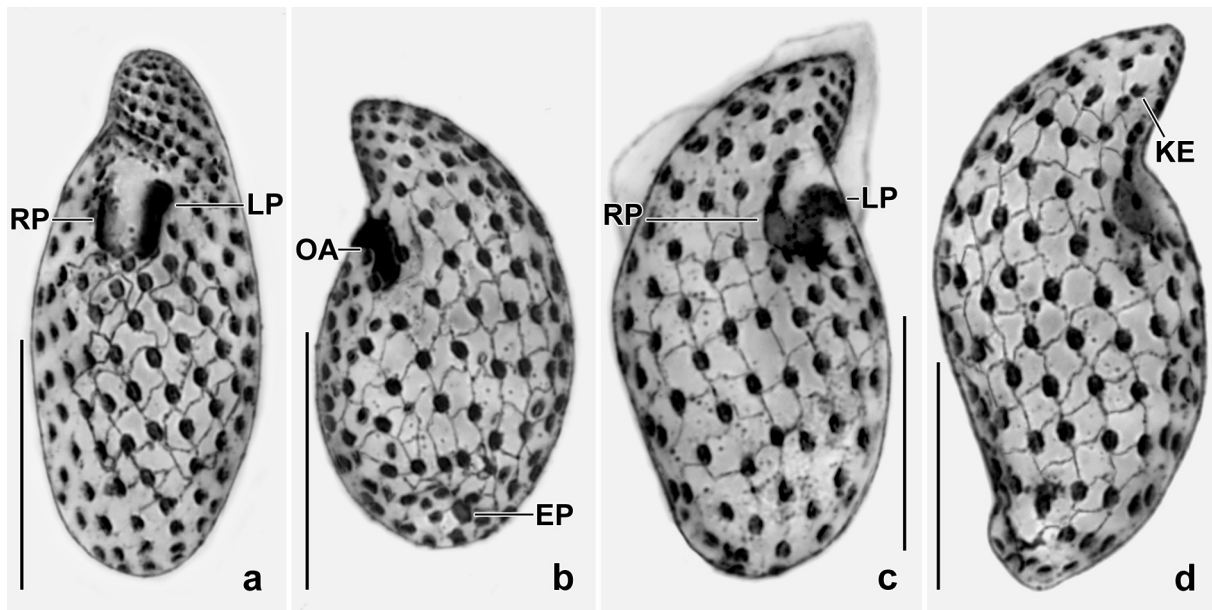


**Fig. 49a–d.** *Exocolpoda augustini* after Chatton-Lwoff silver nitrate impregnation. **a:** Ventral view. Arrow marks the colpodid silverline pattern. **b:** Left side view. **c, d:** Right side views. Figure (c) shows the species-specific boomerang-shaped left oral polykinetid. EP – excretory pore of contractile vacuole, KE – keel, LP – left oral polykinetid, OA – oral apparatus, RP – right oral polykinetid. Scale bars 20  $\mu\text{m}$ .

**Material:** Australian site (32).<sup>1</sup> Six voucher slides of Chatton-Lwoff-impregnated specimens have been deposited in the Biology Centre of the Upper Austrian Museum in Linz (LI). For slides, see Fig. 22a–f in Chapter 5.

**Remarks:** The Australian population (Fig. 49a–d) matches the type population from a *Eucalyptus* forest south of Tel Aviv (Israel). Very likely, *E. augustini* is a cosmopolitan (Foissner 1993, 1998). However, a complex of similar morphospecies is also possible because the resting cysts are rather different: those from the hot Namib desert have a very thick wall while cysts from the temperate Austria have a much thinner wall (Foissner 2011). Unfortunately, I did not investigate the cysts of the type material and the Australian population.

#### 4.2.4 Cyrtophorida

##### *Gastronauta insula* nov. spec.

(Fig. 50a–c, 51a–h; Table 19 on p. 325)

**Diagnosis:** Size in protargol preparations on average  $33 \times 21 \mu\text{m}$ , in vivo  $38 \times 24 \mu\text{m}$  when 15% preparation shrinkage is added. Body broadly ellipsoid, ovoid, or depressed, i.e., right margin distinctly convex, left straight or slightly convex. Macronucleus globular to broadly ellipsoid, micronucleus globular. Two contractile vacuoles in genus-specific location. Eight kineties in right ciliary field, five in left; two preoral and two vertical kineties. Circumoral kinety as typical for genus, long axis of oral cleft on average  $11 \mu\text{m}$ , short axis on average  $2.5 \mu\text{m}$  in protargol preparations. Dorsal brush along margin of anterior body end, composed of three clusters with two bristles each.

**Type locality:** Australian site (27), i.e., surface soil from Green Island east of the town of Cairns,  $17^{\circ}02'07''\text{S}$ ,  $145^{\circ}05'09''\text{E}$ .

<sup>1</sup> Note by H. Berger: I did not find a note by W. Foissner where the Australian sites are listed and described in detail.

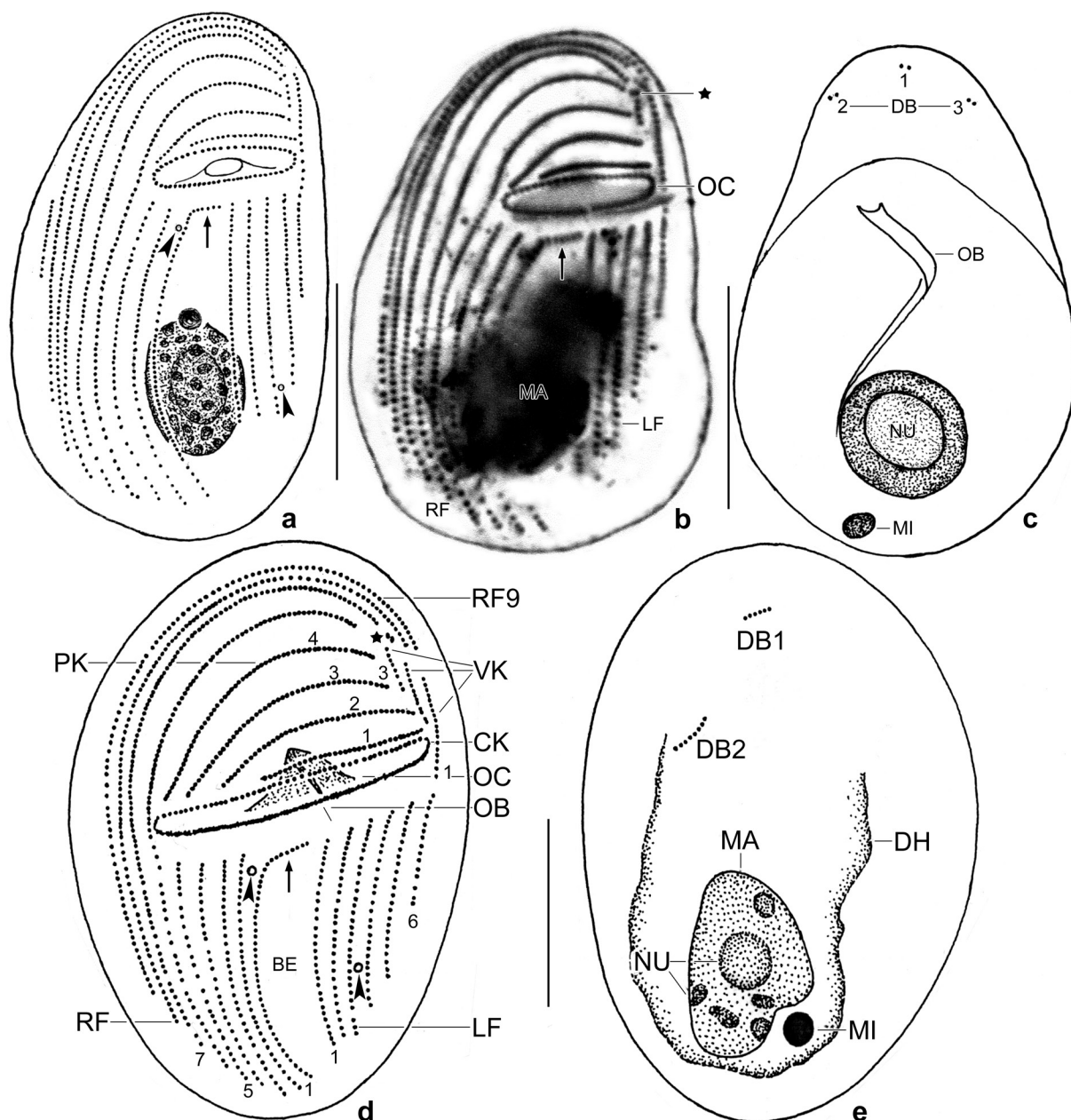


**Fig. 50a–e.** *Gastronauta insula* nov. spec. (a–c) and *G. membranaceus* (d, e; from Foissner 2000), ventral (a, b, d) and dorsal (c, e) views after protargol impregnation, showing *G. membranaceus* (d, e) as example for general organization and terminology. Arrows mark anteriorly curved inner kinety of right ciliary field; arrowheads denote excretory pore of contractile vacuoles; asterisks mark two mono- or dikinetids at anterior end of vertical kinety 2 or 3; numbers in figure (d) mark ciliary rows, preoral kineties are those which abut to the anterior portion of the circumoral kinety. The long oral cleft is associated with the inconspicuous oral basket and the circumoral kinety whose cilia form a conspicuous, lamellar structure in vivo. BE – barren (unciliated) area between right and left ciliary field, CK – circumoral kinety, DB1,2,3 – dorsal brush rows, DH – dorsal hump, LF – left ciliary field, MA – macronucleus, MI – micronucleus, NU – small peripheral nucleoli and a large central nucleolus, OB – oral basket, OC – oral cleft, PK – preoral kineties 1–4, RF – right oral ciliary field, RF9 – kinety 9 of right ciliary field, VK – three vertical kinety fragments. Scale bars 15  $\mu$ m.

**Type material:** The slide containing the holotype and two paratype slides with protargol-impregnated specimens have been deposited in the Biology Centre of the Upper Austrian Museum in Linz (LI). Relevant specimens have been marked by black ink circles on the coverslip.<sup>1</sup> For slides, see Fig. 23a–e in Chapter 5.

<sup>1</sup> Note by H. Berger: According to the labels, these slides also contain  $\rightarrow$  *Oxytricha africana australiensis*.

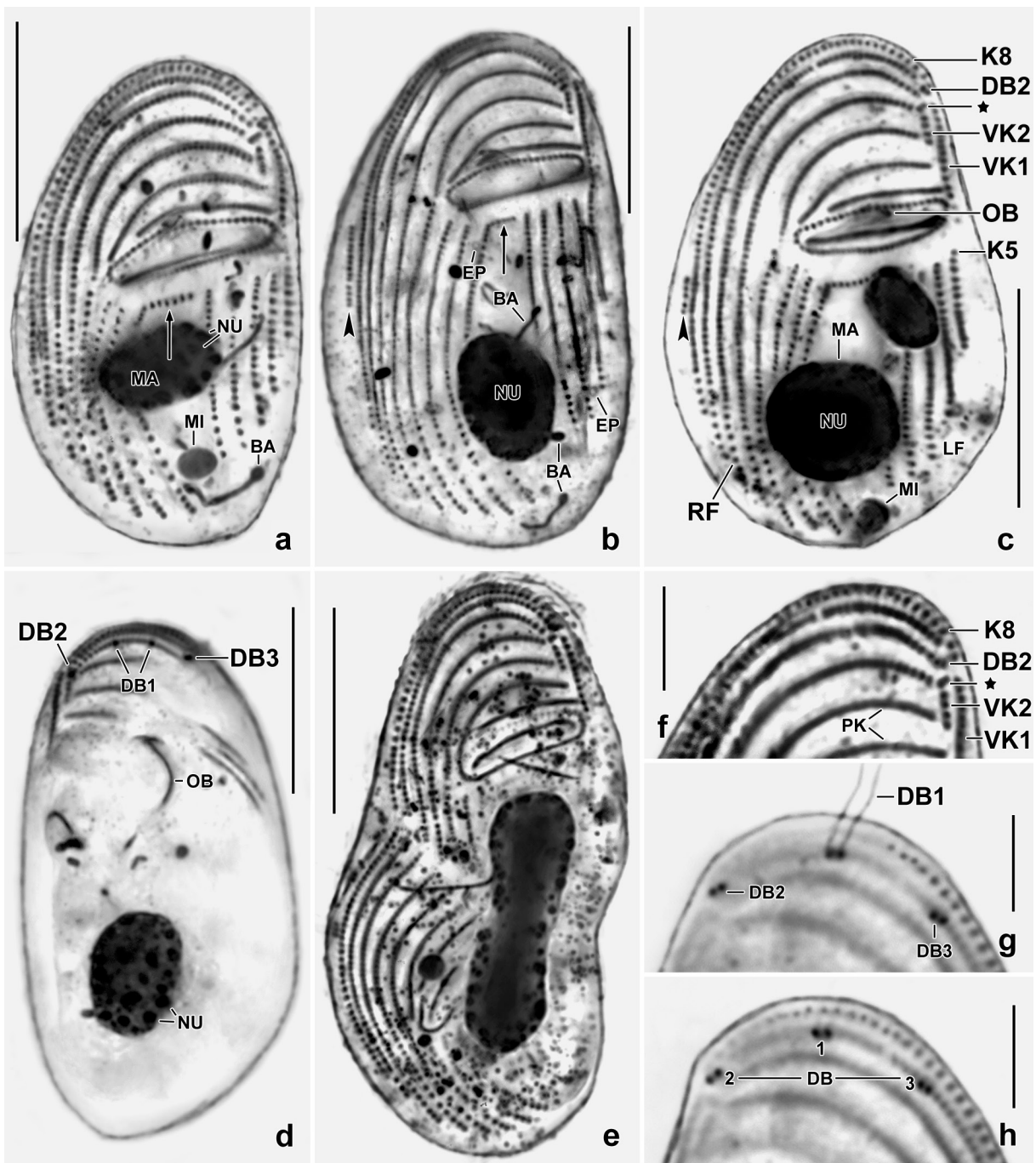


**Fig. 51a-h.** *Gastronauta insula*, ventral (a-c, e, f) and dorsal (d, g, h) views after protargol impregnation. See Fig. 50d, e for further explanation of structures. **a-c, f:** Overviews and a detail (f) of ventral side. Arrows mark the anteriorly curved first kinety of the right ciliary field; arrowheads mark the anlage for the dorsal brush; Fig. (f) is a detail from (a), showing the complex basal body pattern in the left anterior quadrant of the cell. The cytoplasm often contains club-shaped bacteria up to 8  $\mu\text{m}$  long. **d, g, h:** *Gastronauta insula* has a tripartite dorsal brush each cluster being composed of two about 3  $\mu\text{m}$  long bristles (g). Rarely, the bristles of cluster 1 are widely spaced (d). **e:** An early mid-divider. BA – bacteria, DB1,2,3 – clusters of dorsal brush, EP – pore of contractile vacuole, K5 – kinety 5 of left ciliary field, K8 – kinety 8 of right ciliary field, LF – left ciliary field, MA – macronucleus, MI – micronucleus, NU – central and peripheral nucleoli, OB – oral basket, PK – preoral kineties, RF – right ciliary field, VK1,2 – vertical kineties, \* – minute kinety. Scale bars 5  $\mu\text{m}$  (f-h) and 15  $\mu\text{m}$  (a-e).

**Etymology:** The Latin *Insula* (Island) is a noun in apposition and refers to the habitat the species was discovered.

**Description:** This species was very rare and thus recognized only in the protargol preparations. Accordingly, live observations are lacking. However, *Gastronauta insula* is so distinct that description without live observations seems justified.

*Gastronauta insula* is rather variable (many CV's > 15%), for instance, body length varies between 21  $\mu\text{m}$  and 42  $\mu\text{m}$  and most distances (Table 19).

Size in protargol preparations 21–42  $\times$  15–25  $\mu\text{m}$ , on average 33  $\times$  21  $\mu\text{m}$ , in vivo about 38  $\times$  24  $\mu\text{m}$  when 15% preparation shrinkage is added. Body broadly ellipsoid, ovoid or depressed, i.e., right margin distinctly convex, left straight or slightly convex (Fig. 50a–c, 51a–d; Table 19). Both ends broadly rounded, posterior end rarely slightly to distinctly notched. Dorsoventrally flattened 2–4:1, ventral side flat, postoral dorsal side with more or less distinct hump sometimes slightly projecting from body proper. Nuclear apparatus usually in rear body half, rarely in mid-body (Fig. 50a, c, 51a–d; Table 15); globular to broadly ellipsoid, contains a large central nucleolus(?) impregnating faintly and many small, globular to polygonal peripheral nucleoli impregnating deeply. Micronucleus attached to various sites of macronucleus, rarely some micrometers distant from macronucleus; globular to broadly ellipsoid. Two contractile vacuoles located as in congeners, i.e., upper pore subapical between kineties 1 and 2 of right ciliary field, posterior pore between posterior end of kineties 3 and 4 of left ciliary field (Fig. 50a, 51b; Table 19). Cytoplasm usually rather clear because containing only few food vacuoles with flagellates (*Chlamydomonas*?), small euglenids (*Anisonema*?), and fungal spores(?). Most specimens contain 5–10  $\mu\text{m}$  long bacilli with a terminal spore.

Somatic and oral infraciliature as in congeners, differing mainly in morphometric features. Thus, I describe here only some minor specialties and refer the reader to Fig. 50a–e, 51a–h and, especially, to the detailed morphometry (Table 19). Leftmost kinety of left ciliary field usually interrupted at level of circumoral kinety, the upper portion becoming vertical kinety 1; in other cells no break recognizable or only a wider spacing of basal bodies (Fig. 51b). Basal bodies in posterior region of kineties more widely spaced than anteriorly.

Anlage for dorsal brush absent in about one third of cells. Brush extends along anterior curve of cell, composed of three widely spaced clusters each with two up to 10  $\mu\text{m}$  long bristles; basal bodies of middle cluster widely separate in some cells.

Circumoral kinety on average (oral cleft) 10.0  $\times$  2.7  $\mu\text{m}$  in protargol preparations, basal bodies more narrowly spaced in posterior half than in anterior half. Oral basket extends to near posterior body end.

**Occurrence and ecology:** As yet found only at type locality. This is the first terricolous species of the genus. However, I cannot exclude that *Gastronauta insula* is a brackish water species because the sample was taken from the coast of the island.

**Remarks:** In the last revision of the genus, Foissner (2000) recognized three well described species: the common *Gastronauta membranaceus* (Fig. 50d, e), *G. aloisi* as yet found only in activated sludge; and *G. derouxi*, a marine species. *Gastronauta insula* differs from these species, inter alia, by body size and the total number of somatic ciliary rows: *G. insula* 33  $\times$  21  $\mu\text{m}$ , 17; *G. membranaceus* 48  $\times$  28  $\mu\text{m}$ , 22; *G. aloisi* 45  $\times$  35  $\mu\text{m}$ , 23; *G. derouxi* 61  $\times$  38  $\mu\text{m}$ , 23. Further, *G. insula* has a unique dorsal brush: three clusters with a total of six bristles in anterior quarter of cell; *G. membranaceus* has two clusters with a total of 17 bristles in anterior third of cell (Fig. 50e); *G. aloisi* has 3–5 clusters with a total of 12 bristles along anterior body margin; and *G. derouxi* has 5–7 clusters with a total of 12–16 bristles along anterior body margin. These data show that *G. insula* is a distinct, possibly endemic species.

Deroux (1994) founded the monotypic family Gastronautidae. Foissner (2000) agreed and established a new, monotypic genus, *Paragstronauta*, for species without a barren postoral stripe.

## 4.2.5 Hymenostomata

*Protocyclidium namibiense* nov. spec.

(Fig. 52a–d)

2002 *Protocyclidium terricola*, (Kahl, 1931) nov. comb. — Foissner, Agatha & Berger, *Denisia* 5: 525, 529 (Fig. 120d–f, k–p; Table 102; Namibian population, misidentification).

**Diagnosis:** Size in vivo about  $34 \times 19 \mu\text{m}$ ; ellipsoid. One globular macronucleus. Pore of contractile vacuole distinctly subterminal (at 16% of body length) at end of somatic kinety 2. Extrusomes slightly cuneate, about  $5 \mu\text{m}$  long, form bundles between kinetids of somatic kineties. Usually 13 ciliary rows, dorsal rows each composed of an average of six dikinetids ciliated in oral area while anterior basal body barren in postoral region; one caudal cilium. Oral apparatus extends about 76% of body length; adoral membranelle 1 rhomboid, membranelle 2 cuneate and composed of seven ciliary aggregates. Scutica composed of one dikinetid right of cytophyge and slightly posterior to paroral vertex, and of two widely spaced dikinetids left of cytophyge, i.e., almost in line with last ciliary row.

**Type locality:** Namibia, Etosha National Park, dolomitic rock-pools in the surroundings of the Halali rest camp,  $19^{\circ}\text{S}$ ,  $16^{\circ}30'\text{E}$ .

**Type material:** Three slides (accession numbers 84–86/2002) with silver nitrate impregnated (Chatton-Lwoff method) specimens have been deposited in the Biology Centre of the Upper Austrian Museum in Linz (LI). The holotype and relevant paratype specimens are marked by black ink circles on the coverslip.

**Etymology:** Named after the country where it was discovered.

**Remarks:** Foissner et al. (2002, p. 529) did not separate the Namibian population from the European *P. terricola* (p. 525) because of considerable overall similarity. Specifically, they did not

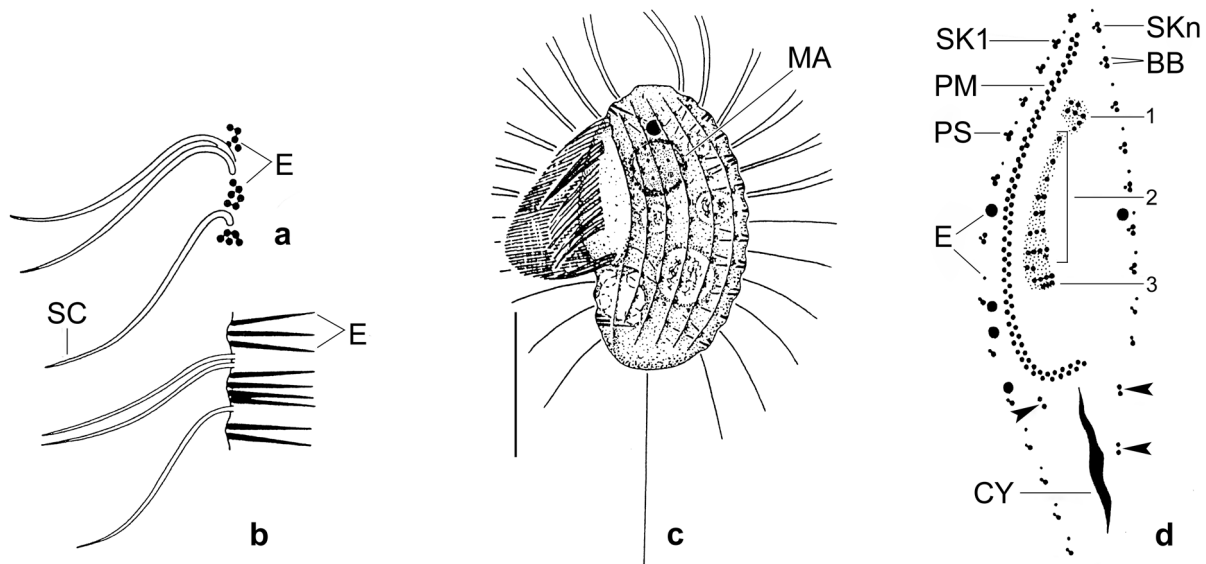


**Fig. 52a–d.** *Protocyclidium namibiense* from life (a–c) and after Chatton-Lwoff silver nitrate impregnation (d). From Foissner et al. (2002); see this monograph for further figures and a morphometric analysis. **a, b:** Surface view and optical section, showing the arrangement of the extrusomes. **c:** Left side view, showing the subterminal contractile vacuole, the macronucleus in the anterior body portion, and the inconspicuous caudal cilium. **d:** Ventral view of oral apparatus. Arrowheads mark the scutica. BB – basal bodies, CC – caudal cilium, CV – contractile vacuole, CY – cytophyge, E – extrusomes, MA – macronucleus, PM – paroral membrane, PS – parasomal sac, SC – somatic cilia, SK1 – somatic kinety 1, SKn – last somatic kinety, 1,2,3 – adoral membranelles. Scale bar  $20 \mu\text{m}$ .

consider the different scutica and extrusome pattern as sufficient for a distinct species. However, the recent progress in ciliate taxonomy (e.g., Kumar & Foissner 2016) and the different biogeographic regions suggest the Namibian population as a distinct species. Foissner et al. (2002) provided the following species comparison: “The Namibian population matches the type and neotype population in most morphometrics (Table 102). It differs, however, in body shape because it is postorally slightly narrowed making cells obovoidal (Fig. 120k, m; 373a–d). Furthermore, the Namibian specimens are more slender (length:width ratio 2.5:1 vs. 2:1 in ventral and 1.9:1 vs. 1.7:1 in lateral view) and usually slightly longer (33  $\mu\text{m}$  vs. 29  $\mu\text{m}$  long on average; Table 102) than the Austrian ones. The extrusomes are often clustered and form a distinct fringe and rather conspicuous tubercles recognizable even at low ( $\times 150$ ) magnification on the cell surface (Fig. 120d–f, k; 373e, f). The last somatic ciliary row is not only shortened by one kinetid posteriorly, as in the Austrian population, but terminates at the level of the peristomial vertex. Additionally, the oral apparatus is larger than in the Austrian specimens (usually terminating 58% vs. 66% back from anterior body end), the adoral membranelles are more posteriorly located (distance to anterior body end 6.7  $\mu\text{m}$  vs. 3.5  $\mu\text{m}$ ), the paroral membrane often forms a small hook distally, and jumping is more pronounced”.

***Protocyclidium bimacronucleatum* nov. spec.**

(Fig. 53a, b, 54a–f; Table 20 on p. 326)

**Diagnosis:** Size in vivo about 33  $\times$  21  $\mu\text{m}$ ; broadly ellipsoid. Two abutting macronuclear nodules. Pore of contractile vacuole distinctly subterminal (at 18% of body length) at end of somatic kinety 2. Extrusomes slightly cuneate, about 4  $\mu\text{m}$  long, one each between kinetids of somatic kineties. Usually 12 ciliary rows, dorsal rows each composed of six dikinetids ciliated in oral half of cell while

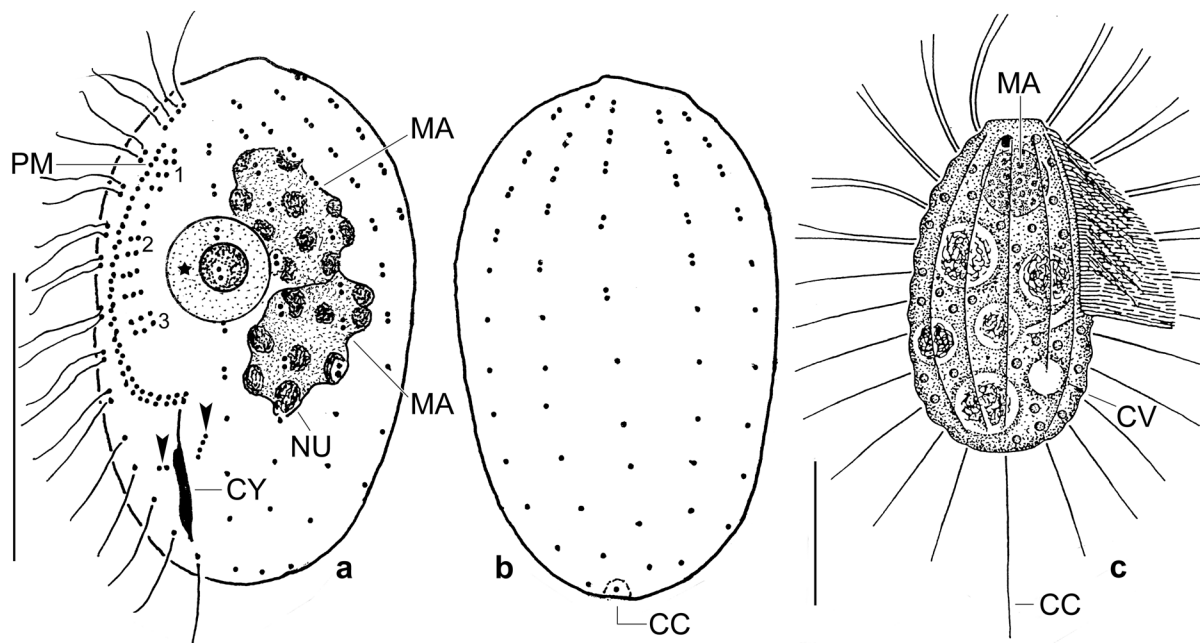


**Fig. 53a–c.** *Protocyclidium bimacronucleatum* (a, b) and *P. terricola* (c, from Foissner et al. 2002) after protargol impregnation (a, b) and from life (c). **a, b:** Ventrolateral views of holotype specimen, showing the two macronuclear nodules, the scutica (arrowheads), and a microsporidium parasite (star) described below. **c:** Right side view. *Protocyclidium bimacronucleatum* and *P. terricola* differ mainly by the number of macronuclear nodules: two in the former, one in the latter. CC – caudal cilium, CV – contractile vacuole, CY – cytophyge, MA – macronuclear nodules, NU – one of several nucleoli in the periphery of the macronuclear nodules, PM – paroral membrane, 1,2,3 – adoral membranelles. Scale bars 15  $\mu\text{m}$ .

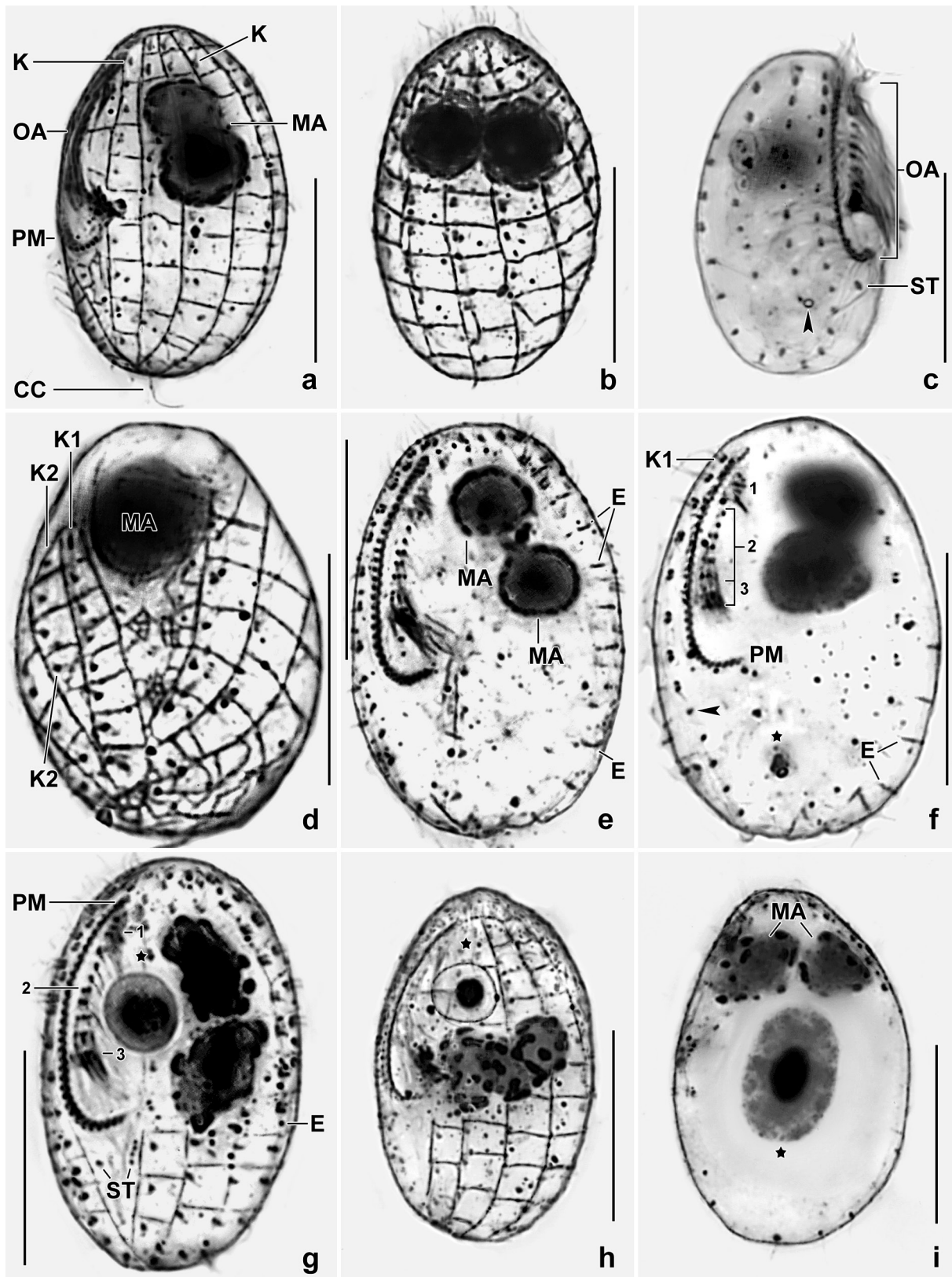


**Fig. 54a–i.** *Protocyclidium bimacronucleatum* (a–i) and *Microsporidium protocyclidicola* (f–i, asterisks) after protargol impregnation. **a, b:** Left side and dorsal view, showing the two macronuclear nodules and a quadrangular fibre system extending right of the ciliary rows and between the cilia (see also Fig. 54d). **c:** The excretory pore of the contractile vacuole is at the end of the shortened ciliary row 2 (arrowhead). **d:** Oblique posterior polar view of a ventrally oriented specimen, showing the complex fibre system, the ciliary pattern, and the shortened somatic kinety 2. **e–g:** Oral structures, showing the cuneate membranelle 2 usually composed of seven ciliary aggregates. Posteriorly, the somatic ciliature likely consists of monokinetics, first marked by an arrowhead in Figure 54f. The microsporidian parasite (asterisk) has a

anterior basal body barren in postoral portion; one caudal cilium. Oral apparatus extends about 77% of body length; adoral membranelle 1 rectangular, membranelle 2 cuneate and composed of six or seven ciliary aggregates. Scutica composed of a single dikinetid right of cytopyge and of two dikinetids left of cytopyge, both clearly separate from proximal end of paroral membrane and somatic kineties.

**Type locality:** Australian site (170), i.e., ephemeral puddles on top of Ayers Rock, 863 m above sea level, Uluru-Kata Tjuta National Park, central Australia, 25°20'42"S, 131°02'10"E.

**Type material:** The protargol slide<sup>1</sup> containing the holotype (Fig. 53a, b) and paratype specimens has been deposited in the Biology Centre of the Upper Austrian Museum in Linz (LI). The holotype and relevant paratype specimens have been marked by black ink circles on the coverslip. For slides, see Fig. 24a, b in chapter 5.

**Etymology:** The Latin *bimacronucleatum* (two macronuclei) refers to the main feature of the species, viz., the two macronuclear nodules.

**Description and remarks:** *Protocyclidium bimacronucleatum* is highly similar – both morphologically and morphometrically – to the Austrian mononucleate neotype of *P. terricola* described by Foissner et al. (2002). Thus, I provide only some notes and photographs and refer the reader to the diagnosis. The main difference is the macronucleus, viz. one nodule in *P. terricola*, two in *P. bimacronucleatum*. Another, but small difference, concerns the scutica which is nearer to the proximal part of the paroral membrane in *P. terricola* than in *P. bimacronucleatum*. Further, the quadrangular cortex structure is more prominent in *P. bimacronucleatum*; however, this is likely a preparation effect.

#### 4.2.6 Microsporidia

##### *Microsporidium protocyclidicola* nov. spec.

(Fig. 54f–i, 55a–h; Table 21 on p. 326)

**Diagnosis** (based on protargol-impregnated, mounted specimens): Two stages of the life cycle were observed. Stage 1 (possibly meronts): globular with an average diameter of about 5 µm and an about 1 µm-sized nucleus; can divide; about 10 parasites/host. Stage 2 (possible sporoblasts): globular to ellipsoid with an average size of 10 × 6 µm and an about 3 µm-sized nucleus; very likely does not divide but originating from stage 1 parasites.

**Type host:** Cytoplasm of the ciliate *Protocyclidium bimacronucleatum* nov. spec. described above.

**Type locality:** Australian site (170), i.e., ephemeral puddles on top of Ayers Rock, 863 m above sea level, Uluru-Kata Tjuta National Park, central Australia, 25°20'42"S, 131°02'10"E.

**Type material:** Three type slides (the slide<sup>2</sup> containing the holotype, two paratype slides) with protargol-impregnated specimens have been deposited in the Biology Centre of the Upper Austrian Museum in Linz (LI). The holotype shows stage 1 and stage 2 parasites (Fig. 55e). Both, the holotype

<sup>1</sup> Note by H. Berger: This slide also contains the holotype of → *Urosomoida uluruensis* and → *Microsporidium protocyclidicola*.

<sup>2</sup> Note by H. Berger: This slide also contains the holotype of → *Urosomoida uluruensis* and → *Protocyclidium bimacronucleatum*.

← very clear cytoplasm in Fig. 54f (thus, only the nucleus is distinct while it is dense and smooth in Fig. 54g). **h:** The microsporidian parasite (asterisk) has a distinct nucleus and a clear cytoplasm. **i:** A meront (asterisk) with granular cytoplasm. CC – caudal cilium, E – extrusomes, K – somatic kinety, K1,2 – somatic kineties, MA – macronuclear nodules, OA – oral apparatus, PM – paroral membrane, ST – scutica, 1,2,3 – adoral membranelles. Scale bars 15 µm.

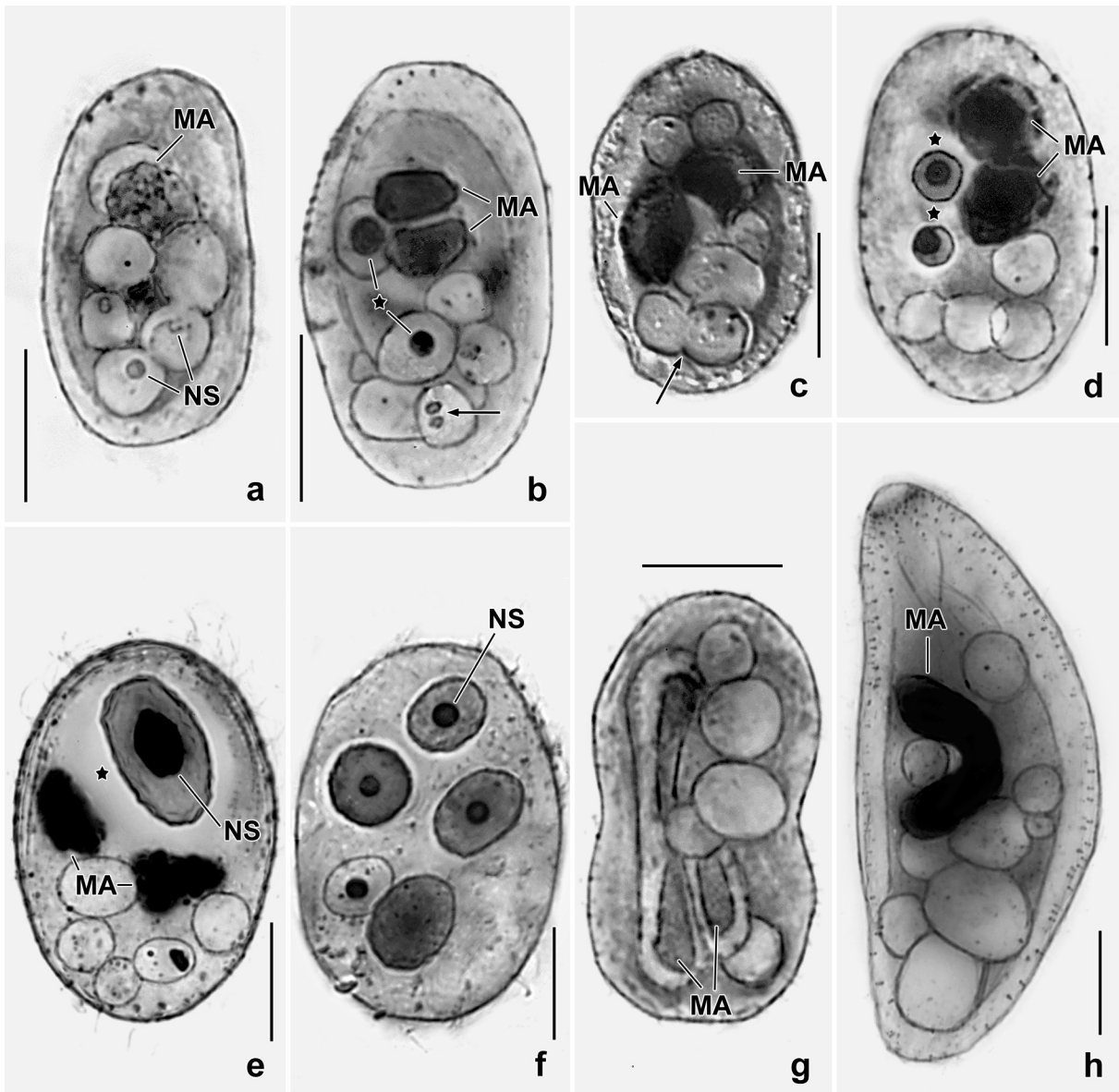


**Fig. 55a–h.** *Microsporidium protocyclidicola* in protargol preparations. **a:** Stage 1 parasites with pale nucleus. **b:** The arrow marks a dividing stage 1 parasite while the starred specimens develop to stage 2 parasites. **c:** One of the stage 1 parasites is dividing (arrow). **d:** Four degenerated stage 1 parasites without nucleus and plasm; two develop to stage 2 (asterisks). **e:** Holotype specimen with five degenerated stage 1 parasites and a fully developed stage 2 parasite (asterisk). **f:** Five developing stage 2 parasites; the smallest has a clear plasm. **g:** Degenerated stage 1 parasites in a dividing host. **h:** *Fuscheria terricola* feeds on *Microsporidium protocyclidicola* which are “empty”, i.e., lost nucleus and plasm. MA – macronuclear nodules of the host ciliate, i.e., *Protocyclus bimacronucleatus*, NS – nucleus of parasite. Scale bars 10  $\mu$ m.

and several paratype specimens have been marked by black ink circles on the coverslip. For slides, see Fig. 24a, b in Chapter 5.

**Etymology:** The species name is a composite of the genus-group name *Protocyclus*, the thematic vowel *-i-*, and the Latin verb *colere* (to live in), referring to the habitat the species was discovered.

**Description:** I observed only protargol-impregnated parasites, and thus I cannot provide the full life cycle. The infection rate was 100% in *Protocyclus bimacronucleatus* both in morphostatic (Fig. 55a–f) and dividing (Fig. 55g) cells. Very likely, the parasite is highly species-specific because 80 other species were not infected in the non-flooded Petri dish culture; however, rapacious ciliates that feed on *P. bimacronucleatus* contain “empty” (without nucleus and plasm) parasites (Fig. 55h).

Stage 1 parasites (possibly early meronts): They have a diameter of 3–9  $\mu\text{m}$  (average 5  $\mu\text{m}$ ), i.e., the cells are small and do not impregnate with the protargol method used except of the nucleus which lightly impregnates. On average, there are 9.5 parasites in each *Protocyclidium* (Fig. 55a–e; Table 21). The nucleus has a diameter of about 1  $\mu\text{m}$  and is usually out of the cell centre (Fig. 55a). The plasm contains some granules. Stage 1 parasites can divide (Fig. 55b, c) and one or several develop to stage 2 while the others degenerate, i.e., lose nucleus and plasm.

Stage 2 (possibly sporoblasts): These develop from stage 1 cells as evident from transition stages (Fig. 55b, d, f). They have an average size of  $10 \times 6 \mu\text{m}$  and a 3–4  $\mu\text{m}$ -sized, deeply impregnating nucleus (Fig. 54i, 55e, f; Table 21). Some have a clear (unstained) cytoplasm (Fig. 54h) while it is rather deeply impregnated and contains some granular material in other specimens (Fig. 54g, h, 55e, f). Dividing stage 2 parasites have been not observed.

**Remarks:** Although I do not have the whole life cycle, I name this organism because (i) the two stages seen appear highly characteristic, (ii) it is highly host-specific, and (iii) well documented by micrographs (Fig. 54f–i, 55a–h; Table 21). The stages observed resemble meronts and sporoblasts as described by Canning & Lom (1986) and a marine fish *Microsporidium* sp. described by Raabe (reviewed in Canning & Lom 1986).

Until 1987 only four microsporidian parasites have been described from ciliates (for a review, see Görtz 1987): “Lutz and Splendore (1908) found ciliates (*Balantidium* ?) in the gut of *Bufo marinus* infected with *Nosema balantidii*. Hovasse (1950) observed a microsporidian, named *Gurleya nova*, in the ciliate *Spirobuetschliella chattoni*, and Krüger (1956) found *Telomyxa campanellae* (*Glugea campanellae*; Sprague 1977) in *Campanella umbellaria*. In this paper, we report on the infection of two ciliates by microsporidia”. None of these closely resembles *Microsporidium protocyclidicola*. More recently, Foissner (1993, 2016) and Foissner & Foissner (1995) described *Ciliatosporidium platyophryae* making little feet in various colpodean ciliates.

#### 4.2.7 Hypotrichida

For some recent comments on this taxon by W. Foissner, see Foissner (2016, p. 487).

### *Gonostomum affine* (Stein, 1859) Sterki, 1878 (Fig. 56a–c)

**Material:** Australian site (32).<sup>1</sup>

**Remarks:** The Australian population highly resembles *Gonostomum affine* (for reviews, see Berger 1999, 2011) and *G. singhii* Kamra et al., 2008 from an Australian site<sup>2</sup> investigated by Foissner (2016, p. 666). *Gonostomum singhii* differs from *G. affine* mainly by the transverse cirral pattern. Here, I show the silverline pattern of *G. affine*. It is very fine-meshed with meshes 0.5–2.5  $\mu\text{m}$  in size (Fig. 56a–c).

### *Afrogonostomum* nov. gen.

**Diagnosis:** Oblong Gonostomatidae with transverse cirri. Ventral cirral pattern very similar to that of *Gonostomum affine*. Specific cortical granules, postoral and caudal cirri absent.

<sup>1</sup> Note by H. Berger: I did not find a note by W. Foissner where the Australian sites are listed and described in detail. In addition, I did not find the silver slides.

<sup>2</sup> Note by H. Berger: I did not find a detailed description of this site. According to Foissner (2016, p. 672), the sample was composed of the upper 5 cm litter and soil under *Nothofagus* trees; pH 4.1, about 200 m above sea-level.

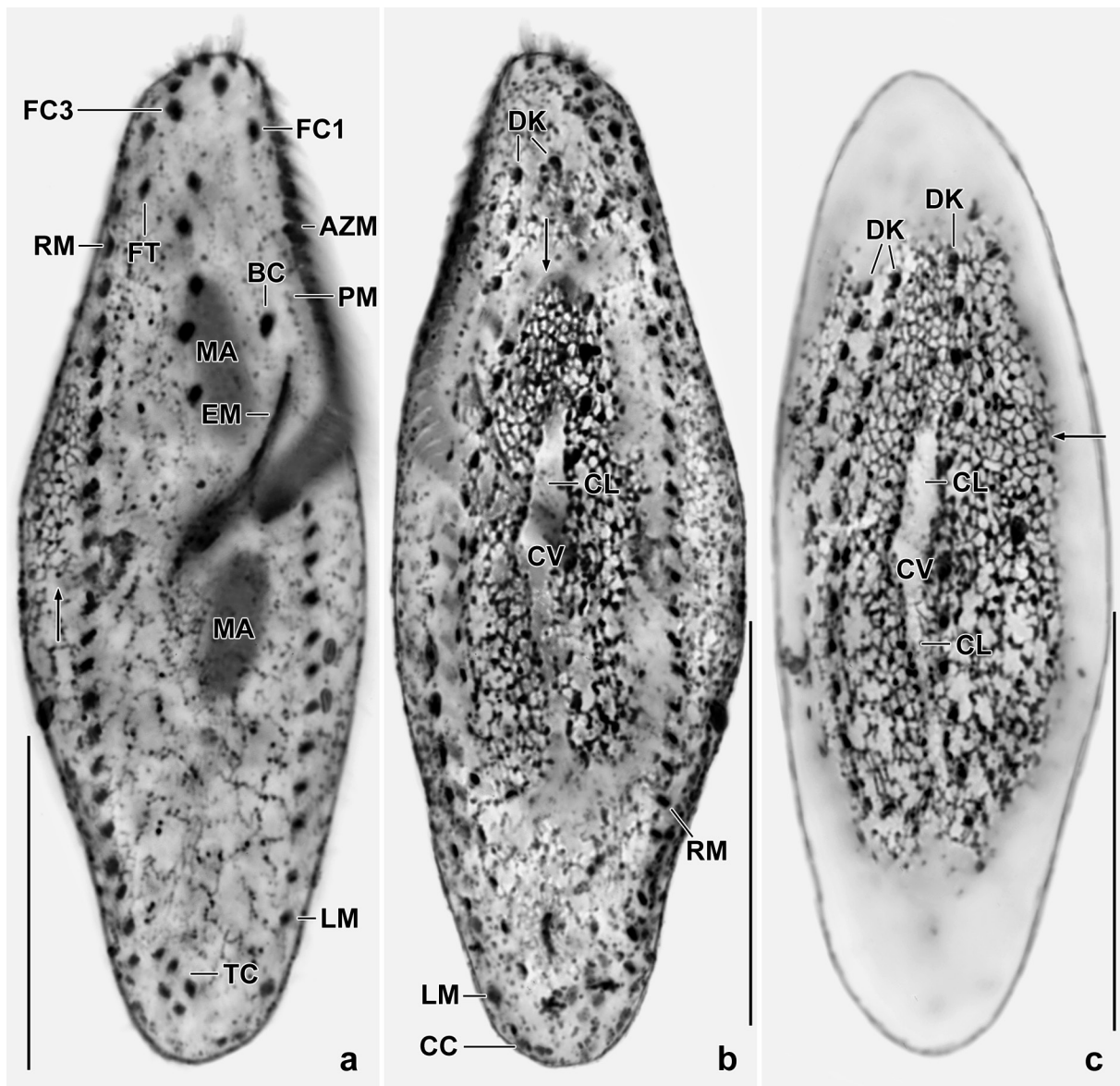


**Fig. 56a–c.** *Gonostomum affine* after Chatton-Lwoff silver nitrate impregnation. Arrows mark sites where the fine, irregularly-shaped silverline meshes can be seen. **a:** Ventral view showing, inter alia, the transverse cirral pattern that is different in *G. shii*. **b, c:** Dorsal views, showing three dorsal kineties and the contractile vacuole with the two collecting canals. AZM – adoral zone of membranelles, BC – buccal cirrus, CC – caudal cirri, CL – canals of the contractile vacuole, CV – contractile vacuole, DK – dorsal kineties, EM – endoral membrane, FC1, 3 – frontal cirri, FT – frontoterminal cirri, LM – left marginal cirral row, MA – macronuclear nodules, PM – paroral membrane, RM – right marginal cirral row, TC – transverse cirri. Scale bars 30 µm.

**Type species:** *Afrogonostomum alveum* nov. spec.

**Etymology:** *Afrogonostomum* is a composite of the Latin noun *Africa*, the thematic vowel ·o-, and the Greek genus-group name *Gonostomum* (angled adoral zone of membranelles). Neuter gender. For details on *Gonostomum*, see Aesch (2001) and Berger (1999, 2011).

**Species assignable:** *Afrogonostomum alveum* nov. spec.

**Remarks:** Foissner (2016, p. 611) established *Apogonostomum* which has transverse cirri while caudal cirri are absent, as in *Afrogonostomum*. However, *Apogonostomum* species are tailed and have many frontoventral and postoral cirral pairs while the oblong *Afrogonostomum* has only two frontal pairs (Bharti et al. 2015; Foissner 2016).

*Gonostomum paronense* Bharti et al., 2015, a species from an Italian paddy field, has the characteristics of *Apogonostomum pantanalense* Foissner, 2016, the type species of *Apogonostomum*. Thus, *G. paronense* is synonymized with *A. pantanalense* Foissner, 2016.<sup>1</sup> Both species match well in all morphological and morphometric features as well as in the habitat, indicating global distribution.

***Afrogonostomum alveum* nov. spec.**  
(Fig. 57a–c, 58a–c; Table 22 on p. 327)

**Diagnosis** (averages are provided): Size in vivo about  $115 \times 27 \mu\text{m}$ ; very elongate rectangular. Four broadly ellipsoid macronuclear nodules and two ellipsoid micronuclei. Specific cortical granules absent. On average three frontal cirri, two frontoterminal cirri, one buccal cirrus at level of begin of paroral membrane, five frontoventral cirri of which four form two pairs, four transverse cirri, 26 cirri in right marginal row, 23 in left. Three dorsal kineties. Adoral zone indistinctly gonostomoid, extends 35% of body length, composed of 27 membranelles. Buccal lip distinctly convex, paroral and endoral membrane distinctly shifted; paroral composed of about 20 dikinetids.

**Type locality:** Soil from the floodplain of the Chobe River, Kabolebole Peninsula, Botswana, 25°S, 17°50'E.

**Type material:** The slide containing the holotype and two paratype slides with protargol-impregnated specimens have been deposited in the Biology Centre of the Upper Austrian Museum in Linz (LI). Relevant specimens have been marked by black ink circles on the coverslip. For slides, see Fig. 25a–f in Chapter 5.

**Etymology:** The Latin noun *alveum* refers to the habitat, viz., soil from the flood plain the species was discovered.

**Description:** *Afrogonostomum alveum* is a rather stable species. Only seven out of 38 features investigated have a CV > 15%, and most of these are distances of low value for species recognition.

Size in vivo  $90\text{--}140 \times 20\text{--}35 \mu\text{m}$ , on average  $115 \times 27 \mu\text{m}$ , as calculated from some in vivo measurements and the morphometric data in Table 22 adding 15% preparation shrinkage. Body slenderly (3.6:1) to very slenderly (5.3:1) rectangular, usually slightly narrower in posterior than anterior third; dorsoventrally flattened about 2:1, posterior third distinctly thinner than anterior third (Fig. 57a–c, 58a, b; Table 22). Usually four ellipsoid to broadly ellipsoid macronuclear nodules, forming an about  $53 \mu\text{m}$  long row postorally and left of body's midline; individual nodules distinctly separate, forming indistinct pairs; average size  $9 \times 6 \mu\text{m}$  in protargol preparations, with inconspicuous nucleoli impregnated very faintly. Usually two ellipsoid micronuclei  $5 \times 3 \mu\text{m}$  in vivo, one each attached to anterior and posterior macronuclear pair (Fig. 57c, 58a; Table 22). Contractile vacuole slightly anterior of mid-body, with two long collecting canals (Fig. 57a). Cortex flexible, specific granules not detectable neither in vivo nor in protargol preparations. Cytoplasm colourless, usually contains many food vacuoles  $4\text{--}8 \mu\text{m}$  across in posterior half (Fig. 57a). Feeds on bacteria, fungal hyphae, and heterotrophic flagellates. Swims and creeps rather fast.

<sup>1</sup> Note by the editor (Helmut Berger): *Gonostomum paronense* was described by Bharti et al. (2015, p. 769) in a work published in an online-only journal. Unfortunately, Bharti et al. (2015) have forgotten to register the work according to ICZN (2012, Article 8.5.3; note that the registration – or at least a hint to the registration – must appear in the work itself!). Thus, the new species (*G. paronense*) described in this work is not available, that is, invalid. Consequently, the synonymy proposed by W. Foissner in the present work is valid (the question is if an invalid species can be synonymised at all?). In 2017, a “corrigendum” (Corrigendum to “Two gonostomatid ciliates from the soil of Lombardia, Italy; including note on the soil mapping project by Bharti et al”; J. Euk. Microbiol. 64, 907) has been published for Bharti et al. (2015). However, this corrigendum is irrelevant because the registration in ZooBank has to be mentioned in the work itself and the corrigendum itself cannot be considered as valid original description of *G. paronense* because it lacks all other details for a valid description. For a valid correction of a similar mistake (Shao et al. 2014), see Shao et al. (2017).

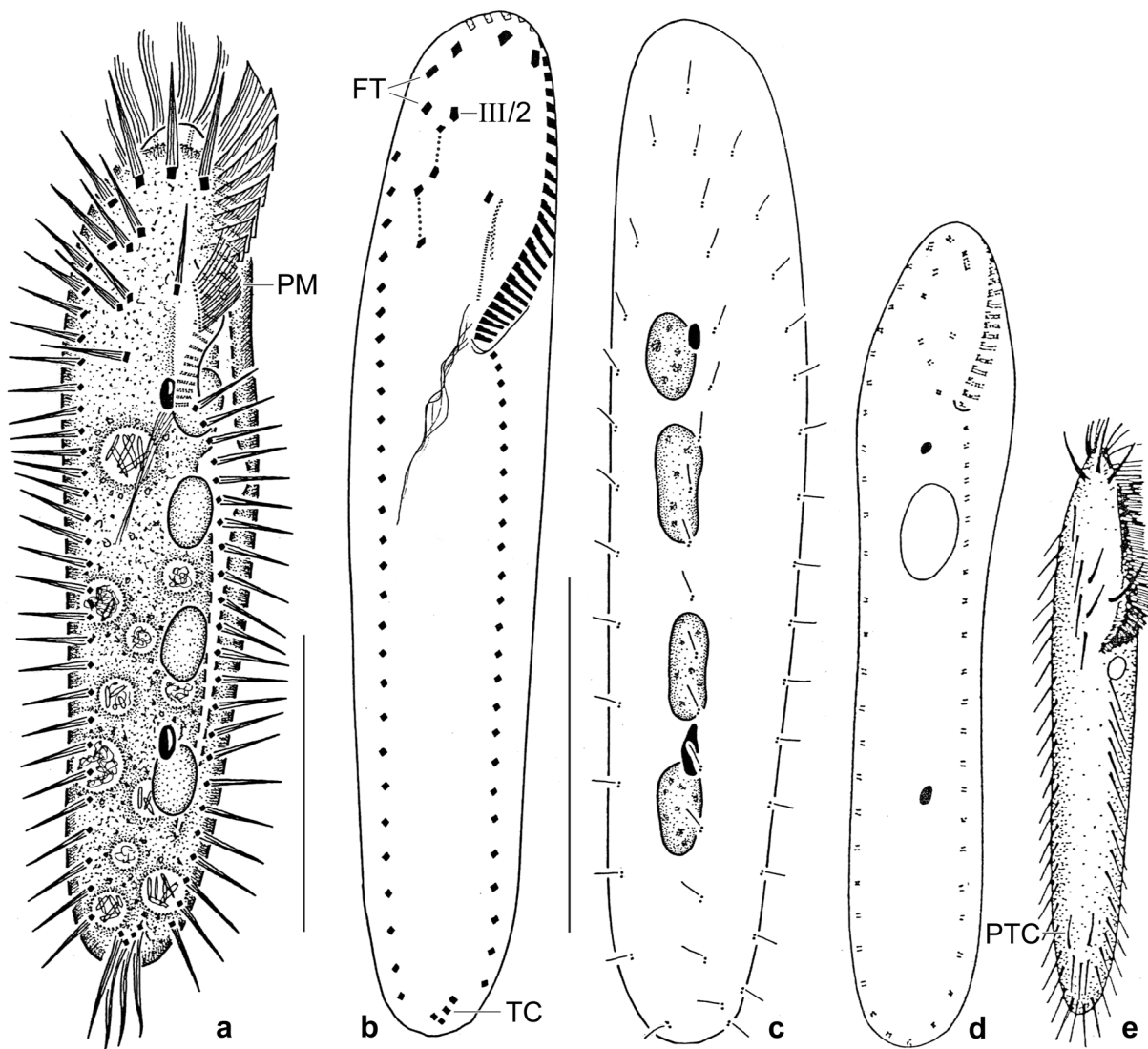


**Fig. 57a–e.** *Afrogonostomum alveum* (a–c) and slender *Gonostomum affine* specimens (d, e) from life (a, e) and after protargol impregnation (b–d). **a:** Ventral view of a representative specimen, length 115  $\mu\text{m}$ . **b, c:** Ventral and dorsal view of holotype specimen, length 117  $\mu\text{m}$ . Ventral cirral pairs connected by dotted lines. Note lack of caudal cirri. **d:** Very likely a post-conjugational *Gonostomum* specimen, length 140  $\mu\text{m}$  (from Berger 1999). **e:** A very slender *Gonostomum* specimen (from Stein 1859 and copied by Berger 1999). FT – frontoterminal cirri, PTC – pretransverse cirri, TC – transverse cirri, III/2 – cirrus III/2. Scale bars 40  $\mu\text{m}$ .

Cirri in *Gonostomum affine* pattern as described in Berger (1999, 2011) and Foissner et al. (2001); fine and short compared to body size, frontoventral and some transverse cirri slightly thickened. Three frontal cirri 15  $\mu\text{m}$  long in vivo, followed by two frontoterminal cirri, cirrus III/2 left of posterior frontoterminal cirrus; four frontoventral cirri in oral area, form two pairs; buccal cirrus right of anterior end of paroral membrane; four transverse cirri only 3  $\mu\text{m}$  distant from posterior body end, thus cilia project distinctly from body proper; each composed of four or six about 15  $\mu\text{m}$  long cilia; marginal cirral rows composed of 26 cirri (right row) and of 22 cirri (left row), each made of four basal bodies with 10  $\mu\text{m}$  long cilia, except of first right marginal cirrus composed of six cilia; intercirral distances increase from anterior to posterior; marginal rows distinctly separate posteriorly (Fig. 57a, b, 58a–c; Table 22).

Dorsal kinety pattern as typical for *Gonostomum*, i.e., three rows of bristles 2.5–3.0  $\mu\text{m}$  long in vivo (Berger 1999, 2011). Middle row composed of 16 dikinetids (Fig. 57c, 58b; Table 22).

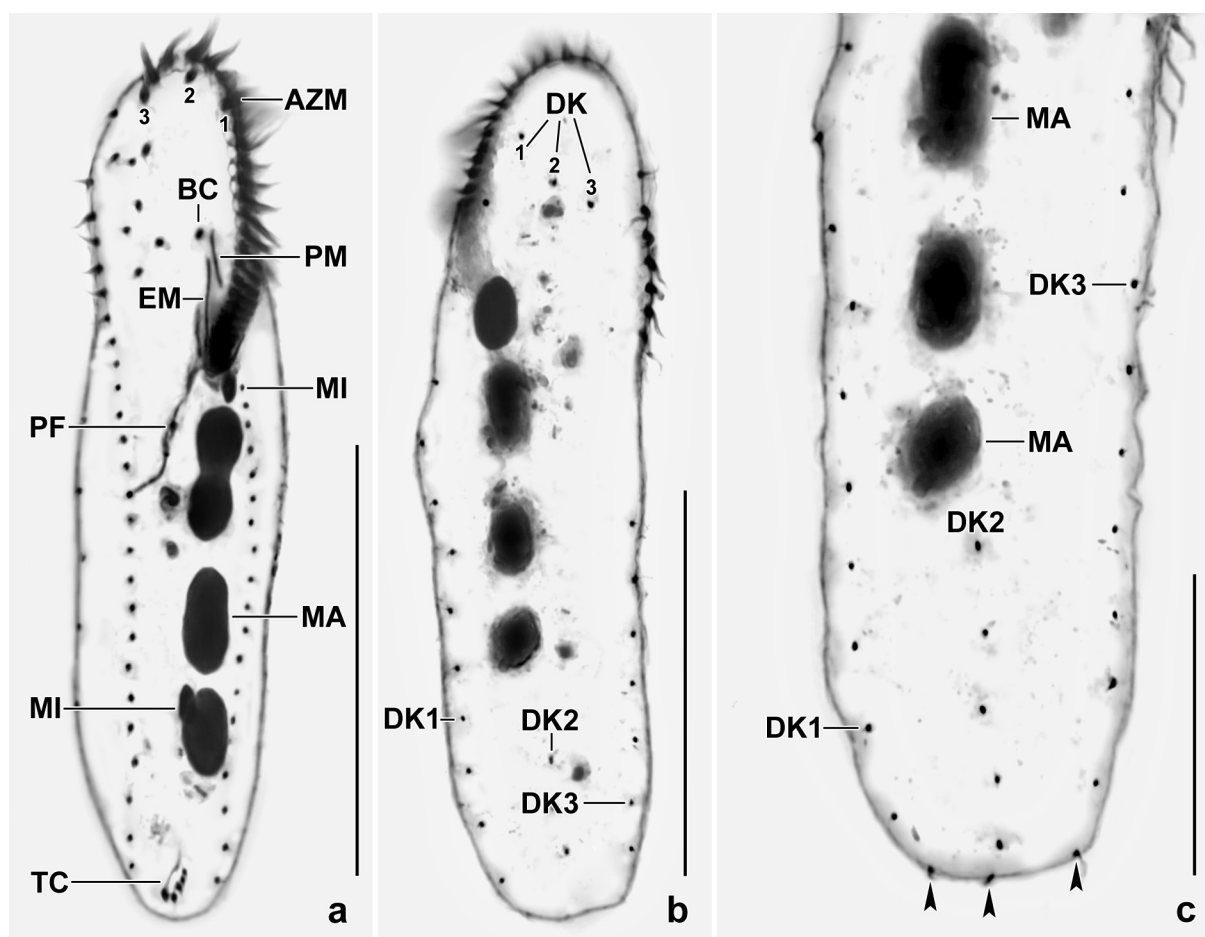


**Fig. 58a–c.** *Afrogonostomum alveum* after protargol impregnation. **a, b:** Ventral and dorsal view of infraciliature and nuclear apparatus. This species has transverse cirri while caudal cirri are absent. The cirral pattern and the adoral zone of membranelles are gonostomoid (see Berger 1999, 2011). The numerals mark the frontal cirri. **c:** Dorsal posterior half, showing the absence of caudal cirri because the last kinetids consist of two basal bodies indicating that they are dorsal kinetids (arrowheads). AZM – adoral zone of membranelles, BC – buccal cirrus, DK1,2,3 – dorsal kineties, EM – endoral membrane, MA – macronucleus, MI – micronucleus, PF – pharyngeal fibres, PM – paroral membrane, TC – transverse cirri. Scale bars 50  $\mu\text{m}$  (a, b) and 25  $\mu\text{m}$  (c).

Oral apparatus indistinctly gonostomoid, i.e., adoral zone of membranelles bends continuously into the cell about 35% of body length, extends on anterior and left margin of body, on average composed of 27 membranelles with, in vivo, up to 15  $\mu\text{m}$  long cilia frontally; intermembranellar distances slightly increase from posterior to anterior (Fig. 57a, b, 58a; Table 22). Buccal cavity in vivo flat and narrow; buccal lip distinctly convex, i.e., about 7  $\mu\text{m}$  wide on top of convexity, covers proximal half of adoral zone (Fig. 57a, b). Paroral membrane slightly curved, near left margin of buccal lip, short, i.e., composed of about 20 very narrowly spaced dikinetids with cilia about 8  $\mu\text{m}$  long in vivo. Endoral membrane straight, longer than paroral membrane, both distinctly shifted, i.e., project over end of endoral anteriorly by about half of its length while endoral projects over paroral in posterior half. Pharyngeal fibres about 25  $\mu\text{m}$  long, extend obliquely to mid-body.

**Occurrence and ecology:** As yet found only at type locality (see above). The species had low abundance and was present only for 2 d.

**Remarks:** *Afrogonostomum alveum* is easily recognizable by the slender body, the four macronuclear nodules, the sparse ciliature in the oral area, and the three rows of dorsal bristles. However, most of these features are found in several genera, especially *Hemisincirra* Hemberger,

1985, e.g., *H. namibiensis* Foissner et al., 2002 which has, as *A. alveum*, a slender body, a similar size, and four macronuclear nodules (for review, see Berger 2008).

I found two figures in the literature which could belong to *Afrogonostomum*. However, the first is very likely a post-conjugate of *Gonostomum affine* that possibly lacks transverse cirri and has an unknown number of macronuclear nodules (Fig. 57d). The second is probably a very slender *Gonostomum affine* because it has two prominent pretransverse cirri and thus cannot be identical with *A. alveum*. See Berger (1999, 2011) for reviews of the taxa mentioned.

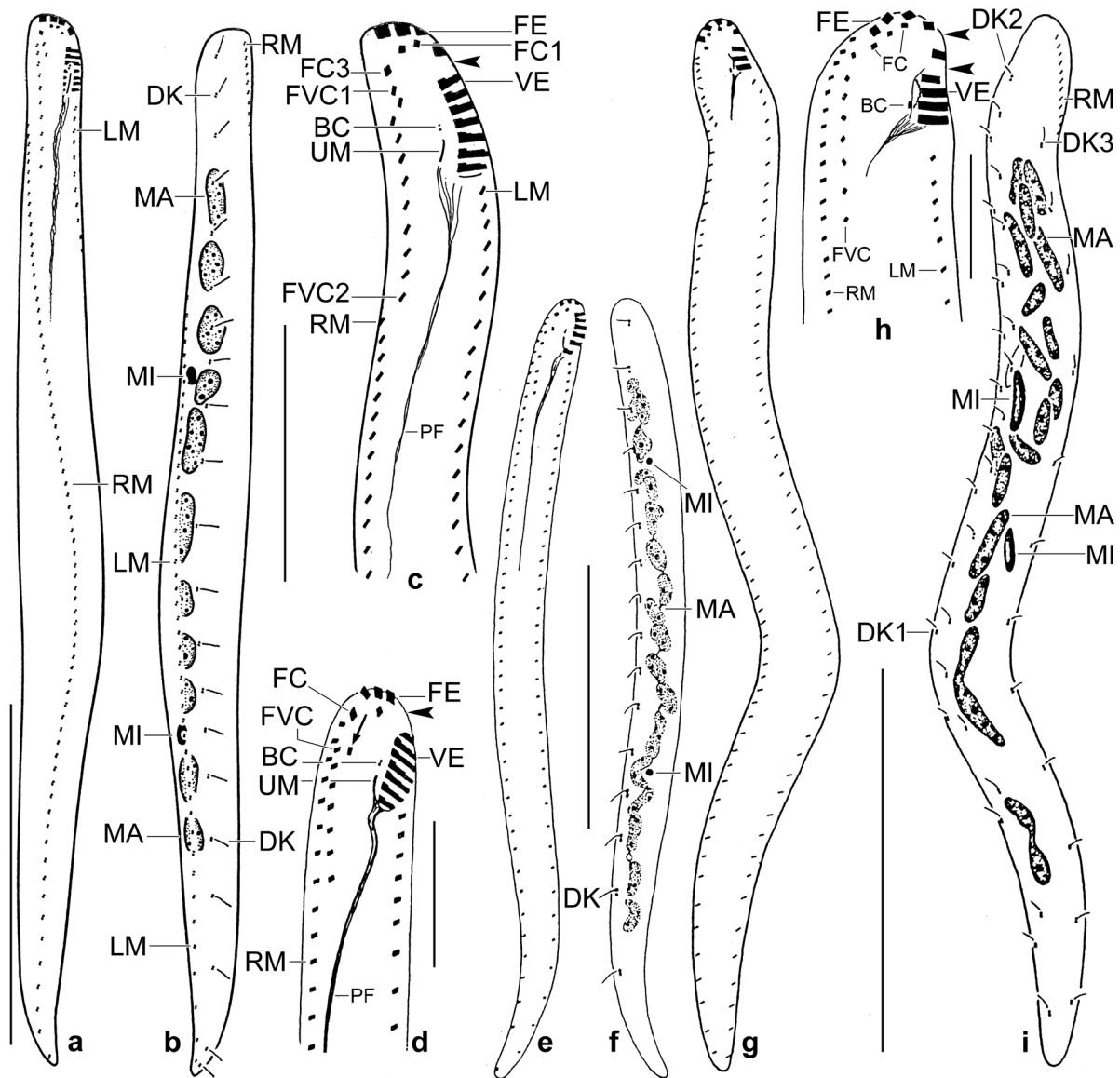


**Fig. 59a-i.** Comparison of *Circinella filiformis australiensis* (a-c), *Circinella filiformis filiformis* (d-f, from Foissner 1982), and *Circinella vettersi* (g-i, from Berger & Foissner 1989) after protargol impregnation. Drawn to scale (a, b, e, f, g, i). Arrowheads mark gap between frontal and ventral adoral membranelles. **a, b:** Ventral and dorsal view of infraciliature and nuclear apparatus. Note the narrow spacing of the marginal cirri and the macronuclear nodules separated from each other. **c:** Oral area at high magnification, showing the two rows of frontoventral cirri. **d:** Oral area at high magnification. The arrow marks supposed frontal cirrus 3 or a reduced row of frontoventral cirri. **e, f:** Ventral and dorsal view of infraciliature and nuclear apparatus. Note the moniliform macronucleus, a main difference to the Australian subspecies (Fig. 59b). **g-i:** *Circinella vettersi*, ventral and dorsal view of infraciliature and nuclear apparatus that shows two peculiarities: the macronuclear nodules are scattered and are of similar size as the micronuclei. BC – buccal cirrus, DK1–3 – dorsal kineties, FC1,3 – frontal cirri, FE – frontal adoral membranelles, FVC1,2 – frontoventral cirral rows, LM – left row of marginal cirri, MA – macronuclear nodules, MI – micronuclei, PF – pharyngeal fibres, RM – right row of marginal cirri, UM – undulating membrane, VE – ventral adoral membranelles. Scale bars 10  $\mu\text{m}$  (d, h), 20  $\mu\text{m}$  (c), and 50  $\mu\text{m}$  (a, b, e–g, i).

*Circinella filiformis australiensis* nov. subspec.

(Fig. 59a–c, 60a–k; Table 23 on p. 328)

**Diagnosis:** Vermiform; on average  $144 \times 12 \mu\text{m}$  in protargol preparations and  $166 \times 14 \mu\text{m}$  when 15% preparation shrinkage is added. On average a row of 10 globular to elongate ellipsoid, distinctly separate macronuclear nodules and 137 right and left marginal cirri; usually, nine cirri in frontoventral row 2. Adoral zone of membranelles extends about 9% of body length, composed of an average of three frontal and seven ventral membranelles, and one membranelle in gap between frontal and ventral membranelles.

**Type locality:** Australian site (30), i.e., upper soil and litter layer (0–5 cm) of a forest in the Eubenangee Swamp National Park about 55 km south of the town of Cairns,  $16^{\circ}50'S$ ,  $145^{\circ}E$ .

**Type material:** The slide containing the holotype and two paratype slides with protargol-impregnated specimens have been deposited in the Biology Centre of the Upper Austrian Museum

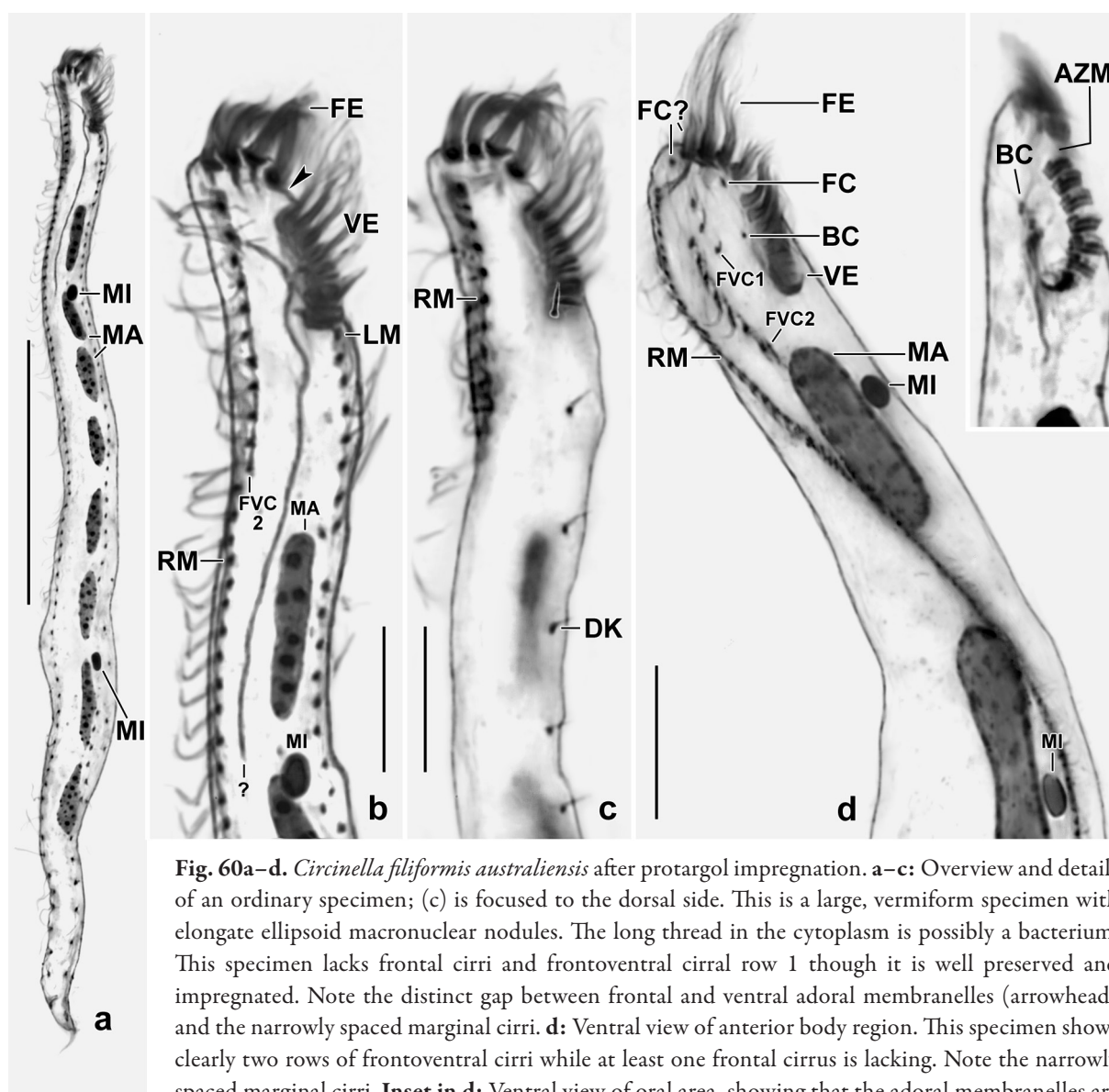


**Fig. 60a–d.** *Circinella filiformis australiensis* after protargol impregnation. **a–c:** Overview and details of an ordinary specimen; (c) is focused to the dorsal side. This is a large, vermiform specimen with elongate ellipsoid macronuclear nodules. The long thread in the cytoplasm is possibly a bacterium. This specimen lacks frontal cirri and frontoventral cirral row 1 though it is well preserved and impregnated. Note the distinct gap between frontal and ventral adoral membranelles (arrowhead) and the narrowly spaced marginal cirri. **d:** Ventral view of anterior body region. This specimen shows clearly two rows of frontoventral cirri while at least one frontal cirrus is lacking. Note the narrowly spaced marginal cirri. **Inset in d:** Ventral view of oral area, showing that the adoral membranelles are composed of only three rows of basal bodies. AZM – gap in adoral zone of membranelles, BC – buccal cirrus, DK – dorsal kinety, FC – frontal cirri, FE – frontal adoral membranelles, FVC1,2 – frontoventral cirral rows, LM – left row of marginal cirri, MA – macronuclear nodules, MI – micronuclei, RM – right row of marginal cirri, VE – ventral adoral membranelles. Scale bars  $10 \mu\text{m}$  (b–d) and  $50 \mu\text{m}$  (a).

in Linz (LI). Relevant specimens have been marked by black ink circles on the coverslip. For slides, see Fig. 26a–f in Chapter 5.

**Etymology:** Named after the country discovered, i.e., Australia.

**Description:** In 1987, when I studied *C. filiformis australiensis* in vivo, I identified it as *C. filiformis* because several main features were rather similar, e.g., body shape and size, the nuclear apparatus, and the number of dorsal kineties and macronuclear nodules. Thus, I did not make live illustrations. In 2017, when I studied the protargol slides, I recognized two distinct differences, viz., the separate macronuclear nodules and the much higher number of marginal cirri, suggesting subspecies rank (Table 23).

Some features of *C. filiformis australiensis* are highly variable (Table 23), viz., the number of frontal cirri (0–3) and the number of frontoventral cirral rows (one or two). Most other features have an ordinary variability ( $CV \leq 15\%$ ) except of, e.g., the length:width ratio; the anterior body end to the proximal end of frontoventral cirral row 2; the length, width, and number of macronuclear nodules; the number and size of the micronuclei; the number of marginal cirri; and the number of frontoventral cirral rows (usually two but short row 1 occasionally lacking).

The following description is based on the misidentification mentioned above and protargol-impregnated specimens.

Size of protargol-impregnated specimens  $130\text{--}210 \times 11\text{--}17 \mu\text{m}$ , on average  $166 \times 14 \mu\text{m}$  when 15% preparation shrinkage is added (Table 23). Body very flexible; serpentine (Fig. 60a, h), rarely rod-shaped (Fig. 59a, 2i), in ordinarily fed specimens slightly flattened laterally; well-fed and overfed specimens about twice as wide as ordinary cells, more or less curved, rarely almost circular (Fig. 60f). Anterior region slightly narrowed, end obliquely truncate (Fig. 59a, 60c–e, i–k); posterior region gradually narrowed, posterior end narrowly rounded, bluntly pointed, or pointed (Fig. 59a, 60a, f–i). On average 10 macronuclear nodules forming a single strand left of body midline, occupies central fifths of cell, leaving free one fifth each anterior and posterior of strand (Fig. 59a, b, 60a, f–i; Table 23). Nodules never connected, globular to very elongate ellipsoid, contain many minute nucleoli. Usually, two bluntly ellipsoid or ellipsoid micronuclei one each attached to anterior and posterior region of macronuclear strand (Fig. 59b, 60a, d; Table 23). Feds on bacteria digested in vacuoles  $3\text{--}5 \mu\text{m}$  across (Fig. 60a, b, i). Glides worm-like between soil particles, showing great flexibility.

Data on somatic and oral infraciliature based on protargol-impregnated specimens for the reasons mentioned above; some features difficult to interpret due to the narrowness of the cells.

All cirri composed of only two basal bodies with about  $8 \mu\text{m}$  long cilia. Three, rarely only two or no frontal cirri; cirrus 3 (= right frontal cirrus) rather far subapical at begin of frontoventral cirral row 1, consisting of one or two cirri and thus extending only to mid-level of buccal cavity (Fig.

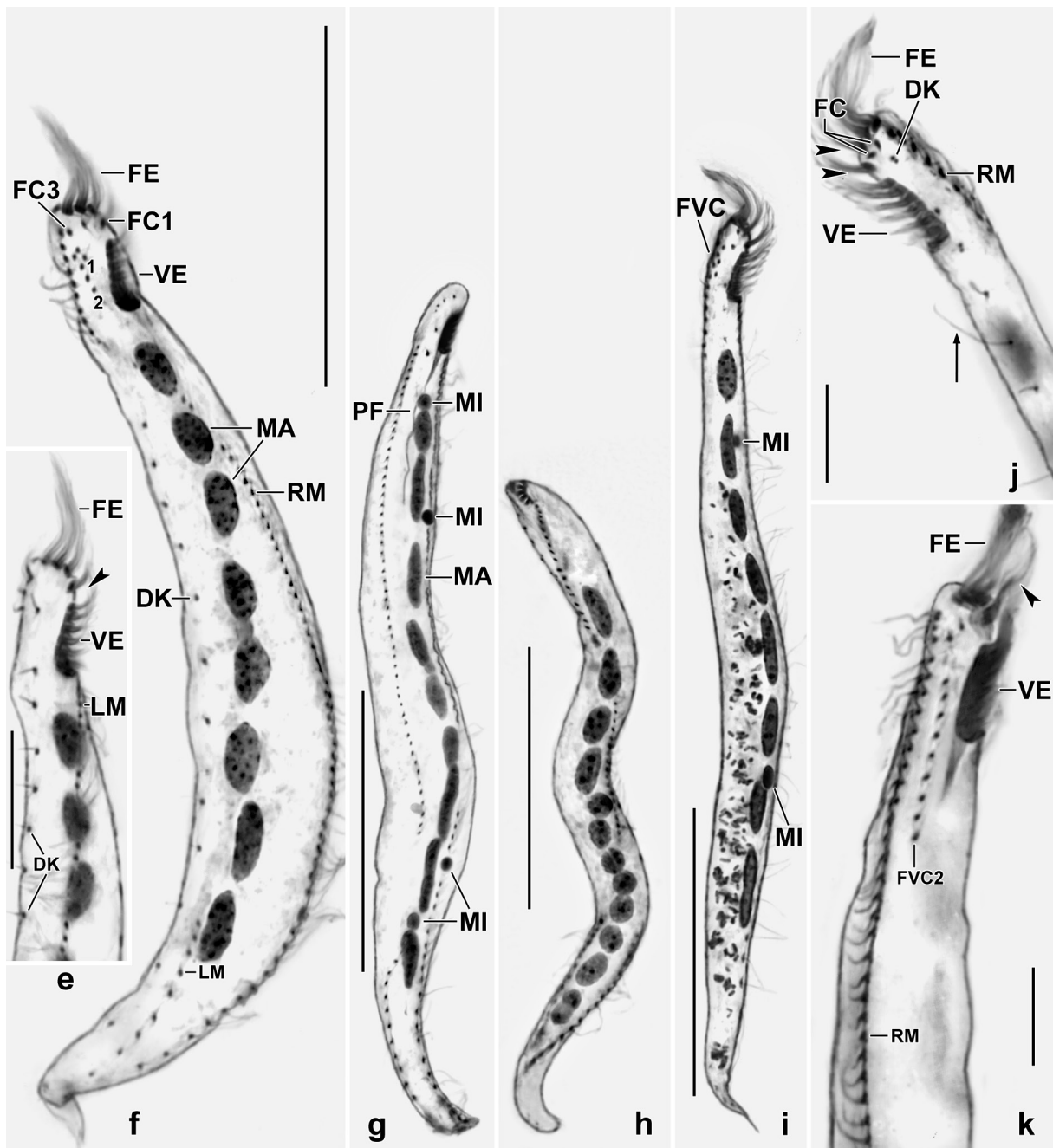
---

**Fig. 60e–k.** *Circinella filiformis australiensis* after protargol impregnation. **e** (focused to dorsal side): Dorsal view of anterior body region. The arrowhead marks the gap between frontal and ventral adoral membranelles. **f**: Ventral view of a slightly spiralized well-fed cell, showing the broad body, three frontal cirri, two rows of frontoventral cirri (1, 2), and the clearly separate macronuclear nodules. **g**: A rather well-fed cell with four micronuclei and elongate macronuclear nodules. **h**: A specimen with incomplete oral apparatus and globular to ellipsoid macronuclear nodules separated from each other. **i, j**: An ordinarily fed specimen in which the wide gap in the adoral zone is occupied by a single membranelle so that a narrow gap is produced anterior and posterior of the membranelle (arrowheads). The macronuclear nodules are distinctly apart and ellipsoid to elongate ellipsoid. The arrow in (j) marks a long dorsal bristle. **k**: Ventral view of a specimen with only one row of frontoventral cirri, very likely row 2. The arrowhead marks an adoral membranelle in the gap between frontal and ventral adoral membranelles. DK – dorsal kinety, FC1–3 – frontal cirri, FE – frontal adoral membranelles, FVC2 – row of frontoventral cirri, LM – left row of marginal cirri, MA – macronuclear nodules, MI – micronuclei, PF – pharyngeal fibres, RM – right row of marginal cirri, VE – ventral adoral membranelles. Scale bars  $10 \mu\text{m}$  (j, k),  $15 \mu\text{m}$  (e),  $50 \mu\text{m}$  (f–i). →

59a, c, 60d, f; Table 23). Frontoventral cirral row 2 near right row of marginal cirri, composed of 6–12, on average of nine cirri and thus much longer than adoral zone of membranelles (Fig. 59a, 60b, d, k; Table 23). Identity of buccal cirrus questionable, i.e., could be the paroral or endoral membrane. Right row of marginal cirri bipolar, left commences at level of proximal end of adoral zone of membranelles and extends to posterior end of body; distance between cirri gradually slightly increasing from anterior to posterior end of cell; postoral and transverse cirri lacking (Fig. 59a–c, 60a–d, f, g, i–k; Table 23).

On dorsal side, slightly left of body midline an average of 19 dikinetids producing a distinct, bipolar row. Anterior basal body of dikinetids associated with an about 3  $\mu\text{m}$  long bristle (Fig. 59b, 60c, e, j; Table 23).

Oral apparatus inconspicuous because extending only 9% of body length (Fig. 59a, c, 60a, f, g, i; Table 23). Adoral zone of membranelles bipartite, i.e., composed of three, very rarely of four frontal membranelles, 5–8 ventral membranelles, and one membranelle between frontal and ventral



membranelles, on average a total of 11 membranelles with largest bases 2–3  $\mu\text{m}$  wide; individual membranelles not composed of four ciliary rows, as usual, but of only three because row 3 is lacking (Fig. 60d, inset; terminology, see Foissner & Al-Rasheid 2006), resembling the genus *Etoschothrix* Foissner et al., 2002. Membranellar cilia up to 15  $\mu\text{m}$  long. Buccal cavity minute and shallow, identity of undulating membranes uncertain (see above); supposed endoral membrane about 3  $\mu\text{m}$  long. Pharyngeal fibres about 20  $\mu\text{m}$  long (Fig. 59a, c, 60a–d, f, k; Table 23).

**Occurrence and ecology:** As yet found only at type locality, i.e., soil from a coastal swamp. The slim body matches the sandy environment (Foissner 1987b).

**Remarks:** *Circinella filiformis australiensis* differs from the nominal subspecies, *C. filiformis filiformis* (Foissner, 1982) Foissner, 1994, by two distinct features (Fig. 59d–f; Table 23): macronucleus in several separate globules vs. moniliform; 137 vs. 94 right and left marginal cirri. Minor differences are (Table 23): the larger body size and the size and site of the first macronuclear nodule.

The in vivo identification of this kind of hypotrichs is difficult because several congeners and species from other genera have a similar shape and size, e.g., *Circinella vettersi* (Berger & Foissner, 1989) Foissner, 1994 (Fig. 59g–i), *Periholosticha lanceolata* Hemberger, 1985 (see also Foissner et al. 2002, p. 582); *Engelmanniella mobilis* (Engelmann, 1862) Foissner, 1982; *Vermioxytricha arenicola* Foissner et al., 2002; *Hemiurosoma terricola* Foissner et al., 2002; *Hemisincirra rariseta* Foissner et al., 2002; *Australothrix fraterculus* Foissner, 2016. All differ from *Circinella filiformis australiensis* by the number of dorsal kineties (two at least, but kinety 2 is often very short and thus difficult to recognize in vivo vs. one).

#### ***Urosoma australiensis* nov. spec.**

(Fig. 61a–e, 62a–h; Tables 24, 31 on p. 329, 337)

**Diagnosis:** Size in vivo about  $200 \times 60 \mu\text{m}$ . Ellipsoid with posterior half gradually narrowed. Two widely separated, elongate ellipsoid macronuclear nodules and an average of three globular micronuclei. Cortical granules in loose rows, colourless, about 0.5  $\mu\text{m}$  across; a reticular mitochondrial layer underneath cortical granules. Buccal cirrus subapical of paroral membrane. Five transverse cirri near posterior body end, last cirrus distinctly apart from penultimate cirri. Marginal cirral rows extend to posterior body end, right row composed of an average of 43 cirri, left of 37; right row commences with a dikinetid having associated a short bristle with the anterior basal body. Four almost bipolar dorsal kineties associated with three caudal cirri. Adoral zone extends 27% of body length on average, composed of about 36 membranelles; buccal cavity narrow and flat, lip narrow and concave. Paroral and endoral membrane each about 15  $\mu\text{m}$  long, half of posterior, respectively, anterior portion side by side.

**Type locality:** Australian site (153), i.e., floodplain soil from a small river between the towns of Alice Springs and Eridunda, central Australia,  $\sim 25^{\circ}30'S$ ,  $133^{\circ}E$ .

**Type material:** The slide containing the holotype (Fig. 61d, e) and two paratype slides with protargol-impregnated specimens have been deposited in the Biology Centre of the Upper Austrian Museum in Linz (LI). Relevant specimens have been marked by black ink circles on the coverslip. For slides, see Fig. 27a–d in Chapter 5.

**Etymology:** The adjective *australiensis* (belonging to Australia) refers to the country the species was discovered.

**Description:** *Urosoma australiensis* has an ordinary variability, i.e., most coefficients of variation are  $\leq 15\%$  (Table 24). None of the features which have a higher variability is diagnostic, e.g., the number of micronuclei (CV = 28.6%) and the distance from anterior body end to the right marginal cirral row (CV = 22.9%).

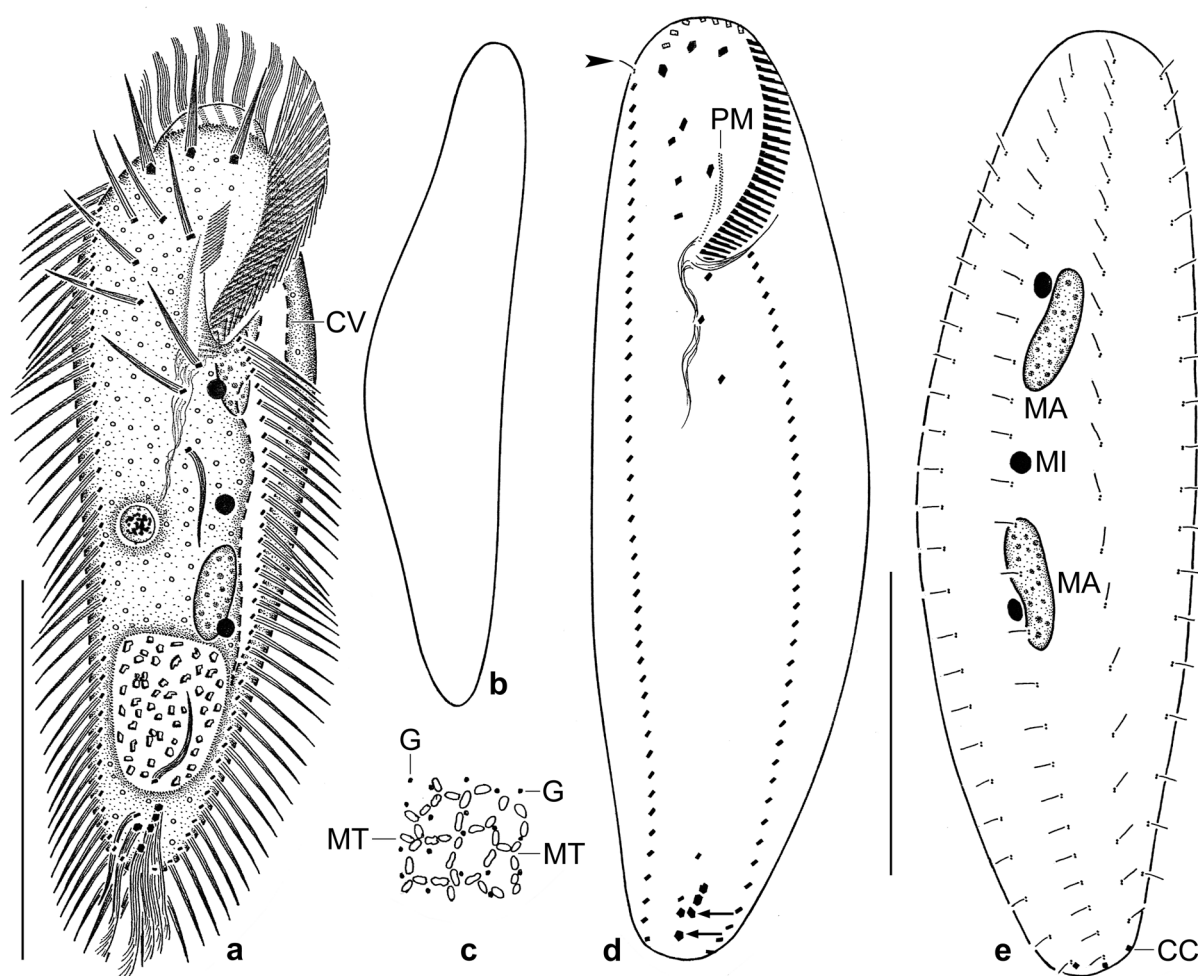


**Fig. 61a–e.** *Urosoma australiensis* from life (a–c) and after protargol impregnation (d, e). **a:** Ventral view of a representative specimen, showing a large vacuole with crystalline contents, possibly from digested hypotrich ciliates. **b:** Lateral view, showing the convex dorsal side. **c:** The cortical mitochondria form a reticular pattern. The cortical granules are very loosely spaced and only  $0.5\ \mu\text{m}$  across. **d, e:** Infra-ciliary view of ventral and dorsal side and nuclear apparatus of holotype specimen. The arrows mark the gap between the last and the penultimate transverse cirri; the arrowhead denotes a single (dorsal?) bristle at anterior end of the right marginal cirral row. CC – caudal cirri, CV – collecting canal of contractile vacuole, G – cortical granules, MA – macronuclear nodules, MI – micronucleus, MT – mitochondria, PM – paroral membrane. Scale bars  $50\ \mu\text{m}$ .

Size in vivo  $150\text{--}250 \times 50\text{--}100\ \mu\text{m}$ , usually about  $200 \times 60\ \mu\text{m}$ . Difficult to preserve and thus strongly shrunken ( $\sim 50\%$ ) in protargol preparations (Table 24). Body basically ellipsoid but gradually narrowed in posterior half with rear end about one third as wide as postoral region (Fig. 61a); narrowing usually also distinct in protargol preparations (Fig. 62b–e); laterally flattened up to 2:1, ventral side flat, dorsal more or less convex, depending on amount of food ingested (Fig. 61b). Nuclear apparatus in central third of cell, nuclear figure about  $60\ \mu\text{m}$  long, consists of two (very rarely three) macronuclear nodules and an average of three micronuclei (Fig. 61a, e, 62b–e; Table 24); nodules wide-spaced, usually elongate ellipsoid, rarely broadly ellipsoid, contain many minute, globular nucleoli. Micronuclei attached to macronuclear nodules and scattered in central third of cytoplasm, usually broadly, rarely slenderly ellipsoid, in vivo about  $5\ \mu\text{m}$ , in protargol preparations about  $4 \times 3\ \mu\text{m}$ . Contractile vacuole distinctly anterior of mid-body, with long, lacunar collecting canals. Cortex flexible, fragile, contains widely spaced, colourless granules about  $0.5\ \mu\text{m}$  across; underneath granular layer a conspicuous reticulum produced by discoidal mitochondria  $2.0 \times 1.5\ \mu\text{m}$  in size (Fig. 61c, 62a). Cytoplasm opaque due to countless, colourless granules about  $0.5\ \mu\text{m}$

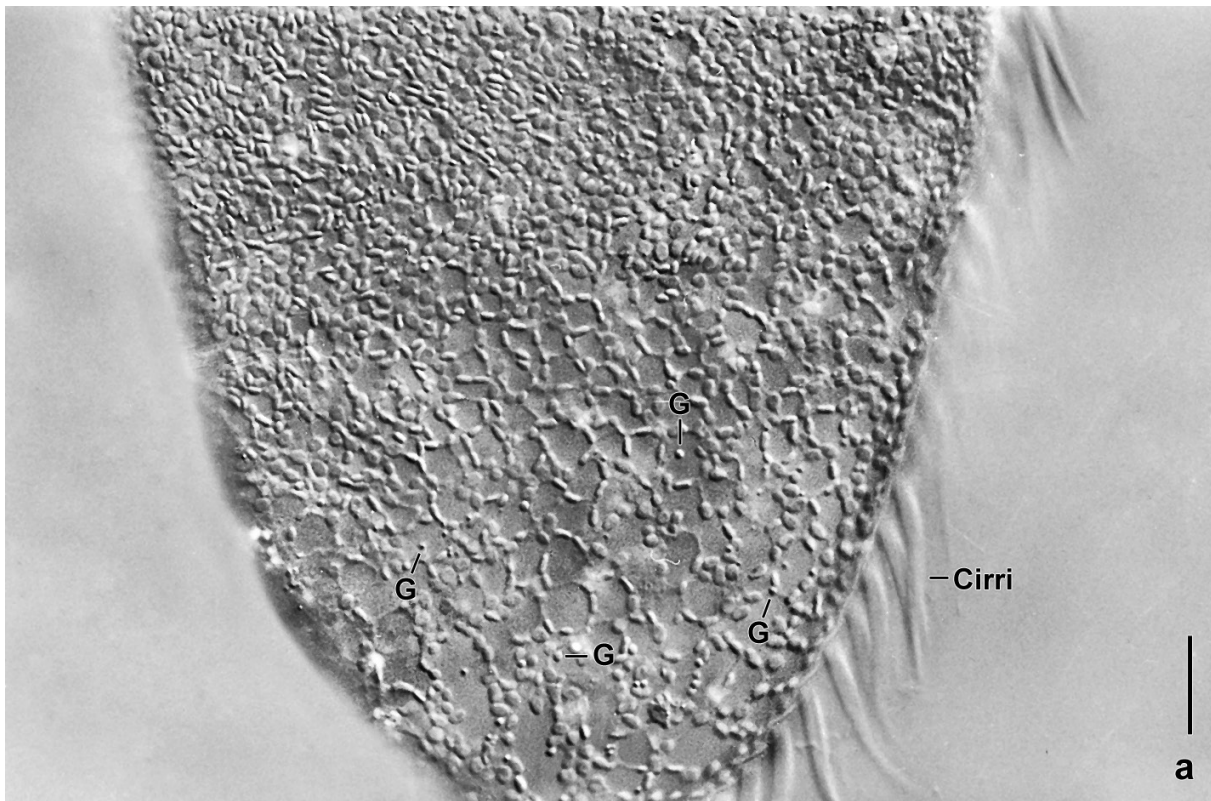


**Fig. 62a.** *Urosoma australiensis* from life. Dorsal view of rear region, showing the conspicuous, reticular pattern produced by the cortical mitochondria. The cortical granules are very inconspicuous because very loosely arranged and only  $0.5\ \mu\text{m}$  across. G – cortical granules. Scale bar  $10\ \mu\text{m}$ .

across, producing a brownish appearance of anterior half of cell under bright field illumination; no lipid droplets. Near posterior end usually a large defecation vacuole containing many small crystals of irregular shape and  $2\text{--}4\ \mu\text{m}$  in size. Feeds on cysts of flagellates and very likely also on ciliates, as indicated by the crystal vacuole. Swims and creeps rather rapidly.

Cirral pattern urosomoid, i.e., cirrus III/2 slightly anterior and left of frontoventral row, usually slightly thickened (Fig. 61a, d, 62b–f; Table 24). Frontal cirri in vivo about  $25\ \mu\text{m}$  long and moderately thickened; only two cirri in one out of 25 specimens investigated. Buccal cirrus subapical of paroral membrane. Postoral cirri almost in line. Transverse cirri in hook-like pattern and near to posterior body end, about  $35\ \mu\text{m}$  long in vivo and thus widely projecting from body proper, fringed distally; last cirrus invariably apart from the others (Fig. 61d, 62d, g, h). Marginal cirri in two rows, about  $25\ \mu\text{m}$  long in vivo, right row commences with a dikinetid of which the anterior basal body bears a  $3\ \mu\text{m}$  long bristle; individual cirri composed of two ciliary rows.

Dorsal bristles  $4\ \mu\text{m}$  long in vivo, in four rows, row 1 commences subapically, the others bipolar. Caudal cirri  $25\ \mu\text{m}$  long in vivo (Fig. 61a, e, 62e, g; Table 24).

Oral apparatus inconspicuous because extending only  $22\text{--}32\%$ , on average  $27\%$  of body length both in vivo and in protargol preparations (Fig. 61a, d, 62b–e; Table 24). Adoral zone in *Oxytricha* or indistinct *Gonostomum* pattern (Fig. 62d), composed of an average of 30 ordinary membranelles with largest bases about  $4\ \mu\text{m}$  wide in protargol preparations. Buccal cavity short, shallow and narrow compared to body size. Paroral and endoral membrane each only about  $10\ \mu\text{m}$  long, in typical *Urosoma* pattern, i.e., posterior half of paroral side by side with anterior half of endoral; paroral cilia in vivo  $7\ \mu\text{m}$  long. Buccal lip inconspicuous, concave. Pharyngeal fibres about  $40\ \mu\text{m}$  long in protargol preparations.

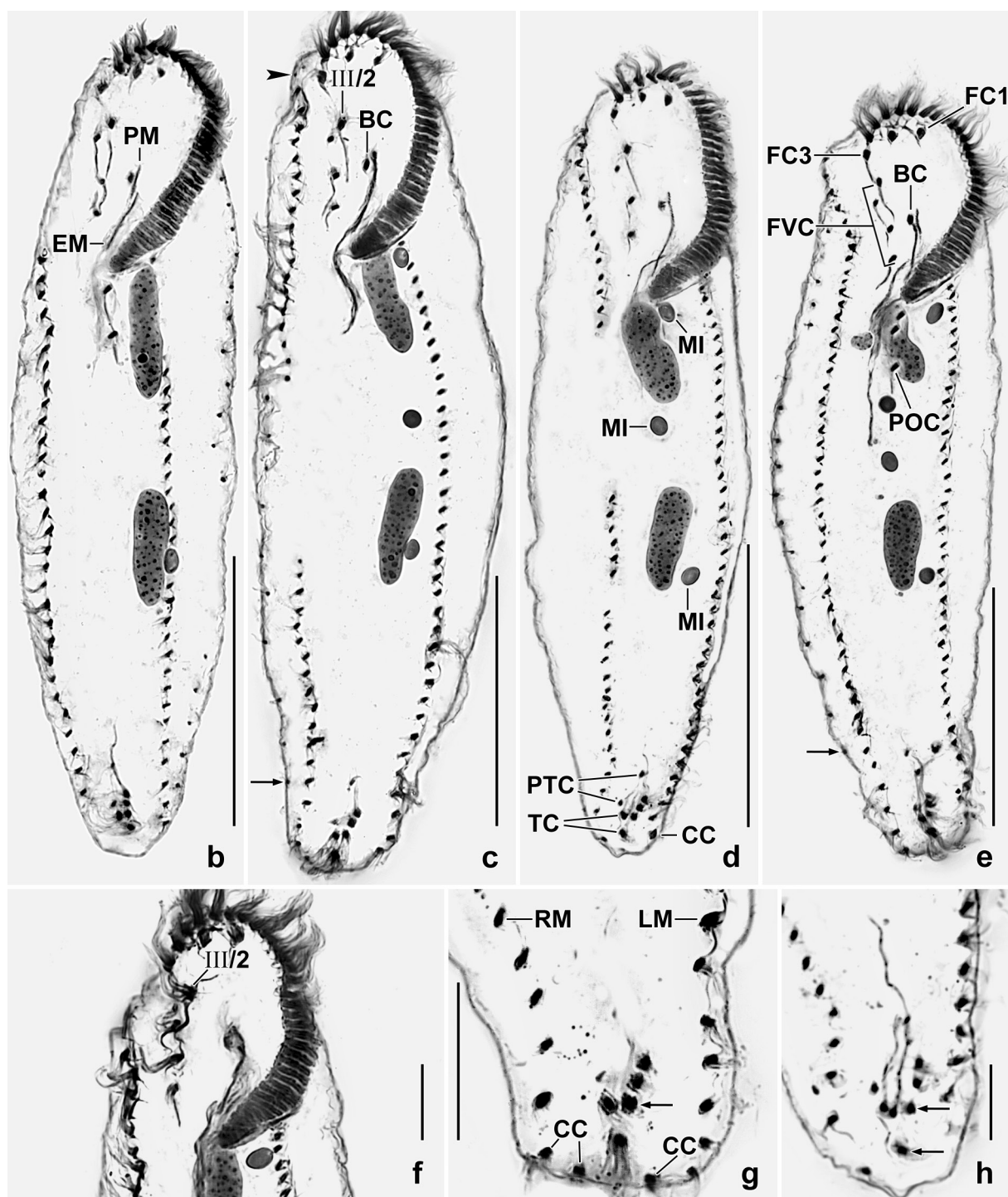


**Fig. 62b–h.** *Urosoma australiensis*, ventral views after protargol impregnation; part of infraciliature out of focal plane in most specimens. **b–e:** Total views, showing the urosomoid cirral pattern and the subterminal end of dorsal kiny 4 (c, e, arrows). **f–h:** Anterior (f) and posterior (g, h) region, showing the gap between the posteriormost and the penultimate transverse cirri (arrows). BC – buccal cirrus, CC – caudal cirri, EM – endoral membrane, FC1,3 – frontal cirri, FVC – frontoventral cirri, LM – left marginal cirral row, MA – macronuclear nodules, MI – micronuclei, PM – paroral membrane, POC – postoral cirri, PTC – pretransverse cirri, RM – right marginal cirral row, TC – transverse cirri. Scale bars 10  $\mu\text{m}$  (h) and 50  $\mu\text{m}$  (b–g).

**Occurrence and ecology:** As yet found only at type locality. The big size and the habitat suggest that *Urosoma australiensis* is more limnetic than edaphic. Possibly it develops in minute floodplain puddles with much organic debris.

**Remarks:** *Urosoma australiensis* has a considerable overall similarity with *Paroxytricha longigranulosa sinensis* Foissner, 2016 (cirri in *Urosoma* vs. *Oxytricha* pattern); *Urosomoida reticulata* Foissner et al., 2002 (cirri in *Urosoma* vs. *Urosomoida* pattern); and, specifically, *Urosoma gigantea* (Horváth, 1933) Kahl, 1935, as redescribed by Berger & Foissner (1987). They differ by the following features: (i) reticular vs. linear pattern of cortical mitochondria; (ii) posteriormost transverse cirrus distinctly vs. ordinarily separated from other transverse cirri; (iii) right marginal cirral row commences with a (dorsal?) bristle vs. an ordinary cirrus; (iv) adoral zone of membranelles extends 27% vs. 37% of body length; (v) 36 vs. 47 adoral membranelles; and (vi) buccal lip concave vs. angularly projecting. Minor differences: contractile vacuole with long vs. short collecting canals; micronuclei 5  $\mu\text{m}$  vs. 3  $\mu\text{m}$  in vivo; buccal cirrus subapical vs. right of anterior end of paroral membrane.

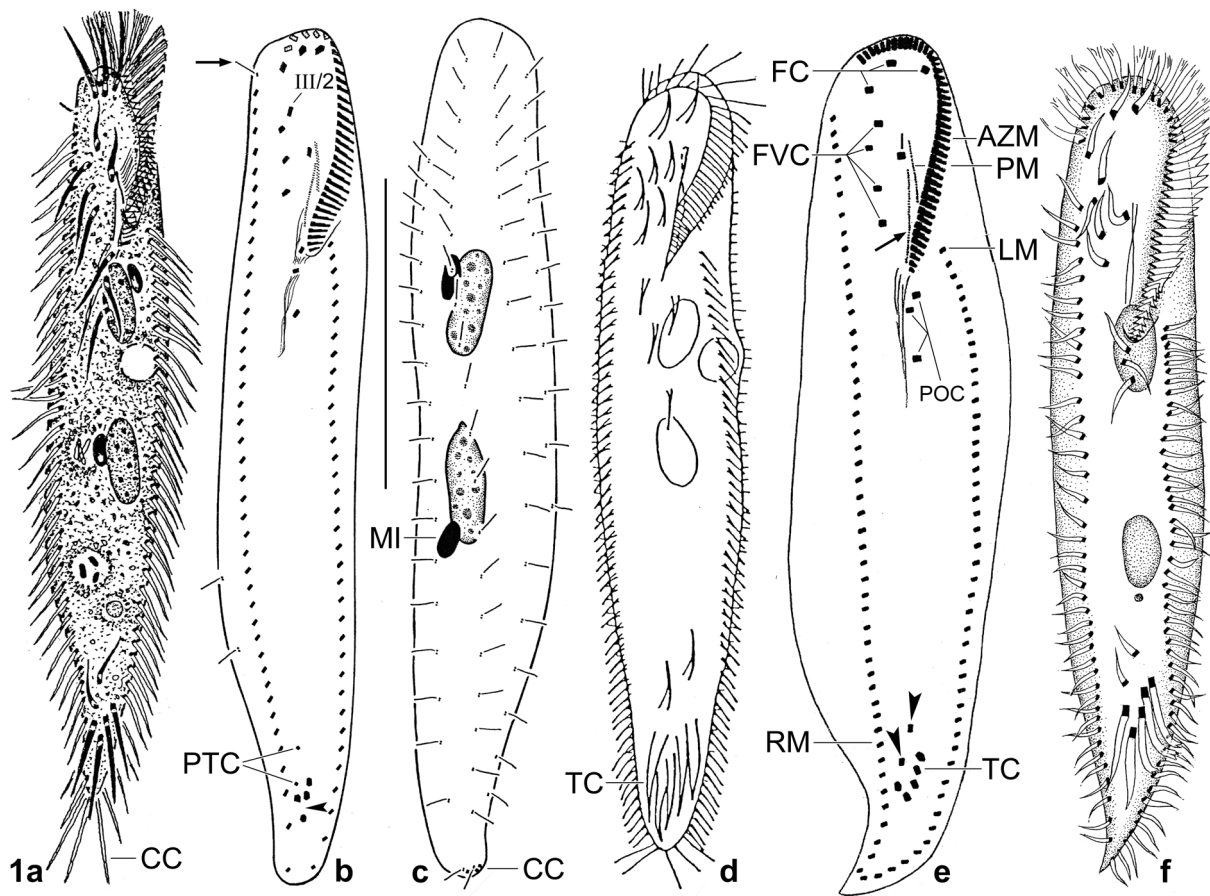


**Fig. 63a–f.** Comparison of *Urosoma pelobia* nov. spec. (a–c) with similar congeners (d–f; see also Table 25) in vivo (a, d, f) and in protargol preparations (b, c, e). **a:** *Urosoma pelobia*, ventral view of a representative specimen, length 150  $\mu\text{m}$ . Note the slender body and the narrowly rounded posterior end. **b, c:** *Urosoma pelobia*, ventral and dorsal view of holotype specimen, length 140  $\mu\text{m}$ . The arrow marks a dikinetid at begin of the right marginal cirral row; the arrowhead denotes the increased space between the last and the penultimate cirrus. See also the large micronuclei. **d:** Ventral view of *U. macrostyla* according to Wrzesniowski (1867; from Berger 1999), length 120  $\mu\text{m}$ . Note the five thick, subterminal transverse cirri. **e:** *Urosoma macrostyla* as described by Qin et al. (2011), length 245  $\mu\text{m}$ . Note the acute posterior end and the fine transverse cirri, indicating misidentification. The arrowheads mark pretransverse cirri; the arrow denotes the endoral membrane. **f:** Ventral view of *U. ambigua* Dragesco & Dragesco-Kernéis, 1986, length 165  $\mu\text{m}$ . Note the acute body end. AZM – adoral zone of membranelles, CC – caudal cirri, FC – frontal cirri, FVC – frontoventral cirri, LM – left marginal cirral row, MI – micronucleus, PM – paroral membrane, POC – postoral cirri, PTC – pretransverse cirri, RM – right marginal cirral row, TC – transverse cirri, III/2 – cirrus in urosomoid location.

***Urosoma pelobia* nov. spec.**

(Fig. 63a–c, 64a–q; Tables 24, 25 on p. 329, 331)

**Diagnosis:** Size in vivo about  $155 \times 25 \mu\text{m}$ . Very slender ( $\sim 6:1$ ) with posterior end narrowly rounded, rarely bluntly acute, never emarginated. Two widely spaced, elongate ellipsoid macronuclear nodules and an average of two large ( $7 \times 3 \mu\text{m}$ ), ellipsoid micronuclei. Distance between frontal cirri 2 and 3 usually twice as large as between 1 and 2. Buccal cirrus subapical of paroral membrane. Four subterminal, fine transverse cirri distinctly projecting from body proper. Marginal rows extend to posterior body end, right row composed of an average of 37 cirri, left of 33; right row commences with a single dikinetid, the anterior basal body associated with a short bristle. Four dorsal kineties, row 4 ends subterminally, i.e., at begin of tail-like narrowing. Adoral zone extends about 26% of body length, composed of an average of 30 membranelles; buccal cavity narrow and flat. Paroral and endoral membrane each about  $10 \mu\text{m}$  long, half of posterior, respectively, anterior portion side by side.

**Type locality:** Australian site (1/2006), i.e., floodplain soil from the Murray River near to the town of Albury, waterside of Ryans road, Australia,  $37^{\circ}\text{S}$ ,  $147^{\circ}\text{E}$ .

**Type material:** Three slides (one slide containing the holotype, two paratype slides) with protargol-impregnated specimens have been deposited in the Biology Centre of the Upper Austrian Museum in Linz (LI). The holotype (Fig. 63b, c) and other relevant specimens have been marked by black ink circles on the coverslip. For slides, see Fig. 28a–d in Chapter 5.

**Etymology:** *pelobia* is Greek and refers to the marshy floodplain habitat.

**Description:** Except of some distances, e.g., anterior body end to right marginal cirral row (CV = 17.9%) and posterior body end to left marginal cirral row (CV = 45.7%), *U. pelobia* has a low to ordinary variability (CV  $\leq 10\%$ ,  $\leq 15\%$ ).

Size in vivo about  $155 \times 25 \mu\text{m}$ , in protargol preparations  $136 \times 23 \mu\text{m}$  on average (Table 24). Body slender (5:1) to very slender (7:1), on average 6:1 (Table 24); parallel-sided or slightly convex, anterior end transversely cut off, posterior region distinctly narrowed especially the right margin, rear end narrowly rounded to bluntly acute; never emarginated (checked in 50 specimens, Fig. 63a, b, 64a, d, f, g–l, o, p); about 2:1 flattened laterally. Two ellipsoid to elongate ellipsoid macronuclear nodules in or near central third of body, usually distinctly apart; with many minute nucleoli. Usually two, rarely three ellipsoid to elongate ellipsoid micronuclei attached to macronuclear nodules at various sites, comparatively large ( $7 \times 3 \mu\text{m}$  in protargol preparations) and thus also conspicuous in vivo (Fig. 63a–c, 64a, b, d, g, o; Table 24). Contractile vacuole slightly anterior of mid-body. Cortex very flexible, possibly contains minute granules. Cytoplasm without peculiarities. Food vacuoles up to  $10 \mu\text{m}$  across, contain bacterial spores, small heterotrophic flagellates, and small resting cysts. Swims and glides elegantly and rapidly on microscope slides.

Cirral pattern urosomoid, i.e., cirrus III/2 slightly anterior and left of frontoventral row (Fig. 63a, b, 64a–c, g, o). All cirri fine compared to body size (Fig. 63a–c, 64a, g–i, m–p). Frontal cirri about  $10 \mu\text{m}$  long in vivo and slightly thickened, cirrus 3 (= right frontal cirrus) usually distinctly apart from cirri two and one (Fig. 63a, b, 64a–c, g, o, p). Buccal cirrus subapical of anterior end of paroral membrane. Postoral cirri in line, first cirrus at level of proximal end of adoral zone of membranelles. Four subterminal transverse cirri in hook-like pattern, in vivo about  $15 \mu\text{m}$  long and thus slightly projecting from body proper, thickened, last cirrus usually slightly apart from the others. Pretransverse cirri minute, the posterior one at hook entrance. Marginal cirri fine, composed of two minute ciliary rows, about  $12 \mu\text{m}$  long in vivo, cirral distance highly variable in rear region; right row commences with a dikinetid of which the anterior basal body has a  $3 \mu\text{m}$  long bristle.

Dorsal bristles about  $5 \mu\text{m}$  long in vivo; row 1 slightly shortened anteriorly and posteriorly; rows 2 and 3 almost bipolar, row 4 ends far subterminal, i.e., where body narrowing commences. Caudal

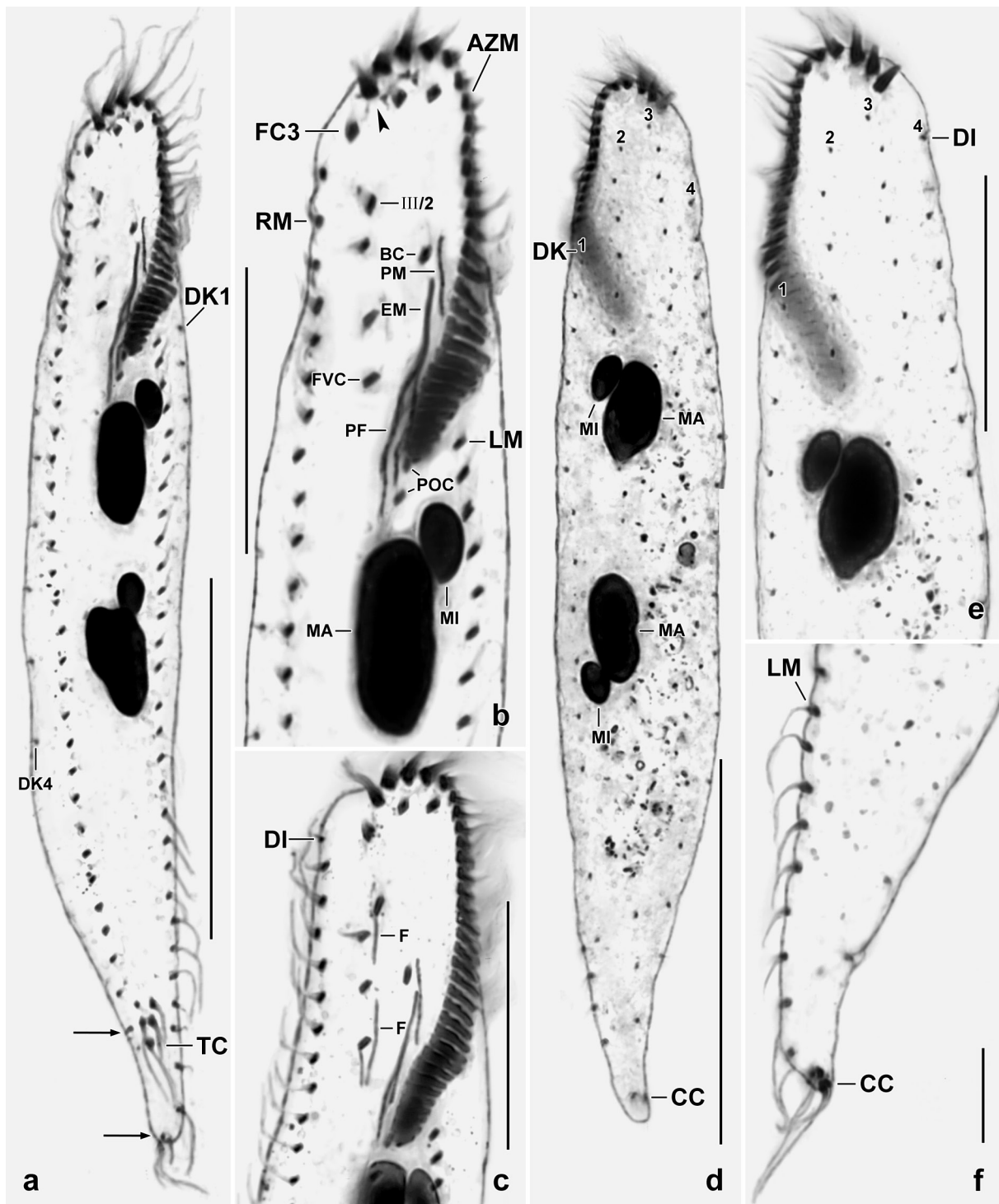


**Fig. 64a–f.** *Urosoma pelobia*, ventral (a–c), dorsal (d, e), and dorsolateral (f) views of protargol-impregnated specimens. Arrows in (a) mark a gap in the right marginal cirral row; the arrowhead in (b) marks the increased distance between frontal cirri 2 and 3. Further important features: the slender body (a, d), the distinctly narrowed posterior region (a, d, f), the narrowly rounded posterior end (a, d), the large micronuclei (a, b, d, e), cirrus III/2 (a–c), the four subterminal transverse cirri (a), and the narrow buccal cavity (a, b). Scale bars 10  $\mu\text{m}$  (f), 25  $\mu\text{m}$  (b, c), and 50  $\mu\text{m}$  (a, d). Explanation of figure abbreviations, see other legends of this species.

cirri about 20  $\mu\text{m}$  long in vivo, close to last dikinetid of dorsal kineties 2 and 3 (Fig. 64a, d, e, g, j–l; Table 24).

Oral apparatus inconspicuous because extending only 23–29%, on average 26% of body length (Table 24). Adoral zone in rather distinct *Gonostomum* pattern, composed of an average of 30

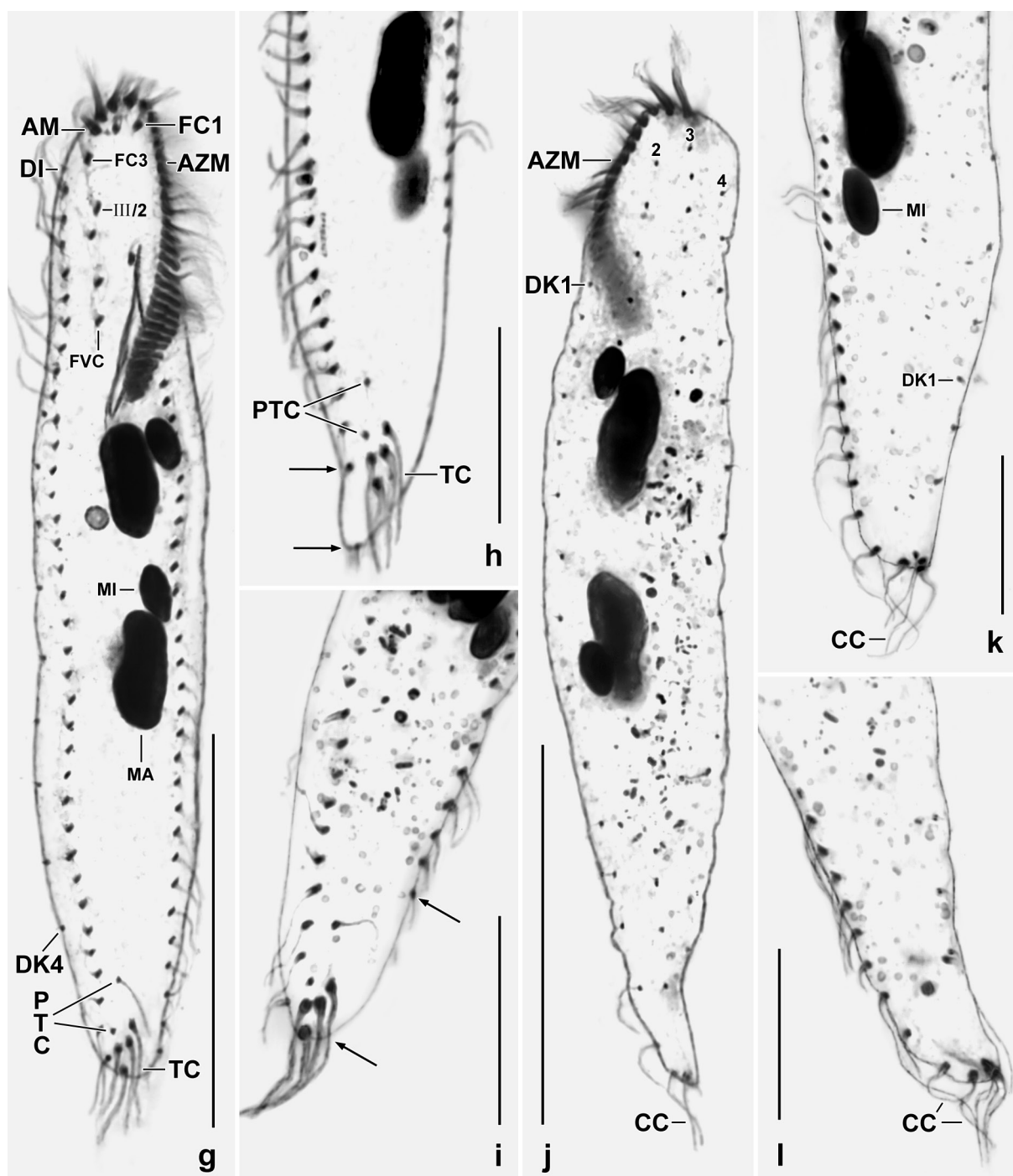


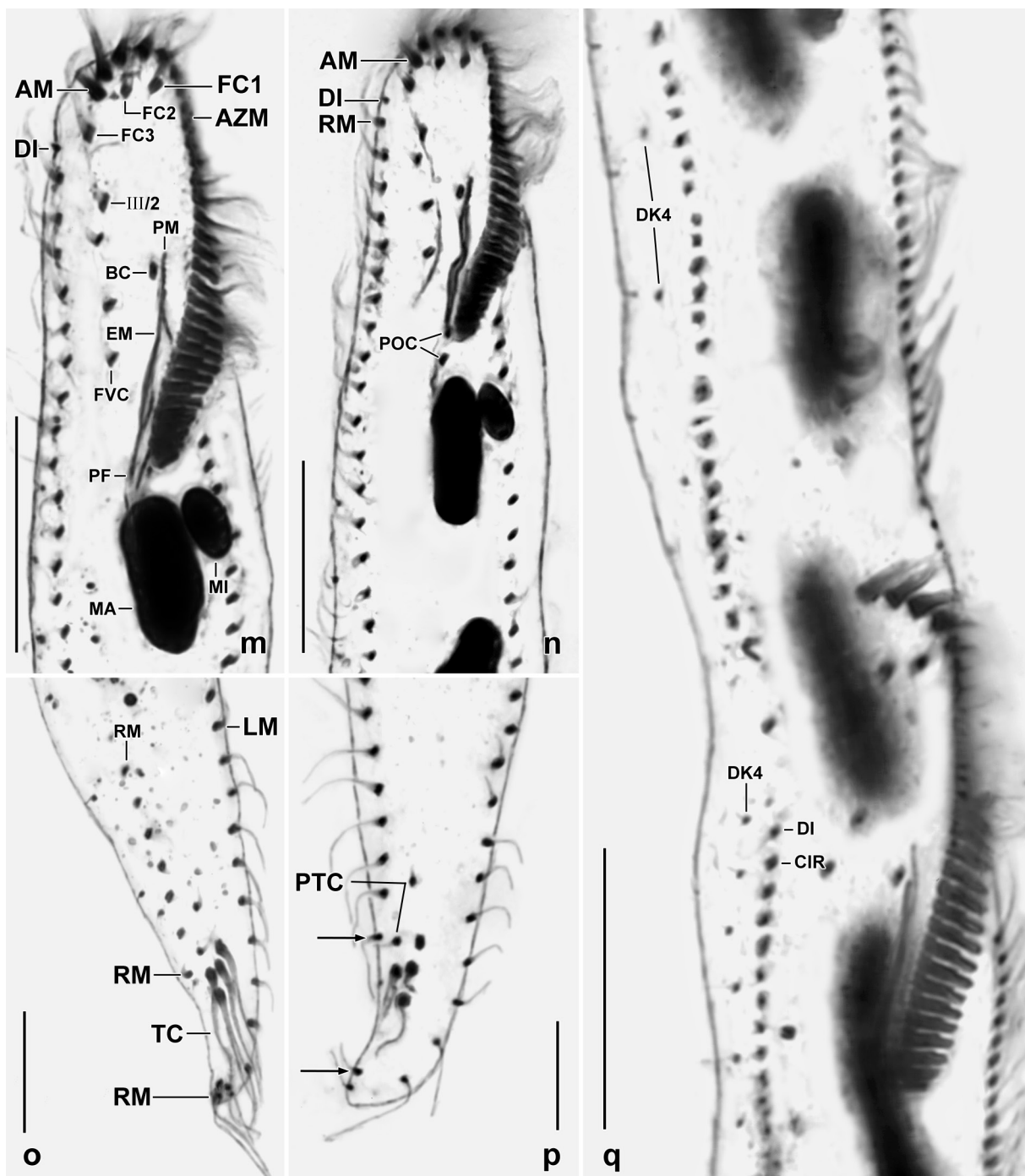
**Fig. 64g-l.** *Urosoma pelobia*, ventral (g-i), dorsal (j), and dorsolateral (k, l) views of protargol-impregnated specimens. **g:** Note the large distance between frontal cirri 2 and 3, the rounded posterior body end, and the large micronuclei. This species has only four transverse cirri (g-i). **h, i, k, l:** Variability of posterior body region and posterior body end. The distance between the posterior body end and the end of the marginal cirral rows is highly variable (h, i, arrows). This applies also to the location of the transverse cirri. **j:** Dorsal view of a rather broad specimen with acute posterior body end. AM – distalmost adoral membranelle, AZM – adoral zone of membranelles, DI – dikinetid at begin of right marginal cirral row, DK1–4 – dorsal kineties, FC1,3 – frontal cirri, FVC – frontoventral cirral row, MA – macronuclear nodule, MI – micronuclei, PTC – pretransverse cirri, TC – transverse cirri, III/2 – cirrus III/2. Scale bars 20  $\mu\text{m}$  (h, i), 25  $\mu\text{m}$  (k, l), and 50  $\mu\text{m}$  (g, j).

ordinary membranelles with largest bases about 4  $\mu\text{m}$  wide in protargol preparations (Fig. 63a, b, 64a–c, g, n, o; Table 24). Buccal cavity short, shallow, and narrow. Paroral and endoral membrane each only about 10  $\mu\text{m}$  long, in typical *Urosoma* pattern, i.e., posterior half of paroral side by side

with anterior half of endoral membrane; form an acute angle because paroral more or less oblique. Buccal lip inconspicuous. Pharyngeal fibres about 20  $\mu\text{m}$  long in protargol preparations.

**Occurrence and ecology:** As yet found only at type locality. A second new species,  $\rightarrow$  *Urosoma australiensis*, occurred in floodplain soil from the red centre of Australia, about 1300 km southeast of the type locality of *U. pelobia*. This shows not only intracontinental diversification but also our ignorance of the ciliate fauna in general (see Berger 1999 and Foissner et al. 2002 for reviews and post-Kahlian *Urosoma* species).

**Remarks:** There are four species which are similar to *Urosoma pelobia* (Table 25). *Urosoma macrostyla* (Fig. 63d), as described by Wrzeńskiowski (1870), is a small ( $120 \times 30 \mu\text{m}$  vs.  $155 \times 25 \mu\text{m}$ ), rather broad (length:width ratio 4:1 vs. 6:1) species with five thick (vs. four thin) transverse cirri. *Urosoma macrostyla* (Fig. 63e), as described by Qin et al. (2011), is a misidentification (see



below). It has an acute (vs. narrowly rounded) posterior end, 41 (vs. 30) adoral membranelles, 48 (vs. 37) cirri in the right marginal row, and 42 (vs. 33) cirri in the left. *Urosoma acuta* Dragesco, 1972 and *U. ambigua* (Fig. 63f), as described by Dragesco & Dragesco-Kernéis (1986), have an acute (vs. narrowly rounded) posterior end, 43 (vs. 30) adoral membranelles, five (vs. four) transverse cirri, and about 50 (vs. 37 and 33) cirri each in the right and left marginal row (Table 25).

Berger (1999) synonymized *U. acuta* Dragesco, 1972 and *U. ambigua* Dragesco & Dragesco-Kernéis, 1986 with *U. macrostyla*. I disagree because a life micrograph of Qin et al. (2011) shows that species with a pronounced acute posterior end really exist. The Chinese species discovered by Qin et al. (2011) differs from the African species described by Dragesco (1972) and Dragesco & Dragesco-Kernéis (1986) mainly by body size (average length 226  $\mu\text{m}$  vs. 120  $\mu\text{m}$  and 150  $\mu\text{m}$ ), indicating that they might be synonymous, especially when assumed that the huge body length of the Chinese specimens results mainly from culture conditions.

### *Hemiurosoma similis* (Foissner, 1982) Foissner, Agatha & Berger, 2002

(Fig. 65a–e, 66a–n; Table 26 on p. 331)

**Material:** Surface soil from the green river bed of the Thamalakane River in the surrounding of the town of Maun, Botswana. Soil dark-grey when dried, black in wet condition, sandy and loamy, covered with a dense grass layer, pH 5.3 in water. Collected and investigated in 2004.

**Material deposited:** Four voucher slides with protargol-impregnated specimens have been deposited in the Biology Centre of the Upper Austrian Museum in Linz (LI). For slides, see Fig. 29a–d in Chapter 5.

**Description:** Except of some distances, e.g., posterior end to right marginal cirral row (CV = 42.5%); and the nuclear apparatus, e.g., the number of micronuclei (CV = 31.6%), *H. similis* has an ordinary variability in all important features (CV  $\leq$  15%).

Size in vivo about 140  $\times$  25  $\mu\text{m}$ , as calculated from some in vivo measurements and the morphometric data in Table 26 adding 15% preparation shrinkage. Body slender (5.8:1 on average) to very slender (7:1) and lanceolate, i.e., rather abruptly narrowed posteriorly; rarely indistinctly sigmoid. Anterior end transverse-truncate, posterior narrowly rounded. About 2:1 flattened laterally (Fig. 65a–e, 66a, g, i, l; Table 26). Nuclear apparatus usually anterior of mid-body, anterior nodule frequently partially covered by proximal third of adoral zone of membranelles (Fig. 65a, e, 66a–c, i; Table 26). Macronuclear nodules in protargol preparations 13  $\times$  5  $\mu\text{m}$  on average, i.e., ellipsoid to elongate ellipsoid (>2.5:1); with many minute nucleoli. 1–4, on average two ellipsoid micronuclei one each attached to macronuclear nodules; of ordinary size, i.e., 3  $\times$  1.5  $\mu\text{m}$  in protargol preparations. Contractile vacuole slightly anterior of mid-body, with short, lacunar collecting canals (Fig. 65a). Cortex very flexible, colourless, cortical granules in vivo not recognizable in five specimens observed but minute, argyrophilic granules around cirri and dorsal

---

← **Fig. 64m–q.** *Urosoma pelobia*, ventral views of morphostatic (m–p) and dividing (q) specimens. **m, n:** These specimens show clearly a single dikinetid at the anterior end of the right marginal row. Note the large micronucleus. In the left specimen, the distance between frontal cirri 2 and 3 is almost thrice as large as between 1 and 2. **o, p:** *Urosoma pelobia* has only four transverse cirri. The arrows in (p) mark a big gap in the right marginal cirral row. **q:** A late mid-divider. Scale bars 10  $\mu\text{m}$  (o, p) and 20  $\mu\text{m}$  (m, n, q). Abbreviations (also for figures 64a–f): AM – distalmost adoral membranelle, AZM – adoral zone, BC – buccal cirrus, CIR – ordinary right marginal cirrus, DI – dikinetid at begin of right marginal row, DK1–4 – dorsal kineties, EM – endoral membrane, F – fibres associated with cirri, FC1–3 – frontal cirri, FVC – row of frontoventral cirri, LM – left marginal cirral row, MA – macronuclear nodule, MI – micronucleus, PF – pharyngeal fibres, PM – paroral membrane, POC – postoral cirri, PTC – pretransverse cirri, RM – right marginal cirral row, TC – transverse cirri, 1–4 – dorsal kineties.

bristles in some protargol-impregnated specimens. Cytoplasm colourless and turbid due to several inclusions (Fig. 65a, b): (i) many compact food vacuoles 5–10  $\mu\text{m}$  across in posterior half of body; (ii) 1–3  $\mu\text{m}$ -sized crystals accumulated in rear end and as small clusters throughout body making cells dark under bright field illumination; (iii) many lipid (?) arrays composed of 0.5–1.0  $\mu\text{m}$ -sized, refractive droplets; and (iv) three, rarely four lithosomes in the pattern shown in Fig.

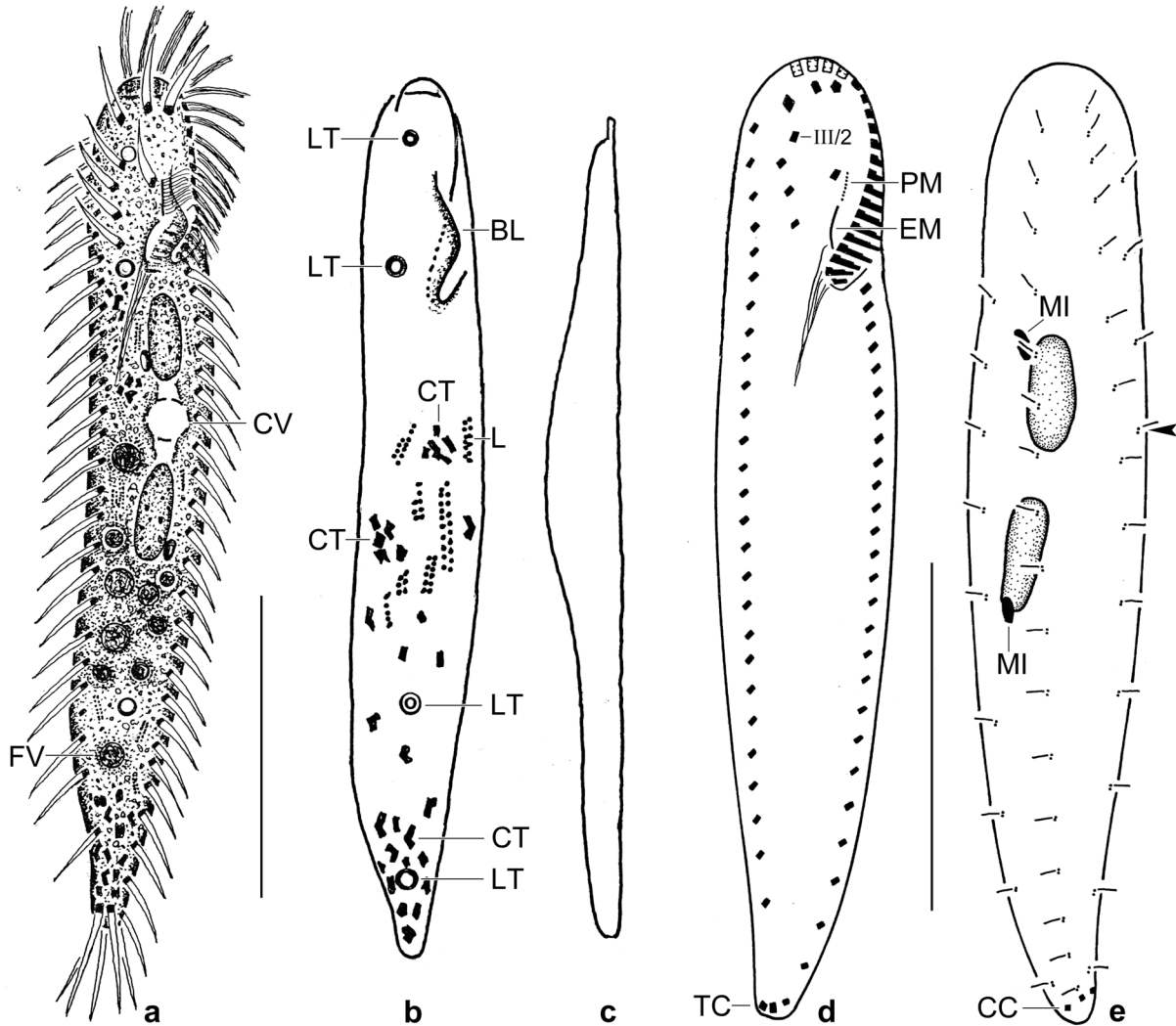
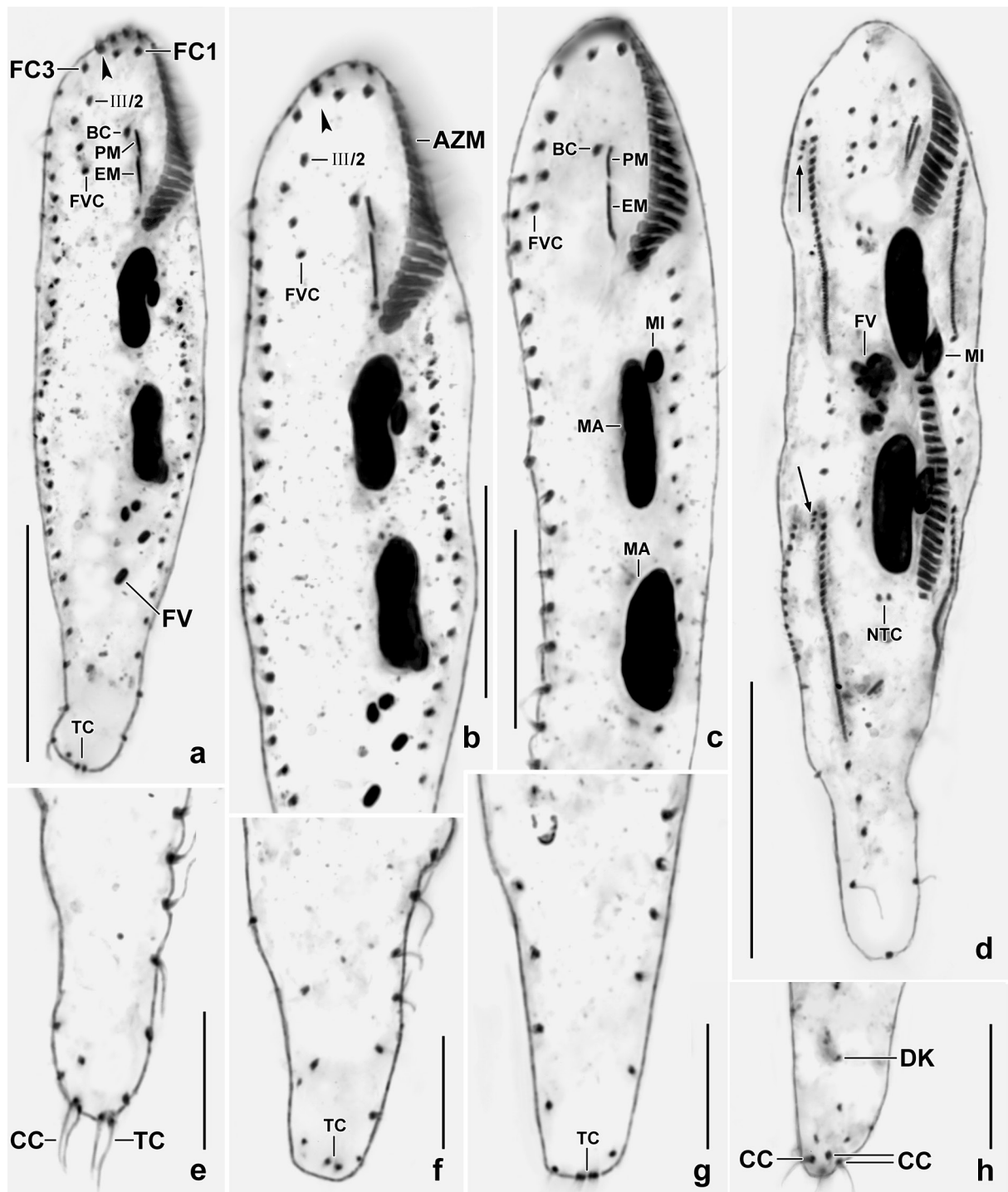


**Fig. 65a–e.** *Hemiurosoma similis*, Botswanan specimens from life (a–c) and after protargol impregnation (d, e). **a–c:** Ventral and lateral view of a representative specimen, length 140  $\mu\text{m}$ . Note the rich diversity of cytoplasmic inclusions. Crystal spots occur not only in the narrowed posterior region but throughout the cell. The anterior macronuclear nodule is usually partially covered by the posterior region of the oral apparatus; in the figure it is more posteriorly located to show the oral structures more clearly. **d, e:** Ventral and dorsal view of infraciliature and nuclear apparatus. The arrowhead in (e) marks the posterior end of dorsal kinety 4. BL – buccal lip, CC – caudal cirri, CT – crystals, CV – contractile vacuole, EM – endoral membrane, FV – food vacuole, LT – lithosomes, MI – micronuclei, PM – paroral membrane, TC – transverse cirri, III/2 – cirrus number. Scale bars 40  $\mu\text{m}$  (d, e) and 50  $\mu\text{m}$  (a–c).

**Fig. 66a–h.** *Hemiurosoma similis*, ventral (a–g) and dorsal (h) views after protargol impregnation. **a–c:** Overview and details of a representative specimen. There is a distinctly increased distance between frontal cirri 2 and 3 (arrowheads) except of the specimen shown in (c). Cirrus III/2 is anterior and left of the other frontoventral cirri except in (c). **d:** A divider, showing dorsal kinety 4 originating dorsomarginally (arrows). **e–g:** Posterior body region, showing transverse cirri very near to posterior body end. **h:** Dorsal view, showing three caudal cirri. AZM – adoral zone, BC – buccal cirrus, CC – caudal cirri, EM – endoral membrane, FC1,3 – frontal cirri, FV – food vacuoles with bacterial spores, FVC – frontoventral cirri, MA – macronuclear nodules, MI – micronuclei, NTC – new transverse cirri, PM – paroral membrane, TC – transverse cirri, III/2 – cirrus number. Scale bars 15  $\mu\text{m}$  (e–h), 20  $\mu\text{m}$  (b, c), 30  $\mu\text{m}$  (d), 35  $\mu\text{m}$  (a).

65b; individual lithosomes 3–4  $\mu\text{m}$  across, center empty, rarely filled. Feed on small, heterotrophic flagellates and possibly also on bacteria. Glides rapidly on microscope slides as well as between and upon soil particles.

Somatic and oral infraciliature as described by Foissner (1982), i.e., in *Urosoma* pattern with cirrus III/2 anterior and slightly left of frontoventral cirral row; postoral cirri absent (Fig. 65a, d, e, 66a–c, e–n; Table 26). Frontal cirri 10–12  $\mu\text{m}$  long in vivo and slightly thickened; distance between frontal cirri 2 and 3 distinctly increased, as in Austrian type (Foissner 1982). Usually two slightly thickened transverse cirri very near to rear body end, about 15  $\mu\text{m}$  long in vivo. Marginal cirri about 10  $\mu\text{m}$  long in vivo, intracirral distances considerably enlarged in posterior region of rows.



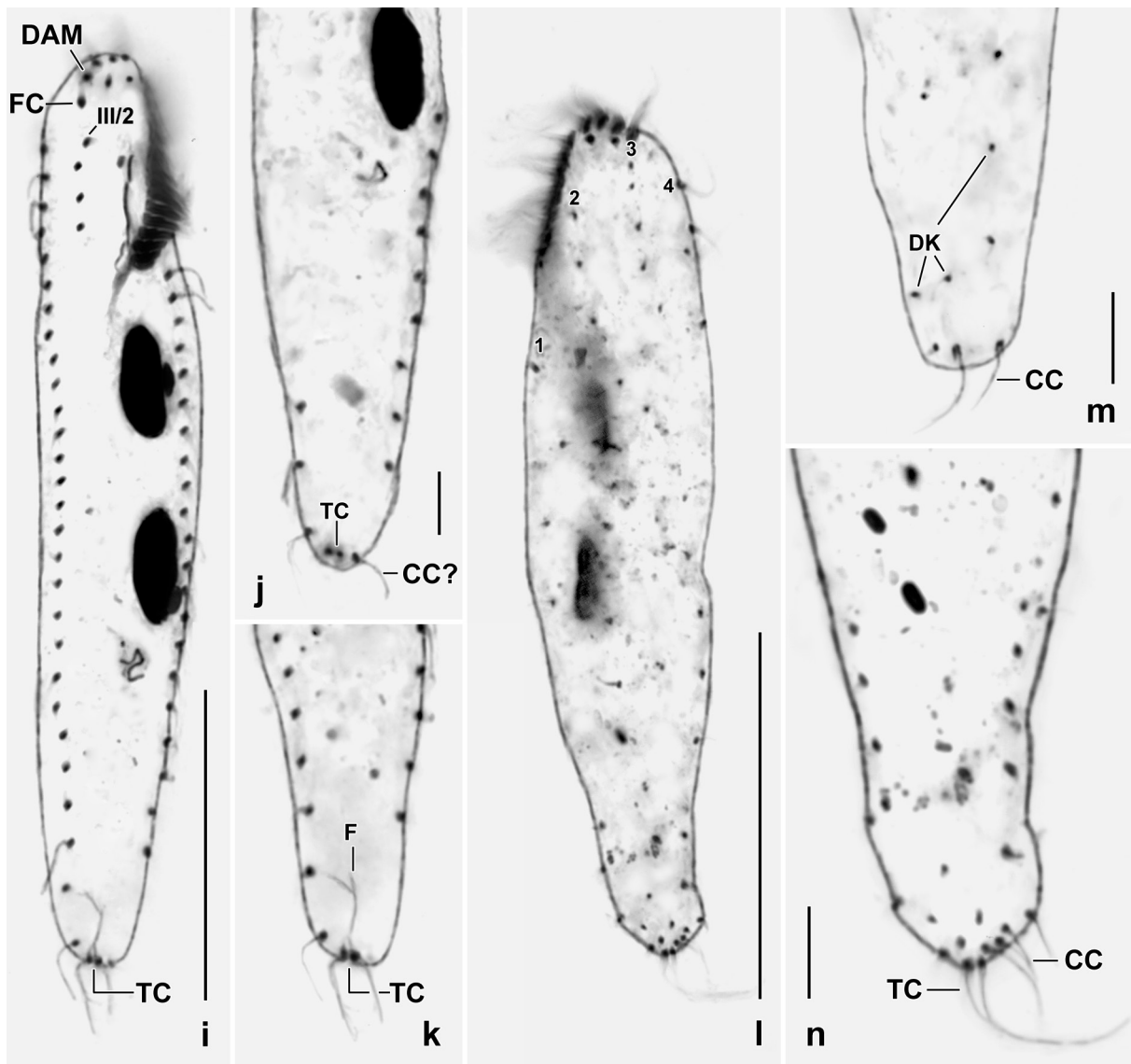


**Fig. 66i–n.** *Hemiurosoma similis*, ventral (i, k, n) and dorsal (j, l, m) views of Botswanan specimens after protargol impregnation. **i:** A typical specimen, showing the entire cirral pattern very clearly. **j, k:** Posterior body region, showing the transverse cirri at end of cell. **l, n:** There are four dorsal kineties. Transverse cirri and caudal cirri are often difficult to identify because the posterior end is very flat. **m:** Possibly, this specimen has only two caudal cirri. CC? – supposed caudal cirrus, DAM – distalmost adoral membranelle, DK – dorsal kineties, F – fibres originating from transverse cirri, FC – right frontal cirrus, TC – transverse cirri, III/2 – parabuccal cirrus, 1, 2, 3, 4 – dorsal kineties. Scale bars 10  $\mu\text{m}$  (j, m, n), 20  $\mu\text{m}$  (k), 40  $\mu\text{m}$  (l), 50  $\mu\text{m}$  (i).

Invariably four dorsal kineties with 2  $\mu\text{m}$  long bristles. Kinety 4 composed of an average of only three dikinetids and thus ending anterior of mid-body. Caudal cirri close to rear body end, about 15  $\mu\text{m}$  long in vivo (Fig. 65a, e, 66e, h, l–n; Table 26).

Oral apparatus inconspicuous because extending only 21% of body length on average, composed of an average of 19 adoral membranelles only up to 5  $\mu\text{m}$  wide in vivo (Fig. 65a, b, d, 66a–c, i; Table 26). Frontal scutum 2–3  $\mu\text{m}$  high. Buccal cavity very flat and narrow, lip distinctly convex and up to 5  $\mu\text{m}$  broad in vivo, bears paroral membrane composed of nine or 10 cilia 5  $\mu\text{m}$  long in vivo. Paroral and endoral membrane one after the other, both only 3–5  $\mu\text{m}$  long in protargol preparations. Pharyngeal fibres about 30  $\mu\text{m}$  long.

**Occurrence and ecology:** Green river beds develop in the tropics during the dry season. The river dries up and grass begins to grow in the bed area. The grass is used by many vertebrates, such

as rhinos, elephants and antelopes. Their faeces is an ideal fertilizer for the organism community, including protists, when the river fills with water during the wet season. Although my experience with this kind of habitat is rather limited, I know that its protist community is extremely diverse and contains hundreds, very likely even thousands of undescribed species.

The Botswanan record confirms the notion of Foissner (1998) that *H. similis* is a cosmopolitan present in all main biogeographic regions except of Antarctica.

**Remarks:** The Botswanan specimens are highly similar to the Austrian ones except for the presence/absence of lithosomes. However, I cannot exclude to have overlooked lithosomes in 1982 when I had much less experience than in 2004. Further, it is not known whether or not lithosomes are a species-specific feature.

The morphometric comparison (Table 26) shows only minor differences in body size (on average  $140 \times 25 \mu\text{m}$  vs.  $130 \times 20 \mu\text{m}$ ), length:width ratio (5.8 vs. 6.6), and in the number of adoral membranelles (19 vs. 22 on average).

### ***Urosomoida uluruensis* nov. spec.**

(Fig. 67a–h, 68a–g; Table 27 on p. 333)

**Diagnosis:** Size about in vivo  $90 \times 25 \mu\text{m}$ ; very elongate obovate (3.4:1). Two ellipsoid, narrowly spaced ( $4 \mu\text{m}$ ) macronuclear nodules with a micronucleus each. Cortical granules in loose rows and around cirri and dorsal bristles, citrine to orange,  $0.5\text{--}1.0 \mu\text{m}$  across. One buccal cirrus rather distinctly posterior of anterior end of paroral membrane; distance between postoral cirri II and III distinctly increased ( $5 \mu\text{m}$ ); four transverse and pretransverse cirri. four dorsal kineties including one dorsomarginal kinety, three caudal cirri. Adoral zone extends about 32% of body length, composed of 24 membranelles on average. Buccal cavity moderately narrow and deep, buccal horn distinct.

**Type locality:** Australian site (170), i.e., ephemeral puddles on top of Uluru, Australia,  $25^{\circ}20'42''\text{S}$ ,  $131^{\circ}02'10''\text{E}$ .

**Type material:** The slide<sup>1</sup> containing the holotype (protargol method) and three paratype slides<sup>2</sup> (protargol method) have been deposited in the Biology Centre of the Upper Austrian Museum in Linz (LI). The holotype and other relevant specimens have been marked by black ink circles on the coverslip. For slides, see Fig. 24a–h in Chapter 5.

**Etymology:** Named after the site discovered, i.e., the aboriginal noun *Uluru* (English colonial name: Ayers Rock) which is type locality.

**Description:** *Urosomoida uluruensis* is rather variable. Of the 41 characteristics investigated, 13 have a  $\text{CV} > 15\%$ , including two diagnostic features, viz., the distance between the macronuclear nodules and the distance between postoral cirri II and III (Table 27).

Size in vivo  $75\text{--}120 \times 20\text{--}40 \mu\text{m}$ , usually about  $90 \times 25 \mu\text{m}$ , as calculated from some in vivo measurements and the morphometric data in Table 27 adding 15% preparation shrinkage. Usually very elongate to elongate obovate, rarely elongate ellipsoid, never tail-like elongated posteriorly (Fig. 67a, b, e, g, h, 68a–c, d, g). Nuclear apparatus in central third of cell left of bodies midline; composed of two macronuclear nodules and two micronuclei on average, anterior nodule begins at level of buccal vertex; nodules close together, on average  $3.9 \mu\text{m}$  ( $\text{CV} = 52.5\%$ !); ellipsoid to broadly ellipsoid, in vivo about  $15 \times 10 \mu\text{m}$ ; with distinct nucleoli (Fig. 67a, d, 68a–d, f, g; Table 27). Micronuclei usually in flat concavities of macronuclear nodules, about  $3 \times 2 \mu\text{m}$  in vivo and

<sup>1</sup> Note by H. Berger: This slide also contains the holotype of  $\rightarrow$  *Protocyclidium bimacronucleatum*. and  $\rightarrow$  *Microsporidium protocyclidicola*.

<sup>2</sup> Note by H. Berger: One of these paratype slides also contains the holotype of *Hausmanniella uluruensis* (this name is disclaimed for nomenclatural purposes; ICZN 1999, Article 8.3; original description not yet published).

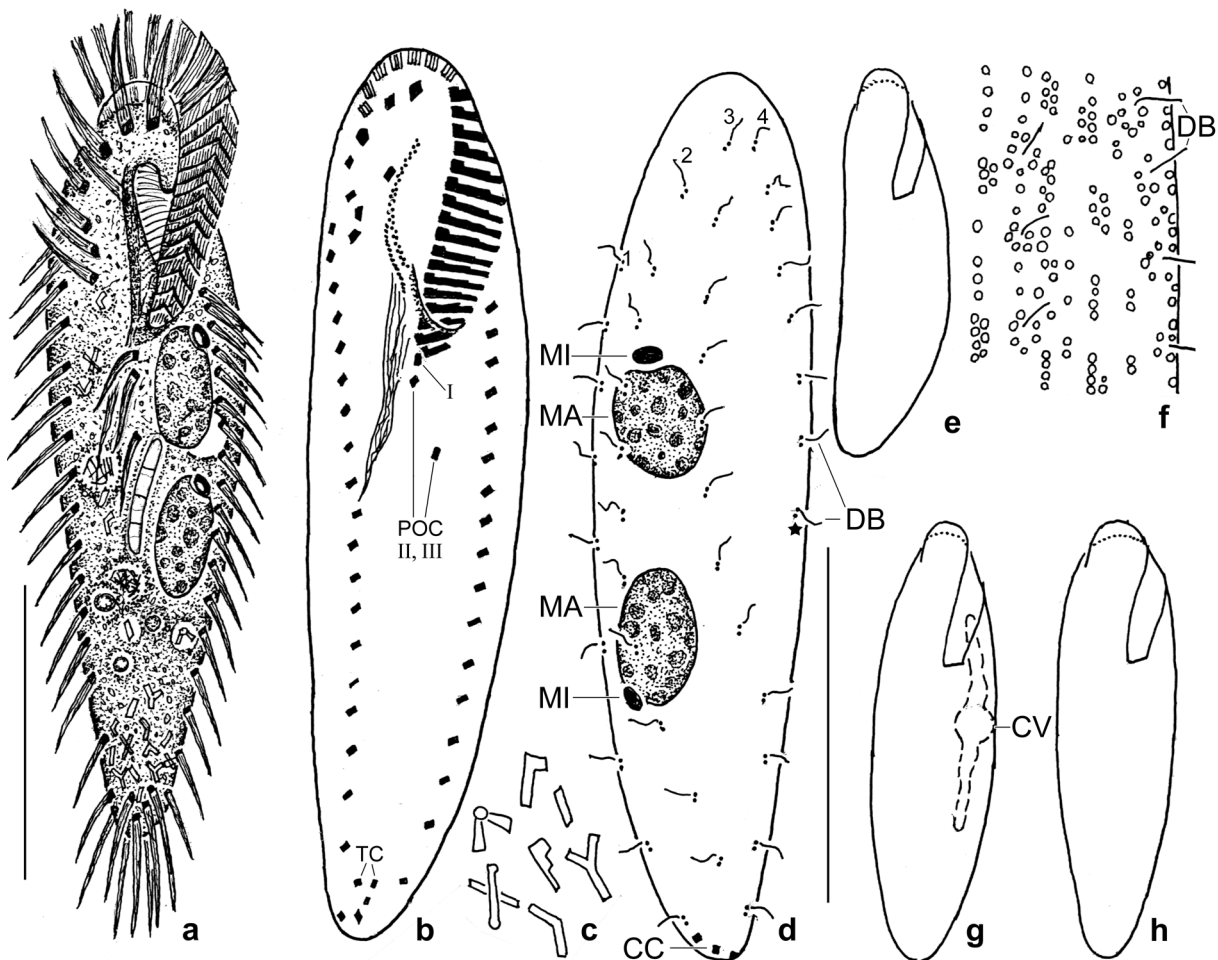


**Fig. 67a–h.** *Urosomoida uluruensis* from life (a, c, e–h) and after protargol impregnation (b, d). **a:** Ventral view of a representative specimen, length 75  $\mu\text{m}$ . **b, d:** Ventral and dorsal view of same specimen, showing the following specific features: the very elongate obovate body, the wide distance between postoral cirri 2 and 3, four transverse and pretransverse cirri, the short adoral zone of membranelles, and the four dorsal kineties of which kinety 4 is shortened posteriorly (asterisk) and produced dorsomarginally. **c:** Cytoplasmic crystals. **e, g, h:** Shape variants. **f:** Cortical granulation. The granules are citrine to orange and are 0.5–1  $\mu\text{m}$  across. CC – caudal cirri, CV – contractile vacuole, DB – dorsal bristles, MA – macronuclear nodules, MI – micronuclei, POCI, II, III – postoral cirri, TC – transverse and pretransverse cirri, 1, 2, 3, 4 – dorsal kineties. Scale bars 30  $\mu\text{m}$ .

in protargol preparations; number highly variable, two on average (Fig. 67a, d, 68c, Table 27). Contractile vacuole slightly anterior of mid-body at left cell margin, with two lacunar collecting canals (Fig. 67a, g). Cortex very flexible, distinctly contractile in anterior half of cell under mild coverslip pressure. Cortical granules in rather loose rows and around bases of cirri and dorsal bristles, citrine to orange making body yellowish at moderate magnification, 0.5–1.0  $\mu\text{m}$  in diameter, do not impregnate with the protargol method used (Fig. 67f). Cytoplasm colourless, studded with ordinary crystals in posterior third of cell often in minute vacuoles, 2–4  $\mu\text{m}$  long (Fig. 67a, c); lipid droplets scattered throughout body, colourless, 1–8  $\mu\text{m}$  in diameter (Fig. 67a). Feeds on bacteria and spores of fungi 10–20  $\times$  2–4  $\mu\text{m}$  in size (Fig. 67a). Glides rapidly on microscope slides.

Most cirri 8–10  $\mu\text{m}$  long in vivo, transverse cirri about 15  $\mu\text{m}$  long; in *Urosomoida* pattern (Berger 1999); frontal and frontoventral cirri slightly thicker than postoral, transverse, and marginal cirri extending to near posterior body end and thus often difficult to separate from transverse cirri and caudal cirri (Fig. 67a, b, d, 68a–e, g). Buccal cirrus distinctly posterior of anterior end of paroral membrane (Fig. 67a, b, 68a–d, g; Table 27). Distance between postoral cirri II and III much larger

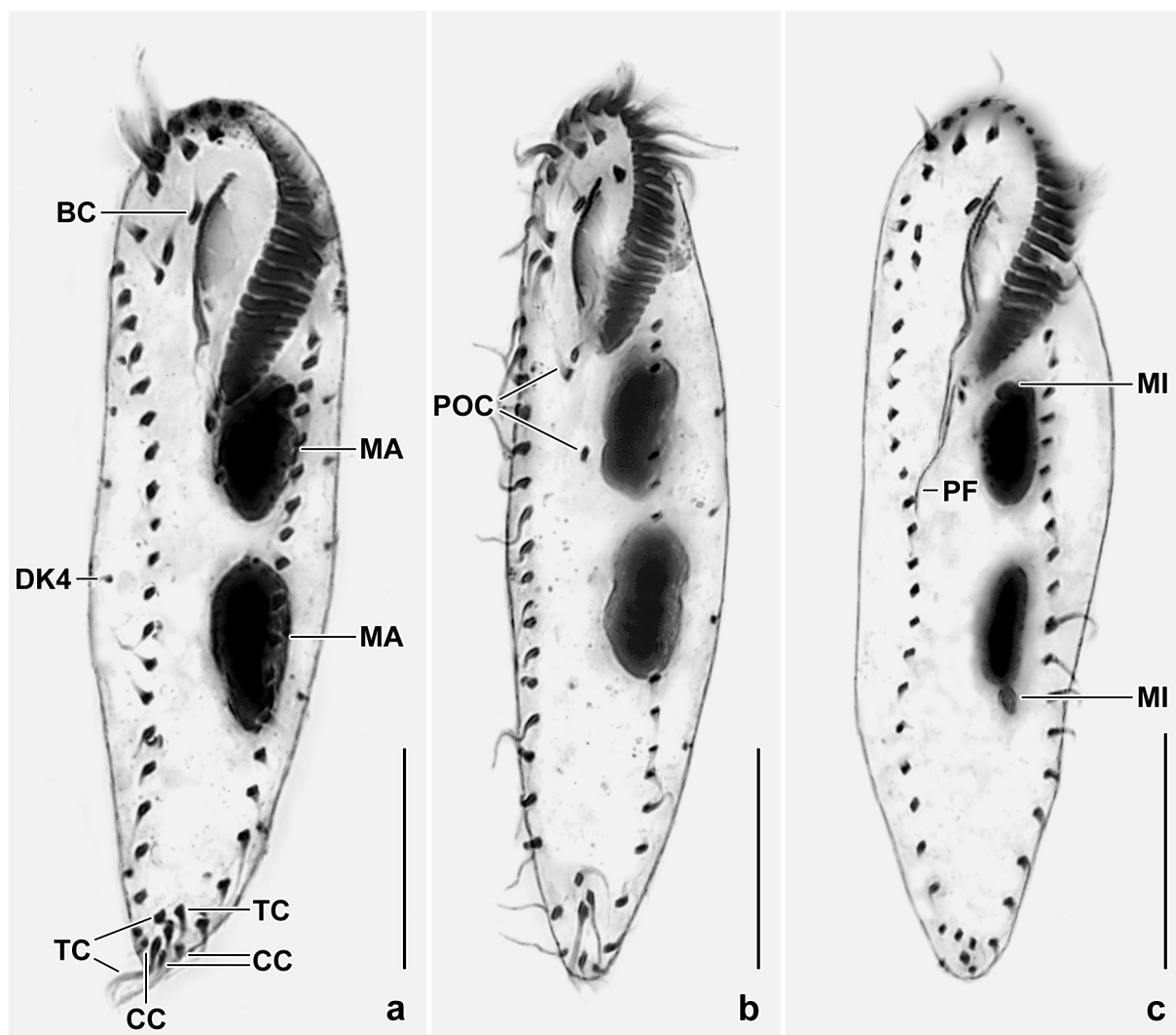
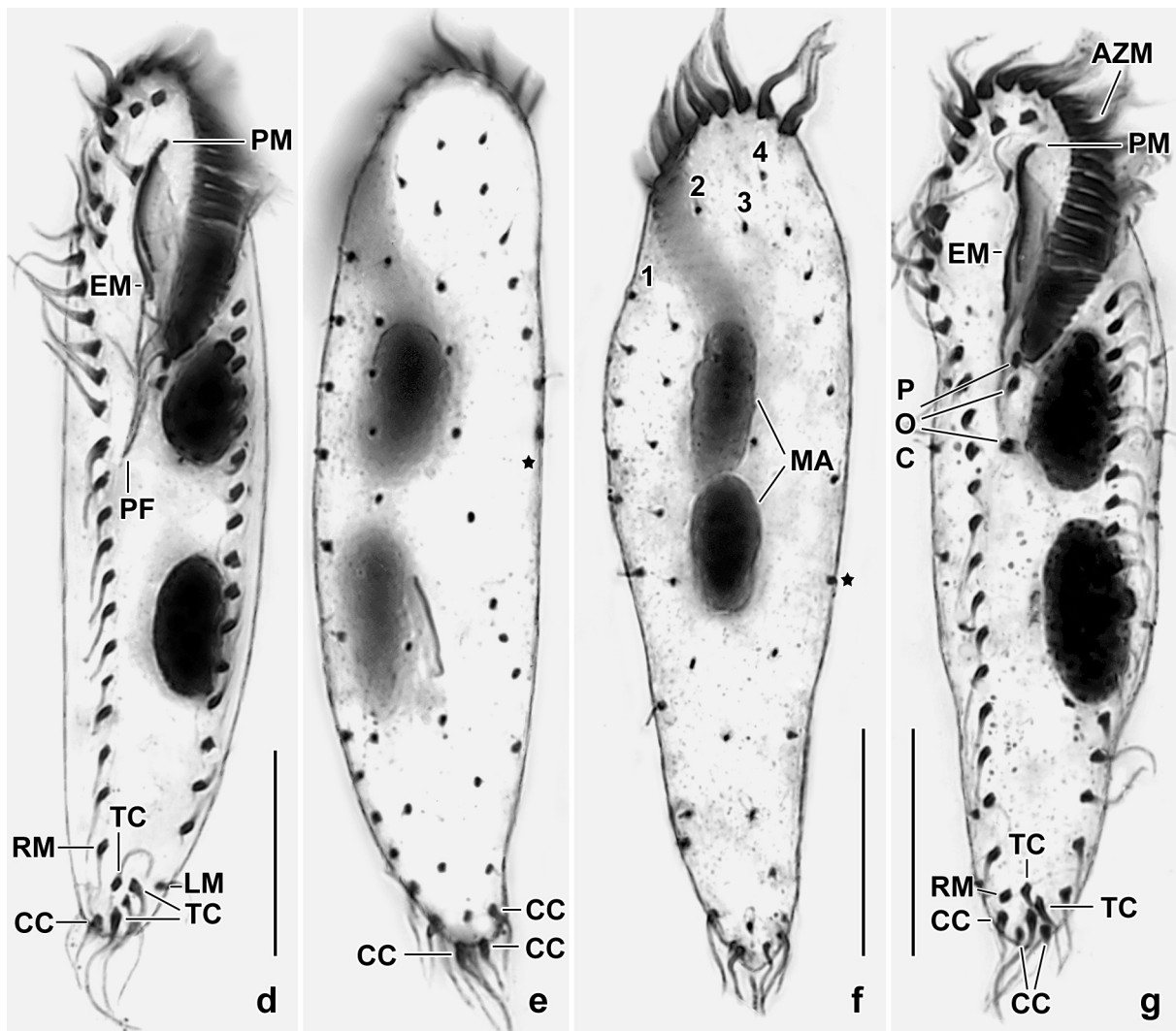


Fig. 68a–c. *Urosomoida uluruensis*, ventral views after protargol impregnation. Important features recognizable: the very elongate obovate body shape, the short adoral zone of membranelles, the narrowly spaced macronuclear nodules, and the large distance between postoral cirri 2 and 3 (b). BC – buccal cirrus, CC – caudal cirri, DK4 – dorsal kinety 4, MA – macronuclear nodules, MI – micronuclei, PF – pharyngeal fibres, POC – postoral cirri, TC – transverse cirri. Scale bars 20  $\mu\text{m}$ .

than between I and II, i.e., 4.0  $\mu\text{m}$  vs. 0.5  $\mu\text{m}$  (Fig. 67a, b, 68b, g; Table 27). Usually four transverse cirri, the upper rightmost very likely a pretransverse cirrus (Fig. 67a, b, 68a–d, g; Table 27). Marginal cirri composed of two ciliary rows, cirral size slightly decreasing near posterior end of body (Fig. 67a, b, 68a–d, g; Table 27). Caudal cirri close to posterior body end (Fig. 67a, b, d, 68a, d, e, g; Table 27). Four dorsal kineties, row 4 extends only in anterior thirds of body and originates dorsomarginally; rows 1–3 each with 8–11 kinetids having 2  $\mu\text{m}$  long bristles (Fig. 67d, 68e, f; Table 27).

Oral apparatus as typical for genus, extends about 32% of body length, composed of 24 membranelles on average with largest bases 8  $\mu\text{m}$  long in vivo and 5  $\mu\text{m}$  in protargol preparations. Buccal cavity moderately narrow and deep, right margin appears thickened (Fig. 67a, b, 68a–d, g; Table 27); buccal horn distinct; buccal lip moderately distinct, covers some proximal membranelles (Fig. 67a, b). Undulating membranes slightly to rather distinctly curved, paroral optically covers anterior region of endoral, paroral cilia in vivo about 5  $\mu\text{m}$  long in anterior quarter, only 3  $\mu\text{m}$  in posterior quarters. Pharyngeal fibres distinct in protargol preparations (Fig. 67a, b, 68a–d, g; Table 27).

**Occurrence and ecology:** As yet found only at type locality. Became rather numerous in the non-flooded Petri dish culture.



**Fig. 68d–g.** *Urosomoida uluruensis*, ventral (d, g) and dorsal (e, f) views after protargol impregnation. **d, e:** Ventral and dorsal view of same specimen having comparatively widely spaced macronuclear nodules. The asterisk marks end of dorsal kinety 4 which is produced dorsomarginally. **f:** A specimen with very narrowly spaced macronuclear nodules. The asterisk marks the posterior end of dorsal kinety 4. **g:** Note the undulating membranes and the narrow spacing of the macronuclear nodules. AZM – adoral zone of membranelles, CC – caudal cirri, EM – endoral membrane, LM – left marginal cirral row, MA – macronuclear nodules, PF – pharyngeal fibres, PM – paroral membrane, POC – postoral cirri, RM – right marginal cirral row, TC – transverse and pretransverse cirri, 1, 2, 3, 4 – dorsal kineties. Scale bars 20  $\mu\text{m}$ .

**Remarks:** There are five *Urosomoida* s.l. species that have cortical granules: *U. agilis* (Engelmann, 1862) Hemberger, 1985, *U. granulifera* Foissner, 1996a, *U. namibiensis* Foissner et al., 2002, *U. galapagensis* Foissner, 2016, and *Paraurosomoida indiensis* Singh & Kamra, 2015. See Berger (1999) for authorship and revision of some species.

*Urosomoida uluruensis* is most similar to *U. agilis* but differs by the number of transverse and pretransverse cirri (four vs. three); the large (vs. ordinary) distance between postoral cirri II and III (as the Indian population of *U. agilis* studied by Singh & Kamra 2015); and the spacing of the macronuclear nodules (only  $\sim 4 \mu\text{m}$  vs. one nodule space between the two nodules; such macronuclear pattern occurs also in *U. galapagensis*, *U. granulifera*, *U. agiliformis* Foissner, 1982, *U. deserticola* Foissner et al., 2002, and in *U. halophila* Foissner, 2016). Body length (around 90  $\mu\text{m}$  vs. 120  $\mu\text{m}$ ) and shape (posterior end narrowly rounded vs. often tail-like elongated) are also slightly different but too variable for a reliable distinction.

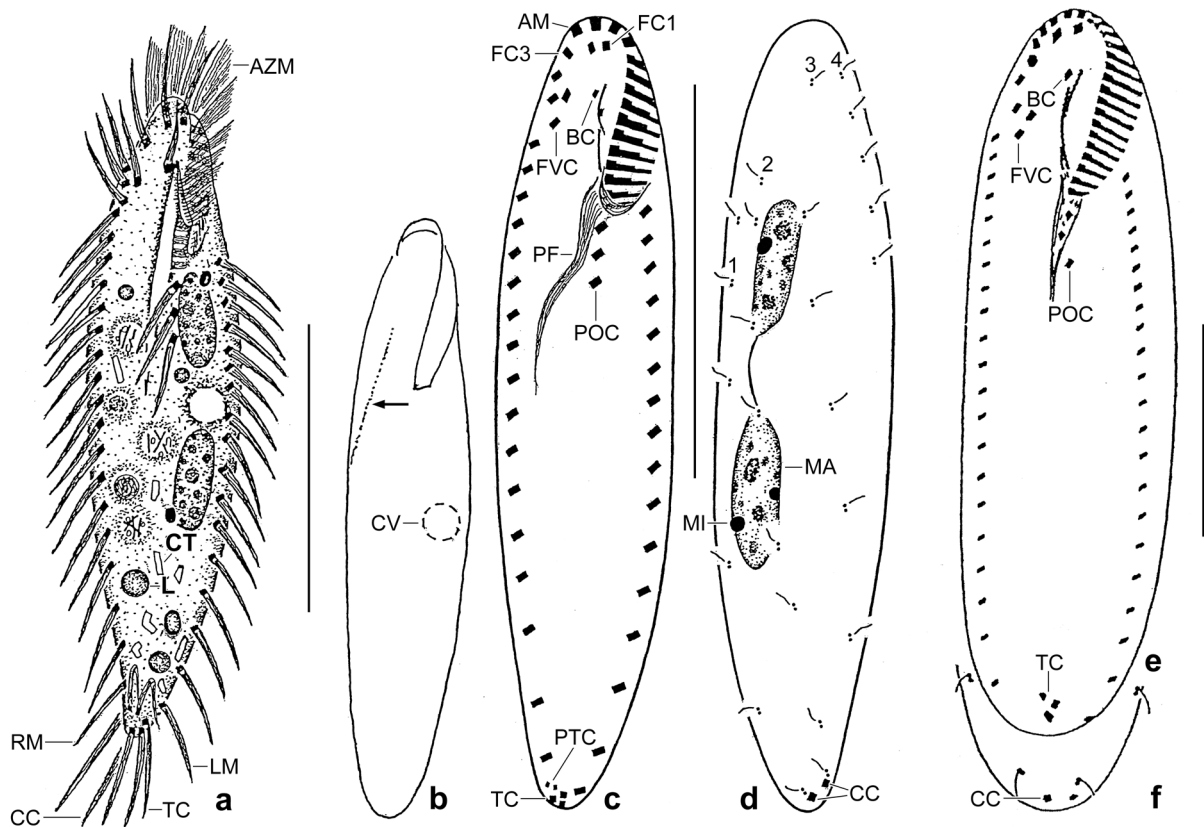


**Fig. 69a–f.** *Urosomoida bromelicola* (a–d) and *U. agiliformis* (e, f; from Foissner 1982) from life (a, b) and after protargol impregnation (c–f). **a:** Ventral view of a representative specimen. The cell has a very hyaline cytoplasm and food vacuoles. The transverse and caudal cirri form a rather conspicuous “bush” at posterior body end. **b:** Elongate ellipsoid shape variant with elevated dorsal body marked by an arrowhead. **c, d:** Ventral and dorsal view of infraciliature and nuclear apparatus of holotype specimen. Note the terminal location of the transverse cirri, the lateral location of the caudal cirri, and the wide distances between the dorsal bristles. **e, f:** Ventral and dorsal view of *U. agiliformis*, a cosmopolitan with considerable overall similarity to *U. bromelicola*. However, there are many distinct and subtle differences, e.g., body shape (elongate ellipsoid vs. very elongate pisciform or elongate ellipsoid; number (3 vs. 5) and location (subterminal vs. terminal) of the pretransverse and transverse cirri; location of cirrus III/2 (slightly posterior of middle cirrus of the frontoventral cirral row vs. left of the middle cirrus); shape of the postoral cirral row (slightly triangular vs. straight); and the wide vs. ordinary spacing of the dorsal bristles. AM – distalmost adoral membranelle, AZM – adoral zone of membranelles, BC – buccal cirrus, CC – caudal cirri, CT – crystals, CV – contractile vacuole, FC1,3 – frontal cirri, FVC – frontoventral cirri, L – lipid droplet, LM – left marginal cirral row, MA – macronuclear nodule, MI – micronucleus, PF – pharyngeal fibres, POC – postoral cirri, RM – right marginal cirral row, TC – transverse cirri, 1,2,3,4 – dorsal kineties. Scale bars 30  $\mu\text{m}$ .

***Urosomoida bromelicola* nov. spec.**

(Fig. 69a–d, 70a–j; Tables 28, 29 on p. 334, 335)

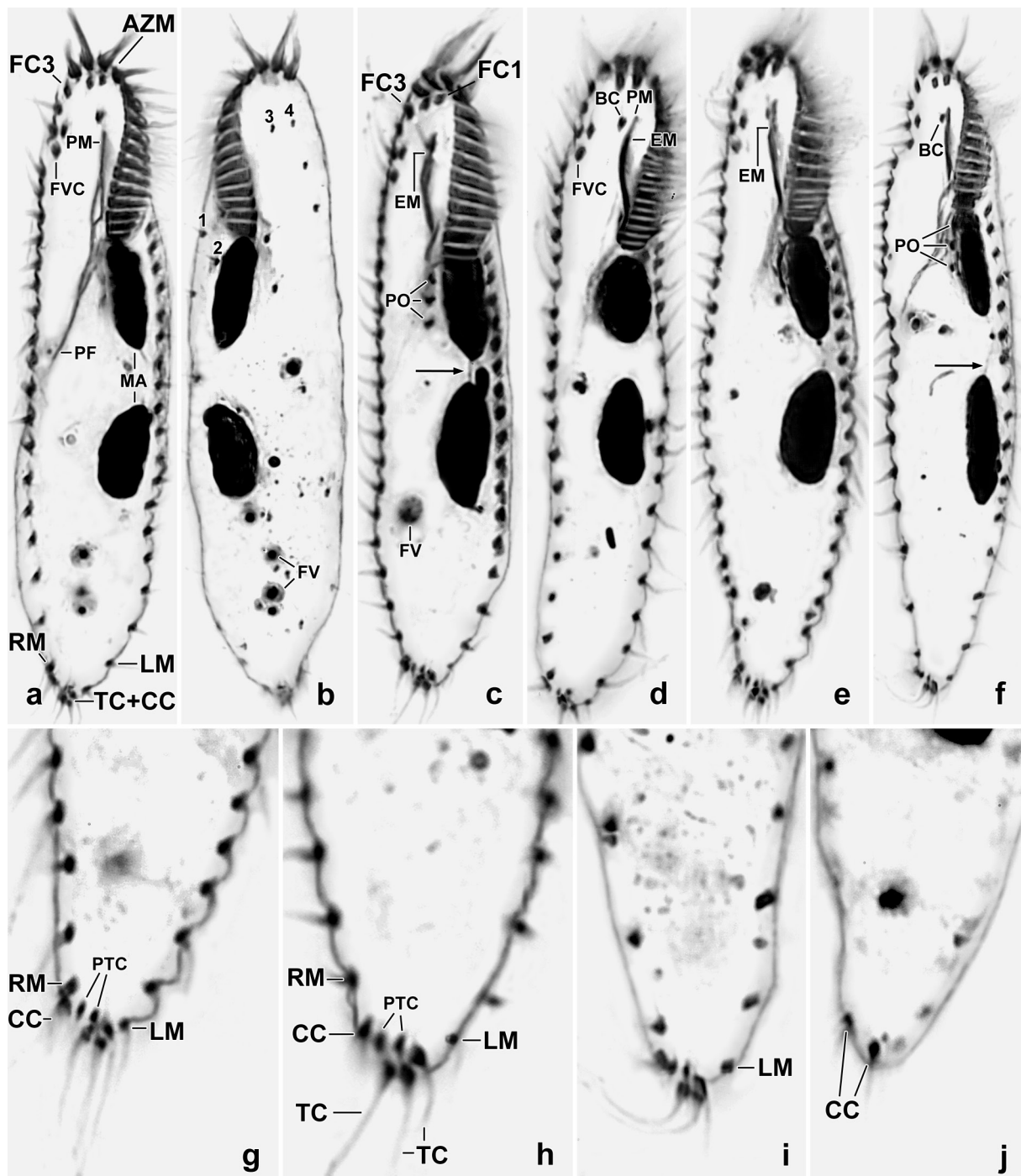
**Diagnosis:** Size in vivo about  $65 \times 15 \mu\text{m}$ . Usually indistinctly pisciform or very elongate ellipsoid, postoral portion usually cuneate because gradually narrowed posteriorly producing a narrowly rounded or bluntly acute posterior end. Two ellipsoid to elongate ellipsoid macronuclear nodules connected by a fine thread and accompanied by an average of two globular micronuclei. Buccal cirrus right of anterior end of paroral membrane; postoral cirri narrowly spaced, form a short, straight line; two fine pretransverse and three terminal transverse cirri. Four dorsal kineties including one dorsomarginal kinety; two laterally located caudal cirri. Adoral zone of membranelles extends about 27% of body length, composed of 16 membranelles on average; buccal cavity only 1–2  $\mu\text{m}$  wide but rather deep, buccal horn inconspicuous.

**Type locality:** Mud from tank bromeliads on the Pico Isabel west of the town of Puerto Plata, Dominican Republic, 19°N, 71°W.

**Type material:** Four slides with protargol-impregnated specimens have been deposited in the Biology Centre of the Upper Austrian Museum in Linz (LI). The holotype (Fig. 69c, d) and other relevant specimens have been marked by black ink circles on the coverslip. For slides, see Fig. 30a–e in Chapter 5.

**Etymology:** *Bromelicola* is a composite of the generic name *Bromus* (Bromeliaceae), the thematic vowel *-i-*, and the Latin verb *colere* (to live in), referring to the habitat the species was discovered.

**Description:** Dry mud was collected from tanks of several bromeliads and treated with the non-flooded Petri dish method (see method section).



*Urosomoida bromelicola* has low variability, i.e., most features investigated have a CV < 15% (Table 28).

Size in vivo about 50–80 × 10–17 µm, usually about 65 × 15 µm, as calculated from some in vivo measurements (Table 29) and the morphometric data in Table 28 adding 15% preparation shrinkage. Usually indistinctly pisciform or very elongate ellipsoid (length:width ratio 4.6:1 on average), postoral portion cuneate because gradually narrowed posteriorly producing a narrowly rounded or bluntly acute posterior end (Fig. 69a–c, 70a–j). Nuclear apparatus in central third of cell left of body midline; composed of two macronuclear nodules and 1–4, on average two micronuclei (Fig. 69a, d, 70a–f; Table 28). Macronuclear nodules ellipsoid to elongate ellipsoid, distinctly separate but connected by a fine thread of argyrophilic material, on average 10.0 × 3.5 µm in protargol preparations; contain many minute (≤ 0.5 µm) and some larger (up to 3 µm) nucleoli. Micronuclei attached to various sites of macronucleus, inconspicuous both in vivo and protargol preparations because only about 2.0 × 1.5 µm in size. Contractile vacuole in or slightly anterior of mid-body at left margin of cell, frequently between macronuclear nodules; without distinct collecting canals (Fig. 69a). Cortex flexible, without specific granules in vivo and in protargol preparations. Cytoplasm conspicuously hyaline, colourless, contains some 2–4 µm-sized crystals and some ellipsoid or globular lipid droplets up to 4 µm across, occur mainly in posterior third of cell. Food vacuoles 4–6 µm in diameter, usually hyaline because containing only few fine bacterial rods up to 6 µm long, rarely compact (Fig. 69a, 70b, c).

Cirral pattern and number as typical for *Urosomoida* (for reviews, see Berger 1999 and Foissner 2016); i.e., not 18 fronto-ventral-transverse cirri but only 16 because two transverse cirri are lacking (Fig. 69a, c, 70a–j; Table 28). Three, rarely only two frontal cirri, cirrus III more widely separate from cirrus II than cirrus I from II. Four frontoventral cirri forming a short row near right margin of cell, cirrus III/2 close to cirrus IV/3, i.e., to middle cirrus of row. Buccal cirrus right or slightly posterior of anterior end of paroral membrane. Postoral cirri close together, forming a short, straight row. Pretransverse cirri close to transverse cirri, fine possibly consisting of only two cilia. Transverse cirri at posterior end of body, each consisting of four cilia about 10 µm long in vivo. Pretransverse, transverse, and caudal cirri form a rather conspicuous bush at end of cell. Marginal cirri about 8 µm long in vivo, distances between cirri gradually increase in posterior third of cell while cirral size decreases. Two caudal cirri at left margin of posterior end of cell, each composed of four cilia about 12 µm long (Fig. 69a, d, 70g, j). Four dorsal kineties composed of comparatively widely spaced dikinetids each associated with an about 2 µm long bristle. Kineties 1 and 2 commence far subapically and end close to the caudal cirri, composed of an average of six and eight bristles, respectively; row 3 commences subapically and ends far subterminally, composed of an average of six bristles; row 4 commences subapically and ends in anterior third of cell, composed of an average of four bristles, originates dorsomarginally (Fig. 69d, 70b; Table 28).

Oral apparatus as typical for genus, inconspicuous because extending only about 27% of body length, on average composed of 16 ordinary membranelles with largest bases only 3–4 µm long in vivo and in protargol preparations; adoral zone of membranelles continuous, i.e., not bipartite (Fig. 69a, c, 70a–f; Table 28). Buccal cavity in vivo only 1–2 µm wide but rather deep; buccal lip

← **Fig. 70a–j.** *Urosomoida bromelicola*, ventral (a, c–i) and dorsal (b, j) views after protargol impregnation. The main features of this species are the narrowly rounded (c–e, h–j) to bluntly pointed (a, b, f, g) posterior end and the terminal location of the transverse cirri (a, c–i). The arrows in (c, f) mark a thread connecting the macronuclear nodules. Note also the lateral location of the caudal cirri (j). Figures (a, b) show the same specimen ventrally and dorsally. AZM – adoral zone of membranelles, BC – buccal cirrus, CC – caudal cirri, EM – anterior end of endoral membrane, FC1,3 – frontal cirri, FV – food vacuole, FVC – frontoventral row, LM – left marginal cirral row, MA – macronuclear nodules, PF – pharyngeal fibres, PM – paroral membrane, PO – postoral cirri, RM – right marginal cirral row, TC – transverse cirri, 1–4 – dorsal kineties. Size of specimens 45–70 µm (a–f).

of angular type, buccal horn indistinct. Undulating membranes short, paroral membrane slightly to rather distinctly curved, cilia in vivo about 3  $\mu\text{m}$  long, optically covers anterior third of endoral membrane. Pharyngeal fibres distinct in protargol preparations, extend to mid-body.

**Occurrence and ecology:** As yet found only at type locality. Became moderately abundant in the non-flooded Petri dish culture.

**Remarks:** This small species lives in a specific habitat, viz. tank bromeliads, and identification requires careful live observation and protargol preparation. The most important features of *U. bromelicola* are body shape (slender, posterior end narrowly rounded or bluntly acute), the number (two) of pretransverse cirri, and the number (three) and location (terminal) of the transverse cirri. See Table 29 of this monograph and Table 2 in Wang et al. (2016) for detailed comparisons with similar species, especially congeners some of which are now classified in different genera (Foissner 2016).

### **Bothrigidae nov. fam.**

**Diagnosis:** Dorsomarginalian hypotrichs with an ontogenetic primordium each for the oral apparatus (between buccal vertex and transverse cirri) and for the ventral cirri between right row of marginal cirri and ventral cirral rows.

**Type genus:** *Bothrix* nov. gen.

**Further genera assignable:** None, except of the type but ontogenetic data are still rare. Thus, further genera might exist.

**Remarks:** This is an outstanding ciliate well appropriate to serve as a representative of a new family. As yet, no hypotrich has been described having the diagnostic feature described. All other oxytrichids and hypotrichs generally have only one primordium, i.e., that between buccal vertex and transverse cirri (for reviews, see Berger 1999, 2006, 2008, 2011; Chen et al. 2017; Song & Shao 2017). However, there is a great number of ontogenetic patterns some resembling that of *Bothrix africana*, e.g., *Pseudoamphisiella* Song, 1996, *Paraurostyla* Borror, 1972; and often transverse cirri are absent and ventral cirral rows produce new cirri without an extra primordium (Berger 1999; Song & Shao 2017).

Very likely, there is some relationship to the genus *Territricha* Berger & Foissner, 1988, viz., the zigzagging cirri of the ventral rows and the genesis of dorsal kinecy 4 by a posterior split of kinecy 3. This applies also to the genus *Apoterritricha* Kim et al., 2014 which belongs to the Neokeronopsidae Foissner & Stoeck, 2008, according to molecular data (Kim et al. 2014).

### ***Bothrix* nov. gen.**

**Diagnosis:** Bothrigidae with semirigid cortex and zigzagging cirri in two ventral rows; buccal cirrus composed of individualized kineties; postoral cirri absent. Paroral membrane composed of zigzagging dikinetids in anterior half and of a membranoid structure in posterior half. Most dorsal kineties develop de novo.

**Type species:** *Bothrix africana* nov. spec.

**Etymology:** The genus name is a composite of *Bo* (Botswana where the genus was discovered) and the Greek noun *thrix* (hair ~ ciliate). Feminine gender.

**Species assignable:** *Bothrix africana* nov. spec.

**Remarks:** Half of the generic diagnostics are unique, viz., the structure of the buccal cirrus and of the paroral membrane. Very likely, both are apomorphies, i.e., developed in a longly undisturbed

area of South Africa. I did not find a ciliate in the literature with the characteristics of the Bothrigidae and *Bothrix*.

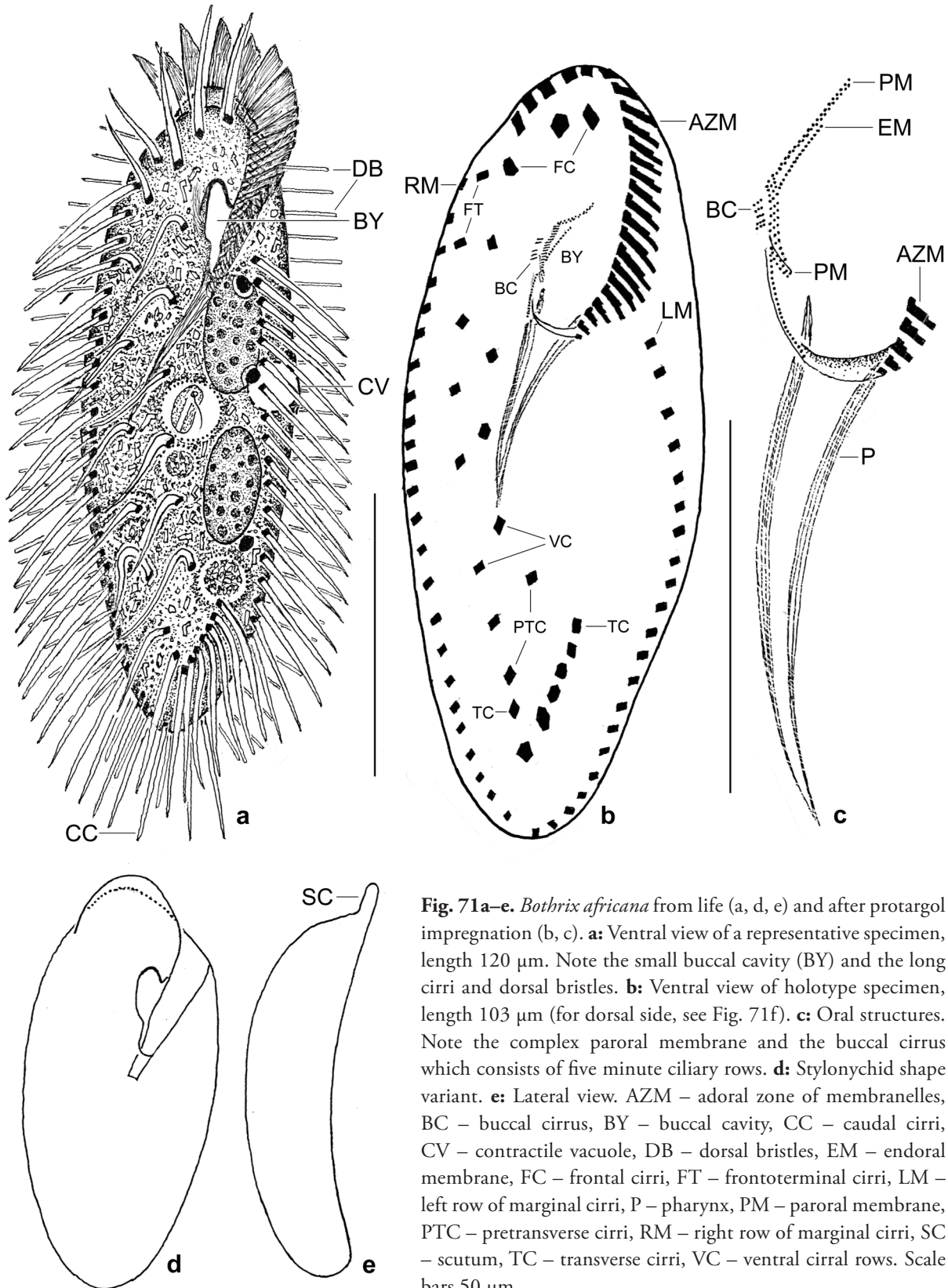


**Fig. 71a–e.** *Bothrix africana* from life (a, d, e) and after protargol impregnation (b, c). **a:** Ventral view of a representative specimen, length 120  $\mu\text{m}$ . Note the small buccal cavity (BY) and the long cirri and dorsal bristles. **b:** Ventral view of holotype specimen, length 103  $\mu\text{m}$  (for dorsal side, see Fig. 71f). **c:** Oral structures. Note the complex paroral membrane and the buccal cirrus which consists of five minute ciliary rows. **d:** Stylonychid shape variant. **e:** Lateral view. AZM – adoral zone of membranelles, BC – buccal cirrus, BY – buccal cavity, CC – caudal cirri, CV – contractile vacuole, DB – dorsal bristles, EM – endoral membrane, FC – frontal cirri, FT – frontoterminal cirri, LM – left row of marginal cirri, P – pharynx, PM – paroral membrane, PTC – pretransverse cirri, RM – right row of marginal cirri, SC – scutum, TC – transverse cirri, VC – ventral cirral rows. Scale bars 50  $\mu\text{m}$ .

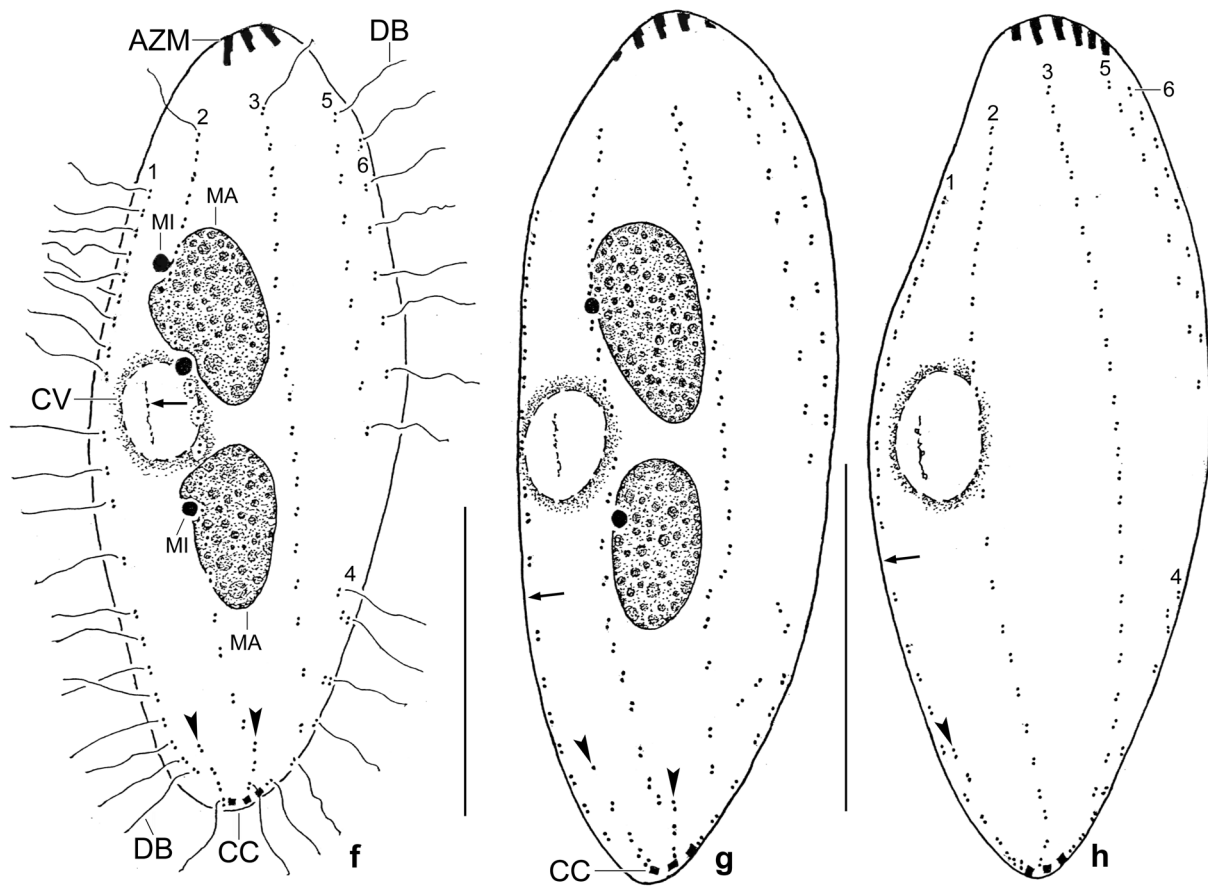


**Fig. 71f-h.** *Bothrix africana*, dorsal views after protargol impregnation. This species has six dorsal kineties, the short kinety 4 is produced by kinety 3, as common in oxytrichids. The arrowheads mark breaks in the posterior region of the kineties. **f:** Holotype, length 103  $\mu\text{m}$  (see Fig. 71b for ventral view). The arrow in (f) marks the slit-like opening of the contractile vacuole. Most specimens have three micronuclei. **g, h:** Variability. The arrows mark a one-bristle-wide gap in dorsal kinety 1. AZM – adoral zone of membranelles, CC – caudal cirri, CV – contractile vacuole, DB – dorsal bristles, MA – macronuclear nodules, MI – micronuclei, 1–6 – dorsal kineties. Scale bars 40  $\mu\text{m}$ .

***Bothrix africana* nov. spec.**

(Fig. 71a–h, 72a–w, 73a–k, 74a–h; Table 30 on p. 336)

**Diagnosis** (averages are provided): Size in vivo about 120  $\times$  45  $\mu\text{m}$ ; ellipsoid. Nuclear apparatus composed of two ellipsoid macronuclear nodules and three globular micronuclei attached to macronuclear nodules. Cortex semirigid, with minute, colourless granules recognizable only in methyl green-pyronin preparations. All cirri rather thick and long, arranged in *Territricha* pattern: three frontal cirri, one buccal cirrus, two frontoterminal cirri, five cirri each in ventral rows 1 and 2, eight distinctly subterminal transverse cirri, two pretransverse cirri, 26 cirri in right marginal row, 23 in left. Oral region inconspicuous in vivo, buccal cavity narrow and flat, anterior portion of paroral membrane very likely covered by cortex. Adoral zone extends 34% of body length, composed of 26 membranelles. Dorsal bristles up to 20  $\mu\text{m}$  long, produce four ordinary rows and two dorsomarginal rows; three caudal cirri.

**Type locality:** Soil from the flood plain of the Chobe River, Kabolebole Peninsula, Botswana, 25°S, 17°50'E.

**Type material:** The slide containing the holotype (Fig. 71b, f) and five paratype slides with protargol-impregnated morphostatic and dividing specimens have been deposited in the Biology

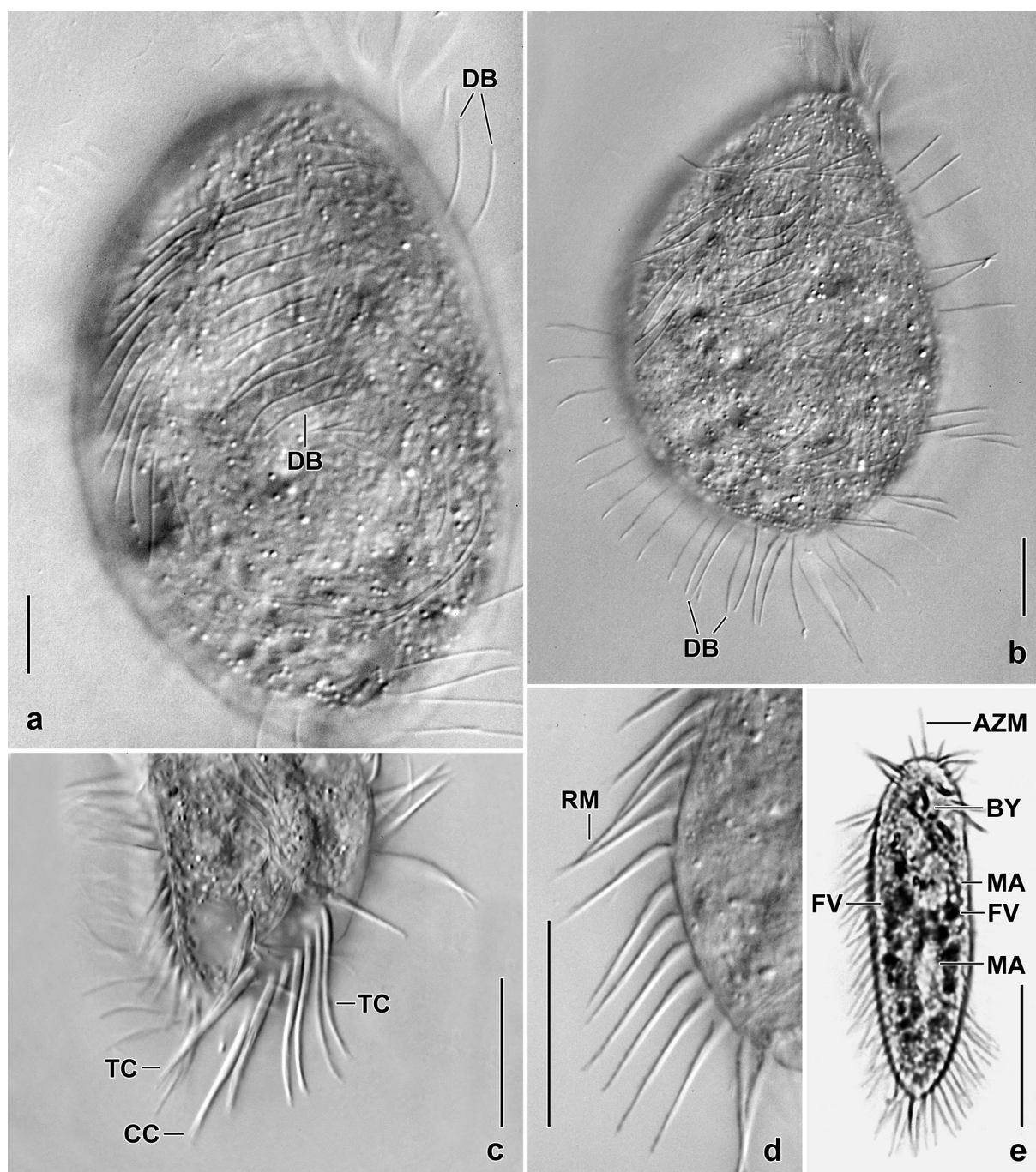


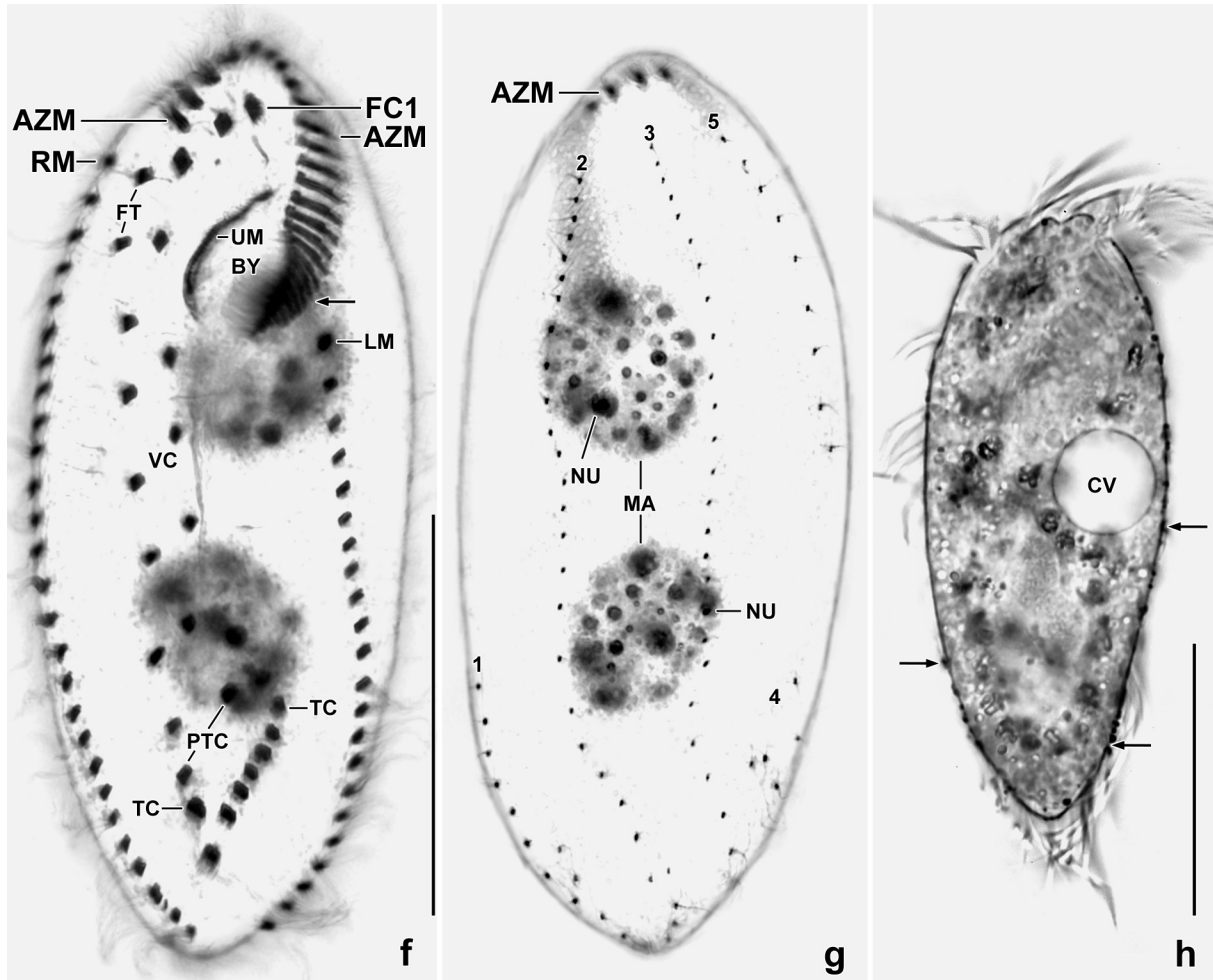
**Fig. 72a–e.** *Botbrix africana* in vivo. **a, b:** Slightly pressed (by coverslip) cells, showing the conspicuous, 10–12  $\mu\text{m}$  long dorsal bristles. **c, d:** Transverse and marginal cirri are 30  $\mu\text{m}$  and 25  $\mu\text{m}$  long, respectively; both have a thin distal third. **e:** Overview of a slender specimen, i.e., length:width ratio 3.5:1. AZM – adoral zone of membranelles, BY – buccal cavity, CC – caudal cirri, DB – dorsal bristles, FV – food vacuoles, MA – macronuclear nodules, RM – right row of marginal cirri, TC – transverse cirri. Scale bars 10  $\mu\text{m}$  (a, b), 30  $\mu\text{m}$  (c, d), and 50  $\mu\text{m}$  (e).

Centre of the Upper Austrian Museum in Linz (LI). Relevant specimens have been marked by black ink circles on the coverslip. For slides, see Fig. 31a–i in Chapter 5.

**Etymology:** Named after the continent (Africa) where it was discovered.

**Description:** Size in vivo about 105–145  $\times$  38–62  $\mu\text{m}$ , on average 120  $\times$  45  $\mu\text{m}$ , as calculated from some in vivo measurements and the morphometric data in Table 30 adding 15% preparation shrinkage. Body slenderly to bluntly ellipsoid (Fig. 71a, b, f–h, 72e–h, l, m, p, s, u; Table 30); many cells slightly narrowed posteriorly and with bluntly acute posterior end; laterally slightly to up to

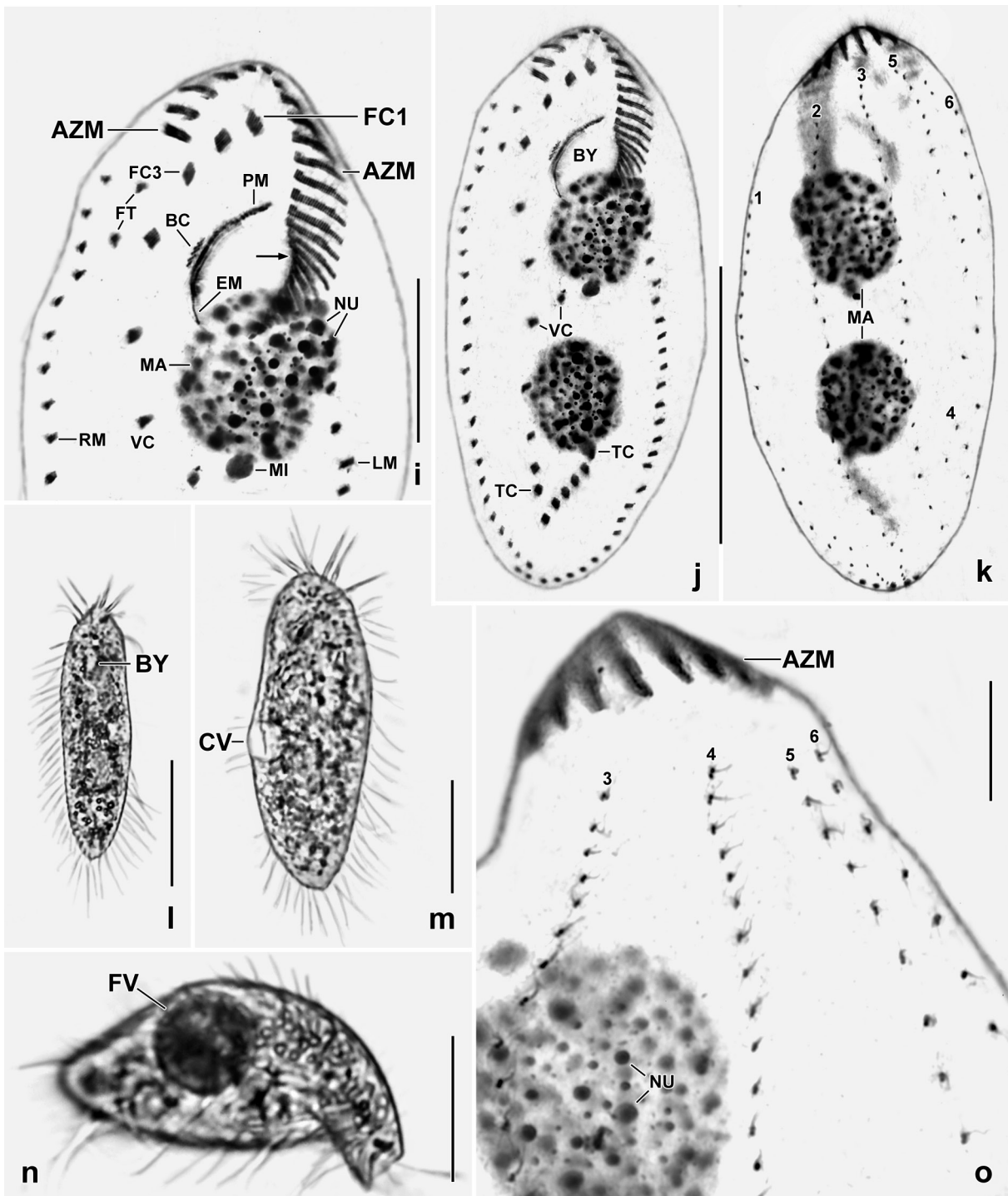
2:1 flattened, ventral side flat, dorsal convex; when feeding distinctly convex and with oral region considerably curved ventrally (Fig. 72n). Further, a stylonychid shape variant occurs (cp. Fig. 71a, e). Nuclear apparatus in central third of cell and left of body's midline (Fig. 71a, f, g, 72e, g, i–k; Table 30). Two macronuclear nodules rather close together and of similar size, in protargol preparations about  $24 \times 12 \mu\text{m}$ ; with many minute nucleoli hardly recognizable in vivo. Three, rarely only two globular micronuclei in minute concavities of macronuclear nodules, third micronucleus usually associated with anterior macronuclear nodule, in vivo about  $5 \mu\text{m}$  across. Contractile vacuole in or



**Fig. 72f–h.** *Bothrix africana* after protargol impregnation (f, g) and methyl green-pyronin staining (h). **f:** Ventral infraciliature of a specimen slightly pressed by a coverslip. The arrow marks the begin of the deepened proximal region of the adoral zone or membranelles. **g:** Dorsal view of the specimen shown in (f). *Bothrix africana* has six dorsal kineties five of which are recognizable. The short kinety 4 originates by a split of kinety 3 (see Fig. 73j). Caudal cirri out of focal plane. **h:** Minute mucocysts (?) are extruded when methyl green-pyronin is added (arrows). AZM – adoral zone of membranelles, BY – buccal cavity, CV – contractile vacuole, FT – frontoterminal cirri, LM – left row of marginal cirri, MA – macronuclear nodules, NU – nucleoli, PTC – pretransverse cirri, RM – right row of marginal cirri, TC – transverse cirri, UM – undulating membranes, VC – rows of ventral cirri, 1–5 – dorsal kineties. Scale bar  $50 \mu\text{m}$ .

**Fig. 72i–o.** *Bothrix africana* from life (l–n) and after protargol impregnation (i–k, o). **i–k:** Ventral and dorsal view of same specimen, overviews (j, k) and oral region (i) at higher magnification. The arrow in (i) marks the begin of the deepened and narrowed proximal region of the adoral zone of membranelles. **l, m:** Shape and size variability. **n:** The oral region can be curved. **o:** Dorsal view of anterior body region. AZM – adoral zone of membranelles, BC – buccal cirrus, BY – buccal cavity, CV – contractile vacuole, EM – endoral membrane, FC1,3 – frontal cirri, FT – frontoterminal cirri, FV – food vacuole, LM – left row of marginal cirri, MA – macronuclear nodules, MI – micronuclei, NU – nucleoli, PM – paroral membrane, RM – right row of marginal cirri, TC – transverse cirri, VC – rows of ventral cirri, 1–6 – dorsal kineties. Scale bars  $10 \mu\text{m}$  (o),  $20 \mu\text{m}$  (i), and  $50 \mu\text{m}$  (j–n).

near mid-body close to left cell margin; collecting canals short; contents released via a vertical slit recognizable in protargol preparations (Fig. 71a, f–h, 72h, m, p, u, 74b, c). Cortex semirigid, but clearly flexible when creeping on soil particles; specific cortical granules not recognizable in vivo but minute, slimy dots released when methyl green-pyronin is added (Fig. 72h). Cytoplasm colourless, usually studded with: up to 30 food vacuoles about 8  $\mu\text{m}$  across containing a small *Chilomonas*; some 8–12  $\mu\text{m}$ -sized food vacuoles containing a colourless euglenid (*Anisonema*?); occasionally an about 20  $\mu\text{m}$ -sized food vacuole containing a small ciliate; rather many vacuoles 3–7  $\mu\text{m}$  across each containing a single crystal; many 0.5–3.0  $\mu\text{m}$ -sized crystals sparkling under interference contrast (Fig. 71a, 72e, m, n, q, s, u). Swims fast becoming bluntly circular in transverse view, interrupted by short jumps.



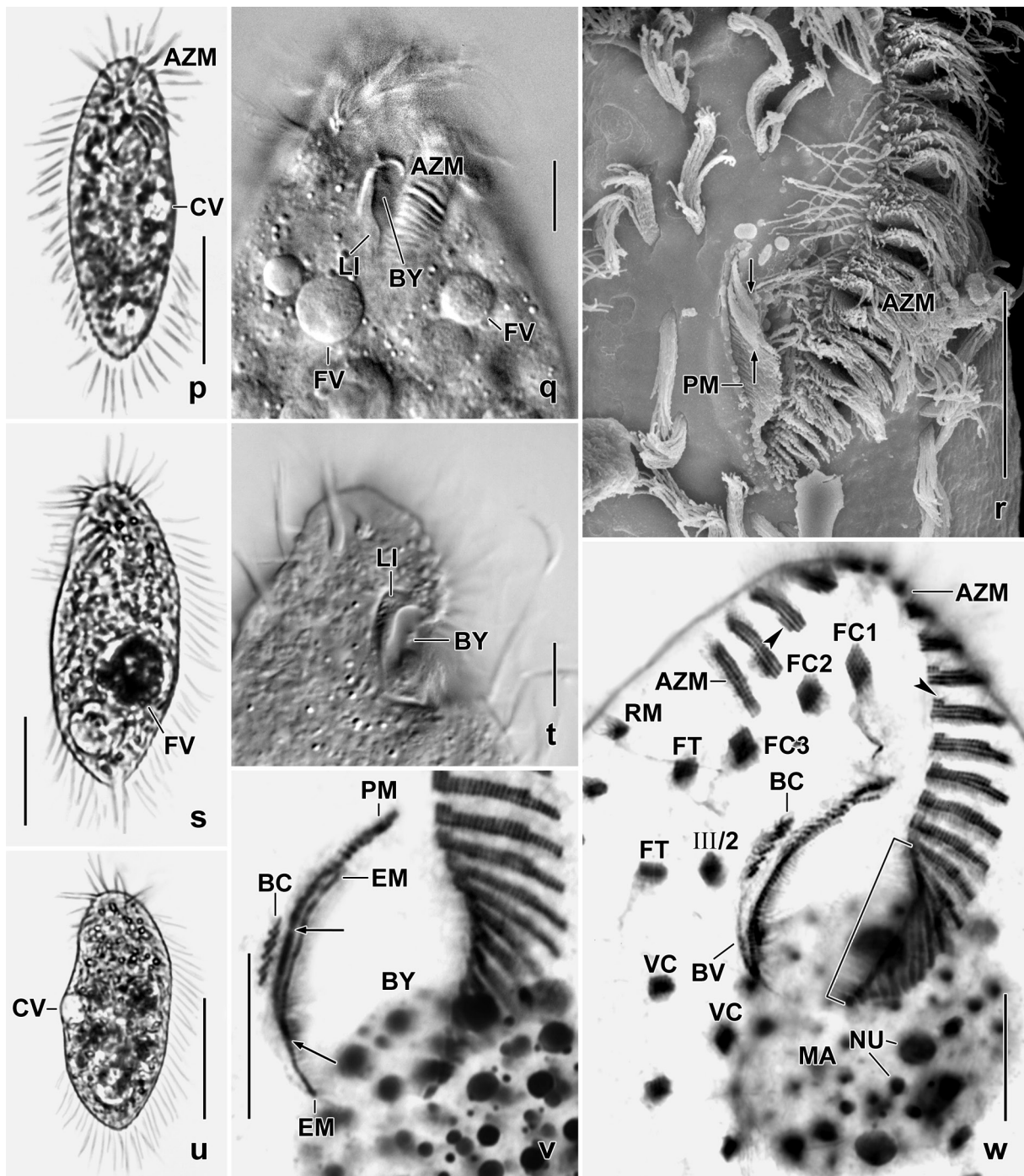


**Fig. 72p-w.** *Botrix africana* from life (p, q, s-u), in the SEM (r), and after protargol impregnation (v, w). **p, s, u:** Variability of body shape and size. **q, r, t:** Oral structures. The oral opening is very small because it is partially covered by the frontal cortex. The arrows in (r) mark the buccal cirrus composed of five minute kineties (v, w). **v, w:** Oral apparatus, showing the adoral zone of membranelles whose proximal region is distinctly narrowed and slightly upright (w, parenthesis). The arrows in (v) mark the thickened, posterior half of the paroral membrane. The arrowheads in (w) mark ciliary row 4 in the frontal and ventral adoral membranelles. AZM – adoral zone of membranelles, BC – buccal cirrus, BV – buccal vertex, BY – buccal cavity, CV – contractile vacuole, EM – endoral membrane, FC1-3 – frontal cirri, FV – food vacuole, LI – buccal lip, MA – macronuclear nodule, NU – nucleoli, PM – paroral membrane, RM – right row of marginal cirri, VC – ventral cirral rows. Scale bars 10  $\mu\text{m}$  (q, t, v, w), 20  $\mu\text{m}$  (r), and 50  $\mu\text{m}$  (p, s, u).

Somatic infraciliature dominated by the up to 30  $\mu\text{m}$  long, distinctly acute cirri and the up to 20  $\mu\text{m}$  long dorsal bristles (Fig. 71a, b, f, 72a-g, l, m, o, p, s, u; Table 30). Three thick frontal cirri, cirrus 3 (= right frontal cirrus) widely separate from cirrus 2, about 25  $\mu\text{m}$  long in vivo. Two frontoterminal

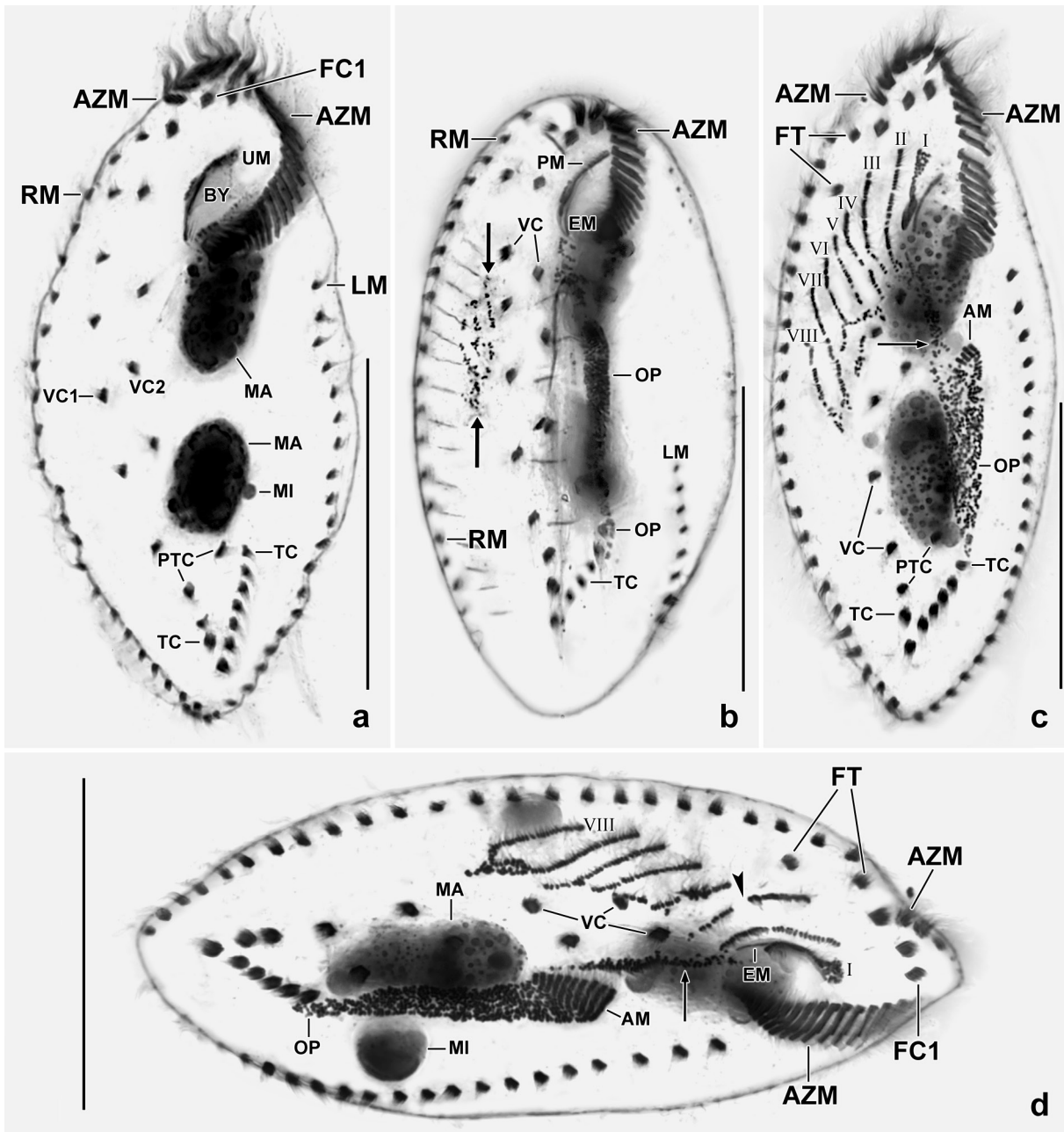


**Fig. 73a–d.** *Botrixis africana*, ventral views of a morphostatic specimen (a) and of early dividers (b–d) after protargol impregnation. **a:** A morphostatic specimen for comparison. **b:** Early divider showing the main feature of the new family Bothrigidae, viz., two “main primordia” instead of one, as is usual: first, the “oral primordium” which extends between the uppermost transverse cirri and the buccal vertex (b, OP); second, the unique “cirral primordium” between the right row of marginal cirri and ventral cirral row 1 (b, arrows). **c:** Eight (I–VIII) cirral anlagen/streaks develop from the cirral primordium, the buccal cirrus, and the upper cirri of the ventral rows. The oral primordium develops a streak of kinetids extending to the buccal vertex (arrow). **d:** Slightly later than (c). The cirral anlagen begin to divide (arrowhead), showing that they are “primary primordia”. The streak of basal bodies (arrows) increase in size and will produce the undulating membranes. In the proter, the parental undulating membrane produces a circular, anarchic field of basal bodies which will become the first frontal cirrus (Fig. 73f). The micronuclei (MI) are now much larger than in the morphostatic specimens (a). AM – adoral membranelles, AZM – adoral zone of membranelles, BY – buccal cavity, EM – endoral membrane, FC1 – first frontal cirrus, FT – frontoterminal cirri, LM – left row of marginal cirri, MA – macronuclear nodules, MI – micronuclei, OP – oral primordium, PTC – pretransverse cirri, RM – right row of marginal cirri, TC – transverse cirri, UM – undulating membranes, VC, VC1, 2 – parental ventral cirri, I–VIII – cirral anlagen. Scale bars 50  $\mu$ m.

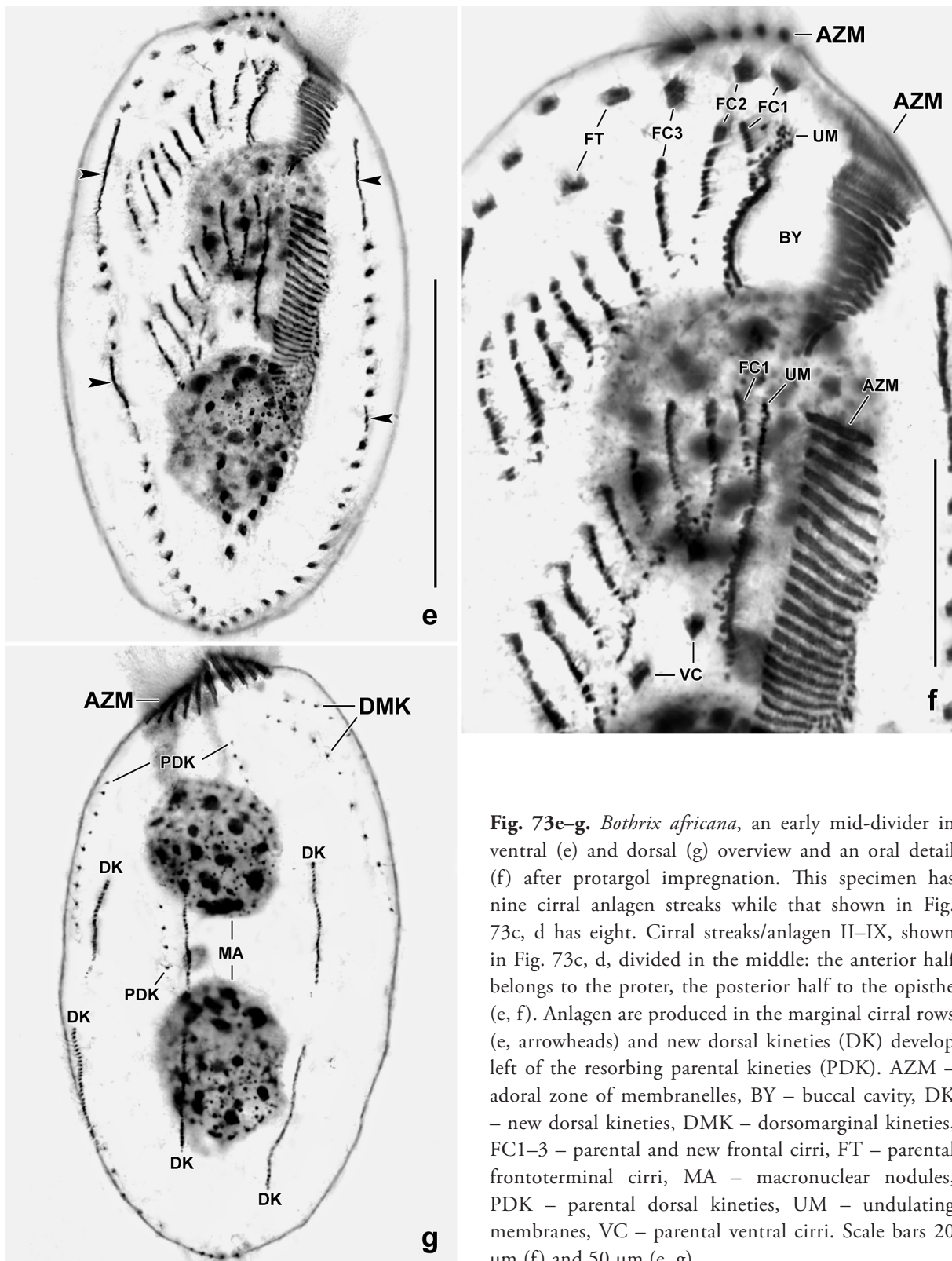


**Fig. 73e–g.** *Bothrix africana*, an early mid-divider in ventral (e) and dorsal (g) overview and an oral detail (f) after protargol impregnation. This specimen has nine cirral anlagen streaks while that shown in Fig. 73c, d has eight. Cirral streaks/anlagen II–IX, shown in Fig. 73c, d, divided in the middle: the anterior half belongs to the proter, the posterior half to the opisthe (e, f). Anlagen are produced in the marginal cirral rows (e, arrowheads) and new dorsal kineties (DK) develop left of the resorbing parental kineties (PDK). AZM – adoral zone of membranelles, BY – buccal cavity, DK – new dorsal kineties, DMK – dorsomarginal kineties, FC1–3 – parental and new frontal cirri, FT – parental frontoterminal cirri, MA – macronuclear nodules, PDK – parental dorsal kineties, UM – undulating membranes, VC – parental ventral cirri. Scale bars 20  $\mu\text{m}$  (f) and 50  $\mu\text{m}$  (e, g).

cirri in ordinary position but difficult to separate from ventral cirral row 1. Buccal cirrus at level of second third of paroral membrane, composed of 5–8 kineties distinctly separate and bearing cilia likely only about 5  $\mu\text{m}$  long (Fig. 71b, 72i, r, v, w); postoral cirri absent. Two rather widely spaced ventral cirral rows<sup>1</sup> right of body's midline, extend between buccal vertex and pretransverse cirri.

<sup>1</sup> Note by the editor H. Berger: Actually, these “ventral rows” are pseudorows (for terminology, see Berger 2008, Fig. 1d–f) because the individual cirri of each row are formed by different anlagen (Fig. 73k). *Bothrix* has, like the urostylids

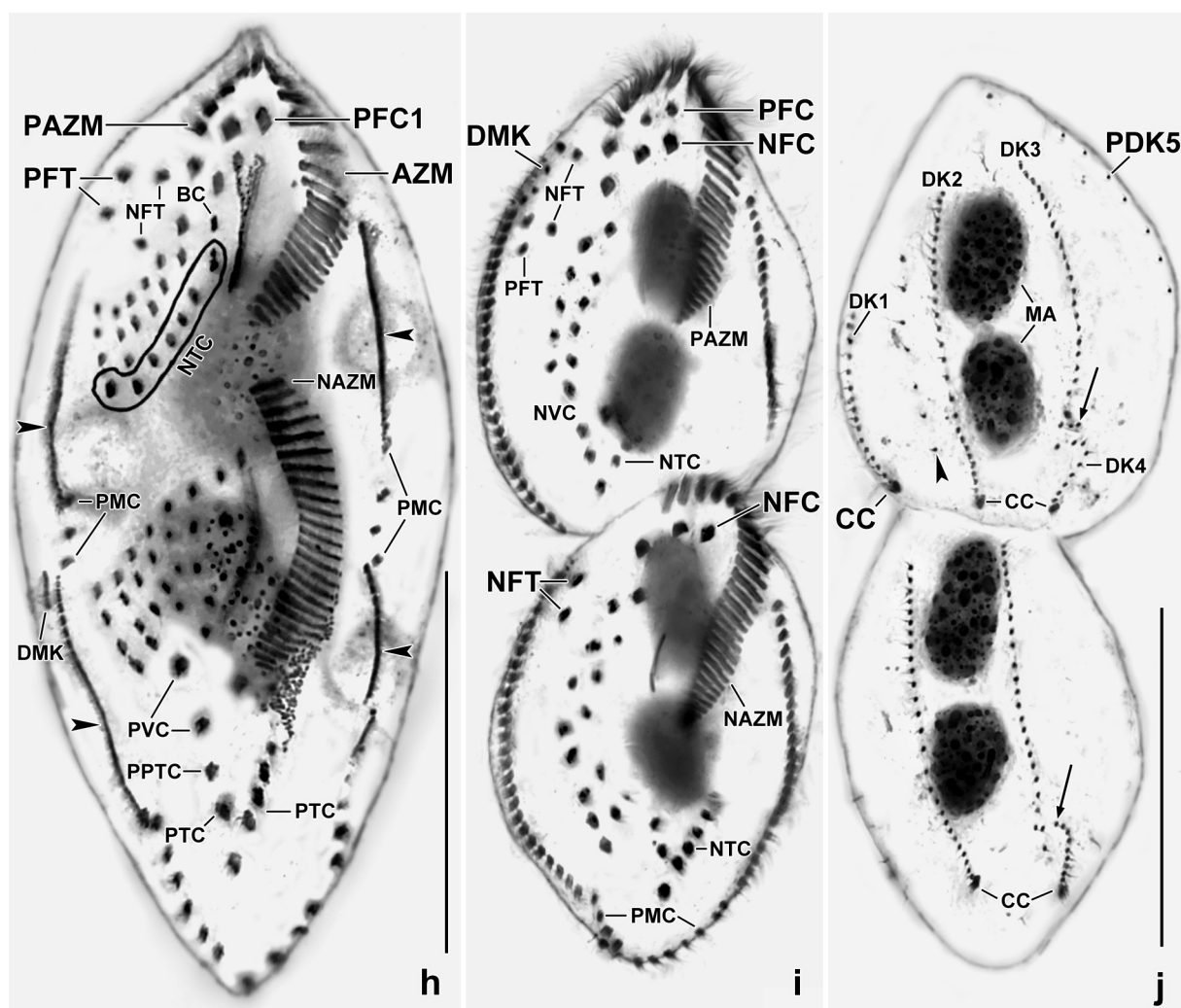


**Fig. 73h–j.** *Botbrrix africana*, ventral view of a mid-divider (h) and ventral and dorsal view of a late divider (i, j) after protargol impregnation. **h:** Very likely, a specimen just before macronuclear fusion. The cirral streaks (Fig. 73c, f) segregate the individual cirri which migrate to the species-specific sites. The arrowheads denote the fully developed anlagen for the marginal cirral rows. **i, j:** In late dividers, i.e., after the second macronuclear division, the division furrow is very distinct and the new cirri migrated to the species-specific sites; parental cirri not involved in anlagen formation, are disappearing. Both adoral zones of membranelles are complete. Three new dorsal kineties (j, DK1–3) have been produced in proter and opisthe; kinety 3 splits subterminally producing a long kinety 3 and a short kinety 4 (j, arrows). New caudal cirri have been produced at end of kineties 1, 2, 4. The arrowhead in (j) marks a resorbing dorsal kinety. AZM – adoral zone of membranelles, BC – buccal cirrus, CC – new caudal cirri, DK1–4 – new dorsal kineties, DMK – new dorsomarginal kinety, MA – macronuclear nodules, NAZM – new adoral zone of membranelles, NFC – new frontal cirri, NFT – new frontoterminal cirri, NTC – new transverse cirri, NVC – new ventral cirri, PAZM – parental adoral zone of membranelles, PDK5 – resorbing parental dorsal kinety, PFC – parental frontal cirri, PFT – parental frontoterminal cirri, PMC – parental marginal cirri, PPTC – parental pretransverse cirrus, PTC – parental transverse cirri, PVC – parental ventral cirri. Scale bars 50  $\mu\text{m}$ .

Two pretransverse cirri, posterior one difficult to separate from last cirrus of ventral row 1 and from rightmost transverse cirrus. Usually eight acute transverse cirri, posteriormost base about 10  $\mu\text{m}$  distant from rear body end, some slightly thickened, 25–30  $\mu\text{m}$  long in vivo and thus distinctly projecting from body proper. Two rows of marginal cirri almost confluent posteriorly, left row occasionally extends over right row (Fig. 72j), 20–25  $\mu\text{m}$  long in vivo (Fig. 71a, b, 72c–f, i, j, l, m, w, 73a; Table 30).

and some other taxa (e.g., the oxytrichid *Neokeronopsis*), a so-called midventral complex (for explanation, see Berger 2006, Fig. 1a), which is, in the present genus, composed of cirral pairs only.

Six dorsal kineties of ordinary structure, rows 1 to 3 commence rather far subapical, one bristle lacking in row 1 subterminally (Fig. 71g, h), short kinety fragments in posterior region; row 4 ends at level of posterior macronuclear nodule, anterior portion usually with scattered bristles; rows 5 and 6 extend dorsomarginally to mid-body. Bristles conspicuous because rod-shaped and 15–20  $\mu\text{m}$

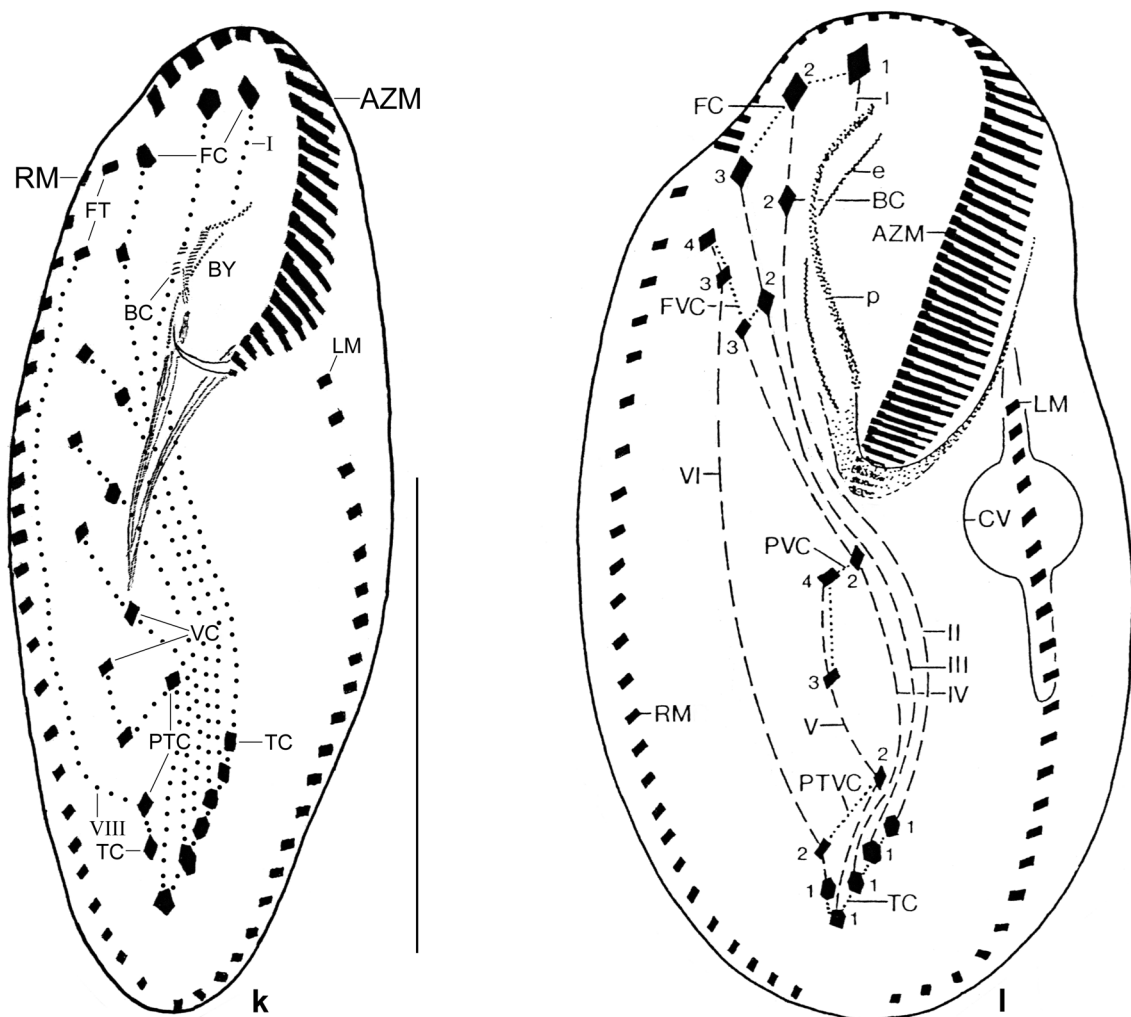
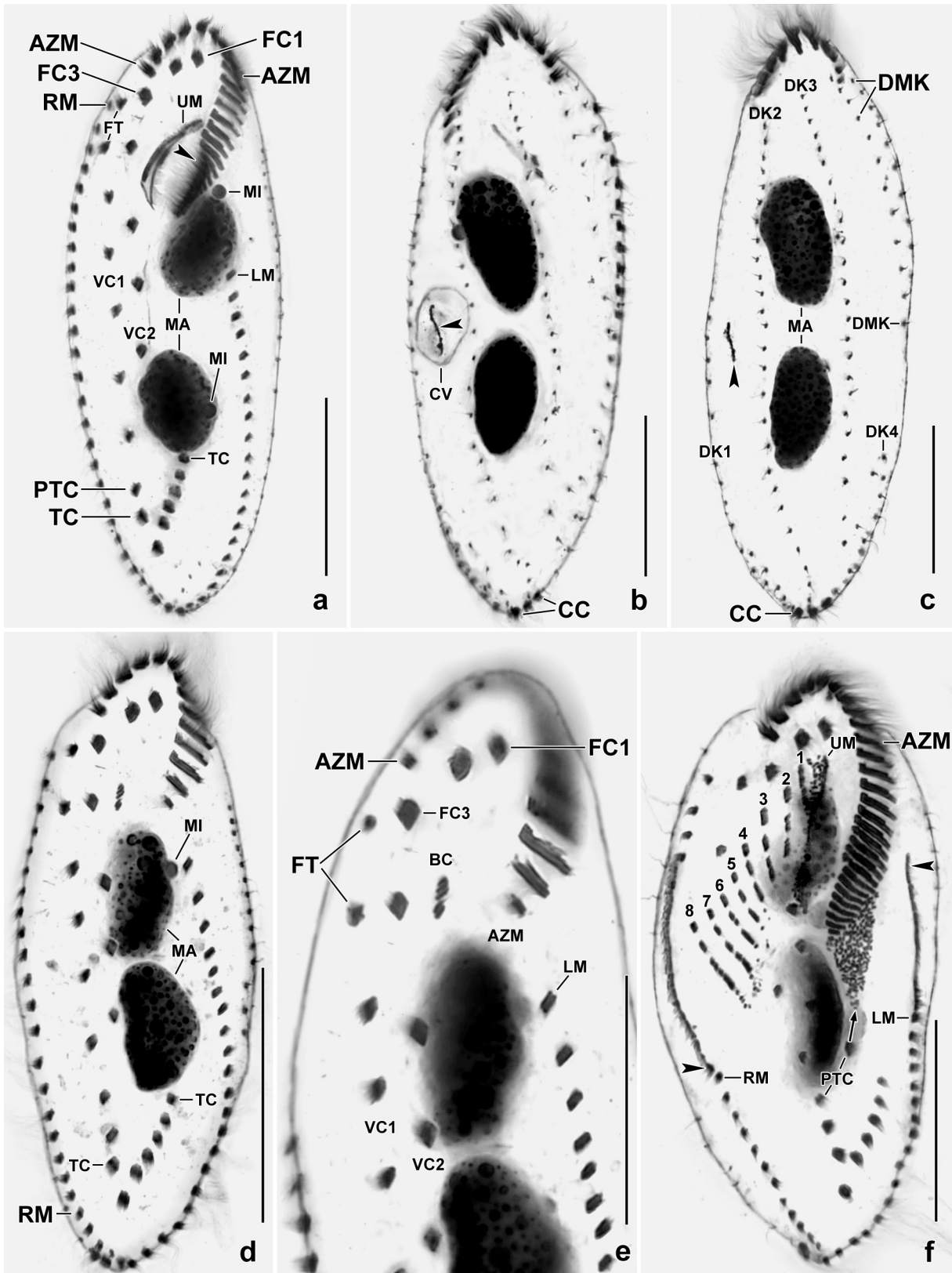


**Fig. 73k, l.** Oxytrichid cirral migration in *Bothrix africana* (k, see also Fig. 73b) and *Sterkiella cavicola* (l, from Berger 1999, slightly modified). In *Bothrix*, cirri originating from the same anlage are connected by dotted lines. In *Sterkiella*, broken lines connect cirri developing from the same streak while dotted lines connect cirri forming more or less typical groups, e.g., transverse cirri. Roman numerals mark anlagen streaks, Latin numerals denote cirri within streaks. AZM – parental adoral zone of membranelles, BC – buccal cirrus, BY – buccal cavity, CV – contractile vacuole, e – endoral membrane, FC – frontal cirri, FVC – frontoventral cirri, FT – frontoterminal cirri, LM – left row of marginal cirri, p – paroral membrane, PTC – pretransverse cirri, PVC – postoral ventral cirri, RM – right row of marginal cirri, TC – transverse cirri.

**Fig. 74a–f.** *Bothrix africana*, morphostatic (a–c) and reorganizing (d–f) specimens after protargol impregnation. **a:** → Ventral view of a morphostatic cell for comparison with reorganizing specimens (d–f). The arrowhead marks the region where the adoral zone of membranelles becomes spiralized. **b, c:** Dorsal views, showing the slit-like opening of the contractile vacuole (arrowheads) and two dorsomarginal kineties. The caudal cirri are slightly right of (b) or in (c) body midline. **d, e:** An early reorganizer that lost the proximal portion of the adoral zone of membranelles and the undulating membranes while the buccal and frontal cirri are preserved. **f:** An early mid-reorganizer with eight cirral anlagen (numerals), reorganizing marginal cirral rows (arrowheads), and an anarchic field of basal bodies (arrow) in the proximal region of the adoral zone of membranelles. AZM – adoral zone of membranelles, BC – buccal cirrus, CC – caudal cirri, CV – contractile vacuole, DK1–4 – dorsal kineties, DMK – dorsomarginal kineties, FC1–3 – frontal cirri, FT – frontoterminal cirri, LM – left row of marginal cirri, MA – macronuclear nodules, MI – micronuclei, PTC – pretransverse cirri, RM – right row of marginal cirri, TC – transverse cirri, UM – undulating membranes, VC1, 2 – rows of ventral cirri. Scale bars 30  $\mu\text{m}$  (a–c, e, f) and 50  $\mu\text{m}$  (d).

long in vivo. Three caudal cirri right of posterior pole centre, 25–30  $\mu\text{m}$  long in vivo (Fig. 71a, f–h, 72a, b, g, k, o).

Oral apparatus slightly depressed, i.e., post-orally higher than orally, extends 34% of body length on average in protargol preparations. Adoral zone of ordinary shape and structure, composed of 25–28 membranelles, largest membranelar bases about 7  $\mu\text{m}$  long, 5–8 membranelles upright in proximal region of zone. Buccal cavity narrow and rather flat, opening conspicuously small



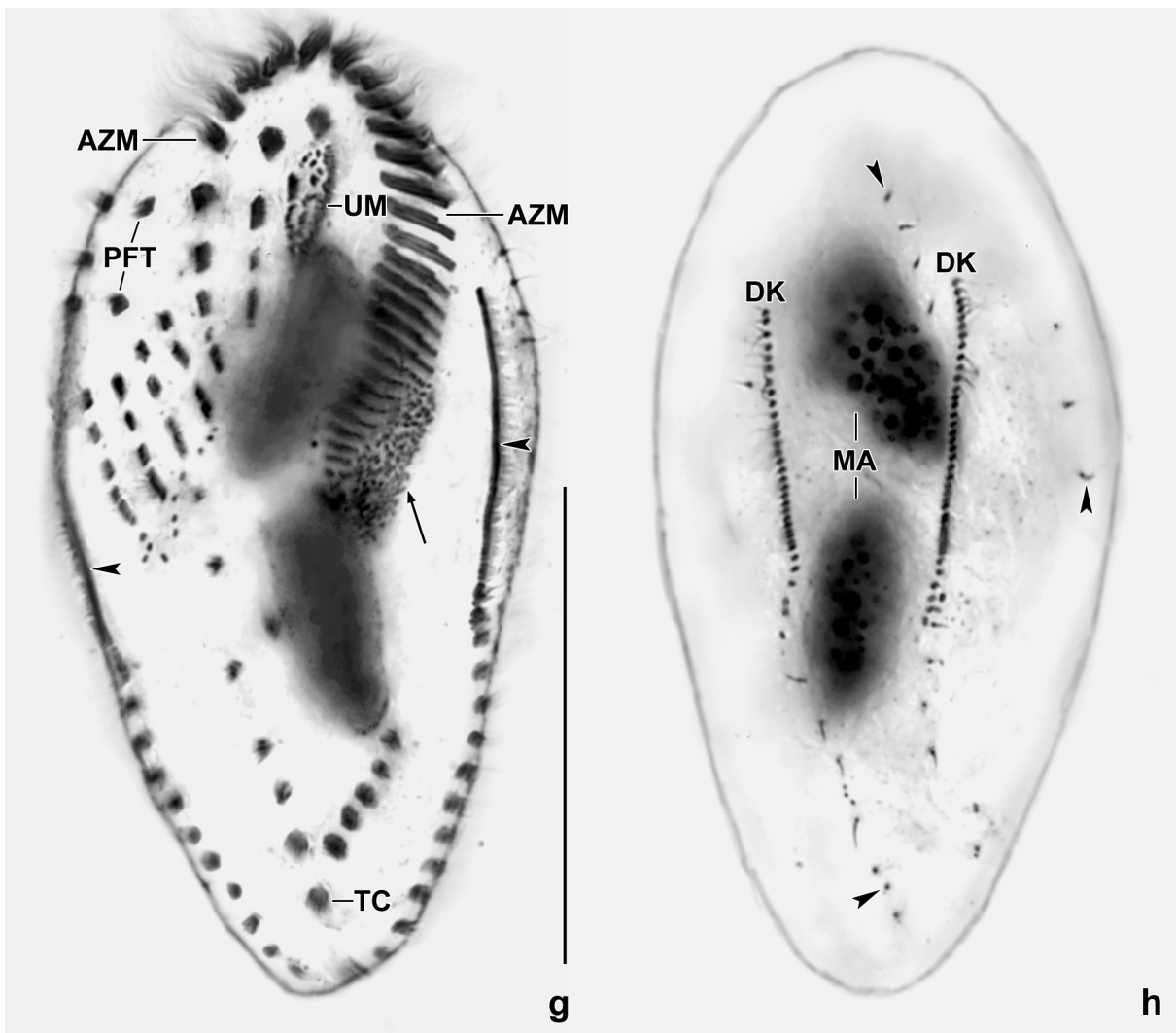


**Fig. 74g, h.** *Bothrix africana*, ventral and dorsal view of an early mid-reorganizer after protargol impregnation. **g:** Similar to the specimen shown in Fig. 74f but cirral segregation more pronounced. The arrowheads mark the primordia for the marginal cirral rows. The arrow denotes an anarchic field of basal bodies in the proximal region of the adoral zone of membranelles. **h:** The dorsal kineties have been reorganized. The arrowheads mark resorbing parental dorsal kineties. Only two of the three new dorsal kineties are recognizable. AZM – adoral zone of membranelles, DK – new dorsal kineties two and three, MA – macronuclear nodules, PFT – parental frontoterminal cirri, TC – transverse cirri, UM – undulating membranes. Scale bar 50  $\mu\text{m}$ .

compared to body size, i.e., about  $20 \times 10 \mu\text{m}$  in vivo, bracket-shaped because suddenly narrowed in posterior third (Fig. 71a–c, 72e, f, i, j, l, n, p–r, t, v, w, 74a; Table 30). Paroral membrane longer than endoral membrane anteriorly, ends far away from buccal vertex, rather distinctly curved, bipartite, i.e., anterior half composed of zigzagging dikinetids, very likely covered by frontal cortex; posterior half extends to mid of buccal cavity, composed of minute, oblique kineties with three basal bodies each, proximal portion turned by about  $180^\circ$ . Endoral membrane curved, commences posterior of paroral and extends to buccal vertex. Pharyngeal fibres extend slightly obliquely to mid-body, usually faintly impregnated (Fig. 71a–c, 72r, v, w; Table 30).

**Occurrence and ecology:** As yet found only at type locality. Can make resting cysts (unfortunately not studied) because the soil was dry when collected. This was a very rich sample containing about 100 species many of which were undescribed. Very likely, hundreds of further species exist in the flood plain and in the “green river bed”.

**Remarks:** This species is easily recognizable by the long dorsal bristles; the long, acute cirri; the small oral opening; the body size; and the nuclear apparatus. Although there are rather many hypotrichs with long dorsal bristles, most are smaller than 100  $\mu\text{m}$  and have only one micronucleus in between the macronuclear nodules (for reviews, see Berger 1999 and Kahl 1932). I could not find a described ciliate with the key features of *Bothrix africana*.

**Ontogenesis:** The protargol preparations contain sufficient dividers to follow the process. *Bothrix* is unique in that there are two primordia, one for the oral apparatus and another for most frontoventral cirri. However, basically it is an oxytrichid ontogenesis, especially on the dorsal side (Fig. 73k, l).

**Oral primordium:** A long anarchic field of basal bodies develops between mid-body and the upper left transverse cirri (Fig. 73b–d). Concomitantly, a very narrow streak of basal bodies projects from the right margin of the oral primordium and extends to the buccal vertex. Further, a club-shaped anlage I is generated in the proter, very likely by the anterior half of the undulating membranes and perhaps also by the streak of basal bodies of the opisthe oral primordium (Fig. 73c, d). Later, an anlage for new undulating membranes is recognizable in proter and opisthe (Fig. 73e, f, h). Concomitantly, new adoral membranelles are generated in the oral primordium of the opisthe while the parental adoral zone of membranelles is completely maintained (Fig. 73c–f, h). Further, a new frontal cirrus 1 is produced by the club-shaped anarchic field of basal bodies in the proter and by the anlage for the undulating membranes in the opisthe (Fig. 73e, f, h). When the cirri are migrating, new undulating membranes are recognizable in proter and opisthe (Fig. 73i).

**Cirral primordium:** This develops slightly anterior of mid-body between the right row of marginal cirri and the right row of ventral cirri (Fig. 73b). Soon, eight or nine long cirral anlagen streaks develop in the proter (Fig. 73c, d). These long streaks are primary primordia that divide in the mid: the anterior half develops to proter cirri, the posterior half produces the opisthe cirri (Fig. 73e, f). Next, cirri develop in the anlagen streaks (Fig. 73b) which then migrate to the species-specific sites (Fig. 73i).

**Marginal cirri and nuclear apparatus:** When the cirral anlagen have been divided, four anlagen are generated for new marginal cirral rows (Fig. 73e, f). Next, the dorsomarginal kineties are produced in the anlagen for the right marginal cirral row (Fig. 73h, i). Nuclear division commences after the production of dorsomarginal kineties (Fig. 73h–j). All these processes are highly similar to those occurring in typical oxytrichids (for a review, see Berger 1999).

**Dorsal infraciliature:** In most oxytrichids and in the type species *Oxytricha granulifera* Foissner & Adam, 1983 the dorsal bristle rows (kineties) originate within the parental kineties (for a review, see Berger 1999). In *Bothrix*, most dorsal kineties develop de novo, i.e., distinctly right of the parental kineties (Fig. 73g, j). In contrast, bristle row 4 is produced as in typical oxytrichids, viz., by terminal segregation of row 3 (Fig. 73j). Caudal cirri develop at posterior end of kineties 1, 2, 4 (Fig. 73j).

**Physiological reorganization:** Three stages were found. First, the proximal, upright portion of the adoral zone of membranelles is resorbed (Fig. 74a, d, e). Then, anlagen are produced for new rows of marginal cirri, the buccal cirrus is resorbed, and eight cirral anlagen streaks are generated. Further, an anarchic field of basal bodies appears in the proximal region of the adoral zone of membranelles (Fig. 74f, g). Dorsally, three new kineties develop right of the parental rows (Fig. 74h) and parental cirri are resorbed ventrally (Fig. 74f, g).

### *Mixophrya* nov. gen.

**Diagnosis:** Large (length usually  $>150 \mu\text{m}$ ), flexible Oxytrichidae with *Oxytricha* cirral pattern (18 fronto-ventral-transverse cirri) and urosomoid dorsal ciliature. Cortex likely semirigid. Oral apparatus stylonychid in vivo, i.e., with short and flat buccal cavity and short undulating membranes

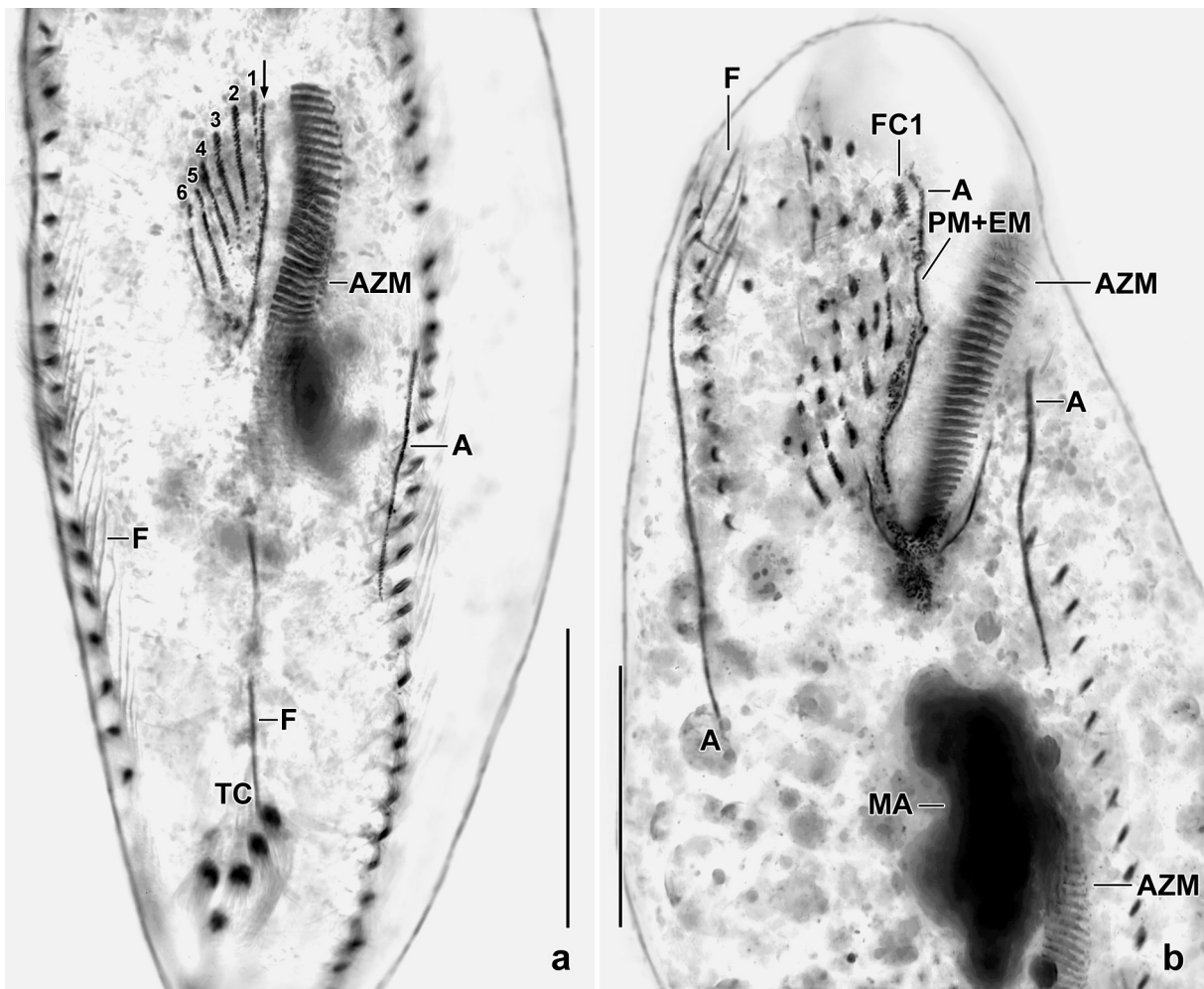


**Fig. 75a, b.** *Mixophrya pantanalensis*, ventral views of dividers after protargol impregnation. **a:** An early opisthe mid-divider, showing six (1–6) anlagen for the production of the fronto-ventral-transverse cirri. The arrow denotes the anlage for the undulating membranes. **b:** A proter mid-divider, showing the formation of cirri in the six anlagen. A – anlagen for the marginal cirral rows, AZM – adoral zone of membranelles, F – fibres, FC1 – new frontal cirrus 1, MA – macronucleus, PM + EM – anlage for the paroral and endoral membrane, TC – transverse cirri. Scale bars 40  $\mu\text{m}$  (a) and 50  $\mu\text{m}$  (b). Note by H. Berger to Fig. 75a–f: Subspecies (*M. pantanalensis pantanalensis* or *M. pantanalensis australiensis*) not indicated by W. Foissner.

in *Oxytricha* pattern; adoral zone of membranelles indistinctly gonostomatid, membranelles narrow compared to body size, i.e., about 12% of body width. Dorsal kineties 1–3 divide without fragmentation; kineties 4–7 originate dorsomarginally. Wall of resting cyst smooth, covered by a voluminous slime formation.

**Type species:** *Mixophrya pantanalensis* nov. spec.

**Etymology:** *Mixophrya* is a composite of the Greek noun *mix* (mingled) and *ophrya* (eyebrow ~ cilia ~ ciliate s.l.) meaning a ciliate group comprising features from two genera, viz., *Oxytricha* and *Urosoma*. Feminine gender.

**Species assignable:** *Mixophrya pantanalensis* nov. spec. with two subspecies, namely, *Mixophrya pantanalensis pantanalensis* nov. sspec.;  $\rightarrow$  *Mixophrya pantanalensis australiensis* nov. ssp.; *Mixophrya gigantea* (Horváth, 1933) nov. comb. (original combination: *Oxytricha gigantea* Horváth, 1933, as redescribed by Berger & Foissner 1987).

Possibly, several large *Oxytricha* species belong to *Mixophrya*, e.g., *Oxytricha longissima* Dragesco & Njine, 1971 and *Oxytricha fallax* Stein, 1859.

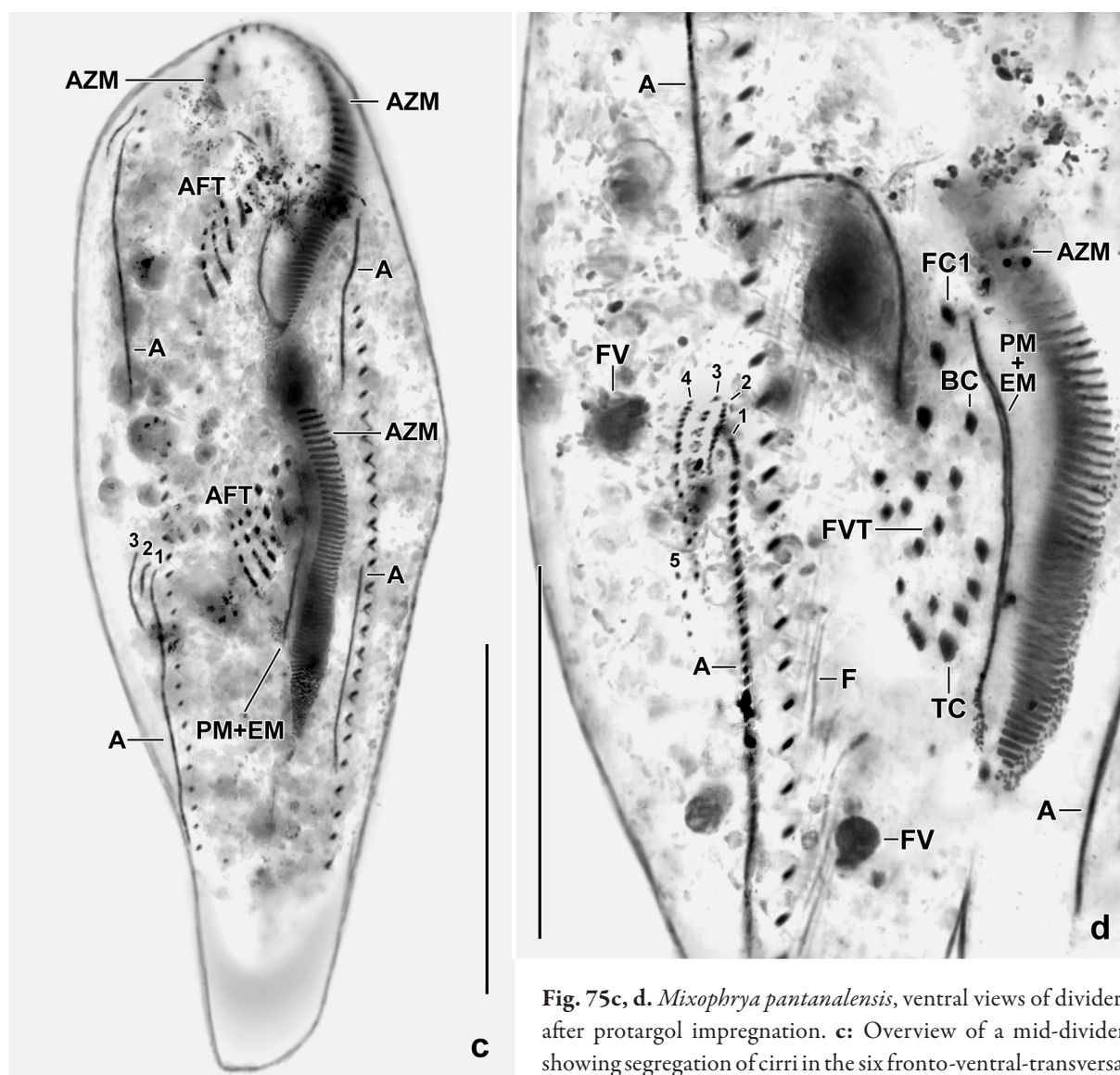
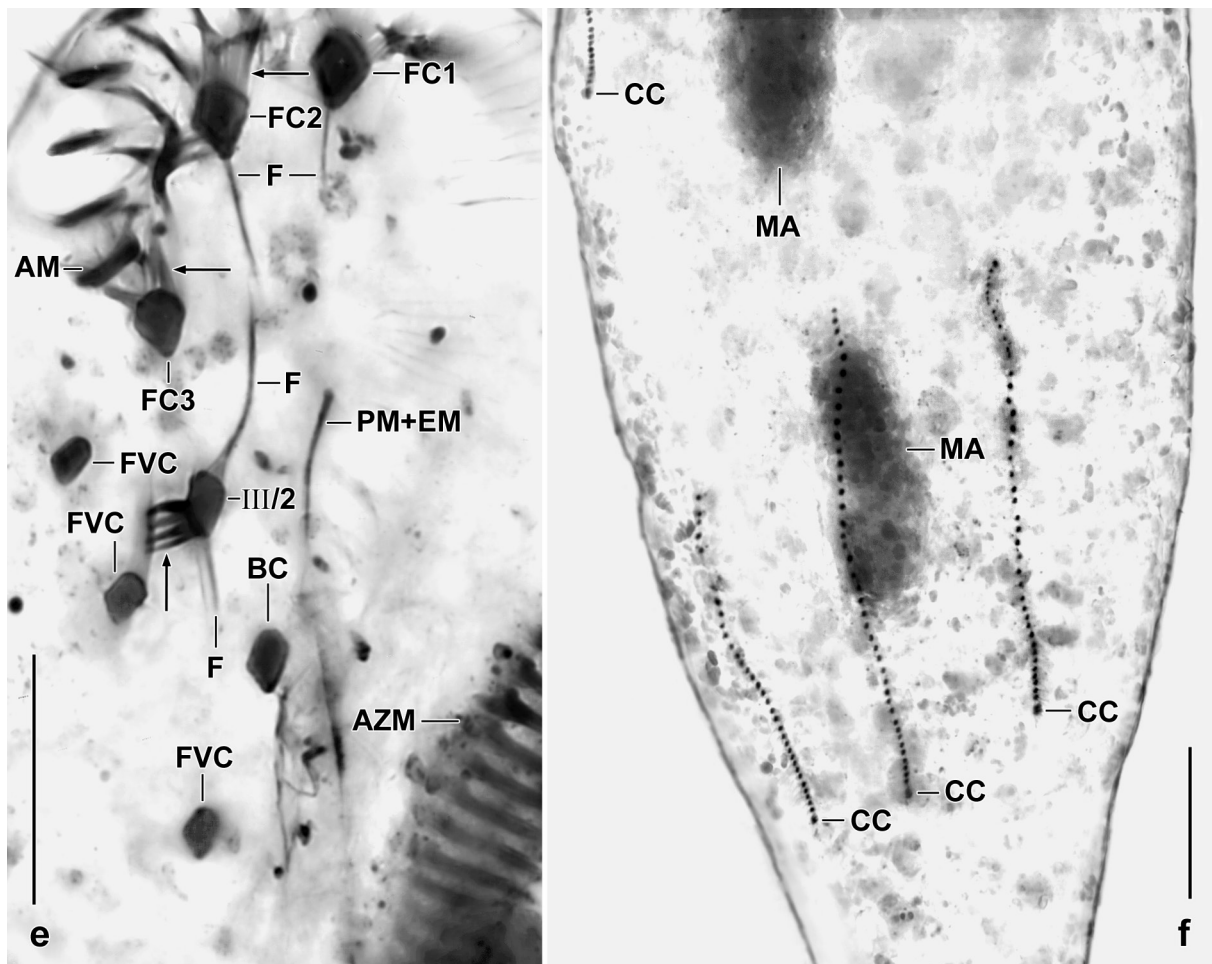


Fig. 75c, d. *Mixophrya pantanalensis*, ventral views of dividers after protargol impregnation. **c**: Overview of a mid-divider, showing segregation of cirri in the six fronto-ventral-transverse cirral anlagen each in proter and opisthe as well as four anlagen

for the new marginal cirral rows. Further, three anlagen (1–3) for dorsomarginal kineties are recognizable. **d**: Opisthe of a late mid-divider, showing cirral migration, the separating undulating membranes, the almost finished adoral zone of membranelles, and five (1–5) anlagen for dorsomarginal kineties; possibly kinety 5 is added to kinety 4 in late dividers. Cirri are generated in the anlagen for the new marginal rows in proter and opisthe. A – anlagen, AFT – anlagen for the fronto-ventral-transverse cirri, AZM – adoral zone of membranelles, BC – buccal cirrus, F – fibres, FC1 – frontal cirrus 1, FV – food vacuoles, FVC – frontoventral cirri, PM + EM – anlage for the undulating membranes, i.e., paroral and endoral membrane, TC – new transverse cirri. Scale bars 50  $\mu$ m.

**Remarks:** Most flexible *Oxytricha* species are medium-sized, i.e., are smaller than  $130 \times 40 \mu$ m in protargol preparations. Here, I report on some large (in vivo up to  $370 \times 115 \mu$ m on average) oxytrichids from Australia, Brazil, and tank bromeliads in Mexico. The main characteristics of these species are compared in Table 31.

The new genus *Mixophrya* has an *Oxytricha* cirral pattern while the dorsal bristles are arranged as in *Urosoma*. This is shown by ontogenetic data (Fig. 75a–d, f, 78h–k, m): there are six cirral anlagen that produce 18 fronto-ventral-transverse cirri, and the posterior postoral cirrus does not form an anlage, as in *Stylonychia* (Fig. 78i, j). Further stylonychid features are the rather rigid cortex, the flat and rather narrow buccal cavity, and an indistinct frontal plate due to the short undulating membranes. The dorsal bristle pattern is as simple as in the oxytrichid *Urosoma*, i.e.,



**Fig. 75e, f.** *Mixophrya pantanalensis*, after protargol impregnation. **e:** High magnification of the right anterior quadrant of a morphostatic specimen, showing cirrus III/2 associated with four thick, short fibres (arrow); similar fibres (arrow) are associated with the three frontal cirri (arrows). Cirrus III/2 forms the *Urosoma* pattern when the three other frontoventral cirri are located more posteriorly. **f:** Dorsal view of a late mid-divider, showing three new kineties with fully formed caudal cirri each consisting of four basal bodies. AM – distalmost adoral membranelle, AZM – adoral zone of membranelles, BC – buccal cirrus, CC – caudal cirri, F – fibres, FC1–3 – frontal cirri, FVC – frontoventral cirri, MA – macronuclear nodules, PM + EM – paroral and endoral membrane. Scale bars 20  $\mu\text{m}$ .

kinety fragmentation is absent. This curious mixture of oxytrichid and stylonychid features justifies the new genus *Mixophrya*.<sup>1</sup>

***Mixophrya pantanalensis* nov. spec.**

(Fig. 75a–f, 76a–i, 77a–u, 78a–m, 79a–e, 80a–n; Tables 31, 32 on p. 337)

**Diagnosis:** Size in vivo about  $370 \times 115 \mu\text{m}$  or  $280 \times 80 \mu\text{m}$ . Body usually broadly clavate. Two distinctly separated elongate ellipsoid or ellipsoid macronuclear nodules and an average of four or three globular micronuclei. Cortical granules in loose rows, sharp-yellowish or bright-citrine,  $0.2\text{--}0.3 \mu\text{m}$  across. Cytoplasm with an average of six conspicuous lithosomes  $6\text{--}11 \mu\text{m}$  across, or lithosomes absent. Buccal cirrus distinctly subapical or subapical of paroral membrane. Five thickened transverse cirri about  $37 \mu\text{m}$  or  $30 \mu\text{m}$  anterior of posterior body end; two fine pretransverse cirri.

<sup>1</sup> Note by H. Berger: W. Foissner found a similar species, likely belonging to *Mixophrya*, in Botswana. According to my terminology, species without kinety 4 fragmentation do not belong to the oxytrichids (see Berger 2008, p. 46).

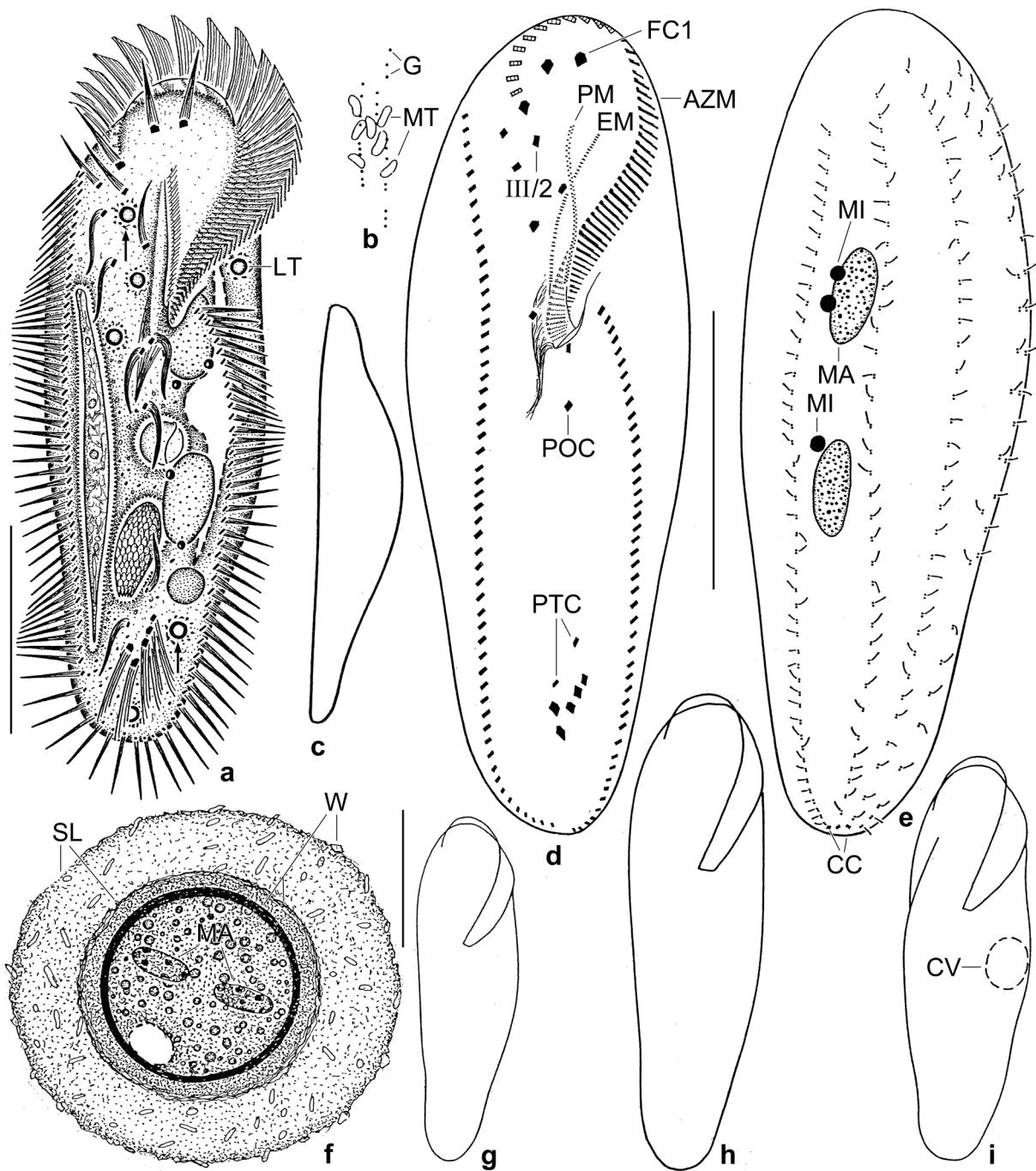


**Fig. 76a-i.** *Mixophrya pantanalensis pantanalensis* from life (a-c, f-i) and after protargol impregnation (d, e). **a:** Ventral view of a representative specimen moderately narrowed posteriorly. It fed on *Chlorogonium*, testate amoeba, and heterotrophic flagellates. The arrows mark some lithosomes. **b:** Cortical granulation. **c:** Lateral view, showing the convex dorsal side. **d, e:** Infra-ciliature of ventral and dorsal side. Note the fine caudal cirri which are not larger than the marginal cirri. **f:** The resting cysts have a voluminous slime cover. The macronuclear nodules are not fused. **g-i:** Shape variability. AZM – adoral zone of membranelles, CC – caudal cirri, CV – contractile vacuole, EM – endoral membrane, FC1 – frontal cirrus 1, G – cortical granules, LT – lithosomes, MA – macronuclear nodule, MI – micronuclei, MT – mitochondria, PM – paroral membrane, POC – postoral cirrus, PTC – pretransverse cirri, SL – slime cover, W – cyst wall, III/2 – cirrus III/2 which has short, thick fibres on the right side (Fig. 75e, 76h, i). Scale bars 50  $\mu\text{m}$  (f) and 100  $\mu\text{m}$  (a, d, e).

Marginal cirral rows extend to posterior body end, right row composed of an average of about 50 cirri, left row of about 40. Six dorsal kineties, including three or four dorsomarginal kineties and three fine caudal cirri associated with kineties 1–3; kinty 1 commences subapical or far subapical, kineties 2–4 bipolar, kineties 5 and 6 (7) shortened posteriorly. Adoral zone extends 30–35% of

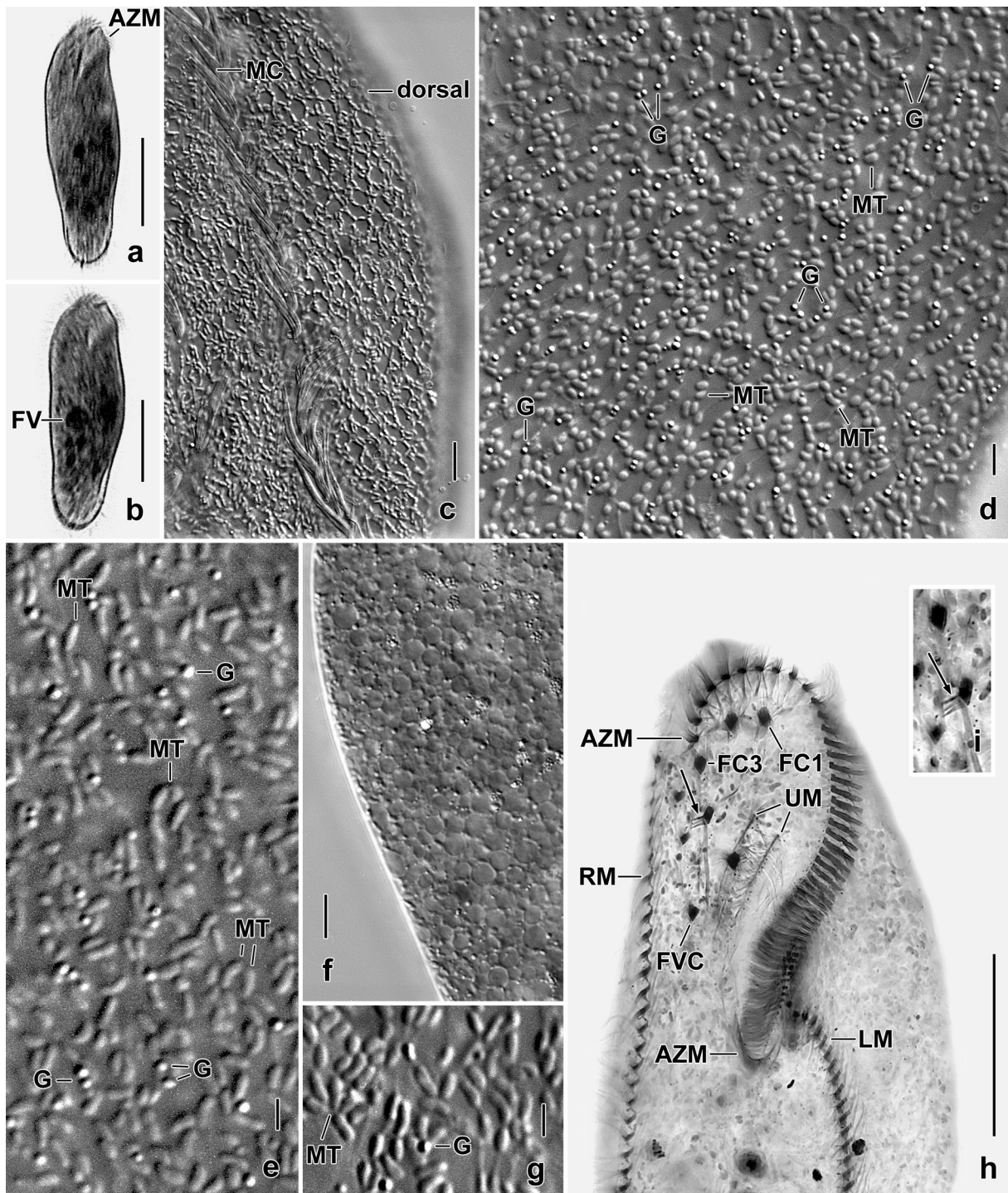


**Fig. 77a–i.** *Mixophrya pantanalensis pantanalensis* from life (a–g) and after protargol impregnation (h, i). **a, b:** Freely motile specimens. **c, d, f:** The mitochondria form a reticulate pattern in carefully prepared specimens (c) while the subcortical cytoplasm is strongly vacuolated (f). Note the loose arrangement (slightly disturbed by the coverslip) of the cortical granules (d). **e, g:** Mitochondrial layer in a squeezed specimen. **h, i:** Ventral view of oral portion. The arrow marks cirrus III/2 which has unique fibres associated at right side. AZM – adoral zone of membranelles, FC – frontal cirri, FVC – frontoventral cirri, FV – food vacuole, G – cortical granules, LM – left row of marginal cirri, MT – mitochondria, RM – right row of marginal cirri, UM – undulating membranes. Scale bars 3  $\mu\text{m}$  (e, g), 4  $\mu\text{m}$  (d), 5  $\mu\text{m}$  (f), 10  $\mu\text{m}$  (c), 50  $\mu\text{m}$  (h), 100  $\mu\text{m}$  (a, b).

body length on average, composed of about 52 membranelles; buccal cavity small, flat, and narrow compared to body size; buccal lip angular. Resting cyst about 70  $\mu\text{m}$  across, wall smooth.

**Remarks:** I split this species into two subspecies, depending on the presence/absence of lithosomes, body size, and biogeographic region (Table 2). Admittedly, the morphological differences are small; the most important being the presence vs. absence of lithosomes.

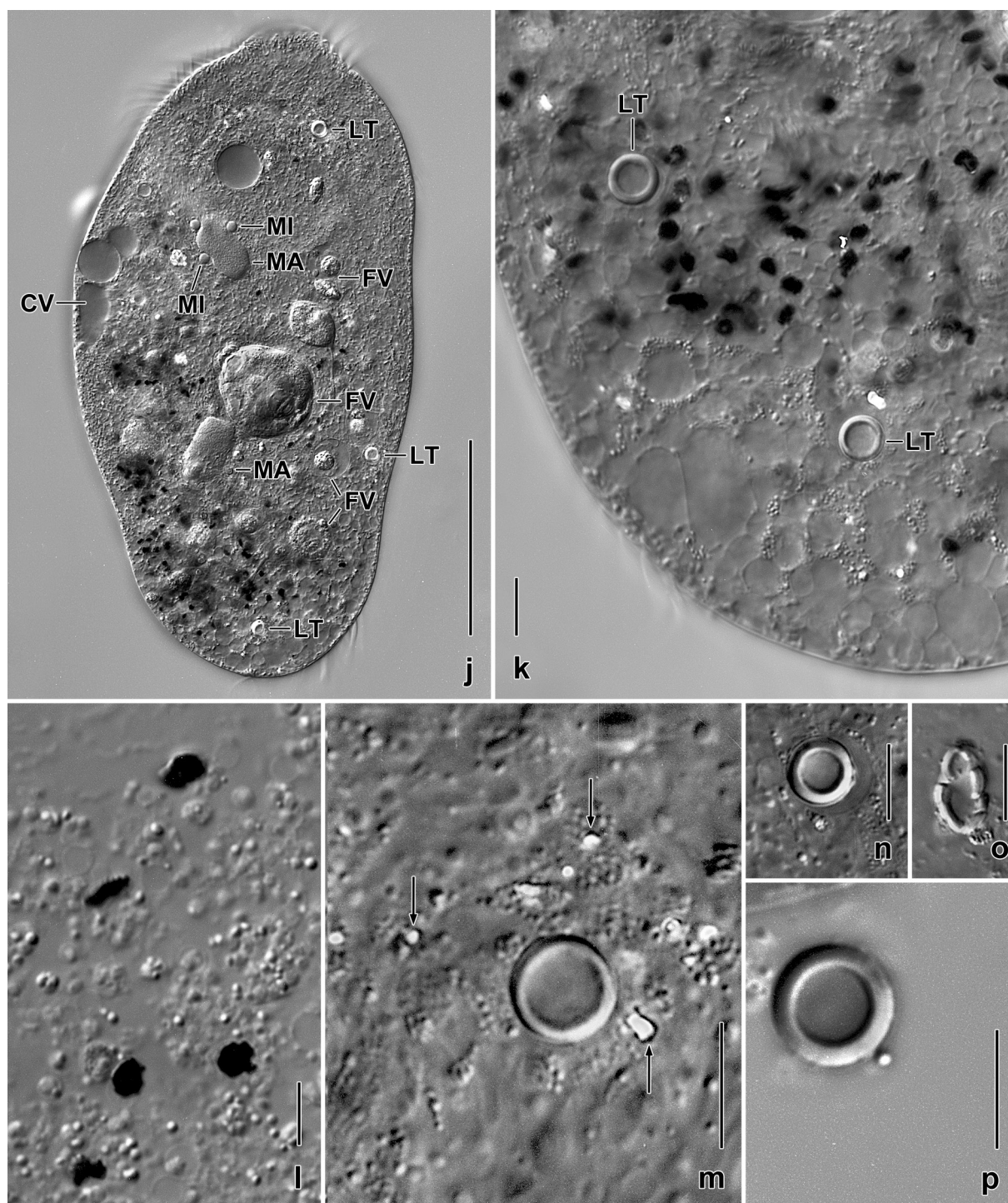


**Fig. 77j–p.** *Mixophrya pantanalensis pantanalensis* from life. **j**: Overview of a squeezed specimen, showing lithosomes and food vacuoles with ciliates and flagellates. The cytoplasm is densely granulated. **k, l**: The cytoplasm is vacuolated (**k**) and contains lithosomes (**k**) and sharp-edged, flattened, dark structures that do not solve when the cell is destroyed, indicating an inorganic nature. **m, p**: The lithosomes have a thick wall and are surrounded by crystalline structures (arrows in **m**) and masses of granules. **n, o**: When lithosomes are strongly squeezed (**n**) they break into sharp-edged pieces (**o**). CV– contractile vacuole, FV – food vacuoles, LT – lithosomes, MA – macronuclear nodules, MI – micronuclei. Scale bars 10  $\mu\text{m}$  (**k–p**) and 100  $\mu\text{m}$  (**j**).

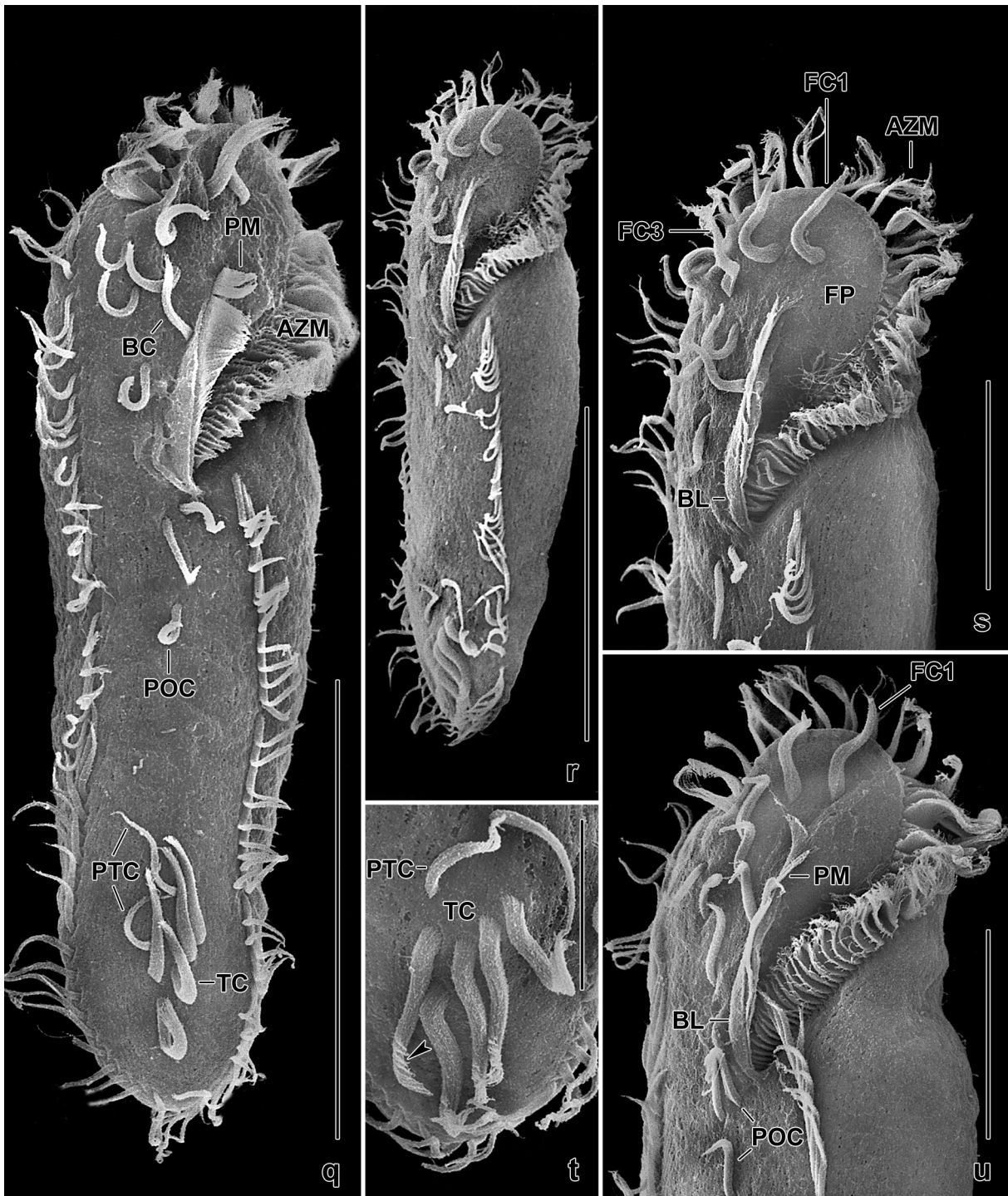


**Fig. 77q–u.** *Mixophrya pantanalensis pantanalensis*, scanning electron micrographs of morphostatic specimens. **q:** Ventral overview, showing the posterior narrowing, the cirral pattern, the short paroral membrane, and the large frontal plate providing the oral area with a stylonychid appearance. **r, s, u:** Overview (**t**) and details of oral area. The buccal seal covers the endoral membrane. **t:** Transverse cirri frequently have a fringed distal end (arrowhead). AZM – adoral zone of membranelles, BC – buccal cirrus, BL – buccal lip, FC1,3 – frontal cirri, FP – frontal plate, PM – paroral membrane, POC – postoral cirri, PTC – pretransverse cirri, TC – transverse cirri. Scale bars 20  $\mu\text{m}$  (**t**), 40  $\mu\text{m}$  (**s, u**), and 100  $\mu\text{m}$  (**q, r**).

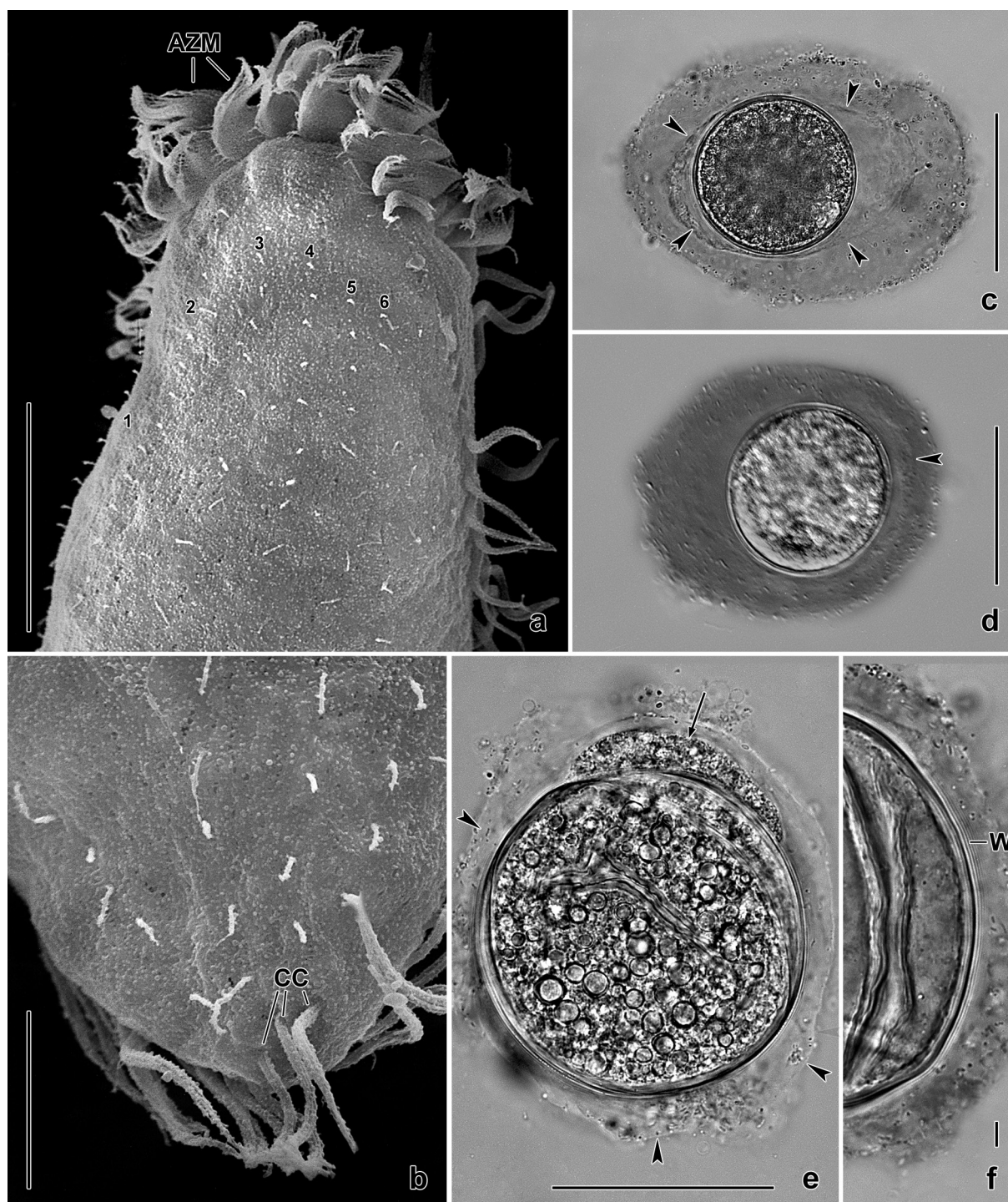
**Fig. 78a–f.** *Mixophrya pantanalensis pantanalensis*, dorsal views in the SEM (**a, b**) and resting cysts from life (**c–f**). **a, b:** Anterior and posterior view of dorsal side, showing six dorsal kineties and three narrowly spaced caudal cirri. **c, d:** The resting cysts are covered by a thick, yellowish slime layer composed of a thin internal (arrowheads) and a thick, fluffy external layer. The cyst content consists of numerous lipid globules. **e:** When the external slime layer is removed, the internal layer remains attached to the cyst wall (arrowheads). The arrow marks cytoplasm out of the cyst which has been slightly pressed by the coverslip. **f:** The cyst wall s. str. is smooth, brownish, and 2–3  $\mu\text{m}$  thick. AZM – adoral zone of membranelles, CC – caudal cirri, W – cyst wall, 1–6 – dorsal kineties. Scale bars 4  $\mu\text{m}$  (**f**), 10  $\mu\text{m}$  (**b**), 30  $\mu\text{m}$  (**a**), 50  $\mu\text{m}$  (**e**), 70  $\mu\text{m}$  (**c, d**).

*Mixophrya pantanalensis pantanalensis* nov. spec.

(Fig. 76a–i, 77a–u, 78a–m; Tables 31, 32 on p. 337)

**Diagnosis:** Size in vivo about  $370 \times 115 \mu\text{m}$ . Macronuclear nodules elongate ellipsoid, four globular micronuclei. Cortical granules sharp-yellowish,  $0.2 \mu\text{m}$  across. Cytoplasm with conspicuous lithosomes. Buccal cirrus distinctly subapical of paroral membrane. Distance between posteriormost transverse cirrus and rear body end  $37 \mu\text{m}$  on average. Resting cyst with a voluminous slime cover.

**Type locality:** Dark soil and litter from the margin of the Aurelio Lagoon associated with the Baia River, a tributary of the Paraná River in Brazil, State of Matu Grosso do Sul, near the town of Maringá,  $22^{\circ}40'S$ ,  $53^{\circ}15'W$ .



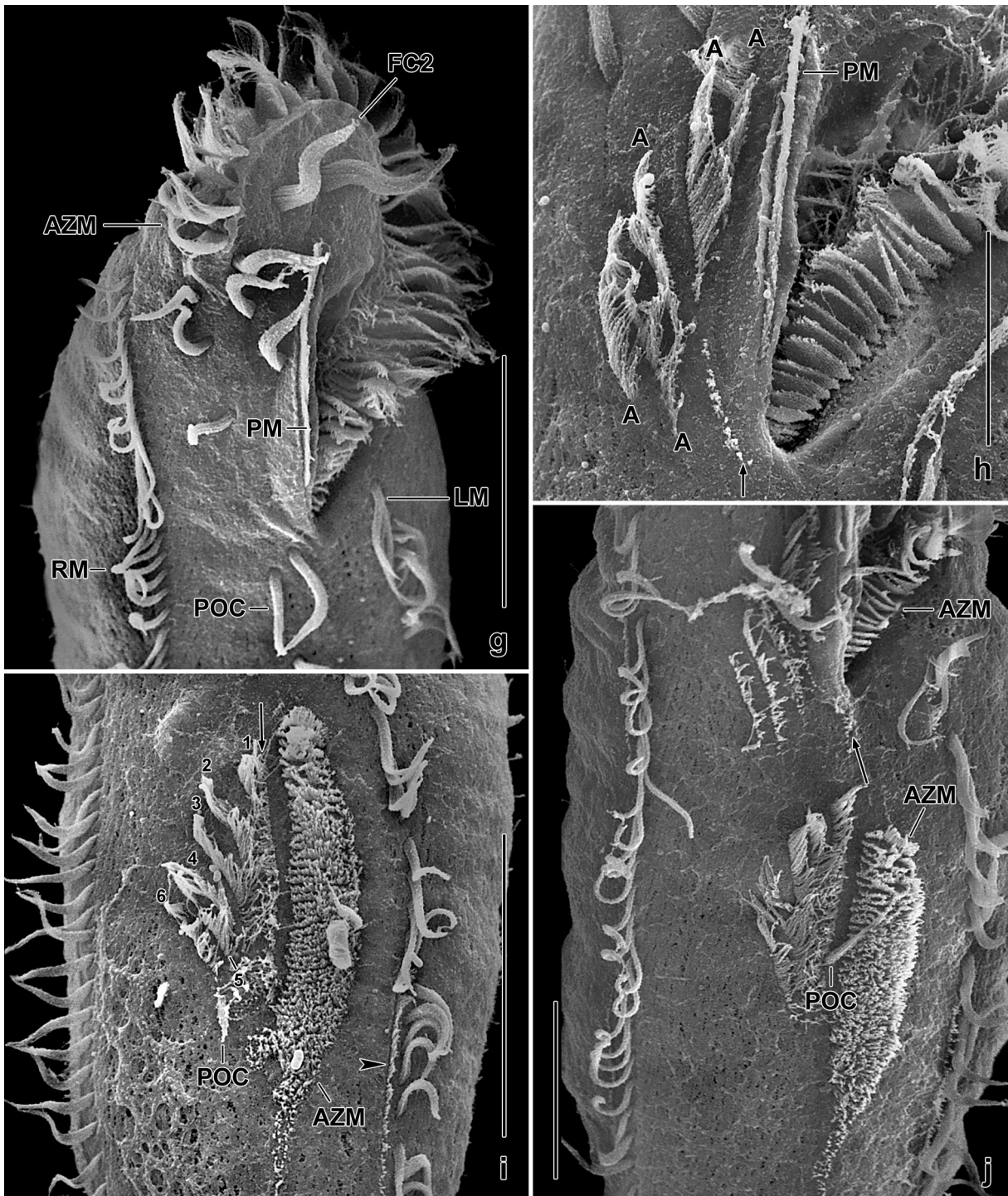


**Fig. 78g–j.** *Mixophrya pantanalensis pantanalensis*, morphostatic (g) and dividing (h–j) specimens in the SEM. **g:** Ventral view of oral region. **h, j:** Early mid-dividers, showing a proter (h) and opisthe (j). Both have five cirral anlagen. The arrows mark a further anlage possibly originating from a postoral cirrus. **i:** Early mid-divider with six cirral anlagen, as typical for oxytrichids. The arrow marks the anlage for the undulating membranes. The arrowhead denotes an anlage for a marginal cirral row. AZM – adoral zone of membranelles, FC2 – frontal cirrus 2, LM – left marginal cirral row, PM – paroral membrane, POC – postoral cirri, RM – right marginal cirral row, 1–6 – cirral anlagen. Scale bars 20  $\mu\text{m}$  (h), 30  $\mu\text{m}$  (j), 40  $\mu\text{m}$  (i), 50  $\mu\text{m}$  (g).

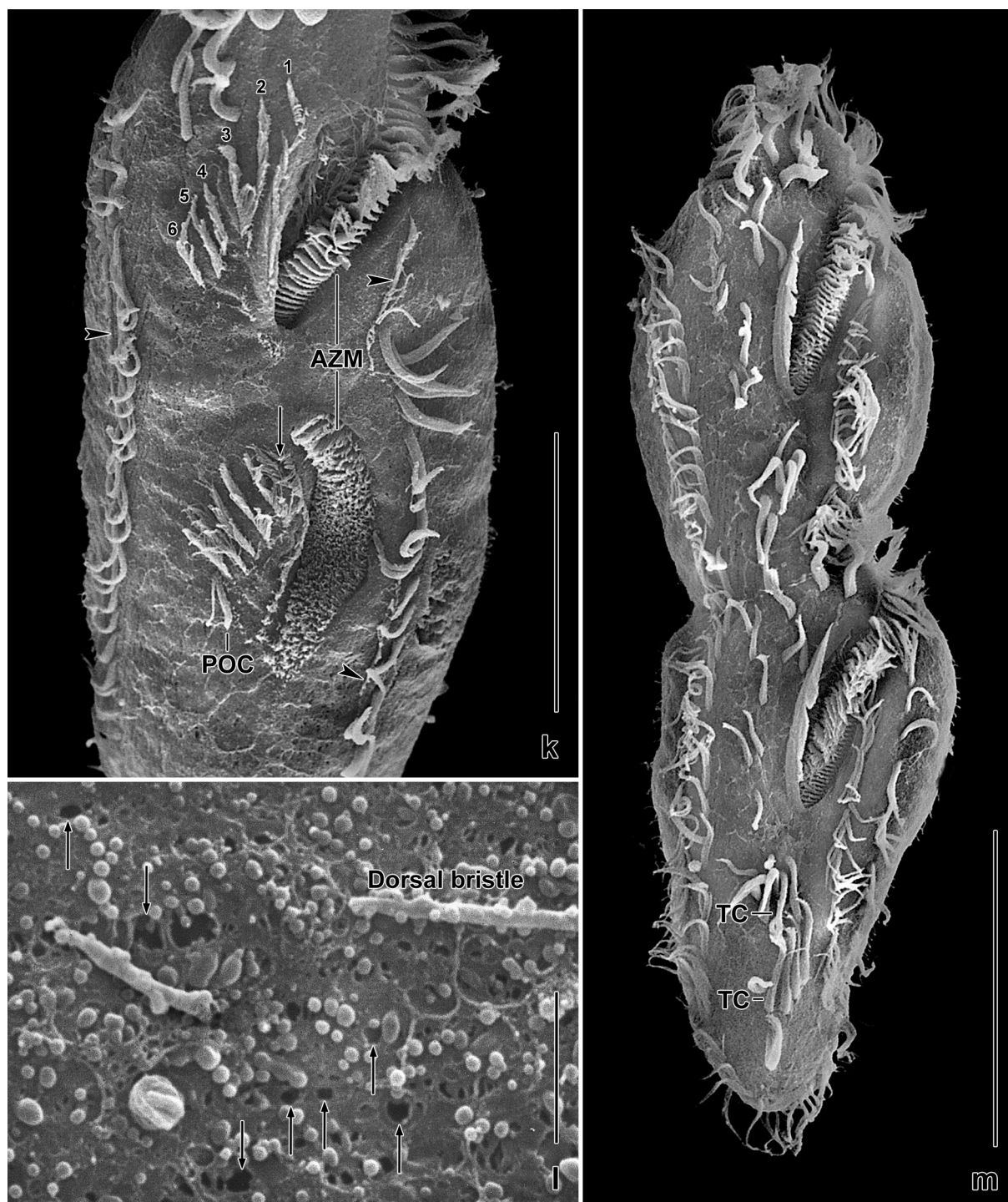
**Fig. 78k–m.** *Mixophrya pantanalensis pantanalensis*, dividers (k, m) and cortex (l) in SEM. **k:** Mid-divider with six cirral anlagen in proter and opisthe. The arrow marks the anlage for the undulating membranes. The arrowheads mark anlagen for the marginal cirri. The posterior postoral cirrus is still recognizable. **l:** Surface of cortex. The arrows mark holes remaining from extruded cortical granules. The minute globules are residues from the cell membrane. **m:** A late divider. The opisthe is distinctly narrowed posteriorly. The parental transverse cirri have not yet resorbed. AZM – adoral zone of membranelles, POC – postoral cirrus, TC – transverse cirri, 1–6 – cirral anlagen. Scale bars 2  $\mu\text{m}$  (l), 50  $\mu\text{m}$  (k), and 100  $\mu\text{m}$  (m).

**Type material:** The slide containing the holotype and four paratype slides with protargol-impregnated specimens have been deposited in the Biology Centre of the Upper Austrian Museum in Linz (LI). The holotype and other relevant specimens have been marked by black ink circles on the coverslip. For slides, see Fig. 32a–f in Chapter 5.

**Etymology:** Named after the area found, i.e., the Pantanal, a famous wetland.

**Description:** *Mixophrya pantanalensis pantanalensis* is difficult to preserve. Good results were obtained with the fixative of Foissner & Dragesco (1996), followed by protargol impregnation with Wilbert's (1975) method.

The preparations are from specimens cultivated in Eau de Volvic, some milliliters from the non-flooded Petri dish culture, and some cracked wheat grains.



*Mixophrya pantanalensis pantanalensis* is moderately variable, i.e., 13 out of 45 features investigated have a coefficient of variation of >15%. However, most of these concern features not used in the diagnosis, such as distances, size of macronuclear nodules and micronuclei. The number of micronuclei and the size and number of lithosomes are highly variable.

Size in vivo 250–350 × 80–100 µm, on average 292 × 110 µm (n = 6, non-flooded Petri dish culture). Cultivated, protargol-impregnated specimens 315–412 × 94–135 µm, on average 370 × 115 µm (including 15% preparation shrinkage; Table 32). Body bluntly clavate, i.e., gradually narrowed in posterior half; rarely elongate ellipsoid, posterior region sometimes slightly head-like; laterally flattened about 2:1, ventral side flat, dorsal more or less convex in middle third, depending on amount of food ingested (Fig. 76a, c, d, g–i, 77a, b, q). Nuclear apparatus in central third of body (Fig. 76a, e; Table 32). Macronuclear nodules widely separate, anterior nodule usually covered by proximal portion of oral apparatus; about 50 × 25 µm in vivo and on average 40 × 18 µm after protargol preparation, i.e., usually ellipsoid, rarely bluntly or elongate ellipsoid; contain many nucleoli 1–3 µm across. 2–10, on average four globular micronuclei attached or near to macronuclear nodules, 5–6 µm in vivo, 4.7 µm on average in protargol preparations. Contractile vacuole in mid-body, with short collecting canals (Fig. 76a, i, 77j). Cortex of specimens from non-flooded Petri dish culture likely semirigid, i.e., does not show flexibility or contractility when swimming or crawling while specimens from semipure culture are soft and flexible. Cortical granules in loose rows, about 0.2 µm across, sharp-yellowish (Fig. 76b, 77d–g, 78l); a second type of cortical granules(?), seen only in protargol preparations, is about 2.0 × 1.5 µm in size and quite similar to those described in → *Mixophrya pantanalensis australiensis*. Mitochondria reniform, 2–3 µm long, produce a conspicuous reticulum close underneath the cortical granules (Fig. 77c). Cytoplasm strongly vacuolated, colourless, contains three remarkable structures: (i) food vacuoles up to 50 µm across; (ii) an average of six scattered lithosomes with a size of 6–11 µm, on average 8.4 µm; and (iii) in posterior body half black, flat, angular structures 3–10 µm in size, do not solve when cell is squashed (Fig. 76a, 77a, b, j, k–p; Table 32). Omnivorous, feeds on a 170 µm long, green, stick-shaped euglenoid (*Astasia?*), fungal hyphae, heterotrophic flagellates, various middle-sized ciliates (*Vorticella*, *Colpoda*), testate amoebae (*Euglypha*, *Arcella*), starch grains from the food added, and even rotifers (Fig. 76a, 77a, b, j–l).

Somatic and oral infraciliature highly similar to that described for → *M. pantanalensis australiensis*, both morphologically and morphometrically. Thus, I refer the reader to the description of → *M. pantanalensis australiensis* and to Fig. 76a, d, e, 77h, i, q–u, 78a, b, g; Tables 31, 32.

**Resting cyst:** Resting cysts globular, with wall on average 70 µm across, with wall and slime cover on average 145 × 128 µm (Table 32). Cyst wall smooth, light brown, 2–3 µm thick, surrounded by a voluminous, yellowish slime cover the internal region of which is more compact and remains on the wall when the cyst is squashed. Macronuclear nodules not fused, plasm studded with 1–5 µm-sized lipid droplets and brown food remnants (Fig. 76f, 78c–f; Table 32).

**Occurrence and ecology:** As yet found only at type locality, i.e., in the soil-water transition zone of a lagoon in the Pantanal of Brazil. Grows well in laboratory cultures (see begin of description). Size, shape and locality suggest that *M. pantanalensis pantanalensis* is a limnetic species.

**Remarks:** See → *Mixophrya pantanalensis australiensis*.

***Mixophrya pantanalensis australiensis* nov. spec.**

(Fig. 79a–e, 80a–n; Tables 31, 32 on p. 337)

**Diagnosis:** Size in vivo about 280 × 80 µm. Macronuclear nodules elongate ellipsoid and an average of three globular micronuclei. Cortical granules bright-citrine, 0.3 µm across. Buccal cirrus subapical

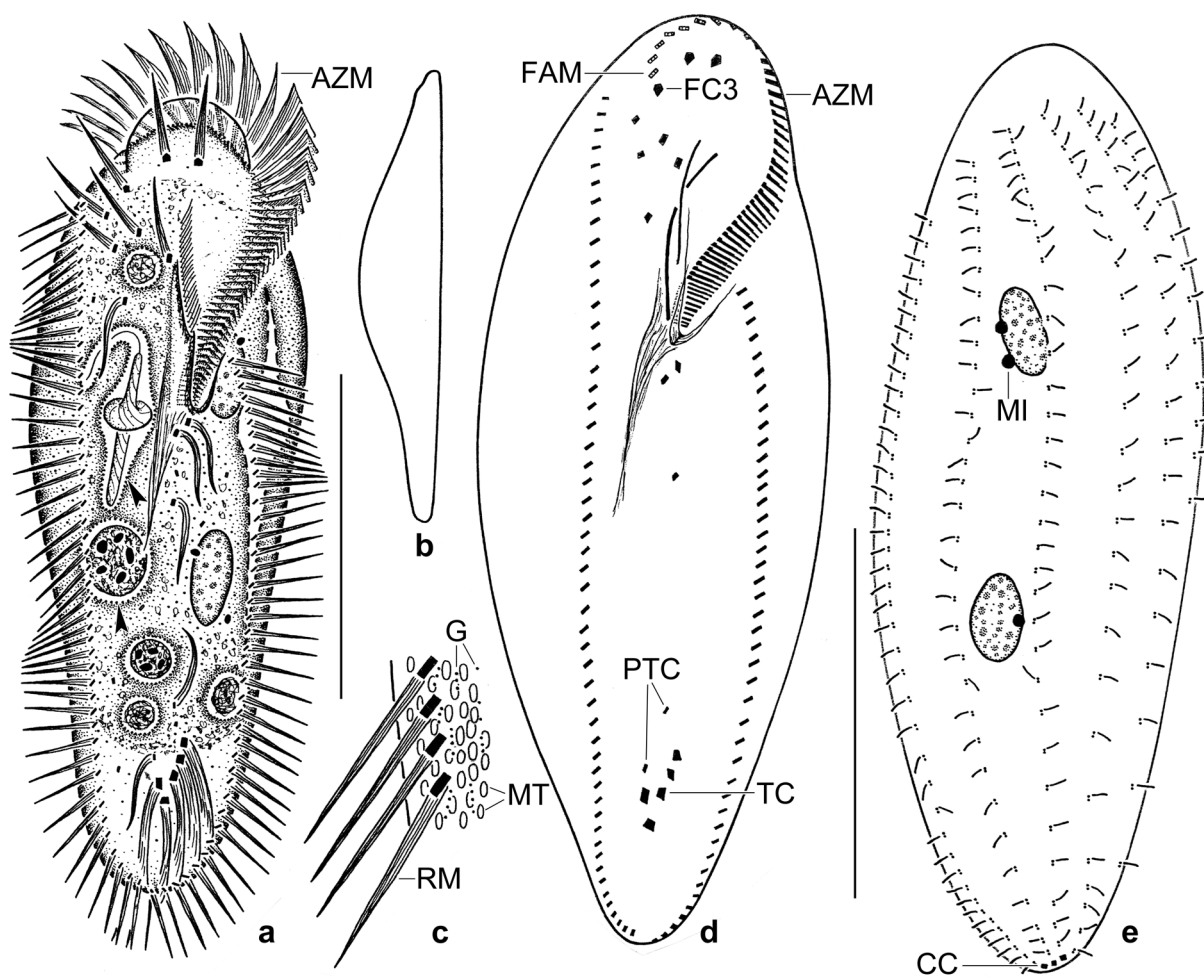


**Fig. 79a–e.** *Mixophrya pantanalensis australiensis* from life (a–c) and after protargol impregnation (d, e). **a:** Ventral view of a representative specimen, length 270  $\mu\text{m}$ . Note the hyaline rear region. The arrowheads mark food vacuoles containing the euglenid flagellate *Peranema*. **b:** Lateral view. **c:** Surface view of cortex, showing minute, citrine cortical granules and pale mitochondria. **d:** Ventral view of holotype specimen, length 250  $\mu\text{m}$ . The undulating membranes were completed with another specimen. Note the subterminal transverse cirri which do not or only slightly project from body proper; the minute pretransverse cirri; and the narrow adoral zone of membranelles. **e:** Dorsal view of a paratype specimen. AZM – adoral zone of membranelles, CC – caudal cirri, FAM – first adoral membranelle, FC3 – frontal cirrus 3, G – cortical granules, MI – micronucleus, MT – mitochondria, PTC – pretransverse cirri, RM – right marginal cirral row, TC – transverse cirri. Scale bars 100  $\mu\text{m}$ .

of paroral membrane. Distance between posteriormost transverse cirrus and rear body end 30  $\mu\text{m}$ .

**Type locality:** Mud of a lithotelma at margin of the Shoalhaven River, surrounding of the town of Bungonia, New South Wales, Australia, 34°50'S, 149°55'E.

**Type material:** The slide containing the holotype (Fig. 79d) and four paratype slides with protargol-impregnated specimens have been deposited in the Biology Centre of the Upper Austrian Museum in Linz (LI). The holotype and other relevant specimens have been marked by black ink circles on the coverslip. For slides, see Fig. 33a–g in Chapter 5.

**Etymology:** The adjective *australiensis* (belonging to Australia) refers to the country the species was discovered.

**Description:** *Mixophrya pantanalensis australiensis* is difficult to preserve. Useable protargol slides were obtained when they were fixed in Stiev's fluid enriched with osmium tetroxide (2% in water) and impregnated with Wilbert's method (Wilbert 1975). Possibly, pure ethanol (70–90%) will give also good results.

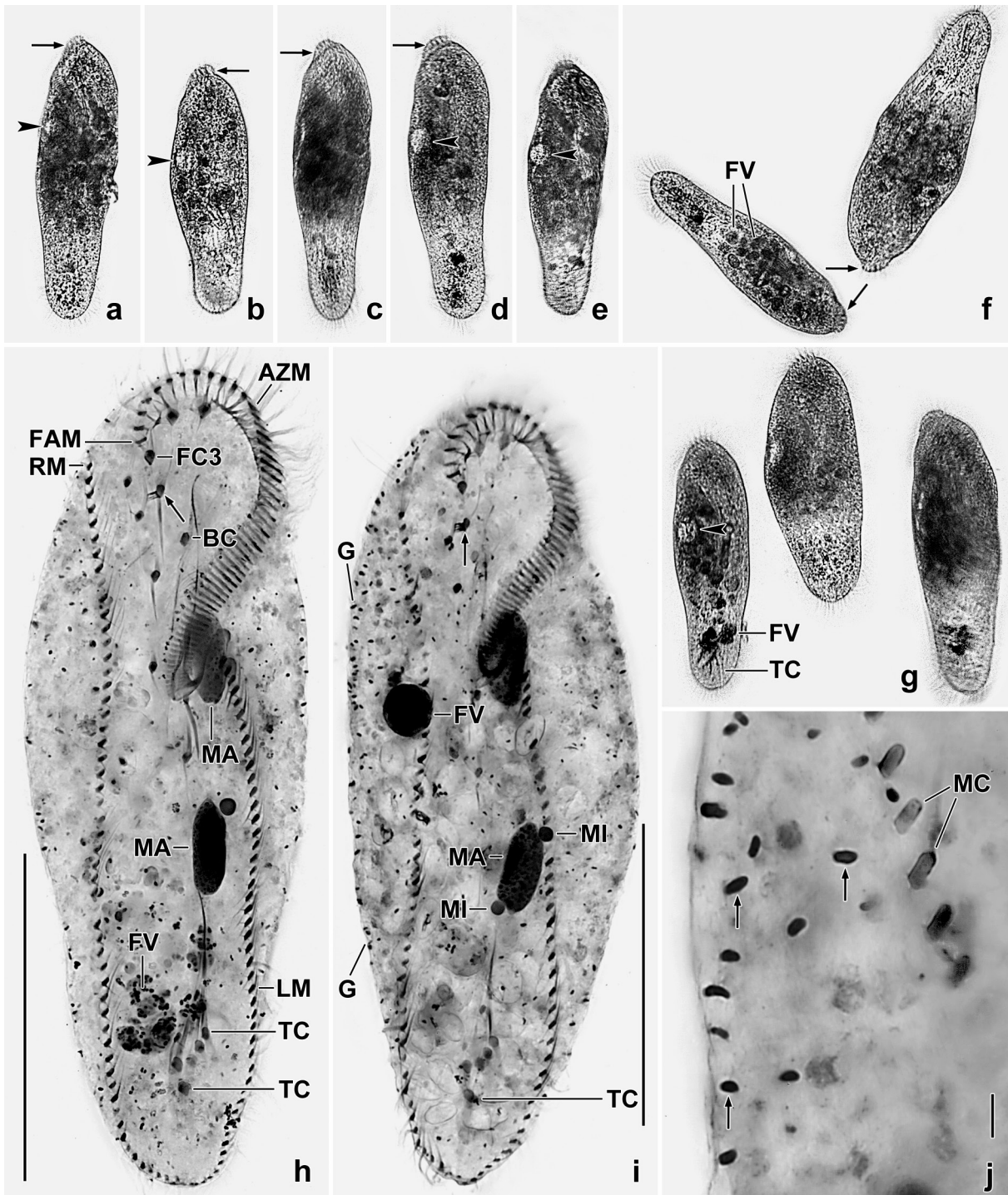


**Fig. 80a–j.** *Mixophrya pantanalensis australiensis* from life (a–g) and after protargol impregnation (h–j). **a–g:** Dorsal view of freely motile specimens, showing the contractile vacuole which is far anterior of mid-body (arrowheads), and the pronounced scutum (arrows); length 210–310  $\mu\text{m}$ . **h–j:** Ventral view of two specimens, showing the oxytrichid cirral pattern, the nuclear apparatus, and cortical granules(?) shown in (j, arrows) at higher magnification. The arrows in (h, i) mark cirrus III/2 shown at higher magnification in Fig. 80m, n. AZM – adoral zone of membranelles, BC – buccal cirrus, FAM – first adoral membranelle, FV – food vacuole, FC3 – frontal cirrus, G – cortical granules(?), LM, RM – left and right marginal cirral row, MA – macronuclear nodules, MC – marginal cirri, MI – micronuclei, TC – transverse cirri. Scale bars 5  $\mu\text{m}$  (j) and 100  $\mu\text{m}$  (h, i).

The preparations are from specimens cultivated with cracked wheat grains, *Tetrahymena mobilis*, *Paramecium aurelia*, and the flagellate *Polytomella* in Eau de Volvic. The cultivated specimens are larger by about 1/3 than those from the non-flooded Petri dish culture.

*Mixophrya pantanalensis australiensis* has an ordinary variability, i.e., most diagnostic features have a  $CV \leq 15\%$  (Table 32). Higher coefficients of variation occur mainly in distances (e.g., anterior body end to right marginal cirral row, posterior body end to right and left marginal cirral row), rarely in sizes and numbers (e.g., size and number of micronuclei, number of bristles in dorsal kineties 5 and 6).

Size in vivo about  $200\text{--}330 \times 70\text{--}90 \mu\text{m}$ , usually about  $280 \times 80 \mu\text{m}$ , as calculated from some in vivo measurements and the morphometric data in Table 32 adding 15% length shrinkage while nothing is added to body width due to the fixation problems; specimens from non-flooded Petri dish culture smaller by about one third than those from pure culture. Body bluntly clavate, i.e., gradually narrowed in posterior half; rarely elongate ellipsoid; laterally flattened about 2:1, ventral side flat, dorsal more or less convex in middle third, depending on amount of food ingested; hungry specimens hyaline in posterior region (Fig. 79a, b, d, 80a–i). Nuclear apparatus in central third of cell (Fig. 79a, e, 80h, i; Table 32). Macronuclear nodules widely separate, anterior nodule usually covered by proximal portion of oral apparatus; elongate ellipsoid, rarely ellipsoid; contain many nucleoli  $1\text{--}10 \mu\text{m}$  across and a quarter of specimens contains some ring-shaped structures  $10\text{--}20 \mu\text{m}$  in size. Usually three globular to broadly ellipsoid micronuclei attached or near to macronuclear nodules. Contractile vacuole distinctly anterior of mid-body, with short collecting canals (Fig. 79a, 80a, b, d, e, g). Cortex very flexible, cells slightly contractile under mild coverslip pressure. Cortical granules in loose rows, bright-citrine, only  $0.2 \mu\text{m}$  across (Fig. 79c); a second type of cortical granules (?), seen only in protargol preparations (Fig. 80j, l), is about  $2.0 \times 1.5 \mu\text{m}$  in size and is probably a special kind of mitochondria which form a dense, subcortical layer (Fig. 79c). Cytoplasm usually studded with food vacuoles and countless, pale globules about  $1 \mu\text{m}$  across, provide cells with a blackish or brownish colour under transmitted light and low magnification ( $\leq \times 100$ ); some about  $2 \mu\text{m}$ -sized crystals scattered throughout body. In the non-flooded Petri dish culture, *M. pantanalensis australiensis* feeds only on a highly metabolic *Peranema* species strongly moving in the food vacuole for some time (Fig. 79a). In raw cultures, feeds on *Polytoma* sp., *Tetrahymena mobilis*, rarely on *Paramecium aurelia*, and on up to  $30 \mu\text{m}$ -sized starch grains. Swims slowly, never stands still.

Somatic ciliature in *Oxytricha* pattern (Fig. 79a, d, 80h, i, k, m, n; Table 32). Frontal cirri thickened, in vivo about  $30 \mu\text{m}$  long, rightmost very near to first adoral membranelle (Fig. 80k, m). Buccal cirrus rather far posterior of anterior end of paroral membrane. Four frontoventral cirri, cirrus III/2 anterior to buccal cirrus and associated with four short, thick fibres anchoring it to the cortex (Fig. 80h, i, m, n); similar fibres very likely associated with frontal cirri. Postoral cirri in vivo about  $30 \mu\text{m}$  long, anterior cirri close together posterior of buccal vertex, third cirrus far posteriorly, i.e., in or near mid-body. Transverse cirri thickened, rather far subterminal, in vivo  $30\text{--}40 \mu\text{m}$  long, do not or only slightly project from body proper, distal end fringed; pretransverse cirri very fine compared to size of cell. Marginal cirri about  $25 \mu\text{m}$  long in vivo, each composed of three rows of basal bodies (Fig. 79a, d, 80h, i, k, m, n; Table 32).

Six dorsal kineties with bristles  $4\text{--}5 \mu\text{m}$  long in vivo and in protargol preparations (Fig. 79e; Table 32). Kintety 1 begins far subapical; kineties 1–4 extend to posterior body end; kintety 5 slightly shortened posteriorly; kintety 6 ends slightly anterior or posterior of mid-body. Three dividers show activity only in kineties 1–3 each producing a thin caudal cirrus; kineties 4–6 originate dorsomarginally.

Oral apparatus in *Oxytricha* (optically crossing undulating membranes) or in vague *Stylonychia* (undulating membranes short, buccal cavity flat and rather narrow, with rather distinct frontal plate) pattern, extends about 35% of body length, composed of about 50 membranelles the largest of which only  $12 \mu\text{m}$  wide in vivo and  $9 \mu\text{m}$  in protargol preparations (Fig. 79a, d, 80h, i; Table 32). Frontal scutum high and thus well recognizable in micrographs (Fig. 80a–d, f). Frontal plate comparatively distinct because undulating membranes begin far posteriorly of anterior body end.

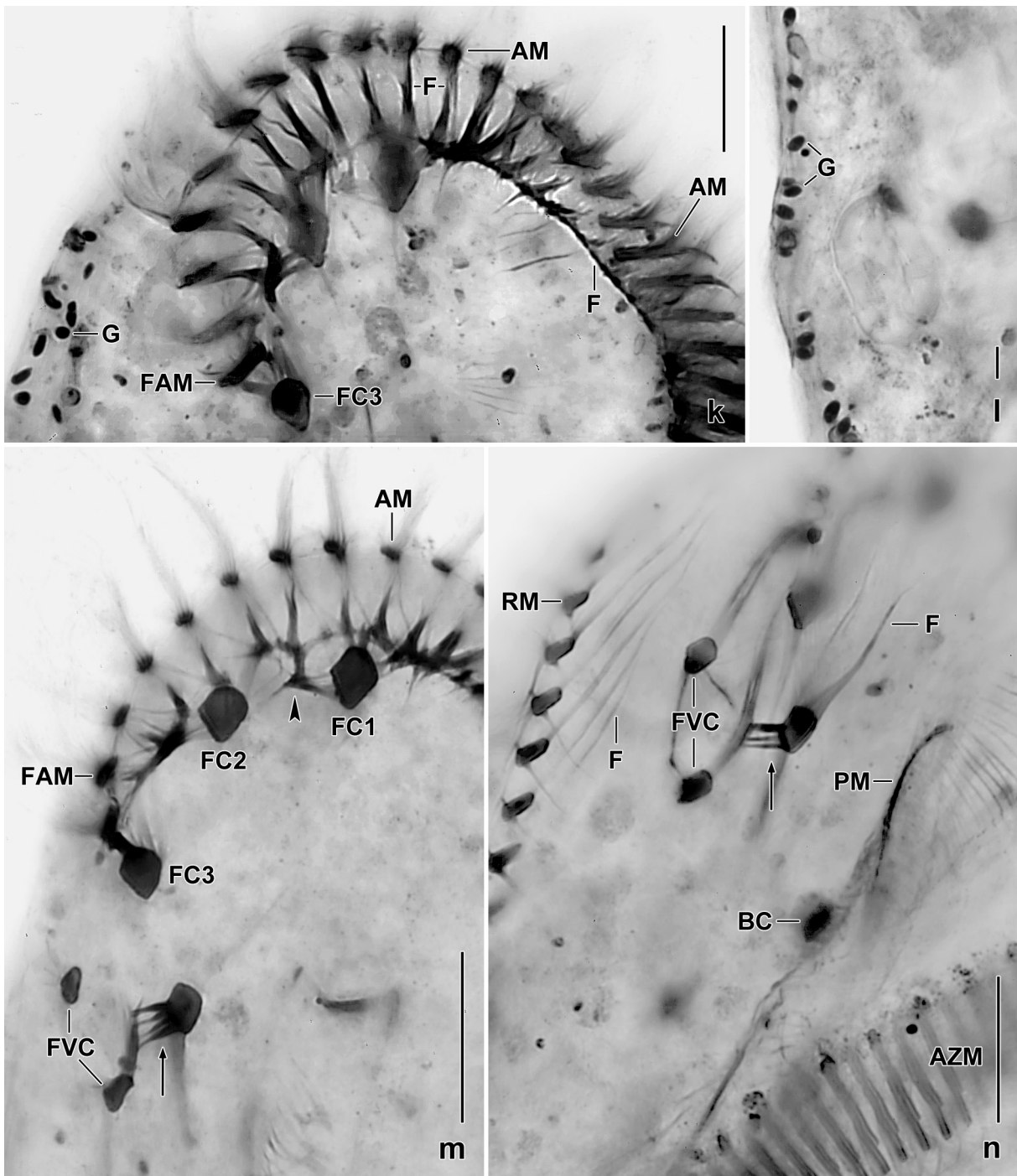


**Fig. 80k–n.** *Mixophrya pantanalensis australiensis* after protargol impregnation. **k, m, n:** Ventral views of oral area. The arrows in (m, n) mark cirrus III/2 which is anchored to the cortex by four short, thick fibres. The arrowhead in (m) denotes a fibre knot connecting the adoral zone of membranelles with frontal cirrus 1 and 2 (for an overview, see Fig. 80h, i). **l:** Large, cortical granules (?) impregnate deeply but were not recognized in vivo possibly due to a very similar refractivity as the mitochondria. AM – adoral membranelles, AZM – adoral zone of membranelles, BC – buccal cirrus, F – fibres, FAM – first adoral membranelle, FC1,2,3 – frontal cirri, FVC – frontoventral cirri, G – cortical granules(?), PM – paroral membrane, RM – right marginal cirral row. Scale bars 5  $\mu\text{m}$  (l), 10  $\mu\text{m}$  (k, m, n).

Buccal cavity flat and comparatively narrow, 21  $\mu\text{m}$  wide on average (Table 32). Buccal lip narrow and slightly convex, of angular type (Foissner & Al-Rasheid 2006). Undulating membranes short, cross optically in or near mid of buccal cavity; paroral cilia 10  $\mu\text{m}$  long in vivo. Buccal vertex and pharyngeal fibres distinct in vivo and in protargol preparations.

**Occurrence and ecology:** As yet found only at type locality. The big size suggests *Mixophrya pantanalensis australiensis* as a limnetic litter species.

**Remarks:** Of the taxa compared in Table 31, *Mixophrya pantanalensis pantanalensis* is most similar to *M. pantanalensis australiensis*. They differ in body size (319  $\mu\text{m}$  vs. 247  $\mu\text{m}$  on average in protargol preparations), the location of the transverse cirri (32  $\mu\text{m}$  vs. 26  $\mu\text{m}$  distant from body end, both about 10% of body length), and the presence vs. absence of lithosomes.

Of the species found in the literature (for a review, see Berger 1999), the African *Oxytricha longissima* Dragesco & Njine, 1971 is rather similar to *M. pantanalensis australiensis*, differing by the length of the macronuclear nodules (26  $\mu\text{m}$  vs. 40  $\mu\text{m}$ ), the number of adoral membranelles (37 vs. 52), the undulating membranes (paroral and endoral same length vs. paroral distinctly shorter than endoral), and the number of dorsal kineties (5 vs. 6). I suggest to reinvestigate the Cameroon species to get better data, for instance, on body shape, cortical granules, and the number of adoral membranelles which is, according to Berger (1999), not 37 but 46 in the figure provided by Dragesco & Njine (1971). This applies also to the North American *O. elongata* (Smith, 1897) Kahl, 1932 of which only body shape and size are useable and match *M. pantanalensis australiensis*.

### Conotrichidae nov. fam.

**Diagnosis:** Dorsomarginalian oxytrichids with unique dorsal ciliature, i.e., long (ordinary) bristle rows each producing “short” rows by growth and terminal segregation in all long kineties; each rightmost short row generates a caudal cirrus. A minute dorsomarginal kinety on ventral side of right anterior quadrant of cell, originates de novo and produces also the right row of marginal cirri. Oral apparatus psilotrichid. Opisthe’s adoral zone of membranelles horizontally oriented in late dividers.

**Type genus:** *Conothrix* nov. gen.

**Genera assignable:** *Conothrix* nov. gen.

**Remarks:** The diagnostic morphological and ontogenetic features are unique and suggest family rank for the single species, *Conothrix australiensis*. This is supported by the bewildering generic characteristics, which occur in various ciliates but not in the combination found in *Conothrix*, indicating a high number of homoplasies. *Conothrix* shows mainly features characteristic for typical oxytrichids and the curious oxytrichid Psilotrichidae reviewed by Heber et al. (2014, 2018). Both are presently supported mainly by morphological and ontogenetic characteristics. An oxytrichid relationship is indicated by the morphology and ontogeny of the dorsal infraciliature and the 18S rRNA of *Urospinula* (Heber et al. 2014). Indeed, the dorsal kinety pattern of *Conothrix* resembles that of typical oxytrichids where (usually) the long kinety 3 produces one or more “short” kineties possibly using the same or a very similar process as *Conothrix* (for a review, see Berger 1999). A rather close relationship of conotrichids and psilotrichids is obvious by the very similar morphology and ontogeny of the highly specific oral apparatus (Foissner 1983b; Heber et al. 2014).

Nonetheless, there is some probability that *Conothrix* belongs to the Psilotrichidae, as re-defined by Heber et al. (2014, 2018). However, psilotrichids lack frontal and buccal cirri. Further, they have a quite different dorsal ciliature, i.e., they lack “short” kineties and the “caudal” cirrus is made by the last cirrus of the left marginal row (Fig. 81g).

### *Conothrix* nov. gen.

**Diagnosis:** Flexible Conotrichidae with frontal, buccal, ventral, and marginal cirri; transverse cirri absent. With distinct frontal plate. Right margin of buccal roof bulge-like thickened. Four ventral

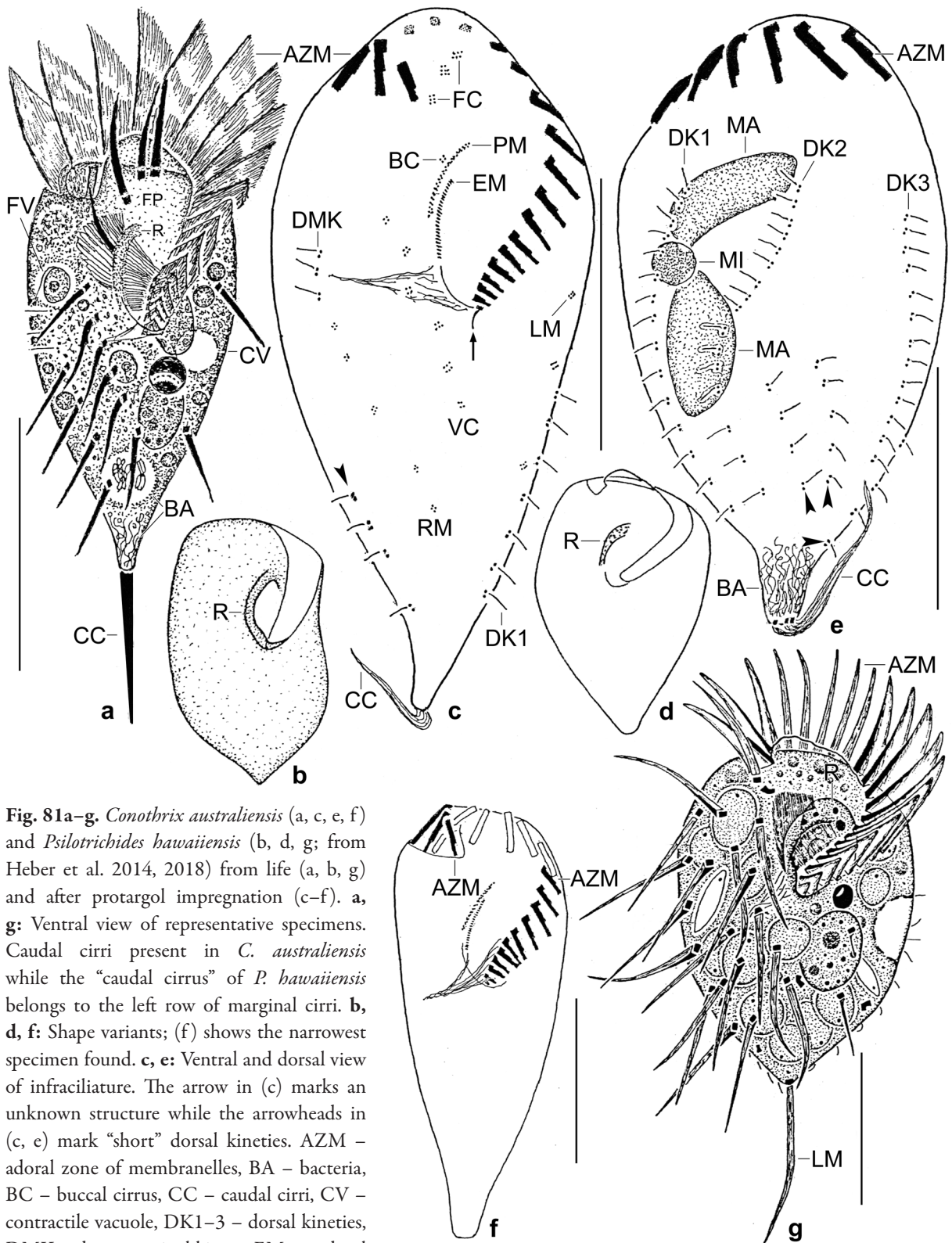
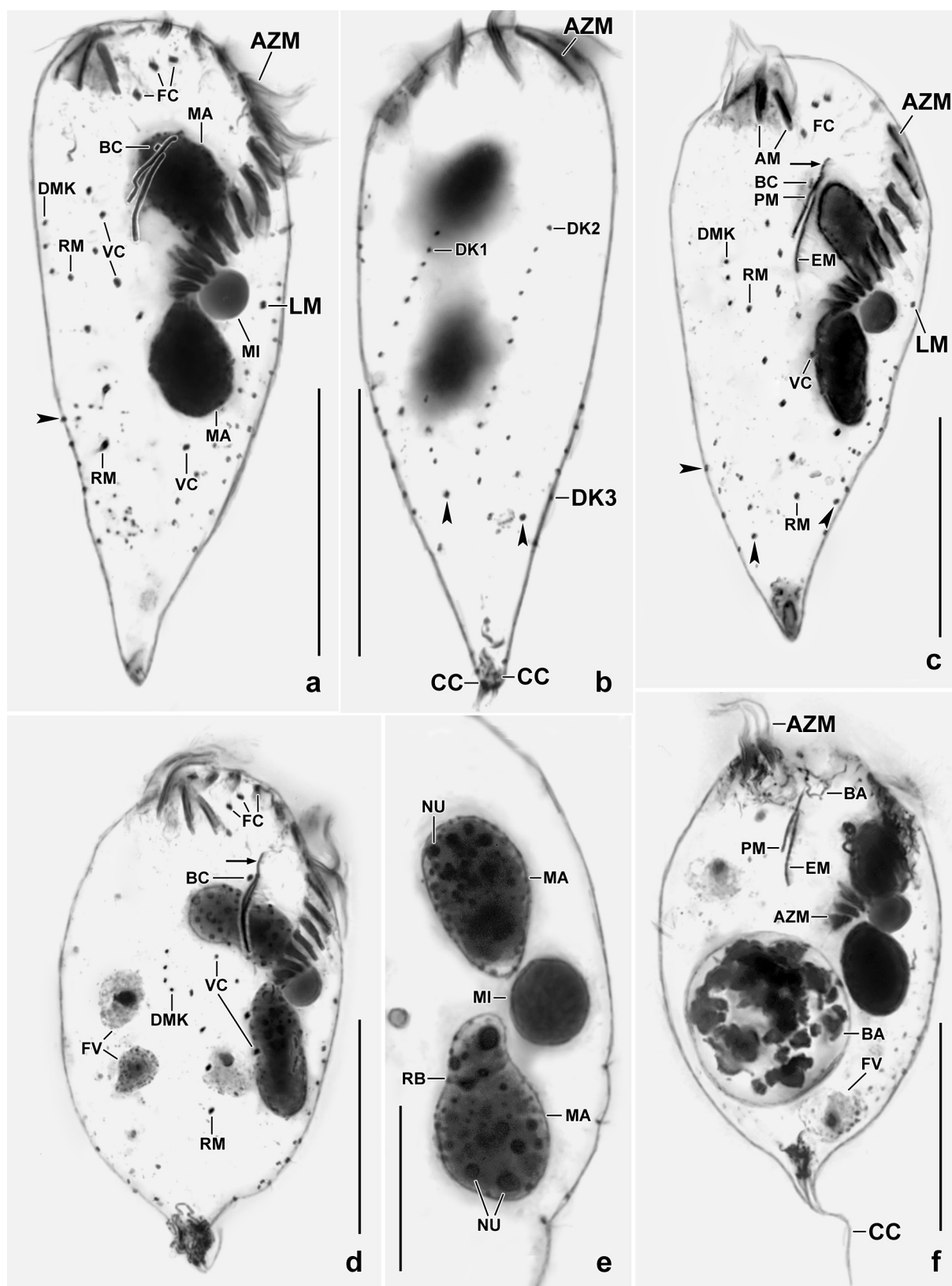


**Fig. 81a–g.** *Conothrix australiensis* (a, c, e, f) and *Psilotrichides hawaiiensis* (b, d, g; from Heber et al. 2014, 2018) from life (a, b, g) and after protargol impregnation (c–f). **a, g:** Ventral view of representative specimens. Caudal cirri present in *C. australiensis* while the “caudal cirrus” of *P. hawaiiensis* belongs to the left row of marginal cirri. **b, d, f:** Shape variants; (f) shows the narrowest specimen found. **c, e:** Ventral and dorsal view of infraciliature. The arrow in (c) marks an unknown structure while the arrowheads in (c, e) mark “short” dorsal kineties. AZM – adoral zone of membranelles, BA – bacteria, BC – buccal cirrus, CC – caudal cirri, CV – contractile vacuole, DK1–3 – dorsal kineties, DMK – dorsomarginal kinety, EM – endoral membrane, FC – frontal cirri, FP – frontal plate, FV – food vacuole, LM – left row of marginal cirri, MA – macronuclear nodules, MI – micronucleus, PM – paroral membrane, R – buccal ridge, RM – right row of marginal cirri, VC – ventral cirri. Scale bars 30  $\mu\text{m}$  (c, e–g) and 50  $\mu\text{m}$  (a).

**Fig. 82a–f.** *Conothrix australiensis* after protargol impregnation. Arrowheads mark “short” dorsal kineties. Note the big micronucleus. **a, b:** Ventral and dorsal view of same specimen, showing the somatic and oral infraciliature and the nuclear apparatus. **c, d:** Slightly right side views, showing, inter alia, the single, short dorsomarginal kinety (DMK) and the spoon-shaped anterior region of the paroral membrane (arrows). The two distalmost adoral membranelles



consist of only three kineties of which the leftmost row is slightly shortened. **e:** Nuclear apparatus and beginning nuclear reorganization (posterior nodule). **f:** A specimen with a very large food vacuole, possibly containing agglutinated bacteria. AM – adoral membranelles, AZM – adoral zone of membranelles, BA – cytoplasmic bacteria, BC – buccal cirri, CC – caudal cirri, DK1–3 – dorsal kineties, DMK – dorsomarginal kinety, EM – endoral membrane, FC – frontal cirri, FV – food vacuoles, LM – left row of marginal cirri, MA – macronuclear nodules, MI – micronucleus, NU – nucleoli, PM – paroral membrane, RB – reorganization band, RM – right row of marginal cirri, VC – ventral rows of cirri. Scale bars 15 µm (e) and 30 µm (a–d, f).

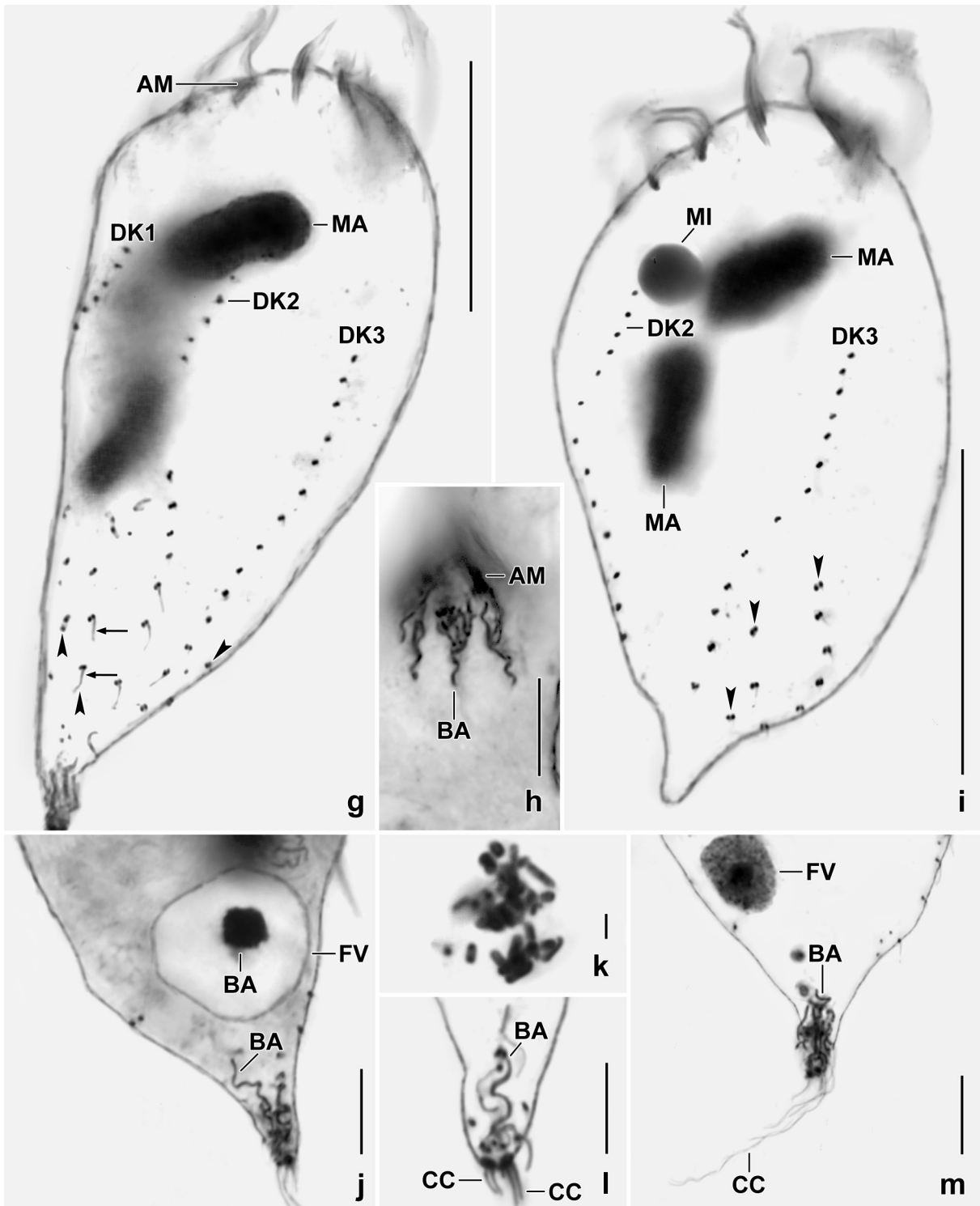


**Fig. 82g–m.** *Conothrix australiensis* after protargol impregnation. Arrowheads mark short dorsal kineties. **g, i:** Dorsal views. Arrows in (g) mark bristles associated with the “short” dorsal kineties. **h, l, m:** Spirochaetes occur under the adoral membranelles (h) and in the tail (j, l, m). **j, k:** In the posterior region occur globular accumulations of bacteria in large vacuoles and spirochaetes in the posterior end. AM – adoral membranelles, BA – bacteria (spirochetes), CC – caudal cirri, DK1–3 – dorsal kineties, FV – food vacuoles, MA – macronuclear nodules, MI – micronucleus. Scale bars 2  $\mu\text{m}$  (k), 10  $\mu\text{m}$  (h, j, l, m), and 30  $\mu\text{m}$  (g, i).

cirral anlagen each in proter and opisthe. Three ordinary (“long”) dorsal kineties each producing two “short” kineties by terminal segregation. Oral primordium in a flat pouch at posterior margin

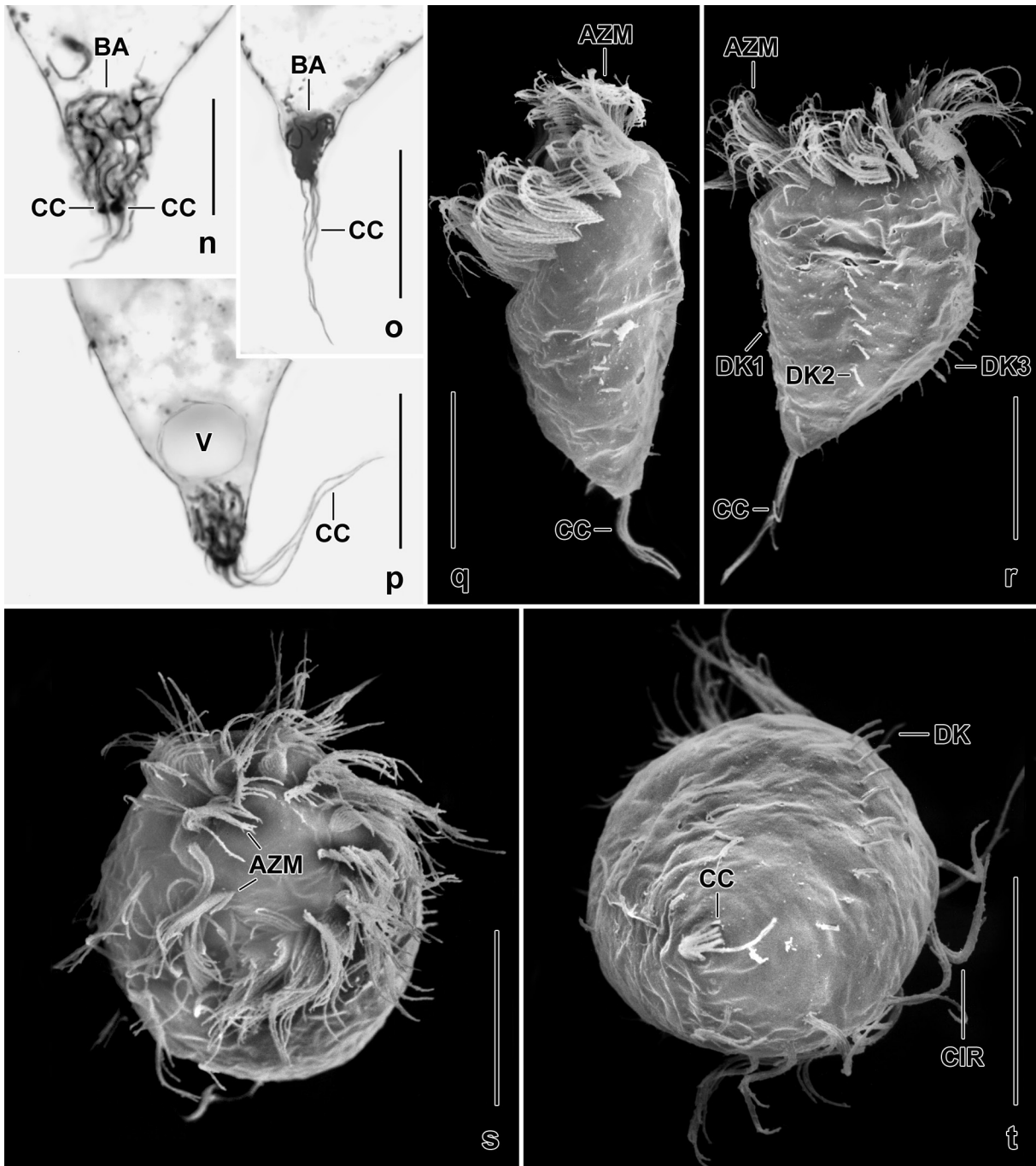


**Fig. 82n-t.** *Conothrix australiensis* after protargol impregnation (n-p) and in the scanning electron microscope (q-t). **n-p:** Posterior regions, showing the up to 25  $\mu\text{m}$  long caudal cirri and the posterior end studded with spirochaetes. In figure (n), the base of the left caudal cirrus is smaller than the base of the right because this is composed of two optically slightly overlapping caudal cirri. **q-t:** When viewed dorsolaterally or dorsally (q, r), the specimens appear flattened which might be an optical artifact because they are circular in anterior and posterior polar view (s, t). AZM – adoral zone of membranelles, BA – bacteria, CC – caudal cirri, CIR – somatic cirri, DK1–3 – dorsal kineties, V – vacuole. Scale bars 10  $\mu\text{m}$  (n) and 20  $\mu\text{m}$  (o-t).

of buccal vertex. The proter endoral membrane very likely produces a new paroral by lateral proliferation of basal bodies.

**Type species:** *Conothrix australiensis* nov. spec.

**Etymology:** Composite of the Latin noun *conus* (cone) and the Greek noun *thrix* (hair ~ ciliate). Feminine gender.

**Remarks:** Most generic characters occur also in other ciliates but not in the combination found in *Conothrix*. A lack of transverse cirri is rather widespread in oxytrichids and, e.g., psilotrichids (Berger 1999; Heber et al. 2014, 2018). A frontal plate is typical for stylonychid oxytrichids (Berger 1999; Kumar & Foissner 2017) and the curious *Rigidothrix* Foissner & Stoeck, 2006. A conspicuously thickened left margin of the buccal roof is typical for psilotrichids (Heber et al. 2014, 2018; Foissner unpubl.). The low number of cirral anlagen is likely connected with the low number of cirri in *Conothrix* while typical oxytrichids usually have six but only five occur, e.g., in

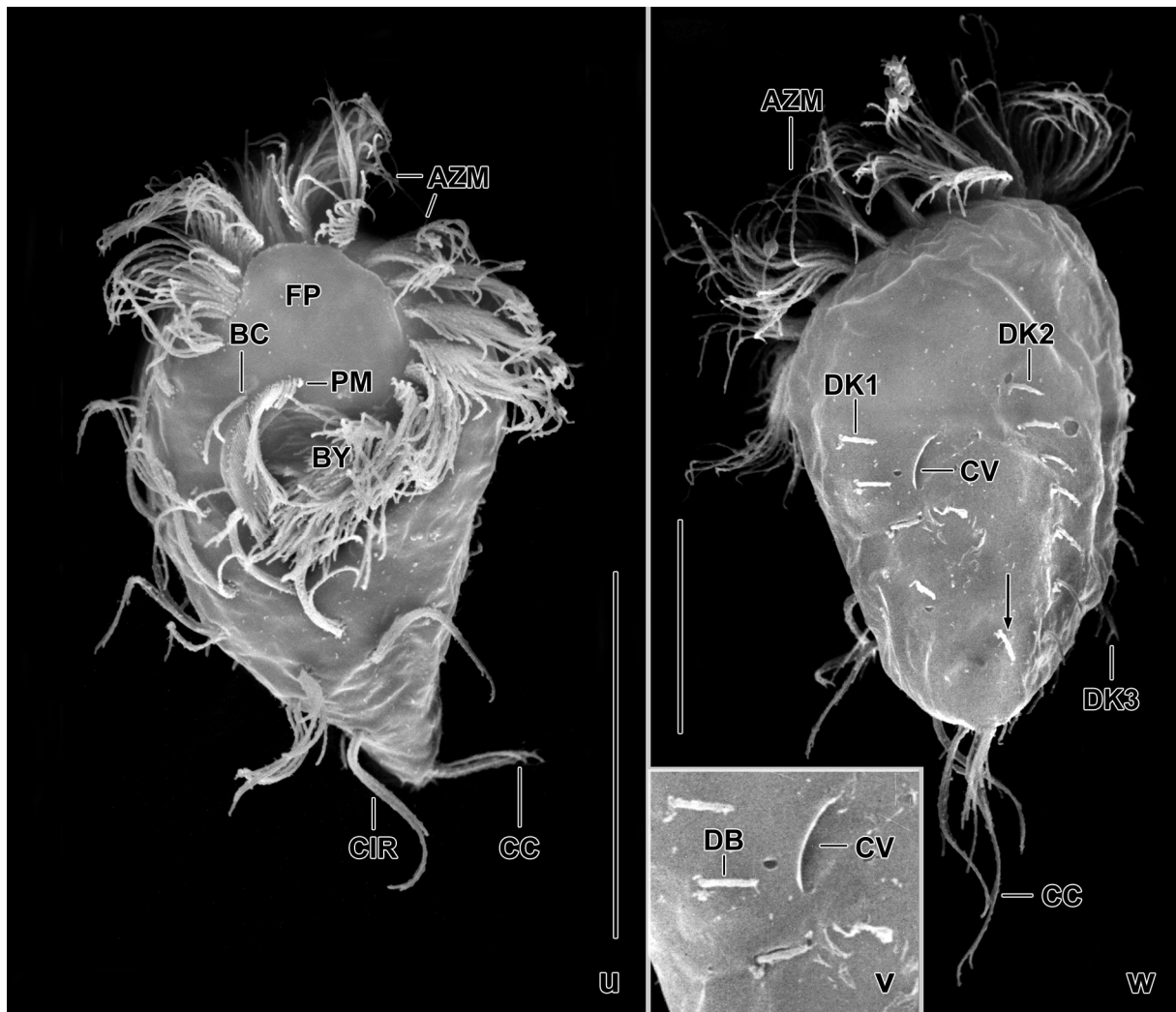


**Fig. 82u–w.** *Conothrix australiensis*, ventral and dorsal view in the scanning electron microscope. The caudal cirri of the left specimen are only partially preserved. Note the conspicuous frontal plate, resembling *Stylonychia*, and the small buccal cavity. The right specimen shows three distinct dorsal kineties which begin far subapically; the arrow marks a single bristle possibly belonging to one of the “short” dorsal kineties usually not recognizable in the SEM for unknown reasons. The slightly curved slit is very likely the opening for the contractile vacuole (v, w). AZM – adoral zone of membranelles, BC – buccal cirrus, BY – buccal cavity, CC – caudal cirri, CIR – somatic cirrus, CV – contractile vacuole, DB – dorsal bristle, DK1–3 – dorsal kineties, FP – frontal plate, PM – paroral membrane. Scale bars 30  $\mu\text{m}$ .

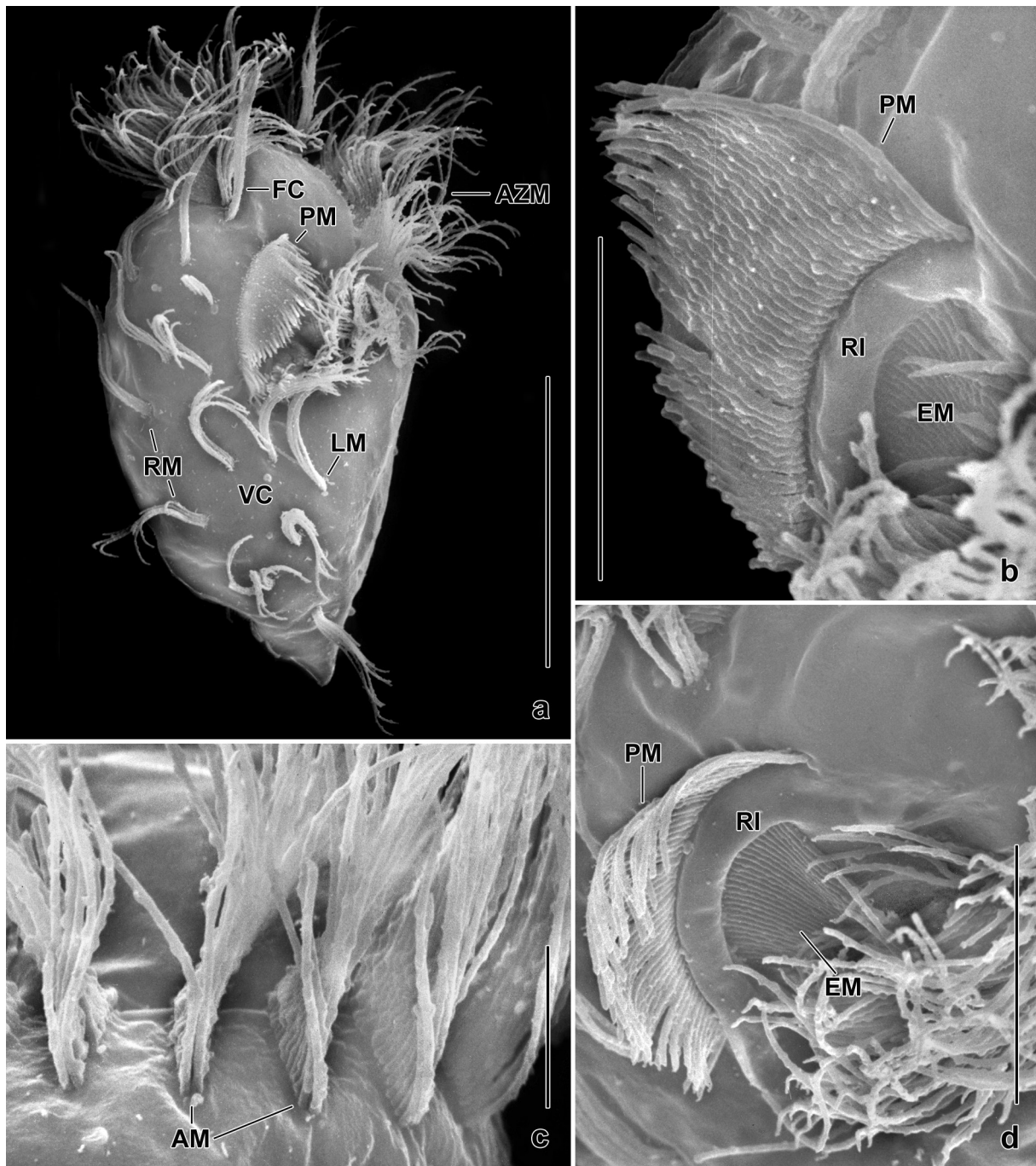
**Fig. 83a–d.** *Conothrix australiensis* in the scanning electron microscope. **a:** Ventral overview; caudal cirri lost by the preparation procedure. The buccal cirrus, the dorsomarginal kinety and the short dorsal kineties are not recognizable. The paroral membrane covers the buccal cavity. **b, d:** The oral apparatus consists of an ordinary adoral zone of membranelles, a sail-shaped paroral membrane, a conical endoral membrane, and a conspicuous “buccal ridge” highly similar to that present in the Psilotrichidae (Heber et al. 2014, 2018). **c:** Distal end of some adoral membranelles each comprising two ciliary rows. AM – adoral membranelles, AZM – adoral zone of membranelles, EM – endoral membrane, FC – frontal cirrus, LM – left row of marginal cirri, PM – paroral membrane, RI – buccal ridge, RM – right row of marginal cirri, VC – ventral cirri. Scale bars 5  $\mu\text{m}$  (c), 10  $\mu\text{m}$  (b, d), and 30  $\mu\text{m}$  (a).

*Vermioxytricha* and *Erimophrya* (Foissner et al. 2002). The oral primordium develops in a more or less deep pouch in psilotrichids (Heber et al. 2014), euplotids (Wise 1965), and oligotrichs (Foissner et al. 1999; Petz & Foissner 1993). The genesis of the proter paroral membrane is as yet unique but resembles the nassulids (Foissner 1996c).

***Conothrix australiensis* nov. spec.**

(Fig. 81a, c, e, f, 82a–w, 83a–u, 84a–h; Table 33 on p. 340)

**Diagnosis** (averages are provided): Size in vivo about  $90 \times 45 \mu\text{m}$ ; funnel-shaped. Nuclear apparatus in mid of left body half, composed of two ellipsoid macronuclear nodules and a conspicuous



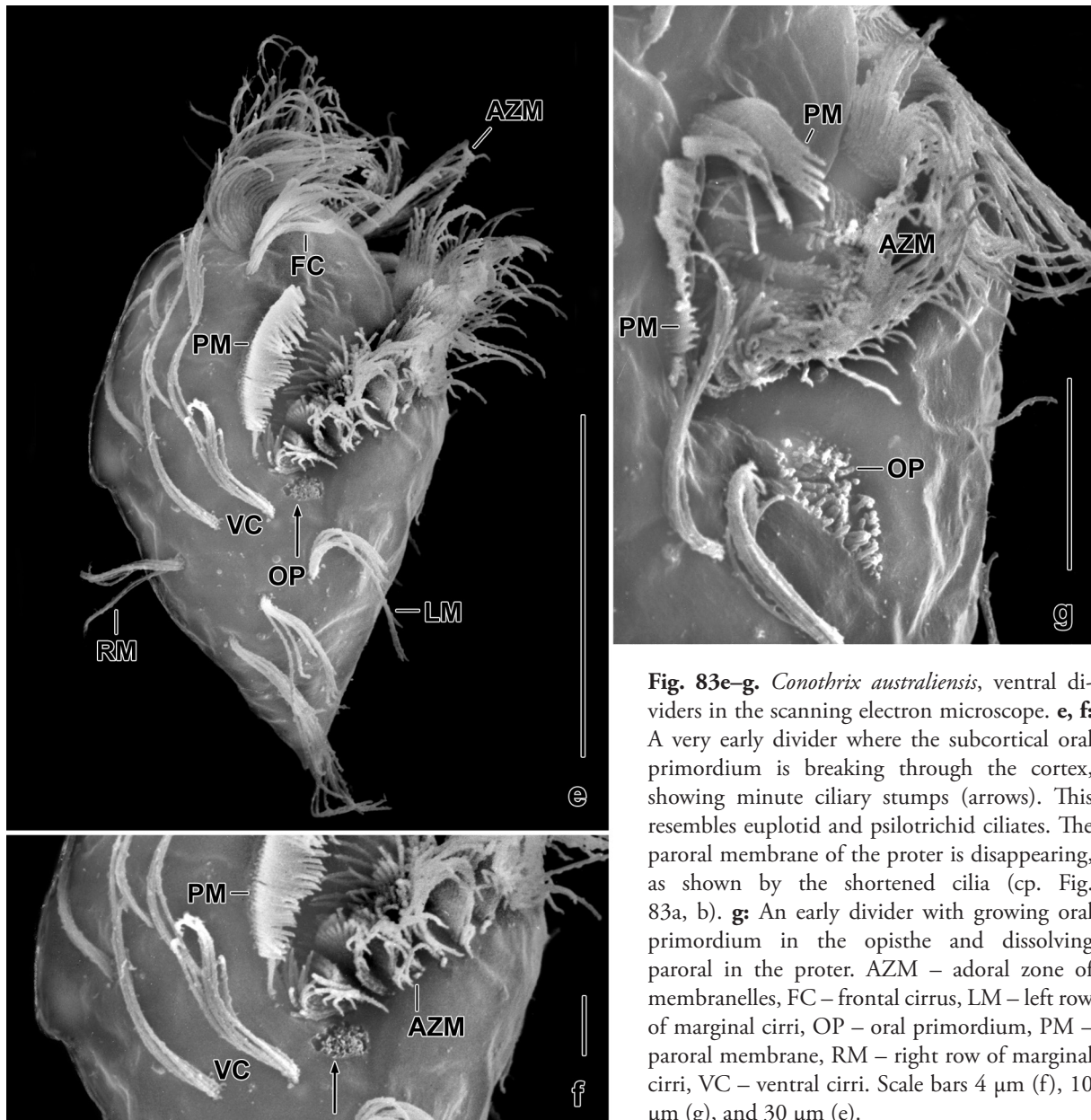


**Fig. 83e–g.** *Conothrix australiensis*, ventral dividers in the scanning electron microscope. **e, f:** A very early divider where the subcortical oral primordium is breaking through the cortex, showing minute ciliary stumps (arrows). This resembles euplotid and psilotrichid ciliates. The paroral membrane of the proter is disappearing, as shown by the shortened cilia (cp. Fig. 83a, b). **g:** An early divider with growing oral primordium in the opisthe and dissolving paroral in the proter. AZM – adoral zone of membranelles, FC – frontal cirrus, LM – left row of marginal cirri, OP – oral primordium, PM – paroral membrane, RM – right row of marginal cirri, VC – ventral cirri. Scale bars 4  $\mu\text{m}$  (f), 10  $\mu\text{m}$  (g), and 30  $\mu\text{m}$  (e).

micronucleus 6–10  $\mu\text{m}$  across in vivo. Contractile vacuole in mid-region, with slit-like opening. Cortex flexible, without specific granules. Swimming resembles oligotrichs. Ventral cirral pattern very sparse, i.e., composed of three frontal cirri, one buccal cirrus and three inconspicuous pairs of ventral cirri, right marginal row composed of four cirri, left of three; dorsomarginal kinety composed of three bristles. Three ordinary rows of dorsal bristles commencing about 20  $\mu\text{m}$  subapically, each accompanied by two “short” bristle rows, each rightmost “short” row produces a caudal cirrus, forming together a conspicuous, about 20  $\mu\text{m}$  long “caudal cirrus” on top of posterior body end. Oral apparatus conspicuous because extending about 40% of body length and membranelar cilia up to 35  $\mu\text{m}$  long in vivo. Adoral zone composed of about 10 membranelles, anteriorly curved to midline of body. Undulating membranes slightly curved and side by side.

**Type locality:** Australian site (106?), i.e., flood plain soil from Murray River near to the town of Albury, waterside of Ryans road, Australia, 37°S, 147°E.

**Type material:** The slide containing the holotype and four paratype slides with protargol-impregnated specimens have been deposited in the Biology Centre of the Upper Austrian Museum

in Linz (LI). The holotype, the ontogenetic stages, and other relevant specimens have been marked by black ink circles on the coverslip.<sup>1</sup> For slides, see Fig. 9a–g, 34a–f in Chapter 5.

**Etymology:** Named after the continent found, i.e., Australia.

**Description of morphostatic cells:** Several ciliated structures present in protargol preparations are not recognizable in the scanning electron microscope, viz., the buccal cirrus, the dorsomarginal kinety, and the “short” dorsal kineties. I do not have an explanation.

The variability is rather high, i.e., 17 out of 39 features have a CV > 15% (Table 33). Size in vivo 70–115 × 35–50 μm, usually about 90 × 45 μm, as calculated from in vivo measurements and the morphometric data in Table 33 adding 15% preparation shrinkage. Conical to pyriform, table tennis racket-shaped when caudal cirral bundle is included (Fig. 81a, c, e, f, 82a–g, i, q–t, 83a, e, h, j); flattened only when undernourished (Fig. 82q, r). Anterior body end transverse truncate or slightly convex, almost completely surrounded by adoral zone of membranelles; posterior region distinctly narrowed to an acute process bearing caudal cirri. Nuclear apparatus in or slightly anterior of mid-body near left margin of cell, consists of two slenderly to broadly ellipsoid macronuclear nodules rather close together, may form a triangular pattern connected by a fine strand in post-dividers; many minute nucleoli up to 4 μm in size. Micronucleus conspicuous because 6–10 μm across in vivo, between and slightly left of macronuclear nodules (Fig. 81a, e, 82a–g, i; Table 33); in some specimens contains about 8 μm long, thin rods, possibly chromosomes or bacterial parasites. Contractile vacuole in or near mid-body at left margin of cell, contents expelled through a slightly curved slit (Fig. 81a, 82v, w). Cortex flexible and rather fragile, without specific granules. Cytoplasm colourless, studded with moderately refractive granules about 1 μm across, some to many food vacuoles up to 30 μm across, and lipid droplets 5–10 μm in size; crystals absent. Contains many spirochetes under frontal membranelles and in narrow posterior end; spirochetes about 10 μm long and deeply impregnating with protargol (Fig. 81a, e, 82h, j, l–p, 83m, o, q, u). Further, 2–3 μm long, deeply impregnating bacteria form aggregates in rather large vacuoles in posterior third of cell (Fig. 81a, 82f, j, k). Feeds on bacteria, green flagellates, and small ciliates (Fig. 81a, 82d, f, m, 83l, n, 84a, b, d). Movement similar to that of oligotrichs, i.e., swims very fast forwards, then suddenly stops swimming backwards for short distances as fast as lightening. Very likely, the frontal adoral membranelles involved in swimming so fast because cirri too thin and sparse.

Somatic ciliature remarkable because sparse and cirri composed of only 2–6 cilia about 15 μm long in vivo; frontal and caudal cirri slightly thickened, the latter 25–30 μm long in vivo (Fig. 81a, c, 82a–d, u, 83e, h). Altogether 20 cirri on average: three subapical frontal cirri in a nearly vertical row; one buccal cirrus subapical of paroral membrane; two short, slightly oblique ventral rows with an average of three cirral pairs showing an indistinct zigzag pattern, commence far subapically and end far subterminally; both marginal rows commence at level of buccal vertex and end far subterminally; right row composed of an average of four cirri, left of three; transverse cirri absent. An average of three “dorsal” bristles in anterior right quadrant of cell, i.e., on margin of ventral side; continue as right row of marginal cirri.

Dorsal infraciliature complex, i.e., three slightly obliquely extending ordinary (“long”) bristle rows commencing about 20 μm subapically and ending about 15 μm subterminally; at right posterior end of each “long” kinety two “short” kineties, each rightmost “short” row generates a 25–30 μm long caudal cirrus together forming a rather thick bundle, caudal cirri 2 and 3 more close than cirri

---

<sup>1</sup> Note by H. Berger: These slides also contain specimens of → *Pseudofuscheria magna*. The sentence “The slide containing the holotype and four paratype slides with protargol-impregnated specimens have been deposited in ...” seems to be not quite correct. I found four slides (one holotype, three paratypes) labelled exclusively with *Conothrix australiensis* (Fig. 34a–f in Chapter 5 of present book). In addition, paratypes of *Conothrix australiensis* are contained in the type slides of → *Pseudofuscheria magna* (Fig. 9a–g in Chapter 5 of present book).

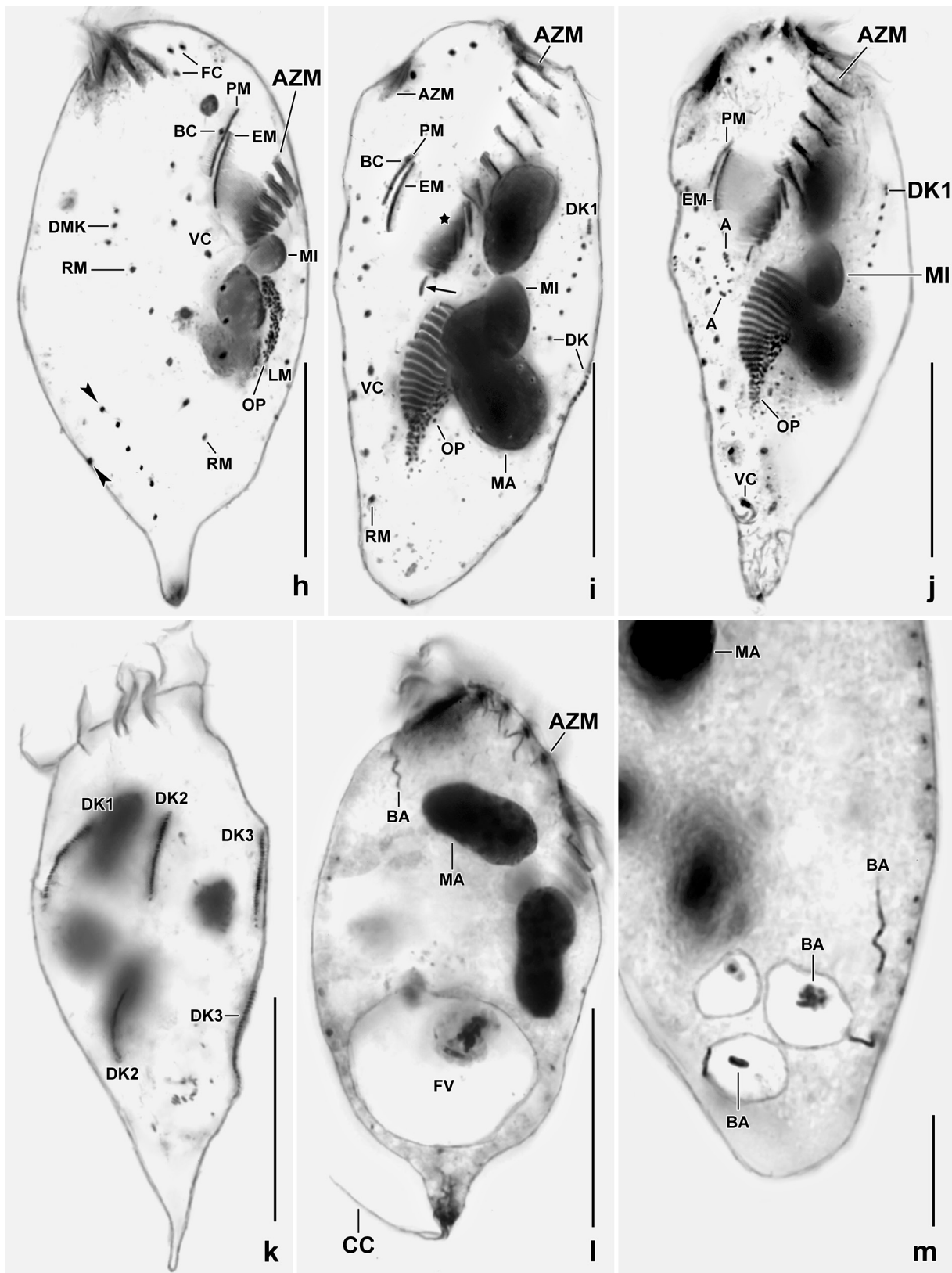


**Fig. 83h–m.** *Conothrix australiensis*, dividing (h–k) and morphostatic specimens (l, m) after protargol impregnation. **h:** Early divider with small oral primordium (see Fig. 83e–g for earlier stages). The arrowheads mark “short” dorsal kineties. **i:** A late early divider, showing developing membranelles in the oral primordium. Anlagen originate in the dorsal kineties. The arrow marks a minute structure associated with the last adoral membranelle. The star denotes the region where the membranelles change direction. **j:** Similar to (i) but cirral Anlagen (A) develop between proter and opisthe. **k:** Dorsal view of a mid-divider, showing that the three dorsal kineties produced Anlagen in proter and opisthe. **l:** A specimen with a large food vacuole in posterior region. **m:** A specimen with three middle-sized

1 and 2; bristles of “long” rows about 3  $\mu\text{m}$  long in vivo, those of “short” rows 2  $\mu\text{m}$ , altogether, i.e., with dorsomarginal kinety 10 bristle rows (Fig. 81c, e, 82a–c, g, i, q, r, t, w; Table 33).

Oral apparatus conspicuous because (i) extending about 40% of body length, (ii) cilia of frontal adoral membranelles 30–35  $\mu\text{m}$  long in vivo, and (iii) due to a conspicuous frontal plate resembling stylonychid Oxytrichidae (Kumar & Foissner 2017). Adoral zone extends to or near to midline of body, on average composed of 19 membranelles with membranelar distance markedly increasing

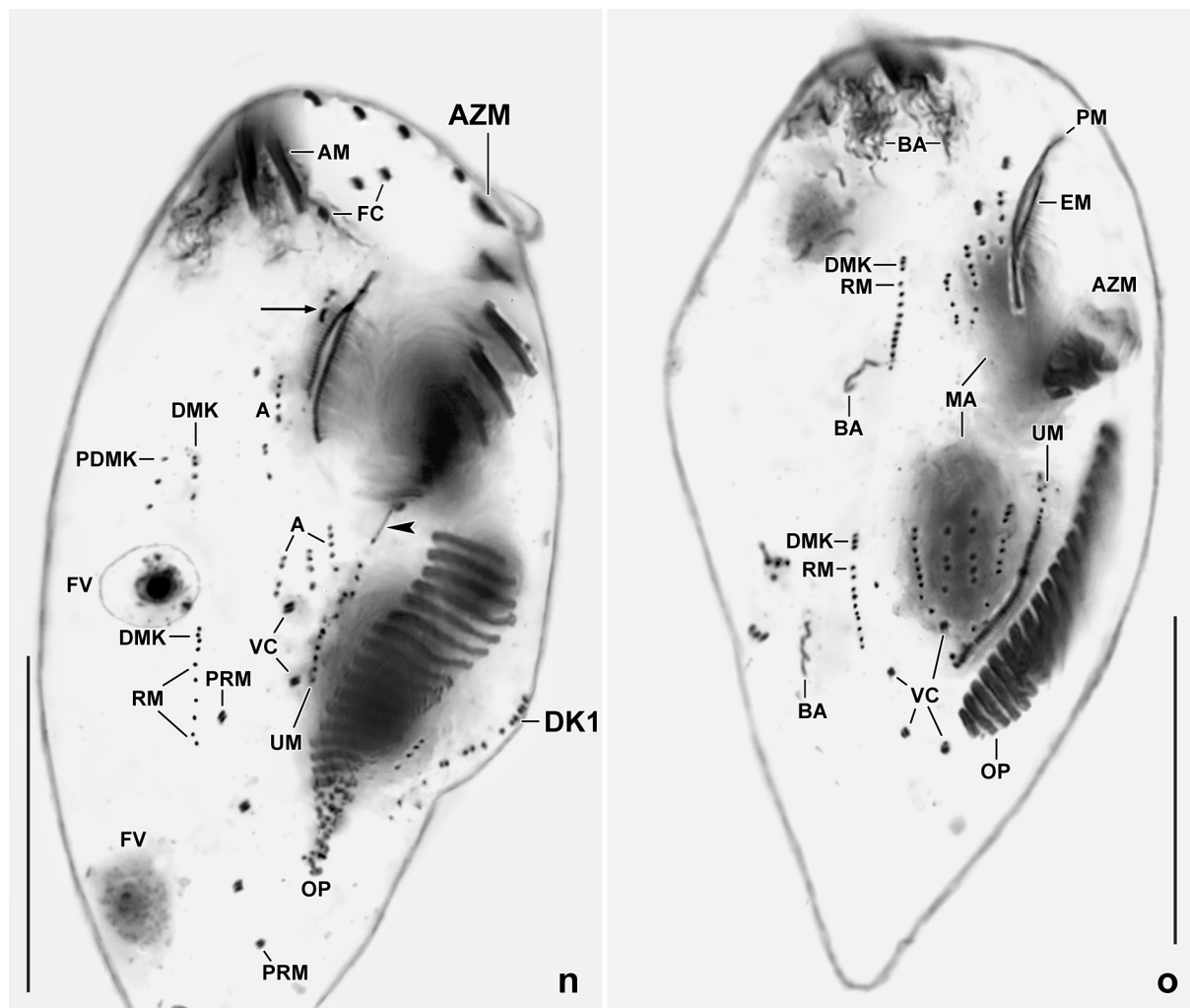


**Fig. 83n, o.** *Conothrix australiensis*, early mid-dividers in protargol preparations. The micrographs show: the de novo origin of the dorsomarginal kinety; the anlagen for the new cirri and undulating membranes are finished earlier in the opisthe than in the proter; four cirral anlagen each develop in proter and opisthe; the adoral membranelles of the oral primordium are almost complete. The arrow in (n) denotes the buccal cirrus which develops to a cirral anlage (o). The arrowhead in (n) marks a minute rod originating from a minute quadrangular structure at the proximal end of the adoral zone of membranelles (cp. Fig. 83i). A – cirral anlagen, AM – adoral membranelles, AZM – adoral zone of membranelles, BA – bacteria, DK1 – dorsal kinety, DMK – dorsomarginal kinety, EM – endoral membrane, FC – frontal cirri, FV – food vacuoles, MA – macronuclear nodules, OP – oral primordium, PDMK1 – parental dorsomarginal kinety, PM2 – paroral membrane, PRM – parental row of right marginal cirri, RM – new right row of marginal cirri, UM – undulating membranes, VC – ventral cirri. Scale bars 30  $\mu\text{m}$ .

← vacuoles containing deeply impregnated, 2–3  $\mu\text{m}$  long bacteria. Some spirochaetes are in the cytoplasm. A – cirral anlagen, AZM – adoral zone of membranelles, BA – bacteria, BC – buccal cirrus, CC – caudal cirri, DK – dorsal kinety, DK1–3 – dorsal kineties, DMK – dorsomarginal kinety, EM – endoral membrane, FC – frontal cirri, FV – food vacuole, LM – left row of marginal cirri, MA – macronuclear nodules, MI – micronucleus, OP – oral primordium, PM – paroral membrane, RM – right row of marginal cirri, VC – ventral cirri. Scale bars 10  $\mu\text{m}$  (m) and 30  $\mu\text{m}$  (h–l).

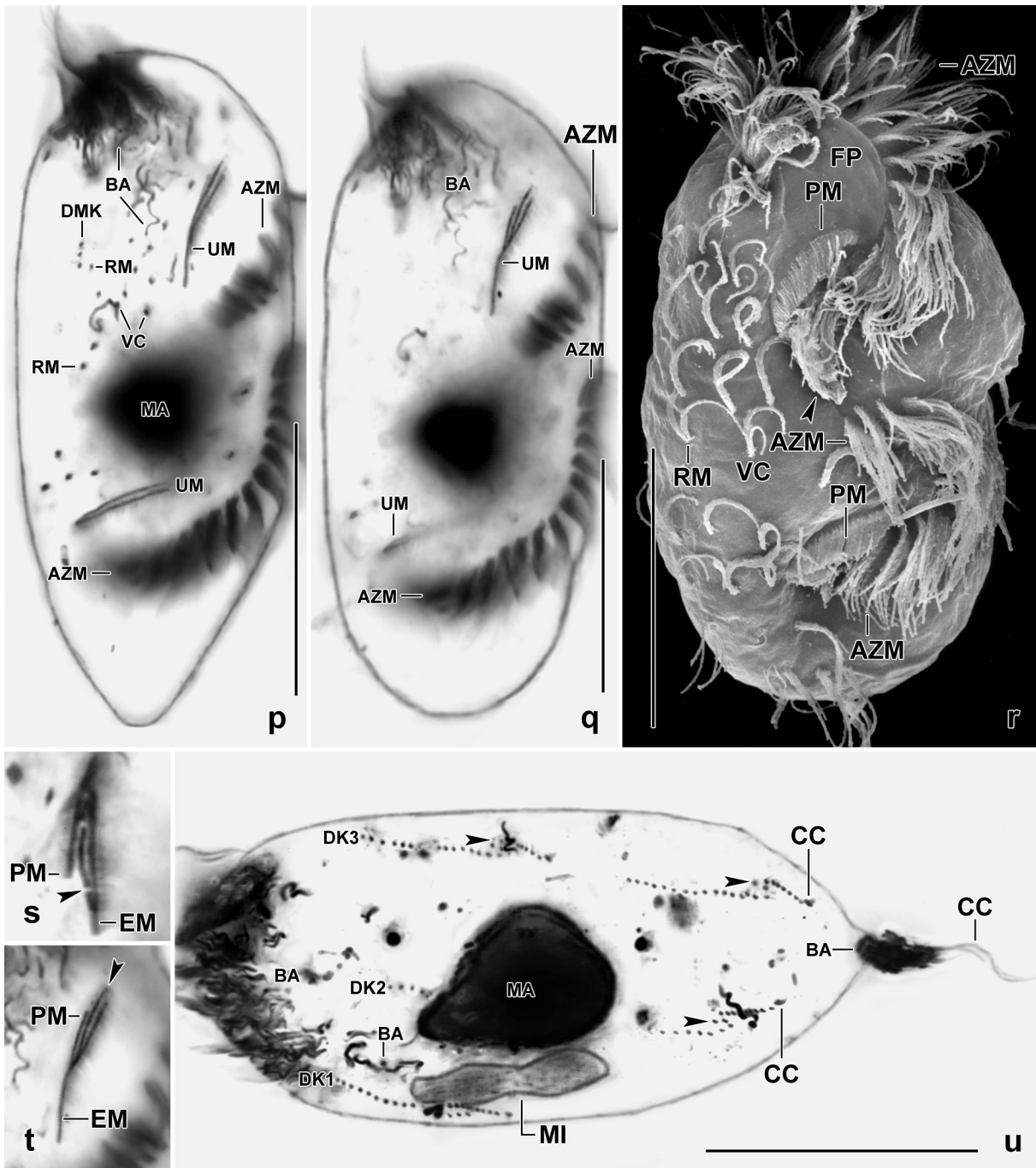
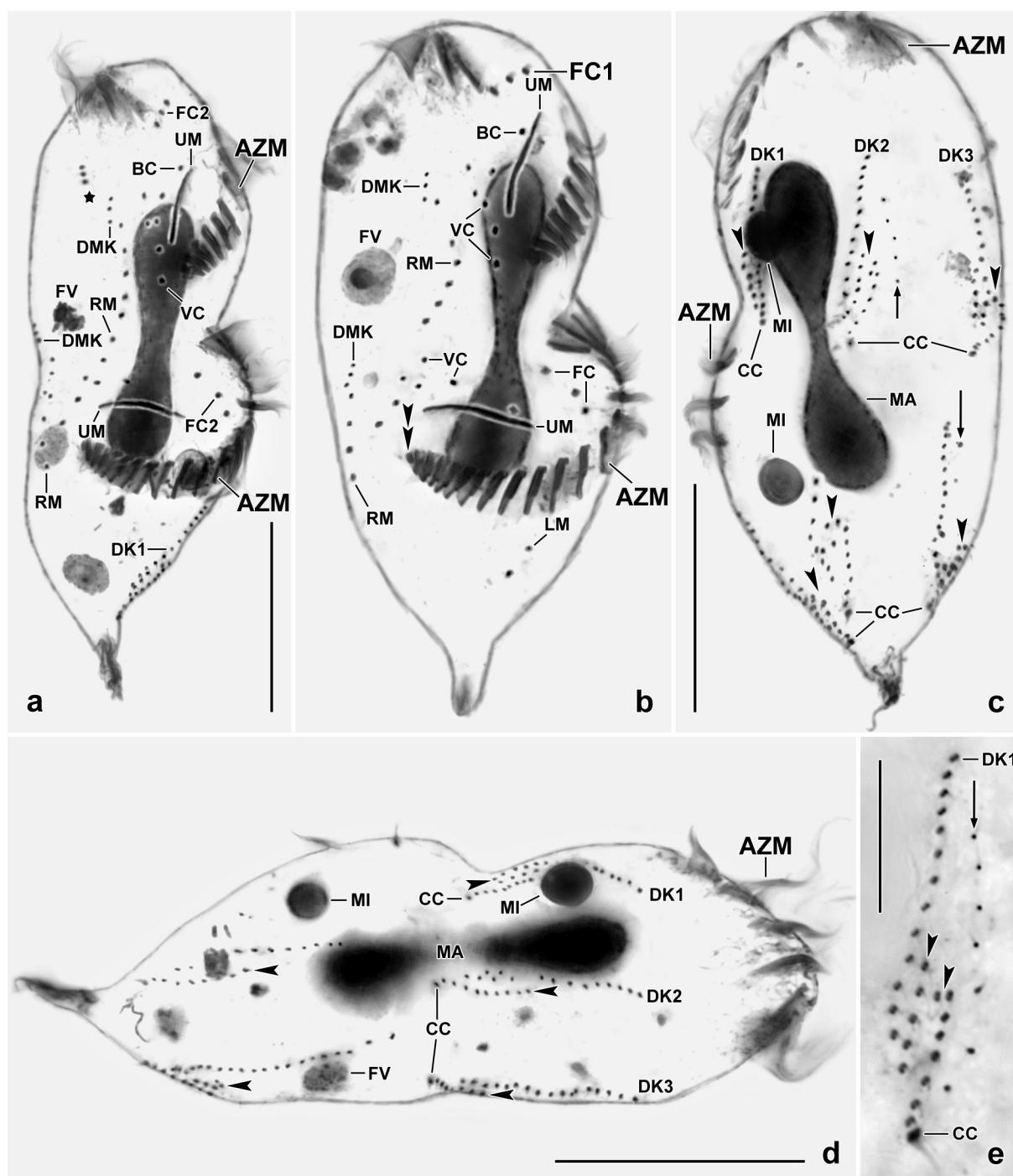


**Fig. 83p–u.** *Conothrix australiensis*, dividers in protargol preparations (p, q, s–u) and in the scanning electron microscope (r). **p–r:** Mid-dividers have fused macronuclear nodules (p, q, u), the micronuclei begin division (u), and the new adoral zone of membranelles becomes horizontally oriented (Fig. 83r, 84f). The arrowhead in (r) marks debris. **s, t:** The endoral membrane of the proter produces a new paroral membrane by lateral proliferation of basal bodies (q, arrowheads in s, t). **u:** Dorsal view of a mid-divider with fused macronuclear nodules, dividing micronucleus, and production of short dorsal kineties (arrowheads). AZM – adoral zone of membranelles, BA – bacteria, CC – caudal cirri, DK1–3 – dorsal kineties, DMK – dorsomarginal kinety, EM – endoral membrane, FP – frontal plate, MA – macronucleus, MI – micronucleus, PM – paroral membrane, RM – right row of marginal cirri, UM – undulating membrane, VC – ventral cirri. Scale bars 30  $\mu\text{m}$ .

**Fig. 84a–e.** *Conothrix australiensis*, early late-dividers in protargol preparations. Ventral view (a), ventral and dorsal view of same specimen (b, c), and dorsal views (d, e). The arrows (c, e) mark remnants of parental dorsal kineties; the arrowheads (c–e) mark “short” dorsal kineties in the posterior half of the long (ordinary) kineties; the doubled arrowhead in (b) denotes a minute, quadrangular structure (adoral membranelle?) associated with a short rod (Fig. 83i). The daughters are almost complete but the proter in (a) still shows the parental dorsomarginal kinety (asterisk). The adoral zone of the opisthe is strongly curved (a, b) while the proter shows the morphostatic pattern. AZM – adoral

from 1–3  $\mu\text{m}$  proximally to 10  $\mu\text{m}$  distally; bases of membranelles about 7  $\mu\text{m}$  (10  $\mu\text{m}$  in vivo) long, proximally only 2–3  $\mu\text{m}$  in protargol preparations; length of cilia decreases from 30–35  $\mu\text{m}$  frontally to 2–3  $\mu\text{m}$  proximally. Individual membranelles basically of ordinary structure but posterior 5–7 membranelles not flat but turned upright; distalmost membranelles composed of only three ciliary rows; last proximal membranelle (?) minute ( $\sim 1 \mu\text{m}$ ) and associated with a deeply impregnating, about 2  $\mu\text{m}$  long rod extending posteriorly (Fig. 81a, c, f, 82a, c, d, q–w, 83a, c, i, n; Table 33). Undulating membranes about 13  $\mu\text{m}$  distant from anterior body end due to frontal plate, side by side and slightly curved, both densely ciliated. Paroral membrane anteriorly slightly to rather



zone of membranelles, BC – buccal cirrus, CC – caudal cirri, DK1–3 – dorsal kineties, DMK – dorsomarginal kinety, FC1, 2 – frontal cirri, FV – food vacuoles, LM – left row of marginal cirri, MA – macronucleus, MI – micronucleus, RM – right row of marginal cirri, UM – undulating membranes, VC – ventral cirri. Scale bars 10  $\mu\text{m}$  (e) and 30  $\mu\text{m}$  (a–d).

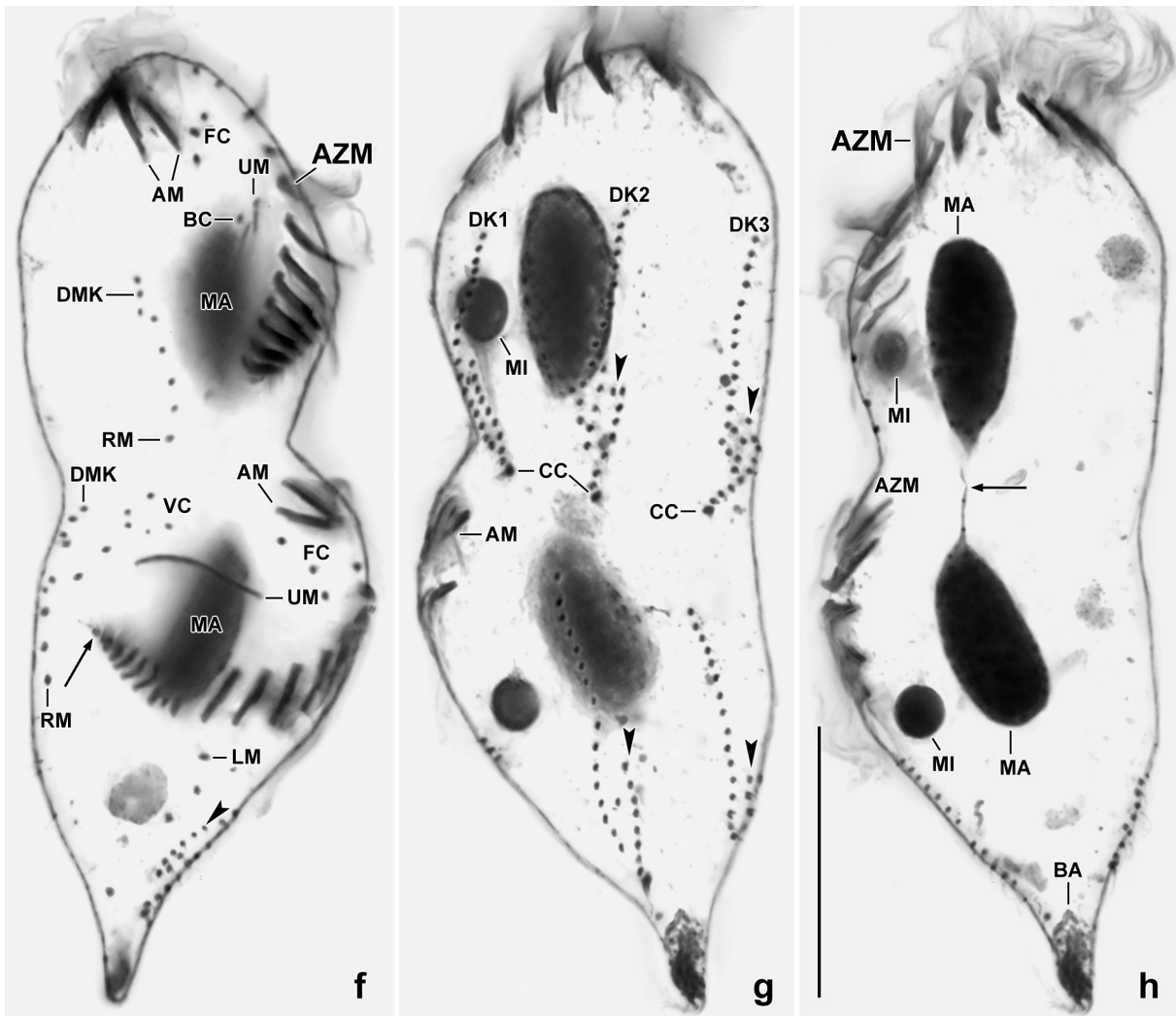


**Fig. 84f-h.** *Conothrix australiensis*, a single, late divider in three focal planes after protargol impregnation. The arrowheads in (f, g) mark “short” dorsal kineties produced by the parental kineties during ontogenesis. **f:** Ventrolateral view, showing two almost fully developed cells except for the opisthe adoral zone of membranelles which is still horizontally oriented in contrast to the vertical orientation in proter and morphostatic cells. The arrow marks a minute quadrangular structure associated with a rod-like process (see also Fig. 83i, n). **g:** Dorsal view showing the new dorsal kineties (DK1–3) while the arrowheads mark the “short” dorsal kineties. **h:** Nuclear apparatus, showing the first division of the macronuclear mass (cp. Fig. 83u) and a fine thread (arrow) connecting the nodules. AM – adoral membranelles, AZM – adoral zone of membranelles, BA – bacteria, BC – buccal cirri, CC – caudal cirri, DK1–3 – dorsal kineties, DMK – dorsomarginal kinety, FC – frontal cirri, LM – left row of marginal cirri, MA – macronuclear nodules, MI – micronuclei, RM – right row of marginal cirri, UM – undulating membranes (paroral and endoral), VC – ventral cirri. Scale bar 30  $\mu\text{m}$ .

distinctly projecting over endoral, projecting portion spoon-shaped in about one third of specimens (Fig. 82c, d), sail-shaped, i.e., cilia in vivo about 10  $\mu\text{m}$  long in anterior third and decreasing to 1–2  $\mu\text{m}$  posteriorly; endoral projecting over paroral posteriorly. Buccal cavity about 10  $\mu\text{m}$  width in protargol preparations, left margin of buccal roof distinctly bulged, a rare pattern as yet found only in psilotrichids (Heber et al. 2014, 2018). Pharyngeal fibres fine, impregnated rarely, extend rectangularly to right body margin (Fig. 81a, c, 82a, c, d, f, u, 83a, b, d–f, h; Table 33).

**Occurrence and ecology:** As yet found only at type locality, i.e., in floodplain soil of Australia. This species very likely lives in the microaerobic bottom plankton, as indicated by the cytoplasmic bacteria and the disappearance when freshwater was added to the non-flooded Petri dish culture. Further, ordinary culture trials failed.

**Remarks:** There is only one described species in vivo highly resembling *Conothrix australiensis*, viz., *Psilotrichides hawaiiensis* (Heber et al. 2014, 2018; Fig. 81b, d, g). They can be clearly distinguished in protargol preparations by the dorsal infraciliature: *C. australiensis* has “long” and “short” dorsal kineties and three caudal cirri while *P. hawaiiensis* has only three “long” kineties and lacks caudal cirri (the elongated last cirrus belongs to left marginal row and is thus not a caudal cirrus). In vivo, the best feature is the posterior body region: distinctly narrowed in *C. australiensis* while bluntly acute in *P. hawaiiensis* (cp. Fig. 81a, c, e, f with 81b, d, g).

**Ventral ontogenesis:** When preserved, the species was in the logarithmic growth phase and thus rather many dividers were present so that the full cycle could be re-constructed. For discussion, see remarks to the diagnoses.

The oral primordium originates in a flat pouch close posterior to the buccal vertex. Concomitantly, the paroral cilia of the proter become disorganized and shorter (Fig. 83e, f). Soon, the oral primordium grows to an oblong structure with disorganized ciliary stumps (Fig. 83g, h). Next, new adoral membranelles and the anlage for the opisthe undulating membranes are produced (Fig. 83i, j, n, o). Concomitantly, four cirral anlagen each are produced in proter and opisthe by the buccal cirrus and some ventral cirri. Further, the dorsomarginal kinety and the right row of marginal cirri originate de novo while the left row of marginal cirri is generated in the ordinary way (Fig. 83n, o). In mid-dividers, which have fused macronuclear nodules, the opisthe oral primordium has produced the anlage for the undulating membranes and most adoral membranelles which form a slightly convex, vertical row. In the proter, a new paroral is generated, very likely by lateral proliferation of basal bodies by the endoral membrane. New cirri are generated in the anlagen (Fig. 83o–t). When cell furrowing commences, the opisthe oral primordium becomes semicircular and extends horizontally in posterior quarters. All cirri have been generated in the anlagen and most moved to the species-specific sites; parental cirri are resorbed. In the proter, the undulating membranes reorganized and are close together (Fig. 84a, b). When furrowing is distinct, the new zone of adoral membranelles is horizontally oriented and the proter undulating membranes are separate. The globular macronuclear mass divided into two nodules connected by a fine strand. The micronucleus also divided (Fig. 84c, d, f, h).

**Dorsal ontogenesis:** *Conothrix australiensis* has three types of dorsal bristle rows: three long rows, as typical for hypotrichs, and two short rows right of the posterior region of each long row. The third type is the ventrally located and de novo generated dorsomarginal kinety (see ventral ontogenesis above).

The dorsal ontogenesis commences in early mid-dividers when the macronuclear nodules are not yet fused. Left of the long rows develop de novo new kineties in the anterior and posterior half of the cell (Fig. 84c, e). The new dikinetids are easily recognizable by their narrow spacing (Fig. 83k). In mid-dividers, the new rows are growing and segregate two short rows in the posterior region of each long row; each rightmost short row forms a caudal cirrus (Fig. 83u, 84c–e). It is unique that all long bristle rows are ontogenetically active and segregate two short kineties.

## Neokeronopsidae Foissner & Stoeck, 2008

### Territrichinae nov. subfam.

**Diagnosis:** Large ( $\geq 150 \mu\text{m}$  in vivo), flexible or rigid Neokeronopsidae Foissner & Stoeck, 2008 often with coloured cortical granules and with *Oxytricha* (18 fronto-ventral-transverse cirri, *Apooxytricha*) or different (*Territricha*, *Apoterritricha*) cirral pattern. Dorsal kinety 3 with multiple fragmentation in posterior half during ontogenesis; the fragments move rightwards to become

ordinary or shortened kineties (*Apoterritricha*), or disperse to scattered dikinetids between kinety 3 and last dorsomarginal kinety (*Territricha*, *Apooxytricha*). Undulating membranes in *Australocirrus* (*Apoterritricha*) or in *Oxytricha* (*Apooxytricha*, *Territricha*) pattern.

**Type genus:** *Territricha* Berger & Foissner, 1988.

**Genera assignable:** *Territricha* Berger & Foissner, 1988; *Apoterritricha* Kim et al., 2014; *Apooxytricha* nov. gen.

**Remarks:** The three genera mentioned form a distinct morphological group within the family Neokeronopsidae Foissner & Stoeck, 2008. The new subfamily differs from the Neokeronopsinae Foissner & Stoeck, 2008 by the cortex (flexible or semirigid) and by the cirral and dorsal bristle pattern.

### ***Apooxytricha* nov. gen.**

**Diagnosis:** Flexible Territrichinae with citrine cortical granules and *Oxytricha* cirral pattern (18 fronto-ventral-transverse cirri). Undulating membranes in *Oxytricha* pattern. During ontogenesis, dorsal kinety 3 produces some small fragments which move rightwards and disperse to scattered dikinetids between kinety 3 and last dorsomarginal kinety.

**Type species:** *Apooxytricha bromelicola* nov. spec.

**Species assignable:** *Apooxytricha bromelicola* nov. spec.

**Etymology:** *Apooxytricha* is a composite of *apo* (derived from) and the genus-group name *Oxytricha*. Feminine gender.

### ***Apooxytricha bromelicola* nov. spec.**

(Fig. 85a–d, 86a–e, 87a–s; Tables 31, 34 on p. 337, 341)

**Diagnosis:** Size in vivo about  $160 \times 60 \mu\text{m}$ . Ellipsoid with distinct indentation where adoral zone enters buccal cavity; about 2:1 flattened; posterior body end bluntly pointed to broadly rounded. Two distinctly separate, ellipsoid macronuclear nodules and an average of three ellipsoid micronuclei. Cortical granules in narrowly spaced rows, colourless, fine, i.e., about  $3.0 \times 0.4 \mu\text{m}$  in vivo. Cirri of appropriate size, transverse cirri, however, 25–30  $\mu\text{m}$  long in vivo and far distant (23%) from body end; posterior end of marginal cirral rows slightly overlapping; buccal cirrus right of anterior end of paroral membrane. Three rows of dorsal bristles on left half of body and three or four rows of dorsomarginal kineties; about 15 scattered dikinetids between bristle rows. Three caudal cirri attached to right posterior end. Adoral zone extends about 35% of body length, composed of an average of 41 membranelles. Buccal cavity narrow and shallow. Undulating membranes slightly convex, optically crossing in anterior third. Resting cyst globular, smooth, ectocyst composed of two thin, brownish layers about 2  $\mu\text{m}$  thick. Macronuclear nodules fused to a globular mass.

**Type locality:** Tanks of the bromeliad *Tillandsia heterophylla* on various trees SE of the town of Coatepec, Veracruz province, Mexico, 19°21'N, 96°47'W. For details, see Durán-Ramírez et al. (2015).

**Type material:** The slide containing the holotype (Fig. 86a) and four paratype slides with protargol-impregnated specimens have been deposited in the Biology Centre of the Upper Austrian Museum in Linz (LI). The holotype and other relevant specimens have been marked by black ink circles on the coverslip. For slides, see Fig. 35a–j in Chapter 5.

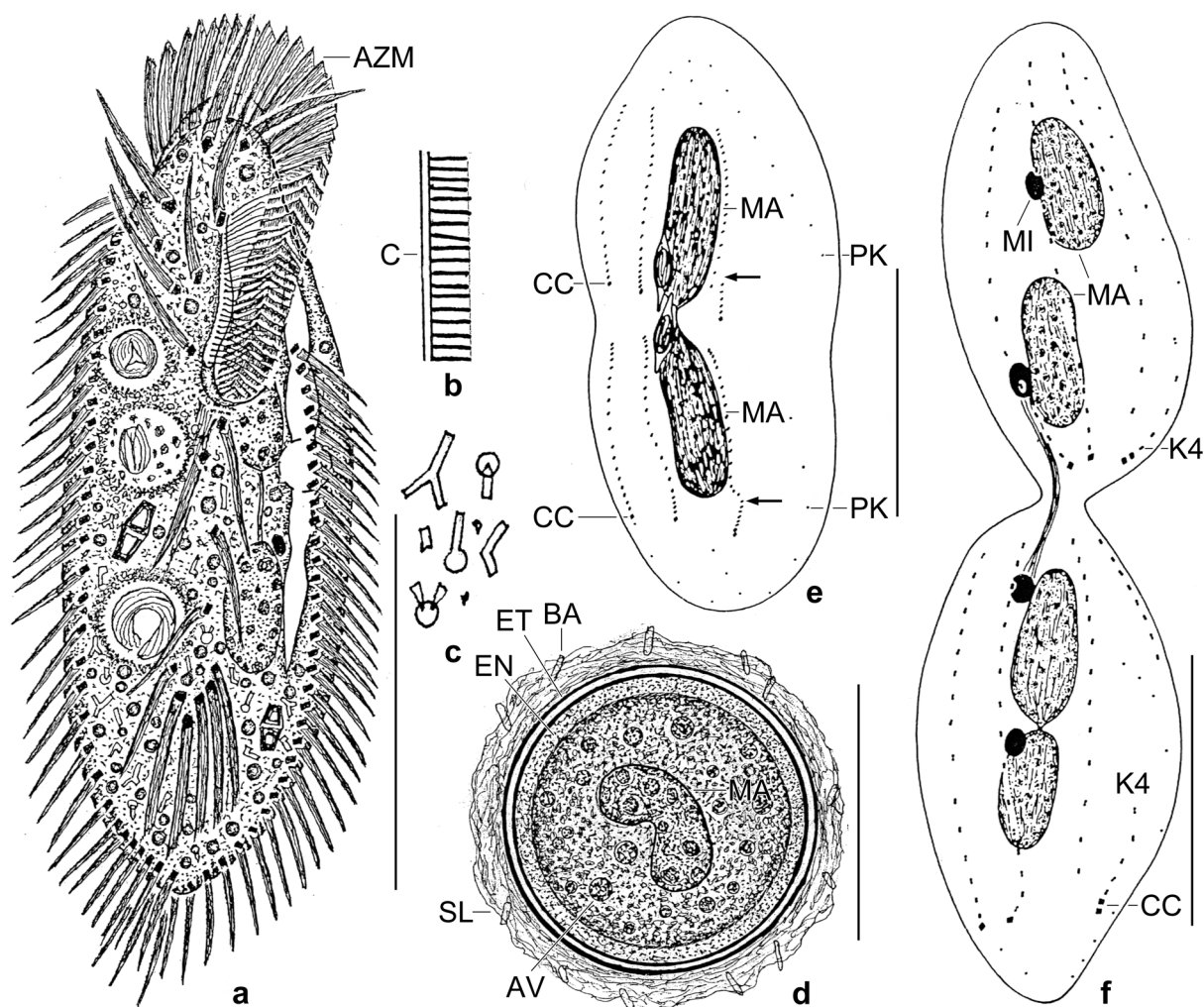


**Fig. 85a–f.** *Apoxytricha bromelicola* (a–d) and dorsal views of dividing *Oxytricha granulifera* (e, f; from Foissner & Adam 1983) from life (a–d) and after protargol impregnation (e, f). **a:** Ventral view of a representative specimen, length 160  $\mu\text{m}$ . The cell is studded with food vacuoles up to 20  $\mu\text{m}$  across and small, slightly orange lipid droplets up to 4  $\mu\text{m}$  in size. Note the far anteriorly placed transverse cirri. **b:** The cortex is densely granulated with rod-shaped mucocysts about  $3.0 \times 0.4 \mu\text{m}$  in size. **c:** Cytoplasmic crystals up to 3  $\mu\text{m}$  in size. **d:** Early resting cyst with many autophagous vacuoles; diameter without slime envelope 50  $\mu\text{m}$  (further details, see description and explanation to Fig. 87i). **e:** A mid-divider with new caudal cirri and splitting dorsal kinety 3 (arrows). **f:** A very late divider, showing that the posterior portion of kinety 3 moved right to become kinety 4. AV – autophagous vacuoles, AZM – adoral zone of membranelles, BA – bacterium, C – cortex, CC – new caudal cirri, EN – endocyst, ET – ectocyst, K4 – dorsal kinety 4, MA – macronuclear nodules, MI – Micronucleus, PK – parental dorsal kineties, SL – slime cover. Scale bars 33  $\mu\text{m}$  (e), 36  $\mu\text{m}$  (f), 40  $\mu\text{m}$  (d), and 80  $\mu\text{m}$  (a).

**Etymology:** The species name is a composite of the genus-group name *Bromelia* (the plant on which the ciliate lives), the thematic vowel *-i-*, and the Latin verb *colere* (to live in), referring to the habitat the species was discovered.

**Description:** Most features of ordinary variability, i.e., with coefficients of variation <15% (Table 34), except of some distances (e.g., posterior body end to right marginal cirral row) and numbers (e.g., micronuclei).

Rather difficult to preserve, tends to become inflated in spite of ethanol-formalin fixation, especially width of body and buccal cavity.

Size in vivo 188  $\times$  84  $\mu\text{m}$  (n = 5, freely motile, rough values; Table 34) or 160  $\times$  60  $\mu\text{m}$  in protargol preparations when 15% preparation shrinkage is added; length:width ratio on average

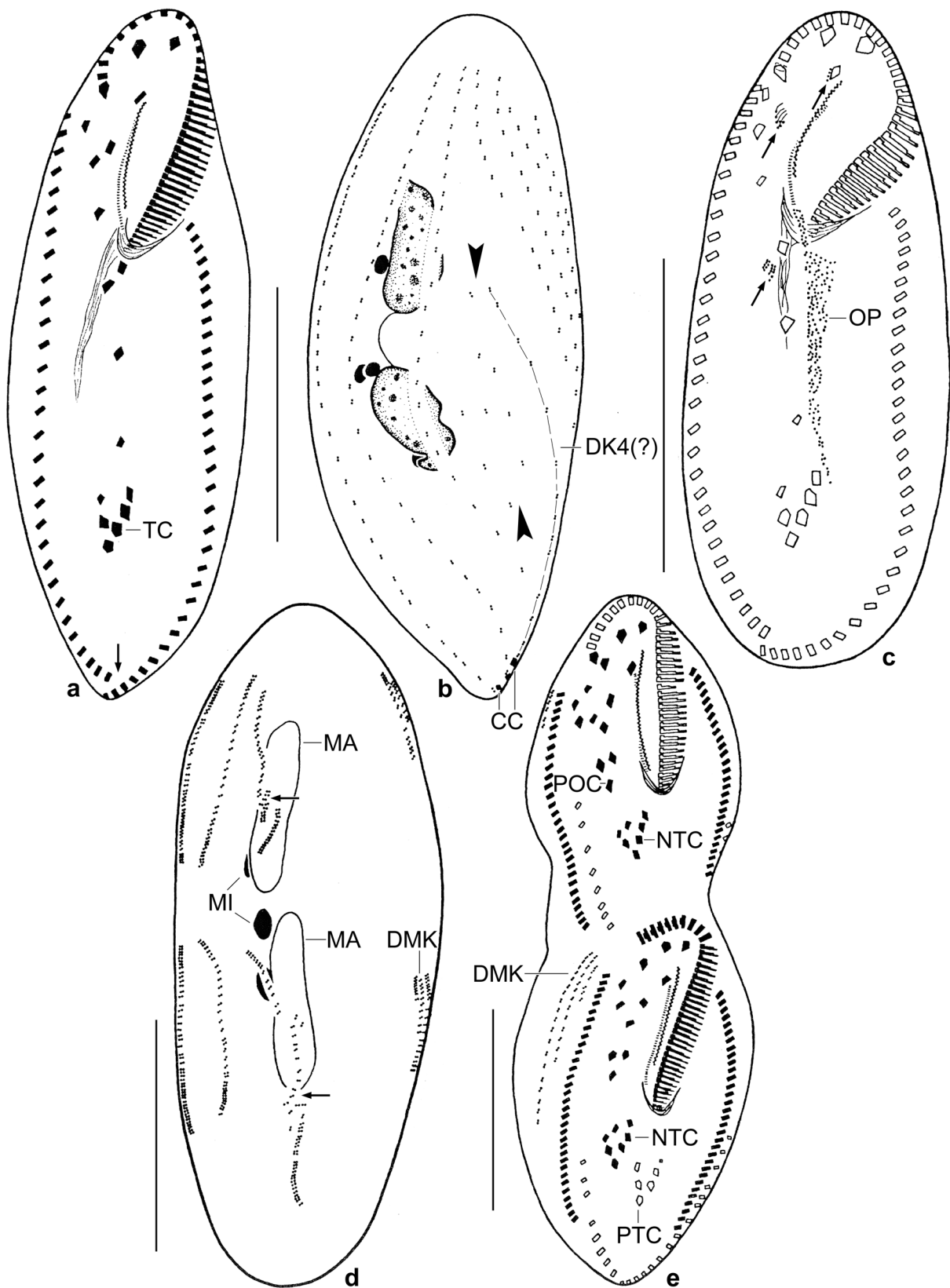


**Fig. 86a–e.** *Apoxytricha bromelicola*, morphostatic (a, b) and dividing (c–e) specimens after protargol impregnation. **a:** Ventral view of holotype specimen, length 135  $\mu\text{m}$ . Note the slightly overlapping marginal cirral rows (arrow). **b:** Dorsal view of a paratype specimen, showing the dispersed kinety 4 (arrowheads). **c:** Ventral view of an early divider with dissolving cirri (arrows) becoming cirral anlagen. **d:** Dorsal view of an early mid-divider where the posterior half of kinety 3 becomes disordered finally producing a field of scattered kinetids between kinety 3 and the last dorsomarginal kinety, as shown in Fig. 86b. **e:** Ventral view of a late divider. CC – caudal cirri, DK4 – dorsal kinety, DMK – dorsomarginal kineties, MA – macronuclear nodules, MI – micronuclei, NTC – new transverse cirri, OP – oral primordium, POC – new postoral cirri, PTC – parental transverse cirri, TC – transverse cirri. Scale bars 50  $\mu\text{m}$ .

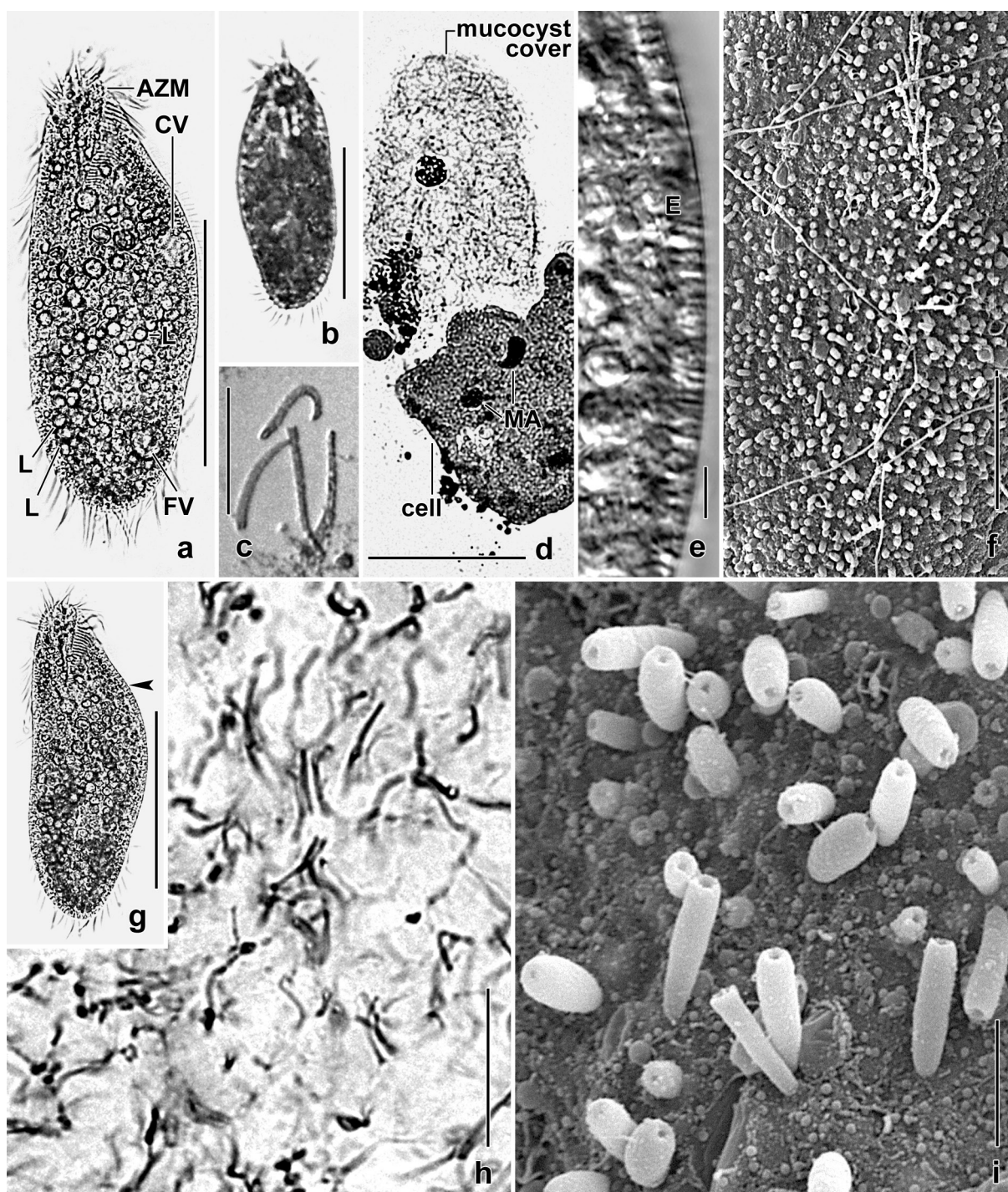


**Fig. 87a–i.** *Apoxytricha bromelicola* from life (a, b, e, g), after methyl green-pyronin staining (c, d, h), and in the SEM (f, i). **a, g:** Ventral views of specimens studded with food vacuoles containing the ciliate *Bromeliothrix*. Arrowhead in (g) marks extrusome fringe. **b:** Dorsal view of a freely motile specimen. **c, h:** Exploded mucocysts. **d:** Cell and mucocyst envelope. **e:** Extrusome fringe. **f, i:** Surface views, showing exploding and exploded mucocysts. AZM – adoral zone of membranelles, CV – contractile vacuole, E – extrusomes, FV – food vacuole, L – lipid droplets, MA – macronuclear nodules. Scale bars 2  $\mu\text{m}$  (i), 4  $\mu\text{m}$  (f), 5  $\mu\text{m}$  (e), 10  $\mu\text{m}$  (c, h), 80  $\mu\text{m}$  (d), 100  $\mu\text{m}$  (a, b, g).

2.7:1 (2.3–3.5:1) in protargol preparations (Table 34). Body shape inconspicuous, i.e., ellipsoid with rather distinct indentation where adoral zone of membranelles enters buccal cavity; posterior body end bluntly pointed to broadly rounded; flattened laterally about 2:1, ventral side flat, dorsal convex (Fig. 85a, 86a, b, 87a, b, g, j, r). Nuclear apparatus in or slightly anterior of central third of cell and in or slightly left of main body axis (Fig. 85a, 86b, 87k, p; Table 34). Invariably two

ellipsoid to elongate ellipsoid macronuclear nodules connected by a fine, argyrophilic strand; in vivo about  $25 \times 15 \mu\text{m}$ ; many minute nucleoli. On average, three globular to bluntly ellipsoid micronuclei in vivo about  $5 \times 4 \mu\text{m}$  attached or near macronuclear nodules. Contractile vacuole in left margin of mid-body, with two lacunar collecting canals. Cortex and cell very flexible. Cortical granules in narrowly spaced rows not always recognizable because very narrowly spaced,

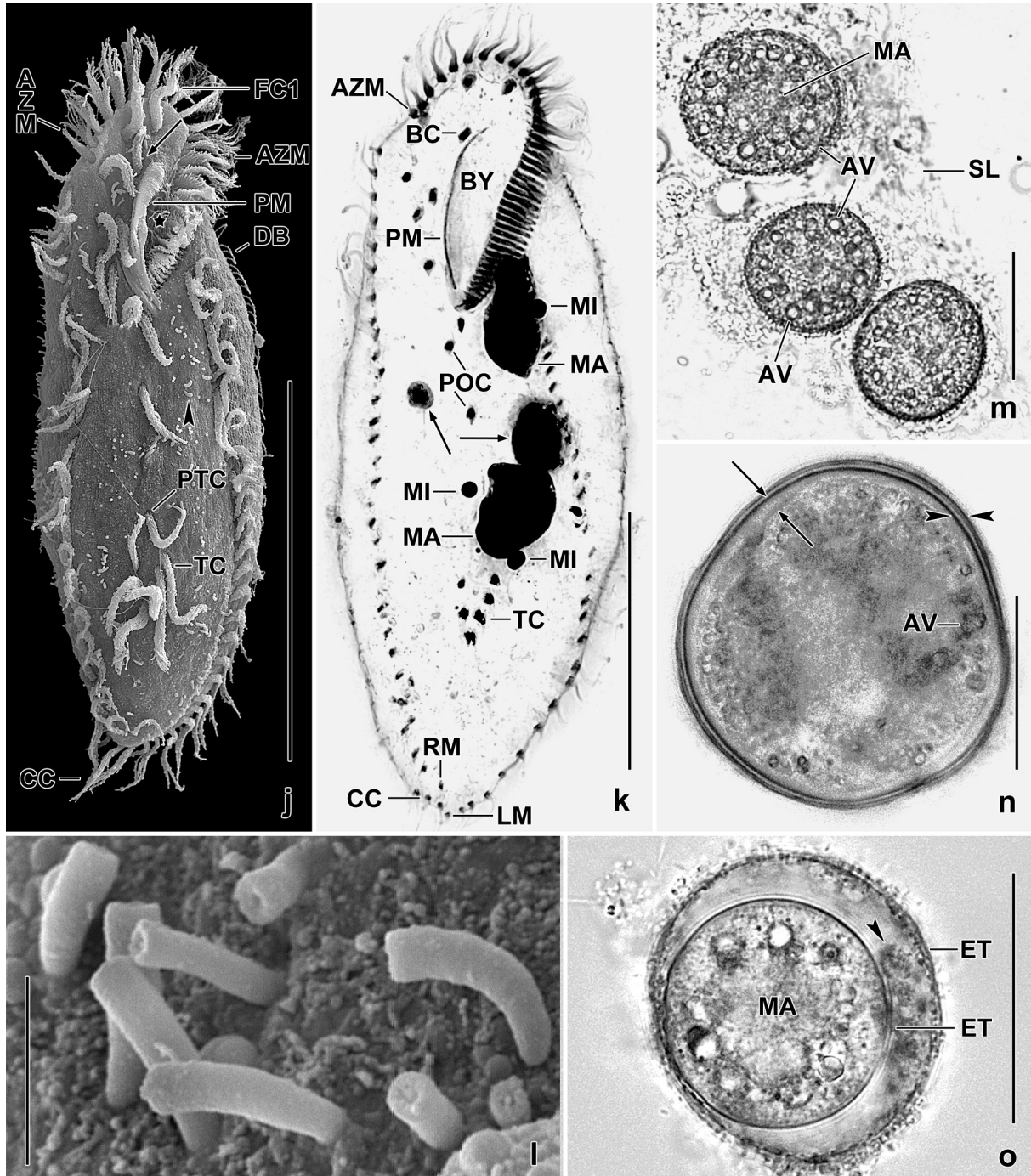


**Fig. 87j–o.** *Apoxytricha bromelicola* from life (m–o), after protargol impregnation (k), and in the scanning electron microscope (j, l). **j, k:** Ventral view of representative specimens, showing the far anteriorly placed transverse cirri and the narrow buccal cavity (star in j), which is slightly inflated in (k). The arrow in (j) marks the buccal cirrus while the arrowhead denotes exploding mucocysts. The arrows in (k) mark argyrophilic food vacuoles. **l:** Exploding and exploded mucocysts with concave distal end. **m:** Young resting cysts are embedded in slime and have many autophagous vacuoles. **n:** Young resting cyst. The opposed arrowheads mark the brownish ectocyst while the opposed arrows denote a bright, structureless zone, possibly the endocyst. **o:** Old cysts frequently have two ectocysts with granular material in between

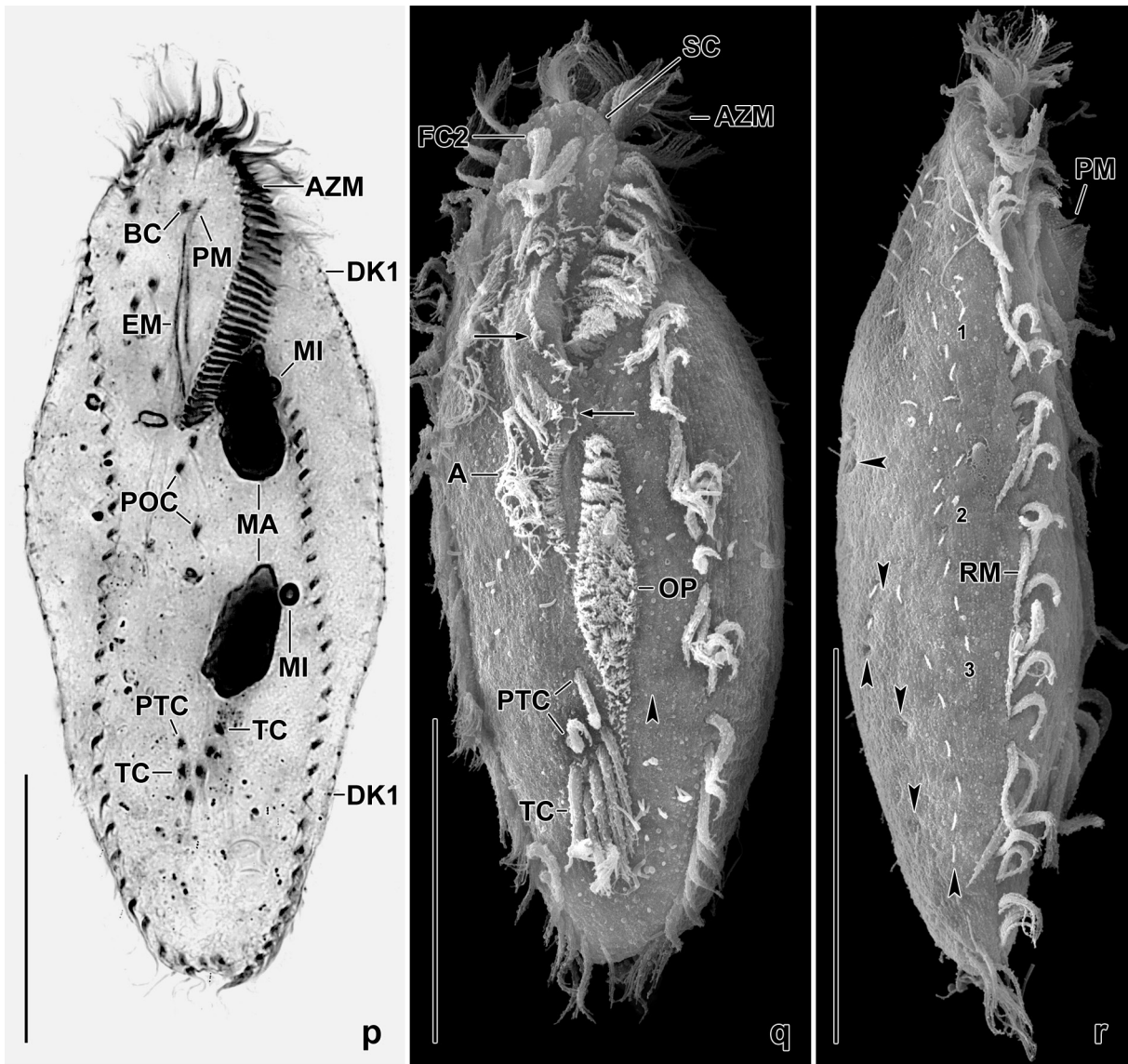
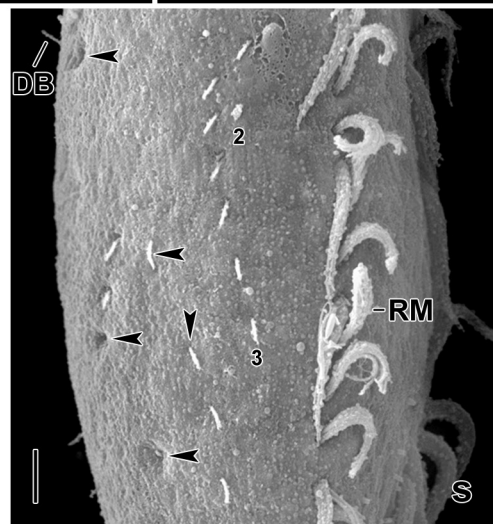


**Fig. 87p-s.** *Apoxytricha bromelicola* after protargol impregnation (p) and in the scanning electron microscope (q-s). **p:** Ventral infraciliature and nuclear apparatus. Note the far anteriorly placed transverse cirri and the buccal cirrus in the corner formed by the anterior end of the undulating membranes. **q:** Ventral view of an early mid-divider, showing the opisthe's oral primordium, cirral anlagen, and an anlage streak (arrows) originating from the oral primordium and becoming the anlage for the proter's undulating membranes. The arrowhead marks exploding mucocyst rows. **r, s:** Right lateral views, showing dorsomarginal kineties (numerals 1-3) and scattered dorsal bristles between dorsal kinety 3 and dorsomarginal kinety 3. A - anlagen, AZM - adoral zone of membranelles, BC - buccal cirrus, DK1 - dorsal kinety 1, EM - endoral membrane, FC2 - frontal cirrus 2, MA - macronuclear nodules, MI - micronuclei, OP - oral primordium, PM - paroral membrane, POC - postoral cirri, PTC - pretransverse cirri, RM - right marginal cirral rows, SC - scutum, TC - transverse cirri. Scale bars 5  $\mu$ m (s), 50  $\mu$ m (p-r).



← (arrowhead). AZM - adoral zone of membranelles, AV - autophagous vacuoles, BC - buccal cirrus, BY - buccal cavity, CC - caudal cirri, DB - row of dorsal bristles, ET - ectocyst, FC1 - first frontal cirrus, L - left row of marginal cirri, MA - macronuclear nodules, MI - micronuclei, PM - paroral membrane, POC - postoral cirri, PTC - pretransverse cirri, RM - right row of marginal cirri, SL - slime. Scale bars 2  $\mu$ m (l) and 50  $\mu$ m (j, k, m-o).

produce a moderately distinct fringe though colourless, thin and short, i.e., about  $3.0 \times 0.4 \mu\text{m}$  in vivo (Fig. 85b, 87a, e, g); do not impregnate with the method used. When methyl green-pyronin is added, they stain red and transform to about  $10 \mu\text{m}$  long, wrinkled cones forming a thin cover on cell (Fig. 87d, h), composed of a thin wall surrounding a rather dense content (Fig. 87c). Exploding cortical granules ellipsoid and quickly transforming to straight or curved cones with concave anterior end in the scanning electron microscope (Fig. 87f, i, j, l). Cytoplasm usually studded with food vacuoles up to  $25 \mu\text{m}$  across in protargol preparations; with many slightly orange lipid(?) droplets  $1\text{--}3 \mu\text{m}$  across in vivo providing cells with an orange shimmer in the bright field microscope; and crystals mainly in posterior half of cell (Fig. 85a, c, 87a, g). Feeds on a variety of items preferring *Bromelothrix metopoides*, a small, bromeliad-specific ciliate (Foissner 2010a). Further, flagellates (*Polytomella*) and euglenoids (*Peranema*, moves five or more minutes in the food vacuoles) have been observed in the food vacuoles; in cultures, also feeds on bacteria, fungal spores, and starch grains. Glides moderately fast on microscope slides and in mud, showing great flexibility.

Cirri in *Oxytricha* pattern with three remarkable specializations (Fig. 85a, 86a, b, 87j, k, p; Table 34): (i) transverse cirri thickened and placed far anteriorly (23% of body length on average or  $31 \mu\text{m}$  distant from body end) never protruding from body proper though  $25\text{--}30 \mu\text{m}$  long in vivo, distal end fringed; (ii) marginal cirral rows slightly overlapping posteriorly (Fig. 85a, 86a, c, 87k); (iii) buccal cirrus slightly anterior or posterior to anterior end of paroral membrane, on average at same level, i.e.,  $13.5 \mu\text{m}$  distant from anterior body end (Table 34). Frontal, ventral, and postoral cirri slightly thickened, these and marginal cirri about  $20 \mu\text{m}$  long in vivo.

Dorsal bristles  $4\text{--}5 \mu\text{m}$  long in vivo, arranged as described in diagnosis of genus, viz., three bipolar kineties in left half of cell and posteriorly curved to right margin; each kinety associated with an about  $25 \mu\text{m}$  long, fine, and lively beating caudal cirrus. Three, rarely four dorsomarginal kineties in right half of cell. About 15 scattered dikinetids between bipolar and dorsomarginal kineties (Fig. 86b, 87r, s; Table 34).

Oral apparatus in *Oxytricha* pattern, of ordinary size, i.e., extends on average 35% of body length, consist of about 41 membranelles with ordinary shape and structure, however, largest membranelar bases only about  $12 \mu\text{m}$  wide in vivo and  $8 \mu\text{m}$  in protargol preparations, i.e., narrow compared to size of body and oral apparatus. Buccal cavity also narrow and shallow. Paroral and endoral membrane optically side by side slightly overlapping or crossing in anterior third; paroral cilia about  $8 \mu\text{m}$  long in vivo, endoral cilia extend into cytopharynx but do not perform wave-like movements. Buccal lip slightly convex, of angular type (Foissner & Al-Rasheid 2006). Pharyngeal fibres extend to or slightly posterior to mid-body (Fig. 85a, 86a, 87a, j, k, p; Tables 31, 34).

**Resting cyst:** Without slime cover about  $50 \times 48 \mu\text{m}$  across in vivo, i.e., on average almost globular and very slightly green-yellow due to the brownish ectocyst (Fig. 85d, 87m, n; Table 34); colour disappears in squeezed cysts. Young cysts covered by an about  $10 \mu\text{m}$  thick slime layer almost disappearing in old cysts (Fig. 87m, n); slime layer colonized by various bacteria, stains red with methyl green-pyronin. Ectocyst smooth, about  $2 \mu\text{m}$  thick, composed of two brownish membranes; followed by a  $1\text{--}2 \mu\text{m}$  thick, bright zone, possibly the endocyst. Old cysts frequently with double ectocyst, usually with a granular heap between walls (Fig. 87o). Macronuclear nodules fused to an irregular mass (Fig. 85d, 87m, o). Cytoplasm of young cysts studded with autophagous vacuoles  $3\text{--}6 \mu\text{m}$  in diameter (Fig. 85d, 87m, n).

**Ontogenesis:** On the ventral side, the ontogenesis of the oral apparatus and the cirral pattern is highly similar to that described for *Oxytricha granulifera*, type species of the genus (for a review, see Berger 1999). Thus, only some key stages are shown. The ontogenesis commences with the proliferation of basal bodies left and slightly anterior of the uppermost transverse cirrus. Further proliferation of basal bodies produces the oral primordium extending from the uppermost transverse

cirrus to the buccal vertex where the primordium has a short streak in the right corner contacting the parental undulating membranes (Fig. 86c). Concomitantly, the buccal cirrus, frontoventral cirrus III/2, and the second postoral cirrus transform to cirral anlagen (Fig. 86c, 87q). The further process, e.g., the production of cirri and their migration to the species-specific sites are shown in Fig. 86e.

The dorsal ontogenesis basically matches the *Oxytricha* mode, i.e., the three bipolar bristles rows on the left half of the cell develop three anlagen each in proter and opisthe (Fig. 85e, f). Concomitantly, three (rarely four) dorsomarginal kineties are generated in proter and opisthe at the anterior end of the right marginal cirral rows (Fig. 86d, e). The anlagen in row 3 show disordered, multiple fragmentation and are slightly longer than those in rows 1 and 2; they migrate rightwards and disperse to scattered dikinetids in midline of body (Fig. 86b, 87r, s). This is rather different to the usual *Oxytricha* mode and a main character of the genus *Apooxytricha* (Fig. 85e, f).

**Occurrence and ecology:** Rare, i.e., as yet found only at type locality. Grows weakly in ordinary cultures with tank water and squeezed wheat grains.

**Remarks:** In vivo, *Apooxytricha bromelicola* is difficult to separate from several middle-sized or large oxytrichids (Table 31). The best features are the far anteriorly placed transverse cirri, the rather large body size, the colourless cortical granules, and the habitat.

***Monomicrocaryon australiense* nov. spec.**

(Fig. 88a–e, g, 89a–f; Table 35 on p. 342)

**Diagnosis:** Size in vivo about  $150 \times 50 \mu\text{m}$ ; parallel-sided or slightly ellipsoid. Buccal cirrus subapical of paroral membrane, last frontoventral cirrus at level of buccal vertex; transverse cirri thickened, about  $40 \mu\text{m}$  long in vivo, do not project from body proper because about 22% anterior from body end. Dorsal bristles 4–5  $\mu\text{m}$  long, arranged in seven kineties with kinety 6 in posterior third of cell and kinety 7 in anterior third; scattered bristles (short kineties?) between kineties 2 and 3. Three comparatively thick caudal cirri 35–40  $\mu\text{m}$  long in vivo. Adoral zone extends about 30% of body length, composed of an average of 25 membranelles with bases up to 10  $\mu\text{m}$  width. Buccal cavity in vivo narrow and flat; paroral and endoral membrane slightly curved and optically one upon the other or close together.

**Type locality:** Australian site (159), i.e., upper, dark brown soil mixed with red gum leaves from the Murray River floodplain below the Hume Dam, Caravan Park, Australia,  $36^{\circ}06'16.0''\text{S}$ ,  $147^{\circ}01'51.3''\text{E}$ .

**Type material:** The slide containing the holotype (Fig. 88b, c) and six paratype slides with protargol-impregnated specimens have been deposited in the Biology Centre of the Upper Austrian Museum in Linz (LI). The holotype and relevant paratype specimens have been marked with black ink circles on the coverslip. For slides, see Fig. 36a–i in Chapter 5.

**Etymology:** Named after the continent found, i.e., Australia.

**Description:** The cortex of *Monomicrocaryon australiense* is rather fragile. Thus, the cells are more or less inflated and wrinkled in the protargol preparations (CV of, e.g., body width on average 16.4; Table 35). Further, the abundance was low. Thus, the dorsal kinety pattern was difficult to study and might be not entirely correct.

The variability is low, i.e., of the 35 features investigated only 10 have a coefficient of variation >15%, and none of these is a diagnostic feature.

Size in vivo  $110\text{--}170 \times 30\text{--}50 \mu\text{m}$ , usually about  $150 \times 50 \mu\text{m}$ , as calculated from in vivo measurements and the morphometric data in Table 35 adding 15% preparation shrinkage. Body elongate ellipsoid or parallel-sided with both ends broadly rounded; moderately flattened laterally

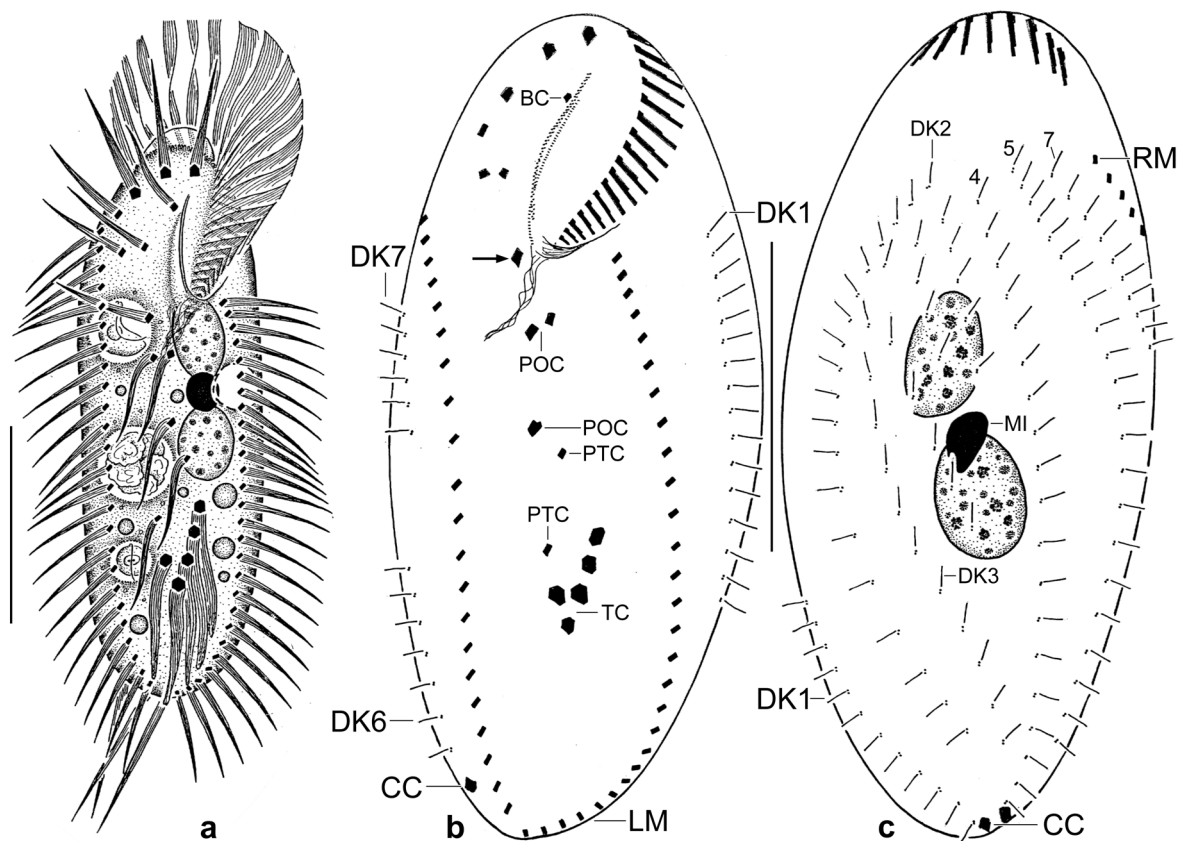


**Fig. 88a–c.** *Monomicrocaryon australiense* from life (a) and after protargol impregnation (b, c). **a:** Ventral view of a representative specimen, length 150  $\mu\text{m}$ . **b, c:** Ventral and dorsal view of holotype specimen, length 137  $\mu\text{m}$ . The arrow marks the last frontoventral cirrus at level of buccal vertex. Note the far anteriorly located transverse cirri, a main feature of this species. Dorsal kinety 6 and leftmost caudal cirrus are recognizable in figure (b). BC – buccal cirrus, CC – caudal cirri, DK1–7 – dorsal kineties, LM – left marginal cirral row, MI – micronucleus, POC – postoral cirri, PTC – pretransverse cirri, RM – right marginal cirral row, TC – transverse cirri. Scale bars 50  $\mu\text{m}$ .

(Fig. 88a, g). Nuclear apparatus in or slightly anterior of mid-body, in vivo conspicuous because comparatively large and the highly refractive micronucleus (Fig. 88a, c, e, 89a–d, f; Table 35). Macronuclear nodules about  $25 \times 15 \mu\text{m}$  in vivo, distance between nodules highly variable, i.e., 2–8  $\mu\text{m}$ , on average 5.3  $\mu\text{m}$  in protargol preparations; many small, globular nucleoli. Micronucleus in between macronuclear nodules, in vivo conspicuous because highly refractive and  $8\text{--}12 \times 7\text{--}10 \mu\text{m}$  in size, and thus usually slightly overlapping one or both macronuclear nodules (Fig. 88e, 89a–d, f). Contractile vacuole anterior of mid-body at left cell margin (Fig. 88a). Cortex fragile and thus difficult to preserve, without specific granules. Cytoplasm colourless, contains food vacuoles up to 30  $\mu\text{m}$  across and, mainly in posterior half, many bright lipid droplets 1–10  $\mu\text{m}$  in size (Fig. 89f); crystals absent. Feeds on ciliates, flagellates, and a euglenoid. Creeps slowly on microscope slides, when swimming rotates about main body axis.

Cirral pattern oxytrichid, i.e., 18 fronto-ventral-transverse cirri; all cirri conspicuously long and thus distinct in vivo (Fig. 88a, b, d, 89a, b; Table 35). Frontal cirri in vivo about 35  $\mu\text{m}$  long, moderately thick, cirrus 3 at level of buccal cirrus subapical of paroral membrane. Last frontoventral cirrus slightly thickened and at level of buccal vertex. Transverse cirri on average 22% anterior of body end, distinctly thickened and up to 40  $\mu\text{m}$  long in vivo, do not project from body proper. Marginal cirral rows almost abutting posteriorly, up to 30  $\mu\text{m}$  long, each composed of three rows of basal bodies (Fig. 88a, b, d, 89a, b; Table 35).

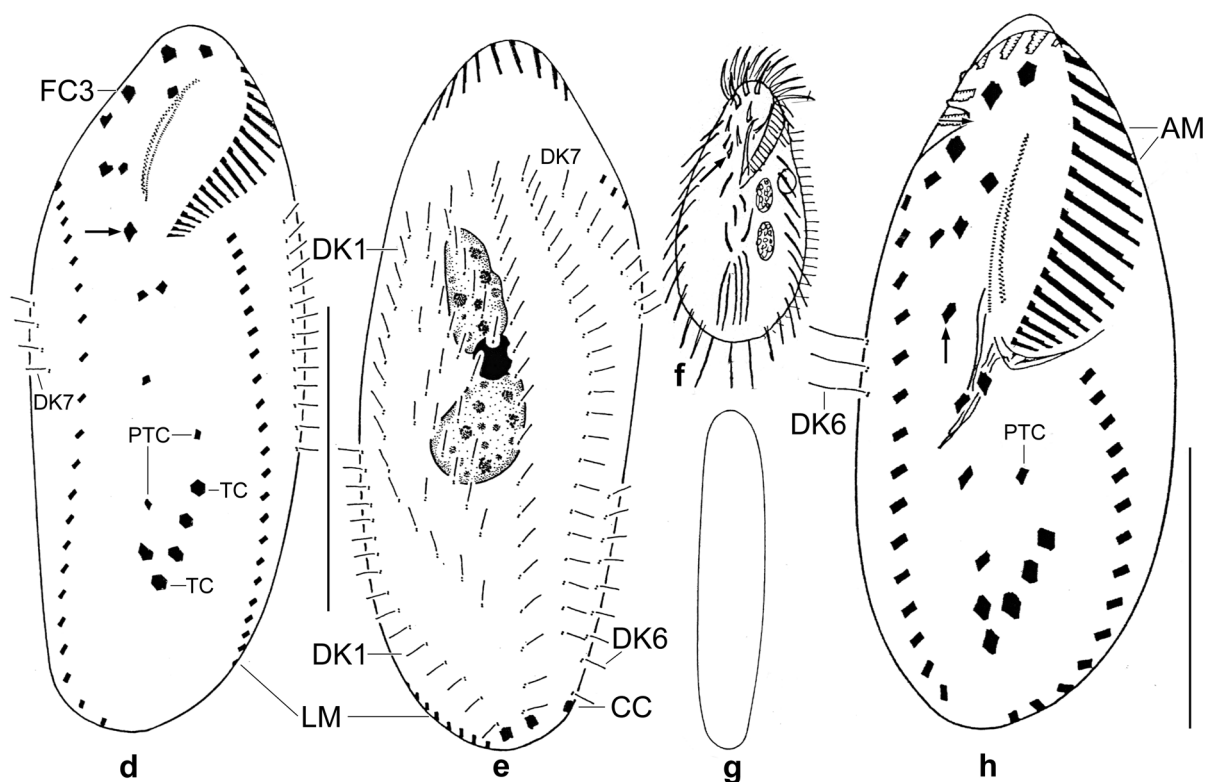


**Fig. 88d–h.** *Monomicrocaryon australiense* (d, e, g), *M. kablovata* (f, from Berger 1999) and *M. crassicirratum* (h, from Foissner 2016) from life (f) and after protargol impregnation (d, e, g, h). **d, e:** Ventral and dorsal view of a paratype specimen. The arrow marks the last frontoventral cirrus at level of buccal vertex. Note the far anteriorly located transverse cirri, a main feature of this species. **f:** This species is 100–120  $\mu\text{m}$  long and has the last frontoventral cirrus (arrow) at level of midbuccal cavity. **g:** Lateral view. **h:** Ventral view. This species resembles *M. australiense* but has, inter alia, a much larger adoral zone of membranelles and the last frontoventral cirrus is slightly anterior of the buccal vertex (arrow). AM – adoral membranelles, CC – caudal cirri, DK6, 7 – dorsal kineties, FC3 – frontal cirrus, LM – left marginal cirral row, PTC – pretransverse cirri, TC – transverse cirri. Scale bars 40  $\mu\text{m}$  (h) and 50  $\mu\text{m}$  (d, e).

Dorsal bristles 3–4  $\mu\text{m}$  long in vivo, likely arranged in seven rows with several peculiarities (Fig. 88b–e; Table 35): (i) all kineties commence far subapical; (ii) a field of scattered bristles between kineties 2 and 3, possibly produced by kinety 2 slightly shortened posteriorly; (iii) kinety 6 extends in posterior third, possibly produced by kinety 5; (iv) kinety 7 extends in anterior body half, likely produced dorsomarginally; and (v) three lively beating, comparatively thick caudal cirri 35–40  $\mu\text{m}$  long in vivo (Fig. 88a–c, 89e).

Oral apparatus extends 30% of body length on average (Fig. 88a, b, d, 89a, b; Table 35). Adoral zone of ordinary shape and structure, twisted in proximal third and thus appearing narrower than it is, composed of an average of 25 rather widely spaced membranelles with largest bases about 10  $\mu\text{m}$  wide in vivo, cilia of frontal membranelles about 35  $\mu\text{m}$  long. Buccal cavity narrow and flat, widened by the preparation procedures; buccal lip also narrow. Paroral and endoral membrane slightly curved and optically one upon the other or close together.

**Occurrence and ecology:** As yet found only at type locality, i.e., floodplain soil from the Murray River, Australia.

**Remarks:** There is only one congener, *Monomicrocaryon kablovata* (Berger, 1999) Foissner, 2016, that has the transverse cirri so far anteriorly as *M. australiense* (Fig. 88f). The two species differ by body shape (distinctly obovate vs. parallel-sided), the last frontoventral cirrus (at level of mid buccal cavity vs. buccal vertex), body size (in vivo 100–120  $\mu\text{m}$  vs. 120–170  $\mu\text{m}$ ), and the transverse cirri (thin vs. thick). Unfortunately, the original description of *M. kablovata* by Kahl (1932, as *Oxytricha (Opisthotricha)*

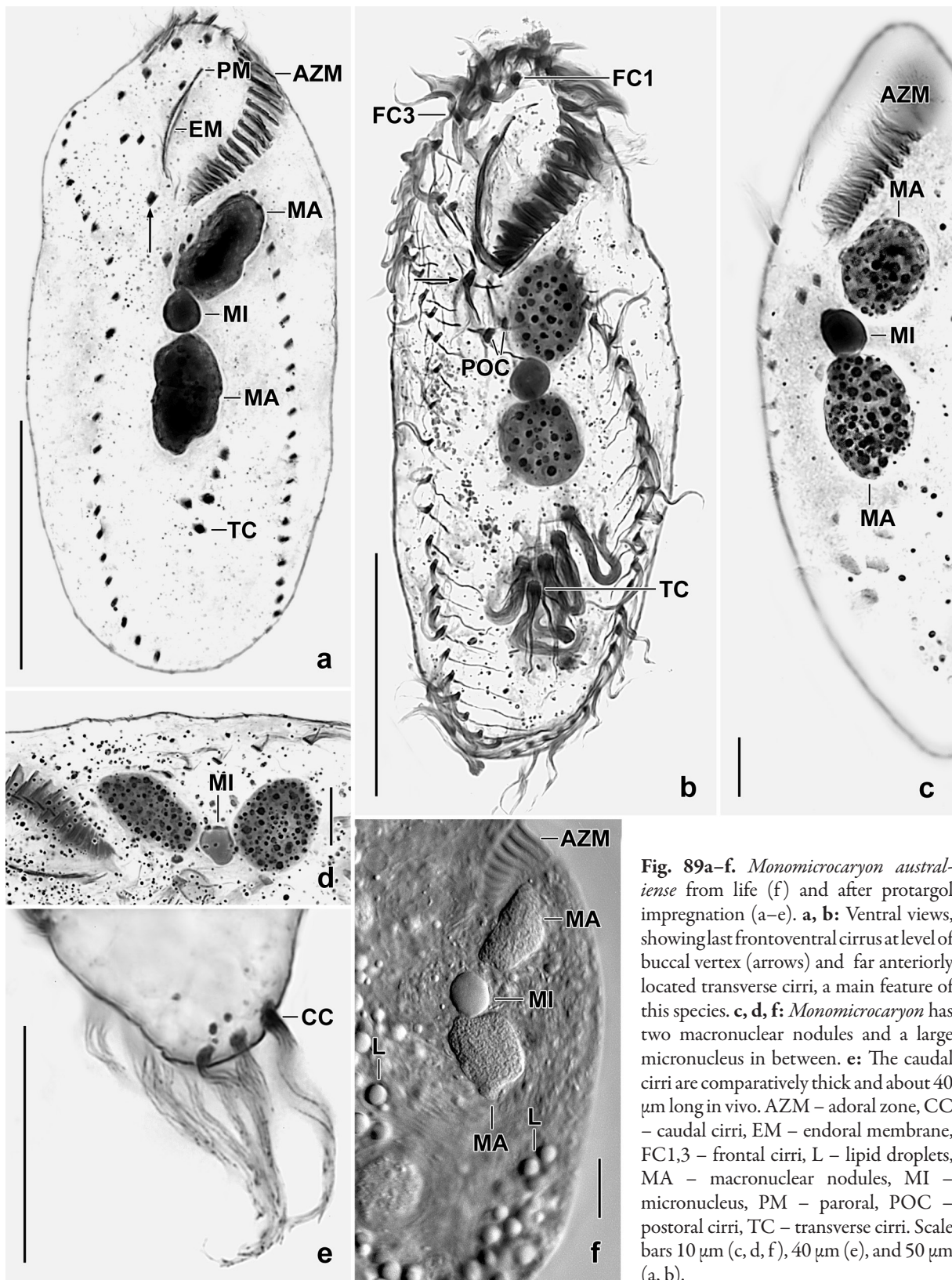
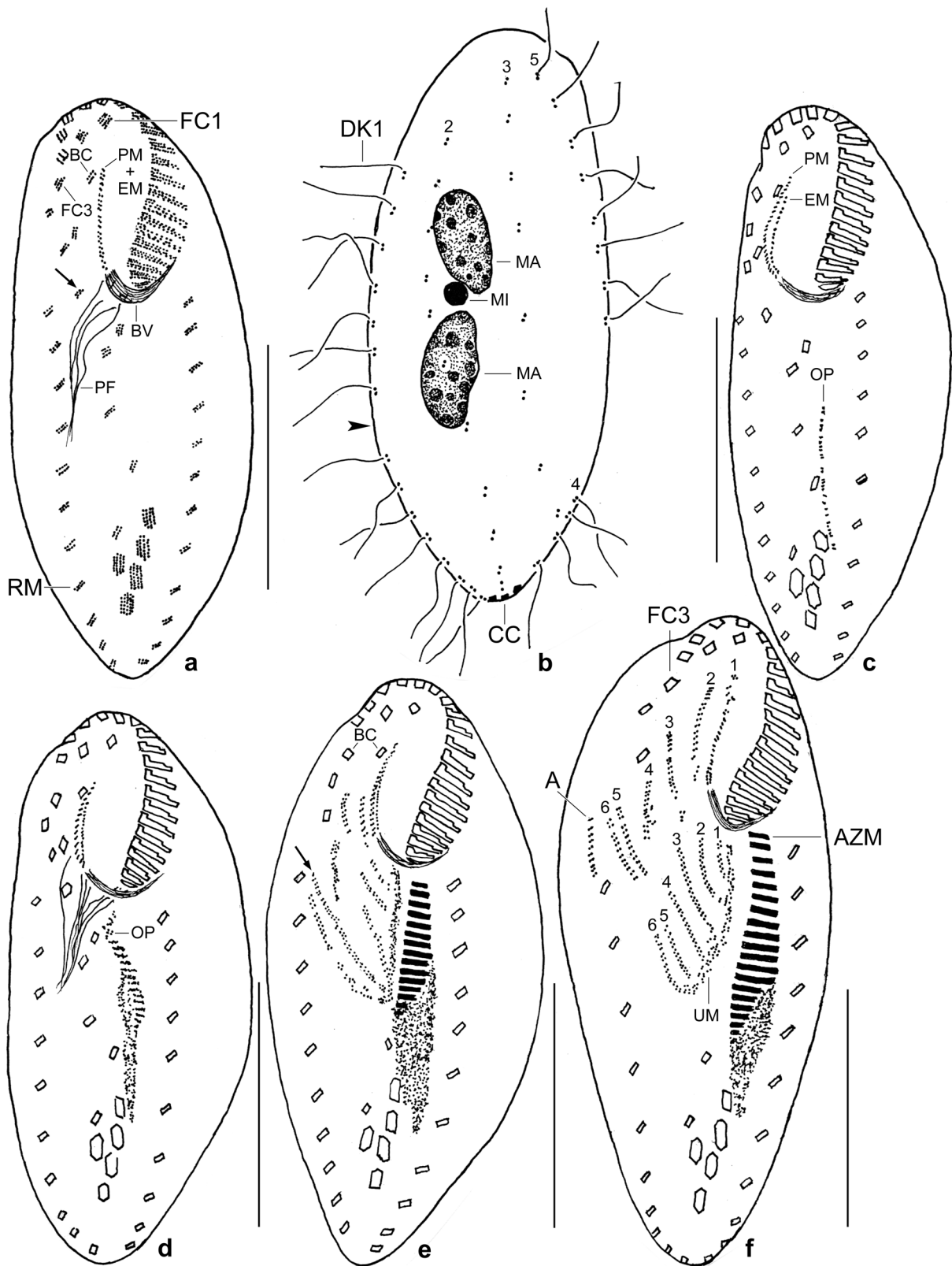


**Fig. 89a–f.** *Monomicrocaryon australiense* from life (f) and after protargol impregnation (a–e). **a, b:** Ventral views, showing last frontoventral cirrus at level of buccal vertex (arrows) and far anteriorly located transverse cirri, a main feature of this species. **c, d, f:** *Monomicrocaryon* has two macronuclear nodules and a large micronucleus in between. **e:** The caudal cirri are comparatively thick and about 40  $\mu\text{m}$  long in vivo. AZM – adoral zone, CC – caudal cirri, EM – endoral membrane, FC1,3 – frontal cirri, L – lipid droplets, MA – macronuclear nodules, MI – micronucleus, PM – paroral, POC – postoral cirri, TC – transverse cirri. Scale bars 10  $\mu\text{m}$  (c, d, f), 40  $\mu\text{m}$  (e), and 50  $\mu\text{m}$  (a, b).

**Fig. 90a–f.** *Monomicrocaryon opisthomuscorum*, morphostatic (a, b) and dividing (c–f) specimens after protargol impregnation. Parental structures shown by contour, newly formed structures shaded black. **a, b:** Ventral and dorsal view of same specimen. The arrow in (a) marks the posteriormost frontoventral cirrus at level of buccal vertex. The buccal cirrus is near to the anterior end of the paroral membrane, an important difference to *Quadrasticha setigera* (Stokes, 1891) Foissner, 2016. Most cirri are thin, but elongate rectangular and thus rather conspicuous. The endoral membrane is optically covered by the paroral membrane in this specimen. The arrowhead in (b) denotes a kinetid-wide-break in dorsal kineity 1. Dorsal kineity 4 is produced by a split of kineity 3. The dorsal cilia (bristles) are up to



10  $\mu\text{m}$  long. **c:** Very early divider, showing the oral primordium originating left of the uppermost transverse cirrus. **d:** Early divider with oral primordium extending from the uppermost transverse cirrus to the buccal vertex. **e, f:** Early mid-dividers showing five (e, buccal cirrus still inactive) or six (f) cirral anlagen streaks in proter and opisthe. Streaks five and six are primary primordia (e, arrow). A – anlage for new marginal cirri, BC – buccal cirrus, BV – buccal vertex, CC – caudal cirri, EM – endoral membrane, FC1,3 – frontal cirri, MA – macronuclear nodules, MI – micronucleus, OP – oral primordium, PF – pharyngeal fibres, PM – paroral membrane, RM – right marginal cirral row, UM – undulating membranes, DK1–5 – dorsal kineties, 1–6 – cirral anlagen streaks. Drawn to scale, bars 25  $\mu\text{m}$ .

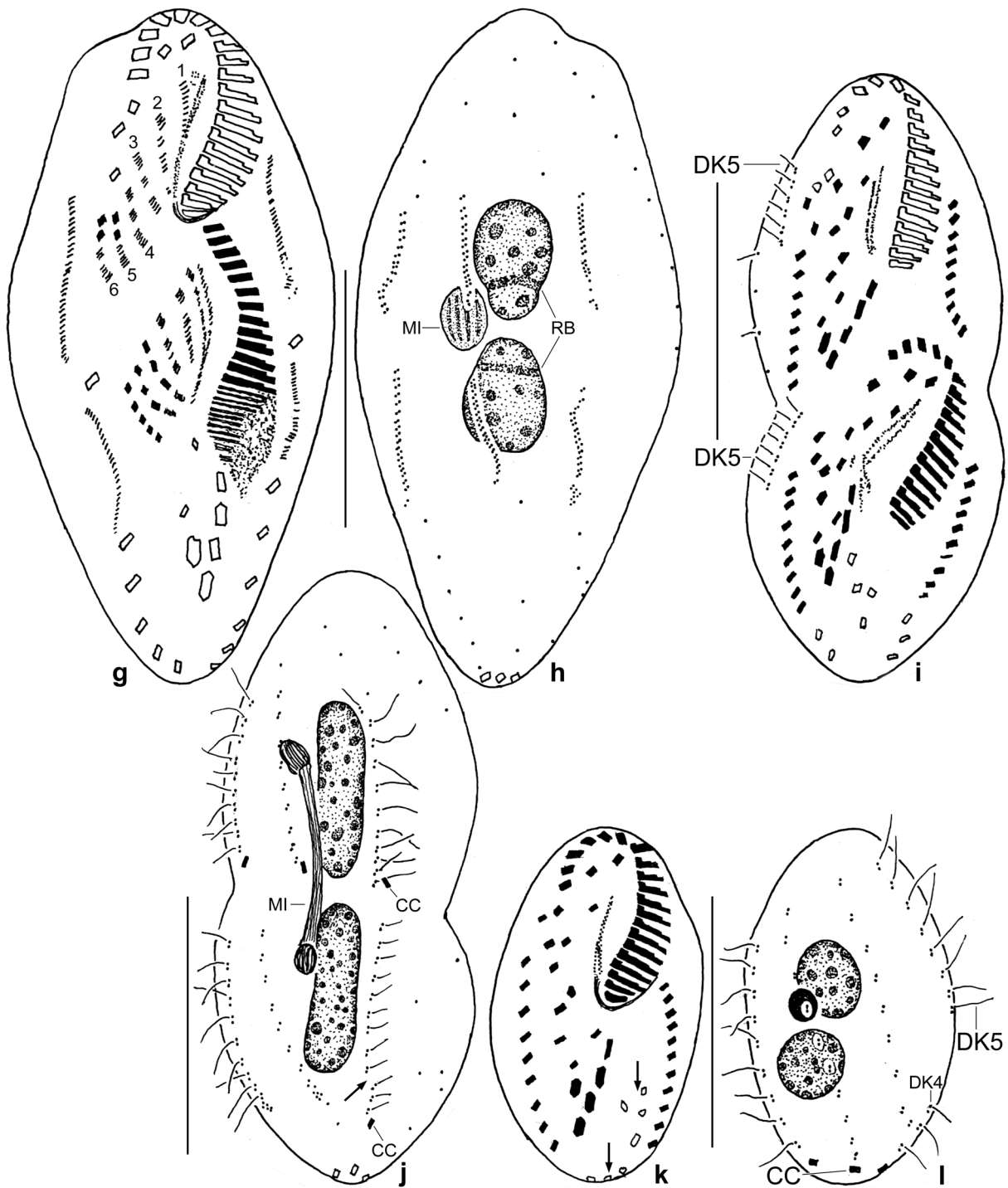


**Fig. 90g-l.** *Monomicrocaryon opisthomuscorum*, dividing specimens after protargol impregnation. Parental structures shown by contour, new structures shaded black. **g, h:** Ventral and dorsal view of a mid-divider. Cirri are forming in six anlagen streaks, and anlagen developed in the marginal rows. New dorsal kineties develop in rows 1-3. **i, j:** Ventral and dorsal view of a late divider with fully developed cirral and oral pattern. Most parental cirri that did not form anlagen have been resorbed. Dorsomarginal kinety 5 very likely developed de novo (i). New caudal cirri have been produced and dorsal kinety 3 is splitting to produce kinety 4 (j, arrow). **k, l:** Ventral and dorsal view of an early opisthe post-divider still having some parental transverse and caudal cirri (k, arrows). Note the small body size (36  $\mu\text{m}$ ). CC – caudal cirri, DK4, 5 – dorsal kineties, MI – micronucleus, RB – reorganization band. Drawn to scale, bars 25  $\mu\text{m}$ .

vacuole, FVC – last frontoventral cirrus, MA – macronuclear nodules, MI – micronucleus, PCC – parental caudal cirri, PM – paroral membrane, POC – postoral cirrus, PTC – pretransverse cirrus, RM – right marginal cirral row, TC – transverse cirri. Scale bars 20  $\mu\text{m}$ .

*ovata*) is meagre, and thus these species are rather difficult to separate. For another similar species, see Fig. 88h. A redescription of a European population of *M. kablovata* is urgently needed.

According to the dorsal kinty pattern, *M. australiense* could represent a distinct genus. However, the data are not entirely clear due to the fragility of the cortex. Thus, data from a second population and about ontogenesis should be available before genus and rank are changed.

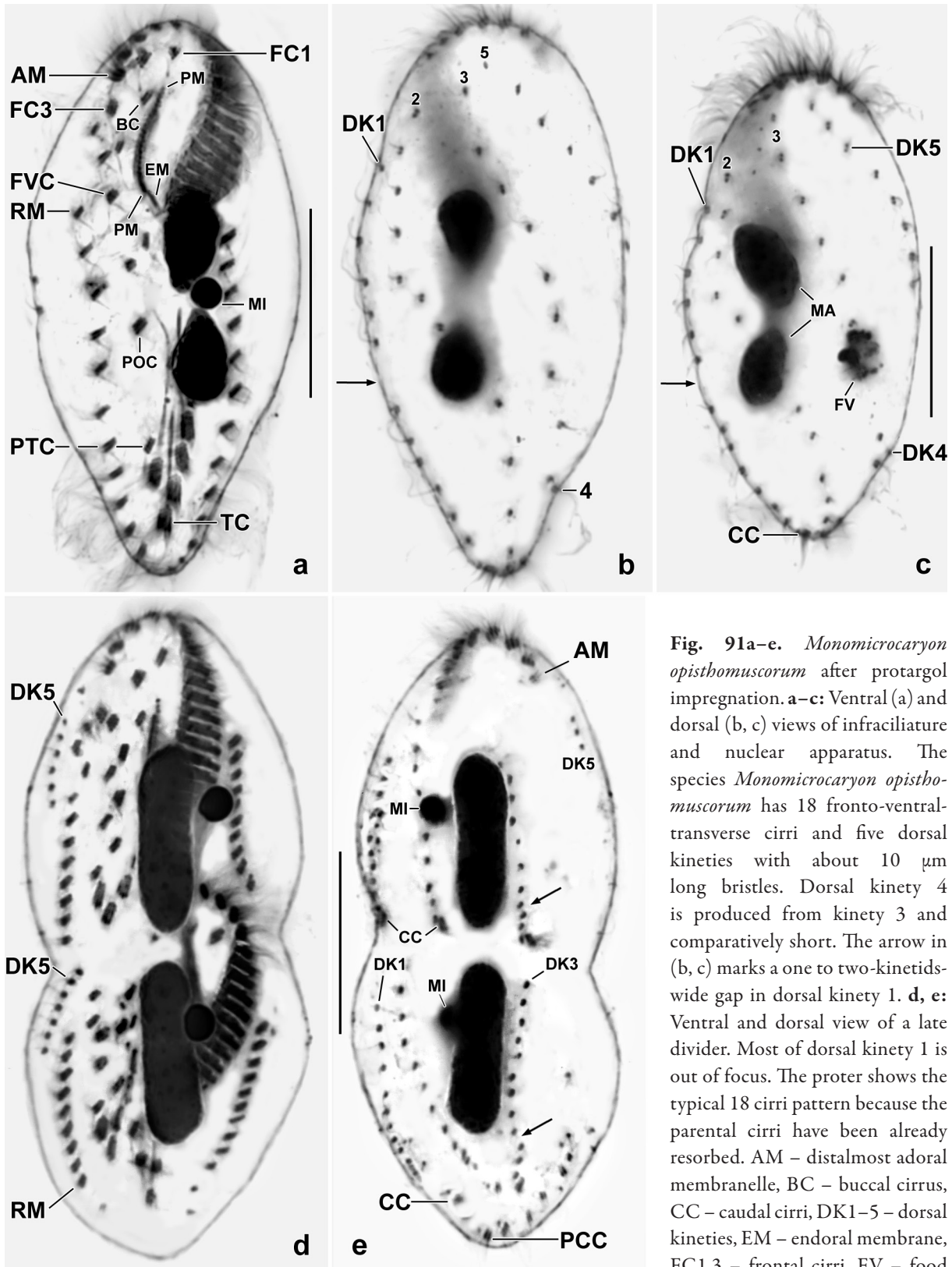


**Fig. 91a-e.** *Monomicrocaryon opisthomuscorum* after protargol impregnation. **a-c:** Ventral (a) and dorsal (b, c) views of infraciliature and nuclear apparatus. The species *Monomicrocaryon opisthomuscorum* has 18 fronto-ventral-transverse cirri and five dorsal kineties with about 10  $\mu\text{m}$  long bristles. Dorsal kinty 4 is produced from kinty 3 and comparatively short. The arrow in (b, c) marks a one to two-kinetids-wide gap in dorsal kinty 1. **d, e:** Ventral and dorsal view of a late divider. Most of dorsal kinty 1 is out of focus. The proter shows the typical 18 cirri pattern because the parental cirri have been already resorbed. AM – distalmost adoral membranelle, BC – buccal cirrus, CC – caudal cirri, DK1–5 – dorsal kineties, EM – endoral membrane, FC1,3 – frontal cirri, FV – food

***Monomicrocaryon opisthomuscorum* (Foissner, Blatterer, Berger & Kohmann, 1991) Foissner, 2016**

(Fig. 90a–l, 91a–e; Table 35 on p. 342)

**Material:** Upper 3 cm soil layer of a dry mangrove forest about 150 m distant from the Atlantic Ocean coast in the surroundings of the village of Maimon, i.e., about 10 km west of the town of Puerto Plata, Dominican Republic (~19°N, 72°W). Soil covered with a 1–3 cm thick litter layer, fluffy because containing many fine roots and only partially decomposed litter, almost black; pH in water 6.2, salinity 5‰. Collected in August 2002, investigated in June 2003.

Three voucher slides with protargol-impregnated specimens have been deposited in the Biology Centre of the Upper Austrian Museum in Linz (LI).<sup>1</sup> Relevant specimens have been marked by black ink circles on the coverslip.

**Description and remarks:** For synonymy, see Berger (1999) and Foissner (2016). The Dominican specimens of *M. opisthomuscorum* match almost perfectly the Antarctic specimens described by Petz & Foissner (1997). I found only two differences worth to be mentioned: the number of dorsal kineties (invariably five vs. five or six with kinety 6 comprising only two or three kinetids) and dorsal kinety 1 which has an up to two-kinetids-wide gap (Fig. 90b) not mentioned in the Antarctic specimens.

In vivo, *M. opisthomuscorum* is difficult to separate from *Oxytricha setigera* (now *Quadrasticha setigera* (Stokes, 1891) Foissner, 2016) because both have a similar size and shape of body and oral apparatus as well as long dorsal bristles. In morphostatic specimens, the main difference is the location of the buccal cirrus: near anterior end of paroral membrane vs. near its posterior end (Fig. 90a, 91a). In dividing specimens, there is a main difference in the genesis of the dorsal ciliature: kinety 3 splits to produce kinety 4 (Fig. 90b, j, 91b, c) vs. without kinety split (Berger 1999).

**Ontogenesis:** *Monomicrocaryon opisthomuscorum* has an oxytrichid ontogenesis. Streaks V and VI are primary primordia. Further details, see figure explanations.

***Oxytricha africana australiensis* nov. sspec.**

(Fig. 92a–e)

**Diagnosis:** Dorsal bristles arranged in five uninterrupted rows, row 1 straight or slightly curved rightwards posteriorly.

**Type locality:** Australian site (27), i.e., surface soil from Green Island east of the town of Cairns, ~17°02'07"S, 145°05'09"E.

**Type material:** The slide containing the holotype (Fig. 92b) and one paratype slide with protargol-impregnated specimens have been deposited in the Biology Centre of the Upper Austrian Museum in Linz (LI).<sup>2</sup> Relevant specimens have been marked by black ink circles on the coverslip. For slides, see Fig. 23a, c, d, 37a–c in Chapter 5.

**Etymology:** The Latin adjective *australiensis* (belonging to Australia) refers to the country the species was discovered.

**Description and remarks:** The new subspecies differs from the nominotypical subspecies *Oxytricha africana africana* Foissner, 1999 by the number of dorsal kineties (five vs. six), the absence of a break in dorsal kinety 1, and the only indistinct (vs. distinct) posterior curve of dorsal kinety 1

<sup>1</sup> Note by H. Berger: These voucher slides have not been in the boxes prepared by W. Foissner for deposition in the museum. I could not locate them in reasonable time, that is, these slides are not yet deposited in Linz (LI).

<sup>2</sup> Note by H. Berger: For further paratypes, see type slides of → *Gastronauta insula* (see Fig. 23a–in Chapter 5 of present book).

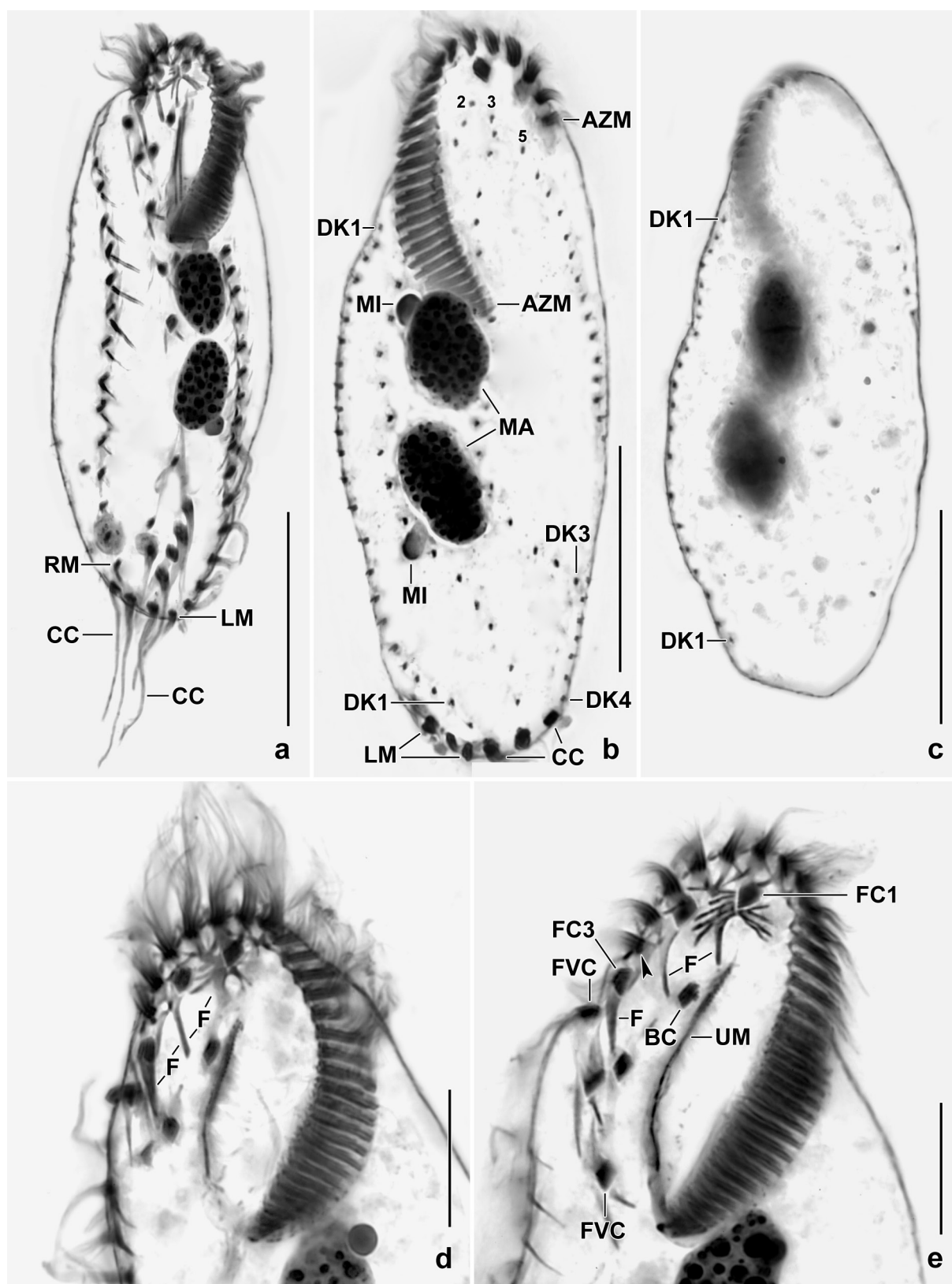


**Fig. 92a–e.** *Oxytricha africana australiensis*, ventral (a, d, e) and dorsal (b, c) views after protargol impregnation. **a:** Ventral overview. Note the long caudal cirri. **b:** Dorsal overview of holotype specimen, showing the five dorsal kineties with kinety 1 uninterrupted and only slightly curved posteriorly. There are only five dorsal kineties. Note the thick caudal cirri. **c:** Dorsal overview, showing the straight, uninterrupted kinety 1. **d, e:** Oral apparatus. Note the conspicuous fibre system associated with frontal cirrus 1. The arrowhead in (e) marks the distal end of the adoral zone of membranelles. AZM – adoral zone of membranelles, BC – buccal cirrus, DK 1–5 – dorsal kineties, F – fibres, FC1–3 – frontal cirri, FVC – frontoventral cirri, LM – left marginal cirral row, MA – macronuclear nodules, MI – micronuclei, RM – right marginal cirral row, UM – undulating membranes. Scale bars 10  $\mu\text{m}$  (d, e) and 30  $\mu\text{m}$  (a–c).

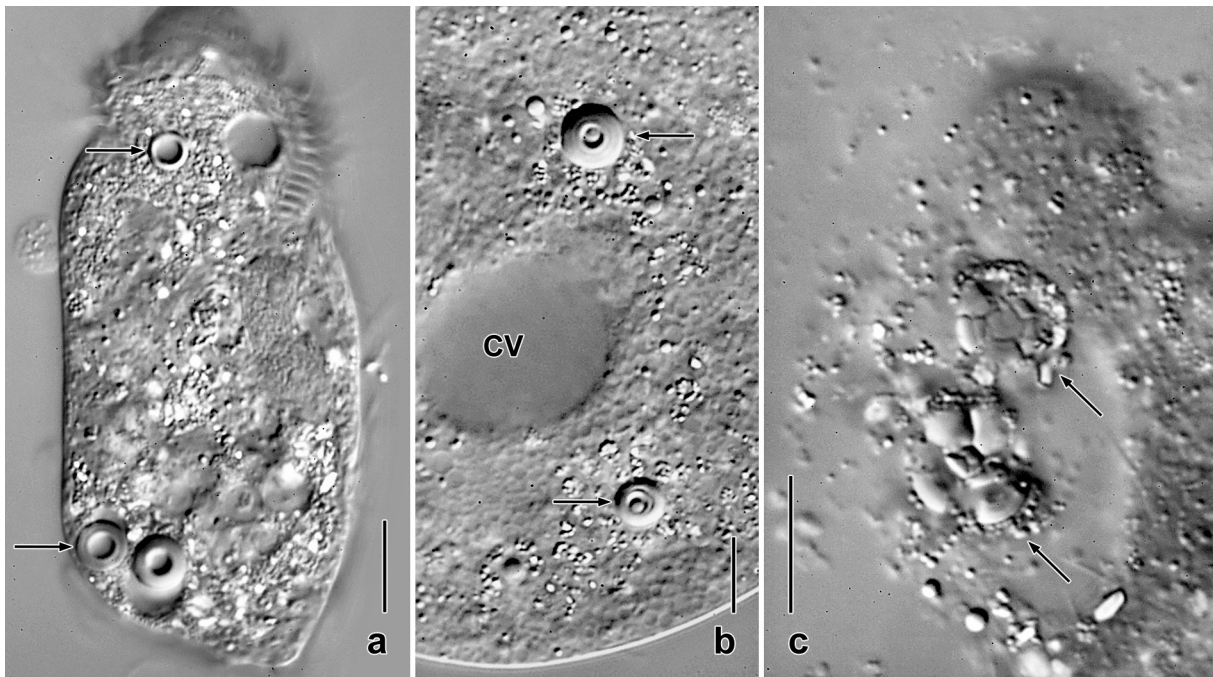


**Fig. 93a–c.** *Oxytricha lithoferana* from life. **a:** Ventral view of a pressed specimen with three lithosomes (arrows). **b:** A specimen with two lithosomes (arrows). **c:** When the specimen shown in (a) is heavily pressed, the lithosomes break into pieces with sharp outlines, indicating an anorganic nature. CV – contractile vacuole. Scale bars 10  $\mu\text{m}$  (b) and 20  $\mu\text{m}$  (a, c).

(Fig. 92b, c). These are rather subtle differences. However, the number and shape of dorsal kineties are widely used as species or subspecies character (for a review, see Berger 1999).

Minor differences: The dorsal bristles of the Australian subspecies are slightly shorter than those of the nominotypical subspecies, i.e., about 6  $\mu\text{m}$  (vs. 10  $\mu\text{m}$ ) in anterior body half and up to 10  $\mu\text{m}$  in posterior half, as in *O. africana africana* (Foissner 1999). The conspicuous fibre system associated with the thick frontal cirri (Fig. 92d, e) has been not described by Foissner (1999). Very likely, its visibility depends on the preparation conditions. All other features are very similar in both subspecies.

### *Oxytricha lithoferana* Foissner, 2016

(Fig. 93a–f)

**Material:** Australian site (170), i.e., ephemeral puddles on top of Uluru (Ayers Rock). Two voucher slides with protargol-impregnated specimens have been deposited in the Biology Centre of the Upper Austrian Museum in Linz (LI). Some specimens are marked by black ink circles on the coverslip. For slides, see Fig. 38a, b in Chapter 5.

**Remarks:** The type population occurred in slightly saline (~10‰) moss from a small cave at the north coast of Venezuela (Foissner 2016). The Australian population is so similar to the type that I provide only some micrographs, showing main features of this species, viz., the lithosomes (Fig. 93a–c), the break in dorsal kinety 1 (Fig. 93f), and the oral apparatus where the straight, oblique undulating membranes are more close to the adoral zone of membranelles anteriorly than posteriorly (Fig. 93d, e). This special arrangement indicates a distinct genus.

When heavily pressed, the lithosomes break into pieces with sharp outlines, and they dissolve in protargol preparations, indicating an anorganic nature. There are two congeners that have two

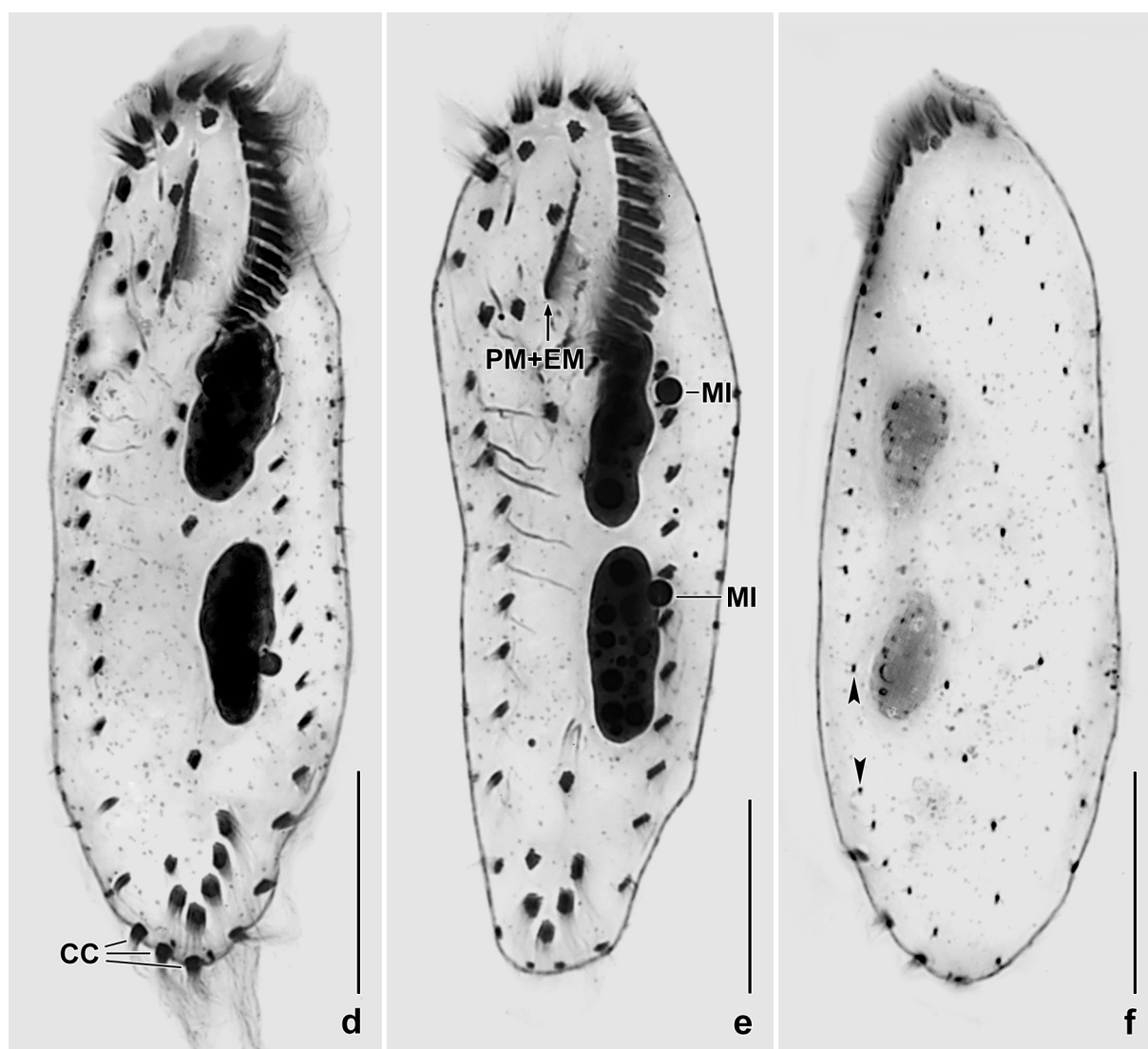


**Fig. 93d–f.** *Oxytricha lithoferana* after protargol impregnation. The lithosomes dissolved due to the preparation procedure indicating an anorganic nature. **d, e:** Ventral views, showing the special arrangement of the undulating membranes, a micronucleus each attached to the macronuclear nodules (d, e), and a specimen (e) with only four transverse cirri. **f:** Dorsal view, showing the break in bristle row 1 (arrowheads). CC – caudal cirri, EM – endoral membrane, MI – micronuclei, PM – paroral membrane. Scale bars 20  $\mu$ m.

lithosomes: *Oxytricha balladyna* and *O. setigera*.<sup>1</sup> Both have a different nuclear pattern, viz., one micronucleus in between two macronuclear nodules (for a review, see Berger 1999).

***Tachysoma setifera* nov. spec.**

(Fig. 94a–c, 95a–h; Tables 36, 37 on p. 344, 345)

**Diagnosis:** Size in vivo about 45  $\times$  20  $\mu$ m; ellipsoid. Two obliquely abutting macronuclear nodules and one micronucleus upon or on side of macronuclear nodules. Buccal cirrus subapical of paroral membrane; four frontoventral cirri three of which form an oblique row; three postoral cirri; five transverse cirri and two pretransverse cirri. Right marginal row composed of an average of three cirri forming a short row in central third of body; left marginal row composed of an average of four

<sup>1</sup> Note by H. Berger: *Oxytricha setigera* is now the type species of *Quadrasticha* Foissner, 2016: *Quadrasticha setigera* (Stokes, 1891) Foissner, 2016.

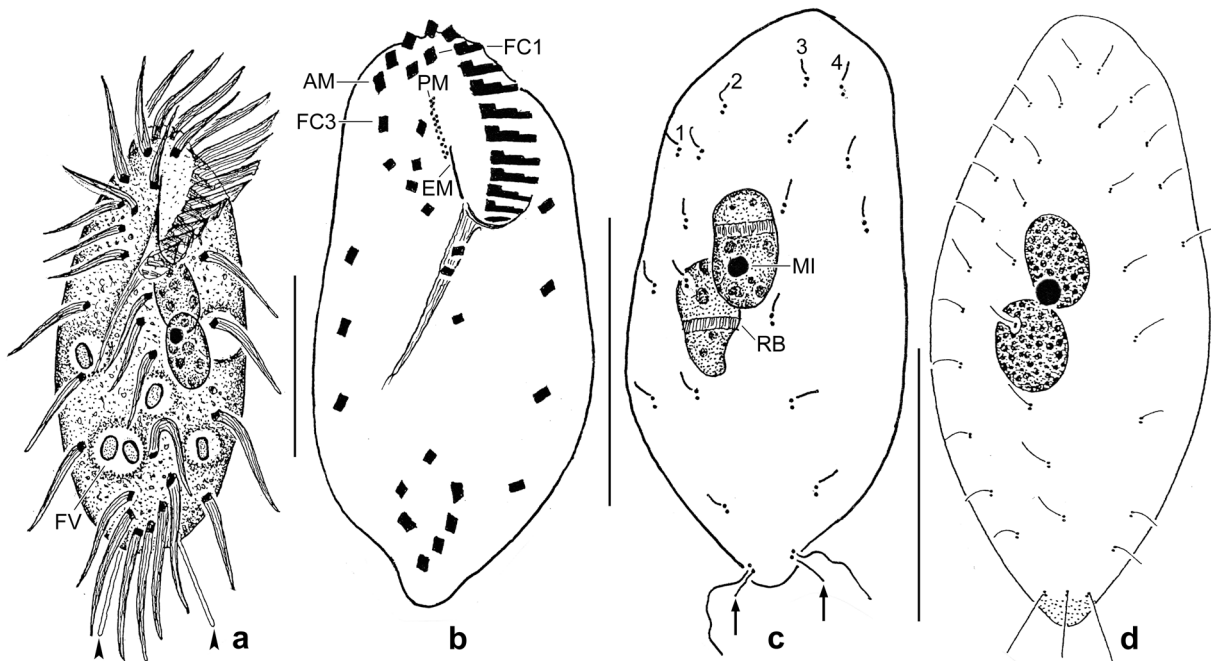


**Fig. 94a–d.** *Tachysoma setifera* (a–c) and *T. humicola longisetum* (d, from Foissner 1998) from life (a) and after protargol impregnation (b–d). **a:** Ventral view of a representative specimen, showing food vacuoles with bacterial spores and the two elongated bristles at end of dorsal kinetids 2 and 3 (arrowheads). **b, c:** Ventral and dorsal view of holotype specimen. Arrows in (c) mark the slightly elongated bristles associated with the posterior kinetid of rows 2 and 3. **d:** *Tachysoma humicola longisetum* has three (vs. two) elongated dorsal bristles and many more dorsal kinetids than *Tachysoma setifera*. AM – distalmost adoral membranelle, EM – endoral membrane, FC1,3 – frontal cirri, FV – food vacuole, MI – micronucleus, PM – paroral membrane, RB – reorganization band, 1, 2, 3, 4 – dorsal kinetids. Scale bars 20  $\mu\text{m}$ .

cirri forming a row extending between level of buccal vertex and uppermost transverse cirrus. Four dorsal kinetids with 2–3  $\mu\text{m}$  long bristles except of last kinetid of kinetids 2 and 3 associated with an about 10  $\mu\text{m}$  long bristle. Adoral zone extends over about 36% of body length, composed of an average of 14 membranelles; paroral and endoral membrane in straight, oblique line.

**Type locality:** Australian site (26), i.e., litter, roots and sandy soil from the palm girdle about 30 m inshore of Green Island east of the town of Cairns, 17°S, 146°E.

**Type material:** The slide containing the holotype (Fig. 94b, c) and three paratype slides with protargol-impregnated specimens have been deposited in the Biology Centre of the Upper Austrian Museum in Linz (LI).<sup>1</sup> Relevant specimens have been marked by black ink circles on the coverslip. Further, I marked some specimens of *Oxytrichella mahadjacola* on one of the paratype slides. For slides, see Fig. 39a–f in Chapter 5.

**Etymology:** The Latin adjective *setifera* (bristle-bearing) refers to the two distinctly elongated bristles of the last kinetid of dorsal kinetids 2 and 3.

**Description:** The main features of *T. setifera* have a low variability, i.e., the CV  $\leq 10\%$ . Thus, the species can be sharply defined.

Size in vivo 35–50  $\times$  15–25  $\mu\text{m}$ , usually about 45  $\times$  20  $\mu\text{m}$ , as calculated from protargol-impregnated specimens (Table 36) adding 15% preparation shrinkage. Body ellipsoid, length:width ratio 2.2:1 on average; often slightly widened posterior of mid-body, rarely almost rectangular; posterior end nipple-like shrunken in about one third of protargol-impregnated specimens, ventral side flat, dorsal more or less convex, depending on amount of food vacuoles (Fig. 94a, b, 95a–e, g, h;

<sup>1</sup> Note by H. Berger: The name on the slides is *Tachysoma bisticha* (this name is disclaimed for nomenclatural purposes; ICZN 1999, Article 8.3).

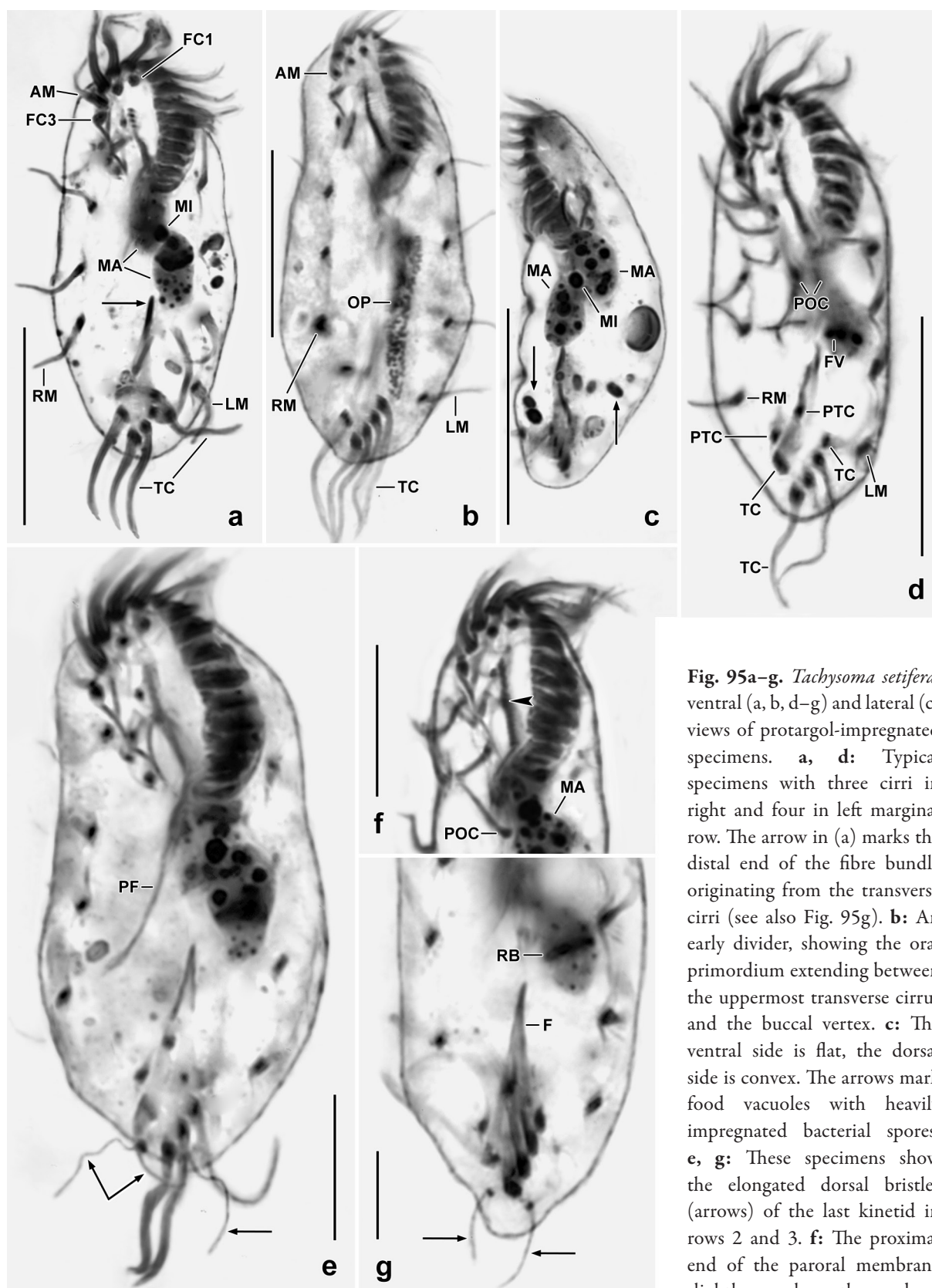


**Fig. 95a-g.** *Tachysoma setifera*, ventral (a, b, d-g) and lateral (c) views of protargol-impregnated specimens. **a, d:** Typical specimens with three cirri in right and four in left marginal row. The arrow in (a) marks the distal end of the fibre bundle originating from the transverse cirri (see also Fig. 95g). **b:** An early divider, showing the oral primordium extending between the uppermost transverse cirrus and the buccal vertex. **c:** The ventral side is flat, the dorsal side is convex. The arrows mark food vacuoles with heavily impregnated bacterial spores. **e, g:** These specimens show the elongated dorsal bristles (arrows) of the last kinetid in rows 2 and 3. **f:** The proximal end of the paroral membrane slightly overlaps the endoral (arrowhead).

AM – distalmost adoral membranelle, F – fibres, FC1, 3 – frontal cirri, FV – food vacuoles, LM – left marginal row, MA – macronuclear nodules, MI – micronucleus, OP – oral primordium, PF – pharyngeal fibres, POC – postoral cirri, PTC – pretransverse cirri, RB – reorganization band, RM – right marginal row, TC – transverse cirri. Scale bars 10  $\mu\text{m}$  (e-g) and 20  $\mu\text{m}$  (a-d).

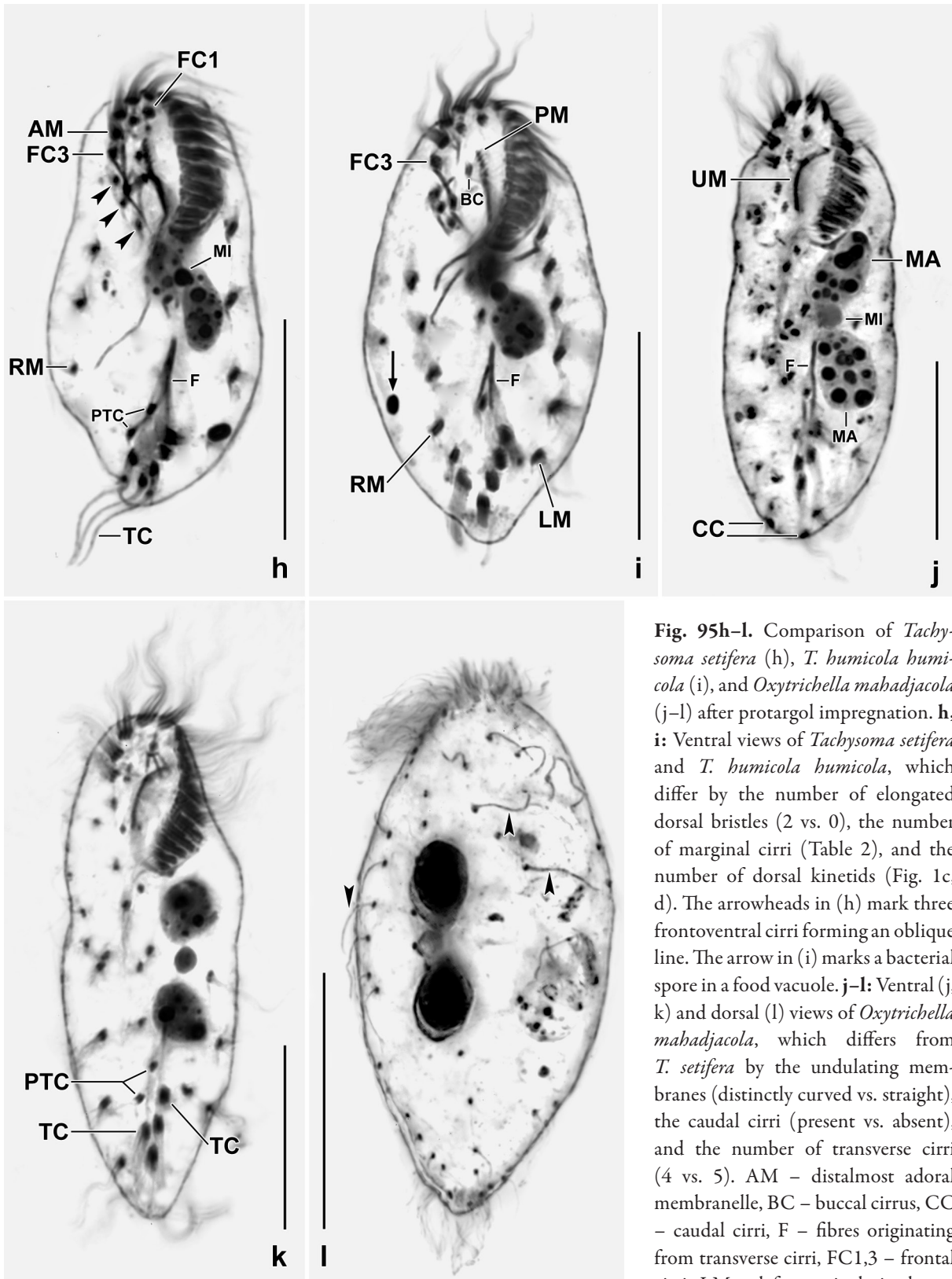


**Fig. 95h-l.** Comparison of *Tachysoma setifera* (h), *T. humicola humicola* (i), and *Oxytrichella mahadjacola* (j-l) after protargol impregnation. **h, i:** Ventral views of *Tachysoma setifera* and *T. humicola humicola*, which differ by the number of elongated dorsal bristles (2 vs. 0), the number of marginal cirri (Table 2), and the number of dorsal kinetids (Fig. 1c, d). The arrowheads in (h) mark three frontoventral cirri forming an oblique line. The arrow in (i) marks a bacterial spore in a food vacuole. **j-l:** Ventral (j, k) and dorsal (l) views of *Oxytrichella mahadjacola*, which differs from *T. setifera* by the undulating membranes (distinctly curved vs. straight), the caudal cirri (present vs. absent), and the number of transverse cirri (4 vs. 5). AM – distalmost adoral membranelle, BC – buccal cirrus, CC – caudal cirri, F – fibres originating from transverse cirri, FC1,3 – frontal cirri, LM – left marginal cirral row,

MA – macronuclear nodules, MI – micronucleus, PM – paroral membrane, PTC – pretransverse cirri, RM – right marginal cirral row, TC – transverse cirri, UM – undulating membranes (paroral and endoral). Scale bars 20  $\mu$ m.

Table 36). Invariably two macronuclear nodules and one micronucleus slightly anterior of mid-body and in left half of cell (Fig. 94a, c, 95a, e, h; Table 36). Macronuclear nodules on average broadly ellipsoid and with many minute and middle-sized, globular nucleoli; overlap more or less widely,

thus no distance in between. Micronucleus upon or on side of macronuclear nodules, globular and of ordinary size. Contractile vacuole slightly anterior of mid-body in left margin of cell. Cortex flexible, without specific granules. Cytoplasm colourless, usually with rather many, about 5  $\mu\text{m}$ -sized food vacuoles containing intensely impregnated bacterial spores about  $1.0 \times 0.7 \mu\text{m}$  in size (Fig. 94a, 95c). Moves moderately rapid on microscope slides and soil particles.

Most cirri 7–10  $\mu\text{m}$  long except of the 15  $\mu\text{m}$  long, slightly thickened transverse cirri; arranged in typical *Oxytricha* pattern (Fig. 94a, b, 95a, b, d–h; Table 36; for a review, see Berger 1999). Three slightly thickened frontal cirri, cirrus 3 far subapical and thus easily misidentified as an adoral membranelle; three of the four frontoventral cirri form an oblique line (Fig. 95h, i); buccal cirrus subapical of paroral membrane; postoral and transverse cirri in ordinary position; right marginal row in middle third of body, composed of an average of three widely spaced cirri; left marginal row extends between level of buccal vertex and uppermost transverse cirrus, composed of an average of four widely spaced cirri.

Invariably four dorsal kineties composed of comparatively wide-spaced, 2–3  $\mu\text{m}$  long bristles except of rows 2 and 3 the last dikinetid of which has an about 10  $\mu\text{m}$  long anterior bristle and a 3–5  $\mu\text{m}$  long posterior bristle sometimes lacking or not impregnated (Fig. 94c, 95e, g; Table 36). Row 1 distinctly shortened anteriorly and posteriorly, rows 2 and 3 slightly shortened anteriorly, row 4 dorsomarginal, consists of only three or four dikinetids thus ending anterior of mid-body.

Oral apparatus of ordinary structure and size (Fig. 94a, b, 95a–f, h; Table 36). Adoral zone extends 36% of body length on average, composed of 12–15 ordinary membranelles, largest membranelar bases 4  $\mu\text{m}$  wide in protargol preparations, cilia up to 12  $\mu\text{m}$  long in vivo. Undulating membranes short, form slightly oblique line directed right. Buccal cavity flat and of ordinary width. Pharyngeal fibres distinct in protargol preparations, extend beyond mid-body (Fig. 95e).

**Occurrence and ecology:** As yet found only at type locality though I investigated several samples from the surroundings. The small size suggests *T. setifera* as a true soil inhabitant.

*Tachysoma setifera* is an impressive Australian endemic. Interestingly, it occurs together with *T. humicola humicola* Gellért, 1957, a supposed cosmopolitan, while the African subspecies, *T. humicola longisetum* Foissner, 1998, has three elongated dorsal bristles and more cirri in the marginal rows and dikinetids in the dorsal kineties (Fig. 94d; Table 36).

**Remarks:** I classify the Australian population as a distinct species because it is more different from the nominal subspecies of *T. humicola* than *T. humicola longisetum* (Table 37).

There are rather many similar species from different genera making in vivo identification difficult. However, all have caudal cirri well recognizable in vivo, for instance,  $\rightarrow$  *Oxytrichella mahadjacola* Foissner, 2016 (only four transverse cirri, long dorsal bristles, undulating membranes distinctly curved; Fig. 95j–l),  $\rightarrow$  *Monomicrocaryon opisthomuscorum* (long dorsal bristles, undulating membranes distinctly curved; Fig. 90a, b), and *Quadristicha setigera* (long dorsal bristles, undulating membranes distinctly curved), all reviewed by Berger (1999) and Foissner (2016).

#### ***Pattersoniella (Pattersoniellides) australiensis* Kumar & Foissner, 2016**

**Remarks:** In this species, I observed that the paroral basal bodies are reduced anteriorly while their fibrillar associates are still present, a very strange feature. Thus, I did what I should have done before publication, i.e., I reinvestigated the type slides of *Pattersoniella vitiphila* Foissner, 1987a. Indeed, they have a paroral as described for *P. australiensis* described by Kumar & Foissner (2016). Thus, this feature should be abandoned from the diagnosis of *Pattersoniellides*.

Based on the new data, the diagnoses of the subgenera *Pattersoniella (Pattersoniella)* Foissner, 1987a and *Pattersoniella (Pattersoniellides)* must be emended.

**Emendation of *Pattersoniella* Foissner, 1987a:** Rigid oxytrichids with three frontal and one buccal cirrus or with distinctly increased fronto-ventral cirri forming a bicorona. Two pretransverse and more than five transverse cirri. One right and one left row of marginal cirri. Undulating membranes in *Australocirrus* pattern; paroral membrane complete or some basal bodies reduced anteriorly while their fibrillar associates still present. Number of fronto-ventral-transverse cirral streaks distinctly increased (7–11 vs. 6 in “typical” oxytrichids). More than six dorsal kineties due to multiple fragmentation of dorsal kinety 3 and two dorsomarginal rows; some parental kinetids retained after division. Caudal cirri present.

**Emendation of *Pattersoniella* (*Pattersoniella*) Foissner, 1987a:** *Pattersoniella* with an increased number of fronto-ventral cirri forming a bicorona.

**Type species:** *Pattersoniella* (*Pattersoniella*) *vitiphila* Foissner, 1987a.<sup>1</sup>

**Emendation of *Pattersoniella* (*Pattersoniellides*) Kumar & Foissner, 2016:** *Pattersoniella* with three frontal and one buccal cirrus arranged in *Oxytricha* pattern.

**Type species:** *Pattersoniella* (*Pattersoniellides*) *australiensis* Kumar & Foissner, 2016.

## Acknowledgements

The technical assistance of Robert Schörghofer, Andreas Zankl, and Michael Gruber is greatly acknowledged. Many thanks to all who collected samples.

## Funding

This work was supported by a grant from the Austrian Science Fund FWF [Project 26325, “Biodiversity of soil ciliates (Protista, Ciliophora) from Australia”].

## References

- Aescht E. (2001): Catalogue of the generic names of ciliates (Protozoa, Ciliophora). — *Denisia* (Linz) **1**: 1–350.
- Apstein C. (1915): Nomina conservanda. — *Sber. Ges. naturf. Freunde Berl.* **1915**: 119–202.
- Bary B.M. (1950): Studies on the freshwater ciliates in New Zealand. Part I. A general morphology of *Bursaria truncatella* Muller. — *Trans. R. Soc. N. Z.* **78**: 301–310.
- Beers C.D. (1952): Observations on the ciliate *Bursaria ovata*, n. sp. — *J. Elish Mitchell scient. Soc.* **68**: 184–190.
- Berger H. (1999): Monograph of the Oxytrichidae (Ciliophora, Hypotrichia). — *Monographiae biol.* **78**: i–xii, 1–1080.
- Berger H. (2006): Monograph of the Urostyloidea (Ciliophora, Hypotricha). — *Monographiae biol.* **85**: i–xvi, 1–1303.
- Berger H. (2008): Monograph of the Amphiellidae and Trachelostylidae (Ciliophora, Hypotricha). — *Monographiae biol.* **88**: i–xvi, 1–737.
- Berger H. (2011): Monograph of the Gonostomatidae and Kahliellidae (Ciliophora, Hypotricha). — *Monographiae biol.* **90**: i–xiv, 1–741.
- Berger H. & Al-Rasheid K.A.S. (2008): Wilhelm Foissner: nomenclatural and taxonomic summary 1967–2007. — *Denisia* **23**: 65–124.

<sup>1</sup> Note by H. Berger: Voucher specimens are contained in the type slides of → *Circinella filiformis australiensis* (see Fig. 26a, b in Chapter 5 of present book). On these slides W. Foissner incorrectly designated this species as “*Pattersoniella* (*Pattersoniellides*) *vitiphila*” (this name is disclaimed for nomenclatural purposes; ICZN 1999, Article 8.3).

- Berger H. & Foissner W. (1987): Morphology and biometry of some soil hypotrichs (Protozoa: Ciliophora). — Zool. Jb. Syst. **114**: 193–239.
- Berger H. & Foissner W. (1988): Revision of *Lamtostyla* Buitkamp, 1977 and description of *Territricha* nov. gen. (Ciliophora: Hypotrichida). — Zool. Anz. **220**: 113–134.
- Berger H. & Foissner W. (1989): Morphology and biometry of some soil hypotrichs (Protozoa, Ciliophora) from Europe and Japan. — Bull. Br. Mus. Nat. Hist. (Zool. Ser.) **55**: 19–46.
- Berger H., Foissner W. & Adam H. (1983): Morphology and morphogenesis of *Fuscheria terricola* n. sp. and *Spathidium muscorum* (Ciliophora: Kinetofragminophora). — J. Protozool. **30**: 529–535.
- Berger H., Foissner W. & Adam H. (1984): Taxonomie, Biometrie und Morphogenese einiger terricoler Ciliaten (Protozoa: Ciliophora). — Zool. Jb. Syst. **111**: 339–367.
- Bharti D., Kumar S. & La Terza A. (2015): Two gonostomatids ciliates from the soil of Lombardia, Italy; including note on the soil mapping project. — J. Euk. Microbiol. **62**: 762–772.
- Borror A.C. (1972): Revision of the order Hypotrichida (Ciliophora, Protozoa). — J. Protozool. **19**: 1–23.
- Canning E.U. & Lom J. (1986): The microsporidia of vertebrates. Academic Press, London.
- Chen X., Lu X., Luo X., Jiang J., Shao C., Al-Rasheid K.A.S., Warren A. & Song W. (2017): The diverse morphogenetic patterns in spirotrichs and philasterids: researches based on five-year-projects supported by IRCN-BC and NSFC. — Eur. J. Protistol. **61**: 439–452.
- Deroux G. (1994): Sous-classe des Cyrtophoria Fauré-Fremiet in Corliss, 1956. In: Puytorac P. de (ed.), Traité de zoologie. Anatomie, systématique, biologie, Tome 2 (2), pp. 401–431. Masson, Paris, Milan, Barcelone.
- Doflein F. & Reichenow E. (1929): Lehrbuch der Protozoenkunde. G. Fischer, Jena.
- Dragesco J. (1960): Ciliés mésopsammiques littoraux. Systématique, morphologie, écologie. — Trav. Stn biol. Roscoff **12**: 1–356.
- Dragesco J. (1972): Ciliés libres de la cuvette tchadienne. — Anns Fac. Sci. Univ. féd. Cameroun **11**: 71–91.
- Dragesco J. & Dragesco-Kerneis A. (1979): Cilies muscicoles nouveaux ou peu connus. — Acta Protozool. **18**: 401–416, Planche I.
- Dragesco J. & Dragesco-Kernéis A. (1986): Ciliés libres de l'Afrique intertropicale. Introduction à la connaissance et à l'étude des ciliés. — Faune tropicale (Éditions de L'ORSTOM, Paris) **26**: 1–559.
- Dragesco J. & Njine T (1971): Compléments à la connaissance des ciliés libres du Cameroun. — Anns Fac. Sci. Univ. féd. Cameroun **7-8**: 97–140.
- Durán-Ramírez C.A., García-Franco J.G., Foissner W. & Mayén-Estrada R. (2015): Free-living ciliates from epiphytic tank bromeliads in Mexico. — Eur. J. Protistol. **51**: 15–33.
- Ehrenberg C.G. (1838): Die Infusionsthierchen als vollkommene Organismen. Ein Blick in das tiefere organische Leben der Natur. L. Voss, Leipzig. 548 pp, Tafeln I–LXIV.
- Engelmann T.W. (1862): Zur Naturgeschichte der Infusionsthierchen. — Z. wiss. Zool. **11**: 347–393, Tafeln XXVIII–XXXI.
- Foissner I. & Foissner W. (1995): *Ciliatosporidium platyophryae* nov. gen., nov. spec. (Microspora incerta sedis), a parasite of *Platyophrya terricola* (Ciliophora, Colpodea). — Eur. J. Protistol. **31**: 248–259.
- Foissner W. (1980): Artenbestand und Struktur der Ciliatenzönose in alpinen Kleingewässern (Hohe Tauern, Österreich). — Arch. Protistenk. **123**: 99–126.
- Foissner W. (1980a): Taxonomische Studien über die Ciliaten des Grossglocknergebietes (Hohe Tauern, Österreich). IX. Ordnungen Heterotrichida und Hypotrichida. — Ber. Nat. med. Ver. Salzburg **5**: 71–117.

- Foissner W. (1981a): Morphologie und Taxonomie einiger neuer und wenig bekannter kinetofragminophorer Ciliaten (Protozoa: Ciliophora) aus alpinen Böden. — Zool. Jb. Syst. **108**: 264–297.
- Foissner W. (1982): Ökologie und Taxonomie der Hypotrichida (Protozoa: Ciliophora) einiger österreichischer Böden. — Arch. Protistenk. **126**: 19–143.
- Foissner W. (1983a): Taxonomische Studien über die Ciliaten des Großglocknergebietes (Hohe Tauern, Österreich) I. Familien Holophryidae, Prorodontidae, Plagiocampidae, Colepidae, Enchelyidae und Lacrymariidae nov. fam. — Annl. naturh. Mus. Wien **84B**: 49–85.
- Foissner W. (1983b): Morphologie und Morphogenese von *Psilotricha succisa* (O. F. Müller, 1786) nov. comb. (Ciliophora, Hypotrichida). — Protistologica **19**: 479–493.
- Foissner W. (1984): Infraciliatur, Silberliniensystem und Biometrie einiger neuer und wenig bekannter terrestrischer, limnischer und mariner Ciliaten (Protozoa: Ciliophora) aus den Klassen Kinetofragminophora, Colpodea und Polyhymenophora. — Stapfia (Linz) **12**: 1–165.
- Foissner W. (1985): Morphologie und Infraciliatur der Genera *Microthorax* und *Stammeridium* und Klassifikation der Microthoracina Jankowski, 1967 (Protozoa: Ciliophora). — Zool. Anz. **214**: 33–53.
- Foissner W. (1987a): Neue und wenig bekannte hypotriche und colpode Ciliaten (Protozoa: Ciliophora) aus Böden und Moosen. — Zool. Beitr. N. F. **31**: 187–282.
- Foissner W. (1987b): Soil protozoa: fundamental problems, ecological significance, adaptations in ciliates and testaceans, bioindicators, and guide to the literature. — Progr. Protistol. **2**: 69–212.
- Foissner W. (1987c): Neue terrestrische und limnische Ciliaten (Protozoa, Ciliophora) aus Österreich und Deutschland. — Sber. öst. Akad. Wiss., Mathematisch-naturwissenschaftliche Klasse, Abt. I **195** (year 1986): 217–268.
- Foissner W. (1988): Gemeinsame Arten in der terricolen Ciliatenfauna (Protozoa: Ciliophora) von Australien und Afrika. — Stapfia **17**: 85–133.
- Foissner W. (1991): Basic light and scanning electron microscopic methods for taxonomic studies of ciliated protozoa. — Eur. J. Protistol. **27**: 313–330.
- Foissner W. (1993): Colpodea (Ciliophora). — Protozoenfauna **4/1**: i–x, 1–798.
- Foissner W. (1994): Morphology and morphogenesis of *Circinella arenicola* nov. gen., nov. spec., a cephalized hypotrich (Ciliophora, Hypotrichida) from sand dunes in Utah, USA. — Eur. J. Protistol. **30**: 156–170.
- Foissner W. (1995): Tropical protozoan diversity: 80 ciliate species (Protozoa, Ciliophora) in a soil sample from a tropical dry forest of Costa Rica, with descriptions of four new genera and seven new species. — Arch. Protistenk. **145**: 37–79.
- Foissner W. (1996a): Faunistics, taxonomy and ecology of moss and soil ciliates (Protozoa, Ciliophora) from Antarctica, with description of new species, including *Pleuroplitoides smithi* gen. n., sp. n. — Acta Protozool. **35**: 95–123.
- Foissner W. (1996b): Terrestrial ciliates (Protozoa, Ciliophora) from two islands (Gough, Marion) in the southern oceans, with description of two new species, *Arcuospathidium cooperi* and *Oxytricha ottowi*. — Biol. Fertil. Soils **23**: 282–291.
- Foissner W. (1996c): Ontogenesis in ciliated protozoa, with emphasis on stomatogenesis. In: Hausmann K. & Bradbury P.C. (eds.), Ciliates: cells as organisms, pp. 95–177. Fischer, Stuttgart, Jena, Lübeck, Ulm.
- Foissner W. (1997c): Infraciliature and systematic position of the marine interstitial ciliates (Protozoa, Ciliophora) *Lopezoterenia torpens* (Kahl, 1931) nov. gen., nov. comb., *Discotricha papillifera* Tuffrau, 1954, and *Paraspathidium fuscum* (Kahl, 1928) Fjeld, 1955. — Rev. Soc. Mes. Hist. Nat. **47**: 41–63.

- Foissner W. (1998): An updated compilation of world soil ciliates (Protozoa, Ciliophora), with ecological notes, new records, and descriptions of new species. — *Eur. J. Protistol.* **34**: 195–235.
- Foissner W. (1999): Notes on the soil ciliate biota (Protozoa, Ciliophora) from the Shimba Hills in Kenya (Africa): diversity and description of three new genera and ten new species. — *Biodivers. Conserv.* **8**: 319–389.
- Foissner W. (2000): Revision of the genera *Gastronauta* Engelmann in Bütschli, 1889 and *Paragastronauta* nov. gen. (Ciliophora: Gastronomitidae). — *Protozoological Monographs* **1**: 63–101.
- Foissner W. (2003): Two remarkable soil spathidiids (Ciliophora: Haptorida), *Arcuospathidium pachyoplites* sp. n. and *Spathidium faurefremietii* nom. n. — *Acta Protozool.* **42**: 145–159.
- Foissner W. (2010): *Enchelys micrographica* nov. spec., a new ciliate (Protista, Ciliophora) from moss of Austria. — *MittBl. Mikroskop. Ges. Wien, Festschrift*: 71–79.
- Foissner W. (2010a): Life cycle, morphology, ontogenesis, and phylogeny of *Bromeliotrix metopoides* nov. gen., nov. spec., a peculiar ciliate from tank bromeliads. — *Acta Protozool.* **49**: 159–193.
- Foissner W. (2011): Dispersal of protists: the role of cysts and human introductions. — In: Fontaneto D. (ed): *Biogeography of microscopic organisms. Is everything small everywhere?* Cambridge Univ. Press, Cambridge, UK: 61–87.
- Foissner W. (2014): An update of ‘basic light and scanning electron microscopic methods for taxonomic studies of ciliated protozoa’. — *Int. J. Syst. Evol. Microbiol.* **64**: 271–292.
- Foissner W. (2016): Terrestrial and semiterrestrial ciliates (Protozoa, Ciliophora) from Venezuela and Galápagos. — *Denisia (Linz)* **35**: 1–912.
- Foissner W. & Adam H. (1981): Morphologie und Infraciliatur von *Parafurgasonia sorex* (Penard, 1922) nov. gen. und *Obertrumia georgiana* (Dragesco, 1972) nov. gen. (Protozoa: Ciliophora). — *Zool. Anz.* **207**: 303–319.
- Foissner W. & Adam H. (1983): Morphologie und Morphogenese des Bodenciliaten *Oxytricha granulifera* sp. n. (Ciliophora, Oxytrichidae). — *Zool. Scr.* **12**: 1–11.
- Foissner W. & Al-Rasheid K. (2006): A unified organization of the stichotrichine oral apparatus, including a description of the buccal seal (Ciliophora: Spirotrichea). — *Acta Protozool.* **45**: 1–16.
- Foissner W. & Al-Rasheid K. (2007): Notes on soil ciliates (Protozoa, Ciliophora) from The Netherlands, with description of *Keronopsis schminkei* nov. spec. and *Apobryophyllum schmidingeri* nov. spec. — *Acta Protozool.* **46**: 201–220.
- Foissner W. & Dragesco J. (1996): Updating the trachelocercids (Ciliophora, Karyorelictea). I. A detailed description of the infraciliature of *Trachelolophos gigas* n. g., n. sp. and *T. filum* (Dragesco & Dragesco-Kernéis, 1986) n. comb. — *J. Euk. Microbiol.* **43**: 12–25.
- Foissner W. & Foissner I. (1985): Oral monokinetids in the free-living haptorid ciliate *Enchelydium polynucleatum* (Ciliophora, Enchelyidae): ultrastructural evidence and phylogenetic implications. — *J. Protozool.* **32**: 712–722.
- Foissner W. & Lei Y.-L. (2004): Morphology and ontogenesis of some soil spathidiids (Ciliophora, Haptoria). — *Linzer biol. Beitr.* **36**: 159–199.
- Foissner W. & O’Donoghue P.J.O. (1990): Morphology and infraciliature of some freshwater ciliates (Protozoa: Ciliophora) from Western and South Australia. — *Invertebrat. Taxon.* **3**: 660–696.
- Foissner W. & Stoeck T. (2006): *Rigidotrix goiseri* nov. gen., nov. spec. (Rigidotrichidae nov. fam.), a new “flagship” ciliate from the Niger floodplain breaks the flexibility-dogma in the classification of stichotrichine spirotrichs (Ciliophora, Spirotrichea). — *Eur. J. Protistol.* **42**: 249–267.
- Foissner W. & Stoeck T. (2008): Morphology, ontogenesis and molecular phylogeny of *Neokeronopsis (Afrokeronopsis) aurea* nov. subgen., nov. spec. (Ciliophora: Hypotricha), a new African flagship ciliate confirms the CEUU hypothesis. — *Acta Protozool.* **47**: 1–33.

- Foissner W. & Xu K. (2007): Monograph of the Spathidiida (Ciliophora, Haptoria). Volume I: Protospathidiidae, Arcuospathidiidae, Apertospathulidae. — Monogr. Biol. **81**: 1–485.
- Foissner W., Blatterer H., Berger H. & Kohmann F. (1991): Taxonomische und ökologische Revision des Saprobiensystems. – Band I: Cyrtophorida, Oligotrichida, Hypotrichia, Colpodea. — Informationsberichte des Bayer. Landesamtes für Wasserwirtschaft **1/91**: 1–478.
- Foissner W., Berger H. & Kohmann F. (1992): Taxonomische und ökologische Revision des Saprobiensystems. – Band II: Peritrichia, Heterotrichida, Odontostomatida. — Informationsberichte des Bayer. Landesamtes für Wasserwirtschaft **5/92**: 1–502.
- Foissner W., Berger H. & Kohmann F. (1994): Taxonomische und ökologische Revision der Ciliaten des Saprobiensystems – Band III: Hymenostomata, Prostomatida, Nassulida. — Informationsberichte des Bayer. Landesamtes für Wasserwirtschaft **1/94**: 1–548.
- Foissner W., Berger H. & Schaumburg J. (1999): Identification and ecology of limnetic plankton ciliates. — Informationsberichte des Bayer. Landesamtes für Wasserwirtschaft **3/99**: 1–793.
- Foissner W., Stoeck T., Schmidt H. & Berger H. (2001): Biogeographical differences in a common soil ciliate, *Gonostomum affine* (Stein), as revealed by morphological and RAPD-fingerprint analysis. — Acta Protozool. **40**: 83–97.
- Foissner W., Agatha S. & Berger H. (2002): Soil ciliates (Protozoa, Ciliophora) from Namibia (Southwest Africa), with emphasis on two contrasting environments, the Etosha region and the Namib Desert. — Denisia (Linz) **5**: 1–1459.
- Foissner W., Berger H., Xu K. & Zechmeister-Boltenstern S. (2005): A huge, undescribed soil ciliate (Protozoa: Ciliophora) diversity in natural forest stands of Central Europe. — Biodivers. Conserv. **14**: 617–701.
- Foissner W., Hess S. & Al-Rasheid K.A.S. (2010): Two vicariant *Semispathidium* species from tropical Africa and central Europe: *S. fraterculum* nov. spec. and *S. pulchrum* nov. spec. (Ciliophora, Haptorida). — Eur. J. Protistol. **46**: 61–73.
- Foissner W., Stoeck T., Agatha S. & Dunthorn M. (2011): Intra-class evolution and classification of the Colpodea (Ciliophora). — J. Euk. Microbiol. **58**: 397–415.
- Gabilondo R. & Foissner W. (2009): Four new fuschieriid soil ciliates (Ciliophora: Haptorida) from four biogeographic regions. — Acta Protozool. **48**: 1–24.
- Ganner B., Foissner W. & Adam H. (1987): Morphogenetic and biometric comparison of four populations of *Urosomoida agiliformis* (Ciliophora, Hypotrichida). — Anns Sci. nat. (Zool.) **8**: 199–207.
- Gelei J. (1936): Beiträge zur Ciliatenfauna der Umgebung von Szeged. Zwei Gymnostomata Arten: *Amphileptus carchesii* Stein und *Bryophyllum hyalinum* n. sp. — Acta biol., Szeged **4**: 1–11.
- Gelei J. & Szabados M. (1950): Tömegprodukción városi esővizpocsolyában (Massenproduktion in einer städtischen Regenwasserpfütze). — Anns biol. Univ. szeged. **1**: 249–294.
- Gellért J. (1957): Néhány hazai lomblevelű és tűlevelű erdő talajának ciliáta-faunája (Ciliatenfauna im Humus einiger ungarischen Laub- und Nadelholzwälder). — Anns Inst. biol. Tihany **24**: 11–34.
- Görtz H.-D. (1987): Infections of *Stentor roeseli* and *S. polymorphus* (Ciliophora, Heterotrichida) by microsporidia. — Parasitol. Res. **74**: 34–35.
- Heber D., Stoeck T., Foissner W. (2014): Morphology and ontogenesis of *Psilotrichides hawaiiensis* nov. gen., nov. spec. and molecular phylogeny of the Psilotrichidae (Ciliophora, Hypotrichia). — J. Euk. Microbiol. **61**: 260–277.
- Heber D., Stoeck T., Foissner W. (2018): Corrigendum: “Morphology and ontogenesis of *Psilotrichides hawaiiensis* nov. gen., nov. spec. and molecular phylogeny of the Psilotrichidae (Ciliophora, Hypotrichia)” by Heber et al. (2014). — J. Euk. Microbiol. **65**: 291–292.

- Hemberger H. (1985): Neue Gattungen und Arten hypotricher Ciliaten. — Arch. Protistenk. **130**: 397–417.
- Hentschel E.J. & Wagner G.H. (1996): Zoologisches Wörterbuch. Tiernamen, allgemeinbiologische, anatomische, physiologische Termini und Kurzbiographien. Gustav Fischer Verlag, Jena
- Horváth J.v. (1933): Beiträge zur hypotrichen Fauna der Umgebung von Szeged. I. — Arch. Protistenk. **80**: 281–302.
- Hovasse R. (1950): *Spirobütschliella chattoni*, nov. gen., nov. sp., cilie astome, parasité en Méditerranée du Serpulen *Potamoceros triquetter* L., et parasité par la microsporidie *Gurleya nova*, sp. n. — Bull. Inst. Oceanogr. (Monaco) **962**: 1–10.
- ICZN (International Commission on Zoological Nomenclature) (1999): International Code of Zoological Nomenclature, 4th edn. — International Trust for Zoological Nomenclature, London: i–xxx, 1–306.
- ICZN (International Commission of Zoological Nomenclature) (2012). Amendment of Articles 8, 9, 10, 21 and 78 of the International Code of Zoological Nomenclature to expand and refine methods of publication. — Bull. Zool. Nom. **69**:161–169.
- Jang S.W., Vd'ačný P., Shazib S.U.A., Shin M.K. (2017): Linking morphology and molecules: integrative taxonomy of spathidiids (Protista: Ciliophora: Litostomatea) from Korea. — J. nat. Hist. **51**: 939–974.
- Jankowski A.V. (2007): Phylum Ciliophora Doflein, 1901. Review of taxa. In: Alimov A.F. (ed.): Protista: Handbook on zoology, Part 2, pp. 415–993. Nauka, St. Petersburg.
- Kahl A. (1927): Neue und ergänzende Beobachtungen holotricher Ciliaten. I. — Arch. Protistenk. **60**: 34–129.
- Kahl A. (1930): Urtiere oder Protozoa I: Wimpertiere oder Ciliata (Infusoria) 1. Allgemeiner Teil and Prostomata. — Tierwelt Dtl. **18**: 1–180.
- Kahl A. (1931): Urtiere oder Protozoa I: Wimpertiere oder Ciliata (Infusoria) 2. Holotricha außer den im 1. Teil behandelten Prostomata. — Tierwelt Dtl. **21**: 181–398.
- Kahl A. (1932): Urtiere oder Protozoa I: Wimpertiere oder Ciliata (Infusoria) 3. Spirotricha. — Tierwelt Dtl. **25**: 399–650.
- Kahl A. (1935): Urtiere oder Protozoa I: Wimpertiere oder Ciliata (Infusoria) 4. Peritricha und Chonotricha. — Tierwelt Dtl. **30**: 651–886, I–V.
- Kahl A. (1943): Infusorien (1. Teil). Ein Hilfsbuch zum Erkennen, Bestimmen, Sammeln und Präparieren der freilebenden Infusorien des Süßwassers und der Moore. Buchbeilage zum Mikrokosmos Jahrgang 1942/43, d. h., erschienen in der Reihe “Handbücher für die praktische naturwissenschaftliche Arbeit”, Band 31/32, 52 pp. Franckh'sche Verlagsbuchhandlung, W. Keller & Co., Stuttgart.
- Kamra K., Kumar S. & Sapra G.R. (2008): Species of *Gonostomum* and *Paragonostomum* (Ciliophora, Hypotrichida, Oxytrichidae) from the Valley of Flowers, India, with descriptions of *Gonostomum singhii* sp nov, *Paragonostomum ghangriai* sp nov and *Paragonostomum minuta* sp nov. — Indian J. Microbiol. **48**: 372–388.
- Kim J.H., Vd'ačný P., Shazib S.U.A. & Shin M.K. (2014): Morphology and molecular phylogeny of *Apoterritricha lutea* n. g., n. sp. (Ciliophora, Spirotrichea, Hypotrichia): a putative missing link connecting *Cyrtohymena* and *Afrokeronopsis*. — J. Euk. Microbiol. **61**: 520–536.
- Krüger F. (1956): Über die Microsporiden-Infektion von *Campanella umbellaria* (Ciliata, Peritricha). — Zool. Anz. **156**:125–129.
- Kumar S. & Foissner H. (2016): High cryptic soil ciliate (Ciliophora, Hypotrichida) diversity in Australia. — Eur. J. Protistol. **53**: 61–95.

- Kumar S. & Foissner W. (2017): Morphology and ontogenesis of *Stylonychia* (*Metastylonychia*) *nodulinucleata* nov. subgen. (Ciliophora, Hypotricha) from Australia. — Eur. J. Protistol. **57**: 61–72.
- Lutz A. & Splendore A. (1908): Über Pebrine und verwandte Mikrosporidien. — Zentralbl. Bakteriol. Parasitenkd. Infektionskr. Hyg. Abt. 1 Orig **46**: 311–315.
- Lynn D.H. (1980): The somatic cortical ultrastructure of *Bursaria truncatella* (Ciliophora, Colpodida). — Trans. Am. microsc. Soc. **99**: 349–359.
- Mermod G. (1914): Recherches sur la faune infusorienne des tourbières et des eaux voisines de Sainte-Croix (Jura vaudois). — Revue suisse Zool. **22**: 31–114, Planches 2, 3.
- Müller O.F. (1773): Vermium Terrestrium et Fluviatilium, seu Animalium Infusoriorum, Helminthicorum et Testaceorum, non Marinorum, Succincta Historia. Heineck & Faber, Havniae & Lipsiae. 135 pp.
- Müller O.F. (1786): Animalcula Infusoria Fluviatilia et Marina, quae Detexit, Systematicè Descripsit et ad Vivum Delineari Curavit. — N. Mölleri, Hauniae: vi + 367 pp.
- Oertel A., Wolf K., Al-Rasheid K., Foissner W. (2008): Revision of the genus *Coriplites* Foissner, 1988 (Ciliophora: Haptorida), with description of *Apocoriplites* nov. gen. and three new species. — Acta Protozool. **47**: 231–246.
- Penard E. (1922): Études sur les infusoires d'eau douce. Georg and Cie, Genève. 331 pp.
- Petz W. & Foissner W. (1993): Morphogenesis in some freshwater tintinnids (Ciliophora, Oligotrichida). — Eur. J. Protistol. **29**: 106–120.
- Petz W. & Foissner W. (1997): Morphology and infraciliature of some soil ciliates (Protozoa, Ciliophora) from continental Antarctica, with notes on the morphogenesis of *Sterkiella histriomuscorum*. — Polar Record **33**: 307–326.
- Petz W., Song W. & Wilbert N. (1995): Taxonomy and ecology of the ciliate fauna (Protozoa, Ciliophora) in the endopagial and pelagial of the Weddell Sea, Antarctica. — Stapfia (Linz) **40**: 1–223.
- Qin Y., Qiu Z., Shao C., Warren A. & Shen Z. (2011): Morphological redescription and morphogenesis of *Urosoma macrostyla* (Wrześniowski, 1866) Berger, 1999 (Ciliophora, Hypotrichida). — Acta Protozool. **50**: 163–174.
- Schewiakoff W. (1892): Ueber die geographische Verbreitung der Süßwasser-Protozoën. — Verh. naturh.-med. Ver. Heidelb. (N. S.) **4**: 544–567.
- Schewiakoff W. (1893): Über die geographische Verbreitung der Süßwasser-Protozoën. — Zap. imp. Akad. Nauk, 7e Série **41**: 1–201, Tafeln I–IV.
- Schewiakoff W. (1896): The organization and systematics of the infusoria Aspirotricha (Holotricha auctorum). — Zap. imp. Akad. Nauk **4**: 1–395.
- Shao C., Li L., Zhang Q., Song W. & Berger H. (2014): Molecular phylogeny and ontogeny of a new ciliate genus, *Paracladotricha salina* n. g., n. sp. (Ciliophora, Hypotrichia). — J. Euk. Microbiol. **61**: 371–380.
- Shao C., Li L., Zhang Q., Song W. & Berger H. (2017): Corrigendum to “Molecular phylogeny and ontogeny of a new ciliate genus, *Paracladotricha salina* n. g., n. sp. (Ciliophora, Hypotrichia) by Shao et al. 2014”. — J. Euk. Microbiol. **64**: 901–902.
- Singh J. & Kamra K. (2015): Molecular phylogeny of *Urosomoida agilis*, and new combinations: *Hemiurosomoida longa* gen. nov., comb. nov., and *Heterourosomoida lanceolate* gen. nov., comb. nov. (Ciliophora, Hypotricha). — Eur. J. Protistol. **51**: 55–65.
- Small E.B. & Lynn D.H. (1981): A new macrosystem for the phylum Ciliophora Doflein, 1901. — BioSystems **14**: 387–401.
- Smith J.C. (1897): Notices of some undescribed infusoria, from the infusorial fauna of Louisiana. — Trans. Am. microsc. Soc. **19**: 55–68, Plate I.

- Song W. (1996): Description of the marine ciliate *Pseudoamphisiella lacazei* (Maupas, 1883) nov. gen., nov. comb. (Protozoa, Ciliophora, Hypotrichida). — *Oceanol. Limnol. Sin.* **27**: 18–22.
- Song W. & Shao C. (2017): Ontogenetic patterns of hypotrich ciliates. Science Press, Beijing.
- Song W. & Wilbert N. (1989): Taxonomische Untersuchungen an Aufwuchsciliaten (Protozoa, Ciliophora) im Poppelsdorfer Weiher, Bonn. — *Lauterbornia* Heft **3**: 2–221.
- Sprague V. (1977): Annotated list of species of microsporidia. In: Bulla L.A. Jr. & Cheng T.C. (Eds): *Comparative pathobiology*, vol 2: Systematics of the microsporidia. Plenum, New York, London, pp 31–334.
- Stechmann A., Schlegel M. & Lynn D. (1998): Phylogenetic relationships between prostome and colpodean ciliates tested by small subunit rRNA sequences. — *Mol. Phyl. Evol.* **9**: 48–54.
- Stein F. (1859): *Der Organismus der Infusionsthier nach eigenen Forschungen in systematischer Reihenfolge bearbeitet. I. Abtheilung. Allgemeiner Theil und Naturgeschichte der hypotrichen Infusionsthier.* Engelmann, Leipzig. I–XII, 206 pp, Tafeln I–XIV.
- Sterki V. (1878): Beiträge zur Morphologie der Oxytrichinen. — *Z. wiss. Zool.* **31**: 29–58, Tafel IV.
- Stokes A.C. (1891): Notes of new infusoria from the fresh waters of the United States. — *Jl R. microsc. Soc.* year **1891**: 697–704, Plate X.
- Strüder-Kypke M.C., Wright A.-D.G., Foissner W., Chatzinotas A. & Lynn D.H. (2006): Molecular phylogeny of litostome ciliates (Ciliophora, Litostomatea) with emphasis on free-living haptorian genera. — *Protist* **157**: 261–278.
- Vďačný P. & Foissner W. (2012): Monograph of the dileptids (Protista, Ciliophora, Rhynchostomatia). — *Denisia (Linz)* **31**: 1–529.
- Vďačný P. & Foissner W. (2013): Synergistic effects of combining morphological and molecular data in resolving the phylogenetic position of *Semispathidium* (Ciliophora, Haptoria) with description of *Semispathidium breviararmatum* sp. n. from tropical Africa. — *Zool. Scr.* **42**: 529–549.
- Vďačný P., Breiner H.-W., Yashchenko V., Dunthorn M., Stoeck T. & Foissner W. (2014): The chaos prevails: molecular phylogeny of the Haptoria (Ciliophora, Litostomatea). — *Protist* **165**: 93–111.
- Vďačný P., Slovák M. & Foissner W. (2014a): Multivariate morphometric analyses of the predatory ciliate genus *Semispathidium* (Ciliophora: Litostomatea), with description of *S. longiararmatum* nov. spec. — *Eur. J. Protistol.* **50**: 329–344.
- Vuxanovici A. (1963): Contributii la sistematica ciliatelor (Nota IV). — *Studii Cerc. Biol., Seria "biologie animala"* **15**: 65–93.
- Wang J., Lyu Z., Warren A. Wang F. & Shao C. (2016): Morphology, ontogeny and molecular phylogeny of a novel saline soil ciliate, *Urosomoida paragiliformis* n. sp. (Ciliophora, Hypotrichia). — *Eur. J. Protistol.* **56**: 79–89.
- Wilbert N. (1975): Eine verbesserte Technik der Protargolimprägung für Ciliaten. — *Mikrokosmos* **64**: 171–179.
- Wirnsberger E., Foissner W. & Adam H. (1984): Morphologie und Infraciliatur von *Perispira pyriformis* nov. spec., *Cranotheridium foliosus* (Foissner, 1983) nov. comb. und *Dileptus anser* (O. F. Müller, 1786) (Protozoa, Ciliophora). — *Arch. Protistenk.* **128**: 305–317.
- Wise B.N. (1965): The morphogenetic cycle in *Euplotes eurytomus* and its bearing on problems of ciliate morphogenesis. — *J. Protozool.* **12**: 626–648.
- Wrzesniowski A. (1867): Przyczynek do historyi naturalnej wymoczków. — *Rocznik ces. król. Towarzystwa Naukowego Krakowskiego, Poczet trzeci* **12** (Ogólnego zbioru, 35): 231–342, Tablica I–VII.
- Wrzesniowski A. (1870): Beobachtungen über Infusorien aus der Umgebung von Warschau. — *Z. wiss. Zool.* **20**: 467–511.

Xu K., Foissner W. (2005): Description of *Protospathidium serpens* (Kahl, 1930) and *P. fraterculum* n. sp. (Ciliophora, Haptoria), two species based on different resting cyst morphology. — J. Euk. Microbiol. **52**: 298–309.

## Tables 1–37 for morphometric characterisation

The morphometric tables are arranged at the end of Chapter 4 because of the high number of illustrations on 204 plates and the relatively low amount of text. The two lists below are fast guides to the individual tables:

<i>Afrogonostomum alveum</i> → Table 22 on p. 327	Table 1 → p. 308
<i>Apobryophyllum pinetum</i> → Tables 9, 10 on p. 315	Table 2 → p. 309
<i>Apooxytricha bromelicola</i> → Tables 31, 34 on p. 337, 341	Table 3 → p. 310
<i>Bophrya costata</i> → Table 13 on p. 318	Table 4 → p. 310
<i>Bothrix africana</i> → Table 30 on p. 336	Table 5 → p. 311
<i>Bryophyllum australiense</i> → Table 11 on p. 316	Table 6 → p. 312
<i>Bursaria africana</i> → Tables 15, 16 on p. 321, 322	Table 7 → p. 313
<i>Bursaria americana</i> → Tables 15, 17 on p. 321, 323	Table 8 → p. 314
<i>Bursaria fluviatilis</i> → Tables 15, 18 on p. 321, 324	Table 9 → p. 315
<i>Bursaria salisburgensis</i> → Tables 15, 17 on p. 321, 323	Table 10 → p. 315
<i>Bursaria truncatella</i> → Tables 15, 16 on p. 321, 322	Table 11 → p. 316
<i>Bursaria uluruensis</i> → Tables 15, 18 on p. 321, 324	Table 12 → p. 317
<i>Circinella filiformis australiensis</i> → Table 23 on p. 328	Table 13 → p. 318
<i>Conothrix australiensis</i> → Table 33 on p. 340	Table 14 → p. 319
<i>Crassienchelys oriclavata</i> → Table 5 on p. 311	Table 15 → p. 321
<i>Enchelariophrya jamaicensis</i> → Table 1 on p. 308	Table 16 → p. 322
<i>Enchelariophrya micrographica</i> → Table 1 on p. 308	Table 17 → p. 323
<i>Enchelys australiensis</i> → Tables 2, 3 on p. 309, 310	Table 18 → p. 324
<i>Enchelys bivacuolata</i> → Table 4 on p. 310	Table 19 → p. 325
<i>Enchelys polynucleata hollandica</i> → Table 2 on p. 309	Table 20 → p. 326
<i>Enchelys polynucleata polynucleata</i> → Table 2 on p. 309	Table 21 → p. 326
<i>Enchelys polyvacuolata</i> → Table 4 on p. 310	Table 22 → p. 327
<i>Gastronauta insula</i> → Table 19 on p. 325	Table 23 → p. 328
<i>Hemiurosoma similis</i> → Table 26 on p. 331	Table 24 → p. 329
<i>Levispatha australiensis</i> → Table 6 on p. 312	Table 25 → p. 331
<i>Microsporidium protocyclidicola</i> → Table 21 on p. 326	Table 26 → p. 331
<i>Mixophrya pantanalensis australiensis</i> → Tables 31, 32 on p. 337	Table 27 → p. 333
<i>Mixophrya pantanalensis pantanalensis</i> → Tables 31, 32 on p. 337	Table 28 → p. 334
<i>Monomicrocaryon australiense</i> → Table 35 on p. 342	Table 29 → p. 335
<i>Monomicrocaryon opisthomuscorum</i> → Table 35 on p. 342	Table 30 → p. 336
<i>Protocyclidium bimacronucleatum</i> → Table 20 on p. 326	Table 31 → p. 337
<i>Pseudofuscheria magna</i> → Tables 7, 8 on p. 313, 314	Table 32 → p. 337
<i>Rimaleptus similis australiensis</i> → Table 12 on p. 317	Table 33 → p. 340
<i>Tachysoma setifera</i> → Tables 36, 37 on p. 344, 345	Table 34 → p. 341
<i>Urosoma australiensis</i> → Tables 24, 31 on p. 329, 337	Table 35 → p. 342
<i>Urosoma pelobia</i> → Tables 24, 25 on p. 329, 331	Table 36 → p. 344
<i>Urosomoida bromelicola</i> → Tables 28, 29 on p. 334, 335	Table 37 → p. 345
<i>Urosomoida uluruensis</i> → Table 27 on p. 333	
<i>Wolfkasia acuta</i> → Table 14 on p. 319	
<i>Wolfkasia pantanalensis</i> → Table 14 on p. 319	

**Table 1.** Comparison of morphometric data of *Enchelariophrya jamaicensis* (JAM) and *E. micrographica* (MIC, from Foissner 2010).

Characteristic <sup>a</sup>	Species	Mean	M	SD	SE	CV	Min	Max	n
Body, length	JAM	118.8	124.0	23.8	10.6	20.0	85.0	150.0	5
	MIC	107.2	103.0	14.0	3.1	13.1	90.0	135.0	21
Body, width	JAM	40.4	35.0	8.7	3.9	21.6	33.0	53.0	5
	MIC	42.4	41.0	7.2	1.6	17.0	35.0	65.0	21
Body length:width, ratio	JAM	3.0	3.1	0.5	0.2	17.1	2.3	3.6	5
	MIC	2.6	2.5	0.3	0.1	10.4	2.0	3.1	21
Oral bulge, width	JAM	8.6	8.0	1.3	0.6	15.6	7.0	10.0	5
	MIC	9.7	9.0	1.4	0.3	14.6	7.0	13.0	21
Oral bulge, height	JAM	2.4	2.0	–	–	–	2.0	3.0	5
	MIC	2.4	2.0	0.5	0.1	22.4	2.0	3.5	21
Oral basket, length <sup>b</sup>	JAM	28.0	25.0	–	–	–	20.0	50.0	5
	MIC	29.3	30.0	–	–	–	15.0	40.0	21
Anterior body end to first macronuclear nodule, distance	JAM	11.0	11.0	1.6	0.7	14.4	9.0	13.0	5
	MIC	13.4	13.0	4.4	1.0	32.8	7.0	27.0	21
Macronuclear nodules, number <sup>c</sup>	JAM	260.0	250.0	–	–	–	130.0	360.0	5
	MIC	116.7	100.0	–	–	–	50.0	210.0	21
Macronucleus nodules, length	JAM	3.8	5.0	1.6	0.6	34.3	3.0	7.0	5
	MIC	6.5	6.0	2.3	0.5	36.1	3.0	12.0	21
Macronucleus nodules, width	JAM	3.2	3.0	–	–	–	3.0	4.0	5
	MIC	4.1	4.0	1.2	0.3	27.8	3.0	7.0	21
Somatic ciliary rows, number	JAM	41.4	40.0	3.0	1.3	7.2	38.0	45.0	5
	MIC	34.9	35.0	2.0	0.4	5.7	32.0	39.0	21
Basal bodies in a lateral kinety, number <sup>d</sup>	JAM	107.0	100.0	23.3	10.4	21.4	80.0	140.0	5
	MIC	84.2	78.0	17.0	3.7	20.2	50.0	128.0	21
Dorsal brush rows, number	JAM	3.0	3.0	0.0	0.0	0.0	3.0	3.0	3
	MIC	3.0	3.0	0.0	0.0	0.0	3.0	3.0	21
Dorsal brush row 1, length	JAM	26.0	–	–	–	–	25.0	27.0	2
	MIC	22.5	23.0	4.1	0.9	18.3	17.0	35.0	21
Dorsal brush row 2, length	JAM	27.5	–	–	–	–	25.0	30.0	2
	MIC	23.4	22.0	4.5	1.0	19.1	17.0	34.0	21
Dorsal brush row 3, length	JAM	8.5	–	–	–	–	7.0	10.0	2
	MIC	9.0	9.5	1.7	0.4	19.3	6.0	12.0	20
Dorsal brush row 1, number of dikinetids	JAM	42.0	–	–	–	–	–	–	1
	MIC	23.7	22.0	4.9	1.1	20.8	18.0	38.0	21
Dorsal brush row 2, number of dikinetids	JAM	40.0	–	–	–	–	–	–	1
	MIC	28.9	30.0	6.2	1.3	21.3	19.0	40.0	21
Dorsal brush row 3, number of dikinetids	JAM	16.0	–	–	–	–	–	–	1
	MIC	11.4	12.0	3.1	0.7	27.4	6.0	17.0	19

<sup>a</sup> Data based on mounted, protargol-impregnated (Foissner 1991, protocol A), and randomly selected specimens from a non-flooded Petri dish culture. Measurements in  $\mu\text{m}$ . CV – coefficient of variation in %, M – median, Max – maximum, Mean – arithmetic mean, Min – minimum, n – number of individuals investigated, SD – standard deviation, SE – standard error of arithmetic mean.

<sup>b</sup> Rough values because faintly and very likely incompletely impregnated.

<sup>c</sup> Rough values because difficult to count.

<sup>d</sup> Ciliated and non-ciliated basal bodies.

**Table 2.** Comparison of Austrian type population (AT) of *Enchelys polynucleata polynucleata* nov. subspec. (see Foissner 1984 and Foissner et al. 2002 for additional data on taxonomy and morphometry) with *E. polynucleata hollandica* nov. subspec. (NH, additional data in Foissner & Al-Rasheid 2007), *E. australiensis* (AU), and *E. polynucleata polynucleata* from the Antarctic (GI, Gough Island).

Characteristic <sup>a</sup>	Species	Mean	M	SD	SE	CV	Min	Max	n
Body, length	AT	119.5	120.0	10.0	2.2	8.3	100.0	140.0	21
	NH	114.4	116.0	12.0	2.6	10.5	96.0	131.0	21
	AU	134.7	132.0	17.5	5.5	13.0	105.0	165.0	10
	GI	121.3	122.0	14.9	3.2	12.3	100.0	145.0	21
Body, width	AT	60.6	60.0	10.6	2.3	17.4	40.0	77.0	21
	NH	53.0	53.0	9.1	2.0	17.1	38.0	66.0	21
	AU	66.1	71.0	24.9	7.9	37.6	51.0	97.0	10
	GI	52.3	52.0	9.1	2.0	17.3	32.0	70.0	21
Body length:width, ratio	AT	2.0	2.0	0.4	0.1	18.9	1.6	3.1	21
	NH	2.2	2.2	0.3	0.1	12.1	1.7	2.6	21
	AU	1.9	1.8	0.4	0.1	21.8	1.3	2.5	10
	GI	2.3	2.6	0.4	0.2	17.4	3.1	13.0	21
Oral bulge, length (width)	AT	20.4	21.0	2.9	0.6	14.1	16.0	26.0	21
	NH	25.0	26.0	3.9	0.6	15.6	20.0	34.0	21
	AU	32.6	35.0	4.7	1.6	14.5	25.0	39.0	9
	GI	27.1	27.0	3.2	0.7	11.9	21.0	35.0	21
Temporary cytostome to ventral margin of oral bulge, distance	AT	11.0	11.0	1.5	0.3	14.1	8.0	14.0	21
	NH	15.0	15.0	2.8	0.6	18.7	10.0	21.0	21
	AU	20.7	22.0	3.1	1.0	14.9	16.0	25.0	9
	GI	14.8	15.0	2.3	0.5	15.4	9.0	20.0	21
Temporary cytostome to dorsal margin of oral bulge, distance	AT	9.6	10.0	1.7	0.4	17.2	7.0	12.0	21
	NH	10.1	10.0	1.9	0.4	18.3	8.0	15.0	21
	AU	11.9	12.0	1.8	0.6	14.8	9.0	14.0	9
	GI	12.3	12.0	1.4	0.3	11.3	9.0	15.0	21
Temporary cytostome, difference between ventral and dorsal margin of oral bulge	AT	1.1	0.0	1.3	0.3	119.2	0.0	4.0	19
	NH	5.5	5.0	1.4	0.3	25.4	4.0	8.0	20
	AU	8.8	9.0	1.7	0.6	19.5	6.0	11.0	9
	GI	3.2	3.0	1.6	0.4	51.0	1.0	7.0	21
Ciliary rows, number	AT	35.1	35.0	3.4	0.5	9.6	30.0	45.0	21
	NH	34.4	35.0	2.4	0.7	7.9	29.0	38.0	12
	AU	42.5	42.5	4.9	1.7	11.5	36.0	50.0	8
	GI	34.1	35.0	3.0	0.6	8.6	31.0	38.0	21

<sup>a</sup> Data based on specimens cultivated with the non-flooded Petri dish method and randomly selected specimens impregnated with Foissner's (1991) protargol method. All measurements in  $\mu\text{m}$ . CV – coefficient of variation in %, M – median, Max – maximum, Mean – arithmetic mean, Min – minimum, n – number of individuals investigated, SD – standard deviation, SE – standard error of arithmetic mean.

**Table 3.** Morphometric data on *Enchelys australiensis* based on mounted, protargol-impregnated, and randomly selected specimens from a non-flooded Petri dish culture. Measurements in  $\mu\text{m}$ . CV – coefficient of variation in %, M – median, Max – maximum, Mean – arithmetic mean, Min – minimum, n – number of individuals investigated, SD – standard deviation, SE – standard error of arithmetic mean.

Characteristic	Mean	M	SD	SE	CV	Min	Max	n
Body, length	134.7	132.0	17.5	5.5	13.0	105.0	165.0	10
Body, width	66.1	71.0	24.9	7.9	37.6	51.0	97.0	10
Body length: width, ratio	1.9	1.8	0.4	0.1	21.8	1.5	2.5	8
Ciliary rows, number	42.5	42.5	4.9	1.7	11.5	36.0	50.0	8
Dorsal brush kineties, number	3.0	3.0	0.0	0.0	0.0	3.0	3.0	10
Dorsal brush row 2, length	27.8	27.0	5.6	1.8	20.0	18.0	38.0	10
First kinety left of dorsal brush, number of basal bodies	89.0	85.0	21.3	6.7	24.0	60.0	120.0	10
Oral bulge, length (width)	32.6	35.0	4.7	1.6	14.5	25.0	39.0	9
Oral bulge, maximum dorsal height	6.3	7.0	0.9	0.2	13.6	5.0	7.0	13
Macronuclear nodules, length	7.3	7.5	1.9	0.6	26.7	4.0	10.0	10
Macronuclear nodules, width	2.6	2.5	0.5	0.2	19.9	2.0	3.0	10
Macronuclear nodules, number	about 150–300							10

**Table 4.** Morphometric data on *Enchelys bivacuolata* (EB) and *Enchelys polyvacuolata* (EP) based on protargol-impregnated specimens from non-flooded Petri dish cultures. Measurements in  $\mu\text{m}$ . CV – coefficient of variation in %, M – median, Max – maximum, Mean – arithmetic mean, Min – minimum, n – number of individuals investigated, SD – standard deviation, SE – standard error of arithmetic mean.

Characteristic	Species	Mean	M	SD	SE	CV	Min	Max	n
Body, length	EB	188.0	184.0	34.3	9.9	18.3	139.0	240.0	12
	EP	232.4	210.0	35.5	10.7	15.3	196.0	280.0	11
Body, width	EB	34.5	34.5	4.5	1.3	13.1	26.0	41.0	12
	EP	40.3	35.0	13.7	4.1	33.9	27.0	75.0	11
Body length: width, ratio	EB	5.5	5.4	1.1	0.3	19.7	3.8	7.7	12
	EP	6.3	6.0	2.0	0.6	32.9	2.7	9.8	11
Oral bulge, width	EB	10.2	10.0	1.4	0.4	13.4	8.0	13.0	10
	EP	12.2	12.0	1.4	0.4	11.5	11.0	15.0	11
Oral bulge, height	EB	2.3	2.5	0.5	0.2	22.1	1.5	3.0	6
	EP	2.3	2.0	0.5	0.4	22.5	2.0	3.0	6
Somatic kineties, number	EB	25.5	25.5	1.6	0.6	6.3	23.0	28.0	8
	EP	20.8	21.0	1.5	0.7	7.1	19.0	23.0	5
Ciliated kinetids in a ventral kinety, number	EB	131.8	136.0	21.6	10.8	16.4	103.0	152.0	4
	EP	131.0	130.0	24.1	10.8	18.4	105.0	160.0	5
Anterior body end to proximal end of dorsal brush row 1, distance	EB	38.4	40.0	7.4	2.8	19.4	26.0	49.0	7
	EP	39.6	39.0	7.9	3.5	19.9	31.0	49.0	5
Anterior body end to proximal end of dorsal brush row 2, distance	EB	36.4	36.0	6.8	2.6	18.7	24.0	45.0	7
	EP	41.8	38.0	8.8	3.6	20.9	35.0	56.0	6
Anterior body end to proximal end of dorsal brush row 3, distance	EB	26.3	26.0	5.2	2.1	19.6	21.0	32.0	6
	EP	24.3	23.0	9.4	3.9	38.8	15.0	39.0	6
Dikinetids in dorsal brush row 1, number	EB	35.4	35.0	2.7	1.2	7.6	32.0	39.0	5
	EP	34.0	35.0	2.0	1.0	5.9	31.0	35.0	4
Dikinetids in dorsal brush row 2, number	EB	33.0	31.5	7.3	3.6	22.0	26.0	43.0	4
	EP	30.3	30.5	1.7	0.9	5.6	28.0	32.0	4
Dikinetids in dorsal brush row 3, number	EB	16.4	13.0	8.0	3.6	48.9	8.0	28.0	5
	EP	20.0	20.5	2.2	1.1	10.8	17.0	22.0	4

**Table 4.** Continued.

Characteristic	Species	Mean	M	SD	SE	CV	Min	Max	n
Dorsal brush rows, number	EB	3.3	3.0	–	–	–	3.0	4.0	8
	EP	3.0	3.0	0.0	0.0	0.0	3.0	3.0	5
Contractile vacuoles, number	EB	2.0	2.0	0.0	0.0	0.0	2.0	2.0	7
	EP	>3 (not fully recognizable in the preparations)						11	
Pores in anterior contractile vacuole, number	EB	4.5	4.0	1.7	0.9	38.5	3.0	7.0	4
	EP	not recognizable							
Pores in posterior contractile vacuole, number	EB	5.0	4.0	1.9	0.8	37.4	3.0	7.0	5
	EP	not recognizable							
Macronuclear nodules, length	EB	5.6	6.0	0.9	0.3	16.3	4.0	7.0	8
	EP	5.6	6.0	1.4	0.4	24.2	4.0	8.0	11
Macronuclear nodules, width	EB	2.1	2.0	0.4	0.1	16.6	2.0	3.0	8
	EP	2.2	2.0	0.4	0.1	19.9	1.5	3.0	11
Macronuclear nodules, number (rough values)	EB	252.9	258.0	46.0	15.3	18.2	193.0	334.0	9
	EP	489.0	500.0	33.0	11.1	6.8	400.0	500.0	9
Micronuclei, diameter	EB	2.1	2.0	0.2	0.1	9.1	2.0	2.5	7
	EP	3.8	4.0	0.9	0.3	23.5	2.8	6.0	11
Micronuclei, number (rough values because difficult to separate from similar cytoplasmic inclusions)	EB	11.3	10.0	3.8	1.4	33.8	7.0	19.0	7
	EP	not recognizable							

**Table 5.** Morphometric data on *Crassienchelys oriclavata*, based on mounted, protargol-impregnated specimens from a non-flooded Petri dish culture. Measurements in  $\mu\text{m}$ . CV – coefficient of variation in %, M – median, Max – maximum, Mean – arithmetic mean, Min – minimum, n – number of individuals investigated, SD – standard deviation, SE – standard error of arithmetic mean.

Characteristic	Mean	M	SD	SE	CV	Min	Max	n
Body, length	127.9	129.5	22.6	4.8	17.7	99.0	189.0	22
Body, width	74.1	73.0	13.2	2.8	17.8	55.0	111.0	22
Body length: width, ratio	1.8	1.7	0.3	0.1	18.3	1.2	2.8	22
Anterior body end to first macronuclear nodule	21.2	20.0	5.9	1.3	27.7	11.0	30.0	21
Oral bulge, length of cord	45.4	46.0	6.2	1.7	13.7	34.0	55.0	13
Oral bulge, width at ventral end	5.3	5.0	0.9	0.3	16.5	4.0	7.0	12
Oral bulge, width at dorsal end	13.1	13.0	2.4	0.7	18.3	9.0	18.0	12
Oral bulge, height near ventral end	2.6	2.0	1.3	0.5	48.9	1.0	5.0	7
Oral bulge, height near dorsal end	6.3	6.5	2.1	0.7	21.1	4.0	10.0	10
Temporary cytostome, distance to ventral margin of oral bulge	34.8	33.0	5.1	1.8	14.7	13.0	43.0	8
Temporary cytostome, distance to dorsal margin of oral bulge	11.9	12.0	2.1	0.7	17.5	8.0	15.0	9
Temporary cytostome, difference between ventral and dorsal margin of oral bulge	23.0	21.0	5.3	1.6	22.9	14.0	32.0	11
Macronucleus figure, length	100.0	99.0	23.3	5.1	5.1	72.0	165.0	21
Macronuclear nodules, length	9.7	9.0	1.5	0.3	15.8	8.0	14.0	21
Macronuclear nodules, width	3.5	4.0	–	–	–	3.0	4.0	21
Macronuclear nodules, number	96.1	92.0	21.7	4.7	22.6	64.0	140.0	21
Ciliary rows, number <sup>a</sup>	61.7	60.0	10.8	2.4	17.6	47.0	89.0	21
Basal bodies (cilia) in a ventral row, number	81.7	84.0	13.4	3.2	16.4	59.0	105.0	17
Dorsal brush, number of rows	3.8	4.0	–	–	–	3.0	4.0	11
Dorsal brush row 1, length	19.4	19.0	8.4	3.2	43.3	11.0	37.0	7
Dorsal brush row 1, number of dikinetids	18.0	16.0	6.2	3.6	34.7	13.0	25.0	3

**Table 5.** Continued.

Characteristic	Mean	M	SD	SE	CV	Min	Max	n
Dorsal brush row 2, length	41.6	35.0	11.8	3.9	28.4	30.0	61.0	9
Dorsal brush row 2, number of dikinetids	46.5	46.5	–	–	–	41.0	52.0	2
Dorsal brush row 3, length	40.4	36.0	10.7	3.6	26.3	31.0	57.0	9
Dorsal brush row 3, number of dikinetids	50.0	50.0	–	–	–	43.0	57.0	2
Dorsal brush row 4, length	21.6	20.5	4.8	1.7	22.1	16.0	31.0	8
Dorsal brush row 4, number of dikinetids	24.3	25.5	5.1	2.6	21.1	17.0	29.0	4
Contractile vacuole, number of pores	9.8	9.0	3.5	1.0	35.5	7.0	20.0	12

<sup>a</sup> Only one side is impregnated because the species is rather thick; values thus doubled.

**Table 6.** Morphometric data on *Levispatha australiensis* based, if not mentioned otherwise, on ethanol-fixed, mounted, protargol-impregnated, and randomly selected specimens from a non-flooded Petri dish culture. Measurements in  $\mu\text{m}$ . CV – coefficient of variation in %, M – median, Max – maximum, Mean – arithmetic mean, Min – minimum, n – number of individuals investigated, SD – standard deviation, SE – standard error of arithmetic mean.

Characteristic	Mean	M	SD	SE	CV	Min	Max	n
Body, length in vivo (rough values)	94.0	100.0	–	–	–	70.0	120.0	11
Body, width in vivo (rough values)	22.0	20.0	–	–	–	12.0	30.0	11
Body length:width, ratio in vivo (rough values)	4.7	4.7	–	–	–	3.3	6.7	11
Body, length	93.0	96.0	14.2	3.1	15.3	50.0	115.0	21
Body, width in ventral or dorsal view	19.3	18.0	5.8	1.3	30.3	11.0	33.0	21
Body, width in lateral view	18.8	16.0	6.0	1.3	32.2	11.0	36.0	21
Body length:width, ratio in ventral or dorsal view	5.2	4.9	1.7	0.4	33.3	3.1	9.1	21
Body, length (Stieve fixation)	88.8	90.0	15.2	3.3	17.1	62.0	115.0	21
Body, width in ventral or dorsal view (Stieve fixation)	15.8	16.0	4.2	0.9	26.8	9.0	22.0	21
Body, width in lateral view (Stieve fixation)	16.2	15.0	4.4	1.0	26.8	10.0	25.0	21
Body length:width, ratio in ventral or dorsal view (Stieve fixation)	6.2	5.8	1.9	0.4	30.7	4.1	11.9	21
Anterior body end to macronucleus, distance	42.2	42.0	7.7	1.7	18.2	30.0	58.0	21
Anterior body end to proximal end of oral bulge, distance	17.4	17.0	3.3	0.7	18.8	12.0	25.0	21
Circumoral kinety to end of brush row 1, distance	13.8	14.0	1.2	0.3	8.6	11.0	16.0	21
Circumoral kinety to end of brush row 2, distance	13.7	13.0	1.2	0.3	8.7	12.0	16.0	21
Circumoral kinety to end of brush row 3, distance	9.4	10.0	0.9	0.2	9.8	7.0	11.0	21
Dorsal brush row 1, number of dikinetids	11.5	12.0	1.2	0.3	10.1	9.0	14.0	21
Dorsal brush row 2, number of dikinetids	12.0	13.0	1.6	0.3	12.9	9.0	14.0	21
Dorsal brush row 3, number of dikinetids	7.4	8.0	0.8	0.2	10.9	5.0	8.0	21
Dorsal brush row 3, number of bristles in posterior tail	7.5	8.0	1.5	0.3	20.6	4.0	10.0	21
Dorsal brush row 1, number of monokinetids in anterior tail	1.5	1.0	–	–	–	1.0	2.0	21
Dorsal brush row 2, number of monokinetids in anterior tail	2.0	2.0	0.5	0.1	22.4	1.0	3.0	21
Dorsal brush row 3, number of monokinetids in anterior tail	2.5	3.0	–	–	–	2.0	3.0	21
Oral bulge, dorsal height	1.5	1.5	–	–	–	1.0	2.0	21
Oral bulge, max. width	1.6	1.5	–	–	–	1.0	2.0	21
Macronucleus, length	22.0	21.0	4.4	1.0	19.8	15.0	33.0	21
Macronucleus, width	4.6	5.0	0.6	0.1	12.0	3.5	5.0	21
Micronucleus, length	3.4	3.5	0.5	0.1	14.0	2.5	4.0	21
Micronucleus, width	3.2	3.0	0.5	0.1	14.4	2.5	4.0	21
Ciliary rows, number	12.9	13.0	1.0	0.2	7.9	11.0	15.0	21
Ciliated monokinetids in a lateral row, number	30.9	30.0	6.9	1.5	22.4	20.0	48.0	21
Dorsal brush, number of rows	3.0	3.0	0.0	0.0	0.0	3.0	3.0	21
Resting cysts, diameter in vivo	34.7	35.0	2.5	0.6	7.3	30.0	39.0	17

**Table 7.** Comparison of *Pseudofuscheria magna* with the congener, *Fuscheria* spp. and other similar genera. Number of specimens investigated in parentheses. Measurements in  $\mu\text{m}$ . Averages are provided. nd – not determined.

Species (Reference)	Size of protargol-impregnated specimens	Number of ciliary rows	Number of dikinetids in brush row 1	Number of dikinetids in brush row 2	Shape of macronucleus
<i>Pseudofuscheria magna</i> nov. spec.	118 × 58 (29)	28	28 (21)	23	oblong and curved
<i>Pseudofuscheria terricola</i> (Berger et al. 1983) (two populations)	56 × 18 (21)	15	10	5	horseshoe-shaped,
<i>Pseudofuscheria terricola</i> (Foissner et al. 2002)	60 × 29 (25)	17	11	nd	filiform, helical
	68 × 22 (21)	15	8	3	oblong
<i>Fuscheria lacustris</i> (Song & Wilbert 1989)	42 × 22 (6)	25	nd	2–3	ellipsoid
<i>Fuscheria marina</i> (Petz et al. 1995)	104 × 60 (6, in vivo)	36	nd	nd	oblong
<i>Fuscheria nodosa</i> (Foissner 1983a)	45–80 × 25–35 (?)	25–30 (?)	19 (1)	15 (1)	oblong and curved
<i>Fuscheria nodosa</i> (Foissner & O'Donoghue 1990) <sup>b</sup>	39 × 23 (10)	26	13 (7)	10 (7)	semicircular
<i>Fuscheria nodosa salisburgensis</i> (Gabilondo & Foissner 2009) <sup>a</sup>	102 × 64 (21)	45	21	13	filiform,
(two populations)	82 × 53 (21)	42	20	14	tortuous strand
<i>Fuscheria uluruensis</i> (Gabilondo & Foissner 2009) <sup>a</sup>	74 × 53 (21)	46	24	14	12 oblong nodules
<i>Fuscheriides tibetensis</i> (Gabilondo & Foissner 2009) <sup>a</sup>	47 × 10 (21)	7	3	6	oblong
<i>Aciculoplites ethiopiensis</i> (Gabilondo & Foissner 2009) <sup>a</sup>	88 × 43 (21)	22	14 (1)	8 (1)	oblong to horseshoe-shaped
<i>Actinorhabdus trichocystifera</i> (Foissner 1984)	48 × 21 (16)	16	7	4	oblong
<i>Diplites telmatobius</i> (Foissner 1998)	51 × 21 (19)	16	3	3	oblong
<i>Diplites arenicola</i> (Foissner et al. 2002)	54 × 17 (19)	9	4	7	oblong
<i>Dioplitophrya otti</i> (Foissner et al. 2002)	93 × 38 (21)	26	nd	nd	horseshoe-shaped
<i>Coriplites terricola</i> (Foissner 1988) (Japanese and Australian population). Three brush rows	62 × 13 (15)	12	6	9, 11	two globular macronuclear nodules with
	55 × 11 (11)	12	7	10, 11	a micronucleus in between
<i>Coriplites grandis</i> (Oertel et al. 2008) (three brush rows)	162 × 38 (21)	26	22	27, 27	two ellipsoidal macronuclear nodules with a micronucleus in between
<i>Coriplites proctori</i> (Oertel et al. 2008) (three brush rows)	42 × 15 (22)	12	7	8, 5	oblong
<i>Coriplites tumidus</i> (Foissner 2016) (three brush rows). Three populations	93 × 20 (21)	11	13	26	two globular macronuclear nodules with
	100 × 16 (11)	9	11	22	a micronucleus in between
	93 × 13 (11)	10	10	19	
<i>Apocriplites lajacola</i> (Oertel et al. 2008)	71 × 18 (24)	12	10	9	two globular macronuclear nodules with a micronucleus in between

<sup>a</sup> Described in Gabilondo & Foissner (2009); <sup>b</sup> Reinvestigated with paratype material.

**Table 8.** Morphometric data on *Pseudofuscheria magna* based on mounted, protargol-impregnated, and randomly selected specimens from a non-flooded Petri dish culture. Measurements in  $\mu\text{m}$ . CV – coefficient of variation in %, M – median, Max – maximum, Mean – arithmetic mean, Min – minimum, n – number of individuals investigated, SD – standard deviation, SE – standard error of arithmetic mean.

Characteristic	Mean	M	SD	SE	CV	Min	Max	n
Body, length	118.2	120.0	15.0	2.7	12.7	85.0	145.0	29
Body, width	58.1	53.0	15.1	2.8	26.0	33.0	95.0	29
Body length:width, ratio	2.1	2.2	0.5	0.1	22.3	1.3	3.2	29
Anterior body end to macronucleus, distance	39.7	35.0	17.5	3.2	44.0	14.0	95.0	29
Macronucleus, length	41.7	40.0	7.2	1.6	17.3	31.0	59.0	21
Macronucleus, width	10.1	10.0	0.8	0.2	8.2	9.0	12.0	21
Micronucleus, length	4.9	5.0	0.8	0.2	15.3	4.0	7.0	21
Micronucleus, width	4.5	4.5	1.0	0.2	21.8	3.0	7.0	21
Micronucleus, thickness	2.5	2.5	0.4	0.1	16.6	2.0	3.0	11
Oral bulge, diameter	9.3	9.0	1.6	0.3	16.7	7.0	15.0	21
Oral bulge, height	2.0	2.0	0.0	0.0	0.0	2.0	2.0	21
Oral basket extrusomes, length	7.1	7.0	0.5	0.1	7.0	6.0	8.0	13
Cytoplasmic extrusomes, length with inflated end	7.0	7.0	1.2	0.3	17.4	9.0	13.0	13
Oral basket, longest rods	41.8	40.0	5.5	1.2	13.2	35.0	50.0	21
Ciliary rows, number	28.4	28.0	1.9	0.4	6.8	25.0	34.0	21
Ciliary rows, distance in mid-body	5.5	5.0	0.9	0.2	16.9	4.0	8.0	21
Kinetids in a ventral kinety, number	55.9	53.0	11.4	2.5	20.4	40.0	80.0	21
Kinetids in 30 $\mu\text{m}$ of mid-body, number	14.2	15.0	3.1	0.7	21.6	9.0	19.0	21
Kinetids in polymerization 1, number	13.0	13.0	3.2	0.7	24.4	8.0	18.0	21
Kinetids in polymerization 2, number	8.9	8.0	1.7	0.4	19.4	6.0	12.0	21
Kineties between dorsal brush row 2 and polymerized region 1, number	5.0	5.0	1.2	0.3	23.2	3.0	7.0	21
Circumoral kinety to proximal end of dorsal brush row 1, distance	28.6	25.0	5.0	1.1	17.6	20.0	40.0	21
Dikinets comprising dorsal brush row 1, number	28.1	28.0	4.7	1.0	16.8	18.0	45.0	21
Circumoral kinety to proximal end of dorsal brush row 2, distance	28.5	27.0	5.2	1.2	17.6	21.0	40.0	21
Dikinets comprising dorsal brush row 2, number	23.0	24.0	5.2	1.1	22.5	16.0	30.0	21
Ordinary somatic cilia, length	8.5	8.0	1.2	0.3	14.0	6.0	10.0	15
Anterior bristle of a dikinetid from brush row 1, length	2.8	2.5	0.9	0.3	33.5	2.0	5.0	9
Posterior bristle of a dikinetid from brush row 1, length	2.4	2.0	1.2	0.4	48.6	1.0	4.0	9
Anterior bristle of a dikinetid from brush row 2, length	1.8	2.0	0.4	0.1	21.0	1.0	2.5	14
Posterior bristle of a dikinetid from brush row 2, length	3.6	3.5	0.6	0.2	17.6	3.0	5.0	14
Bristles of tail of brush row 2, length	3.0	3.0	0.6	0.2	19.9	2.0	4.0	9

**Table 9.** Morphometric data on *Apobryophyllum pinetum* based on mounted, protargol-impregnated, and randomly selected specimens from a non-flooded Petri dish culture. Measurements in  $\mu\text{m}$ . CV – coefficient of variation in %, M – median, Max – maximum, Mean – arithmetic mean, Min – minimum, n – number of individuals investigated, SD – standard deviation, SE – standard error of arithmetic mean.

Characteristic	Mean	M	SD	SE	CV	Min	Max	n
Body, length in vivo	144.0	150.0	19.5	8.7	13.5	120.0	170.0	5
Body, width in vivo	50.0	60.0	10.0	4.5	20.0	40.0	60.0	5
Body length:width, ratio in vivo	3.1	3.1	0.7	0.3	31.3	2.2	3.8	5
Body, length (protargol)	116.9	113.5	21.1	5.0	18.1	88.0	170.0	19
Body, width (protargol)	39.3	39.0	5.8	1.3	14.8	30.0	53.0	19
Body length:width, ratio	3.0	2.0	0.5	0.1	17.8	2.3	4.5	19
Anterior body end to first macronuclear nodule, distance	49.2	47.0	13.8	3.2	28.2	28.0	90.9	19
Anterior body end to end of longest dorsal brush row, distance	34.3	32.0	8.7	2.0	25.3	23.0	55.0	19
Nuclear figure, length of longitudinal axis	40.3	40.0	8.4	1.9	20.8	28.0	60.0	19
Nuclear figure, length of transverse axis	29.0	26.0	9.6	2.2	33.2	16.0	58.0	19
Macronuclear nodules, length	11.5	11.0	2.4	0.6	20.7	7.0	16.0	19
Macronuclear nodules, width	5.4	5.0	0.9	0.2	16.6	4.0	8.0	19
Macronuclear nodules, number	19.0	20.0	4.5	1.0	23.4	10.0	25.0	19
Micronuclei, length	3.5	3.5	–	–	–	3.0	4.0	19
Micronuclei, width	2.9	3.0	–	–	–	2.0	3.5	19
Micronuclei, number	9.0	9.0	2.8	0.7	31.4	3.0	16.0	19
Ciliary rows, number on right side	13.2	14.0	2.0	0.5	15.5	9.0	16.0	19
Ciliary rows, number on left side	13.7	14.0	2.6	0.6	19.0	9.0	21.0	19
Ciliary rows, total number	28.0	28.0	3.4	0.8	12.7	18.0	31.0	19
Dorsal brush rows, number	8.1	8.0	1.1	0.3	13.8	6.0	10.0	19
Main brush row, number of mono- and dikinetids (see Fig. 22l, m)	25.8	26.0	5.2	1.2	20.0	13.0	33.0	19

**Table 10.** Comparison of *Apobryophyllum pinetum* with similar species. All data are based of specimens impregnated with the same protargol method. Measurements in  $\mu\text{m}$ .

Characteristic	<i>Apobryophyllum pinetum</i>	<i>Apobryophyllum schmidingeri</i>	<i>Bryophyllum lingua multistriatum</i>
Body, length	117	167	187
Body, width	39	74	78
Somatic ciliary rows, number	28	33	40
Macronuclear nodules, number	19 (moniliform globular mass)	55 (scattered)	78 (scattered)
Micronuclei, number	9	9	many
Dorsal brush heteromorphic	yes	yes	no
Dorsal brush, number of rows	8	9	9
Oral bulge ends	subterminally	terminally	on dorsal side
Specimens investigated, number	19	8–19	10–12
Data source	This study	Foissner & Al-Rasheid (2007)	Foissner et al. (2002)

**Table 11.** Morphometric data on *Bryophyllum australiense* nov. spec. (BA) and *Neobryophyllum paucistriatum* from Kenya (KE) and Namibia (NA), both from Foissner et al. (2002). Data based on mounted, protargol-impregnated (Foissner's method), and randomly selected specimens from non-flooded Petri dish cultures. Measurements in  $\mu\text{m}$ . CV – coefficient of variation in %, M – median, Max – maximum, Mean – arithmetic mean, Min – minimum, n – number of individuals investigated, Pop – species/population, SD – standard deviation, SE – standard error of arithmetic mean.

Characteristic	Pop	Mean	M	SD	SE	CV	Min	Max	n
Body, length	BA	98.3	100.0	13.8	3.0	14.0	67.0	122.0	21
	KE	86.5	84.0	9.1	2.7	10.5	75.0	102.0	11
	NA	129.5	130.0	29.6	6.8	22.9	76.0	172.0	19
Body, width	BA	28.8	28.0	5.5	1.2	19.0	20.0	38.0	21
	KE	40.5	38.0	6.5	1.9	16.1	34.0	55.0	11
	NA	36.3	38.0	8.8	2.0	24.2	22.0	3.0	19
Body, length:width, ratio	BA	3.5	3.5	0.7	0.2	20.0	2.4	5.0	21
	KE	2.2	2.2	0.4	0.1	16.1	1.5	2.7	11
	NA	3.9	3.2	1.7	0.4	42.7	1.7	7.8	19
Posterior body end to dorsal end of oral bulge, distance	BA	8.8	9.0	2.4	0.5	26.8	6.0	14.0	21
	KE	12.6	12.0	2.4	0.7	19.1	10.0	18.0	11
	NA	8.6	8.0	3.4	0.8	39.0	4.0	17.0	19
Anterior body end to end of longest dorsal brush row, distance	BA	15.9	15.0	3.1	0.7	19.7	11.0	22.0	21
	KE	17.6	17.5	2.5	0.8	14.2	14.0	21.0	10
	NA	18.1	18.0	4.0	0.9	21.8	11.0	24.0	19
Macronucleus, length (spread if coiled; values thus approximations)	BA	58.2	56.0	–	–	–	38.0	84.0	21
	KE	34.4	35.0	–	–	–	28.0	40.0	10
	NA	71.3	65.0	–	–	–	40.0	120.0	19
Macronucleus, width	BA	4.2	4.0	0.8	0.2	18.1	3.0	5.0	21
	KE	7.8	8.0	–	–	–	7.0	8.0	10
	NA	6.4	6.0	1.1	0.2	17.6	5.0	8.0	19
Nodes in macronucleus, number	BA	4.9	5.0	1.1	0.2	21.4	3.0	7.0	19
	KE	0.0	0.0	0.0	0.0	0.0	0.0	0.0	11
	NA	3.9	4.0	2.7	0.6	68.6	0.0	8.0	19
Micronucleus, length	BA	3.6	3.5	0.7	0.2	18.7	3.0	5.0	12
	KE	5.6	5.6	0.9	0.3	16.6	4.0	7.0	10
	NA	5.0	5.0	0.7	0.2	13.9	4.0	7.0	19
Micronucleus width	BA	2.4	2.0	–	–	–	2.0	3.0	12
	KE	4.1	4.0	1.2	0.4	28.	3.0	6.0	10
	NA	3.3	3.0	0.8	0.2	24.4	2.0	5.0	19
Micronuclei, number	BA	1.0	1.0	0.0	0.0	0.0	1.0	1.0	12
	KE	1.0	1.0	0.0	0.0	0.0	1.0	1.0	10
	NA	1.0	1.0	0.0	0.0	0.0	1.0	1.0	19
Ciliary rows, number (including brush rows)	BA	10.3	10.0	0.7	0.2	6.5	9.0	11.0	19
	KE	14.4	14.5	1.4	0.5	9.8	12.0	16.0	10
	NA	10.9	11.0	0.8	0.2	7.2	10.0	12.0	19
Dorsal brush rows, number	BA	3.0	3.0	0.0	0.0	0.0	3.0	3.0	21
	KE	4.6	5.0	–	–	–	4.0	5.0	10
	NA	4.6	5.0	0.7	0.2	1.9	4.0	6.0	19
Dorsal brush kinecy 1, number of dikinetids	BA	12.0	11.0	2.4	0.6	20.2	8.0	16.0	17
Dorsal brush kinecy 1, number of dikinetids	BA	14.5	15.0	2.3	0.6	15.9	10.0	18.0	17
Dorsal brush kinecy 1, number of dikinetids	BA	8.5	8.0	1.2	0.3	14.5	6.0	11.0	17

**Table 12.** Morphometric data on a Costa Rican (CR; from Foissner 1995), a Kenyan (K; from Foissner 1999) and an Australian (AU; original data) population (Pop) of *Rimaleptus similis*, that is, *R. similis australiensis*. Data based on mounted, protargol-impregnated (Foissner's method), and randomly selected specimens from non-flooded Petri dish cultures. Measurements in  $\mu\text{m}$ . CV – coefficient of variation in %, M – median, Max – maximum, Mean – arithmetic mean, Min – minimum, n – number of individuals investigated, SD – standard deviation, SE – standard error of arithmetic mean.

Characteristic	Pop	Mean	M	SD	SE	CV	Min	Max	n
Body, length	CR	218.7	210.0	27.4	7.9	12.5	170.0	280.0	12
	K	245.1	240.0	20.6	6.2	8.4	216.0	288.0	11
	AU	255.7	255.0	39.4	8.6	15.4	197.0	322.0	21
Body, width	CR	56.7	55.0	13.9	4.0	24.6	37.0	83.0	12
	K	43.0	44.0	4.8	1.4	11.2	36.0	50.0	11
	AU	36.0	34.0	7.1	1.5	19.7	25.0	53.0	21
Body length:width, ratio (calculated from original data)	CR	4.0	3.9	1.0	0.3	24.1	2.9	6.2	12
	K	5.7	5.8	0.5	0.1	8.0	5.1	6.7	11
	AU	7.3	6.9	1.3	0.3	18.0	5.4	10.1	21
Anterior body end to oral bulge opening, distance	CR	104.3	102.5	19.2	5.5	18.4	80.0	140.0	12
	K	121.5	120.0	11.5	3.5	9.4	112.0	152.0	11
	AU	110.4	115.0	19.4	4.2	17.6	65.0	144.0	21
Proboscis, % of body length (calculated from original data)	CR	47.5	47.7	5.1	1.5	10.7	39.0	58.5	12
	K	49.6	50.0	2.4	0.7	4.8	46.2	53.3	11
	AU	43.2	44.6	4.8	1.0	11.0	31.0	45.0	21
Nuclear figure, length (calculated from original data)	CR	69.4	70.0	13.4	4.2	19.3	44.0	90.0	10
	AU	58.1	60.0	10.7	2.3	18.3	35.0	80.0	21
Macronuclear nodules, length	CR	36.8	39.0	7.1	2.1	19.3	22.0	45.0	12
	K	32.1	32.0	3.9	1.2	12.0	26.0	38.0	11
	AU	30.1	30.0	4.2	0.9	13.9	24.0	40.0	21
Macronuclear nodules, width	CR	10.5	10.0	1.6	0.5	15.5	8.0	13.0	12
	K	9.4	10.0	0.8	0.2	8.6	8.0	10.0	11
	AU	7.9	8.0	0.7	0.2	8.9	7.0	9.0	21
Macronuclear nodules, number	CR	2.0	2.0	0.0	0.0	0.0	2.0	2.0	12
	K	2.0	2.0	0.0	0.0	0.0	2.0	2.0	11
	AU	2.0	2.0	0.0	0.0	0.0	2.0	2.0	21
Micronucleus, diameter	CR	2.8	3.0	0.6	0.2	22.6	1.5	3.5	12
	K	2.6	2.4	–	–	–	2.4	3.0	11
	AU	2.3	2.5	0.3	0.1	13.1	2.0	3.0	21
Micronucleus, number	CR	1.0	1.0	0.0	0.0	0.0	1.0	1.0	12
	K	1.0	1.0	0.0	0.0	0.0	1.0	1.0	12
	AU	1.0	1.0	0.0	0.0	0.0	1.0	1.0	21
Ciliary rows, number	CR	28.7	28.0	2.6	1.0	9.2	25.0	32.0	7
	K	31.5	31.0	2.2	0.7	7.0	28.0	35.0	11
	AU	19.4	19.0	1.2	0.3	6.4	17.0	22.0	21

**Table 13.** Morphometric data on *Bophrya costata* based on silver-impregnated specimens from a non-flooded Petri dish culture. Measurements in  $\mu\text{m}$ . CV – coefficient of variation in %, M – median, Max – maximum, Mean – arithmetic mean, Met – method, Min – minimum, n – number of individuals investigated, SC – silver carbonate, SD – standard deviation, SE – standard error of arithmetic mean, SN – silver nitrate impregnation (Chatton-Lwoff method), SNI – silver nitrate impregnation + interference contrast.

Characteristic	Met	Mean	M	SD	SE	CV	Min	Max	n
Body, length	SN	47.3	48.0	2.9	0.6	6.1	40.0	51.0	21
Body, preoral width	SN	30.4	30.0	2.7	0.6	9.0	24.0	36.0	21
Body, maximum postoral width	SN	36.7	37.0	3.0	0.4	8.9	29.0	41.0	21
Anterior body end to macronucleus, distance	SN	19.6	20.0	2.0	0.4	10.4	16.0	24.0	21
Macronucleus, length	SN	7.5	7.0	1.0	0.2	13.7	6.0	10.0	21
Macronucleus, width	SN	7.1	7.0	0.7	0.1	9.2	6.0	8.0	21
Anterior body end to deepest site of paroral membrane, distance	SN	18.0	18.0	2.2	0.5	12.2	13.0	28.0	21
Paroral membrane, length	SN	9.0	9.0	0.9	0.2	9.6	7.0	10.0	21
Paroral membrane, number of kinetids	SN	8.7	9.0	0.8	0.2	9.1	7.0	10.0	21
Paroral membrane, number of dikinetids	SC	18.1	18.0	0.9	0.3	10.8	17.0	20.0	10
Oral basket rods, number	SNI	11.6	12.0	0.9	0.2	8.0	9.0	12.0	21
Oral basket, diameter at distal end	SNI	3.7	3.5	0.4	0.1	11.8	3.0	5.0	21
Nassulid organelle 3, number of horizontal ciliary rows	SC	6.0	6.0	0.0	0.0	0.0	6.0	6.0	10
Anterior body end to pore of contractile vacuole	SN	21.9	22.0	2.9	0.6	13.1	17.0	27.0	21
Somatic ciliary rows on right side, number	SN	6.8	7.0	–	–	–	6.0	7.0	21
Somatic ciliary rows on left side, number	SN	7.7	8.0	0.7	1.5	8.6	7.0	9.0	21
Postoral ciliary rows, number	SN	4.0	4.0	0.0	0.0	0.0	4.0	4.0	21
Somatic ciliary rows, total number	SN	18.3	18.0	0.7	0.1	3.6	17.0	19.0	21
Mono- and dikinetids in somatic ciliary row 1, number	SN	18.4	18.0	1.8	0.4	9.8	18.0	23.0	21
Monokinetids in somatic ciliary row 3, number	SN	17.5	17.0	4.6	1.0	26.0	15.0	23.0	21
Monokinetids in somatic ciliary row 10, number	SN	16.0	16.0	1.1	0.2	6.7	14.0	18.0	21
Silverline pattern, mesh size	SN	1.3	1.0	0.6	0.1	42.4	0.5	2.0	21
Extrusomes, length	SNI	10.0	10.0	1.2	0.3	13.2	8.0	12.0	21
Extrusomes, width	SNI	1.2	1.2	0.1	0.02	11.0	1.0	1.5	21

**Table 14.** Morphometric comparison of silver nitrate impregnated (Chatton-Lwoff method) *Wolfkasia acuta* nov. sp. from Africa, Botswana (WA), *W. pantanalensis* nov. sp. from the Pantanal of Brazil (WB), and *W. loeffleri* Foissner et al., 2002 from Costa Rica (WC) and Saudi Arabia (WS). Measurements in  $\mu\text{m}$ . CV – coefficient of variation in %, M – median, Max – maximum, Mean – arithmetic mean, Min – minimum, n – number of individuals investigated, Pop – population, SD – standard deviation, SE – standard error of arithmetic mean.

Characteristic	Pop	Mean	M	SD	SE	CV	Min	Max	n
Body, length	WA	67.1	67.5	3.0	0.8	4.4	60.0	72.0	14
	WB	53.4	52.0	4.7	1.3	8.8	45.0	61.0	13
	WC	41.5	41.5	3.9	0.7	9.3	33.0	48.0	30
	WS	45.2	42.0	9.4	1.7	20.7	38.0	73.0	30
Body, width in lateral view	WA	23.9	23.0	3.2	0.7	39.9	13.5	31.0	9
	WB	23.2	23.5	2.5	1.0	10.7	20.0	26.0	6
	WC	22.2	23.0	2.1	0.6	9.7	19.0	25.0	15
	WS	23.3	24.0	2.3	0.6	9.7	20.0	28.0	15
Body, width in ventral or dorsal view	WA	26.0	24.0	5.8	2.6	9.4	20.0	34.0	5
	WB	22.3	22.0	2.1	0.8	9.6	20.0	26.0	7
	WC	17.1	18.0	2.3	0.6	13.2	14.0	21.0	15
	WS	23.3	21.0	5.4	1.4	23.1	17.0	35.0	15
Body length: width, ratio in lateral view	WA	2.9	2.9	0.3	0.1	11.7	2.3	3.4	9
	WB	2.4	2.4	0.2	0.1	6.2	2.2	2.6	6
	WC	2.0	1.9	0.1	0.1	7.2	1.7	2.2	15
	WS	1.8	1.8	0.2	0.1	8.2	1.6	2.0	15
Body length: width, ratio in ventral or dorsal view	WA	2.6	2.5	0.5	0.3	19.2	2.1	3.3	5
	WB	2.3	2.3	0.2	0.1	6.4	2.1	2.5	7
	WC	2.3	2.3	0.3	0.1	14.2	1.7	3.1	15
	WS	2.1	2.1	0.2	0.1	10.2	1.8	2.4	15
Anterior body end to pore of contractile vacuole, distance	WA	20.0	20.0	1.0	0.1	5.0	18.0	21.0	12
	WB	17.2	17.0	1.1	0.3	6.7	16.0	19.0	13
	WC	12.9	13.0	1.3	0.3	9.9	11.0	15.0	15
	WS	14.2	14.0	3.0	0.8	21.0	9.0	21.0	15
Anterior body end to nassulid organelle 3, distance	WA	12.9	13.0	1.4	0.2	10.6	11.0	16.0	10
	WB	11.5	12.0	1.0	0.3	8.4	10.0	13.0	13
	WC	7.2	8.0	1.2	0.3	16.8	5.0	9.0	15
	WS	7.5	8.0	2.1	0.5	27.9	4.0	12.0	15
Anterior body end to summit of paroral membrane, distance	WA	8.3	8.5	0.8	0.3	9.8	7.0	9.0	6
	WB	8.2	8.0	0.9	0.3	11.3	7.0	10.0	13
	WC	4.4	4.0	1.0	0.3	22.4	3.0	6.0	15
	WS	5.1	5.0	1.4	0.4	27.4	3.0	9.0	15
Anterior body end to somatic kinety 1, distance	WA	4.6	5.0	0.8	0.3	17.1	3.0	5.0	7
	WB	4.9	5.0	0.7	0.2	14.2	4.0	6.0	13
	WC	2.4	2.0	0.8	0.2	34.5	1.0	4.0	15
	WS	3.0	3.0	1.1	0.3	37.8	1.0	6.0	15
Anterior body end to macronucleus, distance	WA	38.3	38.0	10.1	2.8	26.4	27.0	57.0	13
	WB	23.1	22.0	4.9	1.4	21.1	19.0	38.0	13
	WC	13.6	14.0	2.6	0.7	19.2	10.0	19.0	15
	WS	19.6	19.0	4.5	1.2	22.8	15.0	29.0	15
Macronucleus, length	WA	8.7	9.0	0.6	0.2	7.2	8.0	10.0	13
	WB	8.2	8.0	0.7	0.2	8.1	7.5	10.0	13
	WC	8.5	8.0	1.1	0.3	12.4	6.0	10.9	15
	WS	7.0	6.0	1.1	0.3	16.2	6.0	9.0	15

Table 14. Continued.

Characteristic	Pop	Mean	M	SD	SE	CV	Min	Max	n
Macronucleus, width	WA	8.7	9.0	0.6	0.2	7.2	8.0	10.0	13
	WB	8.2	8.0	0.7	0.2	8.1	7.5	10.0	13
	WC	7.5	8.0	0.9	0.2	12.5	6.0	9.0	15
	WS	7.0	6.0	1.1	0.3	16.2	6.0	9.0	15
Somatic ciliary rows, total number	WA	18.2	18.0	0.8	0.2	4.3	17.0	19.0	12
	WB	18.0	18.0	0.8	0.2	4.5	16.0	19.0	13
	WC	14.4	14.5	0.6	0.2	4.5	13.0	15.0	15
	WS	14.6	14.0	1.0	0.5	12.9	13.0	19.0	15
Somatic kinety 1, number of dikinetids	WA	18.3	18.0	1.2	0.4	6.3	16.0	20.0	10
	WB	16.5	16.0	1.4	0.4	8.3	15.0	19.0	11
	WC	9.3	9.0	–	–	–	9.0	10.0	15
	WS			not investigated					
Kinetics in a left side kinety, number	WA	20.5	20.0	1.3	0.4	6.1	19.0	24.0	13
	WB	15.6	15.0	1.2	0.3	7.6	14.0	18.0	13
	WC	11.1	11.0	1.4	0.4	13.0	9.0	14.0	15
	WS	11.4	11.0	2.9	0.8	25.4	9.0	21.0	15
Nassulid organelle 3, number of vertical ciliary rows	WA	10.1	10.0	0.7	0.3	6.8	9.0	11.0	6
	WB	8.3	8.0	–	–	–	8.0	10.0	6
	WC	7.0	7.0	0.9	0.2	12.5	6.0	9.0	15
	WS	6.0	6.0	0.0	0.0	0.0	6.0	6.0	9
Cord of paroral membrane, length	WA	6.0	6.0	1.2	0.4	19.2	5.0	8.0	7
	WB	5.6	6.0	0.7	0.2	13.1	4.0	6.0	9
	WC	5.5	5.0	–	–	–	5.0	6.0	15
	WS			not investigated					
Paroral dikinetids, number	WA	12.7	12.5	2.4	0.9	19.3	10.0	16.0	8
	WB	8.4	8.0	1.7	0.8	19.9	7.0	11.0	5
	WC	12.6	12.5	0.9	0.2	6.8	11.0	14.0	15
	WS			not investigated					
Extrusomes, length	WB	9.0	9.0	0.9	0.2	9.6	8.0	11.0	21
Extrusomes, width	WB	1.4	1.3	0.2	0.1	11.2	1.0	1.5	21

**Table 15.** Comparison of main features in seven *Bursaria* species. Upper line: arithmetic mean, lower line: extremes in parenthesis; number of specimens investigated: 10 – 21. IV – in vivo, P – protargol impregnation, SN – Chatton – Lwoff silver nitrate impregnation.

Characteristic	<i>B. ovata</i> <sup>d</sup> Botswana	<i>B. fluvialilis</i> Australia	<i>B. uluruensis</i> Australia	<i>B. americana</i> USA	<i>B. truncatella</i> Austria	<i>B. africana</i> Botswana	<i>B. salisburgensis</i> Austria
Body, length (µm)	521 (SN) (440–600)	681 (P) (560–800)	442 (SN) (360–510)	655 (SN) (550–830)	376 (SN) (330–460)	305 (SN) <sup>a</sup> (250–380)	444 (P) (360–630)
Body, width (µm)	323 (SN) (270–360)	442 (P) (380–520)	256 (SN) (200–400)	399 (SN) (310–580)	190 (SN) (160–230)	190 (SN) <sup>a</sup> (160–230)	289 (P) (250–330)
Anterior body end to posterior end of oral cleft, % of body length	64 (SN) (52–75)	48 (P) (44–54)	57 (SN) (51–67)	62 (SN) (59–65)	54 (SN) (48–62)	57 (SN) (50–63)	53 (P) (45–63)
Posterior body end to deepest point of adoral polykinetid, % of body length	19 (SN) (13–23)	31 (P) (23–35)	30 (SN) (21–42)	10 (SN) (4–17)	17 (SN) (10–24)	11 (SN) (7–16)	20 (P) (13–28)
Somatic ciliary rows, number	41 <sup>7d</sup> (352–480)	403 (P) <sup>b</sup> (316–474)	328 (P) <sup>b</sup> (166–605)	581 (SN) <sup>b</sup> (450–844)	215 (SN) <sup>b</sup> (160–294)	214 (SN) <sup>b</sup> (182–261)	455 (P) <sup>b</sup> (394–520)
Barren stripe along right oral polykinetid	present	absent	?	present	?	present	250–330
Adoral polykineties in left polykinetid, number	148 (P) (130–160)	71 (P) (58–85)	103 (P) (87–130)	132 (P) (120–168)	83 (SN) (70–100)	91 (P) (65–114)	101 (P) (82–130)
Adoral polykineties, maximum width (µm)	33 (P) (30–40)	63 (P) (50–90)	62 (P) (50–70)	64 (P) (55–75)	50 (SN) (40–60)	49 (P) (35–60)	51 (P) (35–60)
Shape of left oral polykinetid (“adoral zone of membranelles”)	Posterior part distinctly recurved anteriorly	Posterior part not recurved	Posterior part recurved	Posterior part distinctly recurved	Posterior part not distinctly recurved	Posterior part not recurved	Posterior part distinctly recurved
Extrusome fringe, height (µm)	~20 (IV); 14, 10–17 (P)	3–4 (IV); 4, 9, 3–6 (P)	~3, 3–5 (IV); 3, 7, 3–5 (SN)	~10 (IV); 5–8 (P)	~3.2, 3–4 (SN)	~3–4 (IV); 3.6, 3–5 (P)	~3–4 (IV); 5.8, 3–8 (P)
Extrusome shape	cylindroid	globular/ellipsoidal	globular	cylindroid	cylindroid	globular	unstructured plate
Resting cyst, diameter with wall (µm)	193 (IV) (176–212)	232 (IV) (190–280)	223 (IV) (200–250)	328 (IV) (310–380)	140 µm (IV)	153 (IV) (132–188)	not investigated

<sup>a</sup> From a declining culture. Protargol-impregnated specimens from the non-flooded Petri dish culture fixed with Stieve’s solution are considerably larger: 391 µm (310–460 µm) × 291 µm (220–370 µm).

<sup>b</sup> The number of ciliary rows was calculated as follows (*B. uluruensis* as example: cell width = 255.8 µm; 12 ciliary rows in 25 µm; this means 122.8 rows in 255.8 µm. Since both sides are ciliated, the total number is about 146 rows (122.8 × 2). I could roughly count the numbers of ciliary rows in three specimens of *B. truncatella*: 400, 465, 500 (average 216.2, 168–331 when calculated). Thus, the calculated numbers are likely underestimates. However, in *B. africana*, the counted number is higher than the calculated (282 vs. 213.7, Table 2).

<sup>c</sup> Recalculated from Foissner (2016), using strongly flattened specimens: rows in 25 µm × body width × 2.

<sup>d</sup> Recalculated from Foissner (2016).

**Table 16.** Morphometric data on *Bursaria africana* from Botswana (B, fed with *Colpidium kleini*) and environmental specimens of *B. truncatella* from Austria (A). Measurements in  $\mu\text{m}$ . CV – coefficient of variation in %, IV – in vivo, M – median, Max – maximum, Me – method, Mean – arithmetic mean, Min – minimum, n – number of individuals investigated, P – protargol impregnation, Po – population, SD – standard deviation, SE – standard error of arithmetic mean, SN – Chatton – Lwoff silver nitrate impregnation.

Characteristic	Po/Me	Mean	M	SD	SE	CV	Min	Max	n
Body, length	B/IV	364.0	370.0	30.5	13.6	8.4	320.0	400.0	5
	B/SN	305.5	300.0	29.6	6.5	9.7	250.0	380.0	21
	B/P	391.0	390.0	43.9	9.6	11.2	310.0	460.0	21
	A/SN	376.5	375.0	38.7	9.4	10.3	330.0	460.0	17
Body, width	B/IV	264.0	250.0	35.1	15.7	13.3	220.0	300.0	5
	B/SN	190.2	190.0	16.5	3.6	8.7	160.0	230.0	21
	B/P	290.7	300.0	41.7	9.1	14.3	220.0	370.0	21
	A/SN	190.3	190.0	18.2	4.4	9.6	160.0	230.0	17
Body length:width, ratio	B/IV	1.4	1.4	0.1	0.1	6.4	1.3	1.5	5
	B/SN	1.6	1.6	0.1	0.1	6.1	1.4	1.8	21
	B/P	1.3	1.4	0.1	0.1	6.5	1.2	1.5	21
	A/SN	2.0	2.0	0.1	0.1	6.1	1.8	2.2	17
Anterior body end to posterior end of ventral cleft, distance	B/SN	173.9	170.0	18.8	4.1	10.9	125.0	210.0	21
	A/SN	203.8	200.0	26.3	6.4	12.9	160.0	280.0	17
Anterior body end to posterior end of ventral cleft, percent of body length	B/SN	56.6	57.0	3.4	0.8	6.0	50.0	63.0	21
	A/SN	54.2	54.0	4.5	1.1	8.2	48.0	62.0	17
Posterior body end to deepest point of left oral polykinetid, distance	B/SN	32.6	30.0	7.7	1.7	23.6	20.0	50.0	21
	A/SN	64.0	60.0	15.1	4.8	23.5	35.0	90.0	10
Posterior body end to deepest point of left oral polykinetid, percent of body length	B/SN	10.9	10.0	2.7	0.6	25.3	7.0	16.0	21
	A/SN	17.4	18.0	4.1	1.3	23.5	10.0	24.0	10
Macronucleus, entangled length	B/P	847.6	800.0	340.8	74.4	40.2	500.0	2100.0	21
Macronucleus, width	B/P	17.1	17.0	2.1	0.5	12.5	14.0	20.0	21
Micronucleus, length	B/P	5.5	5.0	0.8	0.2	14.5	5.0	8.0	21
Micronucleus, width	B/P	4.4	4.5	0.4	0.1	9.0	4.0	5.0	21
Micronuclei, number	B/P	20.2	20.0	5.5	1.2	27.2	11.0	32.0	21
Extrusome fringe, height	B/P	3.6	3.0	0.7	0.2	18.9	3.0	5.0	21
	A/SN	3.2	3.0	–	–	–	3.0	4.0	5
Somatic kineties in 25 $\mu\text{m}$ , number	B/SN	14.2	14.0	1.5	0.3	10.4	12.0	18.0	21
	A/SN	14.1	13.0	2.4	0.6	16.8	10.0	20.0	18
Somatic kineties, calculated total number; see Table 15	B/SN	214.0	213.0	33.0	7.2	15.2	182.0	261.0	21
	A/SN	213.7	192.0	45.6	11.1	21.3	160.0	294.0	17
Somatic kineties, number counted	B/P	282.0	280.0	25.7	5.6	9.1	250.0	340.0	21
Adoral polykineties in left oral polykinetid, number	B/P	91.3	92.0	12.3	2.7	13.5	65.0	114.0	21
	A/SN	82.9	83.0	8.7	2.5	10.4	70.0	100.0	12
Adoral polykineties, maximum width	B/P	48.6	50.0	6.6	1.4	13.5	35.0	60.0	21
	B/SN	41.0	40.0	4.1	0.9	9.9	35.0	45.0	21
	A/SN	49.6	50.0	5.8	1.7	11.7	40.0	60.0	12
Adoral polykineties, maximum distance in between	B/P	8.2	9.0	1.3	0.3	15.7	6.0	10.0	21
	B/SN	4.3	4.0	0.7	0.1	15.2	3.0	5.0	21
	A/SN	4.3	4.0	–	–	–	4.0	5.0	12
Resting cyst with bright ectocyst, length	B/IV	153.3	154.0	13.8	3.1	9.0	132.0	188.0	20
Resting cyst with bright ectocyst, width	B/IV	151.3	154.0	15.4	3.4	10.2	126.0	188.0	20
Resting cyst without ectocyst, length	B/IV	128.8	132.0	12.0	2.7	9.3	109.0	160.0	20
Resting cyst without ectocyst, width	B/IV	128.5	131.0	11.9	2.7	9.3	109.0	160.0	20
Escape opening, diameter	B/IV	26.5	26.0	3.2	0.7	11.9	20.0	32.0	19
Bridges, diameter	B/IV	7.3	7.0	1.4	0.3	18.7	5.0	10.0	23

**Table 17.** Morphometric data on *Bursaria americana* (BA, fed with *Paramecium aurelia*) and environmental specimens of *B. salisburgensis* (BS). Measurements in  $\mu\text{m}$ . CV – coefficient of variation in %, IV – in vivo, M – median, Max – maximum, Me – method, Mean – arithmetic mean, Min – minimum, n – number of individuals investigated, P – protargol impregnation (Wilbert method), Pop – population, SD – standard deviation, SE – standard error of arithmetic mean, SN – Chatton – Lwoff silver nitrate impregnation.

Characteristic	Pop/Me	Mean	M	SD	SE	CV	Min	Max	n
Body, length	BA/SN	655.4	600.0	95.0	26.3	14.5	550.0	830.0	13
	BA/P	692.1	680.0	82.0	18.8	11.8	510.0	850.0	19
	BS/IV	410.0	400.0	–	–	–	380.0	450.0	3
	BS/P	443.7	420.0	67.3	17.4	15.2	360.0	630.0	15
Body, width	BA/SN	398.8	370.0	75.1	20.8	18.9	310.0	580.0	13
	BA/P	426.8	430.0	57.2	13.1	13.4	330.0	530.0	19
	BS/IV	266.7	250.0	–	–	–	250.0	300.0	3
	BS/P	288.7	280.0	27.5	7.1	9.5	250.0	330.0	15
Body length:width, ratio	BA/SN	1.7	1.6	0.2	0.1	10.6	1.4	2.0	13
	BA/P	1.6	1.6	0.1	0.1	6.4	1.4	1.8	19
	BS/IV	1.5	1.5	–	–	–	1.5	1.6	3
	BS/P	1.6	1.5	0.3	0.1	19.7	0.8	2.1	15
Anterior body end to posterior end of ventral cleft, distance	BA/SN	427.0	420.0	53.1	12.2	12.4	310.0	530.0	19
	BS/P	236.0	220.0	42.7	11.0	18.1	180.0	320.0	15
Anterior body end to posterior end of ventral cleft, percent of body length	BA/SN	61.8	62.0	1.6	0.4	2.6	59.0	65.0	19
	BS/P	53.1	52.0	4.8	1.2	9.0	45.0	63.0	15
Posterior body end to deepest point of left oral polykinetid, distance	BA/SN	66.1	60.0	22.5	5.2	34.0	30.0	125.0	19
	BS/P	86.5	90.0	16.3	4.2	18.8	50.0	118.0	15
Posterior body end to deepest point of left polykinetid, percent of body length	BA/SN	9.6	10.0	3.1	0.7	32.5	4.0	17.0	19
	BS/P	19.7	21.0	4.0	1.0	20.1	13.0	28.0	15
Macronucleus, entangled length	BA/P	1147.1	1100.0	166.9	38.3	14.6	900.0	1500.0	19
	PS/P	636.0	650.0	108.3	28.0	17.0	400.0	900.0	15
Macronucleus, width in mid of length	BA/SN	25.3	25.0	4.2	1.0	16.4	20.0	35.0	19
	BS/P	17.3	17.0	2.1	0.5	12.1	15.0	20.0	15
Micronucleus, length	BA/P	10.2	10.0	1.6	0.5	15.7	7.0	12.0	11
Micronucleus, width	BA/P	8.7	8.0	1.2	0.4	13.7	7.0	11.0	11
Extrusome fringe, height	BA/IV	6.1	6.0	0.8	0.2	13.3	5.0	8.0	19
	BS/IV	5.8	6.0	1.3	0.4	21.5	3.0	8.0	11
Somatic kineties in 25 $\mu\text{m}$ , number	BA/SN	18.2	18.0	3.2	0.7	17.4	12.0	27.0	19
	BS/P	19.7	18.5	4.9	1.4	25.0	14.0	30.0	12
Somatic kineties, calculated total number; see Table 15	BA/SN	581.0	593.0	165.9	38.1	27.4	304.0	972.0	19
	BS/P	455.4	405.5	116.0	33.5	25.7	394.0	660.0	12
Adoral polykineties in left oral polykinetid, number	BA/P	131.7	127.0	12.0	2.8	9.1	120.0	520.0	19
	BS/P	101.4	96.0	13.4	3.5	13.2	82.0	130.0	15
Adoral polykineties, maximum width	BA/P	64.5	65.0	5.2	1.2	8.1	55.0	75.0	19
	BS/P	50.7	50.0	6.5	1.7	12.9	35.0	60.0	15
Adoral polykineties, maximum distance in between	BA/P	11.9	12.0	1.9	0.4	16.1	7.0	15.0	19
	BS/P	6.4	7.0	1.0	0.3	15.4	4.8	8.0	15
Resting cyst, diameter with wall	BA/IV	327.9	320.0	18.0	4.8	5.5	310.0	380.0	14
Resting cyst, diameter without wall	BA/IV	248.9	242.5	19.0	5.1	7.6	230.0	300.0	14

**Table 18.** Morphometric data on *Bursaria uluruensis* (BU, cultivated with *Paramecium aurelia*) and *B. fluviatilis* (BF, environmental culture with wheat grains). Measurements in  $\mu\text{m}$ . CV – coefficient of variation in %, IV – in vivo, M – median, Max – maximum, Me – method, Mean – arithmetic mean, Min – minimum, n – number of individuals investigated, P – protargol impregnation (Foissner method), Pop – population, SD – standard deviation, SE – standard error of arithmetic mean, SN – Chatton – Lwoff silver nitrate impregnation.

Characteristic	Pop/Me	Mean	M	SD	SE	CV	Min	Max	n
Body, length	BU/IV	547.5	540.0	65.8	23.3	12.0	450.0	650.0	8
	BU/SN	442.1	450.0	38.7	8.9	8.8	360.0	510.0	19
	BU/P	616.9	625.0	81.8	20.5	13.3	460.0	760.0	16
	BF/P	681.3	680.0	64.3	14.8	9.4	560.0	800.0	19
Body, width	BU/IV	283.8	300.0	23.3	8.3	8.2	250.0	300.0	8
	BU/SN	255.8	250.0	45.3	10.4	17.7	200.0	400.0	19
	BU/P	341.9	350.0	48.2	12.1	14.1	230.0	420.0	16
	BF/P	441.6	450.0	37.6	8.6	8.5	380.0	520.0	19
Body length:width, ratio	BU/IV	1.7	2.0	0.6	0.2	37.1	1.7	2.2	8
	BU/SN	1.8	1.8	0.3	0.1	15.8	1.1	2.4	19
	BF/P	1.5	1.5	0.1	0.1	3.3	1.5	1.6	19
Anterior body end to posterior end of ventral cleft, distance	BU/SN	253.2	250.0	21.8	5.0	8.6	220.0	300.0	19
	BF/P	327.9	330.0	32.4	7.4	17.9	280.0	400.0	19
Anterior body end to posterior end of ventral cleft, percent of body length	BU/SN	56.8	56.5	4.4	1.1	7.7	51.0	67.0	18
	BF/P	48.1	48.0	3.1	0.7	6.4	44.0	54.0	19
Posterior body end to deepest point of left oral polykinetid, distance	BU/SN	133.6	122.5	37.4	8.8	28.0	80.0	190.0	18
	BF/P	210.0	210.0	37.6	8.6	17.9	130.0	270.0	19
Posterior body end to deepest point of left oral polykinetid, percent of body length	BU/SN	29.8	29.0	6.2	1.5	20.9	21.0	42.0	18
	BF/P	30.6	31.0	3.6	0.8	11.8	23.0	35.0	19
Macronucleus, entangled length	BU/SN	not fully recognizable							
	BF/P	985.0	950.0	221.5	53.7	22.5	600.0	1400.0	17
Macronucleus, width in mid of length	BU/SN	12.4	12.0	1.6	0.4	13.0	10.0	15.0	19
	BF/P	15.7	15.0	2.6	0.6	16.5	11.0	22.0	19
Extrusome fringe, height	BU/SN	3.7	4.0	0.7	0.2	17.5	3.0	5.0	19
	BF/P	4.9	5.0	0.8	0.2	16.5	3.0	6.0	19
Somatic kineties in 25 $\mu\text{m}$ , number	BU/P	12.0	12.0	3.2	0.6	26.5	8.0	21.0	24
	BU/P	11.4	12.0	2.5	0.6	21.9	7.0	16.0	19
Somatic kineties, calculated total number; see Table 15	BU/P	328.0	305.5	106.2	26.5	33.4	166.0	605.0	16
	BF/P	403.0	394.0	82.5	18.9	20.8	347.0	474.0	19
Adoral polykineties in left oral polykinetid, number	BU/P	103.3	100.0	10.9	2.1	10.5	87.0	130.0	28
	BF/P	71.1	72.0	6.0	1.2	8.4	58.0	85.0	27
Adoral polykineties, maximum width	BU/P	61.7	60.0	7.8	1.6	12.6	50.0	70.0	24
	BF/P	62.5	65.0	9.7	2.2	15.5	50.0	90.0	19
Adoral polykineties, maximum distance in between	BU/P	7.1	7.0	1.3	0.3	18.4	5.0	10.0	16
	BF/P	7.5	7.0	1.0	0.2	12.8	6.0	10.0	19
Resting cyst, diameter with wall	BU/IV	223.4	225.0	16.6	3.8	7.4	200.0	250.0	19
	BF/IV	232.0	230.0	21.1	4.3	9.1	190.0	280.0	24
Resting cyst, diameter without wall	BU/IV	185.0	185.0	15.3	3.5	8.3	160.0	215.0	19
	BF/IV	190.0	185.0	18.4	3.8	9.7	160.0	230.0	24
Granular vacuoles in cortex, length	BU/P	15.1	15.0	3.3	0.7	21.9	8.0	20.0	20
Granular vacuoles in cortex, width	BU/P	13.1	13.5	3.4	0.8	25.7	7.0	20.0	20

**Table 19.** Morphometric data on *Gastronauta insula* from a non-flooded Petri dish culture. Data based on mounted, protargol-impregnated, and randomly selected specimens. Measurements in  $\mu\text{m}$ . CV – coefficient of variation in %, M – median, Max – maximum, Mean – arithmetic mean, Min – minimum, n – number of individuals investigated, SD – standard deviation, SE – standard error of arithmetic mean.

Characteristic	Mean	M	SD	SE	CV	Min	Max	n
Body, length	33.0	35.0	6.1	1.5	18.6	21.0	42.0	17
Body, width	20.6	20.0	2.5	0.6	12.1	15.0	25.0	17
Right and left ciliary field, distance in between	4.3	4.0	1.0	0.2	23.9	3.0	6.0	17
Anterior body end to circumoral kinety, distance	10.4	10.0	1.2	0.3	11.3	9.0	13.0	17
Anterior body end to macronucleus, distance	20.7	22.0	3.9	0.9	18.8	13.0	27.0	17
Anterior body end to brush row 1, distance	2.0	2.0	0.6	0.1	28.2	1.0	3.0	17
Brush row 1, number of basal bodies	2.0	2.0	0.0	0.0	0.0	2.0	2.0	17
Anterior body end to brush row 2, distance	3.9	4.0	0.8	0.2	19.3	3.0	5.0	17
Brush row 2, number of basal bodies	2.0	2.0	0.0	0.0	0.0	2.0	2.0	17
Anterior body end to brush row 3, distance	3.5	3.5	1.0	0.2	27.6	2.0	6.0	17
Brush row 3, number of basal bodies	2.0	2.0	0.0	0.0	0.0	2.0	2.0	17
Circumoral kinety, length of long axis	10.1	10.0	1.1	0.3	11.4	8.0	12.0	17
Circumoral kinety, length of short axis	2.5	2.5	0.6	0.1	24.5	1.5	3.5	17
Macronucleus, length	9.1	9.5	1.1	0.3	12.5	7.0	11.0	17
Macronucleus, width	7.4	7.0	0.9	0.2	12.0	6.0	10.0	17
Macronucleus, diameter of central nucleolus	4.3	4.0	1.0	0.3	24.2	3.0	6.0	9
Macronucleus, diameter of peripheral nucleoli	1.6	1.5	0.6	0.1	35.6	1.0	3.0	17
Micronucleus, length	2.5	2.5	–	–	–	2.0	3.0	16
Micronucleus, width	2.4	2.5	–	–	–	2.0	3.0	16
Kineties in right ciliary field, number	8.0	8.0	0.0	0.0	0.0	8.0	8.0	17
Kineties in left ciliary field, number	5.0	5.0	0.0	0.0	0.0	5.0	5.0	17
Postoral kineties in right ciliary field, number	3.0	3.0	0.0	0.0	0.0	3.0	3.0	17
Preoral kineties, number	2.0	2.0	0.0	0.0	0.0	2.0	2.0	17
Vertical preoral kinety fragments, number	2.0	2.0	0.0	0.0	0.0	2.0	2.0	17
Vertical row 2, number of kinetids	3.6	3.0	0.9	0.2	25.3	3.0	6.0	15
Basal bodies at anterior end of vertical row 2, number	2.1	2.0	–	–	–	2.0	3.0	17
Clusters formed by dorsal bristles, number	3.0	3.0	0.0	0.0	0.0	3.0	3.0	17
Anterior body end to upper excretory pore, distance	15.8	16.0	1.6	0.4	10.3	13.0	19.0	17
Posterior body end to lower excretory pore, distance	9.8	10.0	1.6	0.4	16.6	7.0	12.0	16
Dorsal brush, length of bristles	3.6	3.5	0.7	0.2	18.5	2.5	5.0	16

**Table 20.** Morphometric data on *Protocyclidium bimaconucleatum* based on protargol-impregnated (Foissner method) and randomly selected specimens from a non-flooded Petri dish culture. Measurements in  $\mu\text{m}$ . CV – coefficient of variation in %, M – median, Max – maximum, Mean – arithmetic mean, Min – minimum, n – number of individuals investigated, SD – standard deviation, SE – standard error of arithmetic mean.

Characteristic	Mean	M	SD	SE	CV	Min	Max	n
Body, length	28.8	29.0	2.9	0.7	10.2	22.0	33.0	17
Body, width in ventral view	17.8	18.0	2.2	0.5	12.4	15.0	23.0	17
Body, width in lateral view	18.3	18.0	1.3	0.3	7.2	16.0	20.0	17
Body length:width, ratio in ventral view	1.6	1.6	–	–	–	1.2	1.9	17
Body length:width, ratio in lateral view	1.6	1.6	0.2	0.1	11.3	1.2	1.9	17
Anterior body end to macronucleus, distance	5.1	4.0	2.0	0.5	39.6	3.0	9.0	17
Anterior body end to excretory pore, distance	23.6	23.0	3.1	0.9	13.0	18.0	30.0	11
Anterior body end to paroral membrane, distance	2.7	3.0	0.7	0.2	26.5	1.0	3.0	17
Anterior body end to vertex of paroral membrane, distance	17.7	18.0	1.5	0.4	8.7	14.0	19.0	17
Anterior body end to membranelle 1, distance	3.6	4.0	1.0	0.3	28.3	1.0	5.0	17
Anterior body end to proximal end of membranelle 3, distance	13.7	14.0	1.1	0.3	7.6	12.0	15.0	17
Macronuclear nodule, length	7.3	7.0	1.2	0.3	16.6	6.0	10.0	17
Macronuclear nodule, width	6.7	7.0	0.8	0.2	11.5	5.0	8.0	17
Macronuclear nodules, number	2.1	2.0	–	–	–	2.0	3.0	17
Excretory pore, diameter	~1.0	1.0	–	–	–	–	–	9
Ciliary rows, number	11.9	12.0	–	–	–	11.0	12.0	17
Kinetids in a dorsal ciliary row, number	12.1	12.0	–	–	–	12.0	13.0	17
Adoral membranelle 2, number of horizontal kineties	6.5	7.0	–	–	–	6.0	7.0	17
Scutica, number of dikinetids right of cytopyge	1.0	1.0	0.0	0.0	0.0	1.0	1.0	12
Scutica, number of dikinetids left of cytopyge	2.0	2.0	0.0	0.0	0.0	2.0	2.0	12

**Table 21.** Morphometric data on two developmental stages of *Microsporidium protocyclidicola* based on protargol-impregnated specimens. Measurements in  $\mu\text{m}$ . CV – coefficient of variation in %, M – median, Max – maximum Mean – arithmetic mean, Min – minimum, n – number of individuals investigated, SD – standard deviation, SE – standard error of arithmetic mean.

Characteristic	Mean	M	SD	SE	CV	Min	Max	n
<b>Stage 1 (meronts?)</b>								
Body, length	5.3	5.0	1.6	0.3	30.3	3.0	9.0	30
Body, width	5.2	5.0	1.6	0.3	31.0	3.0	8.0	30
Nucleus, diameter	1.2	1.0	0.4	0.1	0.7	0.7	2.0	30
Parasites in a host	9.5	9.5	2.6	0.5	5.0	5.0	14.0	30
<b>Stage 2 (sporoplasts?)</b>								
Body, length	9.2	10.0	2.9	1.0	31.5	5.0	13.0	9
Body, width	6.3	6.0	1.0	0.3	15.8	5.0	8.0	9
Nucleus, largest axis	3.7	3.0	1.4	0.5	38.0	2.5	6.0	9

**Table 22.** Morphometric data on *Afrogonostomum alveum* based on mounted, protargol-impregnated, and randomly selected specimens from a non-flooded Petri dish culture. Measurements in  $\mu\text{m}$ . CV – coefficient of variation in %, M – median, Max – maximum, Mean – arithmetic mean, Min – minimum, n – number of individuals investigated, SD – standard deviation, SE – standard error of arithmetic mean.

Characteristic	Mean	M	SD	SE	CV	Min	Max	n
Body, length	104.4	102.0	10.4	2.3	9.9	86.0	123.0	21
Body, width	23.3	23.0	3.2	0.7	13.7	19.0	30.0	21
Body length:width, ratio	4.5	4.5	0.6	0.1	12.7	3.6	5.3	21
Adoral zone of membranelles, length <sup>a</sup>	36.4	36.0	3.7	0.8	10.0	30.0	43.0	21
Adoral zone of membranelles, % of body length	34.9	35.0	2.2	0.5	6.3	29.0	39.0	21
Adoral membranelles, number	26.7	27.0	2.3	0.5	8.6	23.0	31.0	21
Anterior body end to paroral membrane, distance	19.3	19.0	2.2	0.5	11.5	15.0	23.0	21
Paroral membrane, length	6.7	7.0	1.0	0.2	15.3	5.0	8.0	21
Anterior body end to endoral membrane, distance	22.7	22.0	2.7	0.6	12.0	18.0	27.0	21
Endoral membrane, length	8.2	8.0	0.9	0.2	10.7	7.0	10.0	21
Anterior body end to buccal cirrus, distance	19.1	18.0	2.2	0.5	11.6	15.0	22.0	21
Anterior body end to first macronuclear nodule, distance	29.2	30.0	3.7	0.8	12.8	21.0	35.0	21
Anterior body end to first frontoventral cirrus, distance	9.9	10.0	1.2	0.3	12.5	7.0	12.0	21
Anterior body end to last frontoventral cirrus, distance	26.3	26.0	3.8	0.8	14.4	18.0	34.0	21
Anterior body end to first frontoterminal cirrus, distance	6.9	7.0	1.3	0.3	19.2	5.0	10.0	21
Anterior body end to second frontoterminal cirrus, distance	12.6	12.0	1.3	0.3	10.5	10.0	16.0	21
Posterior body end to transverse cirri, distance	2.9	3.0	1.1	0.2	37.6	1.0	5.0	21
Posterior body end to right marginal row, distance	6.3	6.0	1.6	0.4	25.7	3.0	20.0	21
Posterior body end to left marginal row, distance	4.7	5.0	1.4	0.3	29.8	2.0	7.0	21
Anteriormost macronuclear nodule, length	9.3	9.0	1.5	0.3	16.0	7.0	12.0	21
Anteriormost macronuclear nodule, width	5.5	6.0	0.8	0.2	13.7	4.0	7.0	21
Nuclear figure, length	53.3	54.0	6.6	1.4	12.4	37.0	64.0	21
Macronuclear nodules, number	4.1	4.0	–	–	–	4.0	5.0	21
Micronuclei, length	3.6	4.0	0.8	0.2	20.9	2.0	4.0	21
Micronuclei, width	1.9	2.0	0.3	0.1	15.8	1.0	2.0	21
Micronuclei, number	2.0	2.0	0.3	0.1	15.8	1.0	3.0	21
Frontal cirri, number	3.0	3.0	0.0	0.0	0.0	3.0	3.0	21
Buccal cirri, number	1.0	1.0	0.0	0.0	0.0	1.0	1.0	21
Right marginal cirri, number	26.0	26.0	2.8	0.6	10.7	22.0	30.0	21
Left marginal cirri, number	22.9	22.0	2.6	0.6	11.5	18.0	27.0	21
Frontoventral cirri, number	5.2	5.0	0.8	0.2	14.7	4.0	7.0	21
Frontoventral cirri, number of pairs	2.1	2.0	0.4	0.1	14.7	2.0	3.0	21
Frontoterminal cirri, number	2.0	2.0	0.0	0.0	0.0	2.0	2.0	21
Transverse cirri, number	3.8	4.0	0.6	0.1	16.6	3.0	5.0	21
Dorsal kineties, number	3.0	3.0	0.0	0.0	0.0	3.0	3.0	21
Dorsal kinety 1, number of bristles	12.2	12.0	1.6	0.3	12.9	10.0	15.0	21
Dorsal kinety 2, number of bristles	16.1	16.0	2.0	0.4	12.3	13.0	19.0	21
Dorsal kinety 3, number of bristles	13.1	13.0	1.6	0.4	12.5	11.0	16.0	21

<sup>a</sup> Anterior body end to proximal end of zone.

**Table 23.** Morphometric data on *Circinella filiformis australiensis* (upper line) and *Circinella filiformis filiformis* (lower line; from Foissner 1982) based on mounted, protargol-impregnated and randomly selected specimens from non-flooded Petri dish cultures. Measurements in  $\mu\text{m}$ . CV – coefficient of variation in %, M – median, Max – maximum, Mean – arithmetic mean, Min – minimum, n – number of individuals investigated, SD – standard deviation, SE – standard error of arithmetic mean, – not investigated.

Characteristic	Mean	M	SD	SE	CV	Min	Max	n
Body, length	144.0	145.0	17.4	3.8	12.1	113.0	179.0	21
	108.7	106.0	16.1	5.1	14.9	83.0	140.0	10
Body, width	12.3	12.0	1.6	0.3	12.7	10.0	15.0	21
	7.2	6.8	1.3	0.4	18.1	5.5	10.6	10
Body length: width, ratio	11.9	12.2	2.1	0.5	17.7	7.5	16.3	21
	15.1	–	–	–	–	–	–	10
Anterior body end to proximal end of adoral zone of membranelles, distance	12.9	13.0	1.6	0.4	12.2	9.0	16.0	20
	7.8	8.0	0.6	0.2	8.0	6.6	9.0	10
Body length: length of adoral zone of membranelles (%)	9.0	8.7	1.5	0.3	16.2	6.9	12.3	20
	7.2	–	–	–	–	–	–	10
Anterior body end to buccal cirrus, distance	8.9	9.0	0.9	0.3	9.9	7.0	10.0	9
	–	–	–	–	–	–	–	–
Anterior body end to proximal end of frontoventral row 1, distance	7.3	7.0	1.0	0.3	13.2	6.0	9.0	15
	–	–	–	–	–	–	–	–
Anterior body end to proximal end of frontoventral row 2, distance	19.5	19.5	1.8	0.4	20.2	5.0	13.0	21
	16.2	16.0	2.3	0.7	14.3	13.0	13.0	10
Anterior body end to undulating membrane, distance	8.1	8.0	0.9	0.3	11.4	6.0	9.0	9
	–	–	–	–	–	–	–	–
Anterior body end to first macronuclear nodule, distance	21.4	22.0	2.8	0.6	12.8	17.0	26.0	21
	–	–	–	–	–	–	–	–
Antermost macronuclear nodule, length	9.1	9.0	1.8	0.4	20.2	5.0	13.0	21
	5.8	5.3	1.1	0.3	18.6	4.0	8.0	10
Antermost macronuclear nodule, width	2.8	3.0	0.6	0.1	20.4	2.0	4.0	21
	1.9	1.7	0.5	0.2	26.6	1.4	2.6	10
Macronuclear nodules, number	10.4	11.0	2.1	0.5	20.2	7.0	15.0	21
	16.4	15.5	4.6	1.5	28.4	11.0	20.0	10
Micronuclei, length	3.3	3.0	–	–	–	2.5	4.0	19
	1.6	1.5	0.2	0.1	12.8	1.4	1.9	10
Micronuclei, width	1.9	2.0	–	–	–	1.0	2.0	18
	–	–	–	–	–	–	–	–
Micronuclei, number	1.8	2.0	0.6	0.1	30.8	1.0	3.0 <sup>1</sup>	18
	2.0	2.0	0.0	0.0	0.0	2.0	2.0	10
Adoral membranelles, number	10.6	11.0	0.9	0.2	9.0	8.0	12.0	20
	9.8	10.0	0.9	0.3	8.9	9.0	12.0	10
Frontal adoral membranelles, number	3.0	3.0	0.0	0.0	0.0	3.0	3.0	14
	–	–	–	–	–	–	–	–
Ventral adoral membranelles, number	6.9	7.0	0.6	0.1	8.0	5.0	8.0	19
	–	–	–	–	–	–	–	–
Adoral membranelles between frontal and ventral membranelles, number	1.0	1.0	0.0	0.0	0.0	1.0	1.0	19
	–	–	–	–	–	–	–	–
Largest adoral membranelle, length of base	2.3	2.0	0.4	0.1	16.5	2.0	3.0	19
	–	–	–	–	–	–	–	–
Frontal cirri, number					see text			
	3.0	3.0	0.0	0.0	0.0	3.0	3.0	10

**Table 23.** Continued.

Characteristic	Mean	M	SD	SE	CV	Min	Max	n
Buccal cirri, number	1.0	1.0	0.0	0.0	0.0	1.0	1.0	9
	1.0	1.0	0.0	0.0	0.0	1.0	1.0	10
Frontoventral cirral row 1, number of cirri	1.9	2.0	–	–	–	1.0	2.0	15
	–	–	–	–	–	–	–	–
Frontoventral cirral row 2, number of cirri	8.7	9.0	1.5	0.3	16.8	6.0	12.0	19
	6.6	6.0	0.7	0.3	11.1	6.0	8.0	7
Right marginal row, number of cirri	76.6	76.0	8.1	1.8	10.6	59.0	91.0	21
	52.9	50.0	8.8	2.8	16.6	44.0	74.0	10
Left marginal row, number of cirri	60.1	60.0	7.0	1.5	11.6	46.0	70.0	21
	40.8	39.0	6.7	2.1	16.4	33.0	55.0	10
Dorsal kineties, number	1.0	1.0	0.0	0.0	0.0	1.0	1.0	21
	1.0	1.0	0.0	0.0	0.0	1.0	1.0	10
Dikinetids in dorsal kinety, number	19.1	19.0	2.3	0.5	12.0	13.0	24.0	19.0
	–	–	–	–	–	–	–	–

<sup>a</sup> Rarely four (Fig. 60g).

**Table 24.** Morphometric data on *Urosoma australiensis* (upper line) and *Urosoma pelobia* (lower line) based on mounted, protargol-impregnated, and randomly selected specimens. Measurements in  $\mu\text{m}$ . CV – coefficient of variation in %, M – median, Max – maximum, Mean – arithmetic mean, Min – minimum, n – number of individuals investigated, SD – standard deviation, SE – standard error of arithmetic mean.

Characteristic	Mean	M	SD	SE	CV	Min	Max	n
Body, length	140.5	138.0	11.7	2.6	8.3	121.0	164.0	21
	136.2	137.0	11.7	2.6	8.6	115.0	155.0	21
Body, width	41.1	41.0	3.5	0.8	8.6	35.0	50.0	21
	22.6	23.0	1.3	0.3	5.7	21.0	25.0	21
Body length:width, ratio	3.4	3.4	0.2	0.1	6.9	3.0	3.9	21
	6.1	6.1	0.5	0.1	7.7	5.2	7.0	21
Anterior body end to first macronuclear nodule, distance	37.5	38.0	3.1	0.7	8.3	32.0	44.0	21
	38.5	39.0	2.3	0.5	6.0	34.0	43.0	21
Anterior body end to paroral membrane, distance	19.9	20.0	2.1	0.5	10.5	16.0	23.0	21
	16.8	17.0	1.8	0.4	10.7	13.0	20.0	21
Anterior body end to endoral membrane, distance	–	–	–	–	–	–	–	–
	20.2	20.0	1.5	0.3	7.1	18.0	23.0	21
Anterior body end to buccal cirrus, distance	23.1	23.0	2.3	0.5	10.0	19.0	26.0	21
	18.1	18.0	1.6	0.4	9.1	15.0	21.0	20
Anterior body end to last frontoventral cirrus, distance	29.7	29.0	2.4	0.5	8.0	26.0	34.0	21
	27.0	27.0	1.8	0.4	6.7	24.0	30.0	21
Anterior body end to last postoral cirrus, distance	51.3	52.0	4.7	1.0	9.1	42.0	60.0	21
	46.5	47.0	3.2	0.7	6.8	41.0	51.0	21
Anterior body end to right marginal cirral row, distance	8.8	9.0	2.0	0.5	22.9	4.0	12.0	20
	7.7	7.0	1.4	0.3	17.9	5.0	10.0	21
Posterior body end to right marginal cirral row, distance	3.5	3.0	2.1	0.5	59.9	1.0	8.0	21
	13.1	13.0	1.9	0.4	14.7	9.0	16.0	21
Posterior body end to left marginal cirral row, distance	2.4	2.0	1.6	0.3	64.6	1.0	6.0	21
	1.6	2.0	0.7	0.2	45.7	1.0	4.0	21
Posterior body end to rearmost transverse cirrus, distance	3.8	4.0	1.1	0.2	27.8	2.0	6.0	21
	11.2	11.0	1.6	0.4	14.3	8.0	14.0	21

Table 24. Continued.

Characteristic	Mean	M	SD	SE	CV	Min	Max	n
Anterior macronuclear nodule, length	19.5	20.0	2.4	0.5	12.5	15.0	23.0	21
	15.7	16.0	1.8	0.4	11.3	13.0	20.0	21
Anterior macronuclear nodule, width	6.3	6.0	0.9	0.2	13.5	5.0	8.0	21
	6.4	6.0	0.9	0.2	14.4	5.0	8.0	21
Macronuclear nodules, number	2.0	2.0	0.0	0.0	0.0	2.0	2.0	20
	2.0	2.0	0.0	0.0	0.0	2.0	2.0	21
Micronuclei, length	4.1	4.0	0.4	0.1	9.5	3.0	5.0	21
	6.9	7.0	0.8	0.2	11.5	5.0	8.0	15
Micronuclei, width	2.9	3.0	0.3	0.1	10.4	2.0	3.0	21
	3.4	3.0	0.5	0.1	14.4	3.0	4.0	15
Micronuclei, number	2.9	3.0	0.8	0.2	28.6	1.0	4.0	21
	2.1	2.0	–	–	–	2.0	3.0	15
Nuclear figure, length	–	–	–	–	–	–	–	–
	43.0	43.0	4.2	0.9	9.9	37.0	52.0	21
Body length:adoral zone length, ratio in %	27.4	27.1	2.3	0.5	8.3	22.3	31.5	21
	25.7	25.5	1.7	0.4	6.7	23.1	28.8	21
Adoral membranelles, number	36.0	36.0	2.1	0.5	5.8	32.0	40.0	21
	29.8	30.0	1.9	0.4	6.2	26.0	32.0	21
Adoral zone, width of bases in largest membranelles	–	–	–	–	–	–	–	–
	4.1	4.0	–	–	–	4.0	5.0	21
Frontal cirri, number	3.0	3.0	0.0	0.0	0.0	3.0	3.0	20
	3.0	3.0	0.0	0.0	0.0	3.0	3.0	21
Buccal cirri, number	1.0	1.0	0.0	0.0	0.0	1.0	1.0	21
	1.0	1.0	0.0	0.0	0.0	1.0	1.0	21
Frontoventral cirri, number	4.0	4.0	0.0	0.0	0.0	4.0	4.0	21
	4.0	4.0	0.0	0.0	0.0	4.0	4.0	21
Postoral cirri, number	3.0	3.0	0.0	0.0	0.0	3.0	3.0	21
	3.0	3.0	0.0	0.0	0.0	3.0	3.0	20
Right marginal cirri, number	43.0	42.5	3.6	0.8	8.4	37.0	53.0	20
	36.7	36.0	3.2	0.7	8.8	31.0	44.0	21
Left marginal cirri, number	36.7	37.0	3.5	0.8	9.4	28.0	43.0	21
	32.8	33.0	2.2	0.5	6.7	29.0	36.0	21
Transverse cirri, number	5.0	5.0	0.0	0.0	0.0	5.0	5.0	21
	4.0	4.0	0.0	0.0	0.0	4.0	4.0	21
Pretransverse cirri, number	2.0	2.0	0.0	0.0	0.0	2.0	2.0	21
	2.0	2.0	0.0	0.0	0.0	2.0	2.0	21
Dorsal kineties, number	4.0	4.0	0.0	0.0	0.0	4.0	4.0	21
	4.0	4.0	0.0	0.0	0.0	4.0	4.0	21
Bristles in dorsal kinety 1, number	–	–	–	–	–	–	–	–
	15.8	16.0	1.6	0.4	9.9	13.0	19.0	20
Bristles in dorsal kinety 2, number	–	–	–	–	–	–	–	–
	19.6	20.0	2.0	0.4	10.4	16.0	23.0	21
Bristles in dorsal kinety 3, number	–	–	–	–	–	–	–	–
	18.0	18.0	1.7	0.4	9.6	15.0	22.0	21
Bristles in dorsal kinety 4, number	–	–	–	–	–	–	–	–
	13.0	13.0	1.4	0.3	10.9	11.0	16.0	21
Caudal cirri, number	3.0	3.0	0.0	0.0	0.0	3.0	3.0	21
	3.0	3.0	0.0	0.0	0.0	3.0	3.0	21

**Table 25.** Comparison of main characteristics of *Urosoma pelobia* with similar species. Arithmetic means and extremes, if available, in parenthesis. All based on protargol-impregnated specimens, if not mentioned otherwise.

Characteristic	<i>Urosoma pelobia</i> nov. spec. (present work)	<i>U. macrostyla</i> (from Wrzesniowski 1870)	<i>U. macrostyla</i> (from Qin et al. 2011)	<i>U. acuta</i> (from Dragesco 1972)	<i>U. ambigua</i> (from Dragesco & Dragesco- Kernéis 1986)
Body, size in vivo ( $\mu\text{m}$ )	~155 × 25	120 × 30	180–300 × 30–60	?	?
Body, size ( $\mu\text{m}$ )	136 × 23 (115–155 × 21–25)	?	226 × 40 (182–270 × 29–49)	120–170	150 (130–168)
Body, length: width ratio	6:1 (5–7:1)	4:1	5.6:1	~5.2:1	4.5:1
Adoral membranelles, number	29.8 (26–32)	?	41 (33–49)	43–53	43 (38–45)
Transverse cirri, number	4 (4–4)	5	4.4 (2–5)	likely 5	5
Right marginal cirri, number	37 (31–44)	?	48 (31–63)	42–63	50 (40–59)
Left marginal cirri, number	33 (29–36)	?	42 (25–58)	39–62	50 (45–55)
Number of specimens analysed	21	?	40	?	5
Site	Australia	Poland	China	Chad	Benin

**Table 26.** Morphometric comparison of a Botswanan (original data, upper line) and an Austrian (Foissner 1982, lower line) population of *Hemiurosoma similis* based on mounted, protargol-impregnated, and randomly selected specimens from a raw culture. Measurements in  $\mu\text{m}$ . CV – coefficient of variation in %, M – median, Max – maximum, Mean – arithmetic mean, Min – minimum, n – number of individuals investigated, SD – standard deviation, SE – standard error of arithmetic mean; – not investigated.

Characteristic	Mean	M	SD	SE	CV	Min	Max	n
Body, length	120.5	119.0	11.7	2.6	9.7	97.0	152.0	21
	113.3	110.0	13.1	4.6	13.8	83.0	140.0	17
Body, width	21.0	21.0	2.5	0.5	11.6	17.0	27.0	21
	17.1	17.0	1.7	0.4	9.9	14.0	20.0	17
Body length:width, ratio	5.8	5.7	0.5	0.1	8.1	5.3	7.2	21
	6.6	–	–	–	–	–	–	21
Anterior body end to first macronuclear nodule, distance	13.6	13.0	1.8	0.4	13.0	11.0	18.0	21
	–	–	–	–	–	–	–	–
Anterior body end to paroral membrane, distance	12.2	12.0	1.1	0.2	8.8	10.0	14.0	21
	–	–	–	–	–	–	–	–
Anterior body end to endoral membrane, distance	15.2	15.0	1.1	0.3	7.4	13.0	17.0	21
	–	–	–	–	–	–	–	–
Anterior body end to buccal cirrus, distance	11.6	12.0	0.8	0.2	7.0	10.0	13.0	21
	–	–	–	–	–	–	–	–
Anterior body end to begin of frontoventral cirral row, distance	8.3	8.0	0.9	0.2	10.2	7.0	10.0	21
	–	–	–	–	–	–	–	–
Anterior body end to end of frontoventral cirral row, distance	18.9	19.0	0.9	0.2	4.7	17.0	21.0	21
	15.9	16.0	1.8	0.4	11.3	11.0	20.0	17
Anterior body end to right marginal cirral row, distance	6.7	6.0	2.2	0.5	33.7	3.0	15.0	21
	–	–	–	–	–	–	–	–

Table 26. Continued.

Characteristic	Mean	M	SD	SE	CV	Min	Max	n
Posterior body end to right marginal cirral row, distance	8.0	8.0	3.4	0.8	42.5	2.0	15.0	21
	–	–	–	–	–	–	–	–
Posterior body end to left marginal cirral row, distance	3.9	4.0	2.9	0.7	74.6	1.0	10.0	21
	–	–	–	–	–	–	–	–
Anterior macronuclear nodule, length	13.6	13.0	1.8	0.4	13.1	11.0	18.0	21
	11.8	12.0	1.7	0.4	14.5	9.3	15.0	17
Anterior macronuclear nodule, width	5.0	5.0	0.8	0.2	15.6	3.0	6.0	21
	3.9	4.0	0.6	0.1	15.1	2.4	5.3	17
Macronuclear nodules, number	2.0	2.0	0.0	0.0	0.0	2.0	2.0	21
	2.0	2.0	0.0	0.0	0.0	2.0	2.0	17
Macronuclear nodules, distance in between	9.4	9.0	3.3	0.7	34.6	5.0	18.0	21
	–	–	–	–	–	–	–	–
Nuclear figure, length	37.1	36.0	4.0	0.9	11.5	32.0	47.0	21
	–	–	–	–	–	–	–	–
Micronuclei, length	3.3	3.0	0.5	0.1	15.3	2.5	4.0	20
	2.9	2.8	0.2	0.1	8.2	2.7	3.5	13
Micronuclei, width	1.7	1.5	0.3	0.1	17.6	1.0	2.0	20
	1.9	2.0	0.2	0.1	8.2	1.4	2.4	13
Micronuclei, number	2.2	2.0	0.7	0.2	31.6	1.0	4.0	21
	2.0	2.0	0.0	0.0	0.0	2.0	2.0	13
Anterior body end to proximal end of adoral zone of membranelles, distance	24.8	25.0	1.3	0.3	5.4	22.0	27.0	21
	24.3	24.0	1.5	0.4	6.3	20.0	27.0	17
Body length: adoral zone length, ratio in %	20.7	20.8	1.7	0.4	8.1	17.1	23.7	21
	21.4	–	–	–	–	–	–	17
Adoral zone, number of membranelles	19.1	19.0	1.1	0.2	5.7	16.0	21.0	21
	21.6	22.0	0.7	0.2	3.1	20.0	23.0	17
Paroral membrane, length	3.1	3.0	–	–	–	3.0	4.0	21
	–	–	–	–	–	–	–	–
Endoral membrane, length	5.3	5.0	–	–	–	5.0	6.0	20
	–	–	–	–	–	–	–	–
Frontal cirri, number	3.0	3.0	0.0	0.0	0.0	3.0	3.0	21
	3.0	3.0	0.0	0.0	0.0	3.0	3.0	17
Buccal cirri, number	1.0	1.0	0.0	0.0	0.0	1.0	1.0	21
	1.0	1.0	0.0	0.0	0.0	1.0	1.0	17
Frontoventral cirri, number	3.9	4.0	–	–	–	3.0	4.0	21
	3.5	4.0	–	–	–	1.0	4.0	17
Right marginal cirri, number	28.3	28.0	1.9	0.4	6.7	25.0	31.0	21
	33.6	34.0	2.8	0.7	8.4	27.0	37.0	17
Left marginal cirri, number	23.8	24.0	1.8	0.4	7.6	21.0	27.0	21
	27.6	27.0	2.1	0.5	7.8	24.0	32.0	17
Transverse cirri, number	1.9	2.0	–	–	–	1.0	2.0	17
	2.1	2.0	–	–	–	2.0	3.0	17
Dorsal kineties, number	4.0	4.0	0.0	0.0	0.0	4.0	4.0	19
	4.0	4.0	0.0	0.0	0.0	4.0	4.0	17
Bristles in dorsal kinety 1, number	7.7	8.0	0.9	0.2	11.8	6.0	10.0	18
	8.0	–	–	–	–	–	–	1

**Table 26.** Continued.

Characteristic	Mean	M	SD	SE	CV	Min	Max	n
Bristles in dorsal kinety 2, number	14.3	15.0	1.5	0.4	10.7	12.0	17.0	18
	13.0	–	–	–	–	–	–	1
Bristles in dorsal kinety 3, number	14.1	14.0	1.3	0.3	9.0	12.0	16.0	18
	15.0	–	–	–	–	–	–	1
Bristles in kinety 4, number	3.3	3.0	0.7	0.2	20.6	2.0	5.0	18
	3.0	–	–	–	–	–	–	1
Caudal cirri, number	3.6	3.0	–	–	–	3.0	4.0	18
	3.0	–	–	–	–	–	–	1

**Table 27.** Morphometric data on *Urosomoida uluruensis* based on mounted, protargol-impregnated and randomly selected specimens from a non-flooded Petri dish culture. Measurements in  $\mu\text{m}$ . CV – coefficient of variation in %, M – median, Max – maximum Mean – arithmetic mean, Min – minimum, n – number of individuals investigated, SD – standard deviation, SE – standard error of arithmetic mean.

Characteristic	Mean	M	SD	SE	CV	Min	Max	n
Body, length	77.0	78.0	5.6	1.2	7.2	66.0	85.0	21
Body, width	22.9	23.0	3.0	0.7	13.2	19.0	28.0	21
Body length:width, ratio	3.4	3.3	0.3	0.1	10.1	2.0	4.0	21
Anterior body end to right marginal cirral row	13.8	14.0	2.5	0.6	18.2	8.0	18.0	21
Anterior body end to posterior postoral cirrus	31.5	31.0	1.9	0.4	6.2	27.0	35.0	21
Anterior body end to buccal cirrus	8.9	9.0	0.8	0.2	9.0	8.0	10.0	21
Anterior body end to last fronto ventral cirrus	13.9	14.0	1.2	0.3	8.8	12.0	16.0	21
Posterior body end to transverse cirri	1.9	2.0	0.7	0.2	36.8	1.0	3.0	21
Posterior body end to right marginal cirral row	4.3	4.0	2.4	0.5	55.3	1.0	11.0	21
Posterior body end to left marginal cirral row	3.3	3.0	1.8	0.4	55.4	1.0	8.0	21
Anterior body end to first macronuclear nodule	23.1	23.0	1.5	0.3	6.4	20.0	25.0	21
Anterior macronuclear nodule, length	12.5	12.0	1.6	0.3	12.6	9.0	16.0	21
Anterior macronuclear nodule, width	7.1	7.0	1.0	0.2	13.5	6.0	9.0	21
Macronuclear nodules, distance in between	3.9	3.0	2.0	0.4	52.5	1.0	8.0	21
Macronuclear nodule, number <sup>a</sup>	2.0	2.0	0.0	0.0	0.0	2.0	2.0	21
Anteriormost micronucleus, length	2.6	3.0	0.4	0.1	17.0	2.0	3.0	21
Anterior most micronucleus, width	2.1	2.0	–	–	–	2.0	2.5	21
Micronuclei, number	1.8	2.0	0.9	0.2	53.6	0.0	5.0	21
Adoral zone of membranelles, length	24.6	24.0	1.5	0.3	6.1	23.0	28.0	21
Body length: adoral zone length, %	32.1	33.3	2.7	0.6	8.4	27.1	35.9	21
Largest adoral membranelle, width	5.1	5.0	0.4	0.1	7.0	5.0	6.0	21
Adoral membranelles, number	23.9	24.0	1.4	0.3	5.9	21.0	26.0	21
Anterior body length to paroral	6.3	6.0	1.1	0.2	17.5	4.0	8.0	21
Paroral membrane, length	11.3	11.0	1.5	0.3	13.5	7.0	14.0	21
Anterior body end to endoral	8.5	8.0	1.1	0.2	12.7	7.0	10.0	21
Endoral membrane length	11.7	12.0	2.0	0.4	17.1	7.0	16.0	21
Frontal cirri, number	3.0	3.0	0.0	0.0	0.0	3.0	3.0	21
Frontoventral cirri, number	3.6	4.0	0.6	0.1	16.3	2.0	4.0	21
Buccal cirri, number	1.0	1.0	0.0	0.0	0.0	1.0	1.0	21
Postoral cirri, number	2.9	3.0	0.5	0.1	16.7	2.0	4.0	21
Postoral cirri, distance between 1 and 2	0.6	0.5	0.3	0.2	44.0	0.1	1.0	20
Postoral cirri, distance between 2 and 3	4.2	4.0	0.9	0.2	21.0	3.0	6.0	20
Transverse and pretransverse cirri, number	3.9	4.0	–	–	–	3.0	4.0	21

Table 27. Continued.

Characteristic	Mean	M	SD	SE	CV	Min	Max	n
Caudal cirri, number	3.0	3.0	0.0	0.0	0.0	3.0	3.0	21
Right marginal cirri, number	19.5	19.0	2.8	0.6	14.1	13.0	24.0	21
Left marginal cirri, number	18.7	19.0	2.1	0.5	11.3	15.0	23.0	21
Dorsal kineties, number	4.0	4.0	0.0	0.0	0.0	4.0	4.0	21
Bristles in dorsal kinety 1	8.0	8.0	1.3	0.3	16.6	5.0	10.0	21
Bristles in dorsal kinety 2	11.4	11.0	1.5	0.3	12.9	9.0	15.0	21
Bristles in dorsal kinety 3	10.5	11.0	1.3	0.3	12.3	8.0	13.0	21
Bristles in dorsal kinety 4	8.1	8.0	1.0	0.2	12.9	7.0	10.0	21

<sup>a</sup> Three nodules and only two frontal cirri in one of 25 individuals investigated.

**Table 28.** Morphometric data on *Urosomoida bromelicola* based on mounted, protargol-impregnated and randomly selected specimens from a raw culture. Measurements in  $\mu\text{m}$ . CV – coefficient of variation in %, M – median, Max – maximum, Mean – arithmetic mean, Min – minimum, n – number of individuals investigated, SD – standard deviation, SE – standard error of arithmetic mean.

Characteristic	Mean	M	SD	SE	CV	Min	Max	n
Body, length	55.3	56.0	6.2	1.4	11.3	44.0	70.0	21
Body, width	12.1	12.0	1.3	0.3	10.8	10.0	15.0	21
Body length:width, ratio	4.6	4.5	0.4	0.1	7.9	4.0	5.5	21
Adoral zone of membranelles, length <sup>a</sup>	14.9	15.0	0.8	0.2	5.6	14.0	17.0	21
Body length: adoral zone length (%)	27.1	27.0	2.4	0.5	8.8	23.0	32.0	21
Largest adoral membranelle, width	3.5	3.5	–	–	–	3.0	4.0	21
Buccal field, width <sup>b</sup>	1.4	1.0	–	–	–	0.0	2.0	21
Anterior body end to right marginal cirral row, distance	8.7	8.0	1.0	0.2	11.6	7.0	11.0	21
Anterior body end to paroral membrane, distance	4.3	4.0	–	–	–	3.5	5.0	21
Anterior body end to endoral membrane, distance	6.0	6.0	0.6	0.1	9.5	5.0	7.0	21
Anterior body end to buccal cirrus, distance	4.7	5.0	0.6	0.1	13.3	4.0	6.0	21
Anterior body end to first macronuclear nodule, distance	14.4	14.0	1.0	0.2	7.2	12.0	17.0	21
Anterior body end to first postoral cirrus, distance	14.8	15.0	1.2	0.3	7.8	13.0	18.0	21
Anterior body end to last postoral cirrus, distance	20.0	20.0	1.4	0.3	7.2	18.0	24.0	21
Anterior body end to first frontoventral cirrus, distance	5.1	5.0	0.6	0.1	11.1	4.0	6.0	21
Anterior body end to last frontoventral cirrus, distance	8.2	8.0	0.6	0.1	6.8	7.0	9.0	21
Macronuclear nodules, length	9.9	10.0	1.4	0.3	14.0	7.0	13.0	21
Macronuclear nodules, width	3.5	3.5	–	–	–	3.0	4.0	21
Macronuclear nodules, number	2.0	2.0	0.0	0.0	0.0	2.0	2.0	21
Micronuclei, number	2.0	2.0	0.9	0.2	44.7	1.0	4.0	21
Micronuclei, length	1.4	1.5	–	–	–	1.0	2.0	21
Micronuclei, width	1.3	1.5	–	–	–	1.0	1.5	21
Adoral membranelles, number	15.6	16.0	0.7	0.1	4.3	15.0	17.0	21
Frontal cirri, number	3.0	3.0	0.0	0.0	0.0	3.0	3.0	21
Buccal cirri, number	1.0	1.0	0.0	0.0	0.0	1.0	1.0	21
Transverse cirri, number	3.0	3.0	0.0	0.0	0.0	3.0	3.0	21
Pretransverse cirri, number	1.9	2.0	0.4	0.1	22.9	1.0	3.0	21
Right marginal cirri, number	18.4	18.0	1.1	0.2	6.1	16.0	20.0	21
Left marginal cirri, number	17.7	18.0	1.3	0.3	7.6	15.0	20.0	21
Postoral cirri, number	3.0	3.0	0.0	0.0	0.0	3.0	3.0	21
Frontoventral cirri, number	4.0	4.0	0.0	0.0	0.0	4.0	4.0	21
Caudal cirri, number	2.0	2.0	0.0	0.0	0.0	2.0	2.0	21

**Table 28.** Continued.

Characteristic	Mean	M	SD	SE	CV	Min	Max	n
Dorsal kineties, number	4.0	4.0	0.0	0.0	0.0	4.0	4.0	21
Dorsal kinety 1, number of bristles	6.1	6.0	0.5	0.1	8.8	5.0	7.0	21
Dorsal kinety 2, number of bristles	8.1	8.0	0.7	0.1	8.0	7.0	10.0	21
Dorsal kinety 3, number of bristles	5.9	6.0	0.8	0.2	14.1	4.0	7.0	21
Dorsal kinety 4, number of bristles	4.3	4.0	0.6	0.1	13.3	3.0	5.0	21

<sup>a</sup> Anterior body end to proximal end of zone.

<sup>b</sup> Distance between centre of paroral membrane and right margin of adoral zone of membranelles.

**Table 29.** Comparison of *Urosomoida bromelicola* with similar species. Extremes and median (in brackets) are provided. Measurements in  $\mu\text{m}$ . All from prepared (mostly protargol) specimens. nd = no data available.

Characteristic	<i>Urosomoida bromelicola</i>	<i>Oxytricha longa</i>	<i>Oxytricha longa</i>	<i>Hemiurosomoida longa</i>	<i>Urosomoida halophila</i>
Size in vivo	50–80 × 10–17 (66 × 15), n = 6	nd	60–100 × 25–35	50–75 × 15–22	55–84 × 15– 25 (70 × 20)
Size in preparations	44–70 × 10–15 (50 × 12)	80–100 × 25–40 (nd)	47–75 × 13– 30 (59 × 19)	51–69 × 16–21 (59 × 17)	45–67 × 14– 23 (56 × 20)
Location of transverse cirri	terminal	subterminal	subterminal	subterminal	subterminal
Adoral membranelles, number	15–17 (16)	21–22 (nd)	18–22 (20)	18–22 (21)	15–18 (17)
Pretransverse cirri, number	1–3 (2)	nd (2)	nd (2)	2–2 (2)	2–3 (2)
Transverse cirri, number	3–3 (3)	nd (4)	3–5 (nd)	4–5 (4)	3–5 (4)
Right marginal cirri, number	16–20 (18)	20–22 (nd)	23–25 (21)	17–23 (20)	19–23 (21)
Left marginal cirri, number	15–20 (18)	19–21 (nd)	17–23 (20)	14–21 (16)	17–24 (20)
Dorsal kineties, number	4–4 (4)	nd (4)	4–4 (4)	4–5 (4)	4–5 (4)
Dikinetids in dorsal kinety 1, number	5–7 (6)	nd	nd	10–14 (12)	6, n = 1
Dikinetids in dorsal kinety 2, number	7–10 (8)	nd	nd	10–13 (12)	7, n = 1
Dikinetids in dorsal kinety 3, number	4–7 (6)	nd	nd	8–12 (10)	8, n = 1
Dikinetids in dorsal kinety 4, number	3–5 (4)	nd	nd	4–6 (5)	3–5 (nd)
Caudal cirri, number	2–2 (2)	nd	2–2 (2)	2–3 (2)	2–2 (2)
Specimens investigated, number	21	nd	25	20	21
Reference	present work	Gelei & Szabados (1950)	Ganner et al. (1987), population 3	Singh & Kamra (2015)	Foissner (2016)

**Table 30.** Morphometric data on *Bothrix africana* based on mounted, protargol-impregnated, and randomly selected specimens from a non-flooded Petri dish culture. Measurements in  $\mu\text{m}$ . CV – coefficient of variation in %, M – median, Max – maximum, Mean – arithmetic mean, Min – minimum, n – number of individuals investigated, SD – standard deviation, SE – standard error of arithmetic mean.

Characteristic	Mean	M	SD	SE	CV	Min	Max	n
Body, length in vivo	116.7	110.0	19.7	8.0	16.8	100.0	150.0	6
Body width in vivo	47.5	47.5	3.1	16.0	6.5	40.0	60.0	6
Body, length (protargol)	106.9	107.0	6.9	1.5	6.5	93.0	120.0	21
Body, width (protargol)	37.8	37.0	5.0	1.1	13.2	32.0	55.0	21
Body length:width, ratio	2.9	2.9	0.3	0.1	10.3	2.1	3.4	21
Anterior body end to right marginal row, distance	15.0	15.0	1.9	0.4	12.6	12.0	20.0	21
Right marginal row, number of cirri	25.9	26.0	2.0	0.4	7.6	23.0	29.0	21
Left marginal row, number of cirri	23.2	23.0	1.3	0.3	5.4	21.0	26.0	21
Anterior body end to ventral row 1, distance <sup>a</sup>	14.5	15.0	1.6	0.3	11.1	11.0	18.0	21
Anterior body end to ventral row 2, distance	22.0	22.0	1.9	0.4	8.5	18.0	26.0	21
Anterior body end to anterior macronuclear nodule, distance	26.8	27.0	1.9	0.4	7.0	24.0	30.0	21
Anterior macronuclear nodule, length	23.6	24.0	2.1	0.5	8.9	17.0	27.0	21
Anterior macronuclear nodule, width	12.4	13.0	1.3	0.3	10.4	10.0	15.0	21
Posterior macronuclear nodule, length	22.5	23.0	3.3	0.7	14.6	12.0	27.0	21
Posterior macronuclear nodule, width	11.6	12.0	1.5	0.3	12.9	8.0	14.0	21
Macronuclear nodules, distance in between	6.7	7.0	3.7	0.8	53.3	0.0	13.0	21
Nuclear figure, length	53.1	52.0	4.4	1.0	8.3	44.0	60.0	21
Posteriormost micronucleus, length	3.1	3.0	0.2	0.1	7.6	3.0	3.8	21
Posteriormost micronucleus, width	3.1	3.0	0.3	0.1	9.8	2.5	3.8	21
Micronucleus, number	2.9	3.0	0.3	0.1	10.4	2.0	3.0	21
Posterior body end to lowermost transverse cirrus, distance	10.3	10.0	2.4	0.5	23.6	5.0	15.0	21
Posterior body end to anteriormost transverse cirrus, distance	28.9	28.0	2.7	0.6	9.5	23.0	34.0	21
Posterior body end to ventral row 1, distance	26.4	27.0	2.9	0.6	11.0	20.0	30.0	21
Posterior body end to ventral row 2, distance	32.1	32.0	3.6	0.8	11.3	27.0	44.0	21
Anterior body end to proximal end of adoral zone, distance	36.1	36.0	1.4	0.3	3.9	33.0	39.0	21
Anterior body end to proximal end of adoral zone (%)	34.0	34.0	2.6	0.6	7.8	30.0	40.0	21
Adoral membranelles, number	26.6	26.0	0.8	0.2	3.1	25.0	28.0	21
Base of longest adoral membranelles, length	7.0	7.0	0.7	0.1	9.5	6.0	8.0	21
Buccal cavity, width	7.0	7.0	1.7	0.4	24.4	5.0	11.0	21
Anterior body end to paroral membrane, distance	17.8	18.0	1.6	0.4	9.2	14.0	20.0	21
Paroral membrane, length	13.6	13.0	2.8	0.6	20.9	10.0	22.0	21
Anterior body end to endoral membrane, distance	21.2	21.0	1.3	0.3	6.1	18.0	23.0	21
Endoral membrane, length	13.7	14.0	1.0	0.2	7.3	12.0	15.0	21
Frontal cirri, number	3.0	3.0	0.0	0.0	0.0	3.0	3.0	21
Frontoterminal cirri, number	2.0	2.0	0.0	0.0	0.0	2.0	2.0	21
Buccal cirrus, number of ciliary rows	5.7	5.0	1.1	0.2	18.5	5.0	8.0	21
Buccal cirrus, length of base	3.9	4.0	0.6	0.1	14.1	3.0	5.0	21
Buccal cirri, number	1.0	1.0	0.0	0.0	0.0	1.0	1.0	21
Transverse cirri, number	7.8	8.0	0.5	0.1	6.9	7.0	8.0	21
Pretransverse cirri, number	2.0	2.0	0.0	0.0	0.0	2.0	2.0	19
Ventral row 1, number of cirri <sup>b</sup>	4.8	5.0	0.6	0.1	13.1	3.0	6.0	21
Ventral row 1, length (with pretransverse and frontoterminal cirri)	63.9	65.0	5.4	1.2	8.4	55.0	74.0	21
Ventral row 2, number of cirri	4.5	5.0	0.5	0.1	11.1	4.0	5.0	21
Ventral row 2 length with pretransverse cirrus	50.4	53.0	8.3	1.8	16.4	27.0	61.0	21
Dorsal kineties, number	6.0	6.0	0.0	0.0	0.0	6.0	6.0	21

**Table 30.** Continued.

Characteristic	Mean	M	SD	SE	CV	Min	Max	n
First dorsal kinety, number of bristles	24.7	25.0	2.3	0.5	9.3	21.0	29.0	21
Sixth dorsal kinety, number of bristles	8.7	8.0	1.8	0.4	21.2	6.0	12.0	21
Caudal cirri, number	3.0	3.0	0.0	0.0	0.0	3.0	3.0	21

<sup>a</sup> Includes two frontoterminal cirri at begin of row.

<sup>b</sup> Without frontoterminal and pretransverse cirri.

**Table 31.** Comparison of main characteristics in some large oxytrichs. The median and extremes are given. Distances and sizes in  $\mu\text{m}$ . Most data based on protargol-impregnated specimens.

Characteristic	<i>Mixophrya pantanalensis australiensis</i>	<i>Mixophrya pantanalensis pantanalensis</i>	<i>Apooxytricha bromelicola</i>	<i>Paroxytricha longigranulosa sinensis</i>	<i>Urosoma australiensis</i>
Body, length	247 (202–289)	319 (274–358)	137 (130–161)	146 (124–161)	138 (121–164)
Body length: width, ratio	3.1 (2.6–3.7)	3.2 (2.7–3.8)	2.7 (2.3–3.5)	3.1 (2.6–3.7)	3.4 (3.0–3.9)
Posterior body end to rearmost transverse cirrus, distance	26 (20–37)	32 (17–46)	31 (27–35)	15 (9–21)	4 (2–6)
Right marginal cirri, number	50 (41–58)	53 (47–58)	31 (27–35)	37 (32–48)	43 (37–53)
Adoral zone of membranelles, % of body length	35 (30–39)	35 (29–40)	35 (30–38)	38 (25–46)	27 (22–32)
Adoral zone, number of membranelles	50 (45–56)	52 (49–58)	41 (35–44)	40 (29–45)	36 (32–40)
Largest adoral membranelle, base width	9 (8–11)	12 (11–13)	8 (7–8)	6 (6–7)	~12
Dorsal kineties, number	6 (6–6)	6 (6–6)	6 (6–6)	5 (5–5)	4 (4–4)
Cortical granules	bright citrine, about 0.2 $\mu\text{m}$	sharp yellowish, globular, 0.3 $\mu\text{m}$	colourless rods ~3.0 $\times$ 0.4 $\mu\text{m}$	colourless, ~1.5 $\times$ 0.5 $\mu\text{m}$	colourless, ~0.5 $\mu\text{m}$ across
Lithosomes	absent	present	absent	absent	absent
Number of specimens investigated	21	21	21	21	21

**Table 32.** Comparison of morphometric data on *Paroxytricha longigranulosa sinensis* from China (CH, from Foissner 2016), *Mixophrya pantanalensis pantanalensis* from Brazil (BR), and *Mixophrya pantanalensis australiensis* from Australia (AUS). Data based on mounted, protargol-impregnated, and randomly selected specimens from raw cultures. Measurements in  $\mu\text{m}$ . CV – coefficient of variation in %, M – median, Max – maximum, Mean – arithmetic mean, Min – minimum, n – number of individuals investigated, SD – standard deviation, SE – standard error of arithmetic mean.

Characteristic	Pop	Mean	M	SD	SE	CV	Min	Max	n
Body, length	CH	145.6	146.0	11.1	2.4	7.6	124.0	161.0	21
	BR	319.6	319.0	22.4	4.9	7.0	274.0	358.0	21
	AUS	247.1	245.0	23.7	5.2	9.6	202.0	289.0	21
Body, width	CH	48.2	48.0	7.2	1.6	15.0	32.0	68.0	21
	BR	101.5	101.0	8.8	1.9	8.6	82.0	117.0	21
	AUS	82.9	82.0	6.3	1.4	7.7	74.0	97.0	21

**Table 32.** Continued.

Characteristic	Pop	Mean	M	SD	SE	CV	Min	Max	n
Body length: width, ratio	CH	3.1	3.1	0.5	0.1	15.0	2.4	4.6	21
	BR	3.2	3.1	0.3	0.1	9.4	2.7	3.8	21
	AUS	3.0	2.9	0.3	0.1	9.3	2.6	3.7	21
Anterior body end to proximal end of adoral zone of membranelles, distance	CH	50.2	51.0	5.3	1.2	10.6	37.0	57.0	20
	BR	109.3	109.0	5.1	1.2	4.7	98.0	119.0	19
	AUS	85.3	84.3	7.5	1.7	8.8	73.0	97.5	20
Adoral zone of membranelles, percentage of body length	CH	37.0	38.0	5.2	1.1	14.0	25.0	46.0	21
	BR	34.7	33.5	2.1	0.5	5.9	29.0	40.0	19
	AUS	35.0	35.0	2.4	0.5	6.9	30.0	39.0	20
Largest adoral membranelle, base width	CH	6.4	6.0	–	–	–	6.0	7.0	21
	BR	12.1	12.0	0.5	0.1	4.5	11.0	13.0	21
	AUS	9.0	9.0	0.7	0.2	8.1	8.0	10.5	21
Buccal cavity, width	CH	6.7	7.0	2.4	0.5	36.3	2.0	12.0	21
	BR	22.5	22.8	2.0	0.5	8.9	18.5	26.5	20
	AUS	21.1	21.0	3.1	0.7	14.5	15.0	27.0	21
Anterior body end to right marginal cirral row, distance	CH	19.0	20.0	4.1	0.9	21.6	10.0	26.0	21
	BR	39.3	39.0	6.1	1.3	15.5	30.0	51.0	21
	AUS	23.4	23.0	5.4	1.2	22.9	14.0	35.0	21
Anterior body end to paroral membrane, distance	CH	21.1	22.0	4.0	0.9	19.1	13.0	29.0	21
	BR	37.8	38.0	2.8	0.6	7.4	33.5	45.0	21
	AUS	31.4	31.0	5.1	1.1	16.3	23.0	43.0	21
Anterior body end to endoral membrane, distance	CH	26.6	27.0	4.4	1.0	16.5	18.0	33.0	21
	BR	43.4	42.0	6.9	1.5	15.9	36.0	67.0	21
	AUS	36.1	35.0	4.4	1.0	12.1	31.0	46.5	21
Anterior body end to buccal cirrus, distance	CH	18.8	19.0	2.2	0.5	12.0	14.0	23.0	21
	BR	55.5	57.0	5.5	1.2	9.9	41.0	63.0	21
	AUS	41.4	41.0	5.4	1.2	13.1	35.0	55.0	21
Anterior body end to first macronuclear nodule, distance	CH	37.6	37.0	3.1	0.7	8.1	31.0	43.0	21
	BR	86.3	85.0	6.3	1.4	7.3	76.0	100.0	21
	AUS	60.3	60.5	7.2	1.6	12.0	50.0	74.0	21
Posterior body end to transverse cirri, distance	CH	14.8	15.0	3.0	0.7	20.1	9.0	21.0	21
	BR	32.3	33.5	6.6	1.4	20.4	16.5	46.0	21
	AUS	26.4	27.5	4.4	1.0	16.7	20.0	36.5	21
Posterior body end to right marginal cirral row, distance	CH	4.1	4.0	1.8	0.4	45.0	0.5	8.0	21
	BR	3.8	4.0	1.6	0.3	41.7	1.5	7.0	21
	AUS	3.4	3.0	1.6	0.3	45.8	1.0	8.0	21
Posterior body end to left marginal cirral row, distance	CH	1.3	1.0	1.0	0.2	73.4	0.5	4.0	21
	BR	1.5	1.5	0.6	0.1	38.1	1.0	3.0	21
	AUS	1.1	1.0	0.5	0.1	45.0	0.5	2.0	21
Anterior macronuclear nodule, length	CH	19.8	20.0	1.9	0.4	9.5	17.0	24.0	21
	BR	40.5	40.0	7.6	1.7	18.7	31.0	66.0	21
	AUS	32.5	33.0	6.6	1.4	20.3	22.0	48.0	21
Anterior macronuclear nodule, width	CH	10.8	10.0	1.5	0.3	13.8	8.0	14.0	21
	BR	17.6	17.0	3.7	0.8	21.0	13.0	27.0	21
	AUS	11.9	11.5	1.9	0.4	15.7	10.0	17.0	21
Macronuclear nodules, number	CH	2.0	2.0	0.0	0.0	0.0	2.0	2.0	21
	BR	2.0	2.0	0.0	0.0	0.0	2.0	2.0	21
	AUS	2.0	2.0	0.0	0.0	0.0	2.0	2.0	21

Table 32. Continued.

Characteristic	Pop	Mean	M	SD	SE	CV	Min	Max	n
Micronuclei, number	CH	2.1	2.0	0.5	0.1	22.3	2.0	4.0	21
	BR	4.0	3.0	2.1	0.5	52.4	2.0	10.0	21
	AUS	3.3	3.0	1.4	0.3	42.8	1.0	6.0	21
Anterior micronucleus, length	CH	3.9	5.0	0.7	0.2	17.9	3.0	5.0	21
	BR	4.7	4.5	1.2	0.3	24.9	3.0	7.0	21
	AUS	4.1	4.0	1.4	0.3	33.9	3.0	10.0	21
Anterior micronucleus, width	CH	3.1	3.0	–	–	–	3.0	4.0	21
	BR	4.7	4.5	1.2	0.3	24.9	3.0	7.0	21
	AUS	3.3	3.0	0.4	0.1	11.2	3.0	4.0	21
Lithosomes, number	BR	6.1	6.0	1.5	0.4	25.2	4.0	10.0	17
Lithosomes, diameter	BR	8.4	8.5	1.4	0.3	17.0	6.5	11.0	18
Adoral membranelles, number	CH	39.0	40.0	4.2	0.9	10.8	29.0	45.0	21
	BR	52.2	52.0	2.7	0.6	5.2	49.0	58.0	21
	AUS	49.4	50.0	2.9	0.6	5.9	45.0	56.0	21
Frontal cirri, number	CH	3.0	3.0	0.0	0.0	0.0	3.0	3.0	21
	BR	3.0	3.0	0.0	0.0	0.0	3.0	3.0	21
	AUS	3.0	3.0	0.0	0.0	0.0	3.0	3.0	21
Buccal cirri, number	CH	1.0	1.0	0.0	0.0	0.0	1.0	1.0	21
	BR	1.0	1.0	0.0	0.0	0.0	1.0	1.0	21
	AUS	1.0	1.0	0.0	0.0	0.0	1.0	1.0	21
Right marginal cirri, number	CH	37.2	37.0	3.8	0.8	10.3	32.0	48.0	21
	BR	53.3	53.0	2.6	0.6	4.9	47.0	58.0	21
	AUS	49.4	50.0	5.0	1.1	10.1	41.0	58.0	21
Left marginal cirri, number	CH	34.9	34.0	3.5	0.8	10.0	28.0	42.0	21
	BR	41.6	41.0	3.5	0.8	8.5	33.0	46.0	21
	AUS	40.1	39.0	3.9	0.9	9.8	34.0	49.0	21
Frontoventral cirri, number	CH	4.0	4.0	0.0	0.0	0.0	4.0	4.0	21
	BR	4.0	4.0	0.0	0.0	0.0	4.0	4.0	21
	AUS	4.0	4.0	0.0	0.0	0.0	4.0	4.0	21
Postoral cirri, number	CH	3.0	3.0	0.0	0.0	0.0	3.0	3.0	21
	BR	3.0	3.0	0.0	0.0	0.0	3.0	3.0	21
	AUS	3.0	3.0	0.0	0.0	0.0	3.0	3.0	21
Transverse cirri, number	CH	5.0	5.0	0.0	0.0	0.0	5.0	5.0	21
	BR	5.0	5.0	0.0	0.0	0.0	5.0	5.0	21
	AUS	5.0	5.0	0.0	0.0	0.0	5.0	5.0	21
Pretransverse cirri, number	CH	2.0	2.0	0.0	0.0	0.0	2.0	2.0	21
	BR	2.0	2.0	0.0	0.0	0.0	2.0	2.0	21
	AUS	2.0	2.0	0.0	0.0	0.0	2.0	2.0	21
Caudal cirri, number	CH	3.2	3.0	–	–	–	3.0	4.0	21
	BR	3.0	3.0	0.0	0.0	0.0	3.0	3.0	21
	AUS	3.0	3.0	0.0	0.0	0.0	3.0	3.0	21
Dorsal kineties, number	CH	5.0	5.0	0.0	0.0	0.0	5.0	5.0	21
	BR	6.0	6.0	0.0	0.0	0.0	6.0	6.0	21
	AUS	6.0	6.0	0.0	0.0	0.0	6.0	6.0	21
Dorsal kinety 1, number of kinetids	AUS	39.1	39.0	3.9	0.9	10.0	32.0	45.0	15
Dorsal kinety 2, number of kinetids	AUS	34.9	36.0	4.1	1.2	11.6	27.0	40.0	11
Dorsal kinety 3, number of kinetids	AUS	35.9	36.0	2.8	0.6	7.8	32.0	41.0	7
Dorsal kinety 4, number of kinetids	AUS	30.4	31.0	3.4	1.5	11.1	25.0	34.0	5

Table 32. Continued.

Characteristic	Pop	Mean	M	SD	SE	CV	Min	Max	n
Dorsal kinety 5, number of kinetids	AUS	18.5	19.0	3.3	1.2	18.0	12.0	23.0	8
Dorsal kinety 6, number of kinetids	AUS	9.5	10.0	3.2	1.0	33.9	5.0	14.0	11
Resting cyst with wall, length	BR	71.4	71.0	6.2	0.6	8.6	58.0	80.0	18
Resting cyst with wall, width	BR	70.2	70.0	5.0	1.2	7.1	58.0	76.0	18
Resting cyst with slime cover, length	BR	145.7	145.0	22.5	5.3	15.4	120.0	176.0	18
Resting cyst with slime cover, width	BR	128.4	128.0	16.9	4.0	13.2	100.0	152.0	18

**Table 33.** Morphometric data on *Conothrix australiensis* based on mounted, protargol-impregnated, and randomly selected specimens. Measurements in  $\mu\text{m}$ . CV – coefficient of variation in %, M – median, Max – maximum, Mean – arithmetic mean, Min – minimum, n – number of individuals investigated, SD – standard deviation, SE – standard error of arithmetic mean.

Characteristic	Mean	M	SD	SE	CV	Min	Max	n
Body, length	76.6	75.0	10.6	2.3	13.8	60.0	100.0	21
Body, width	37.8	38.0	4.3	0.9	11.3	30.0	45.0	21
Body length:width, ratio	2.0	2.0	0.2	0.0	10.7	1.6	2.4	21
Anterior body end to anterior macronuclear nodule, distance	14.7	14.0	2.8	0.6	18.9	11.0	22.0	21
Anterior body end to proximal end of adoral zone of membranelles, distance	31.7	31.0	2.6	0.6	8.1	28.0	36.0	21
Anterior body end to frontal cirrus 3, distance	8.0	8.0	1.7	0.4	21.7	4.0	12.0	21
Anterior body end to right row of marginal cirri, distance	32.7	32.0	4.3	0.9	13.0	26.0	42.0	21
Anterior body end to buccal cirrus, distance	15.0	15.0	2.4	0.5	15.8	10.0	19.0	21
Anterior body end to paroral membrane, distance	12.8	12.0	2.8	0.6	21.9	8.0	18.0	21
Anterior body end to endoral membrane, distance	15.6	15.0	2.6	0.6	16.9	11.0	20.0	21
Paroral membrane, length	9.8	10.0	1.6	0.4	16.8	7.0	12.0	21
Endoral membrane, length	11.9	11.0	2.1	0.5	17.6	10.0	16.0	21
Buccal cavity, width	10.5	10.0	1.6	0.3	15.3	8.0	15.0	21
Anterior macronuclear nodule, length	15.6	15.0	3.1	0.7	19.9	11.0	23.0	21
Anterior macronuclear nodule, width	8.5	9.0	0.9	0.2	10.9	7.0	10.0	21
Macronuclear nodules, distance in between	4.2	3.0	2.9	0.6	69.7	2.0	15.0	21
Macronuclear nodules, number	2.0	2.0	0.0	0.0	0.0	2.0	2.0	21
Nuclear figure, length	35.0	35.0	5.5	1.2	15.8	25.0	51.0	21
Micronucleus, length	6.5	6.0	1.1	0.2	17.2	5.0	10.0	21
Micronucleus, width	6.2	6.0	1.1	0.2	17.7	5.0	9.5	21
Micronucleus, number	1.0	1.0	0.0	0.0	0.0	1.0	1.0	21
Long dorsal kineties, number	3.0	3.0	0.0	0.0	0.0	3.0	3.0	21
Dorsal kineties in posterior third, number	10.3	10.0	1.3	0.3	12.7	8.0	13.0	21
Dorsomarginal kineties, number	1.0	1.0	0.0	0.0	0.0	1.0	1.0	21
Dorsomarginal kinety, number of bristles	3.2	3.0	0.4	0.1	12.6	3.0	4.0	21
Anterior body end to dorsal kinety 2, distance	21.2	21.0	2.7	0.6	13.0	13.0	25.0	21
Posterior body end to dorsal kinety 2, distance	14.3	14.0	3.3	0.7	22.9	10.0	20.0	21
Dorsal kinety 2, length	40.1	39.0	7.3	1.6	18.2	30.0	56.0	20
Dorsal kinety 2, number of bristles	14.4	14.0	1.4	0.3	9.5	12.0	17.0	21
Caudal cirri, number	3.0	3.0	0.0	0.0	0.0	3.0	3.0	14
Posterior bundle of caudal cirri, length	19.9	20.0	2.9	0.6	14.6	15.0	25.0	21
Adoral membranelles, number	18.5	19.0	1.1	0.2	5.8	17.0	21.0	21
Largest ventral adoral membranelle, length	7.1	7.0	1.0	0.2	14.2	5.0	9.0	21
Frontal cirri, number	3.0	3.0	0.0	0.0	0.0	3.0	3.0	21

**Table 33.** Continued.

Characteristic	Mean	M	SD	SE	CV	Min	Max	n
Buccal cirri, number	1.0	1.0	0.0	0.0	0.0	1.0	1.0	21
Right marginal cirri, number	4.4	4.0	0.7	0.2	16.9	3.0	6.0	21
Left marginal cirri, number	2.8	3.0	0.7	0.2	25.4	2.0	5.0	21
Ventral rows, number of cirri	6.2	6.0	0.7	0.2	11.2	5.0	8.0	21
Largest food vacuole, diameter	17.0	15.0	6.2	1.3	36.2	8.0	28.0	21

**Table 34.** Morphometric data on *Apooxytricha bromelicola* based, if not mentioned otherwise, on mounted, protargol-impregnated and randomly selected specimens from a raw culture. Measurements in  $\mu\text{m}$ . CV – coefficient of variation in %, M – median, Max – maximum, Mean – arithmetic mean, Min – minimum, n – number of individuals investigated, SD – standard deviation, SE – standard error of arithmetic mean, VR – ventral row.

Characteristic	Mean	M	SD	SE	CV	Min	Max	n
Body length in vivo (freely motile)	188.0	180.0	29.5	13.2	15.7	150.0	230.0	5
Body width in vivo (freely motile)	83.0	75.0	15.6	7.0	18.9	70.0	100.0	5
Body, length	138.6	137.0	7.6	1.7	5.5	130.0	161.0	21
Body, width	50.9	50.0	5.0	1.1	9.8	41.0	60.0	21
Body length:width, ratio	2.7	2.7	0.3	0.1	11.3	2.3	3.5	21
Adoral zone of membranelles, length <sup>a</sup>	48.4	48.0	3.6	0.8	7.4	40.0	56.0	21
Body length: adoral zone length %	34.9	35.0	2.0	0.4	5.7	30.0	38.0	21
Largest membranelar basis, length	7.7	8.0	–	–	–	7.0	8.0	21
Buccal field, width <sup>b</sup>	8.8	9.0	1.2	0.3	13.5	5.0	11.0	21
Anterior body end to buccal cirrus, distance	13.5	13.0	1.8	0.4	13.4	10.0	16.0	21
Anterior body end to paroral membrane, distance	13.5	13.0	2.0	0.4	14.8	10.0	18.0	21
Anterior body end to endoral membrane, distance	19.3	19.0	2.2	0.5	11.4	15.0	22.0	21
Anterior body end to right marginal row, distance	18.1	19.0	3.8	0.8	20.7	11.0	24.0	21
Anterior body end to first macronuclear nodule, distance	36.2	37.0	3.5	0.8	9.6	30.0	46.0	21
Posterior body end to transverse cirri, distance	31.3	31.0	2.2	0.5	7.2	27.0	35.0	21
Posterior body end to transverse cirri, distance in % of body length	22.7	23.0	1.3	0.3	6.0	20.0	25.0	21
Posterior body end to right marginal cirral row, distance	3.9	4.0	1.9	0.4	48.7	0.0	7.0	21
Posterior body end to left marginal cirral row, distance	0.6	0.0	0.0	0.2	159.6	0.0	3.0	21
Anterior macronuclear nodule, length	24.0	23.0	2.7	0.6	11.1	20.0	29.0	21
Anterior macronuclear nodule, width	10.5	11.0	0.9	0.2	8.8	9.0	12.0	21
Micronuclei, length	3.6	4.0	–	–	–	3.0	4.0	21
Micronuclei, width	3.2	3.0	–	–	–	3.0	4.0	21
Nuclear figure, length	57.4	57.0	3.9	0.9	6.8	52.0	68.0	21
Macronuclear nodules, number	2.0	2.0	0.0	0.0	0.0	2.0	2.0	21
Micronuclei, number	2.8	3.0	1.2	0.3	42.7	1.0	4.0	21
Adoral membranelles, number	40.8	41.0	2.7	0.6	6.7	35.0	44.0	21
Frontal cirri, number	3.0	3.0	0.0	0.0	0.0	3.0	3.0	21
Frontoventral cirri, number	4.0	4.0	–	–	–	4.0	5.0	21
Postoral cirri, number	3.0	3.0	0.0	0.0	0.0	3.0	3.0	21
Buccal cirri, number	1.0	1.0	0.0	0.0	0.0	1.0	1.0	21
Right marginal cirri, number	31.0	31.0	1.7	0.4	5.6	27.0	35.0	21
Left marginal cirri, number	33.0	33.0	2.9	0.6	8.9	28.0	39.0	21
Transverse cirri, number	5.0	5.0	0.0	0.0	0.0	5.0	5.0	21
Pretransverse cirri, number	2.0	2.0	0.0	0.0	0.0	2.0	2.0	21
Caudal cirri, number	3.0	3.0	–	–	–	2.0	3.0	21
Dorsal kineties, number					see text			

Table 34. Continued.

Characteristic	Mean	M	SD	SE	CV	Min	Max	n
Dorsal kinety 1, number of bristles	43.9	46.0	4.9	1.1	11.2	32.0	50.0	21
Dorsal kinety 2, number of bristles	33.6	34.0	4.3	0.9	121.7	26.0	40.0	21
Resting cyst, length (without slime cover)	49.9	50.9	5.5	1.3	11.0	40.0	60.0	19
Resting cyst, width (without slime cover)	48.4	48.0	3.9	0.9	8.1	40.0	55.0	19

<sup>a</sup> Anterior body end to proximal end of zone.

<sup>b</sup> Distance between centre of paroral membrane and right margin of adoral zone.

**Table 35.** Morphometric data on *Monomicrocaryon opisthomuscorum* (upper line) and *Monomicrocaryon australiense* (lower line) based on mounted, protargol-impregnated and randomly selected specimens from non-flooded Petri dish cultures. Measurements in  $\mu\text{m}$ . CV – coefficient of variation in %, M – median, Max – maximum, Mean – arithmetic mean, Min – minimum, n – number of specimens investigated, SD – standard deviation, SE – standard error of arithmetic mean.

Characteristic	Mean	M	SD	SE	CV	Min	Max	n
Body, length	54.8	55.0	6.0	1.6	10.9	42.0	65.0	15
	130.3	132.0	12.0	2.9	9.3	100.0	149.0	18
Body, width	25.0	26.0	2.8	0.8	11.3	19.0	29.0	14
	49.7	49.0	8.2	2.5	16.4	32.0	60.0	11
Body length:width, ratio	2.2	2.2	0.2	0.1	8.6	1.9	2.6	14
	2.7	2.7	0.3	0.1	11.8	2.1	3.1	11
Anterior body end to right marginal cirral row, distance	18.5	18.0	1.6	0.4	8.9	16.0	21.0	15
	22.1	22.0	4.6	1.3	21.1	14.0	31.0	17
Anterior body end to anterior postoral cirrus, distance	22.2	22.0	1.9	0.5	8.4	19.0	25.0	15
Anterior body end to posterior postoral cirrus, distance					not measured			
	29.6	30.0	3.6	0.9	12.1	21.0	35.0	15
Anterior body end to last frontoventral cirrus, distance	69.5	71.0	7.2	1.8	10.4	55.0	81.0	17
	18.4	18.0	1.8	0.5	9.6	15.0	21.0	15
Anterior body end to uppermost pretransverse cirrus, 33.1 distance	42.5	42.0	6.3	1.5	14.7	33.0	58.0	17
	32.0	5.3	1.4	16.0	25.0	42.0	15	
Anterior body end to upper macronuclear nodule, distance					not measured			
	16.3	16.0	2.2	0.6	13.6	12.0	19.0	15
Nuclear figure, length	36.6	36.0	5.8	1.4	15.7	26.0	47.0	18
	22.3	22.0	2.4	0.6	10.9	18.0	26.0	15
Macronuclear nodules, distance in between	46.6	45.5	5.1	1.2	10.9	38.0	55.0	18
	2.0	2.0	1.1	0.3	53.5	0.0	4.0	15
Anterior macronuclear nodule, length	5.3	6.0	1.7	0.4	31.5	2.0	8.0	18
	10.1	10.0	1.0	0.3	9.8	8.0	11.0	15
Anterior macronuclear nodule, width	21.3	22.0	2.5	0.6	11.7	15.0	25.0	18
	6.5	6.0	1.1	0.3	16.2	6.0	10.0	15
Macronuclear nodules, number	13.8	13.5	1.9	0.4	13.5	10.0	17.0	18
	2.0	2.0	0.0	0.0	0.0	2.0	2.0	15
Micronucleus, length	2.0	2.0	0.0	0.0	0.0	2.0	2.0	18
	3.3	3.0	0.8	0.2	23.8	3.0	6.0	15
Micronucleus, width	8.3	8.0	0.8	0.2	10.0	7.0	11.0	18
	3.2	3.0	0.5	0.1	16.5	3.0	5.0	15
Micronuclei, number	7.2	7.0	0.9	0.2	12.0	6.0	9.0	18
	1.0	1.0	0.0	0.0	0.0	1.0	1.0	15
	1.0	1.0	0.0	0.0	0.0	1.0	1.0	18

Table 35. Continued.

Characteristic	Mean	M	SD	SE	CV	Min	Max	n
Adoral zone of membranelles, length	19.6	20.0	1.1	0.3	5.4	18.0	22.0	15
	38.7	38.5	4.4	1.0	11.4	30.0	46.0	18
Body length: adoral zone length (%)	27.9	28.0	3.0	0.8	33.3	23.0	33.0	15
	29.8	30.2	2.8	0.7	9.4	24.8	34.6	18
Adoral membranelles, number	19.3	19.0	0.6	0.2	3.1	18.0	20.0	19
	24.9	25.0	0.9	0.2	3.6	23.0	26.0	17
Anterior body end to paroral membrane, distance	7.2	7.0	0.9	0.2	13.1	5.0	9.0	15
	10.6	10.0	2.2	0.5	20.4	7.0	15.0	15
Paroral membrane, length	10.1	10.0	1.2	0.3	11.5	8.0	12.0	15
Anterior body end to endoral membrane, distance	not measured							
	8.2	8.0	1.4	0.4	17.4	6.0	10.0	15
Endoral membrane, length	14.5	14.0	2.7	0.7	18.6	11.0	20.0	15
	9.0	9.0	1.9	0.5	21.4	6.0	14.0	15
Anterior body end to buccal cirrus, distance	not measured							
	7.4	8.0	1.0	0.3	13.3	5.0	9.0	15
Anterior body end to frontal cirrus 3, distance	15.6	15.0	3.2	0.8	20.6	11.0	21.0	16
	8.3	8.0	0.8	0.2	9.8	6.0	9.0	15
Posterior body end to posteriormost transverse cirrus, distance	not measured							
	4.8	5.0	0.9	0.2	18.0	3.0	6.0	15
Posterior body end to right marginal cirral row, distance	28.4	28.0	3.5	0.8	12.4	23.0	36.0	18
	not measured							
Posterior body end to left marginal cirral row, distance	3.1	2.5	1.9	0.5	62.0	1.0	9.0	18
	not measured							
Frontal cirri, number	1.2	1.0	–	–	–	1.0	2.0	18
	3.0	3.0	0.0	0.0	0.0	3.0	3.0	15
Frontoventral cirri, number	3.0	3.0	0.0	0.0	0.0	3.0	3.0	17
	4.0	4.0	0.0	0.0	0.0	4.0	4.0	15
Buccal cirri, number	4.0	4.0	0.0	0.0	0.0	4.0	4.0	17
	1.0 <sup>a</sup>	1.0	0.0	0.0	0.0	1.0	1.0	15
Postoral cirri, number	1.0	1.0	0.0	0.0	0.0	1.0	1.0	17
	3.5	3.0	0.9	0.2	25.9	3.0	5.0	15
Pretransverse cirri, number	3.0	3.0	0.0	0.0	0.0	3.0	3.0	17
	2.0	2.0	0.0	0.0	0.0	2.0	2.0	15
Transverse cirri, number	2.0	2.0	0.0	0.0	0.0	2.0	2.0	17
	5.0	5.0	0.0	0.0	0.0	5.0	5.0	15
Caudal cirri, number	5.0	5.0	0.0	0.0	0.0	5.0	5.0	17
	3.0	3.0	0.0	0.0	0.0	3.0	3.0	15
Right marginal row, number of cirri	3.0	3.0	0.0	0.0	0.0	3.0	3.0	17
	9.9	10.0	1.4	0.4	14.0	6.0	11.0	15
Left marginal row, number of cirri	25.1	25.0	2.1	0.5	8.3	22.0	28.0	18
	11.7	12.0	0.6	0.2	5.3	11.0	13.0	15
Dorsal kineties, number	26.8	27.0	3.6	0.9	13.4	16.0	32.0	18
	5.0	5.0	0.0	0.0	0.0	5.0	5.0	15
Dorsal kineity 1, number of bristles	see text							
	8.2	8.0	0.7	0.2	8.3	7.0	9.0	15
Dorsal kineity 2, number of bristles	27.4	28.5	3.7	1.2	13.6	18.0	31.0	10
	9.2	9.0	0.9	0.2	10.2	8.0	11.0	15
no data								

Table 35. Continued.

Characteristic	Mean	M	SD	SE	CV	Min	Max	n
Dorsal kinety 3, number of bristles	9.5	9.0	1.2	0.3	12.9	7.0	11.0	17
			no data					
Dorsal kinety 4, number of bristles	3.1	3.0	0.7	0.2	22.3	2.0	4.0	17
			no data					
Dorsal kinety 5 (Mo) or 6 (Ma), number of bristles	8.3	8.0	0.8	0.2	9.3	7.0	10.0	17
	12.2	12.5	3.3	0.9	27.0	6.0	16.0	12
Dorsal bristles, length	7.1	7.0	1.3	0.3	18.4	5.0	10.0	17
			no data			3.0	4.0	17

<sup>a</sup> Three in one out of 25 specimens.

**Table 36.** Morphometric data on *Tachysoma setifera* based on mounted, protargol-impregnated and randomly selected specimens. Measurements in  $\mu\text{m}$ . CV – coefficient of variation in %, M – median, Max – maximum, Mean – arithmetic mean, Min – minimum, n – number of individuals investigated, SD – standard deviation, SE – standard error of arithmetic mean.

Characteristic	Mean	M	SD	SE	CV	Min	Max	n
Body, length	38.2	38.0	3.0	0.7	7.8	32.0	43.0	19
Body, width	17.7	18.0	1.7	0.4	9.4	15.0	20.0	19
Body length:width, ratio	2.2	2.2	0.1	0.1	5.5	1.9	2.3	19
Anterior body end to first macronuclear nodule, distance	12.2	12.0	0.7	0.2	5.8	11.0	14.0	19
Anterior body end to buccal cirrus, distance	6.0	6.0	0.9	0.2	14.7	4.0	8.0	19
Anterior body end to last frontoventral cirrus, distance	11.8	12.0	0.8	0.2	6.7	11.0	13.0	19
Anterior body end to last postoral cirrus, distance	18.7	19.0	0.8	0.2	4.3	17.0	20.0	19
Posterior body end to posteriormost transverse cirrus, distance	2.0	2.0	1.1	0.3	55.2	1.0	5.0	19
Anterior macronuclear nodule, length	7.3	7.0	1.2	0.3	15.8	6.0	11.0	19
Anterior macronuclear nodule, width	4.8	5.0	0.5	0.1	11.2	4.0	6.0	19
Macronuclear nodules, space in between	0.0	0.0	0.0	0.0	0.0	0.0	0.0	19
Nuclear figure, length	12.0	12.0	1.8	0.4	15.0	9.0	17.0	19
Macronuclear nodules, number	2.0	2.0	0.0	0.0	0.0	2.0	2.0	19
Micronucleus, length	1.9	2.0	0.2	0.1	11.0	1.5	2.2	19
Micronucleus, width	1.8	1.8	0.2	0.1	13.7	1.2	2.0	19
Micronucleus, number	1.0	1.0	0.0	0.0	0.0	1.0	1.0	19
Anterior body end to proximal end of adoral zone, distance	14.0	14.0	0.9	0.2	6.3	12.0	15.0	19
Adoral zone, number of membranelles	14.4	14.0	0.8	0.2	5.3	12.0	15.0	19
Adoral zone, width of largest membranelle	3.9	4.0	–	–	–	3.5	4.0	19
Body length: adoral zone length, ratio in %	36.8	35.9	3.0	0.7	8.0	33.0	42.0	19
Paroral membrane, length	4.5	5.0	1.1	0.3	24.0	3.0	6.0	19
Endoral membrane, length	3.5	3.0	0.6	0.1	17.4	3.0	5.0	19
Frontal cirri, number	3.0	3.0	0.0	0.0	0.0	3.0	3.0	19
Frontoventral cirri, number	4.0	4.0	0.0	0.0	0.0	4.0	4.0	19
Buccal cirri, number	1.0	1.0	0.0	0.0	0.0	1.0	1.0	19
Postoral cirri, number	3.0	3.0	0.0	0.0	0.0	3.0	3.0	19
Pretransverse cirri, number	2.0	2.0	0.0	0.0	0.0	2.0	2.0	19
Transverse cirri, number	5.0	5.0	0.0	0.0	0.0	5.0	5.0	19
Right marginal cirri, number	3.1	3.0	–	–	–	3.0	4.0	19
Left marginal cirri, number	4.0	4.0	–	–	–	3.0	4.0	19
Dorsal kineties, number	4.0	4.0	0.0	0.0	0.0	4.0	4.0	19
Bristles in dorsal kinety 1, number	3.2	3.0	0.5	0.1	15.9	3.0	5.0	19

**Table 36.** Continued.

Characteristic	Mean	M	SD	SE	CV	Min	Max	n
Bristles in dorsal kinety 2, number	6.3	6.0	–	–	–	6.0	7.0	19
Bristles in dorsal kinety 3, number	7.1	7.0	–	–	–	7.0	8.0	19
Bristles in dorsal kinety 4, number	3.1	3.0	–	–	–	3.0	4.0	19
Bristle length in anterior body half	2.2	2.0	0.3	0.1	14.6	1.7	3.0	19
Last bristles of dorsal kineties 2 and 3, length	8.3	8.0	1.4	0.3	16.6	7.0	11.0	19
Elongated dorsal bristles, number	2.0	2.0	0.0	0.0	0.0	2.0	2.0	19

**Table 37.** Morphometric comparison of some main features of *Tachysoma humicola humicola* from Austria (THA, from Foissner 1984); *T. humicola humicola* from Australian site 27 (TAU, original data), *T. humicola longisetum* from Kenya (THL, from Foissner 1998); and → *T. setifera* nov. spec. (TS) from Australian site (26). All based on same protargol method. Averages and extremes are given.

Characteristic	THA	TAU	THL	TS
Body, length (µm)	42.5 (38–50)	43.8 (36–50)	44.0 (37–50)	38.2 (32–43)
Adoral membranelles, number	14.8 (14–16)	15.0 (15–15)	15.0 (15–15)	14.4 (12–15)
Right marginal row, number of cirri	6.5 (6–8)	5.6 (5–6)	6.0 (6–6)	3.1 (3–4)
Left marginal row, number of cirri	7.2 (7–8)	6.7 (6–7)	7.1 (7–8)	4.0 (3–4)
Elongated dorsal bristles, number	0 (0–0)	0 (0–0)	3 (3–3)	2 (2–2)
Specimens investigated, number	11	21	13	19

